TRANSPORTATION RESEARCH

# RECORD

## No. 1377

*Pavement Design, Management, and Performance*

---

# Nondestructive Deflection Testing and Backcalculation for Pavements

*Proceedings of a Symposium*
*August 19–21, 1991*
*Nashville, Tennessee*

*A peer-reviewed publication of the Transportation Research Board*

TRANSPORTATION RESEARCH BOARD
NATIONAL RESEARCH COUNCIL
NATIONAL ACADEMY PRESS
WASHINGTON, D.C. 1992

**Transportation Research Record 1377**
Price: $35.00

Subscriber Category
IIB pavement design, management, and performance

TRB Publications Staff
*Director of Records and Editorial Services*: Nancy A. Ackerman
*Senior Editor*: Naomi C. Kassabian
*Associate Editor*: Alison G. Tobias
*Assistant Editors*: Luanne Crayton, Norman Solomon, Susan E. G. Brown
*Graphics Specialist*: Terri Wayne
*Office Manager*: Phyllis D. Barber
*Senior Production Assistant*: Betty L. Hawkins

Printed in the United States of America

**Library of Congress Cataloging-in-Publication Data**
National Research Council. Transportation Research Board.

Nondestructive deflection testing and backcalculation for pavements: proceedings of a symposium, August 19–21, 1991, Nashville, Tennessee.
p. cm.—(Transportation research record ISSN 0361-1981; no. 1377)
ISBN 0-309-05420-6
1. Pavements—Testing. 2. Non-destructive testing.
I. National Research Council (U.S.). Transportation Research Board. II. Series: Transportation research record: 1377.
TE7.H5 no. 1377
[TE250]
388 s—dc20 92-47094
[625.8] CIP

**Sponsorship of Transportation Research Record 1377**

**GROUP 2–DESIGN AND CONSTRUCTION OF TRANSPORTATION FACILITIES**
*Chairman: Charles T. Edson, New Jersey Department of Transportation*

**Pavement Management Section**
*Chairman: Joe P. Mahoney, University of Washington*

Committee on Strength and Deformation Characteristics of Pavement Sections
*Chairman: Albert J. Bush III, USAE Waterways Experiment Station*
*Gilbert Y. Baladi, Richard D. Barksdale, Robert C. Briggs, Stephen F. Brown, George R. Cochran, Ronald J. Cominsky, Billy G. Connor, Mark P. Gardner, John P. Hallin, Dennis R. Hiltunen, Lynne H. Irwin, Starr D. Kohn, Robert L. Lytton, Michael S. Mamlouk, Soheil Nazarian, Rasmus S. Nordal, Gonzalo Rada, J. Brent Rauhut, Byron E. Ruth, Larry A. Scofield, Tom Scullion, Stephen B. Seeds, R. N. Stubstad, Marshall R. Thompson, Per Ullidtz, Jacob Uzan, Thomas D. White, Haiping Zhou*

Frank R. McCullagh, Transportation Research Board staff

The organizational units, officers, and members are as of December 31, 1991.

# Transportation Research Record 1377

## Contents

# Foreword

TRB conducted a symposium on "Capabilities and Limitations of Nondestructive Deflection Testing (NDT) and Backcalculation for Estimating Stiffness of Paving Materials" in August 1991. As part of that symposium, a workshop was held to reach consensus on current capabilities and limitations, and directions to pursue for improvements.

This Record contains 13 technical papers presented at that symposium and 7 other papers related to the theme of the symposium. In addition, the Record contains reports prepared by Irwin, Thompson, and Smith, who led the discussion groups on practical limitations and what can be done to overcome them, backcalculation limitations and future improvements, and current and future applications of nondestructive deflection measurements, respectively.

Darter et al. summarize the theory and practice of backcalculation for portland cement concrete pavements, present results from pavement testing around the United States, and discuss portland cement pavement evaluation and design. Maestas and Mamlouk compare four backcalculation programs for determining material properties and asphalt concrete overlay needs. Janoo and Berg present results of a study in which frozen and thawed pavement sections are compared with respect to deflections and backcalculated layer moduli.

Rada, Rabinow et al. present quality assurance software and methodology to evaluate falling weight deflectometer (FWD) data collected on the Strategic Highway Research Program (SHRP) Long Term Pavement Performance (LTPP) test sections. Rauhut and Jordahl discuss the variability of layer thicknesses and material properties on selected SHRP test sections and their effects on measured deflections and backcalculated moduli. Siddharthan et al. quantify the effects of random error in pavement deflection measurements on backcalculated pavement moduli and pavement performance parameters. Hossain and Scofield compare laboratory measured and in situ backcalculated asphalt moduli, discuss differences, and provide recommendations regarding their uses.

Rada et al. describe SHRP's methodology for selecting software and developing a procedure to perform backcalculation on the FWD data contained in the SHRP database. Sebaaly et al. compare pavement moduli backcalculated from deflections obtained with the FWD and under moving trucks using strain gauges and multidepth deflectometers. Brunton and de Almeida describe an updated layered-elastic pavement modeling program incorporating a nonlinear subgrade model. Uzan et al. present a procedure for backcalculating the rigidity of portland cement slabs and modulus of subgrade reaction from nondestructive test results at center slab or at a free edge and present results from selected SHRP sections. Briggs et al. present results of ground penetrating radar testing on SHRP LTPP sections and its role in reducing variability in backcalculated material properties. Kim et al. use the multidepth deflectometer to evaluate the accuracy of layered-elastic pavement models as used with the FWDs.

Jackson and Murphy evaluate a procedure to load-zone light pavement structures using the FWD. Zhou et al. discuss a procedure developed and used in Oregon to determine pavement material properties and overlay requirements. Yuan and Nazarian document the development of an algorithm using spectral analysis of surface waves to characterize stiffness of pavement materials and determine pavement layer thickness. Hossain and Scofield describe the use of nondestructive test and backcalculation techniques to characterize material properties and perform pavement designs on cracked and seated PCC pavements. Nazarian and Chai examine the effect of errors and inaccuracies in nondestructive testing and their effects on pavement design. Jung and Stolle present an alternative to layered-elastic procedures for analyzing severely damaged and cracked pavements with nondestructive test devices. Zaniewski and Hossain discuss the sensitivity of structural analyses of pavements to variations in pavement layer thicknesses and temperature correction factors.

# Report of the Discussion Group on Practical Limitations and What Can Be Done To Overcome Them

LYNNE H. IRWIN

This discussion group identified a number of limitations associated with the state of the practice of backcalculation and nondestructive deflection testing (NDT). We did not attempt to make a distinction regarding whether the limitations were separately associated with backcalculation or NDT or were associated with both.

## LIMITATIONS

The methodology is not sensitive to

- Thin layers (the meaning of thin varies with depth beneath the surface),
- Adjacent layers of similar modulus,
- Large modular ratios (soft layers beneath concrete are a particular problem), or
- The degree of bonding between layers.

The methodology is both too complicated and not sophisticated enough.

The results are only representative of the point tested, at the time tested, under the conditions prevailing at the time.

Parameters that are known to matter are not taken into consideration adequately, are not properly considered, or must be assumed, such as

- Accurate layer thickness data,
- Depth to bedrock or a hard layer,
- The vertical gradient of modulus in the subgrade,
- The gradient of temperature in the surface layer,
- The moisture content of granular layers,
- Poisson's ratio for the materials, and
- The stress sensitivity of granular materials.

There are no adequate criteria for evaluating the reasonableness of the moduli arising from backcalculation. Goodness-of-fit criteria are not adequate.

Layered elastic models are not closely enough related to the realities of a pavement. (For instance, subgrades are not infinitely deep at constant modulus.)

It is difficult to apply the methodology in an urban street environment. (Because of subsurface utilities and utility cuts, the correspondence of the models to the realities of the pavements is poor, traffic is a problem, and productivity is poor.)

We do not know exactly when (time of day or year) or where (in or between the wheelpath) to perform FWD tests in order to get the "right" answer to questions such as overlay thickness design.

Pavements suffer from too much variability, both in distance (along and beneath the road) and over time.

It is hard to apply the current science to the complexity of pavements.

## OVERCOMING THE LIMITATIONS

Without any intent to be humorous or flippant, the group suggested we may need to overhaul our expectations for the methodology. Maybe we want more than it is able to provide.

Ideas on ways to overcome the limitations fell into two major categories: (a) improvement of the equipment and (b) improvement of the analytical models. The group attempted to look into the future to try to identify how the methodology might be changed to make it more useful.

### Better Equipment

Field testing should provide coverage over 100 percent of the pavement surface. This would help to identify the weak areas that are likely to fail first. The need for precision on the part of such an initial screening tool might be somewhat reduced. More detailed testing could be focused on the critical points thereby identified.

Future testing methods should perhaps involve a rolling wheel load. The significance of this was not absolutely clear, but it is known that current methods do not involve any rotation of principal stresses (which occurs at a point as the moving wheel approaches).

Future equipment should provide data on temperature gradients, moisture gradients, and density and modulus gradients.

In terms of applications of the equipment the concept of "fingerprinting" (through initial NDT testing) was advanced. This could be followed by retesting, perhaps annually. The subsequent tests would be compared with the first tests to determine areas of changed conditions, rates of change, and so forth.

Cornell University, 420 Riley-Robb Hall, Ithaca, N.Y. 14853.

### Better Analytical Methods

In the future we need to integrate analytical and empirical approaches with pavement evaluation. The objective should be to yield answers to practical questions such as overlay thickness needs, remaining life, pavement strength, pavement maintenance needs, and so forth.

Future methods should be more able to deal with mixed traffic loading (cars and trucks). The use of the equivalent single-axle load should be reduced or eliminated.

Future methods should be more capable of dealing with the various sources of variability (over time and space) and be able to yield answers based on reliability concepts.

## MAJOR VARIABLES

The discussion group identified three major independent variables that have to be addressed in pavement evaluation: environment, traffic, and construction and maintenance quality.

There is also a need to provide the proper education and training for those who will do the pavement evaluation. This was believed to have the most potential for overcoming many of the limitations that were identified.

The group discussed, but did not resolve, whether NDT and backcalculation were sciences or arts. We agreed, however, that it has evolved over a period of 35 to 40 years, going back to the emergence of the Benkelman beam. The investment that has led to the present state of the practice should be considered a sunk cost. Future developments should take into consideration current and anticipated needs and objectives. They should not necessarily be limited to minor refinements of the present methodology.

The group believed that we should carefully consider why we are doing NDT and backcalculation. Then we should look for better ways to accomplish the objectives. In this context, better does not have to mean less expensive or less sophisticated, but it should mean that it would yield more accurate and more complete results with fewer limitations.

In short, the methodology must be responsive to the mission.

# Report of the Discussion Group on Backcalculation Limitations and Future Improvements

MARSHALL R. THOMPSON

Initial breakout group discussions identified the more frequently encountered problems and limitations associated with the use of existing NDT data and BC procedures. They include

1. How to accommodate depth to stiff layer effects,
2. The need to accommodate nonlinear material behavior,
3. The inability to detect the contribution of "thin layers," and
4. The fact that BC moduli are "effective" moduli that reflect and include the impact of the pavement system, and are not unique material/soil properties.

More details concerning specific issues covered in the breakout group deliberations are summarized below.

## *k* (MODULUS OF SUBGRADE REACTION) VERSUS *E*

*k* is the preferred method of characterizing slab support for rigid pavement analyses and design. Slab theory can also accommodate an elastic modulus subgrade characterization, but the *k* characterization approach is more versatile and useful. BC procedures for *k* based on slab theory are available. Identified difficulties in *k* BC procedures include the accommodation of "layered support systems" (subbase/subgrade) and defining the "degree of bonding" between the various layers of a composite pavement. A breakout group straw vote conducted at the end of the discussion indicated a preference for *k*.

## DATA BASE—ITERATIVE PROCEDURES

Current BC procedures use either an iterative approach (each deflection basin is analyzed in an iterative manner until the assigned layer moduli provide calculated deflection basins that are comparable to the measured basin) or a data base approach (layer moduli are established by matching the measured deflection basin with a data base of precalculated basins based on a range of pavement layer and subgrade moduli).

University of Illinois at Urbana-Champaign, 1211 Newmark Lab, 205 N. Mathews, Urbana, Ill. 61801.

The data base of deflection basins is established for given thickness and thus cannot readily accommodate thickness variability. The iterative approach can accommodate the pavement thicknesses and other material and cross-section details for the specific pavement section under consideration. Iterative approach advocates emphasize that the procedure does not force a moduli solution, but seeks moduli that are most appropriate for the pavement section. The group believed that both procedures are needed and have relevant and appropriate applications.

## SPECTRAL ANALYSIS OF SURFACE WAVES

Various symposium presentations indicated that significant improvements in hardware and computational capabilities and procedures have enhanced spectral analysis of surface waves (SASW) analysis techniques. A particularly useful SASW capability is the identification of material layer boundaries (thickness). A frequently expressed concern is the ability to scale up the SASW BC low strain moduli to the strain levels associated with actual loading conditions. The group expressed an appreciation of SASW capabilities and endorsed the continued pursuit of SASW BC applications. SASW can provide results that are helpful and useful in a broad-based NDT testing and BC effort.

## EXPERT SYSTEMS

BC moduli based on the analyses of a given NDT data base are user dependent (i.e., different results may be achieved by different users). The use of expert systems in BC activities facilitates the achievement of more uniform results. Through the expert system, it is possible to use state-of-the-art technology and provide competent guidance to the broad spectrum of BC system users. The NCHRP MODULUS program and its application in SHRP is an example. Specific guidelines (incorporated into the BC computer programs) have been established to guide the SHRP regional contractors in their analysis of SHRP NDT data. The continued development of expert system applications in BC is encouraged. However, qualified materials/soils/pavement engineers should continue to be involved in BC developments and applications. BC moduli must always stand the test of reasonableness.

## FUTURE IMPROVEMENTS

### Layer Thickness Determination

BC layer moduli are dependent on the assigned layer thicknesses (including the subgrade). High modulus layers (asphalt concrete and PCC) are particularly sensitive to this effect. Improved techniques for establishing pavement layer thicknesses will provide for refined moduli estimates. Some promising techniques discussed at the symposium were ground penetrating radar and SASW applications.

### Stress Dependent Material Characterization

The resilient moduli of cohesive soils and granular materials are stress dependent. Many BC systems are based on constant modulus conditions. It was the group consensus that future developments in BC procedure development should encourage the accommodation of stress dependent modulus conditions.

### Rigid Pavements—Composite Pavements

The effect of FWD loading location (i.e., interior slab, transverse joint, corner, or edge), the definition of appropriate slab support conditions (curling and warping effects and loss of slab support), and the characterization of a composite pavement section complicate BC procedures for rigid and composite pavements. Considerable additional effort is required to develop improved procedures and techniques to overcome these limitations.

### FWD Data—Pavement Performance

Increased efforts should be directed toward establishing procedures that use NDT pavement response data or derived quantities (e.g., asphalt concrete layer curvature estimates and deflection basin area) data to characterize pavement performance potential. For example, flexible pavement surface deflection is an excellent indicator of future performance, and FWD deflection variability can be used to capture within project structural section variability.

### Technology Transfer—Expert Systems

Strong support should be provided to developing technology transfer concerning NDT testing, BC procedures and their applications and limitations, and other NDT data applications and uses.

# Report of the Discussion Group on Current and Future Applications of Nondestructive Deflection Measurements

ROGER E. SMITH

The group tried to address how and what applications of nondestructive deflection testing (NDT) measurements are used currently and envisioned in the future. Specific areas suggested for consideration were pavement performance, pavement management, pavement design, bridge evaluation, and material property determination.

## CURRENT USES

Several current uses of NDT were identified.

### Design

In pavement design, deflection testing is used in subgrade evaluation for new design and in overlay design to determine acceptable deflections, elastic layer characterization, and structural numbers.

### Construction

During or shortly after construction, NDT is used to determine variations through the project with an emphasis on locating areas of localized problems and in relative characterization of structural capacity.

### Pavement Performance

NDT measurements are used in analysis of performance in the following areas: seasonal load limits on paved and unpaved roads, nonlinearity of subgrade materials, joint load transfer across joints and cracks, and loss of support for portland cement concrete pavement slabs.

### Pavement Management

In pavement management, the following areas were identified as currently being used: quantification of effects of material modifications such as stabilization of subgrades, relative characterization of structural capacity, and need for rehabilitation or overlay based on changes in deflections.

Texas Transportation Institute, Texas A&M University, College Station, Tex. 77840.

## FUTURE USES

Several future uses were also identified. These are uses that the group plan, expect, or hope to use NDT measurements for in the future.

### Design

Several participants expressed an interest in using NDT data for design. The areas of interest included mechanistic design, reliability-based design, verification of structural equivalence of different designs, determination of material properties, and evaluation of layer properties used in design.

In addition, the following were identified particularly for rehabilitation design: structural capacity of existing pavement and evaluation of crack and seat overlay thickness.

### Construction

In construction, the following areas were identified as expected uses of NDT: acceptance criteria, especially for end result specifications, and the determination of layer thicknesses, stiffnesses, moisture contents, and densities.

### Performance

Several areas are planned for performance, including load restrictions, prediction of future performance, prediction of remaining life, and changes in layer properties.

### Pavement Management

In pavement management, several items were identified in addition to those mentioned previously, including continuous NDT measurements, high-speed measurements, and forensic engineering (failure analysis).

### Bridges

The following items were identified for bridges: delaminations in bridge decks and dynamic analysis for new bridges and over time.

## CONCERNS

The following were identified as particular concerns:

- The NDT must provide uniform results if it will be used in end result specifications.
- The level of complexity of operation and interpretation must be matched to the level of sophistication of the user.
- The forward calculation problem must be addressed.
- Implementation of NDT and research and development are occurring at the same time.

# Concrete Pavement Backcalculation Results from Field Studies

MICHAEL I. DARTER, KURT D. SMITH, AND KATHLEEN T. HALL

Deflection testing and backcalculation have been conducted on all types of concrete highway and airfield pavements for many years. Backcalculation of the in situ slab elastic modulus and the effective $k$-value or elastic solid subgrade modulus (beneath the slab) from deflection basins was first proposed by Westergaard in 1925 and actually conducted in the 1930s. Over the past decade, backcalculation has greatly improved and is now extremely rapid, highly automated, and reliable. The results from concrete pavement deflection testing and backcalculation have been used for several purposes: to compute the load-carrying capacity of concrete pavement for aircraft and truck loadings, to design structural overlays, and to detect loss of support beneath slab corners. Thus, deflection testing and backcalculation of in situ concrete pavement properties have proven to be very beneficial. The theory and practice of backcalculation for concrete pavements as they have developed over the years are summarized, results from a wide variety of pavements throughout the United States are presented, and implications for evaluation and design of concrete pavements are discussed.

Deflection data have proven to be very useful in the evaluation and structural rehabilitation of concrete pavements. Deflection testing has been conducted on all types of concrete pavements over the past 10 to 15 years on many highways and airfields throughout the United States. The Dynatest falling weight deflectometer (FWD) has been used frequently on such pavements with weights ranging from 5 to 50 kips. The analysis of the deflection basins has greatly improved over the years and is now highly automated and reliable.

The results from deflection testing of concrete pavements and backcalculation have been used for several purposes: to compute the load-carrying capacity of the concrete pavement for aircraft and truck loadings, to design structural overlays, and to detect loss of support beneath slab corners. These results have in turn been used in the selection and design of rehabilitation treatments for many highway and airfield projects.

It is no longer necessary to remove slabs to conduct expensive and time-consuming plate load tests, because the in situ (effective) $k$-value can best be computed from deflections measured at the top of the slab using the FWD. In addition, the in situ elastic modulus of the concrete slab can be directly backcalculated from the same data. If no cores or beams can be taken from the pavement, the flexural strength of the concrete can be roughly estimated as well. These values can be used in the structural evaluation and design of overlays.

The results of many backcalculation studies have led to the conclusion that the in situ $k$-value that actually supports the slab is not necessarily the same as that obtained using the traditional procedures for obtaining the effective $k$-value on top of the base/subbase (where the $k$-value measured on top of the subgrade is increased depending on the thickness and stiffness of the base/subbase layers placed on the subgrade). It is, therefore, not appropriate to describe a $k$-value "on top of a base or subbase layer," only "a $k$-value beneath the slab." This has significant implications for design of new pavements and evaluation of existing pavements.

This paper describes the theory and practice of backcalculation for concrete pavements, presents results from many field studies on diverse pavement and subgrade sections, and discusses implications for evaluation and design of concrete pavements.

## BACKCALCULATION THEORY AND PROCEDURES

Concrete pavements have long been characterized using plate theory, in which the slab is characterized by a thickness $h$ and a modulus of elasticity $E$, and the foundation is characterized as a dense liquid $k$-value. Westergaard developed stress and deflection equations that have been verified and used to the present day in concrete pavement design (*1,2*). In addition, Hogg (*3*) and Holl (*4*) developed the theory to model a slab as a plate on an elastic solid foundation. Equations for deflection basins for a plate on a dense liquid and elastic solid subgrade were presented by Losberg in 1960 (*5*).

Westergaard introduced the term "radius of relative stiffness" to describe the stiffness of a concrete slab relative to that of the subgrade, given by the following equation:

$$\ell_k = \sqrt[4]{\frac{E_{pcc} h_{pcc}^3}{12\,(1 - \mu_{pcc}^2)k}} \qquad (1)$$

where

$\ell_k$ = dense liquid radius of relative stiffness (in.),
$E_{pcc}$ = concrete elastic modulus (lb/in.$^2$),
$h_{pcc}$ = concrete thickness (in.),
$\mu_{pcc}$ = concrete Poisson's ratio, and
$k$ = modulus of subgrade reaction (lb/in.$^2$/in.).

Westergaard (*1*) actually proposed in 1925 that the subgrade $k$-value should be backcalculated from deflections at the sur-

ERES Consultants, Inc., 8 Dunlap Court, Savoy, Ill. 61874-9501.

face of the slab rather than measured from load tests on the subgrade:

> It is true that tests of bearing pressures on soils have indicated a modulus, $k$, which varies considerably depending on the area over which the pressure is distributed. Yet, so long as the loads are limited to a particular type, that of wheel loads on top of the pavement, it is reasonable to assume that some constant value of the modulus, $k$, determined empirically, will lead to a sufficiently accurate analysis of the deflections and stresses. . . . The modulus, $k$, enters in the formulas for the deflections of the pavements, and may be determined empirically, accordingly, for a given type of subgrade, by comparing the deflections found by tests of full-sized slabs with the deflections given by the formulas.

To support the statement that bearing tests produce varying $k$-values depending on the loaded area, Westergaard cited the results of field test reported by Bijls in 1923 (*6*), Goldbeck in 1925 (*7*), and Goldbeck and Bussard in 1925 (*8*). However, Westergaard's 1925 paper (*1*) contained only a center-slab deflection equation for a concentrated load. The center deflection equation for a distributed load of radius $a$ was presented in Westergaard's 1939 paper (*2*):

$$d_0 = \left(\frac{P}{8k\ell_k^2}\right) \times \left\{1 + \left(\frac{1}{2\pi}\right)\left[\ln\left(\frac{a}{2\ell_k}\right) + \gamma - 1.25\right]\left(\frac{a}{\ell_k}\right)^2\right\} \qquad (2)$$

where

$d_0$ = maximum deflection at center of load (in.),
$P$ = load,
$a$ = load radius, and
$\gamma$ = Euler's constant (0.57721566490).

The first known attempts at backcalculation of slab and support properties were at the Arlington, Virginia, experimental tests conducted in the 1930s by the Bureau of Public Roads as part of a major test program to verify the Westergaard equations for stress and deflection. One portion of the program was to develop procedures to determine an appropriate $k$-value. Two different procedures were evaluated: (a) load-deflection testing with a loaded plate directly on the subgrade and (b) load-deflection testing on top of the slab and the use of Westergaard's equations to determine a value for the in situ $k$-value and the in situ slab elastic modulus $E$. The description of the tests and the results of the studies were reported by Teller and Sutherland (*9,10*).

The plate bearing tests conducted directly on the subgrade soil were done using several plate diameters between 2 and 84 in. The test results demonstrated "the important effect of plate area on the pressure intensity required to produce a given plate displacement on the soil in question," particularly for plate diameters less than 26 in. (*10*).

The elastic modulus of the concrete slabs at the Arlington test site was determined by two methods: (a) laboratory testing of cores and beams from the pavement and (b) backcalculation from deflection measurements. Radius of relative stiffness values were determined by matching slab deflection basin measurements to contours developed by Westergaard (*1*) for deflection versus distance from load. This required preparing two-dimensional diagrams of the deflection basins and varying both the horizontal and vertical scales until the measured deflection basins matched the theoretical basins as closely as possible. The subgrade $k$-value could then be backcalculated using Westergaard's deflection equations, and the concrete slab modulus could be backcalculated from the definition of radius of relative stiffness. The backcalculation results are shown in Table 1. Teller and Sutherland (*10*) summarized the results of the backcalculation of $k$ and $E$ from interior, edge, and corner defections:

> For a given slab thickness, values of the radius of relative stiffness, $\ell$, are in good agreement for the three cases of loading (interior, edge, and corner). For conditions that are comparable there is rather good agreement also between the values of modulus of subgrade reaction, $k$, as determined by pavement deflection (on top of the slab), for the interior and edge loadings but the value for the corner loading is consistently lower.
>
> The values of the modulus of elasticity for the concrete, $E$, as determined from the slab deflections are in the same general range as the values that were obtained from the tests of the laboratory specimens (at edge and interior positions).

Although Westergaard proposed backcalculating $k$-values from deflection measurements on full-size slabs in 1925, the fact that he did not present a direct method for doing so, in the words of J. P. Sale (*11*), "has through the years caused Corps' researchers and, we believe, many others considerable concern." The laborious method used to analyze the Arlington test data, in which theoretical and measured deflection basins were matched by hand, was certainly not suited to analysis of large deflection data sets.

It is perhaps because of this lack of a backcalculation method that $k$-values came to be measured by subgrade plate load tests. When bases came into widespread use, it then seemed logical to increase the $k$-value to account for various base types and thicknesses. In time, because of the high costs and long testing times involved, actual plate load testing of subgrades and bases became more uncommon, and typical ranges of $k$-values were identified for various subgrade soils and bases. When very stiff (i.e., stabilized) bases began to come into use, it was naturally expected that the $k$-value would be very high because of the support that this type of base would provide.

Backcalculation methods for multilayer elastic pavement systems first appeared in the 1970s, starting with Scrivner's solution for elastic moduli in a two-layer pavement system in 1973 (*12*). Because of the integral nature of the deflection equations given by elastic layer theory (*13,14*), these backcalculation methods relied on rather complex graphical or computerized solution methods.

A simple two-parameter approach to backcalculation of surface and foundation moduli for a two-layer pavement system was proposed by Hoffman and Thompson in 1981 for flexible pavements (*15*). They proposed the AREA, given by the equation below, to characterize the deflection basin:

$$\text{AREA} = 6 * \left[1 + 2\left(\frac{d_{12}}{d_0}\right) + 2\left(\frac{d_{24}}{d_0}\right) + \left(\frac{d_{36}}{d_0}\right)\right] \qquad (3)$$

**TABLE 1 Backcalculation of *k*-Value and Concrete Modulus from Interior and Edge Deflections and Comparison with Subgrade *k*-Value and Laboratory *E* Values, Arlington Test Site, 1930 (*10*)**

| Load Position | Season | Slab Thick | Effective k-value | Slab E |
|---|---|---|---|---|
| Interior | Late summer | 6 in | 195 psi/in | 4,140,000 psi |
| | Winter | 7 | 238 | 5,750,000 |
| | Summer | 7 | 222 | 4,670,000 |
| | Winter | 8 | 260 | 5,500,000 |
| | Late fall | 9 | 203 | 5,490,000 |
| | Summer | 9 | 220 | 4,210,000 |
| | Means | | 223 | 4,960,000 |
| Edge | Late summer | 6 | 171 | 4,235,000 |
| | Winter | 7 | 212 | 5,125,000 |
| | Winter | 8 | 279 | 5,175,000 |
| | Late fall | 9 | 243 | 5,220,000 |
| | Means | | 226 | 4,339,000 |

Comparisons: Field static plate bearing tests (using 30-in plate and 0.05-in deflection) directly on subgrade soil:

k-value = 166 (January) to 233 (June) psi / in.

Laboratory static concrete E modulus tests determined from flexural tests on specimens cut from slabs:

Dried for 12 months at normal atmosphere of the laboratory = 4,500,000 psi

Immersed for 10 months in water at laboratory temperature = 6,000,000 psi

where

$d_0$ = maximum deflection at the center of the load plate (in.) and
$d_i$ = deflections at 12, 24, and 36 in. from plate center (in.).

AREA has units of length, rather than area, since each of the deflections is normalized with respect to $d_0$ to remove the effect of various load levels and to restrict the range of values obtained. AREA and $d_0$ are thus independent parameters, from which the surface and foundation elastic moduli may be determined. Hoffman and Thompson developed a nomograph for backcalculation of flexible pavement surface and subgrade moduli from $d_0$ and AREA.

During the early 1980s, the AREA concept was applied to backcalculation of slab *E* values and subgrade *k*-values for many concrete pavements (*16*). The ILLISLAB finite element program was used to compute a matrix of maximum deflections and AREA solutions by varying the *k*-value and *E* for a given slab thickness. A family of curves was then plotted, as shown in Figure 1, for a given slab thickness. Individual mid-slab deflection basins (AREA and maximum deflection) measured with the falling weight deflectometer could then be plotted on the matrix, and the slab *E* and foundation's *k*-value determined directly. This procedure was used to backcalculate hundreds of concrete pavement deflection basins during the 1980s and produced very reasonable and consistent results for many highway and airfield projects. The only drawback to this approach was its excessive labor intensiveness. An improvement in efficiency came in 1985 when the procedure was computerized by Foxworthy (*17*) using a vectoring scheme. However, the finite element program still had to be run several times to achieve a backcalculated *k*-value and slab *E* modulus (*17*).

The next major advancement was the development of a closed-form solution for backcalculation of the slab *E*, subgrade *k*-value, and subgrade *E* to replace the graphical procedures used previously. This solution was made possible by research by Barenberg and Petros (*18*) and by Ioannides (*19*), which demonstrated that, for a given load radius and sensor arrangement, a unique relationship exists between AREA and the "dense liquid" radius of relative stiffness of the pavement. A different unique relationship was also shown to exist between AREA and the "elastic solid" radius of relative stiffness of the pavement (in which the subgrade is characterized by an elastic modulus and a Poisson's ratio). In 1989, Ioannides et al. (*20*) demonstrated the application of this closed-form approach using the computer program ILLIBACK, which was developed to provide rapid analysis of deflection basins.

Recently, Hall (*21*) developed highly accurate equations for the dense liquid and elastic radii of relative stiffness versus AREA, using the plate-on-a-dense-liquid and plate-on-an-elastic-solid deflection equations presented by Losberg (*5*).

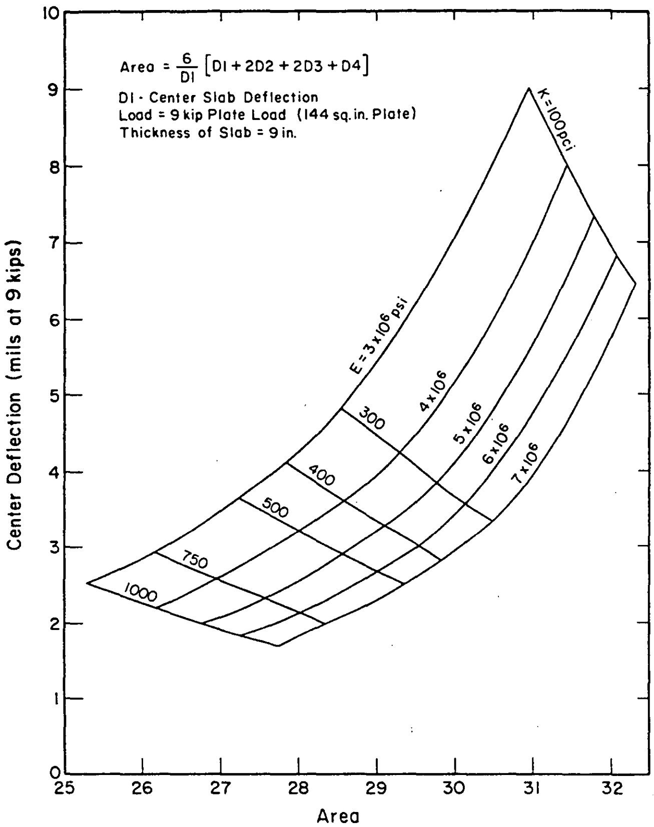


**FIGURE 1 Graphical simultaneous solution of $E$ and $k$ for a known slab thickness.**

The curve obtained for $\ell_k$ as a function of AREA is illustrated in Figure 2 and is given by the following equation:

$$\ell_k = \left[\frac{\ln\left(\dfrac{36 - \text{AREA}}{1812.279}\right)}{-2.55934}\right]^{4.387} \tag{4}$$

Either the ILLIBACK program or the equations presented in this paper may be used to backcalculate the slab $E$ and subgrade $k$-value. AREA is calculated from deflection basin measurements (Equation 3) and used to determine $\ell_k$ (Equation 4). The $k$-value may then be determined using Westergaard's deflection equation (Equation 2). With $\ell_k$ and $k$-value known, the slab $Eh^3$ value may then be computed from the definition of $\ell_k$ (Equation 1), and for a known slab thickness $h$, the concrete modulus $E$ may be determined.

To illustrate this backcalculation procedure, Figure 3 was developed for determination of $k$-value for a load of $P$ = 9,000 lb and an FWD load plate radius $a$ = 5.9 in. The maximum deflection $d_0$ measured at loads within about 2,000 lb more or less than 9,000 lb may be scaled to an equivalent 9,000-lb maximum deflection (the AREA is the same regardless of whether the deflections are normalized to 9,000 lb), or the $k$-value may be determined from Equation 2. Figure 4 was developed for determination of slab $E$ for a load radius of 5.9 in. and a concrete Poisson's ratio of 0.15.

The validity of using center-slab backcalculated $k$-values and slab $E$ values at the slab edge was studied by Foxworthy and Darter (*17,22*). Results from several pavement sections showed that when the backcalculated $k$-value and slab $E$ values obtained at the slab center were used at the slab edge, the edge deflections computed by ILLISLAB finite element program (for full contact conditions) agreed with the measured FWD edge deflections, after adjustment for load transfer. The deflections at the slab edge were predicted very well using this procedure, and it was concluded that it was entirely appropriate to backcalculate $k$ and $E$ from the center deflections and to use these values at the edge for stress calculations. This result is consistent with the finding that center and edge $k$-values at the Arlington test site were very similar.

Very little information is available from side-by-side tests to compare pavement responses backcalculated from FWD deflections measured on concrete pavement slabs to static plate load tests conducted on pavement subgrades. Foxworthy (*17*) compared backcalculated $k$-values and plate load $k$-values for seven sites and found that the backcalculated $k$-values exceeded the plate load $k$-values by a factor of 2.3 on average. This phenomenon is probably the result of a combination of differences between the two test methods, including testing on the subgrade versus testing on the top of the concrete slab,

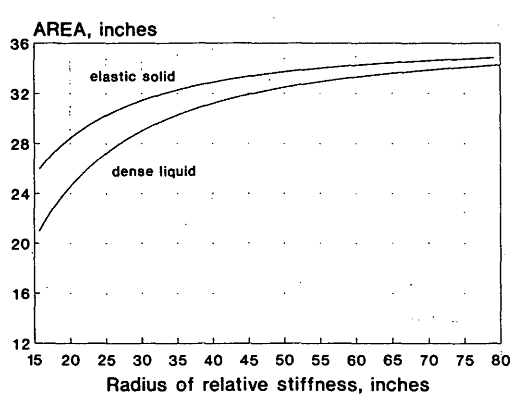


**FIGURE 2 AREA versus dense liquid radius of relative stiffness (*21*).**

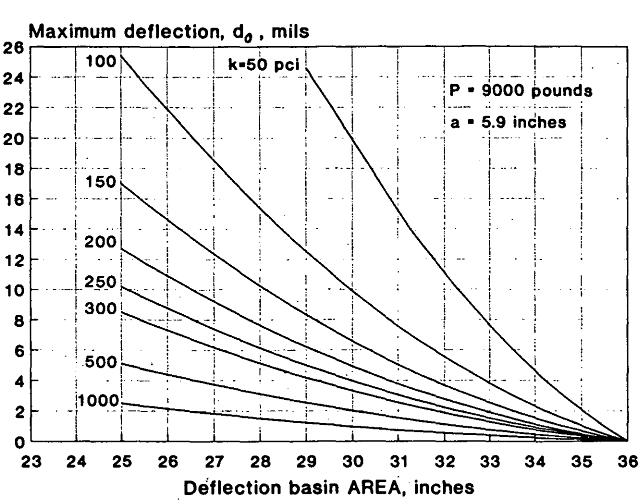


**FIGURE 3 Determination of $k$-value from maximum deflection $d_0$ and AREA.**

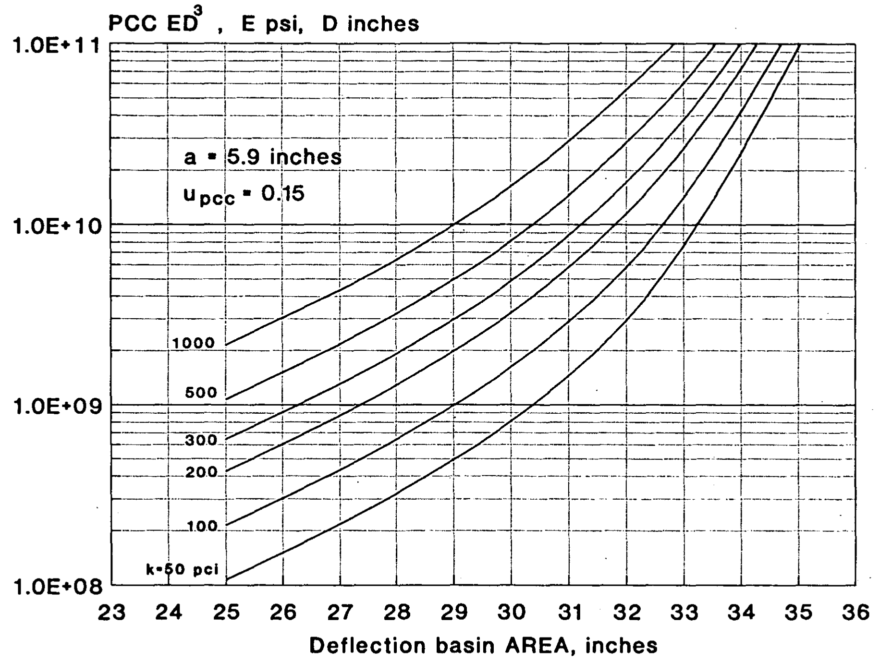


**FIGURE 4 Determination of slab *E* from *k*-value, AREA, and slab thickness.**

and the dynamic loading of the FWD versus the static loading of the plate load test. The possibility that static versus dynamic loading plays some role is also suggested by plate load tests conducted at the AASHO Road Test (*23*) in which repeated-load *k*-values on the subgrade were found to exceed static *k*-values on the subgrade by a factor of 1.77. Dividing back-calculated dynamic *k*-values by a factor of two to estimate static, plate load *k*-values for use in conventional design procedures (that require the static *k*-value) has yielded very reasonable results in analysis of many highway and airfield pavements over the past 10 years.

## FIELD RESULTS FOR SLAB *E* AND SUPPORT *k*-VALUE

Field evaluations were recently conducted on 95 in-service jointed plain concrete pavement (JPCP) and jointed reinforced concrete pavement (JRCP) highway pavements located throughout the United States for FHWA (*24*). These pavements represented a diverse set of designs and climatic conditions. Deflection testing was conducted on these pavements using a Dynatest Model 8000 FWD with a target load of 9,000 lb. The deflection testing was conducted on 10 slabs for each project at slab centers and at joints and corners. The slab center locations were used to backcalculate in situ slab *E* and effective *k*-values using the plate theory concepts described in this paper. The backcalculation results are given in Table 2. This section summarizes the findings from the backcalculation.

### In Situ Slab *E* Modulus

A histogram of all in situ slab *E* moduli obtained from back-calculation is shown in Figure 5. The mean of all values was

**TABLE 2 Backcalculation Results from Field Studies (*24*)**

| SECTION | SLAB THICK (IN) | *IN SITU* SLAB E (MPSI) | CONCRETE FLEX STR (PSI) | BASE TYPE | SUBGRADE TYPE | *IN SITU* K-VALUE (PSI/IN) |
|---|---|---|---|---|---|---|
| MN 1-1 | 9.0 | 7.09 | N/A | AGG | A-6 | 191 |
| MN 1-2 | 9.0 | 7.75 | 801 | AGG | A-6 | 172 |
| MN 1-3 | 8.0 | 6.66 | N/A | AGG | A-6 | 217 |
| MN 1-4 | 8.0 | 6.92 | 552 | AGG | A-6 | 222 |
| MN 1-5 | 8.0 | 9.13 | N/A | ATB | A-6 | 304 |
| MN 1-6 | 8.0 | 9.36 | 587 | ATB | A-6 | 314 |
| MN 1-7 | 9.0 | 8.30 | N/A | ATB | A-6 | 207 |
| MN 1-8 | 9.0 | 7.88 | 689 | ATB | A-6 | 278 |
| MN 1-9 | 9.0 | 6.67 | N/A | CTB | A-6 | 291 |
| MN 1-10 | 9.0 | 6.74 | 735 | CTB | A-6 | 285 |
| MN 1-11 | 8.0 | 8.03 | N/A | CTB | A-6 | 245 |
| MN 1-12 | 8.0 | 7.79 | 763 | CTB | A-6 | 239 |

(*continued on next page*)

TABLE 2 *(continued)*

| SECTION | SLAB THICK (IN) | *IN SITU* SLAB E (MPSI) | CONCRETE FLEX STR (PSI) | BASE TYPE | SUBGRADE TYPE | *IN SITU* K-VALUE (PSI/IN) |
|---|---|---|---|---|---|---|
| MN 5 | 9.0 | 7.56 | N/A | AGG | A-6 | 156 |
| MN 2-1 | 9.0 | 6.78 | 682 | AGG | A-2-7 | 128 |
| MN 2-2 | 8.0 | 8.01 | N/A | AGG | A-2-6 | 127 |
| MN 2-3 | 9.0 | 7.32 | 743 | AGG | A-2-6 | 162 |
| MN 2-4 | 9.0 | 6.62 | N/A | AGG | A-2-6 | 178 |
| MN 3 | 9.0 | 8.81 | N/A | AGG | A-4 | 256 |
| MN 4 | 7.5 | 6.30 | 832 | AGG | A-2-6 | 222 |
| MN 6 | 8.0 | 6.57 | 616 | PATB | A-2-4 | 199 |
| AZ 1-1 | 9.0 | 3.14 | 687 | CTB | A-4 | 546 |
| AZ 1-2 | 13.0 | 3.44 | 649 | NONE | A-6 | 492 |
| AZ 1-4 | 13.0 | 3.49 | 702 | NONE | A-6 | 344 |
| AZ 1-5 | 11.0 | 3.29 | 761 | NONE | A-6 | 439 |
| AZ 1-6 | 9.0 | 3.09 | 853 | LCB | A-6 | 621 |
| AZ 1-7 | 9.0 | 3.69 | 868 | LCB | A-6 | 584 |
| AZ 2 | 10.0 | 5.56 | 725 | LCB | A-6 | 174 |
| CA 1-1 | 8.4 | 6.61 | N/A | CTB | A-1-a | 232 |
| CA 1-3 | 8.4 | 5.24 | 723 | CTB | A-2-4 | 349 |
| CA 1-5 | 11.4 | 5.28 | 918 | CTB | A-1-a | 335 |
| CA 1-7 | 8.4 | 6.48 | 781 | LCB | A-1-a | 433 |
| CA 1-9 | 8.4 | 6.95 | 802 | CTB | A-1-a | 298 |
| CA 7 | 10.2 | 6.26 | 552 | CTB | A-2-4 | 326 |
| CA 2-2 | 8.4 | 7.04 | 730 | PCTB | A-4 | 1423 |
| CA 2-3 | 8.4 | 4.98 | 644 | CTB | A-4 | 572 |
| CA 8 | 10.2 | 6.42 | 727 | ATB | A-7 | 339 |
| CA 6 | 9.0 | 6.71 | 791 | LCB | A-2-4 | 294 |
| MI 1-1a | 9.0 | 5.45 | 745 | AGG | A-2-4 | 353 |
| MI 1-1b | 9.0 | 5.79 | N/A | AGG | A-2-4 | 300 |
| MI 1-4a | 9.0 | 5.88 | 756 | PATB | A-2-4 | 468 |
| MI 1-7a | 9.0 | 6.34 | 744 | AGG | A-2-4 | 292 |
| MI 1-7b | 9.0 | 6.09 | N/A | AGG | A-2-4 | 269 |
| MI 1-10a | 9.0 | 6.23 | N/A | ATB | A-2-4 | 436 |
| MI 1-10b | 9.0 | 5.28 | N/A | ATB | A-2-4 | 502 |
| MI 3 | 10.0 | 4.38 | 810 | PAGG | A-2-4 | 186 |
| MI 4-1 | 9.0 | 4.83 | 596 | AGG | A-4 | 283 |
| MI 4-2 | 9.0 | 4.53 | 756 | AGG | A-4 | 189 |
| MI 5 | 10.0 | 4.49 | 671 | PAGG | A-2-4 | 233 |
| NY 1-1 | 9.0 | 3.81 | N/A | ATB | A-2-4 | 549 |
| NY 1-3 | 9.0 | 3.89 | 809 | ATB | A-2-4 | 503 |
| NY 1-4 | 9.0 | 3.89 | 658 | AGG | A-2-4 | 534 |
| NY 1-6 | 9.0 | 4.02 | N/A | AGG | A-1-a | 619 |
| NY 1-8a | 9.0 | 4.10 | 684 | ATB | N/A | 638 |
| NY 1-8b | 9.0 | 3.88 | N/A | ATB | A-2-4 | 548 |
| NY 2-3 | 9.0 | 5.10 | 864 | AGG | A-1-a | 341 |
| NY 2-9 | 9.0 | 5.09 | 705 | AGG | A-1-a | 471 |
| NY 2-11 | 9.0 | 6.12 | 812 | AGG | A-1-a | 296 |
| NY 2-15 | 9.0 | 5.52 | N/A | AGG | A-1-a | 273 |
| OH 1-1 | 9.0 | 4.43 | 686 | AGG | A-6 | 449 |
| OH 1-3 | 9.0 | 5.31 | N/A | ATB | A-4 | 440 |
| OH 1-4 | 9.0 | 5.23 | N/A | ATB | A-4 | 525 |
| OH 1-6 | 9.0 | 4.06 | 761 | AGG | A-4 | 431 |
| OH 1-7 | 9.0 | 4.43 | 848 | AGG | A-4 | 340 |
| OH 1-9 | 9.0 | 3.40 | 833 | AGG | A-6 | 351 |
| OH 1-10 | 9.0 | 4.51 | 788 | AGG | A-6 | 405 |
| PA 1-1 | 10.0 | 4.21 | 731 | CTB | A-2-4 | 731 |
| PA 1-2 | 10.0 | 3.39 | 720 | PATB | A-4 | 1040 |
| PA 1-3 | 10.0 | 3.23 | 709 | PAGG | A-4 | 538 |
| PA 1-4 | 10.0 | 4.53 | 870 | PAGG | A-2-4 | 747 |
| PA 1-5 | 10.0 | 3.62 | 704 | AGG | A-4 | 540 |

*(continued on next page)*

**TABLE 2** *(continued)*

| SECTION | SLAB THICK (IN) | *IN SITU* SLAB E (MPSI) | CONCRETE FLEX STR (PSI) | BASE TYPE | SUBGRADE TYPE | *IN SITU* K-VALUE (PSI/IN) |
|---|---|---|---|---|---|---|
| NJ 2-1 | 10.0 | 6.72 | 700 | AGG | A-4 | 234 |
| NJ 3-1 | 9.0 | 5.40 | 681 | PAGG | A-1-a | 356 |
| NJ 3-2 | 9.0 | 5.33 | 726 | PATB | A-2-4 | 210 |
| NC 1-1 | 9.0 | 4.63 | 736 | AGG | A-2-4 | 538 |
| NC 1-2 | 9.0 | 5.19 | 674 | CTB | A-2-4 | 347 |
| NC 1-3 | 9.0 | 3.97 | 705 | CTB | A-2-6 | 494 |
| NC 1-4 | 9.0 | 4.21 | 709 | AGG | A-2-6 | 570 |
| NC 1-5 | 9.0 | 5.50 | 674 | CTB | A-4 | 628 |
| NC 1-6 | 9.0 | 5.14 | 559 | ATB | A-2-6 | 672 |
| NC 1-7 | 8.0 | 5.09 | 644 | AGG | A-2-4 | 128 |
| NC 1-8 | 9.0 | 4.22 | 705 | AGG | A-2-6 | 513 |
| NC 2 | 11.0 | 5.89 | 712 | LCB | A-4 | 293 |
| FL 2 | 13.0 | 5.55 | 664 | AGG | A-3 | 378 |
| FL 3 | 9.0 | 4.16 | 599 | LCB | A-3 | 529 |
| CA 3-1 | 9.0 | 3.53 | N/A | CTB | A-4 | 286 |
| CA 3-2 | 9.0 | 4.17 | 796 | CTB | A-4 | 312 |
| CA 3-5 | 9.0 | 4.38 | 842 | CTB | A-4 | 397 |

Note:
AGG = untreated aggregate base
PAGG = permeable aggregate base
ATB = asphalt-treated base
PATB = permeable asphalt-treated base
CTB = cement-treated base
PCTB = permeable cement-treated base
LCC = lean concrete base
SAND = sand base

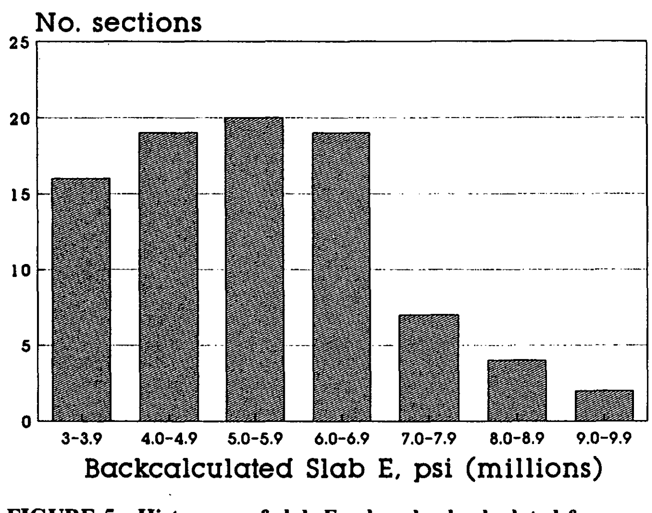


**FIGURE 5 Histogram of slab *E* values backcalculated from field studies.**

5.4 million lb/in.$^2$ with a range of 3 to 9.4 million lb/in.$^2$. These slabs have a mean age of 15 years; therefore, the slab moduli should be expected to be greater than elastic moduli corresponding to typical 28-day-strength values assumed in design.

A comparison of the mean in situ slab elastic moduli for each base type may be made from these data. The results shown below indicate no effect of base stiffness on the backcalculated slab moduli.

| *Base Type* | *No. of Sections* | *In Situ Slab E (lb/in.$^2$)* |
|---|---|---|
| Aggregate or no base | 40 | 5,400,000 |
| Asphalt-treated | 19 | 5,700,000 |
| Cement-treated | 20 | 5,600,000 |
| Lean concrete | 7 | 5,100,000 |

A correlation between in situ slab *E* and the estimated flexural strength of the concrete (from indirect tensile tests on cores) was attempted using the data from Table 2, but no correlation was found. However, this may be partially because only two cores were tested for each section for strength determination. A better correlation was achieved by Foxworthy using data from nine pavement sections, as shown in Figure 6 (*17*).

$$FS = 43.5 \left(\frac{E}{10^6}\right) + 488.5 \tag{5}$$

where

$FS$ = flexural strength, estimated from indirect tensile strength (lb/in.$^2$) and
$E$ = in situ modulus of elasticity, backcalculated from FWD data (lb/in.$^2$).

When Foxworthy's prediction model was plotted on the *E*-versus-*FS* graph, the curve passed through the center of the scatter of data. This estimate is approximate and should be used with caution when it is not feasible to obtain and test concrete cores.

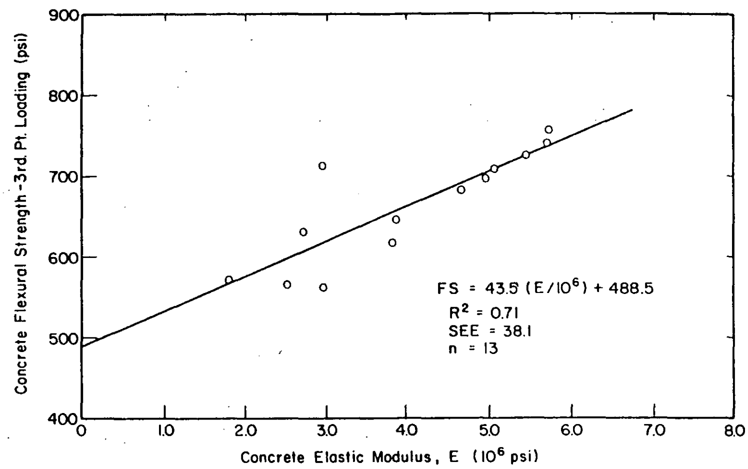


**FIGURE 6 Correlation of concrete flexural strength to backcalculated *E*-value from Foxworthy (*17*).**

### In Situ *k*-Value

A summary of the in situ *k*-values (below the slab) obtained from various sections, sorted by base type and subgrade type, is shown in Table 3. The following observations may be made concerning the results:

1. The in situ *k*-value does not correlate well with subgrade soil classification. The mean *k*-value was computed for fine-grained and coarse-grained soils for each base type. Only the asphalt-treated base course showed a higher *k*-value for coarse-grained subgrade than fine-grained soil. The others were approximately the same.

2. Pavements with asphalt-treated, cement-treated, and lean concrete base layers generally have higher *k*-values than pavements with untreated bases, as shown in the frequency distributions in Figure 7. For example, a high percentage of sections with treated bases had in situ *k*-values greater than 500 lb/in.$^2$/in.

3. The estimated static *k*-values are shown in parentheses. These were obtained by dividing the backcalculated *k*-values by two. For sections with no base or with granular base, the static *k*-values were similar to typical recommended values. For sections with treated bases, the mean values are lower than those that would normally be obtained by conventional methods (e.g., elastic layer program simulation of a plate

**TABLE 3 Summary of Backcalculated *k*-Values Obtained from Field Testing (*24*)**

| Base Type | Backcalculated Mean k-value (psi/in) | Range | Number of Sections |
|---|---|---|---|
| No base | 425 (213)* | 344-492 | 3 |
| Aggregate | 318 (159) | 127-619 | 35 |
| Permeable-Aggregate | 258 (129) | 186-356 | 3 |
| Asphalt-treated | 447 (224) | 207-672 | 14 |
| Permeable-Asphalt | 534 (267) | 199-1040 | 6 |
| Cement-treated | 384 (192) | 232-731 | 19 |
| Permeable-Concrete | 1423 (711) | 1423 | 1 |
| Lean concrete | 418 (209) | 174-621 | 7 |

*Estimated static k-value (backcalculated/2)

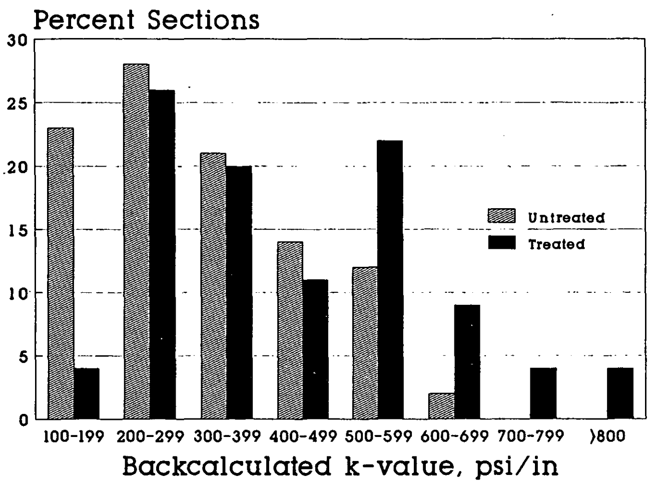


**FIGURE 7 Histogram of backcalculated *k*-values from field studies for untreated aggregate and treated bases.**

load test) for determining the effective *k*-value on top of a treated base.

## IMPLICATIONS FOR PAVEMENT DESIGN AND EVALUATION

For structural evaluation or overlay design, the in situ *k*-value and slab elastic modulus may be easily backcalculated using the techniques presented in this paper or by the ILLIBACK program. The *k*-value and slab *E* backcalculated from FWD deflections should be considered as the moduli that the layers exhibit under moving loads. If the pavement under design is subject to static loads, or if the design procedure requires the input of a static *k*-value (e.g., the FAA and AASHTO procedures), the backcalculated *k*-value should be reduced by approximately 50 percent. The subgrade soil type (fine or coarse-grained) did not appear to significantly affect the in situ *k*-value.

The flexural strength of the slab may be roughly estimated from the slab *E* modulus, but it is preferable to take cores, test them for indirect tensile strength, and estimate the flexural strength. These values, along with the transverse and longitudinal joint load transfer, may then be used to determine the load-carrying capacity of the pavement as well as the required overlay thickness.

For new design, where no slab of similar design exists in the vicinity from which backcalculated slab and support values may be determined, the following *k*-values and the slab moduli shown in Figure 5 may be used as reasonable approximate values.

| *Base Type* | *Backcalculated Mean k-value (lb/in.²/in.)* | *Estimated Static k-value (lb/in.²/in.)* |
|---|---|---|
| No base | 425 | 213 |
| Aggregate | 318 | 159 |
| Permeable aggregate | 258 | 129 |
| Asphalt-treated | 447 | 224 |
| Permeable asphalt | 534 | 267 |
| Cement-treated | 384 | 192 |
| Lean concrete | 418 | 209 |

Existing conventional methods for estimating *k*-values for use in new design may also produce reasonable results, especially for slabs with no base or only untreated aggregate base. However, when a very stiff base is being constructed, the *k*-value used to design the concrete pavement should not be increased to the extent that conventional practice to date suggests.

The *k*-value is not a unique material property but depends on several factors such as slab and loading parameters. The only legitimate way to define a *k*-value is "beneath a slab," and not "on top of a base layer."

## CONCLUSIONS

The backcalculation procedures described in this paper provide a rapid and reliable method to determine the in situ slab *E* modulus and the effective *k*-value supporting the slab. These slab and support values should be considered representative of the pavement's response to moving wheel loads. In situ *k*-values backcalculated from FWD deflections must be modified for use in design procedures that are based on static plate load test *k*-values or for design for static loads. Dividing the FWD backcalculated *k*-value by approximately two gives a reasonable estimate of the static *k*-value. It is not necessary to remove slabs and conduct static plate load tests to obtain a reasonable static *k*-value for use in design.

In situ slab *E* moduli were found to vary from 3 to 9 million lb/in.$^2$, with a mean of 5.4 million lb/in.$^2$, in the field tests summarized in this paper. The Arlington tests showed that the backcalculated slab moduli (for static loads) were very close to those obtained from static laboratory testing of samples from slabs.

Further research is needed to develop methods for backcalculation of the *E* moduli of two stiff layers over a dense liquid subgrade (e.g., a concrete slab and a treated base). It is recommended that when a slab and stiff base layer are present they be modeled as two plates over a dense liquid subgrade, instead of as one plate over a dense liquid subgrade.

Further research is also needed to improve methods for estimation of the subgrade *k*-value for pavements with stiff bases. Currently there is no method available to determine the correct *k*-value for use in design of a new concrete pavement when backcalculation of existing similar pavements cannot be done. Conventional methods (plate bearing tests, correlation with soil properties, or estimation from elastic layer analyses) may produce reasonable results for slabs on grade or on untreated aggregate bases. However, increasing the *k*-value to account for a stiff base layer is likely to produce a value higher than the actual in situ value.

One final comment is made regarding the use of elastic layer theory for backcalculating the moduli of concrete slabs and underlying layers. Although this method has been used with reasonable success by the authors and other researchers, the values obtained can be used only with elastic layer theory to compute interior stresses, strains, and deformations. They cannot be used to compute edge or corner stresses because the moduli are not compatible. In addition, no unique relationship exists between the elastic subgrade *k*-value, because the *k*-value also depends on the loading configuration and other factors.

## GLOSSARY

The following definitions are given for terms used in this paper.

- Static $k$-value on subgrade: determined from static plate load tests performed on the subgrade using a 30-in.-diameter plate, lb/in.$^2$/in.
- In situ $k$-value beneath slab: backcalculated from FWD deflections on top of the slab at an interior position using Westergaard's center-slab deflection equation, lb/in.$^2$/in.
- Static modulus of elasticity ($E$) of slab concrete: determined from samples cut from the pavement and tested in flexure in the laboratory under static load.
- In situ slab modulus of elasticity ($E$): backcalculated from FWD deflections at the center of the slab using backcalculation techniques.

## REFERENCES


1. H. M. Westergaard. Stresses in Concrete Pavements Computed by Theoretical Analysis. *Public Roads*, Vol. 7, No. 2, April 1926.
2. H. M. Westergaard. Stresses in Concrete Runways of Airports. *HRB Proc.*, Vol. 19, 1939.
3. A. H. A. Hogg. Equilibrium of a Thin Plate, Symmetrically Loaded, Resting on an Elastic Foundation of Infinite Depth. *London, Edinburgh, and Dublin Philosophical Magazine and Journal of Science*, Series 7, Vol. 25, March 1938.
4. D. L. Holl. Equilibrium of a Thin Plate, Symmetrically Loaded, on a Flexible Subgrade. *Iowa State College Journal of Science*, Vol. 12, No. 4, July 1938.
5. A. Losberg. *Structurally Reinforced Concrete Pavements*, Doktorsavhandlingar Vid Chalmers Tekniska Högskola, Göteborg, Sweden, 1960.
6. A. Bijls. Essais de Résistance et D'Élasticité du Terrain de Fondation de la Nouvelle Ecluse Maritime D'Ymuiden (Hollande). *Le Génie Civil*, Vol. 82, 1923.
7. A. T. Goldbeck. Researches on the Structural Design of Highways by the United States Bureau of Public Roads. *Transactions, American Society of Civil Engineers*, Vol. 88, 1925.
8. A. T. Goldbeck and M. J. Bussard. The Supporting Value of Soil as Influenced by the Bearing Area. *Public Roads*, Vol. 5, No. 11, 1925.
9. L. W. Teller and E. C. Sutherland. The Structural Design of Concrete Pavements, Part 1—A Description of the Investigation. *Public Roads*, Vol. 16, No. 8, 1935.
10. L. W. Teller and E. C. Sutherland. The Structural Design of Concrete Pavements, Part 5—An Experimental Study of the Westergaard Analysis of Stress Conditions in Concrete Pavement Slabs of Uniform Thickness. *Public Roads*, Vol. 23, No. 8, 1943.
11. J. P. Sale. Rigid Pavement Design for Airfields. *Proc., 1st International Conference on Concrete Pavement Design*, Purdue University, West Lafayette, Ind. 1977.
12. F. H. Scrivner, C. H. Michalak, and W. M. Moore. Calculation of the Elastic Moduli of a Two-Layer Pavement System from Measured Surface Deflection. In *Highway Research Record 431*, HRB, National Research Council, Washington, D.C., 1973.
13. D. M. Burmister. The Theory of Stress and Displacements in Layered Systems and Applications to the Design of Airport Runways. *HRB Proc.*, 1943.
14. D. M. Burmister. The General Theory of Stresses and Displacements in Layered Systems. Parts I, II, and III. *Journal of Applied Physics*, Vol. 16, 1945.
15. M. S. Hoffman and M. R. Thompson. *Mechanistic Interpretation of Nondestructive Pavement Testing Deflections*. Transportation Engineering Series No. 32, Illinois Cooperative Highway and Transportation Research No. 190. University of Illinois at Urbana-Champaign, 1981.
16. ERES Consultants, Inc. *Nondestructive Structural Evaluation of Airfield Pavements*. U.S. Army Corps of Engineers Waterways Experiment Station, Vicksburg, Miss., 1982.
17. P. T. Foxworthy. *Concepts for the Development of a Nondestructive Testing and Evaluation System for Rigid Airfield Pavements*. Ph.D. thesis. University of Illinois at Urbana-Champaign, 1985.
18. E. J. Barenberg and K. A. Petros. Evaluation of Concrete Pavements Using NDT Results. Project IHR-512. Report UILU-ENG-91-2006. University of Illinois and Illinois Department of Transportation, 1991.
19. A. M. Ioannides. Dimensional Analysis in NDT Rigid Pavement Evaluation. *Transportation Engineering Journal*, American Society of Civil Engineers, Vol. 116, 1990.
20. A. M. Ioannides, E. J. Barenberg, and J. A. Lary. Interpretation of Falling Weight Deflectometer Results Using Principles of Dimensional Analysis. *Proc., 4th International Conference on Concrete Pavement Design and Rehabilitation*, Purdue University, West Lafayette, Ind., 1989.
21. K. T. Hall. *Performance, Evaluation, and Rehabilitation of Asphalt-Overlaid Concrete Pavements*. Ph.D. thesis. University of Illinois at Urbana-Champaign, 1991.
22. P. T. Foxworthy and M. I. Darter. A Comprehensive System for Nondestructive Testing and Evaluation of Rigid Airfield Pavements. In *Transportation Research Record 1070*, TRB, National Research Council, Washington, D.C., 1986.
23. *Special Report 61E: The AASHO Road Test, Report 5, Pavement Research*. HRB, National Research Council, Washington, D.C., 1962.
24. K. D. Smith, D. G. Peshkin, M. I. Darter, A. L. Mueller, and S. H. Carpenter. *Performance of Jointed Concrete Pavements, Phase I, Volume IV—Appendix A, Project Summary Reports and Summary Tables*. FHWA-RD-89-139. FHWA, U.S. Department of Transportation, 1990.

# Comparison of Pavement Deflection Analysis Methods Using Overlay Design

JOSEPH M. MAESTAS AND MICHAEL S. MAMLOUK

Four pavement deflection analysis methods, in the form of personal computer software programs, were evaluated and compared from the practitioner's perspective on the basis of calculated overlay design thickness, common characteristics, and performance. These programs are ELSDEF, MODCOMP2, MODULUS4, and ISSEM4. Each program applies the concept of backcalculation, which is the determination of in situ material properties of a pavement structure from its response to dynamic surface loading. A total of 29 in-service, flexible pavement sections, requiring significant rehabilitation, were selected from areas of various environmental conditions, traffic loading, and subgrade soil types in Arizona. Through backcalculation, actual falling weight deflectometer field deflections were used to estimate layer moduli of all pavement sections. The moduli results were then used in the overlay design of each section in accordance with the 1986 AASHTO *Guide for Design of Pavement Structures*. Although the four backcalculation programs are characteristically different, neither layer modulus nor overlay thickness results were statistically different in most cases. However, from a practical perspective, backcalculation, as represented by these programs, is not adequate for use by the practitioner. Additional research is needed to refine the backcalculation process.

The need to standardize and adopt a mechanistic overlay design procedure for flexible pavement has led to the proliferation of PC-compatible backcalculation software programs used for pavement structure evaluation and, potentially, for mechanistic overlay design. These programs require data from common, dynamic nondestructive (NDT) testing devices. Generally, a falling weight deflectometer (FWD) is preferred. Although NDT applications show much promise in pavement evaluation, more research is needed in the areas of backcalculation and overlay design.

Some general similarities among backcalculation programs are that they are iterative in nature, require essentially the same input parameters, and produce the elastic modulus for each pavement layer by equating measured NDT deflections with those calculated. Several recent studies have been conducted on various backcalculation programs. These studies address sources and effects of backcalculation error and performance comparisons of backcalculation programs. They have specifically evaluated the source, degree, and effect of error attributed to deflection measurement, the NDT device used, program user expertise, and the accuracy of program input data (i.e., depth to rigid layer, "seed moduli," moduli limits, etc.) (*1–4*). Many studies have compared certain backcalculation programs on the basis of moduli results [see, for example, Ali and Khosla (*5*)]. However, a limited number of studies have evaluated the effect and comparison of various backcalculation programs on the basis of overlay design. Mahoney et al. (*6*) compared certain backcalculation programs by overlay design using an assumed fixed traffic level and applying the asphalt strain criterion.

If various backcalculation programs result in the same practical overlay design for a particular pavement section, it may mean that we have reached the ultimate level of backcalculation needed for the current highway practice. However, if various overlay designs are the result, caution should be exercised when backcalculation is performed. Additional work would be needed to refine the backcalculation methodology. This paper serves to evaluate the backcalculation effect among various programs through the application of the AASHTO overlay design procedure using actual field data. This paper also provides an in-depth look into each program's relative capabilities and performance. The backcalculation programs used in this study were selected on the basis of their availability to the authors, adequate cross section of common programs, and compatibility with an IBM PC or equivalent.

## BACKGROUND

### Backcalculation

Backcalculation, the "inverse" problem of determining material properties of a flexible pavement structure from its response to surface loading, has not been fully resolved. No direct, closed-form solution is currently available to determine the layer moduli of a multilayered system given the surface deflections and layer thicknesses. Therefore, it is currently necessary to employ iteration or optimization schemes to calculate theoretical deflections by varying the material properties (i.e., layer moduli) until a tolerable "match" of measured deflections is made. Because Poisson's ratios of pavement layers do not significantly affect calculated deflections, they are not iteratively modified like the layer moduli.

Several backcalculation computer programs are available and used by various highway agencies. Initial or "seed" layer moduli values are either assumed by the user or estimated by the program, and the corresponding deflections are computed by a particular analysis (multilayer elastic or finite element) subroutine in the program. The layer moduli are then adjusted using an iterative or optimization process until the computed deflections match the measured deflections within a certain tolerance. This is the extent of similarities among the programs whose unique characteristics create many differences.

J. M. Maestas, Office of Engineering, FHWA, Room 3118, HNG-42, 400 Seventh St., S.W., Washington, D.C. 20590. M.S. Mamlouk, Department of Civil Engineering, Arizona State University, Tempe, Ariz. 85287.

Some differences involve (a) iteration convergence methodologies, (b) consideration of nonlinear material behavior, (c) the need for and affect of seed moduli, (d) predesignated, allowable ranges of calculated layer elastic moduli, (e) a variety of input parameters and assumptions, and (f) the depth to bedrock.

Backcalculation is an ill-posed process in which minor deviations between measured and computed deflections usually result in significantly different moduli. In many cases, self-compensation of moduli results in obtaining various combinations of moduli producing essentially the same deflection basin. Compensation between depth to bedrock and subgrade modulus can also occur.

### Overlay Design

Current overlay design methods range from engineering judgment to mechanistic (or mechanistic-empirical) approaches. Evaluating the material properties of existing pavement layers is a prerequisite for any rational overlay design process.

One of the most commonly used methods of overlay design is the AASHTO procedure. The 1986 AASHTO guide (*7*) recommends the use of layer moduli as a basis for material characterization. Layer moduli can be obtained by either laboratory testing or, where the latter is more practical, backcalculation. The AASHTO guide has recognized the improved accuracy of NDT in structurally evaluating existing pavement systems by allowing a method that uses a backcalculation technique that applies the "multielastic theory" to calculate layer moduli. Since the backcalculation problem has not been fully resolved, errors in backcalculation might result in different overlay thickness designs for the same pavement structure. This uncertainty in overlay thickness might result in millions of dollars in material costs as a result of over- or underdesign of the pavement.

Although the 1986 AASHTO guide emphasizes the use of a resilient modulus as a basis for material characterization, the procedure recommends the use of correlations of questionable accuracy between the modulus and the structural layer coefficients ($a_i$). Also, the AASHTO overlay procedure does not consider the depth to bedrock. Thus, if there is a compensation between the subgrade modulus and depth to bedrock, inconsistent overlay thicknesses will result.

## RESEARCH METHODOLOGY

### Selection of Test Sites

To adequately compare backcalculation programs on the basis of AASHTO overlay thickness, actual NDT data would be required from typical flexible pavement structural sections that require significant rehabilitation. To accomplish this, 29 in-service test sites were selected from the Arizona Department of Transportation (ADOT) construction schedule of pavement rehabilitation projects. These sites are located in areas with various traffic loading, environmental conditions, and subgrade soil types within the state (Figure 1). Preliminary information regarding these sites, shown in Table 1, was obtained from existing ADOT materials pavement design memorandums. These sites are specific locations within the limits of projects scheduled for pavement rehabilitation between late 1989 and the present. They are located only on Interstate and primary highways (United States and Arizona state routes).

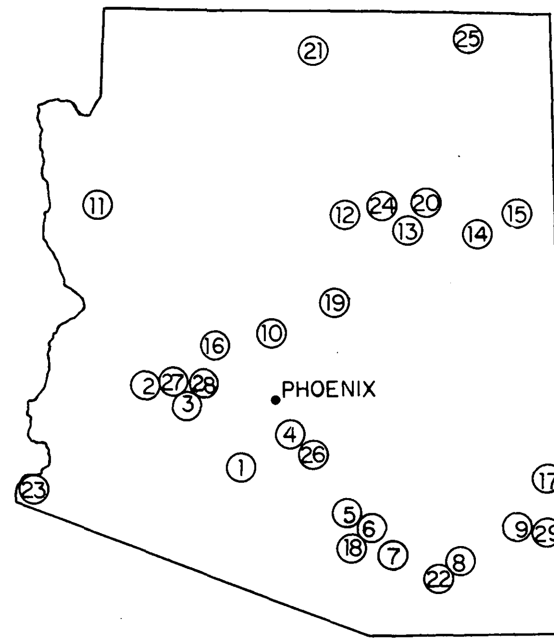


**FIGURE 1 Location of test sites.**

Test sites within the project limits were selected on the basis of the extent of rehabilitation, which included either mill and overlay or just overlay. After selecting test sites, required information for each site was obtained from ADOT's Pavement Management System, Project History, Subgrade *R*-value, and NDT deflection data bases. Specific site locations coincide with locations of actual deflection measurement data selected for backcalculation analysis. Cumulative, 10-year, 18-kip equivalent single axle load (ESAL) in the design lane for each site was obtained from the NDT deflection data base. Deflection and pavement data including the Arizona seasonal variation factor (SVF), percent pavement surface cracking, and pavement surface temperature during NDT were also obtained from the NDT deflection data base. The SVF is an Arizona climate-based, regional factor used to determine percent of time of saturation exposure and ultimately used to select the AASHTO layer drainage coefficients. Layer thicknesses and material types of each site are shown in Table 2. Thicknesses of all surface layers were obtained from pavement coring results, whereas those of all other layers were of "plan" thicknesses obtained from the Project History data base. The AASHTO soil classification of subgrade material at each site was obtained from the subgrade *R*-value data base.

### FWD Deflection Testing

ADOT routinely performs project-level FWD deflection testing. All FWD deflection data are collected and maintained in a computer data base. Currently, five deflection tests are performed per mile for each lane. A set of seven deflections,

**TABLE 1 Location and Characteristics of Test Sites**

| Site No. | Route/ Direction | Milepost | SVF[1] | 1990 | | Surface Temperature | Cumulative ESAL[3] |
|---|---|---|---|---|---|---|---|
| | | | | Cracking (%) | Rough-ness[2] | @NDT (°F) | (1000) |
| 1 | I-8/EB | 135.0 | 1.2 | 1 | 76 | 72 | 6,840 |
| 2 | I-10/EB | 71.0 | 0.8 | 1 | 121 | 118 | 19,364 |
| 3 | I-10/WB | 91.4 | 1.0 | 25 | 100 | 80 | 21,758 |
| 4 | I-10/WB | 170.0 | 1.0 | 2 | 144 | 58 | 15,202 |
| 5 | I-10/EB | 240.6 | 1.6 | 2 | 125 | 100 | 28,439 |
| 6 | I-10/WB | 250.7 | 1.6 | 0 | 134 | 102 | 21,654 |
| 7 | I-10/EB | 273.1 | 1.7 | 0 | 109 | 77 | 17,118 |
| 8 | I-10/WB | 315.7 | 1.9 | 8 | 153 | 60 | 14,179 |
| 9 | I-10/EB | 368.6 | 1.7 | 8 | 141 | 107 | 10,689 |
| 10 | I-17/SB | 247.6 | 2.5 | 6 | 104 | 88 | 9,709 |
| 11 | I-40/WB | 51.6 | 1.7 | 4 | 183 | 82 | 21,072 |
| 12 | I-40/WB | 213.0 | 2.9 | 0 | 90 | 76 | 12,539 |
| 13 | I-40/WB | 255.6 | 1.7 | 0 | 99 | 100 | 14,119 |
| 14 | I-40/WB | 307.6 | 1.8 | 1 | 204 | 108 | 18,108 |
| 15 | I-40/WB | 333.3 | 2.0 | 0 | 224 | 106 | 16,849 |
| 16 | US60/WB | 109.6 | 1.5 | 15 | 268 | 113 | 1,321 |
| 17 | SR75/NB | 380.6 | 1.7 | 20 | 264 | 99 | 98 |
| 18 | SR86/WB | 168.2 | 1.7 | 20 | 157 | 59 | 2,280 |
| 19 | SR87/NB | 265.0 | 3.8 | 2 | 190 | 58 | 2,488 |
| 20 | SR87/NB | 363.0 | 1.8 | 4 | 263 | 70 | 177 |
| 21 | US89A/NB | 531.6 | 1.7 | 4 | 145 | 50 | 258 |
| 22 | SR90/EB | 315.8 | 2.2 | 0 | 138 | 54 | 254 |
| 23 | US95/NB | 11.6 | 0.4 | 3 | 201 | 99 | 1,156 |
| 24 | SR99/NB | 60.3 | 1.6 | 30 | 372 | 110 | 224 |
| 25 | US160/EB | 409.6 | 1.8 | 15 | 341 | 100 | 868 |
| 26 | SR387/NB | 4.2 | 1.3 | 8 | 113 | 70 | 3,948 |
| 27 | I-10/WB | 78.0 | 0.8 | 2 | 95 | 100 | 19,364 |
| 28 | I-10/EB | 92.6 | 1.0 | 30 | 173 | 94 | 21,758 |
| 29 | I-10/EB | 376.0 | 1.7 | 6 | 243 | 107 | 10,689 |

Notes: 1. Arizona seasonal variation factor
2. Mays roughness meter reading
3. Projected 10-year equivalent single axle loads in the design lane

which comprise a single deflection "bowl" or basin, are measured by sensors placed at 1-ft spacings. Multiple load drops are made at various load heights during FWD testing at a single location providing a wide range of load levels. The particular deflection basins used in this study have already been "normalized" to 9 kips by ADOT. This normalized deflection basin is an actual basin measured at the load level nearest to 9 kips and proportionally modified to coincide with a deflection basin produced at a load level of exactly 9 kips.

Because specific test sites were selected from within actual pavement sections scheduled for rehabilitation, FWD deflection data were readily available. In an effort to select a representative deflection basin of the pavement section, a single basin similar to the average basin for that particular pavement section was selected. A single deflection basin was selected for analysis instead of an average because the authors believe the average does not adequately represent an actual basin. Another consideration in selecting a particular deflection basin was the extent of cracking at the NDT location. Nearly every deflection basin selected to represent an individual test site was measured on pavement surface areas having 10 percent cracking or less. This was done in an effort to minimize errors associated with deflection testing of cracked pavements. The selected deflection basins were then used for the backcalculation of layer moduli.

## Backcalculation

### *Unique Characteristics and Observations of Programs*

The following common PC software programs were evaluated in this research: ELSDEF, MODCOMP2, MODULUS4, and ISSEM4. Table 3 includes a comparison of common characteristics of these backcalculation programs. To supplement Table 3, the following sections are included to briefly address some general information, unique characteristics, and observations regarding the use of each program.

**ELSDEF** The ELSDEF program, developed by Bush (*8*), incorporates ELSYM5 as a subprogram to calculate stresses, strains, and deformations in the pavement structure. This technique is explicitly a linear elastic analysis procedure. Subgrade thickness can be assumed as semi-infinite or given a certain thickness by the user. The program iteratively adjusts the layer moduli until the calculated deflections match the measured deflections within a certain error tolerance (see Table 3). To assist the user in satisfactory convergence, each set of iteration results offers layer moduli with and without consideration of designated moduli limits. In the sole case of this program, it may not be extremely important to use core

TABLE 2 Layer Thicknesses and Material Types

| Site No. | Pavement Layer Number: Material Type/Thickness (in.) 1 | 2 | 3 | AASHTO Subgrade Soil Classification |
|---|---|---|---|---|
| 1 | AC/8.0 | AB/4.0 | SM/8.0 | A-1-b(o) |
| 2 | AC/6.4 | AB/4.0 | SM/15.0 | NA |
| 3 | AC/8.1 | AB/4.0 | SM/8.3 | A-2-7(o) |
| 4 | AC/6.0 | AB/4.0 | SM/15.0 | A-6(2) |
| 5* | AC/8.0 | AB/4.0 | CB/6.0 | A-4(o) |
| 6* | AC/8.0 | AB/4.0 | CB/6.0 | A-6(5) |
| 7 | AC/5.5 | AB/3.0 | SM/6.0 | A-1-a(o) |
| 8 | AC/5.3 | AB/4.0 | SM/24.0 | A-1-b(o) |
| 9 | AC/8.0 | AB/4.0 | SM/15.0 | A-2-4(o) |
| 10* | AC/11.5 | AB/4.0 | SM/11.0 | A-2-7(o) |
| 11 | AC/9.7 | SM/3.0 | -- | A-1-b(o) |
| 12 | AC/6.6 | AB/2.0 | SM/12.0 | A-2-4(o) |
| 13 | AC/13.5 | SM/6.0 | -- | A-1-b(o) |
| 14 | AC/6.6 | BB/5.0 | SM/4.0 | A-2-4(o) |
| 15 | AC/8.8 | CB/10.0 | SM/8.0 | A-2-4(o) |
| 16 | AC/4.5 | -- | -- | NA |
| 17 | AC/5.0 | AB/4.0 | SM/9.0 | NA |
| 18 | AC/4.0 | AB/4.0 | SM/15.0 | A-2-7(o) |
| 19 | AC/3.5 | -- | -- | A-4(o) |
| 20 | AC/2.0 | AB/4.0 | SM/15.0 | NA |
| 21 | AC/2.8 | SM/6.0 | -- | NA |
| 22 | AC/4.6 | AB/4.0 | SM/12.0 | A-2-4(o) |
| 23 | AC/4.7 | CB/7.0 | SM/14.0 | A-7-6(31) |
| 24 | AC/3.0 | -- | -- | NA |
| 25 | AC/4.0 | -- | -- | A-3(o) |
| 26 | AC/4.5 | AB/6.0 | SM/20.0 | A-1-b(1) |
| 27 | AC/10.0 | AB/4.0 | SM/10.0 | NA |
| 28 | AC/7.5 | AB/4.0 | SM/13.3 | A-2-4(o) |
| 29 | AC/7.5 | AB/6.0 | SM/21.0 | NA |

Legend: AC - Asphalt Concrete, AB-Aggregate Base
BB - Bituminous Treated Base,CB-Cement Treated Base
SM - Select Material (Granular Subbase)
NA - Not available to authors
*Two layers were combined during backcalculation in order to change the 5-layer system to a 4-layer system which were combined

thicknesses for the surface or any other layers because input values are rounded to the nearest inch. ELSDEF is the only program of the four evaluated that allows the user to estimate the subgrade layer thickness between the range of 0 and 999 in. and its moduli limits. For the purposes of this study, the following typical trial subgrade thicknesses of 999 in. representing a semi-infinite layer, 240 in., and 120 in. were used to obtain the optimum (minimal deflection match error) set of layer moduli. Also, a semi-infinite subgrade layer can be designated by simply entering zero as its thickness.

**MODCOMP2** MODCOMP2, Version 2.4, originally developed by Irwin (*9*), was used for this research. This backcalculation program also uses an iterative approach to compute a final set of layer moduli. In each iteration, the difference between each measured and calculated deflection expressed as a percentage of the measured deflection is compared with a specified tolerance (see Table 3). The program allows the use of up to eight layers and applies the root mean square (RMS) as the error criterion. It incorporates the Chevron elastic layer analysis as a subprogram to compute stresses, strains, and deformations in the pavement structure. No subroutine exists explicitly for data entry. Input data required must be structured in accordance with a prescribed format. The program will terminate if the error tolerance is met or if the prespecified maximum number of iterations is reached.

**MODULUS4** MODULUS, Version 4.0, is a backcalculation program developed by the Texas Transportation Institute (*10*). Its methodology applies a pattern search algorithm to minimize the sum of squares for error between measured and calculated deflections. This method replaces direct deflection computation with an interpolation process that guarantees convergence. It detects nonlinearity in the subgrade and automatically selects the optimum number of sensors for backcalculation use. It incorporates the U.S. Army Corps of Engineers WES5 linear elastic program to compute stresses, strains, and deformations in the pavement system. As shown in Table 3, MODULUS4 is the only program evaluated that does not require user-designated "seed" moduli or maximum number of iterations per basin evaluation. It is also the only program that automatically calculates the subgrade depth on the basis of measured deflections and offers default values for load plate radius, number of deflections, and deflection sensor spacing. Not indicated in Table 3 is the fact that this program provides all measured and calculated deflections only for final

**TABLE 3 Comparison of Common Characteristics Among Backcalculation Programs**

| Program Characteristic | Backcalculation Program: ELSDEF | MODCOMP2 | MODULUS4 | ISSEM4 |
|---|---|---|---|---|
| ***INPUT*:** | | | | |
| Error Tolerance* | (10%) | √ | X | X |
| Max No. of Iterations | (3) | √ | X | (6) |
| No. of Load Levels | ≯5 | ≯6 | X | X |
| Load Magnitude | √ | √ | √ | X |
| Load Plate Radius | X | X | (5.91 in.) | √ |
| Load Pressure | √ | √ | X | √ |
| No. of Deflections | ≯10 | ≯8 | (7) | ≯7 |
| Deflection Readings | √ | √ | √ | √ |
| Deflection Sensor Spacing | √ | √ | (12 in.) | √ |
| No. of Layers | ≯5 | ≯8 | ≯4 | ≯4 |
| Pavement Layer: | | | | |
| Thickness | √ | √ | √ | √ |
| Poisson's Ratio | √ | √ | √ | √ |
| Modulus Limits | √ | X | √ | X |
| Seed Modulus | √ | √ | X | √ |
| Fixed/Variable Modulus | X | √ | X | X |
| Linear/Nonlinear Response | X | √ | √ | X |
| Subgrade Thickness | ≯999 in. | Semi -infinite | (Calculated) | Semi-infinite |
| Subgrade Modulus Limits | √ | X | X | X |
| Subgrade Seed Modulus | √ | √ | √ | √ |
| ***OUTPUT*:** | | | | |
| (Per Iteration) | | | | |
| Deflections: | | | | |
| Measured | √ | √ | X | X |
| Calculated | √ | √ | X | X |
| Percent Difference* | √ | √ | X | X |
| Absolute Sum | √ | X | √ | X |
| Root Mean Square | X | √ | X | X |
| Final Moduli: | √ | √ | √ | √ |
| Percent Difference Between Iterations | X | X | X | Pre-set @3.5 |

* - Cumulative absolute difference between each measured and calculated deflection expressed as a percentage of the measured deflection
( ) - Default values which can be overwritten by the user.
√ - Applicable
X - Not Applicable

moduli results, unlike some other programs that provide such data on a per-iteration basis.

**ISSEM4** In situ stress-dependent elastic moduli, 4 (maximum layers) (ISSEM4) program was originally developed by Stubstad (*11*) with technical assistance from Florida and Arizona DOT engineers. It was originally designed to evaluate only deflection data of the Dynatest FWD. ISSEM4 is the only program that applies nonlinear relationships for "finite cylinders within conically-shaped volume of influence of the applied FWD load" as described in the user's guide. It iteratively backcalculates modulus values of a layered, nonlinear elastic system. Process algorithms are based on Boussinesq's equations and a version of the equivalent thickness method (*12*). ELSYM5 is used as a subroutine to adjust the subgrade moduli until a match of measured and calculated deflections is made. ISSEM4 provides various analysis options or "iteration mode identifiers" that include fixing the modulus of the surface layer and calculating the surface layer thickness.

The program analysis option selected for this research, considered the most typical, was one that assumed that input layer thicknesses are correct and that all layer modulus values are to be calculated. Multiple iterations are performed by the program until the percent difference between individual layer modulus values of two consecutive iterations is less than 3.5 percent if the designated maximum number of iterations are performed or if divergence persists. This convergence error criterion is unique because it does not involve matching calculated and measured deflections. The following are unique characteristics of ISSEM4:

1. ISSEM4 does not provide a comparison and analysis of measured and calculated deflections as part of intermediate or final results.
2. This program will not function if the evaluated pavement section does not have increasing layer thicknesses with depth. This lack of layers necessitated the consolidation of layers of like material, providing only two- and three-layer systems. This was a predominant problem because the typical test site pavement section had a 4-in.-thick base course layer (Layer 2) that was usually thinner than the surface layer.
3. Only five deflections, some NDT-measured and some interpolated by the program, are required for three- and four-

layer systems. Four deflections are required for two-layer systems.

4. Input data must be provided in metric units.

5. In this study, results were almost always obtained only when sites were treated as two- and three-layer pavement systems.

6. The program accepted seed modulus values of underlying layers that were less than those of overlying layers; this occurred despite the warning in the program user's manual that such circumstances could render results unreliable.

7. The program would not accept adjacent pavement layers that had identical seed modulus values.

### *Selection of Parameters*

Common input layer moduli ranges, applicable only to ELSDEF and MODULUS4, and Poisson's ratios used in this study are shown in Table 4. For other backcalculation programs not requiring moduli limits, final moduli were selected with the lowest convergence error or best "goodness of fit" results despite the moduli values being outside the practical moduli input limits in Table 4. Also, selection of input values of Poisson's ratios for the asphaltic concrete and bituminous base were based on the pavement surface temperature at the time of NDT. Such temperatures ranged from 50°F to 118°F. Since backcalculation programs are not significantly sensitive to Poisson's ratio input values, the following general relationships for the bituminous-bound layers were applied with other values obtained by interpolation and extrapolation: Poisson's ratio = 0.30, 0.35, and 0.40 at 40°F, 70°F, and 100°F, respectively. Poisson's ratios used for all other layers were considered as commonly used values.

### *Analysis and Comparison of Results*

A comparison of the overall average layer modulus results of each program is included in Figure 2. Figure 2 indicates that ELSDEF produced the lowest average modulus of the surface layer, whereas ISSEM4 produced the highest. Also, average modulus results of MODCOMP2 and MODULUS4 are similar for Layers 1 and 2. All four programs provided similar average modulus results of Layers 2 through 4. Figure 2 does not include ISSEM4 average modulus results of Layer 3; this layer was combined with Layer 2 or 4. Modulus results from iterations yielding these minimal covergence error results were used in the overlay design portion of this research.

### *Comparison of Program Error Criterion*

Because the error criterion of each program is different, except for ELSDEF and MODULUS4, a valid comparison of programs on the basis of given convergence error results was not possible. However, the absolute sum (ABS) of MODCOMP2 and ISSEM4 convergence error can be calculated using final moduli results and an elastic layer program such as ELSYM5 and Chevron. These programs can calculate the theoretical deflections using pavement layer data (e.g., layer thickness, Poisson's ratio, moduli, etc.). The ABS of the differences between the theoretical and measured deflections can be obtained and could provide a complete comparison of the programs on the basis of convergence error results.

## AASHTO Overlay Design

### *Moduli Corrections and Selection of Design Parameters*

A PC-compatible AASHTO overlay design program, developed by Mamlouk (*13*), was used for this study. Overlay design was performed by using standard AASHTO layer coefficients from each program's final backcalculated layer moduli values of each site's pavement structural section. The only modulus correction applied involved only bituminous-bound layers. Using actual temperatures at NDT, this modulus correction simultaneously computes the average asphalt pavement layer temperature and adjusts the modulus for the standard temperature of 70°F. This temperature correction procedure, as outlined in the AASHTO guide, was applied, assuming that the asphalt pavement surface temperature at the time of NDT is equal to the mean air temperature of the 5 days before NDT. No modulus corrections were made on the predominant granular base and subbase layers to reflect variable stress states. Also, data required to estimate AASHTO's effective subgrade soil resilient modulus was not available to the authors. Instead, the actual backcalculated modulus value for the subgrade was directly used in each overlay design.

After correcting the bituminous-bound layer moduli for temperature, structural layer coefficients for each non-

**TABLE 4 Backcalculation and AASHTO Overlay Design Parameters**

| Layer Material | Modulus (ksi) | | Poisson's Ratio | Structural Coefficient | |
|---|---|---|---|---|---|
| | Min. | Max. | at 70°F | Min. | Max. |
| Asphaltic Concrete | 50 | 1000 | 0.35 | 0.20 | 0.45 |
| Base: | | | | | |
| bituminous | 5 | 400 | 0.35 | 0.10 | 0.30 |
| cement | 90 | 1000 | 0.25 | 0.10 | 0.27 |
| granular | 3 | | 0.35 | 0.05 | 0.17 |
| Subbase: | | | | | |
| granular | 3 | 110 | 0.35 | 0.05 | 0.15 |
| Subgrade | 5 | 40 | 0.40 | | |

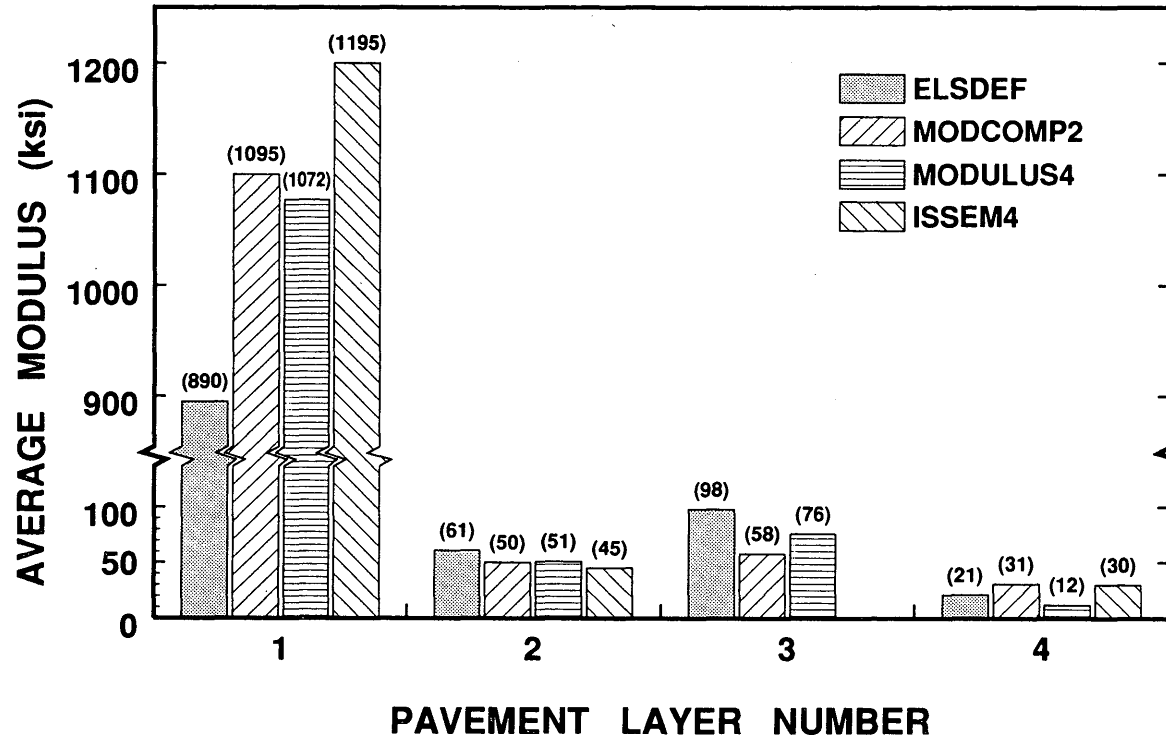


**FIGURE 2 Comparison of pavement layer moduli among backcalculation programs.**

subgrade layer were obtained using the AASHTO correlations given their backcalculated or corrected modulus values, or both, as shown in Table 4.

Using an empirical relationship developed by ADOT (*14*), base and subbase drainage coefficients were estimated as a function of drainage quality and the previously mentioned SVF. Drainage quality was assumed to be "fair" for all overlay designs. Because the primary objective is to compare backcalculation programs, the need to perform an exact overlay design to suit each site was not considered essential. Consequently, some required AASHTO overlay design parameters were assumed and used in each site's overlay design. These parameters are 99.9 percent reliability, 0.45 overall standard deviation, 4.5 overlay initial serviceability index, 3.0 overlay terminal serviceability index, and 0.45 structural layer coefficient of overlay. However, the design ESALs, SVF, layer thicknesses, moduli, and coefficients were parameters characteristic to each site and used for each overlay design.

Milling existing asphaltic concrete pavement prior to overlay was considered in the automated overlay design of applicable sites. Milling is a typical rehabilitation strategy employed by ADOT on most existing flexible pavements on the interstate highway system. In this study, milling 3 in. before overlay was assumed for these particular sites.

### *Results*

Overlay thicknesses, rounded to the nearest ½ in., required for each test site are shown in Table 5. Table 5 also indicates whether milling was considered and includes the average overlay thickness of all test sites for each program.

A comparison of overlay thickness results by backcalculation program per site in Table 5 reveals significant differences between programs. Sites 1 through 3, 9, 11, 23, and 28 each have a maximum overlay thickness difference of over 3 in. From a practical perspective, these differences could translate into a significant amount of money on a large overlay construction project.

## ANALYSIS OF RESULTS

An analysis of variance (ANOVA) was performed to test the null hypothesis that all programs are the same. A completely randomized design was applied where extraneous sources of variability were not controlled. Five ANOVAs were performed to individually consider the following factors: backcalculated modulus results of each layer and overlay thickness results. In considering a level of significance of 0.05 for this research, the results indicate that the backcalculation programs are significantly different on the basis of subgrade layer modulus ($E_4$) results. However, results also reveal that the backcalculation programs are not significantly different considering the other individual factors (modulus results of Layers 1 through 3 and overlay thickness).

Knowing only that the programs are significantly different on the basis of $E_4$, the procedure of multiple comparisons was further performed using Tukey's method as described in Ott (*15*) to determine how each program relatively differed on this basis. Multiple comparisons, using results of the ANOVA, determine the relative difference of the $E_4$ sample means of each program on the basis of a particular critical value. Results of the multiple comparisons indicate that MODULUS4 yields

**TABLE 5 Summary of AASHTO Overlay Design by Backcalculation Program and Test Site**

| Site No. | Milled? | Overlay (in.) by Backcalculation Program | | | |
|---|---|---|---|---|---|
| | | ELSDEF | MODCOMP2 | MODULUS4 | ISSEM4 |
| 1 | YES | 3.5 | 4.5 | 5.5 | 0 |
| 2 | YES | 2.5 | 3.0 | 6.5 | 2.5 |
| 3 | YES | 3.0 | 3.0 | 8.5 | 4.0 |
| 4 | YES | 6.5 | 6.5 | 8.0 | 6.0 |
| 5 | YES | 7.5 | 7.5 | 9.0 | 7.0 |
| 6 | YES | 5.5 | 5.0 | 7.0 | 4.0 |
| 7 | YES | 7.0 | 7.0 | 9.5 | 7.5 |
| 8 | YES | 3.5 | 3.5 | 5.0 | 3.5 |
| 9 | YES | 0 | 0.5 | 3.5 | 0.5 |
| 10 | YES | 0 | 0 | 0 | 0 |
| 11 | YES | 9.0 | 3.5 | 8.0 | 9.0 |
| 12 | YES | 7.5 | 4.5 | 7.5 | 4.5 |
| 13 | YES | 0.5 | 0 | 0.5 | 0 |
| 14 | YES | 8.0 | 7.5 | 7.5 | 8.5 |
| 15 | YES | 2.5 | 4.5 | 5.5 | 7.5 |
| 16 | NO | 5.5 | 5.5 | 6.0 | 5.5 |
| 17 | NO | 0.5 | 0.5 | 1.0 | 0.5 |
| 18 | NO | 2.5 | 1.5 | 2.0 | 1.0 |
| 19 | NO | 5.5 | 5.5 | 6.0 | 5.5 |
| 20 | NO | 0 | 2.5 | 3.0 | 2.5 |
| 21 | NO | 3.0 | 3.5 | 4.5 | 3.0 |
| 22 | NO | 0 | 0 | 0.5 | 0 |
| 23 | NO | 0 | 2.5 | 1.5 | 4.0 |
| 24 | NO | 4.5 | 5.0 | 5.5 | 4.0 |
| 25 | NO | 5.0 | 5.0 | 6.0 | 4.5 |
| 26 | NO | 0 | 0 | 3.0 | 1.5 |
| 27 | YES | 2.5 | 3.0 | 4.5 | 3.5 |
| 28 | YES | 3.5 | 2.0 | 7.0 | 2.0 |
| 29 | YES | 1.0 | 1.0 | 2.5 | 0 |
| Average | | 3.45 | 3.38 | 4.98 | 3.52 |

subgrade layer modulus results significantly lower than those of the other programs.

In addition to the ANOVA, average overlay thickness results were evaluated and found to be not statistically different, considering an allowable level of significance of 0.05. However, in reality, the large differences in overlay thickness between programs per site are very serious.

MODULUS4 results contributed to overlay design thicknesses larger than those from other backcalculation programs, whereas ELSDEF resulted in smaller thicknesses, as shown in Table 5. The larger overlay thicknesses produced by MODULUS4 were attributed to its backcalculated subgrade moduli ($E_4$) results that were determined to be significantly lower than those of other programs. These results are because MODULUS4 automatically calculates a subgrade thickness that was usually not semi-infinite, as was assumed in the cases of MODCOMP2 and ISSEM4. This lower subgrade thickness estimation resulted in higher strains in the subgrade, consequently reducing the layer modulus. In the AASHTO overlay design procedure, the lower the modulus, the higher the required thickness. Because the AASHTO overlay design procedure does not consider the subgrade thickness or depth to rigid layer, excessive overlay thicknesses will result when using backcalculation programs such as MODULUS4.

## SUMMARY AND CONCLUSIONS

Several backcalculation programs are currently available and used to evaluate the structural condition of existing pavements. Because pavement structural evaluation results significantly affect overlay design results, the main objective of this study was to evaluate the effect of backcalculation program differences on overlay thickness. Secondary objectives were to conduct a comprehensive comparison of program characteristics and performance and simulate the use of backcalculation programs by practitioners.

Four common, PC-compatible, backcalculation programs (ELSDEF, MODCOMP2, MODULUS4, and ISSEM4) were compared and used to backcalculate layer moduli from 29 typical, in-service, flexible pavement sites within projects that required significant rehabilitation. FWD field deflections from each test site were used to estimate layer moduli by backcalculation. The estimated moduli were used in the design of required overlays in accordance with the 1986 AASHTO design guide.

Although the various backcalculation programs produced various layer moduli, these differences were not statistically significant except for the subgrade. The overlay thickness results between programs were not statistically different. However, the variability of overlay thickness results per site were serious considering practical applications.

In summary, "state of the art" in backcalculation, as represented by the programs evaluated in this research, is not adequate for use by the practitioner. Despite favorable statistical results, reliable and realistic results will not be obtained using such programs in conjunction with the AASHTO overlay design method. Backcalculation programs must still be used with extreme caution.

Additional research is needed to further refine the backcalculation process to reduce the effects of extraneous sources of error and dependence on user experience. When all effects on moduli results are identified and quantified, perhaps a more intricate statistical analysis can be applied when similarly comparing programs to accurately account for the effects of extraneous sources of error. The method of considering the depth to rigid layer should be improved and standardized among programs. Also, the criteria for evaluating the degree of deflection match should be standardized among all programs. More research is needed to provide a more rational

overlay design procedure that relates the elastic layer moduli to overlay thickness without the need to apply empirical structural layer coefficients. The correlation between AASHTO structural layer coefficients and layer moduli serves to "mask" or reduce the true differences between the programs evaluated on the basis of overlay design thickness results. The AASHTO procedure should be modified to compensate for the depth to the rigid layer in the overlay thickness design procedure.

## ACKNOWLEDGMENTS

The authors would like to express their sincere appreciation and gratitude to the Materials Section of ADOT for their cooperation and assistance in obtaining the necessary data for this study. Special thanks go to Jim Delton for his role as ADOT liaison throughout the study. Thanks are also extended to A. Bush, L. Irwin, T. Scullion, R. Stubstad, and N. Coetzee for providing the backcalculation programs and helpful advice during the study.

## REFERENCES

1. Y. J. Chou and R. L. Lytton. Accuracy and Consistency of Backcalculated Pavement Layer Moduli. Presented at 70th Annual Meeting of the Transportation Research Board, Washington, D.C., 1991.
2. L. H. Irwin, W. S. Yang, and R. N. Stubstad. *Deflection Reading Accuracy and Layer Thickness Accuracy in Backcalculation of Pavement Layer Moduli.* ASTM STP 1026. ASTM, Philadelphia, Pa., 1989, pp. 229–244.
3. T. Rwebangira, R. G. Hicks, and M. Truebe. Sensitivity Analysis of Selected Backcalculation Procedures. In *Transportation Research Record 1117*, TRB, National Research Council, Washington, D.C., 1987, pp. 25–37.
4. R. C. Briggs and S. Nazarian. Effects of Unknown Rigid Subgrade Layers on Backcalculation of Pavement Moduli and Projections of Pavement Performance. In *Transportation Research Record 1227*, TRB, National Research Council, Washington, D.C., 1989, pp. 183–193.
5. N. A. Ali and N. P. Khosla. Determination of Layer Moduli Using a Falling Weight Deflectometer. In *Transportation Research Record 1117*, TRB, National Research Council, Washington, D.C., 1987, pp. 1–10.
6. J. P. Mahoney, N. F. Coetzee, R. N. Stubstad, and S. W. Lee. *A Performance Comparison of Selected Backcalculation Computer Programs.* ASTM STP 1026. ASTM, Philadelphia, Pa., 1989, pp. 452–467.
7. *AASHTO Guide for Design of Pavement Structures.* AASHTO, Washington, D.C., 1986.
8. A. J. Bush III. Nondestructive Testing for Light Aircraft Pavements, Phase II, *Development of Nondestructive Evaluation Methodology.* Final Report FAA-RD-80-9-II. FAA, Washington, D.C., Nov. 1980.
9. L. H. Irwin. *User's Guide to MODCOMP2.* Cornell Local Roads Program Report 83-8. Cornell University Local Roads Program, Ithaca, N.Y., Nov. 1983.
10. T. Scullion and C. Michalak. *MODULUS 4.0: User's Manual.* Research Report 1123-4F. Texas Transportation Institute, Texas A&M University, College Station, Tex., Jan. 1990.
11. R. Stubstad. *Description of and User's Guide for the Dynatest ISSEM4 Computer Program.* Dynatest Consulting, Inc., Ojai, Calif., 1988.
12. P. Ullidtz. *Pavement Analysis.* Elsevier, Amsterdam, 1987.
13. M. S. Mamlouk. *Simplified AASHTO Design Method of Flexible Pavements for City of Phoenix.* Contract 47961, P-875518. Arizona State University, Tempe, June 1988.
14. *Materials Preliminary Engineering and Design Manual*, 3rd ed., Chapter 2. Arizona Department of Transportation, Phoenix, March 1989.
15. L. Ott. *An Introduction to Statistical Methods and Data Analysis*, 3rd ed. PWS-Kent, Boston, Mass., 1988.

---

# Layer Moduli Determination During Freeze-Thaw Periods

VINCENT C. JANOO AND RICHARD L. BERG

In seasonal frost areas, a frozen pavement structure undergoes a complex change in its ability to support traffic as the subgrade and base thaw. In an attempt to quantify this change, several test sections of various cross sections were built in the Frost Effects Research Facility at the Cold Regions Research and Engineering Laboratory. These test sections were subjected to freeze-thaw cycles, and changes in their structural capacity were monitored. The performance of only one of these, TS1, is discussed. The structural capacity during the thaw cycles was characterized nondestructively using a falling weight deflectometer (FWD). Other measurements, such as frost and thaw depths, were obtained from subsurface temperature and resistivity gauges. The Corps of Engineers computer program WESDEF was used to backcalculate layer moduli from the FWD data. On the basis of temperature and resistivity gauge measurements, the pavement layers were appropriately subdivided to reflect the thawed and frozen layers. The backcalculated moduli were used to calculate the horizontal strains at the bottom of the asphalt concrete layer and the vertical strain at the top of the subgrade. These results were compared with those of similar strains obtained when the thawed and frozen layers were combined into a single composite layer. It was found that the thicknesses of the frozen and thawed layers were critical in backcalculating layer moduli and damage to pavement structures. Larger errors were introduced between measured and theoretical deflection basins when the frozen and thawed layers were considered as a single composite layer. The horizontal strains at the bottom of the asphalt layer were not greatly affected by ignoring the thawed layer. The damage to pavements with respect to vertical strains was grossly underestimated when the thawed and frozen layers were not considered separately.

Surface deflections obtained with a falling weight deflectometer (FWD) are now routinely used in evaluating the load-bearing capacity of highway and airport pavements. It has become an integral part of many "remaining life" and overlay design procedures. The modulus of the various layers are "backed out" using the measured FWD deflections and theory of elasticity. This procedure of backing out the layer moduli is referred to as backcalculation. Current backcalculation procedures are characterized in one of the following groups: (a) multilayered (e.g., WESDEF, MODCOMP3, EVERCALC, ELSDEF, and MODULUS) and (b) equivalent thickness (e.g., ELMOD, SEARCH, and BOUSDEF). The pavement materials in most of the models are characterized as linear elastic, although it is generally recognized that most materials in a pavement system do not behave in this fashion.

In this study, the pavement structure was divided into multilayers. The materials in these layers were then characterized by two elastic constants: the layer stiffness ($E_i$) and Poisson's ratio ($\upsilon_i$). The idealization is shown in Figure 1. The backcalculation procedure officially used by the U.S. Army Corps of Engineers is WESDEF. The maximum number of layers that can be modeled by WESDEF is five, with the fifth layer automatically set as a rigid layer. Best backcalculated moduli results are obtained if the number of unknown layers is limited to three. WESDEF uses the WESLEA layered elastic programs for calculating stresses and strains and deflections in the pavement system. WESLEA was developed by Van Cauwelaert et al. (*1*) for the U.S. Army Corps of Engineers.

The backcalculation of the various layer moduli is an iterative procedure. The solution from WESDEF is a set of layer moduli ($E_i$) values that will minimize the error between the measured and computed surface deflections. WESDEF is terminated when the absolute sum of the errors between the measured and calculated deflections is less than 10 percent or when the change in modulus is within the specified tolerance of 10 percent. This limit was developed by the Waterways Experiment Station (WES) on the basis of their experience with the 71-kN Road Rater. The Road Rater measured only four deflections, and it was judged that if the individual deflection error was less than 2.5 percent, the computed deflection basin was good. We used this 2.5 percent error for all the seven FWD sensors. Our criterion for a good fit was when the absolute sum of the errors was ≤ 17.5 percent. Past experience by WES found that the best fits between measured and calculated deflections were obtained when an artificial rigid layer was placed at a depth of 9.5 m from the surface. In WESDEF, the location of the rigid layer can be changed by the user.

WESDEF has been used quite successfully in nonfrost areas, where the number of layers in a pavement structure remains

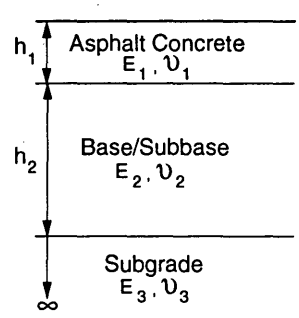


**FIGURE 1 Idealization of pavement structure in backcalculation analysis.**

Cold Regions Research and Engineering Laboratory, Corps of Engineers, Department of the Army, Hanover, N.H. 03755-1290.

fairly constant throughout the year. The pavement structures in these areas could be idealized as three and, at most, four layers without much loss of accuracy in the results. The situation is much more complex in seasonal frost areas where pavement structures are subjected to freezing and thawing. During thaw, the pavement foundation can become saturated with water from the thawing ice lenses, thus creating weak layers in the base or subgrade. It is possible that a subgrade modeled as a single layer before freeze-thaw needs to be subdivided into three layers or more during thaw. Figure 2 shows the annual possible changes in a pavement structure in a seasonal frost area. Most of the pavement damage in seasonal frost areas occurs during the winter or the spring thaw. The failure will manifest itself on the surface in the form of cracking or rutting (caused by deformation in the base or subgrade). The period and severity of thaw weakening varies, depending on the soil type, degree of saturation, drainage conditions and pavement surface temperatures. Therefore, it is important that any backcalculation procedure used for modeling pavement behavior in seasonal frost areas has the flexibility to manage the complex layer changes.

The backcalculation procedure, being iterative, leads to a number of combinations of layer moduli producing the same deflection basin. Therefore, the user must have a reasonable idea of the modulus of the various layers. Other critical information required for backcalculation are layer material and thicknesses. Therefore, even though the FWD test is advertised as nondestructive, a carefully planned boring program should be a standard part of FWD testing. The results from the boring program should include (a) layer thicknesses; (b) material samples for resilient modulus testing; and (c) location of rigid layers, if any.

As part of the development of a design-evaluation method for pavements in cold regions, several test sections were built in the Frost Effects Research Facility (FERF) at the U.S. Army Cold Regions Research and Engineering Laboratory (CRREL) and subjected to freeze-thaw cycles. During the thawing period, deflection measurements were conducted every day with an FWD. The use of FWD deflection data to characterize the thaw weakening of pavements in seasonal frost areas has been previously presented (*2–5*). The deflection measurements obtained during the first and second thaw period were also used to mechanistically characterize (i.e., in terms of layer moduli and strains) the effect of the thawed layer on pavement performance.

Initially we had planned to backcalculate the layer moduli from all the test sections. The test sections ranged from full depth to conventional pavements. Preliminary results showed large errors in the backcalculated moduli during the thaw period. This was especially true for the conventional pavement cross sections. We decided to use a simple full-depth pavement structure to study how WESDEF, or for that matter any of the other backcalculation procedures (multilayered), would work with thawed and frozen layers.

## DESCRIPTION OF TEST SECTION

A test section (TS-1) was constructed in FERF; information on FERF can be found in Janoo and Berg (*2*) and Eaton (*6*). A detailed description of the test section can be found in Janoo and Berg (*2*). The test section was 610 $cm^2$ and 160 cm deep with full-depth asphalt concrete pavements. TS-1 consisted of 15 cm of asphalt concrete over 145 cm of compacted clay soil. The natural foundation under TS-1 was a fine sand (SM) subgrade. Information from drill logs showed no rigid layers to a depth of approximately 20 m.

The compacted clay soil was classified as an inorganic clay of high plasticity (CH) using the Unified Soil Classification System. On the basis of grain size analysis and Atterberg limits, the clay was classified as an F3 soil with respect to frost susceptibility. The compacted clay soil California bearing ratio (CBR) values ranged from 18 percent to 27 percent.

The test section was instrumented with thermocouples, CRREL resistivity gauges and psychrometers. A detailed description of the instrumentation can be found in Janoo and Berg (*2*). Frost and thaw locations were determined from the position of the 0°C isotherm. Frost penetration depths were also determined using the CRREL electrical resistivity gauges. These gauges were especially useful in locating thaw depths when the subsurface temperatures became nearly isothermal at 0.0°C.

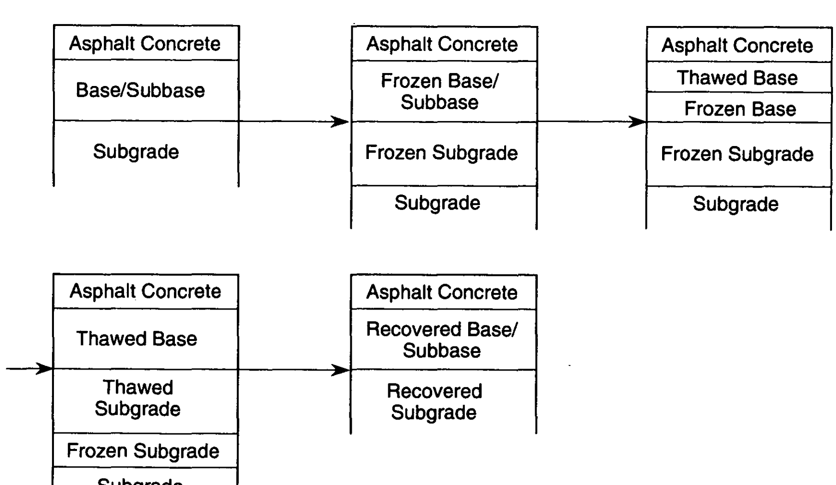


**FIGURE 2 Change in pavement structure during freeze-thaw cycling.**

## TESTING PROGRAM

The test section was frozen from the top down by placing cooling panels on the surface of the pavements. The 0°C isotherms in the test section during the first and second freeze-thaw cycle are presented in Figure 3. The temperature measurements were taken at a single point and were assumed to be representative throughout the respective test sections. The test section was frozen to a depth of 122 cm for the first cycle and 152 cm for the second cycle. Thawing of the test section was done by removing the cooling panels, and the pavement sections were heated by the ambient FERF temperature.

Surface deflection measurements were taken once a day during the thaw periods using a Dynatest 8000 falling weight deflectometer. FWD measurements were taken at four locations on the test section. These locations are illustrated in Figure 4. The FWD measurements were conducted using a 30-cm-diameter plate. The geophones were located at 0, 17.5, 30, 70, 110, 150, and 245 cm from the center of the loading plate. The tests were conducted using four load levels, which ranged from 20 to 67 kN.

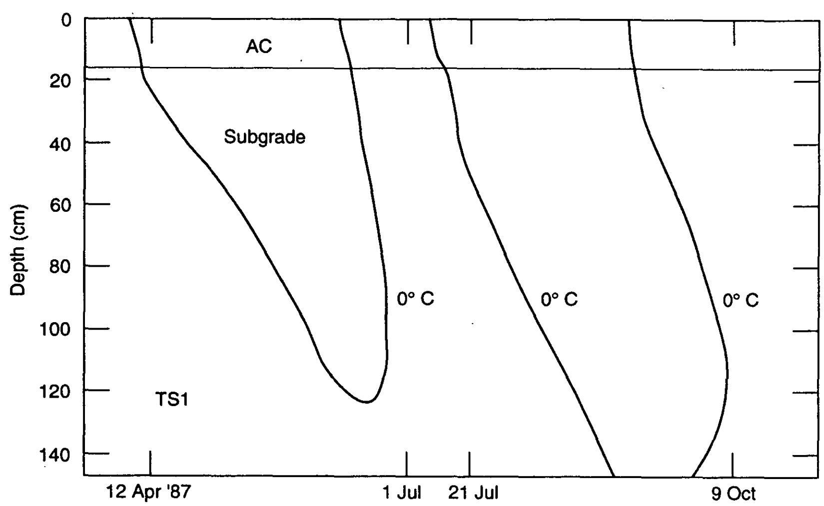


**FIGURE 3 Zero degree isotherm in test section.**

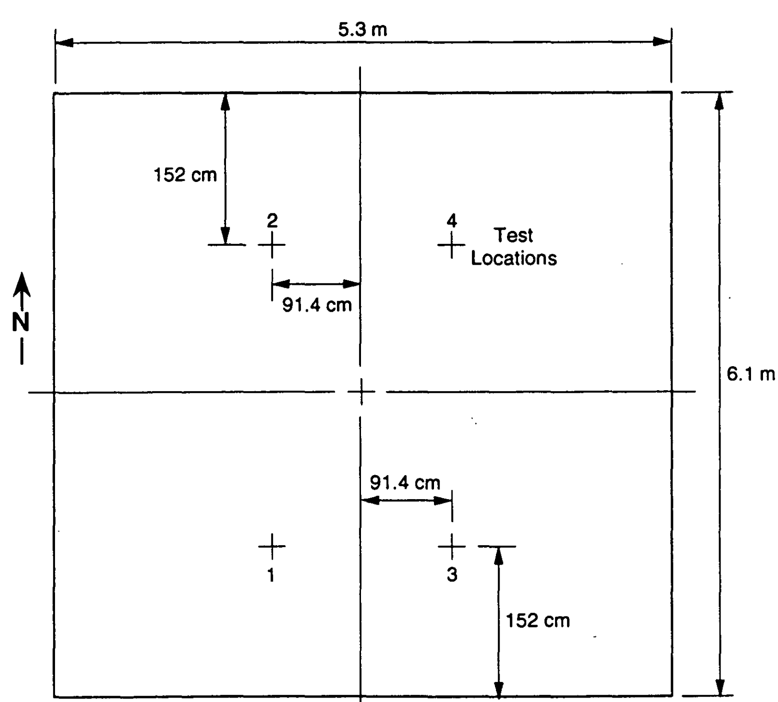


**FIGURE 4 Typical FWD location points in test sections.**

## BACKCALCULATION OF LAYER MODULI

The layer moduli were backcalculated from a normalized 40-kN deflection basin at the four locations in the test section (Figure 4). The normalization was done by plotting the load-deflection data from the first three load levels and applying a linear regression to the data. The representative deflection basin for each test section was obtained using BASIN and the normalized deflection basins from the four FWD points. BASIN, a computer program developed at WES, averages the deflections at each sensor location for a given load level and calculates an average deflection basin area. It then chooses a measured deflection basin that is closest to the averaged basin deflections and area as the representative basin.

Before the application of the first freeze-thaw cycle, FWD measurements were conducted on the newly constructed test sections. The following are seed moduli and Poisson's ratios used in WESDEF for the various layers:

| *Material Type* | *Elastic Modulus (MPa)* | *Poisson's Ratio* |
|---|---|---|
| Asphalt concrete | 2413.25 | 0.35 |
| Clay subgrade | 03.43 | 0.40 |
| Natural sand subgrade | 206.85 | 0.40 |

These were the suggested values in WESDEF. This feature of suggested modulus values of the various pavement materials and their possible range is a useful tool for the new user.

In the initial attempt, prior to freezing, TS-1 was idealized as a three-layer system. The layers were the asphalt concrete (AC) layer (15 cm), the compacted clay layer (145 cm), and an infinite sandy subgrade. The backcalculated values were as follows: AC, 3,292 ± 127 MPa; clay, 140 ± 17 MPa; sand, 114 ± 23 MPa. The mean absolute error was 18.63 ± 11.8, which was greater than the 17.5 percent desired. In the second attempt, the clay layer was divided into two layers. The top and bottom layers were 74 and 71 cm thick. The backcalculated values were as follows: AC, 3,445 ± 540 MPa; top clay, 132 ± 40 MPa; bottom clay, 159 ± 14 MPa; and sand, 110 ± 20 MPa. The mean absolute error was 9.53 ± 6 percent, which was well within the specified requirement of 17.5 percent. Although the error was reduced by half, the changes in the mean modulus were only 5 percent and 3 percent, respectively, for the AC and the sand subgrade. The average of the two-clay layer moduli (145 MPa) was similar to the value of the single clay layer modulus calculated when the system was modeled as a three-layer system. With respect to the calculated strains using either the three- or four-layer system, the difference in the vertical strain at top of the subgrade was approximately 0.3 percent and less for the horizontal strain at the bottom of the AC layer. Because WESDEF is able to accommodate only up to four layers, the mean of the composite clay moduli was used as the baseline. The following are the moduli that were used as the prefrozen (baseline) moduli in TS-1:

| *Material* | *Modulus (MPa)* |
|---|---|
| Asphalt concrete | 3,445 ± 540 |
| Unfrozen clay | 145 ± 50 |
| Sand subgrade | 110 ± 20 |

The backcalculated modulus of the natural sand subgrade was found to be lower than expected. However, since the sand subgrade did not undergo any substantial freeze-thaw cycling, we assumed that the modulus of this layer remained the same throughout the two freeze-thaw cycles. The mean layer moduli for TS-1, in conjunction with NELAPAV (*7*), were used to calculate the horizontal strain at the bottom of the asphalt concrete layer ($Z = -152$ mm) and the vertical strain at top of the clay layer ($Z = -153$ mm) where $Z$ is the depth from the surface. The load level used in calculating the strains was 40 kN. The computed strains were 0.00022 and −0.00067 for the horizontal and vertical strains, respectively. These values were used as reference values during the freeze-thaw cycles.

## BACKCALCULATION OF LAYER MODULI DURING THAW PERIODS

We selected several days during the first and second thaw period to backcalculate the layer moduli for two cases. The first case involved backcalculating the layer moduli, if we assumed no knowledge of the thicknesses of the frozen or thawed layers. Basically, the frozen, thawed, and unfrozen layers were lumped as a single layer. The scenario is identified as Case 1 in all future discussions. In the second case, backcalculation of the layer moduli was made with the knowledge of the thicknesses of the frozen and thawed layers (Case 2).

Before conducting the backcalculation of the various layer moduli, a literature review was done to obtain any data on the frozen and thawed moduli of base, subbase, subgrade, and asphalt concrete. The results of the review for the base, subbase, and subgrade materials are tabulated in Table 1. These moduli values were used as a guide for selecting the seed modulus for the frozen and thawed clay layer. The data presented in Table 1 are from laboratory resilient modulus tests (*8–13*), with the exception of data furnished by Stubstad and Connors (*12*). The modulus values for frozen soils generally increase with decreasing temperatures. The lowest values are at about −2°C and the highest are at a temperature of about −8°C. Because the lowest resilient modulus values in the table are for temperatures about −2°C, values lower than those shown here are expected to be closer to 0°C.

Resilient modulus values for thawed materials generally increase with decreasing moisture content. The lowest values are near saturation and the highest values in the table are in the range of 50 percent to 80 percent of saturation. It was not possible to conduct laboratory resilient modulus tests on some of the fine-grained soils immediately after thawing because they were unstable. Therefore, the lowest values in the table are not the lowest that these materials may exhibit.

Modulus values in the thawed state are also generally stress dependent. Values for fine-grained materials usually decrease with increasing stress but granular materials generally increase with increasing stress. Modulus values for all materials generally increase with increasing density.

The asphalt concrete modulus can be estimated using the Asphalt Institute (AI) equation

$$\log E = 5.553833 + 0.028829\frac{P_{200}}{f^{0.17033}} - 0.03476(V_v) + 0.07037(n_{70°\mathrm{F},10^6}) + 0.000005\left(t_p^{(1.3 + 0.49825 \log f)} P_{ac}^{0.5}\right) - 0.00189\left(t_p^{(1.3 + 0.49825 \log f)} \frac{P_{ac}^{0.5}}{f^{1.1}}\right) + 0.931757\frac{1}{f^{0.02774}}$$

**TABLE 1  Frozen and Thawed Resilient Modulus Values for Pavement Materials**

| Material | USCS Classification | Resilient Modulus Frozen (MPa) | Resilient Modulus Thawed (MPa) |
|---|---|---|---|
| Winchendon, MA dense graded stone | GM-GP | 930 - 56,390 | |
| Albany County Airport TW A, subbase | GW-GM | 100 - 34,970 | 34 - 272 |
| Albany County Airport TW B, subbase | GW-GM | 1,520 - 19,280 | 55 - 366 |
| Minnesota Test Road Class 6 base | GW | | 74 - 972 |
| Minnesota Test Road Class 3 subbase | SW | 1,448 - 46,098 | 25 - 5,433 |
| Albany County Airport TW A, base course | SW-SM | 340 - 24,100 | 43 - 259 |
| Winchendon, MA Graves sand | SM | 650 - 20,590 | 21 - 158 |
| Winchendon, MA Hart Bros. sand | SM | 650 - 20,590 | 21 - 396 |
| Winchendon, MA Hyannis sand | SM | 1,300 - 56,840 | 27 - 141 |
| Albany County Airport TW A, subgrade | SM | | 41 - 209 |
| Albany County Airport TW B, subgrade | SM | 180 - 39,430 | 41 - 192 |
| Albany County Airport TW B, subgrade never frozen | SM | | 42 - 240 |
| Winchendon, MA Ikalanian sand | SM-SP | 660 - 22,750 | 8 - 282 |
| Winchendon, MA Sibley till | SM-SC | 1,050 - 45,590 | 31 - 164 |
| Minnesota Test Road 1206 Subgrade | CL | 924 - 10,928 | 6 - 1,455 |
| Ft. Edward, NY Ft. Edward clay | CL-CH | 450 - 6,220 | 7 - 149 |
| Base Course | | | (13) 20,685<br>(12) 1,034 |
| Subbase | | | (13) 20,685<br>(12) 1,034 |
| Subgrade | | | (13) 3,448<br>(12) 1,034 |

where

$E$ = dynamic modulus of asphalt concrete,
$P_{200}$ = percent aggregate passing Number 200 sieve,
$f$ = frequency,
$V_v$ = percent air voids,
$h_{70°F,10^6}$ = absolute viscosity at 70°F (poise × $10^6$),
$P_{ac}$ = asphalt content (percent by weight of mix), and
$t_p$ = midpavement temperature (°F).

The following assumptions were used in calculating the modulus of the AC using the preceding equation:

$P_{200}$ = 5 percent,
$V_v$ = 4 percent (the acceptable range was 3 to 5 percent),
$\eta_{70°F,10^6}$ = 2.5-AC 20 asphalt (*14*), and
$P_{ac}$ = 6 percent (the acceptable range was 5 to 7.5 percent).

The frequency ($f$) used was 20 Hz, which is commonly assigned to FWD loading. Temperature measurements were taken at 5, 10, and 15 cm from the surface of the AC layer. The midpoint temperature was interpolated linearly between the three temperature measurements.

To reiterate, Case 1 is the three-layer system. WESDEF was used to backcalculate the modulus of the asphalt concrete, composite (thawed and frozen and unfrozen) clay and the sand subgrade layers. When the frozen and thawed layers were accounted for in Case 2, there were different structures in the first and second thaw cycles. At the end of the first freeze cycle, the frost front was located at a depth of 122 cm from the asphalt concrete surface. Thaw was basically downward. The pavement structure was divided into five layers. The structure consisted of an asphalt concrete layer, a variable thickness thawed lawyer ($h_t$), a variable thickness frozen layer ($h_f$), an unfrozen clay layer ($h_{uf}$), and the infinite sand subgrade (Figure 5*a*). At the end of the second freeze cycle, the frost depth was down to 152 cm from the asphalt concrete surface. In the early stages of the second thaw cycle, the pavement structure was idealized as that shown in Figure 5*b*. The structure consisted of an asphalt concrete layer, a variable thickness of the thawed ($h_t$) and frozen layers ($h_f$), and the sand subgrade. Partially through the second thaw cycle, thawing of the pavement structure was occurring simultaneously from the top and bottom. This pavement structure is shown in Figure 5*c*.

The idealized pavement structures used in WESDEF are shown in Figure 6. In the first thaw cycle (Case 1), the structure shown in Figure 5*a* was modeled by the structure shown in Figure 6*a*. Because of the limitation of four layers in WESDEF, it became necessary to combine the unfrozen clay layer with the sand subgrade. The modulus of this composite (clay/sand subgrade) layer was fixed at an average of the two-layer moduli of 128 MPa. In the early stages of the second thaw cycle, the pavement structure shown in Figure 5*b* was idealized by the structure in Figure 6*b*. The modulus of the layer below the frozen layer (sand subgrade) was fixed at 110 MPa. For the late stages of the second thaw cycle, the limitation of four layers in WESDEF meant that the thawing layer below the frozen layer could not be included in the idealization. It was idealized by the structure shown in Figure 6*c*.

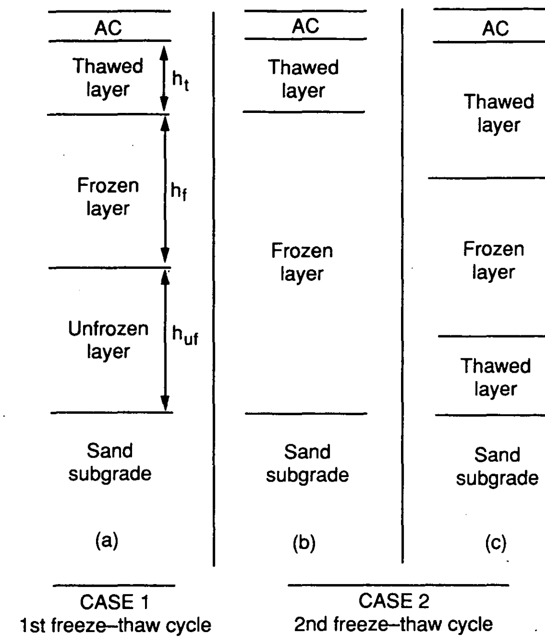


**FIGURE 5 Actual pavement structures in TS-1 during thaw cycles.**

The results from the backcalculation follow. Every attempt was made to minimize the error between the measured and calculated deflections. The absolute arithmetic (AA) errors in the backcalculation of the layer moduli for both cases are shown in Figure 7. The AA errors for most of the days are larger in the first case than in the second. The error was reduced when the thawed and frozen layers were separated. It was found that the largest deflection errors occurred at the sixth and seventh sensors in Case 2, probably because of the constant values assigned to the composite subgrade in the later stages of thawing. However, in both cases, with an exception of a few days, the AA error exceeded our criterion of 17.5 percent. The data in Figure 7 show the best fit between measured and calculated deflection basins that were attainable with WESDEF.

An attempt was made to isolate the source of the large errors in Case 1 (Figure 7). It was found that the backcalculated sand subgrade modulus in Case 1 was similar to its mean prefrozen value. This value gives confidence to our assumption that the modulus of this layer remains constant during the thaw cycles. The backcalculated modulus of the sand subgrade for the two thaw cycles is shown in Figure 8. We found that most of the values were within one standard deviation of its mean prefrozen value, which suggests that the errors are in the upper layers; it also reinforces the need to separate the frozen and thawed layers in the backcalculation process.

The backcalculated asphalt concrete moduli for both cycles with respect to midpavement temperatures are shown in Figure 9. For comparison, the modulus values obtained from AI (*14*) are also shown in the same figure. The backcalculated AC moduli from both cases were consistently lower than the AI predicted modulus. The exception to this is at low temperatures. Also the backcalculated AC modulus appears to

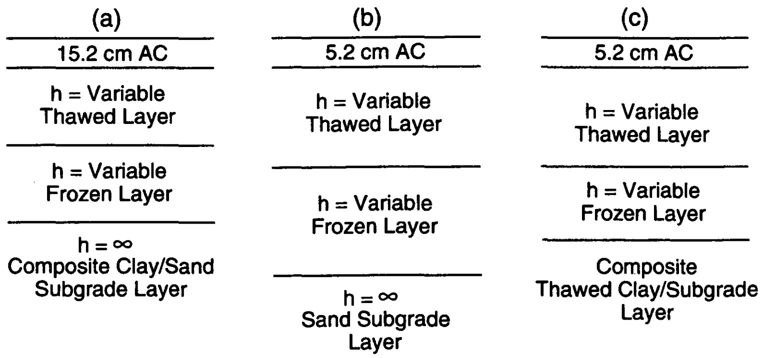


**FIGURE 6 Idealized pavement structure used in WESDEF.**

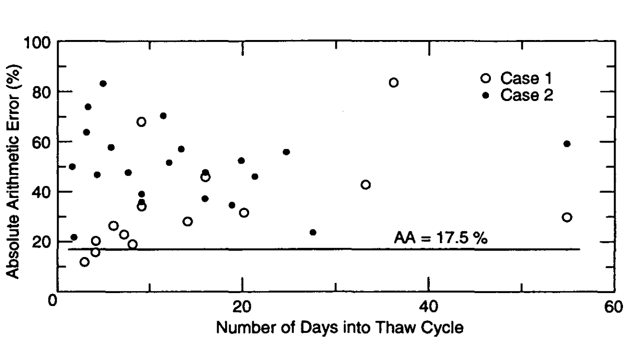


**FIGURE 7 Absolute arithmetic error distribution in backcalculation of layer moduli during thaw periods.**

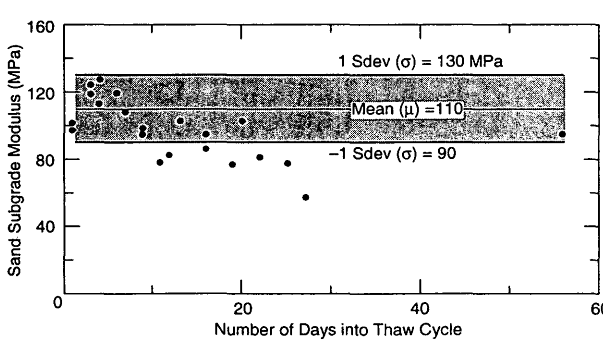


**FIGURE 8 Variation of sand subgrade modulus in both thaw cycles.**

be unaffected by how the pavement system was modeled. Therefore, we can conclude that the larger errors in Case 1 result from the lumping of the frozen and thawed layers as one single layer. Attempts to fix the asphalt concrete modulus in WESDEF for both thaw cycles for both cases with the predicted AI modulus only increased further the AA error. A regression equation ($r$ = 0.54) was developed for the AC modulus in seasonal frost areas (Figure 9$c$):

$$ACMOD = 5{,}944 - 242(T_P)$$

where $ACMOD$ is the AC modulus in megapascals and $T_p$ is the midpavement temperature (°C). This regression can be

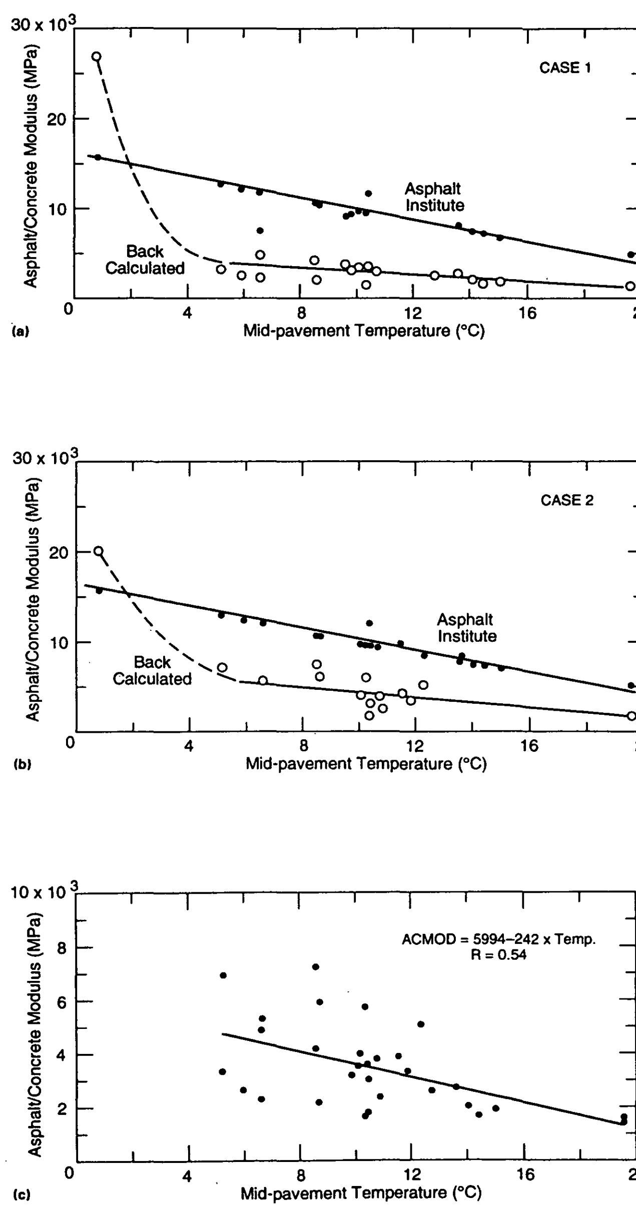


**FIGURE 9 Variation of asphalt concrete modulus in both thaw cycles.**

used as a guide for selecting asphalt concrete moduli in seasonal frost areas.

Several interesting trends were noticed between the clay layer modulus for the two cases. For discussion purposes, the composite clay modulus in Case 1 is designated as $E_c$, and the thawed clay layer modulus in Case 2 as $E_t$. In Figure 10, Case 1 is identified as composite and Case 2 as thawed layer. It becomes apparent in Figure 10 that as soon as thawing of the subgrade commences $E_t \ll E_c$. The difference is approximately 96 percent when $E_t \approx 10$ MPa; this compares with $E_c \approx 280$ MPa at the beginning of thaw (76-mm-thick thawed layer). At the same time, with respect to its prefrozen strength, $E_c$ was about two times greater, and $E_t$ was approximately a quarter of its prefrozen strength. $E_c$ decreases rapidly to a thaw depth of 800 mm from the top of the clay layer, after which it starts to increase (Figure 10). $E_t$ shows a gradual increase with thaw depth. $E_c$ and $E_t$ have approximately the same value when the thaw depth is greater than 1 m ($\approx$80 MPa). However, this value is still less than the prefrozen value of 145 MPa.

The effect of neglecting the thawed layer (Case 1) on pavement performance can be shown by the calculated horizontal and vertical strains at the bottom of the asphalt concrete and at the top of the clay layer, respectively. The horizontal and vertical strains were calculated using NELAPAV (linear). The horizontal strains were calculated at a depth of 152 mm and the vertical strain at 153 mm depth from the surface. The horizontal strains were also calculated with Jung's (*15*) method of using the center and first FWD deflection measurements. The horizontal strain ($H_s$) is calculated from

$$H_s = \frac{h(d_0 - d_1)}{r^2}$$

where

$H_S$ = horizontal strain at the bottom of the asphaltic layer,
$h$ = thickness of asphalt concrete layer (mm),
$d_0$ = surface deflection under center of load (mm),
$d_1$ = surface deflection at edge of plate (mm), and
$r$ = radius of loaded plate (mm).

Jung found that the horizontal strains obtained from this equation compared well with those calculated using linear elasticity. The horizontal strains with respect to thaw depth for both freeze-thaw cycles are shown in Figure 11. Also shown in this figure are the horizontal strains calculated from Jung's equation. The horizontal strains calculated from Jung's method were higher than those from NELAPAV. Similar results were reported by Jung (*15*) for non-frost conditions. However, this equation can be used to estimate reasonably well the horizontal strains. Because it is larger than those

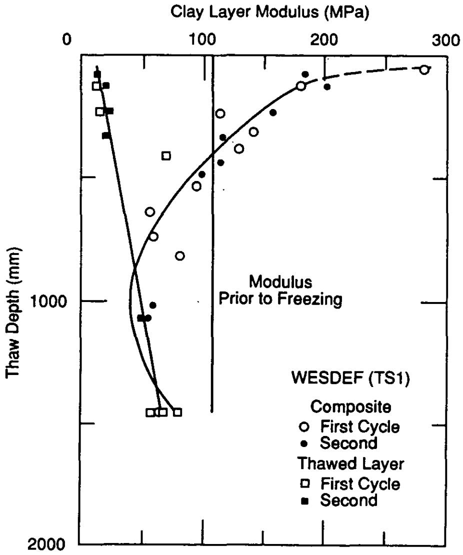


**FIGURE 10 Change in clay layer modulus with thaw depth for both cycles.**

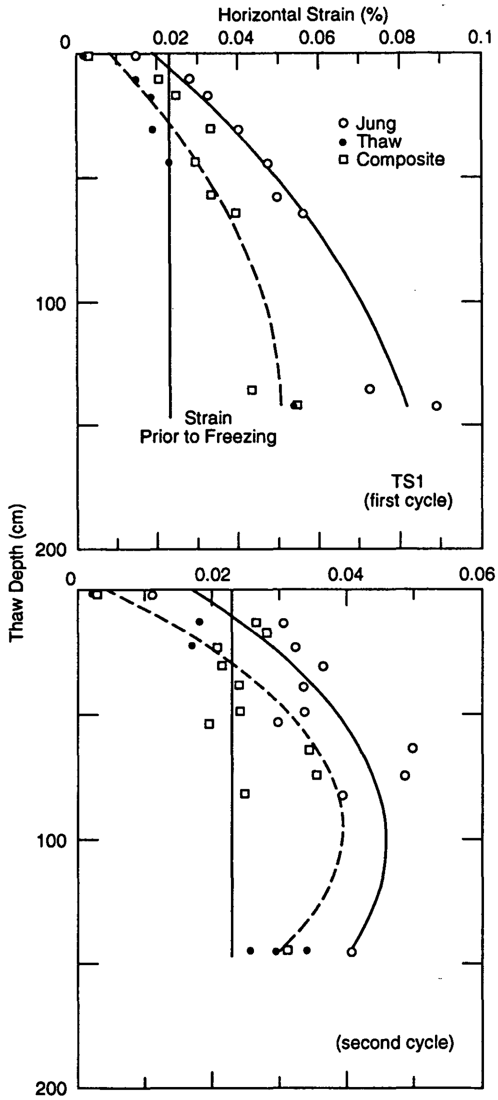


**FIGURE 11 Change in horizontal strain with thaw depth for both cycles.**

calculated from layer elastic theory, the damage calculated from these strains will be larger and therefore conservative. The calculated strains were as high as 1.5 times their prefrozen values during thaw. Another interesting observation in the horizontal strains in Figure 11 is the negligible difference between the two cases. This suggests that the condition of the subgrade has only a small effect on the horizontal strain at the bottom of the AC layer, 0.00022 and −0.00067 for Cases 1 and 2.

The calculated vertical strains with thaw depth for Case 1 ($\varepsilon_{vc}$) and Case 2 ($\varepsilon_{vt}$) for the two cycles are shown in Figure 12. At the beginning of thaw, there was a dramatic increase in ($\varepsilon_{vt}$). It was found to be about four times larger than $\varepsilon_{vc}$. With respect to its prefrozen value, $\varepsilon_{vt}$ was approximately 3.5 times larger at the beginning of the thaw period. With time, as thaw progressed downward, $\varepsilon_{vc}$ increased rapidly, whereas after the initial rapid increase, $\varepsilon_{vt}$ started to recover. This was substantiated later during trafficking of the test sections, when the change in rut depth with traffic was large soon after the beginning of loading. At a depth of about 1 m, the strains $\varepsilon_{vc}$ and $\varepsilon_{vt}$ become the same.

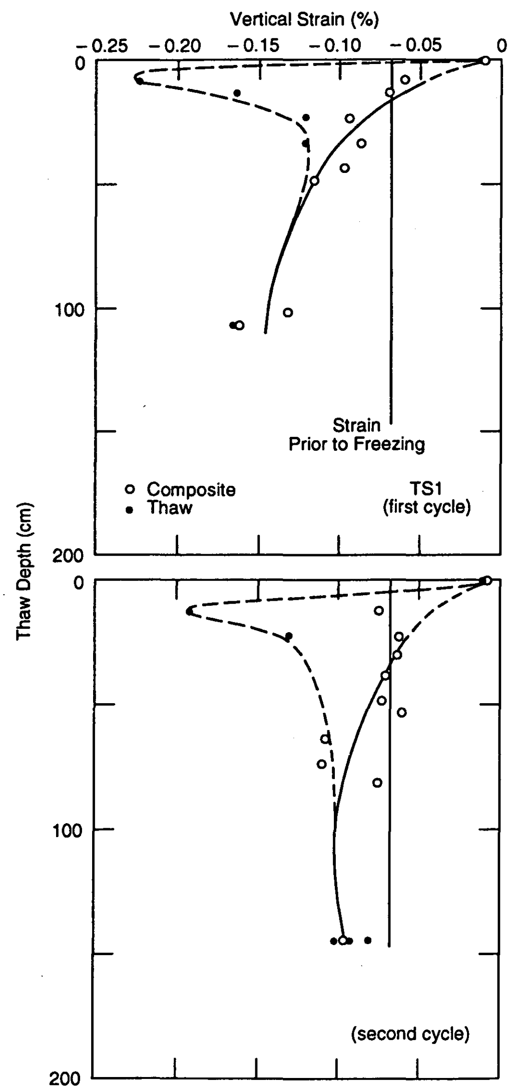


**FIGURE 12 Variation of the vertical strain with thaw depth for both cycles.**

## CONCLUSIONS

From the results of this study, the following conclusions can be drawn regarding the effect of the frozen and thawed layers when backcalculating pavement layer moduli from FWD data:

1. The study showed that the thicknesses of the frozen and thawed layers are critical in backcalculating layer moduli and damage to pavement structures.
2. Larger errors are introduced between measured and theoretical deflection basins when the frozen and thawed layers are considered as a single composite layer. The errors can be attributed to the frozen and thawed layers being lumped together as one layer. These errors were reduced when the thawed and frozen layers were considered as separate layers. However, there were times, even when the deflections were within a specified tolerance, that the backcalculated moduli were unreasonably low or high. At other times, the backcalculated moduli of the thawed and frozen layers were inverse to what was expected. It was also found that it is possible to reduce the AA error by 50 percent and not change the horizontal or vertical strains significantly.
3. The backcalculated asphalt concrete modulus was lower than that predicted by the Asphalt Institute empirical equation. A regression equation was developed to help in selecting seed moduli in seasonal frost areas. It was also found that the asphalt modulus was independent of the modeled support.
4. The horizontal strains at the bottom of the asphalt layer were not greatly affected by ignoring the thawed layer. The horizontal strains as calculated by the Jung method using FWD deflections directly showed a trend similar to that calculated from layer elasticity during thaw periods. The strains from the Jung method were found to be slightly high but will produce conservative results.
5. The damage to pavements with respect to vertical strains was grossly underestimated when the thawed and frozen layers were not considered separately. The difference in the calculated vertical strain could vary by a factor of 4.
6. Finally, the backcalculated moduli for the two cases are the product of the mathematical linear elastic model used and may not truly represent the actual field conditions. Partial verification has been done, but additional research is needed to verify the reductions in the moduli and strains seen in this study during thaw periods in the field.

## REFERENCES

1. F. J. Van Cauwelaert, D. R. Alexander, T. D. White, and W. R. Barker. Multilayer Elastic Program for Backcalculating Layer Moduli in Pavement Evaluation. In *Nondestructive Testing of Pavements and Backcalculation of Moduli* (A. J. Bush III and G. Y. Baladi, eds.) ASTM STP 1026. ASTM, pp. 171–188, 1989.
2. V. C. Janoo and R. L. Berg. *Predicting the Behavior of Asphalt Concrete Pavements in Seasonal Frost Areas Using Nondestructive Techniques*. Report DOT/FAA/RD-90/33. U.S. Department of Transportation, 1990.
3. V. C. Janoo and R. L. Berg. Thaw Weakening of Pavement Structures in Seasonal Frost Areas. In *Transportation Research*

*Record 1286*, TRB, National Research Council, Washington, D.C. 1990, pp. 217–233.
4. V. C. Janoo and R. L. Berg. *Performance of Asphalt Concrete Airport Pavements During Thaw Weakening Periods, A Field Study*. Report DOT/FAA RD-91/16. FAA, U.S. Department of Transportation, 1991.
5. R. L. Berg, S. Bigl, J. Stark, and G. Durell. *Resilient Modulus Testing of Minnesota Materials*. Report to Minnesota Department of Transportation, 1992.
6. R. A. Eaton. A Unique New Cold Weather Testing Facility. *Proc., Test Technology Symposium*, Jan. 1988.
7. L. H. Irwin and D. Speck. *NELAPAV User's Guide*. Report 86-1. Cornell Local Roads Program, Jan. 1986.
8. D. Cole, D. Bentley, G. Durell, and T. Johnson. *Resilient Modulus of Freeze-Thaw Affected Granular Soils for Pavement Design and Evaluation. Part 1. Laboratory Tests on Soils from Winchendon, Massachusetts, Test Sections*. CRREL Report 86-4, 1986.
9. D. Cole, D. Bentley, G. Durell, and T. Johnson. *Resilient Modulus of Freeze-Thaw Affected Granular Soils for Pavement Design and Evaluation. Part 3. Laboratory Tests on Soils from Albany County Airport*. CRREL Report 87-2, 1987.
10. T. C. Johnson, D. Bentley, and D. M. Cole. *Resilient Modulus of Freeze-Thaw Affected Granular Soils for Pavement Design and Evaluation. Part 2. Field Validation Tests at Winchendon, Massachusetts, Test Sections*. CRREL Report 86-12, 1986a.
11. T. C. Johnson, D. Bentley, and D. M. Cole. *Resilient Modulus of Freeze-Thaw Affected Granular Soils for Pavement Design and Evaluation. Part 4. Field Validation Tests at Albany County Airport*. CRREL Report 86-13, 1986b.
12. R. N. Stubstad and W. Connors. Prediction of Damage Potential on Alaskan Highways During Spring Thaw Using the Falling Weight Deflectometer. Report AK-RD-83-11. State of Alaska, DOT&PF, 1983.
13. C. R. Marek and B. J. Dempsey. A Model Utilizing Climatic Factors For Determining Stresses and Deflections in Flexible Pavement Systems. *Proc., 3rd International Conference on the Structural Design of Asphalt Pavements*, Vol. 1, 1972, pp. 101–114.
14. *Research and Development of The Asphalt Institute's Thickness Design Manual (MS-1)*, 9th ed. Research Report 82-2. Asphalt Institute, 1982.
15. W. F. Jung. Direct Calculation of Maximum Curvature and Strain in Asphalt Concrete Layers of Pavements from Load Deflection Basin Measurements. In *Transportation Research Record 1196*, TRB, National Research Council, Washington, D.C., 1988, pp. 125–132.

# Strategic Highway Research Program Falling Weight Deflectometer Quality Assurance Software

G. R. RADA, S. D. RABINOW, M. W. WITCZAK, AND C. A. RICHTER

Nondestructive deflection testing using falling weight deflectometers (FWDs) is one element of the monitoring effort currently under way by the Strategic Highway Research Program (SHRP) for the Long-Term Pavement Performance (LTPP) study. Because accurate data are key to the success of the LTPP study, SHRP has implemented a number of measures to ensure the quality of deflection data. They include equipment comparison and calibration, standardized field testing procedures and field data checks, and quality assurance software. SHRP FWD quality assurance software is the focus—specifically the FWDSCAN and FWDCHECK computer programs. Program FWDSCAN has been developed to verify the integrity and completeness of the FWD deflection data after they have been delivered to the SHRP regional offices. Program FWDCHECK has been developed to analyze deflection data for test section homogeneity, the degree to which test pit data are representative of the section, the presence of data outliers within the section, and overall reasonableness from a structural capacity viewpoint.

The Long-Term Pavement Performance (LTPP) study of the Strategic Highway Research Program (SHRP) involves intensive monitoring of numerous pavement sections located throughout North America. One aspect of the LTPP data collection is deflection testing, which provides information on structural capacity and material properties. Four falling weight deflectometers (FWDs) manufactured by Dynatest are used in the SHRP deflection testing.

Because accurate data are the key to the success of the LTPP study, SHRP has implemented a number of measures to ensure the quality of deflection data. They include equipment comparison and calibration, standardized field testing procedures and field data checks, and quality assurance software. This paper focuses on the quality assurance software.

Equipment calibration and field data checks built into the FWD data acquisition software are the first line of defense against invalid deflection data. The second line of defense is a computer program, called FWDSCAN, which verifies the integrity, completeness, and compliance with the established test pattern of the field data after they are delivered to the SHRP regional office (*1*). For the final stage in the quality assurance process, a computer program called FWDCHECK has been developed to analyze deflection data for test section homogeneity, the degree to which test pit data are representative of the section, the presence of data outliers within the section, and overall reasonableness from a structural capacity viewpoint (*2*). As a rule, the checks embodied in FWDCHECK will not eliminate data, but instead will flag potential problems.

The remainder of this paper provides a brief overview of SHRP's deflection testing program (to facilitate the understanding of the software), followed by detailed descriptions of the FWDSCAN and FWDCHECK computer programs. Typical analysis results are also presented and discussed.

## SHRP DEFLECTION TESTING PROGRAM

SHRP is conducting two basic types of deflection tests: basin tests, which are conducted on all pavement types, and load transfer tests, which are conducted only on portland cement concrete (PCC) pavements. Pertinent details of the testing program are as follows. The full testing program is described in the SHRP field manual for FWD testing (*3*).

A single sensor configuration is used for all deflection basin tests, regardless of pavement type, to minimize the probability of sensor location errors. The sensors are located at radii of $r$ = 0, 8, 12, 18, 24, 36, and 60 in. from the loading plate center. A similar sensor configuration is used for all load transfer tests, except that the sensor at $r$ = 8 in. is moved to the rear of the loading plate 12 in. from the center of the loading plate.

A uniform drop sequence is used at all test points within a test section. This drop sequence begins with a series of three drops at a load of 12,000 to 14,000 lbf for seating purposes, followed by four repeat drops at each drop height (load level) used. For flexible [i.e., asphalt concrete (AC)] pavements, four drop heights are used, producing nominal loads of 6,000, 9,000, 12,000, and 16,000 lb. On rigid (jointed and continuously reinforced concrete) pavements, only three drop heights are employed, producing nominal loads of 9,000, 12,000, and 16,000 lb.

Testing within the section is completed in two or three passes at various lateral (transverse) locations in the lane: midlane, defined as 6.0 ± 0.05 ft from the pavement edge; outer wheel path, defined as 2.5 ± 0.25 ft from the pavement edge; and pavement edge, where the load plate is located within 3 in. of the pavement edge. All testing in a given lateral

G. R. Rada and S. D. Rabinow, PCS/Law Engineering, 12240 Indian Creek Court, Suite 120, Beltsville, Md. 20705-1242. M. W. Witczak, Department of Civil Engineering, University of Maryland, College Park, Md. C. A. Richter, Strategic Highway Research Program, 818 Connecticut Ave., N.W., Suite 400, Washington, D.C. 20006.

location is completed in a single pass over the section for reasons of ease, efficiency, and error reduction. The midlane locations are tested first, followed by the edge locations where applicable, and the outer wheel path locations.

Deflection basin tests at two test pit locations, approximately 50 ft outside the section boundaries, are also conducted for all pavement types. The function of these tests is to provide a basis for "linking" test pit information (i.e., laboratory characterization) with the overall section response. Test pit locations are tested first (i.e., before the within-section testing) so that drilling operations can commence.

All testing uses station 0+00 of the test section as the reference point for the FWD distance measuring instrument to ensure that test locations can be accurately located in the future. The specific test pattern used on the test sections varies with pavement type and is summarized in Table 1. The approximate longitudinal test point spacing for all pavement types is 25 ft, resulting in a minimum of 20 test points per pass per section.

Air and pavement surface temperatures are also monitored by sensors mounted on the FWD trailer; these data are recorded with the deflection data for each test point. Additional temperature data are obtained by manual monitoring of temperatures at three depths (bottom, middle, and surface) in the pavement surface layer at two locations, one at each end of the test section, just beyond the section boundaries. These manual measurements are obtained at the start of testing, at the end of testing, and at hourly intervals during testing.

Because of large file size and the need for back-up copies, data are backed up in the field using commercial back-up software, then restored to the original form on arrival at the SHRP regional office.

## PROGRAM FWDSCAN

All deflection data collected in the field and received by SHRP are checked to ensure that they have been restored to their original form, that all data are present, complete and in a readable form, and that they comply with the established test pattern. This is accomplished by means of the FWDSCAN program.

Each FWD data file can be thought of as being composed of two primary parts. The first part consists of 36 lines of header information. The second part of the data file, known as the data block, consists of the loads, deflections, temperatures, and stations collected during a given pass.

Verifying the contents of the header information consists of two distinct parts. The first part involves the comparison of the data items in the file to either lists of possible values or specified values—for example, that the load plate radius is the correct value. The second part of the verification procedure consists of checking that the remaining items contain reasonable values for what they represent—for example, that calibration factors are between 0.98 and 1.02 for all deflectors.

The data block of the FWD data file consists of a repeating series of lines defining the testing at each station. For each station, the following data should be present: a line containing station identification, lane specification, and other information that occurs once at each station; 12 or 16 lines (depending on the pavement type) of load and deflection data; operator comments (optional); and 151 or 301 line blocks containing load and deflection time history data for a single drop height at this station, repeated up to three or four times at each station, depending on the pavement type being tested.

Accordingly, verification of the data block contents consists of scanning each line of the remainder of the FWD data file to ensure its readability and completeness. In addition, to ensure the reasonableness of the data, the verification procedure also entails a comparison of the data with valid data ranges; that is, lane specification codes must be from the list specified in the SHRP FWD manual, deflection values must range from 0.1 to 80.0 mils, loads must range from 500 to 32,000 lbf, and air and surface temperatures must range from 0°F to 160°F.

**TABLE 1 FWD Test Plan Summary**

| Pavement Type | Transverse Location (Pass) | Longitudinal Location | Interval | Test Type | Number of Points |
|---|---|---|---|---|---|
| Flexible | Mid-Lane<br>Wheel Path** | -<br>- | 25 feet<br>25 feet | Basin<br>Basin | 23*<br>21 |
| Rigid -Jointed Plain or Reinforced Concrete | Mid-Lane<br>Edge<br>Edge<br>Wheel Path** | Mid-Panel<br>Corner<br>Mid-Panel<br>Joint | Each Panel<br>Each Panel<br>Each Panel<br>Each Panel | Basin<br>Basin<br>Basin<br>Load Transfer | 22*<br>20<br>20<br>40 |
| Rigid - Continuously Reinforced Concrete | Mid-Lane<br>Edge<br>Edge<br>Wheel Path** | Mid-Panel<br>Center/Crack<br>Mid-Panel<br>Crack | ± 25 feet<br>± 25 feet<br>± 25 feet<br>± 25 feet | Basin<br>Basin<br>Basin<br>Load Transfer | 22*<br>20<br>20<br>40 |

* Includes 2 test pit locations ± 50 feet from section limits.
** Wheel path testing is in the outer (rightmost) wheel path.

A list of the specific data items that are checked during the scanning process follows:

1. Miscellaneous checks: report scan start time and date, verify line length for each line, report number of skipped records, report total number of records processed, and report scan end time and date.
2. Checks of header information: determine units for data collection, report total expected number of records, determine data collection date, verify use of edition 10 of Dynatest software, determine number of active deflectors, determine deflector range, determine FWD serial number, determine deflection filtering mode, determine load cell gain, determine deflector gains, and determine operator's name.
3. Checks at each station: determine peak data block, verify use of a valid lane, determine specification, verify that stations are increasing, verify that stations are within the 500-ft limits of the test section, determine number of peak records recorded, verify that temperatures are within acceptable range, verify that deflections are within deflector limits, verify that deflections decrease at increasing distance from the load plate, verify that load is within the acceptable range, check for comments, check for unidentifiable data, check for new subsection identification, check for an unexpected end to the file.
4. History data block: determine number of history records recorded, verify that deflections are within deflector limits, verify that load is within acceptable range, check for comments, check for unidentifiable data, check for new subsection identification, check for an unexpected end to the file.

Some checks are for the presence of specific data items, other checks are for data within an acceptable range of numbers, and other checks simply report what was present in the data file.

The results of these scanning procedures are written to an output file as a permanent record of this process having been performed. Erroneous or inconsistent data items are noted by lines beginning with an asterisk or exclamation mark. These lines fully describe which data element is incorrect or inconsistent. Some errors in the data file generate more than one warning message, and sometimes they affect whether subsequent data are interpreted correctly. Table 2, an excerpt from one of these files, contains two warnings, only the first of which is truly an error. In this case, the unrecognized lane specification at station 219 causes the lane specification at station 231 to appear to be out of the normal sequence of testing.

Depending on the results of the verification procedure, a number of scenarios are possible. For all scenarios in which the file is corrupted, the first two remedial steps are the same. The first consists of redoing the restore procedure and repeating the verification, because the original data restoration may have been the cause of the data corruption, and repeating it may eliminate the problem. If this step fails to remedy the problem, the second step is to request that the FWD operator transmit another copy of the data to SHRP and repeat the verification process. If this step also fails, then additional steps are taken, depending on the exact nature of the problem with the data. When errors are not from corruption in the data file but are from erroneously recorded data, the FWD data file may be edited to correct these errors.

**TABLE 2 Excerpt of FWDSCAN Output File Containing Errors**

| |
|---|
| 150 history records successfully read in block 2 at station 207 |
| 150 history records successfully read in block 3 at station 207 |
| * Undefined lane specification (J3]) at station 219 |
| 12 peak records successfully read at station 219 |
| 150 history records successfully read in block 1 at station 219 |
| 150 history records successfully read in block 2 at station 219 |
| 150 history records successfully read in block 3 at station 219 |
| * Test sequence locations not in expected order at station 231 |
| Testing J2 (RIGID) at station 231 |
| 12 peak records successfully read at station 231 |
| 150 history records successfully read in block 1 at station 231 |
| 150 history records successfully read in block 2 at station 231 |
| 150 history records successfully read in block 3 at station 231 |
| Testing J3 (RIGID) at station 238 |
| 12 peak records successfully read at station 238 |
| 150 history records successfully read in block 1 at station 238 |

## PROGRAM FWDCHECK

Program FWDCHECK has been developed to analyze deflection data for test section homogeneity, the degree to which test pit data are representative of the section, the presence of data outliers with the section, and overall reasonableness from a structural capacity viewpoint. The objective of these checks is to flag potential problems and areas in which reality may deviate from assumptions. FWDCHECK is intended for the analysis of midslab deflection basin test data (not load transfer) for rigid pavements and outer-wheel path deflection data for flexible pavements.

For purposes of describing this program, this section has been subdivided into four subsections: preliminary data analysis, section homogeneity analysis, nonrepresentative data analysis, and structural capacity analysis. The order in which these subsections are presented corresponds with the FWDCHECK analysis sequence.

### Preliminary Data Analysis

Before any checks are performed, the deflection data in question is normalized to provide a uniform basis for comparison. Various normalized deflection statistics—mean, standard deviation, and coefficient of variation for each geophone number and drop height combination—are also calculated for the pavement section in question.

Uncorrected normalized deflections are calculated by means of the following relation:

$$\hat{\delta}_u = \frac{\sum_{i=1}^{n}\left(\frac{\delta_{mi}}{P_i}\right)}{n} \qquad (1)$$

where

$\hat{\delta}_u$ = uncorrected normalized mean deflection (mils/lb),
$i$ = repeat drop in question,

$n$ = number of repeat drops used,
$\delta_{mi}$ = measured deflection for $i$th repeat drop, and
$P_i$ = applied load (lb).

For flexible pavements, temperature-corrected normalized deflections are also computed in the manner described above, except that the measured deflections are first corrected to a standard temperature of 68°F (*2*). These corrections are applicable only to the maximum deflections (i.e., under load center) and are made on the basis of temperature-depth data measured in the field.

### Section Homogeneity Analysis

Because pavements are inherently variable, the nondestructive evaluation of any pavement test section will yield variable deflection data. The first data check in the FWDCHECK program is aimed at evaluating the homogeneity of the test section (i.e., determine whether one or more pavement subsections are present based on a comparison of means and standard deviations).

This particular data check is subjective because, on the basis of a visual assessment of the deflection profile, the user selects the boundaries, if any, delimiting pavement subsections. To aid the user in the definition of these boundaries, tabular summaries of the uncorrected and temperature-corrected normalized deflection statistics and deflection plots versus station are generated by the program. Figure 1 is an example of a deflection versus station plot.

If two or more subsections are identified, the program computes the mean normalized deflection (temperature corrected for AC pavements) and standard deviation of Geophone 1 for each subsection. The section uniformity analysis is based only on the analysis of the (nominal) 9,000-lb load data, which closely simulate the "standard" 18-kip single axle load often used in pavement analyses. FWDCHECK then performs a statistical comparison of the means and variances for each pair of adjacent subsections to determine whether they are statistically different. The statistical test of the means assumes that the normalized deflections for each subsection follow a Student's $t$ distribution and that the true standard deviations are unknown and unequal. Furthermore, the test for equal means uses a 95 percent level of probability (two-tailed). An $F$-test is used for the comparison of the variances for each pair of adjacent subsections. The subsections are considered different if either (or both) the means or the variances are statistically different.

Figure 2 is an example of an SHRP section where subsections may exist. As shown, this section can be divided into three subsections at Stations 130 and 290. Subsection 1 (Stations 0 to 130) has a relatively low maximum deflection. Subsection 2 (Stations 130 to 290) has much higher deflections than Subsection 1, with its overall average about 50 percent higher than that for Subsection 1. Subsection 3 (Station 290 to 500) has a more uniform maximum deflection than Subsection 2, with its overall average similar to that of Subsection 1. Although not shown, the hypothesis tests for these subsections indicated that the means are statistically different, but that the variances are not. Thus, subsections are indeed present within the overall section according to the established criteria.

Depending on the outcome of the analysis, one or more messages are sent to the screen and to the program output file; for example, a message indicating that a pair of adjacent subsections have equal means but unequal variances. If two or more subsections are found to be equal by both means and variances, the subsection boundaries are redefined before proceeding with the program.

### Nonrepresentative Data Analysis

The LTPP testing program relies on the assumption that materials from the area adjacent to the monitored section are representative of those within a test section. Deflection data obtained at the time of materials sampling provides an opportunity to evaluate this assumption.

This evaluation, and a check for "outliers" within the section, are accomplished through comparison of normalized de-

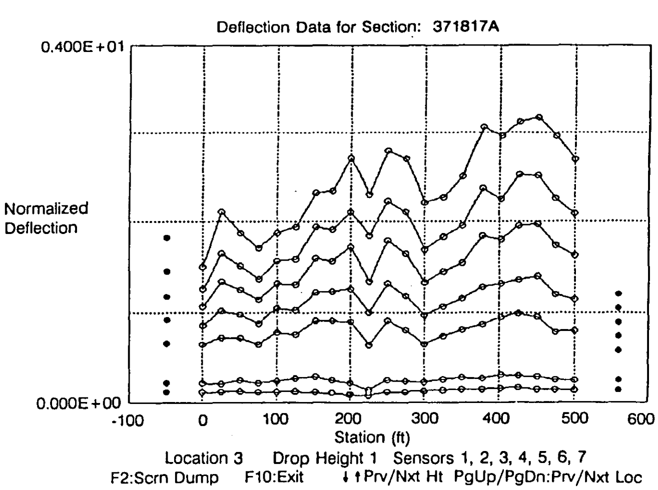


**FIGURE 1 Uncorrected normalized deflection versus station plot.**

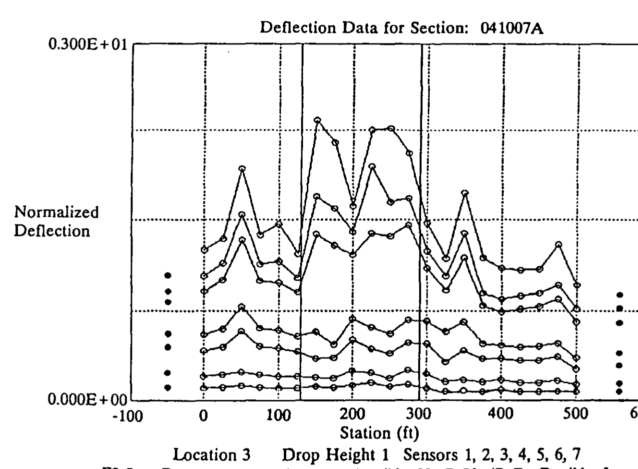


**FIGURE 2 Sample subsection delineation: Section 041007A.**

flection statistics for all geophone and drop height combinations. For the test pit location, normalized deflection data are first compared with the corresponding section means. In those cases in which two or more subsections have been identified, the test pit data are compared with the means for the adjacent subsection. In either case, warnings are automatically generated by the program when the test pit data differ from the section or subsection means by more than two standard deviations.

As in the test pit analysis, the check for data outliers within a section entails the comparison of the normalized deflections for each geophone and drop height combination at each station to the section or corresponding subsection mean. Warning messages are generated by the program when the difference from the section or subsection mean is more than two standard deviations; a tabular summary of the nonrepresentative data found within a section is sent to the output file that includes, for each data point, the station, drop height, geophone number, and number of standard deviations away from the section or subsection mean.

The program also generates normalized deflection-versus-station plots for each combination of geophone and drop height. An example of these plots is given in Figure 3. As shown, a series of lines indicating the mean, mean ± 1 standard deviation, mean ± 2 standard deviations, and so on are superimposed on these plots. Based on these plots, the user can, if desired, include additional messages in the output file in the form of running comments.

### Structural Capacity Analysis

The last set of FWDCHECK data checks deals with the overall reasonableness of the deflection data from a structural capacity viewpoint. It involves the computation of pavement structural capacity and the comparison of the results to what one might expect on the basis of layer thicknesses and material properties.

Because the main objective of this last set of data checks is to verify the general reasonableness of the data, a direct

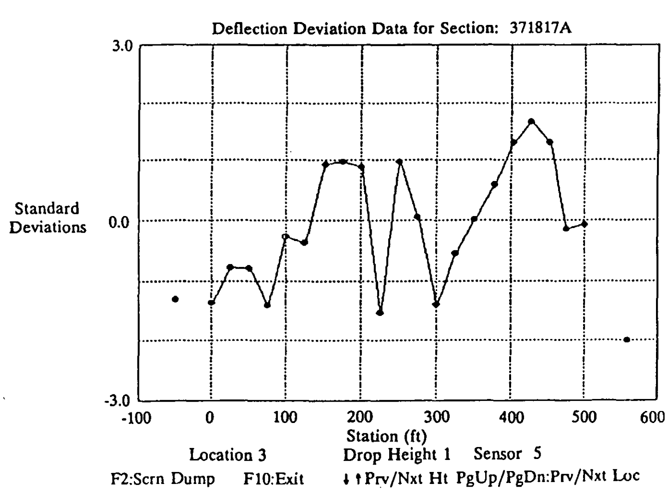


**FIGURE 3 Sample deflection deviation versus station plot for nonrepresentative data analysis.**

structural capacity approach was selected for implementation in the program. The particular analysis procedure used is dependent on the pavement type, as described next.

#### *Rigid Pavement Analysis*

Structural capacity estimates for rigid pavements are derived on the basis of a modified Westergaard solution for interior deflections. The analysis is predicated on the assumption that the slab is "relaxed" (i.e., no curling). The specific model used in this analysis is given by Ioannides et al. (*4*):

$$\delta = \frac{P}{8K\ell^2}\left[1 + \left(\frac{1}{2\pi}\right)\left(\log_e\left(\frac{a}{2\ell}\right) + \gamma - 1.25\right)\left(\frac{a}{\ell}\right)^2\right] \qquad (2)$$

with

$$\ell = \sqrt[4]{\frac{Eh^3}{12(1 - \mu^2)K}}$$

where

$\delta$ = maximum deflection (i.e., under load center);
$a$ = radius of loaded area;
$P$ = total applied load;
$K$ = composite modulus of subgrade reaction;
$\gamma$ = 0.57721566490, Euler's constant;
$\ell$ = radius of relative stiffness;
$E$ = elastic modulus of portland cement concrete;
$h$ = slab thickness; and
$\mu$ = Poisson's ratio of portland cement concrete.

Assuming an elastic modulus of $E$ = 5,000,000 lb/in.$^2$ and a Poisson's ratio of $\mu$ = 0.15 for portland cement concrete, Westergaard's solution is used in an iterative mode to calculate the effective thickness ($h$) of the slab at the time of testing. Because the maximum deflection, applied load, and radius of loaded area are all known, the only unknown parameter is the composite modulus of subgrade reaction or $K$.

The $K$ value is determined from the applied load and the volume of the deflection basin. This approach assumes that the slab is incompressible and, as a consequence, the volume of soil or other materials, or both, displaced by the load is equal to the volume of the deflection basin. Accordingly, the $K$ value is calculated as follows:

$$K = \frac{P}{V} \qquad (3)$$

where $P$ is the applied load and $V$ is the effective volume of deflection basin. The effective volume of the deflection basin is limited to approximately the dimension of half of the lane width (72 in.) and is determined by rotating the deflection basin area through 360 degrees.

Composite modulus of subgrade reaction and effective slab thickness values are determined for all possible location, station, and drop height combinations. The resulting thickness data are then compared with the expected range of thickness to assess the reasonableness of the deflection data. The expected range is defined as 0.65 (to allow for deterioration of

the slab) to 1.15 (to allow for hardening of the concrete) times the actual slab thickness. Warnings are generated by the program and sent to the output file when the estimated effective thickness falls outside the expected range.

The program also generates the following information: (a) plot of equivalent thickness versus station (with the expected thickness range superimposed) for each drop height; (b) plot of composite modulus of subgrade reaction versus station for each drop height; (c) plots of composite modulus (i.e., single value representation of the overall pavement stiffness) versus radial distance for all drop heights at any given station; and (d) tabular summaries of $K$ and thickness values as well as corresponding statistics at each drop height for the pavement section or subsections. An example of the thickness-versus-station plot is given in Figure 4. On the basis of this and other information, the user can, if desired, include additional warning messages in the output file in the form of running comments.

### Flexible Pavement Analysis

The structural capacity analysis of flexible pavements follows the AASHTO direct structural number procedure, which is based on the premise that the overall pavement structural capacity is the result of the combined stiffness influence of each layer (*5*). Accordingly, the maximum deflection may be viewed as being composed of two separate components: (a) pavement structural capacity and (b) subgrade support.

The procedure implemented in FWDCHECK uses outer deflection basin data to estimate the subgrade modulus and then uses this parameter, along with the maximum deflection, to directly estimate the effective structural number (*SN*) of the pavement system. The specific evaluation technique used involves the following major steps.

1. An estimate of the radius of influence ($a_{3e}$) at the pavement-subgrade interface is made on the basis of composite modulus at each geophone location; deflections obtained beyond this value are assumed to be caused by subgrade deformations only. Composite moduli are calculated in the program as follows:

$$E_c = \frac{2 * (1 - \mu_{sg}^2) * p_c * a_c}{\delta} \qquad \text{if } r \leq 0.25a_c \tag{4a}$$

or

$$E_c = \frac{(1 - \mu_{sg}^2) * p_c * a_c^2}{\delta * r} * C \qquad \text{if } r > 0.25a_c \tag{4b}$$

where

$E_c$ = composite modulus,
$r$ = radial distance,
$p_c$ = contact pressure applied by NDT device,
$a_c$ = radius of contact of NDT device,
$\mu_{sg}$ = Poisson's ratio of the subgrade,
$\delta$ = measured deflection at given radial distance, and
$C$ = the lower of $1.1*\log(r/a_c) + 1.15$ and $0.5*\mu_{sg} + 0.875$.

2. If a stiff layer is present beneath the pavement structure, it will have a major influence on the measured deflections and hence structural capacity analysis. To overcome this, a number of assumptions are first made: (a) the deflections measured at distances beyond the radius of influence ($a_{3e}$) are solely a function of the subgrade and stiff layers; (b) the stiff layer has an elastic modulus of $E$ = 1,000,000 lb/in.$^2$ and a Poisson's ratio of $\mu$ = 0.35; and (c) a typical layer modulus and Poisson's ratio is assigned to each layer in the pavement structure (exclusive of subgrade) on the basis of material type, as shown in Table 3.

The assumed layer moduli and Poisson's ratios, along with the known layer thicknesses and depth to stiff layer, are then input into CHEVRON *N*-layer code (*6*) to predict surface deflections at all geophone locations beyond the radius of influence, for subgrade modulus values of 5,000, 15,000 and 30,000 lb/in.$^2$. In turn, these results are used to develop log-log regression equations of surface deflection versus subgrade modulus for each geophone location beyond $a_{3e}$. Finally, the surface deflection versus subgrade modulus correlations are used to determine the subgrade modulus that yields a surface deflection equal to that measured in the field for each geophone location beyond $a_{3e}$. Although only an estimate, the resulting values represent the subgrade moduli at each geophone location, independent of the stiff layer.

3. If the subgrade soil is perfectly elastic, the subgrade moduli derived from the stiff layer analysis for distances beyond the radius of influence will be the same. If nonlinear, however, there will be some degree of stress softening; that is, as the stresses increase, the subgrade modulus decreases. Because the structural analysis is based on the AASHTO structural number as calculated from the maximum measured deflection and the subgrade modulus, it is critical that the best possible estimate of the subgrade modulus underneath the load center be made.

Accordingly, the layer modulus and Poisson's ratio assumed for each layer in the pavement structure, along with the known layer thicknesses and subgrade moduli predicted from the stiff layer analysis, are first input into the CHEVRON *N*-layer code to predict deviator stresses at the pavement-subgrade

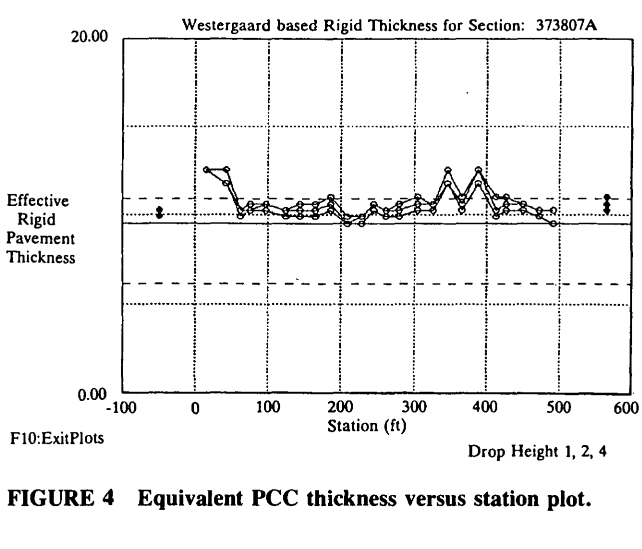


**FIGURE 4 Equivalent PCC thickness versus station plot.**

**TABLE 3 Typical Modulus, Poisson's Ratio, and Layer Coefficient Values Used in FWDCHECK**

| Material Type | Elastic Modulus (ksi) | Poisson's Ratio | Layer Coefficient | |
|---|---|---|---|---|
| | | | Minimum | Maximum |
| Uncrushed Gravel | 20.0 | 0.40 | 0.07 | 0.17 |
| Crushed Stone | 45.0 | 0.40 | 0.11 | 0.21 |
| Crushed Gravel | 30.0 | 0.40 | 0.09 | 0.18 |
| Crushed Slag | 50.0 | 0.40 | 0.12 | 0.22 |
| Sand | 10.0 | 0.40 | 0.05 | 0.15 |
| Fine Soil-Agg. Mixture | 15.0 | 0.40 | 0.06 | 0.16 |
| Coarse Soil-Agg. Mixture | 20.0 | 0.40 | 0.07 | 0.17 |
| Sand Asphalt | 200.0 | 0.40 | 0.10 | 0.30 |
| Asphalt Treated Mixture | 300.0 | 0.35 | 0.15 | 0.35 |
| Cement Aggregate Mixture | 750.0 | 0.30 | 0.25 | 0.45 |
| Econocrete | 1,500.0 | 0.25 | 0.40 | 0.60 |
| Cement Treated Soil | 100.0 | 0.35 | 0.10 | 0.25 |
| Lean Concrete | 1,500.0 | 0.25 | 0.40 | 0.60 |
| Sand-Shell Mixture | 75.0 | 0.40 | 0.15 | 0.25 |
| Limerock, Caliche | 200.0 | 0.35 | 0.15 | 0.30 |
| Lime Treated Soil | 75.0 | 0.35 | 0.10 | 0.25 |
| Soil Cement | 200.0 | 0.35 | 0.15 | 0.30 |
| Pozzolanic-Agg. Mixture | 500.0 | 0.35 | 0.20 | 0.40 |
| Cracked & Seated PCC | 1,000.0 | 0.25 | 0.35 | 0.45 |
| Asphaltic Concrete | 450.0 | 0.35 | 0.35 | 0.45 |
| Portland Cement Concrete | 5,000.0 | 0.15 | 0.60 | 0.80 |

interface at all geophone locations beyond $a_{3e}$ and directly under the load center. The deviator stresses predicted for distances beyond $a_{3e}$ and the subgrade moduli computed in the stiff layer analysis are then used to develop a log-log regression equation of subgrade modulus versus deviator stress. Finally, the predicted deviator stress at a radial distance of zero is input into the subgrade modulus-deviator stress correlation to determine the subgrade modulus directly under the load center.

4. Once the subgrade modulus under the load center has been established, the effective structural number of the pavement is determined through an iterative process. Assuming that the pavement structure can be represented by a one-layer system resting on the subgrade and that crushed stone ($a_s$ = 0.14, $E_s$ = 30,000 lb/in.$^2$, and $\mu_s$ = 0.35) is the standard material, the equivalent modulus of the one-layer system (for a given $SN$ value) and hence the theoretical maximum deflection can be derived using Equations 5 through 9 (5):

$$E_e = \left(\frac{SN}{0.0043h_T}\right)^3 (1 - \mu_e^2) \tag{5}$$

where

$E_e$ = elasticity modulus of equivalent one-layer system,
$SN$ = pavement structural number,
$\mu_e$ = Poisson's ratio of equivalent one-layer system, and
$h_T$ = total pavement thickness;

$$\delta_0 = \frac{2p_c a_c(1 - \mu_{sg}^2)}{E_{sg}} \tag{6}$$

where $\delta_0$ is the maximum measured deflection and $E_{sg}$ is the elastic modulus of subgrade;

$$F_w = \frac{E_{sg}(1 - \mu_e^2)}{E_e(1 - \mu_{sg}^2)} + F_b\left[1 - \left(\frac{E_{sg}}{E_e}\right)\right] \tag{7}$$

where $F_w$ is Burmeister's two-layer deflection factor;

$$F_b = \left[\sqrt{\left(1 + \frac{h_e^2}{a_c}\right)} - \frac{h_e}{a_c}\right] \times \left[1 + \frac{\frac{h_e}{a_c}}{2(1 - \mu_{sg})\sqrt{\left(1 + \frac{h_e^2}{a_c}\right)}}\right] \tag{8}$$

where $F_b$ is Boussinesq's one-layer deflection factor; and

$$h_e = 0.9h_T \sqrt[3]{\frac{E_e(1 - \mu_{sg}^2)}{E_{sg}(1 - \mu_e^2)}} \tag{9}$$

where $h_e$ is transformed thickness of pavement in terms of the subgrade modulus.

Therefore, by iterating on the *SN* value, the structural number that results in a predicted deflection equal to the measured value adjusted to a standard temperature of 68°F is determined. The resulting *SN* data are then compared with those in the expected range to assess the reasonableness of the deflection data. The expected range is defined for each pavement section on the basis of the combination of material types and layer thicknesses as follows:

$$SN = \sum_{i=1}^{n} (a_i * h_i) \tag{10}$$

where

$n$ = number of layers in the pavement (exclusive of subgrade);
$i$ = pavement layer in question;
$a_i$ = structural layer coefficient of the $i$th layer; and
$h_i$ = thickness of the $i$th layer.

Minimum and maximum material layer coefficients used to generate the expected *SN* range are summarized in Table 2.

As with the rigid pavement structural analysis, warnings are generated by the program and sent to the output file when the predicted structural number falls outside the expected range. The program also generates the following information: (a) plot of structural number versus station (with the expected *SN* range superimposed) for each drop height; (b) plot of subgrade modulus (under the load plate) versus station for each drop height; (c) plots of composite modulus versus radial distance for all drop heights at any given station; and (d) tabular summaries of subgrade modulus and *SN* values as well as corresponding statistics at each drop height for the pavement section or subsections. An example of the structural number versus station plot is given in Figure 5. On the basis of this and other similar information, the user can, if desired, include additional warning messages in the output file in the form of running comments.

## FWDCHECK Messages

The FWDCHECK program provides both tabular and graphical data displays for the four major factors evaluated. Examples of these displays have been shown throughout the paper. In addition, the program generates an output file containing a detailed summary of the analysis results. Included at the end of this file are summary remarks that will be stored in the SHRP data base and that will be of significant benefit to users of the SHRP data base. These remarks will be provided automatically to those who request SHRP deflection data. Table 4 provides an example of the summary remarks generated by FWDCHECK for a rigid pavement section.

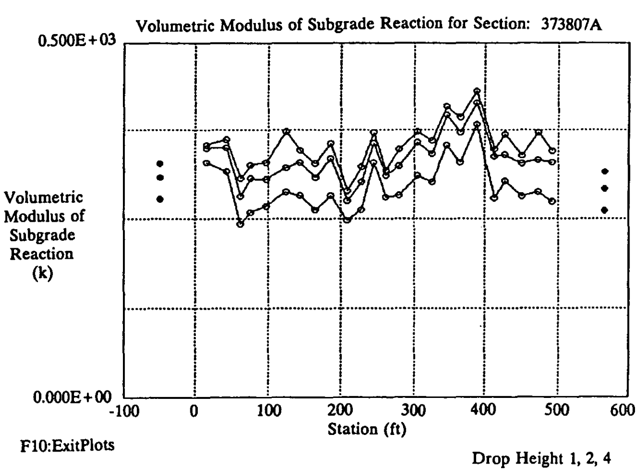


**FIGURE 5 Structural number versus station plot.**

**TABLE 4 Excerpt of FWDCHECK Output File—Summary Remarks**

<u>Section uniformity</u>:
Subsections were identified within the section.
Subsection 1 boundaries occur at 0 ft. and 320 ft.
Subsection 2 boundaries occur at 320 ft. and 410 ft.
Subsection 3 boundaries occur at 410 ft. and 500 ft.

<u>Comparing subsections</u>:
Subsections 1 and 2: UNEQUAL means and EQUAL variances.
Subsections 2 and 3: UNEQUAL means and EQUAL variances.

<u>Outliers - Test pits</u>: 21 combinations at each test pit.
All TP 1 data appears representative of section data.
6 height/sensor combinations at TP 2 DO NOT appear representative of section data.

<u>Outliers - Section data</u>: 546 total combinations within the section.
14 height/sensor/station combinations are data outliers in subsection 1.
There are NO data outliers within subsection 2.
There are NO data outliers within subsection 3.

<u>Structural capacity - Test pits</u>: 3 combinations at each test pit
All results for TP 1 are within the range of expected values.
1 height(s) for TP 2 are NOT within the range of expected values.

<u>Structural capacity - Section data</u>: 78 total combinations within the section.
17 height/station combinations are NOT within the range of expected values.

## SUMMARY AND CONCLUSIONS

SHRP has established standard nondestructive deflection test procedures for monitoring pavement structural properties and has invested significant effort to ensure the quality of the data obtained using these procedures. Measures implemented by SHRP to ensure the quality of the deflection data include equipment comparison and calibration, standard testing procedures and field data checks, and quality assurance software.

This paper focused on the SHRP FWD quality assurance software developed for use with the SHRP LTPP deflection data. The program FWDSCAN is used to verify the integrity, completeness, and compliance with the established test pattern of the field data after being delivered to the SHRP regional offices, whereas the FWDCHECK program performs more detailed analyses to check the deflection data for section homogeneity, nonrepresentative data (from either the destructive sampling area or within the section), and general reasonableness (or agreement with expectations) from a structural capacity point of view.

These programs, used in conjunction with solid equipment calibration and field data collection procedures, will help to

ensure the integrity of the deflection data entered into the SHRP LTPP data base and provide future users of those data with valuable flags regarding section uniformity, structural capacity, and the relationship between deflection data and data obtained from materials testing.

Although specifically developed to meet SHRP needs, these programs could also be of value to state highway agencies and other organizations involved in deflection testing of pavements. Because of the large quantity of data collected within a single set of guidelines, a program such as FWDSCAN is highly valuable. In any other testing environment in which test conditions are likely to vary from site to site, such a program is much less valuable. FWDCHECK, on the other hand, could be greatly useful to other agencies, after some features specific to SHRP are removed. For example, removing the 500-ft test section assumption, lane specification requirements, and test pit comparisons would greatly enhance the usefulness of FWDCHECK.

## ACKNOWLEDGMENTS

The work described in this paper was performed by PCS/Law Engineering under contract to SHRP, National Research Council. The authors gratefully acknowledge the cooperation and assistance of the SHRP Expert Task Group on Deflection Testing and Backcalculation, which is chaired by A. J. Bush III, and the SHRP Regional Coordination Contractors.

## REFERENCES

1. Pavement Consultancy Services/Law Engineering. *Data Readability and Completeness; Program FWDSCAN Version 1.30.* Technical Report. SHRP, June 1990.
2. Pavement Consultancy Services/Law Engineering. *Analysis of Section Homogeneity, Non-Representative Test Pit and Section Data, and Structural Capacity; Program FWDCHECK, Version 2.00.* Technical Report. SHRP, Washington, D.C., Jan. 1991.
3. *SHRP-LTPP Manual for FWD Testing: Operational Field Guidelines, Version 1.0.* SHRP, Washington, D.C., Jan. 1989.
4. A. M. Ioannides, M. R. Thompson, and E. J. Barenberg. Westergaard's Solutions Reconsidered. In *Transportation Research Record 1043*, TRB, National Research Council, Washington, D.C., 1985.
5. *AASHTO Guide for Design of Pavement Structures.* AASHTO, Washington, D.C., 1986.
6. J. Michelow. Analysis of Stresses and Displacement in an N-Layered Elastic System under a Load Uniformly Distributed over a Circular Area. California Research Corporation, California, 1983.

# Variability in Measured Deflections and Backcalculated Moduli for the Strategic Highway Research Program Southern Region

J. BRENT RAUHUT AND PETER R. JORDAHL

It is well known that excessive variability in subgrade characteristics, layer thicknesses, material characteristics, and other such construction variables are major causes of distress and loss of performance in pavements. As the use of deflection measurements to characterize pavement structural capacity and to determine the elastic moduli of the separate layers increases, variability in the deflection measurements and the resulting estimates of the elastic moduli become more important. One study reported was intended as a preliminary evaluation of the amount of variability in deflections that may be expected in relatively short test sections (500 ft for the Strategic Highway Research Program test sections studies), and to learn what characteristics of pavements contribute to this variability. The relative causes of the variability were studied using correlations of variations in deflections with various characteristics of the pavements, such as layer thicknesses, layer stiffnesses, and asphalt viscosity. These studies indicate that the typical coefficients of variation for deflections range between 4 and 18 percent of the mean deflections, but some coefficients of variation for specific test sections will run over 40 percent of the mean deflections. A second study identified variations in backcalculated moduli for four test sections. This limited set of backcalculated moduli indicates that variability in backcalculated moduli for base layers is much higher than that for the asphalt concrete (AC) layers and subgrade and that the coefficients of variation for backcalculated AC moduli appear to be proportional to those for measured deflections. Some causes of the variability appear to have been identified, but variability in deflection measurements were found to result from a multitude of pavement characteristics, each resulting in minor effects to create the whole.

The design of pavement structures typically assumes that a pavement structure will be constructed of materials having certain assumed or expected properties or characteristics. This pavement structure is selected after study of any existing materials in place, new materials that may be specified, expected traffic, and the environment in which the pavement is to exist and function. Variability from these expectations in the field is a major cause of distress and loss of performance in pavements.

Because the material sampling for the Strategic Highway Research Program (SHRP) Long-Term Pavement Performance (LTPP) studies has been conducted at only two general locations (both close to but outside the test section), the only within-section measure of variability available will be from falling weight deflectometer (FWD) deflection measurements at close intervals throughout the test sections. The variations in measured deflections result from variability in layer thicknesses and in material properties, as well as from discontinuities, such as cracks, that usually begin at the bottom of bound layers and propagate toward the surface. Therefore, the variability in measured deflections is important, even though it will be difficult to differentiate among potential causes.

The LTPP data base for the SHRP Southern Region includes Dynatest FWD measurements at close intervals for over 260 general pavement studies (GPS) test sections 500 ft in length. Analysis of the variability in deflections for these test sections offers an opportunity for characterizing typical variability for various types of pavements and exploring apparent variations in moduli within test sections and between similar test sections.

All FWD measurements used in this study were made with the load 6 ft from the outer edge of the pavement. For flexible pavements, measurements were made every 25 ft. For jointed concrete pavements, tests were made at midpanel, except when a transverse crack occurred near that point. In that case, the measurement was made midway between the crack and a joint, within the largest "subpanel" between the crack and a joint. For continuously reinforced concrete pavements, tests were made approximately every 25 ft and midway between cracks.

Deflection data from the SHRP Southern Region Information Management System (RIMS) were extracted, and test section means, standard deviations, and coefficients of variation were calculated for the measured deflections for all seven sensors. After studying the distributions of the coefficients of variation, it was decided to continue studies for Sensor 1 directly under the load and Sensor 6 located 36 in. from the load. Plots were developed to show distributions of coefficients of variability separately for Sensor 1 and for Sensor 6 and for flexible and rigid pavements. Plots were also developed for deflections and backcalculated moduli along typical flexible pavement test sections to indicate how these quantities vary within test sections. Other plots showed coefficient of variation versus various pavement properties for 77 flexible pavements for which a "practice data base" had been developed. A correlation study was also conducted with the deflection data for the 77 flexible pavements and the practice data base to indicate levels of correlation between

Brent Rauhut Engineering, Inc., 8240 Mopac, Suite 220, Austin, Tex. 78759.

coefficients of variation of deflections and various other pavement characteristics.

The results from these studies have been evaluated and the conclusions reported about typical levels of variation of deflections and what pavement parameters may influence levels of variability.

## DISTRIBUTIONS OF VARIABILITY FOR PAVEMENTS IN THE SHRP SOUTHERN REGION

The coefficients of variation (CV) have been calculated individually for Sensors 1 and 6 for 132 flexible pavement test sections and 88 rigid pavement test sections. Coefficients of variation are called CV1 for Sensor 1 and CV6 for Sensor 6. Histograms were developed to indicate distributions of levels of variation and appear as follows:

1. Figures 1 and 2: distributions of CV1 and CV6, respectively, for 132 flexible pavements from Experiments GPS-1, Asphalt Concrete with Granular Base; GPS-2, Asphalt Concrete with Bound Base; and GPS-6, AC Overlay of AC Pavement; and
2. Figures 3 and 4: distributions of CV1 and CV6, respectively, for 88 rigid pavements from Experiments GPS-3, Jointed

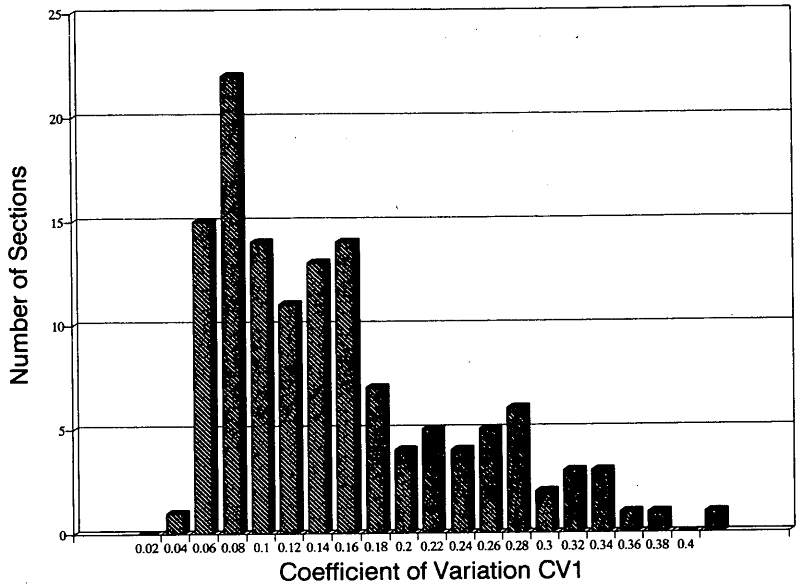


**FIGURE 1 Distribution of Sensor 1 coefficients of variation for 132 flexible pavement test sections in the SHRP southern region, Experiments GPS-1, 2, and 6.**

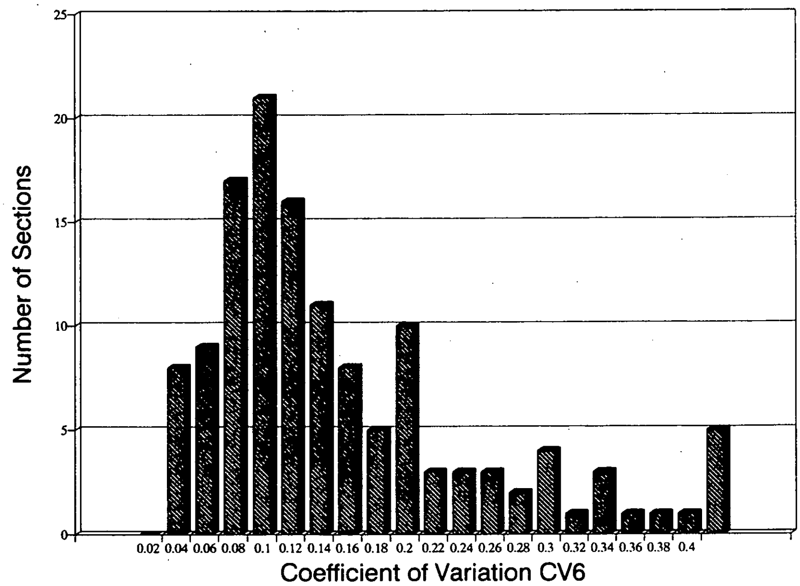


**FIGURE 2 Distribution of Sensor 6 coefficients of variation for 132 flexible pavement test sections in the SHRP southern region, Experiments GPS-1, 2, and 6.**

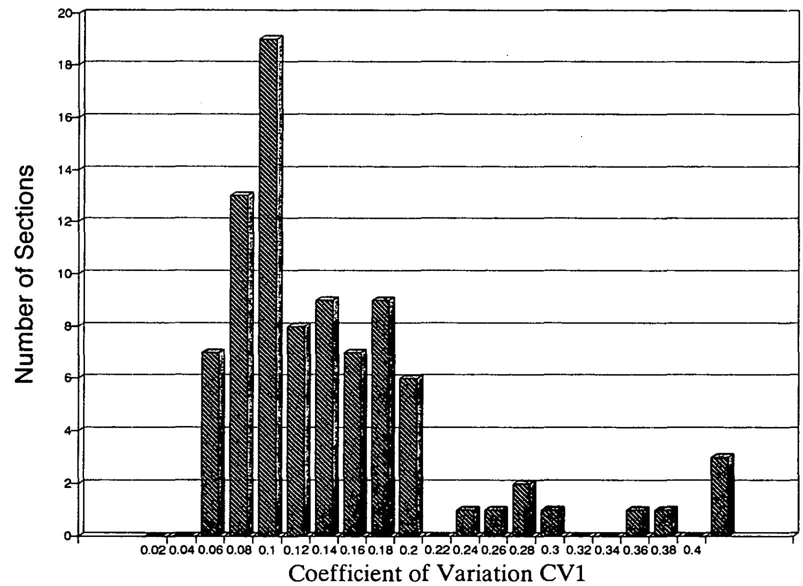


**FIGURE 3 Distribution of Sensor 1 coefficients of variation for 88 rigid pavement test sections in the SHRP southern region, Experiments GPS-3, 4, and 5.**

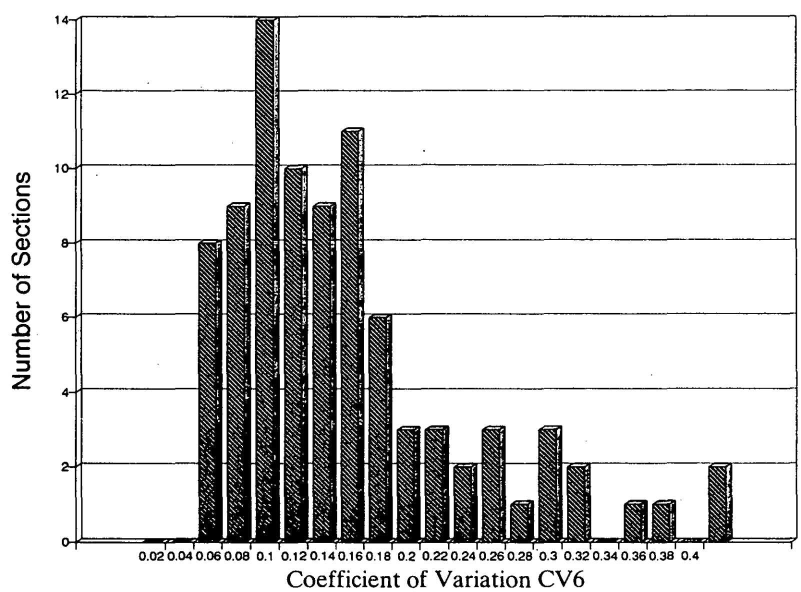


**FIGURE 4 Distribution of Sensor 6 coefficients of variation for 88 rigid pavement test sections in the SHRP southern region, Experiments GPS-3, 4, and 5.**

Plain Concrete Pavements; GPS-4, Jointed Reinforced Concrete Pavements; and GPS-5, Continuously Reinforced Concrete Pavements.

Because the coefficients of variation are simply the ratios of standard deviations from the means to the means, the intervals shown on Figures 1 through 4 represent intervals of standard deviation expressed as fractions of the means. All of the distributions are skewed. The evaluation of the deflections for the majority of the test sections resulted in standard deviations between 4 and 18 percent of the mean deflections for the test sections. However, there were for all pavements and sensors a lesser number of standard deviations ranging from 18 to over 40 percent of the mean deflections. The incidence of standard deviations above 20 percent of the mean deflections for Sensor 1 (below the load) was much greater for flexible than for rigid pavements; this difference for Sensor 6 was negligible.

## DISTRIBUTIONS OF DEFLECTIONS WITHIN TEST SECTIONS

Four flexible pavements from Experiment GPS-1 (AC over granular base) were selected to include (a) two test sections with relatively heavy structures, one on coarse-grained and

one on fine-grained soils, and (b) two sections with moderate structures, one on coarse-grained and one on fine-grained soils.

The measured deflections were not reviewed before selection of the test sections, so the selections were random with relation to measured deflection variability.

Plots of midlane deflections at 25-ft intervals for Drop Height 2 (approximately 9,000 lb normalized to mils/1,000 lb of load) appear in

1. Figure 5 (*top*) for SHRP ID 014126—13.0 in. of HMAC, 18.4 in. of coarse soil aggregate base, and subgrade of clayey sand, located in Alabama;
2. Figure 6 (*top*) for SHRP ID 471023—5.4 in. of HMAC and 6.1 in. of ATB (asphalt-treated base), 6.0 in. of crushed stone base, and a sandy clay subgrade, located in Tennessee;
3. Figure 7 (*top*) for SHRP ID 481065—8.6 in. of HMAC, 4.8 in. of crushed stone, and a sandy clay subgrade, located in Texas; and
4. Figure 8 (*top*) for SHRP ID 481076—4.7 to 6.1 in. of HMAC, 8.4 in. of crushed stone base, and a sand subgrade, located in Texas. (For backcalculations, two different structures were used and will be explained subsequently.)

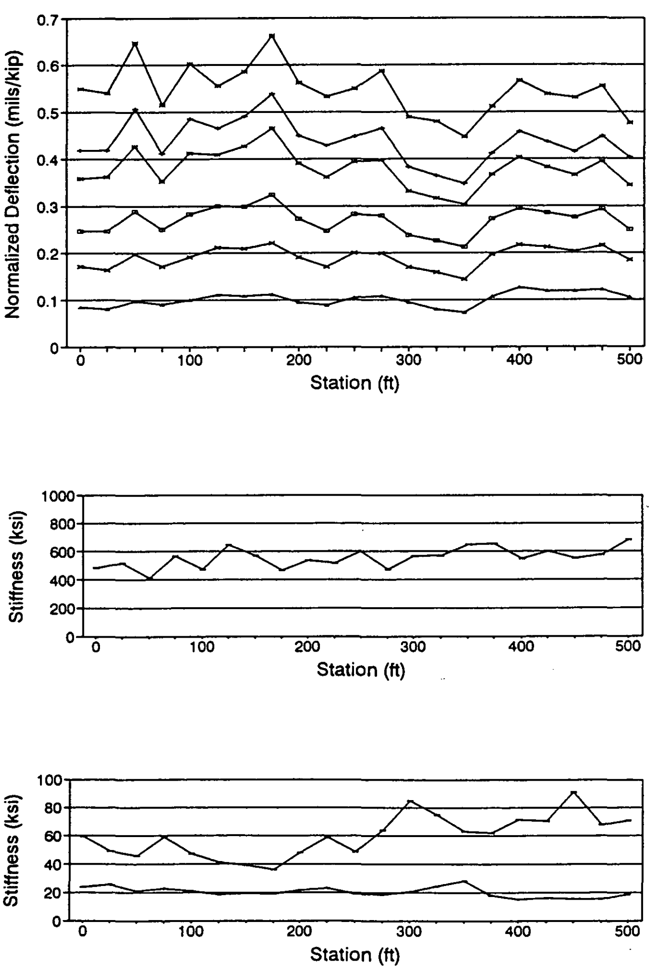


**FIGURE 5 Measured midlane deflections (in mils per 1,000 lb) and backcalculated moduli, GPS Test Section 014126: *top*, deflections across test section, sensor spacings of 0, 8, 12, 24, 36, and 60 in. from center of load; *middle*, moduli for AC; and *bottom*, moduli for base and subgrade.**

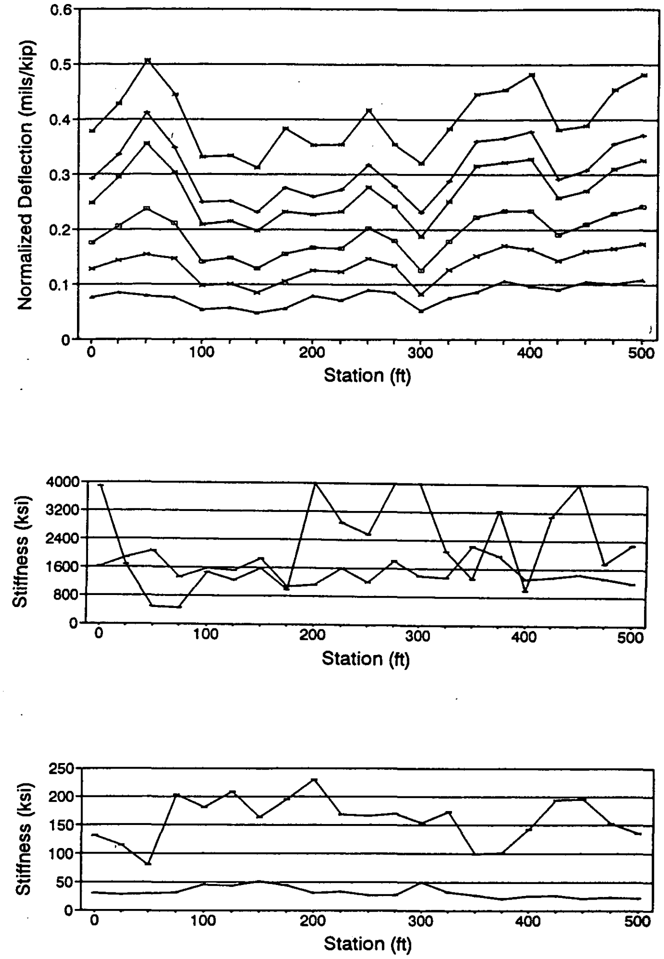


**FIGURE 6 Measured midlane deflections (in mils per 1,000 lb) and backcalculated moduli, GPS Test Section 471023: *top*, deflections across test section, sensor spacings of 0, 8, 12, 24, 36, and 60 in. from center of load; *middle*, moduli for AC and granular base; and *bottom*, moduli for asphalt-treated base and subgrade.**

These plots show the average deflections (over four drops at Drop Height 2) per 1,000 lb of load. (Drop Height 2 yields loads of about 9,000 lb.) The deflection measurements were made with the seven standard SHRP sensor spacings. Because the software package allowed only six dependent variables within a plot, Sensor 4 measurements 18 in. from the center of load were omitted from the plots (but not from the backcalculations).

The coefficients of variation for these test sections are as follows:

| *SHRP ID* | *Sensor 1* | *Sensor 6* |
|---|---|---|
| 014126 | 0.104 | 0.108 |
| 471023 | 0.140 | 0.197 |
| 481065 | 0.248 | 0.106 |
| 481076 | 0.314 | 0.073 |

Variations for Sensors 1 and 6 in deflections throughout a test series can vary markedly.

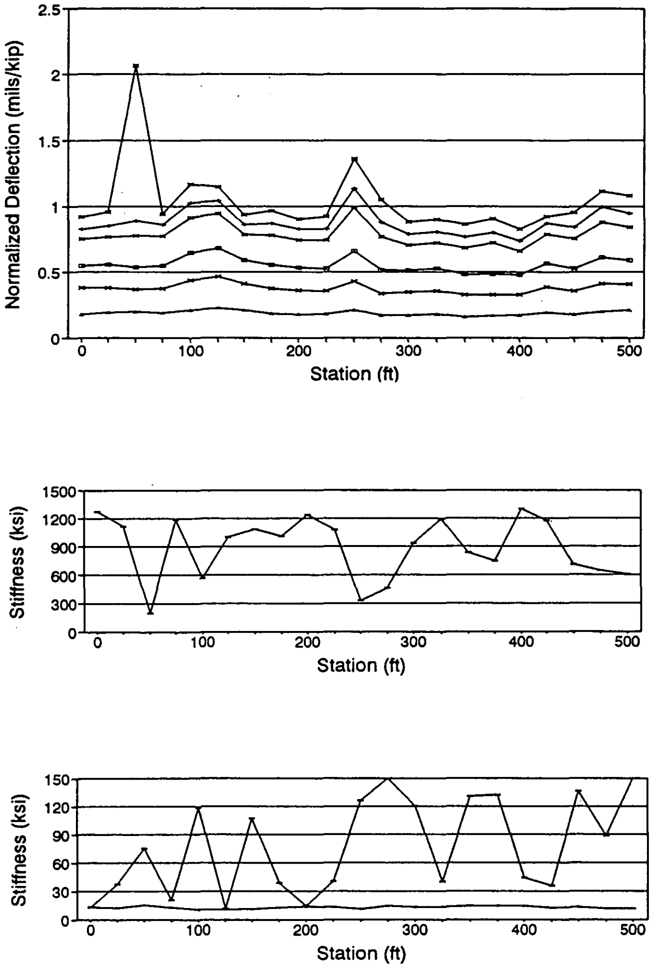


**FIGURE 7 Measured midlane deflections (in mils per 1,000 lb) and backcalculated moduli, GPS Test Section 481065: *top*, deflections across test section, sensor spacings of 0, 8, 12, 24, 36, and 60 in. from center of load; *middle*, moduli for AC; and *bottom*, moduli for base and subgrade.**

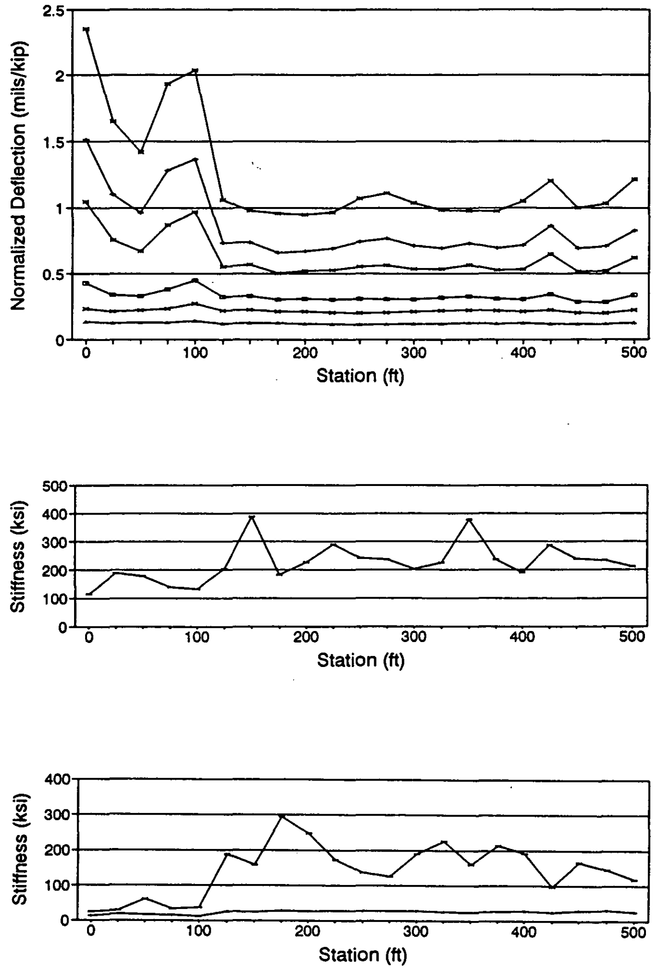


**FIGURE 8 Measured midlane deflections (in mils per 1,000 lb) and backcalculated moduli, GPS Test Section 481076: *top*, deflections across test section, sensor spacings of 0, 8, 12, 24, 36, and 60 in. from center of load; *middle*, moduli for AC; and *bottom*, moduli for base and subgrade.**

Inspection of the plots indicates that the magnitudes of deflections for the separate sensors generally appear to follow the same trends from point to point along the test sections. Also, the measured deflections vary substantially, even in a short test section of 500 ft.

In Figure 7 (*top*) the deflections measured for Sensor 1 at Station 0 + 50 were relatively high and atypical for the trends reflected by the other sensors. It is likely that this sensor rested very near a crack or some other anomaly in the pavement.

It also may be noted in Figure 8 (*top*) that deflections measured between Stations 0 + 00 and 1 + 00 for Sensors 1 through 4 were substantially higher than those for the remainder of the test section. Review of the data from the material sampling indicated that the pavement structures differed between sampling points off the ends of the test section as follows:

| *Location* | *AC Thickness (in.)* | *Base Thickness (in.)* |
|---|---|---|
| Approach | 6.1 | 8.4 |
| Leave | 4.7 | 8.4 |

The plots of deflections in Figure 8 (*top*) appear to indicate that the change in structure occurred between Stations 1 + 00 and 1 + 25, but the higher deflections occurred for the thicker structure. However, review of the laboratory test results indicated that the base material on the approach end was a clayey sand, whereas that on the leave end was a crushed gravel, and the silty clay subgrade on the approach end has 25.6 percent passing the No. 200 sieve compared with 9.8 percent passing the No. 200 sieve on the leave end. The substantial differences in deflections between the two subsections then result from several differences in pavement structure. Although the facts are indeterminate, it appears likely that the layer thicknesses also may have changed between Stations 1 + 00 and 1 + 25, so the backcalculations can be conducted separately for the subsections.

## DISTRIBUTIONS OF BACKCALCULATED LAYER MODULI WITHIN TEST SECTIONS

Backcalculations have been conducted for the same test sections for which distributions of deflections were discussed

earlier. These distributions for calculated moduli appear as Figures 5 through 8 (*middle*) for AC moduli and as Figures 5 through 8 (*bottom*) for base and subgrade moduli. MODULUS 4, developed by the Texas Transportation Institute for the NCHRP and the Texas State Department of Highways and Public Transportation, was used for the backcalculations. Because a 20-ft auger boring by each of the test sections indicated no rigid layer, the estimates for depths to effective stiff layers by MODULUS 4 were used, although other depths to effective stiff layers (including infinity) were tried. The errors in fit were less for three of the test sections when infinity was used, but the calculated moduli appeared illogical.

No reasonable moduli were calculated for Test Section 471023 (Figure 6). Trials included three layers (HMAC and ATB combined) and four layers (HMAC and ATB as separate layers), with combinations of 300 in. (for a single point), infinity (for a single point), and the depths selected by MODULUS 4 to effective stiff layer. As seen from the results plotted in Figure 6 (*middle* and *bottom*), the backcalculated values were not logical. The calculated granular base moduli exceeded those for the AC surface and ATB layers, which is not sensible. The results plotted were for the four-layer structure with a depth to effective stiff layer from the pavement surface of 165 in. Such results indicate that the use of measured deflections to estimate layer moduli is not yet a technique that can be applied without careful examination and evaluation of the results.

Nick Coetzee conducted backcalculations on the same four deflection data sets (unpublished data), with no stiff layers in the subgrade (infinite depth). Table 1 shows approximate ranges of backcalculated moduli across the test sections from ELMOD by Coetzee and from MODULUS 4 by Jordahl. Although the values varied, the trends were generally similar. Coetzee also experienced difficulties with Section 471023, although the moduli for his three-layer solution were less illogical than those from the four-layer solution with MODULUS. In general, lower values for a layer derived from one computer program than from the other would be reflected in higher numbers for another layer. These results further emphasize the need for more development before backcalculation of layer moduli from measured deflections can be considered reliable.

Coetzee later ran the backcalculations on the same data sets but allowed ELMOD to select depths to effective stiff layers. In all cases, the result was a worse fit to the measured deflections than when using an infinite depth.

The mean values of backcalculated moduli, the absolute errors per sensor, and the coefficients of variation for the asphalt concrete, base, and subgrade layers for the four test sections discussed previously appear in Table 2. The ranges for the backcalculated layer moduli appear in Table 1. Judgments were required in selection of the results from the multiple runs, because the best fit (as indicated by a lower value of absolute errors per sensor) often occurred when the resulting calculated moduli were illogical.

The following conclusions were drawn from study of the graphs for backcalculated moduli and Tables 1 and 2:

1. The error checks for the moduli backcalculated with MODULUS 4 indicated good fits between measured deflections and those calculated with the backcalculated moduli when no effective stiff layer was included in the subgrade, but the resulting moduli did not appear to be logical. More reasonable values of moduli were derived using MODULUS 4 estimates of depth to an effective stiff layer, but the fits were not as good.
2. For this limited set of test sections, the variabilities in moduli calculated for base layers are substantially higher than those for asphalt concrete and subgrade layers.
3. The coefficients of variation for asphalt concrete moduli, for this limited sample, appear to be approximately proportional to the variations in Sensor 1 deflections reported previously.
4. The ranges in values for backcalculated moduli may be expected to be substantial, even when the coefficients of variation appear to be relatively small.

Although the lack of data on variability in layer thicknesses within the test sections cause assignment of all of the variability to the moduli, it is believed that variations from the layer

**TABLE 1 Results of Backcalculations on Deflections, SHRP Test Sections 014126, 471023, 481065, and 481076**

| Test Section | Computer Program | Ranges of Backcalculated Moduli in KSI | | |
|---|---|---|---|---|
| | | AC | Granular Base | Subgrade |
| 014126 | ELMOD | 500 to 800 | 20 to 65 | 32 to 50 |
| | MODULUS | 410 to 683 | 36 to 91 | 15 to 29 |
| 471023 | ELMOD | 700 to 900 | 90 to 570 | 44 to 93 |
| | MODULUS | 1000 to 2300 (ATB)<br>80 to 210 (AC) | 446 to 4000 | 21 to 52 |
| 481065 | ELMOD | 80 to 1900 | 8 to 70 | 15 to 22 |
| | MODULUS | 330 to 1298 | 11 to 150+ | 11 to 15 |
| 481076 | ELMOD | 50 to 1900 | 30 to 160 | 20 to 39 |
| | MODULUS | 116 to 388 | 24 to 294 | 13 to 29 |

**TABLE 2 Approximate Ranges for Backcalculated Layer Moduli from Programs ELMOD and MODULUS 4**

| SHRP ID | Average Pavement Temp. (°F) | Absolute[1] Error/Sensor (Percent) | Mean Values of Moduli (KSI) | | | Coefficients of Variation (Percent) | | | Average Depth to Stiff Layers (Inches) |
|---|---|---|---|---|---|---|---|---|---|
| | | | AC | Base | Subgrade | AC | Base | Subgrade | |
| 014126 | 61 | 2.21 | 555 | 60 | 20 | 13 | 25 | 18 | 103 |
| 471023 | 95 | 1.94 | 1537 (ATB)<br>160 (AC) | 2284 | 32 | 21<br>24 | 54 | 30 | 147 |
| 481065[2] | 70 | 3.80 | 890 | 78 | 13 | 32 | 67 | 9<br>10 | 139 |
| 481076[3]<br>0-100 | 76 | 2.40 | 150 | 37 | 15 | 21 | 40 | 18 | 60 |
| 125-500 | | 9.3[4] | 248 | 177 | 26 | 24 | 29 | 6 | 153 |

Notes: [1] = Average over seven sensors of the absolute value of percent error in deflections.

[2] = The one very high deflection data point for Sensor 1 at Station 0+50 was omitted from statistical calculations (see Figure 7).

[3] = Different structures were used for Stations 0+00 to 1+00 and 1+25 to 5+00 (see discussions in "Distributions of Deflections Within Test Sections").

[4] = Sensor 7 was fit very poorly in this case.

thicknesses measured at the ends and outside of the test sections cause a substantial amount of the variability. The results of one study on the effects on calculated moduli from errors in layer thicknesses have been published previously (*1*). Two possibilities for improvement exist for future backcalculations using layer thickness data specific to measurement stations:

1. Some experiments in Texas with calibrating radar output to the known layer thicknesses at each end of four SHRP GPS test sections appear to have resulted in measured layer thicknesses within the test section to reasonable accuracy. Holes were bored in an adjacent lane to check the point-to-point radar estimates. This success has led to a broader experiment funded by SHRP. If successful, radar measurement of all SHRP GPS test sections is probable. [Very accurate layer thickness measurements are being made for some overlays in GPS and all specific pavement studies (SPS) test sections.]
2. As GPS test sections reach a point requiring overlay, cores of the surface material and bound layers could be taken within the test sections before overlay in the existing pavements. Similarly, base material could be augered to establish its thickness. The deflection data will still be available, so new backcalculations could be conducted.

## GPS-1 PRACTICE DATA BASE

A "practice data base" has been developed by the authors for use in conducting practice sensitivity analyses to develop procedures to be used for SHRP Contract P-020, LTPP Data Analysis. This practice data base includes inventory data now available in the southern RIMS for experiment GPS-1, rough measurements of distress by SHRP regional contractor personnel when first visiting the test sections, rough estimates of cumulated ESALs [based on original estimates of ESALs per year by state highway agencies (SHAs)], estimated environmental data from isobar climatic maps, and realistic estimates where data were missing. The estimated values primarily supplemented materials data not furnished (generally not available) by the SHAs, such as estimations for dry densities based on other data available and plasticity indexes based on AASHTO soils classifications. All layer moduli other than those for the subgrade were estimated on the basis of other data available and experience with previous measurements. Moduli for subgrades were obtained from Sensor 6 deflection measurements using the equation for estimating subgrade moduli in the AASHTO Design Guide, with rough reductions reflecting a modification to reflect stress sensitivity imbedded in Program FWDCHECK. All asphaltic layers were combined and all granular base and subbase layers were combined to result in three-layer structures. On the basis of combined results of significance ratings by experts, data were not sought for the many missing data items that were not expected to be significant for predicting pavement performance.

Although the estimated data elements in this data base limit its accuracy in predicting performance, the data base was considered to be adequate for correlation studies to obtain preliminary information on what variables were correlated with variability in measured deflections. The results of these studies are described subsequently. A similar but broader study should be conducted when the actual data become available in the National Pavement Data Base.

## CORRELATION STUDIES

Data from the GPS-1 practice data base described above were used to relate the coefficients of variation CV1 and CV6 in deflections measured by Sensors 1 and 6 (S1 and S6) to a number of other variables. The Statistical Analysis System (SAS) software was used to conduct a correlation analysis and determine Pearson correlation coefficients between CV1 and CV2 and other variables in the data base. The results from this study appear in Table 3.

A positive magnitude for coefficient of correlation indicates that increases in that variable tend to cause increased variability in measured deflections, and vice versa for negative magnitudes. The absolute magnitude of the coefficient indicated the degree of the variable's effect on variability in mesured deflections. The absolute magnitudes for the correlation coefficients ranged from zero to 0.35, except for one at 0.59. To assign some different levels for the effects of variable increases in magnitude on the variability in measured deflections, an arbitrary system was established as follows (this system was also used for each variable in Table 3):

| *Range of Correlation Coefficients* | *Level of Effect* |
|---|---|
| $CV_i > 0.20$ | Significant (S) |
| $0.10 < CV_i \leq 0.20$ | Moderate (M) |
| $0 < CV_i \leq 0.10$ | Nominal (N) |

The greatest correlation appears to be between CV1 and the SHRP ID numbers of the test sections. Once the skepticism stage runs its course and logic returns, it can be noticed that the first two digits of the ID numbers are the state codes, with the highest in the southern region being 48 for Texas, which has 38 of the 77 GPS-1 test sections. Considering that clay subgrades are relatively common in Texas and that CV1 appears to increase with plasticity index of the subgrade soil and the amount of the subgrade soil passing the No. 200 sieve, the correlation between CV1 and SHRP ID number seems more reasonable. Also, the state code for Tennessee is 47, and considerable variability in layer thicknesses was noted between approach and leave ends during material sampling.

If the magnitudes of the correlation coefficients indicate trends, although their accuracy is limited by the limitations of the practice data base, the following tendencies may be noted for effects rated as significant.

1. The higher the amount and plasticity of the clay fractions in subgrades, the higher CV1 is likely to be.
2. The higher the annual precipitation, the lower CV1 is likely to be.
3. High levels of traffic (ESALs) in pavements tend to reduce CV1 (this is probably because of the thicker structures that are designed for pavements expected to experience heavy traffic).
4. CV1 and CV6 appear to decrease for rutted pavements (possibly related to properties of materials that rut, or related to high traffic levels discussed above).
5. The occurrence of low-severity transverse cracking appears to increase CV1, but moderate or high-severity cracking does not. (This is probably a consequence of very limited occurrence of transverse cracking in the southern region, of which the great majority was of low severity.)
6. Increasing air temperatures when testing appears to increase CV1.
7. AADT appears to decrease CV1 (consistent with Item 3).
8. Increasing asphalt concrete thickness tends to decrease both CV1 and CV6.
9. Increasing asphalt viscosity in HMAC appears to decrease variability for Sensor 1 deflections (affects stiffness of the AC layer).
10. Increasing subgrade stiffness tends to decrease CV1 and increase CV6 (note that the effect is greater for Sensor 6, which primarily reflects subgrade characteristics).
11. Increased moisture content in the subgrade tends to increase both CV1 and CV6 (this does not appear to be consistent with Item 2).

Because the correlations between CV1 and CV6 and other variables were not generally strong, it appeared appropriate to conduct regressions to see how much of the variations could be explained with different combinations of the variables. Consequently, 15 variables were selected from the results of the correlation studies and SAS PROC REG, Option RSQUARE, was used to obtain the values of $r^2$, the proportion of variance in CV1 or CV6 explained by various combinations of variables. The SHRP ID number was omitted from this study.

Models for predicting CV1 with only one independent variable each resulted in values of $r^2$ equal to the square of the associated correlation coefficients, as would be expected. Using PROC REG, option STEPWISE, the values of $r^2$ increased moderately as more variables were included in the models, until four variables were included. The $r^2$ for the best model with four variables was 0.32, whereas the $r^2$ for the best model with 13 variables was only 0.39. The variables in the best four-variable model were thickness of the AC layer, Thornthwaite index, annual precipitation, and air temperature at time of testing. The software advised that no other variables were significant at the default value of the "*F* statistic for entry" of 0.15. Note on Table 1 that three of the individual correlation coefficients are negative and one is positive. Two of the four were rated to have significant effect and the other two moderate. The equation is

$$\begin{aligned} \text{CV1} = {} & 0.29479 - 0.00691 \text{ (AC thickness)} \\ & + 0.00211 \text{ (Thornthwaite index)} \\ & - 0.00533 \text{ (annual precipitation)} \\ & + 0.00106 \text{ (air temperature at testing).} \end{aligned}$$

The best five-variable model for CV6 had an $r^2$ of 0.29; the inclusion of nine additional variables increased the $r^2$ only to 0.34. The variables included were thickness of the AC layer, subgrade stiffness, subgrade soil passing the No. 200 sieve, Thornthwaite index, and annual precipitation. Three of the five also appeared in the equation for CV1, but only one was rated as having a substantial effect on CV6. The equation for

**TABLE 3 Correlation Coefficients for Coefficients of Variation for Sensors 1 (S1) and 6 (S6) Deflections and Various Variables**

| Variable | Correlation Coefficients | | Effects on Variability of Increases in Magnitude of Variable | | | |
|---|---|---|---|---|---|---|
| | | | S1 | | S6 | |
| | S1 Deflections | S6 Deflections | Effect | Level | Effect | Level |
| Subgrade Plasticity Index | 0.25 | 0.04 | Increases | S | Increases | N |
| Subgrade, Passing #200 | 0.21 | 0.11 | Increases | S | Increases | M |
| Thornthwaite Index | - 0.15 | 0.15 | Decreases | M | Increases | M |
| Annual Precipitation | - 0.35 | 0.04 | Decreases | S | Increases | N |
| Days Temp. > 90F | 0.04 | - 0.05 | Increases | N | Decreases | N |
| Days Temp. < 32F | 0.20 | 0.01 | Increases | M | Increases | N |
| Cumulative ESAL's | - 0.12 | - 0.07 | Decreases | M | Decreases | N |
| Annual ESAL's (Rate) | - 0.21 | - 0.15 | Decreases | S | Decreases | M |
| Alligator Cracking | | | | | | |
| Low Severity | 0.19 | 0.06 | Increases | M | Increases | N |
| Medium Severity | - 0.12 | 0.02 | Decreases | M | Increases | N |
| High Severity | - 0.09 | - 0.04 | Decreases | N | Decreases | N |
| Rut Depth | - 0.30 | - 0.22 | Decreases | S | Decreases | S |
| Transverse Cracking | | | | | | |
| Low Severity | 0.34 | - 0.10 | Increases | S | Decreases | N |
| Medium Severity | - 0.08 | 0.00 | Decreases | N | --- | O |
| High Severity | 0.00 | - 0.07 | --- | O | Decreases | N |
| Air Temp. When Testing | 0.30 | - 0.07 | Increases | S | Decreases | N |
| AADT | - 0.28 | - 0.14 | Decreases | S | Decreases | M |
| Percent Trucks | - 0.13 | - 0.20 | Decreases | M | Decreases | M |
| Asphalt Concrete Thickness | - 0.16 | - 0.32 | Decreases | M | Decreases | S |
| Asphalt Concrete Stiffness | - 0.14 | 0.07 | Decreases | M | Increases | N |
| Base Thickness | - 0.15 | - 0.12 | Decreases | M | Decreases | M |
| Base Stiffness | 0.03 | 0.17 | Increases | N | Increases | M |
| Percent Voids in A.C. | - 0.12 | - 0.06 | Decreases | M | Decreases | N |
| Asphalt Viscosity (140F) | - 0.26 | - 0.06 | Decreases | S | Decreases | N |
| Asphalt Content | 0.11 | - 0.10 | Increases | M | Decreases | N |
| Subgrade Stiffness | - 0.14 | 0.21 | Decreases | M | Increases | S |
| Functional Class | - 0.18 | - 0.23 | Decreases | M | Decreases | S |
| Subgrade Moisture Content | 0.23 | - 0.21 | Increases | S | Decreases | S |
| SHRP I.D. Number | 0.59 | 0.29 | Increases | S | Increases | S |

**Legend:**
S1 = Sensor 1 Deflection
S6 = Sensor 6 Deflection
S = Substantial Effect = $CV_i > 0.20$
M = Moderate Effect = $0.10 < CV_i \leq 0.20$
N = Nominal Effect = $0 < CV_i \leq 0.10$

**Note:** Assignments of "levels of effect" are arbitrary.

CV6 is

$$\begin{aligned} CV6 = 0.2832 &- 0.01249\ (\text{AC thickness}) \\ &+ 0.00093\ (\text{subgrade stiffness}) \\ &+ 0.00062\ (\text{passing No. 200 sieve}) \\ &+ 0.00024\ (\text{Thornthwaite index}) \\ &- 0.00374\ (\text{annual precipitation}) \end{aligned}$$

Although the fractions of the variance of CV1 and CV6 explained by these equations (as indicated by the values for $r^2$) are quite low, this is partially a consequence of using a very simple linear equation form in the regressions. If the objective had been to develop predictive equations, variables could have been transformed to produce more realistic equation forms. Improvements in $r^2$ might have resulted from including interaction terms between the independent variables. Substantial unexplained error might still have existed because of such factors as limitations of the practice data base, testing error, and use of specific layer thicknesses for all locations within a test section when they are really variable.

To continue the search for identities of variables that affected magnitudes of CV1 and CV6, the independent variables in the equations were individually plotted for each test section against CV1 and CV6, respectively. Simple linear models were regressed from the data, using procedures in the spread sheet software, and plotted to give some insight as to the overall effects of the data represented by the very scattered points on the plots. These plots appear in Figure 9 for CV1 and Figure 10 for CV6.

None of the plots offer much in the way of a definite relationship, so it appears that the levels of variability for the measured deflections are not heavily influenced by any of the variables studied but appear to result from small effects from a number of sources, probably including some that were omitted from this study. Although these plots did not produce any strong candidate as a major cause of variability in deflections, it is comforting to note that the senses and magnitudes of the slopes for the simple linear relationships plotted are consistent with results from the correlation studies displayed in Table 3.

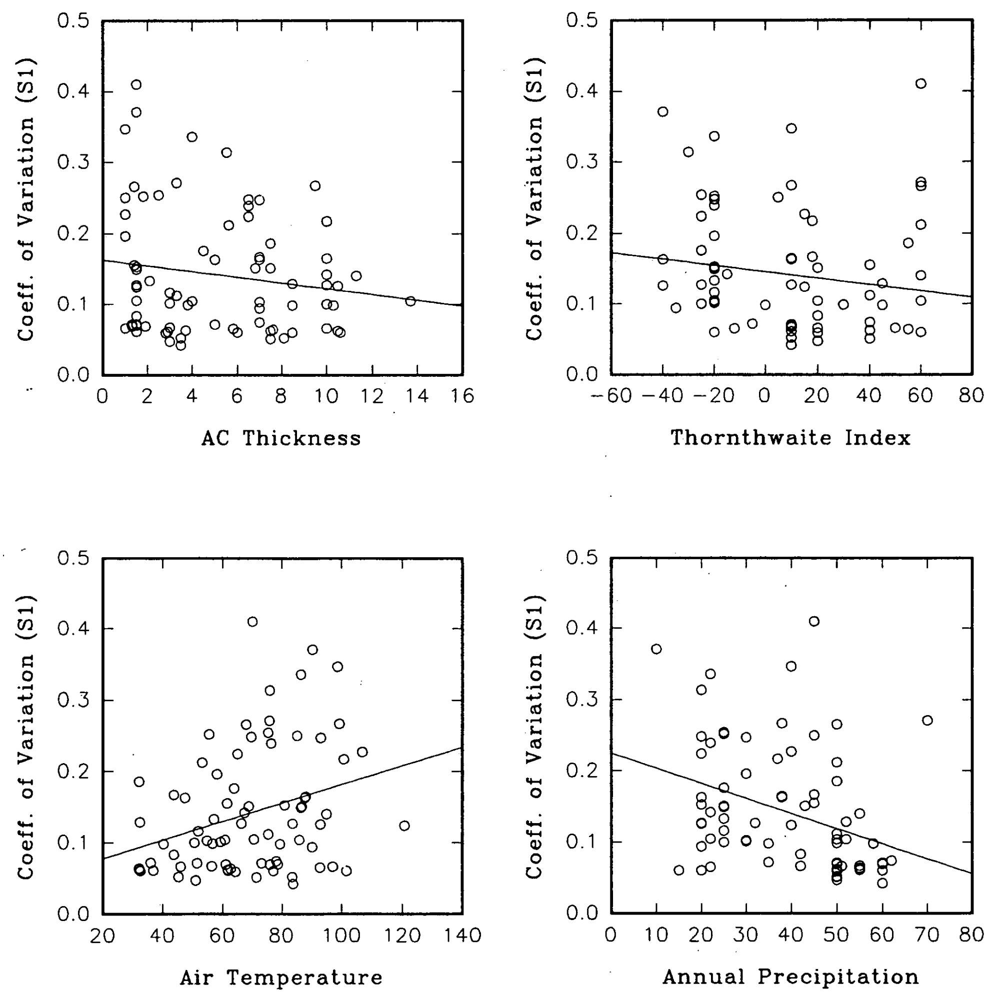


**FIGURE 9 Plots of coefficients of variation CV1 of deflections measured by Sensor 1 (directly below the load) to other variables found to significantly affect the variations: *top left*, CV1 versus AC thickness; *top right*, CV1 versus Thornthwaite index; *lower left*, CV1 versus air temperature at testing; and *lower right*, CV1 versus annual precipitation.**

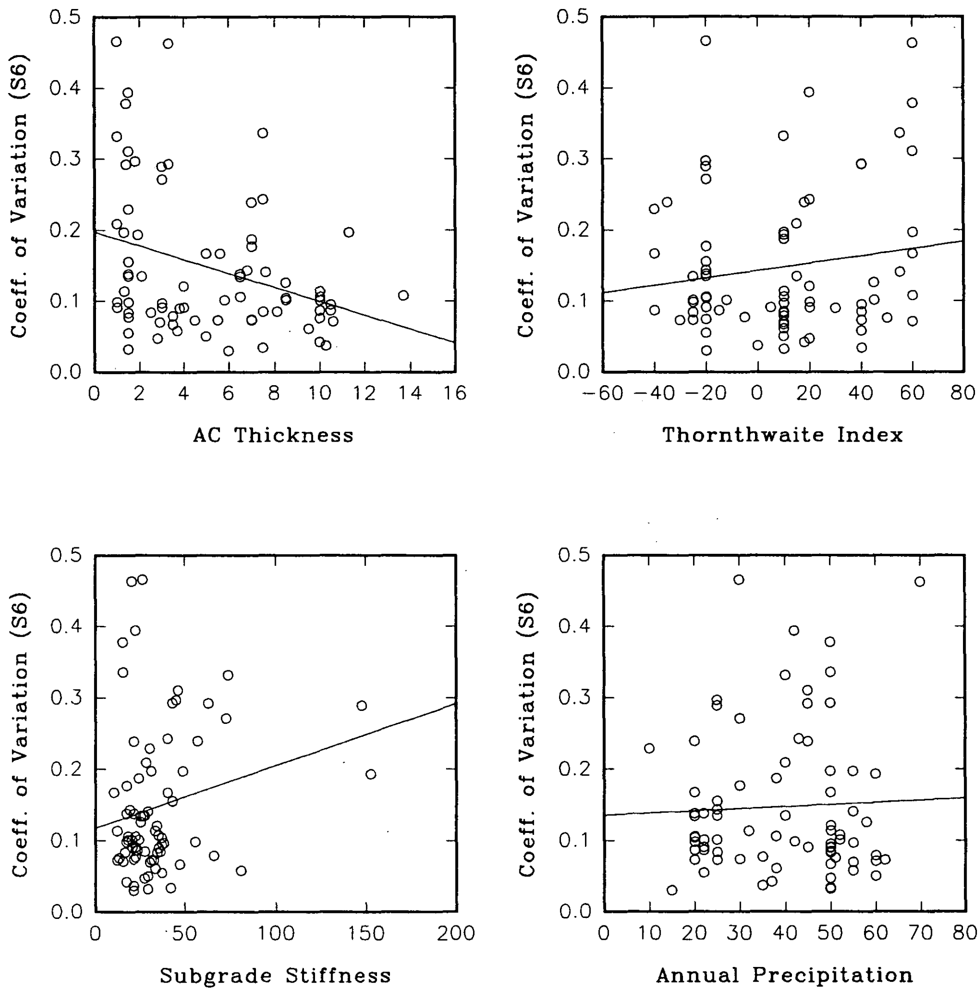


**FIGURE 10 Plots of coefficients of variation CV1 of deflections measured by Sensor 6 (36 in. from the center of loading) to other variables found to significantly affect the variations: *top left*, CV6 versus AC thickness; *top right*, CV6 versus Thornthwaite index; *lower left*, CV6 versus subgrade stiffness; and *lower right*, CV6 versus annual precipitation.**

## CONCLUSIONS

These limited preliminary studies resulted in the following conclusions:

1. The distributions of coefficients of variation in measured deflections for 132 flexible and 88 rigid pavements indicate that the majority of the test sections reflected coefficients of variation from 4 percent to 18 percent of the mean deflections. However, a number of the coefficients of variation ranged from 18 percent to over 40 percent.
2. For the limited set of four test sections, the variations in backcalculated base moduli were much higher than those for asphalt concrete layers and the subgrade.
3. The coefficients of variation for asphalt concrete appear to be approximately proportional to the variations in Sensor 1 deflections.
4. Even when the coefficients of variability appear to be relatively small, the ranges in backcalculated moduli may be expected to be relatively large.
5. Increases in moisture content, clay fraction, and plasticity index for subgrade soils appear to result in increased variability in deflection measurements.
6. Increased annual precipitation appears to reduce variability in deflection measurements.
7. Increased asphalt concrete thickness, as well as overall structure, appears to reduce variability in measured deflections.
8. Variability in measured deflections appears to increase as the air temperature during testing increases (probably caused by reduced stiffness of the asphalt concrete).
9. The presence of transverse cracking in the pavement appears to increase variability in measured deflections.
10. Increasing viscosity in HMAC appears to reduce variability in Sensor 1 deflections (increases stiffness of AC layer).
11. Increased subgrade stiffness tends to decrease variability in measured deflections.
12. On the basis of the various analyses, the variables that most significantly contribute to the magnitudes of variability are (a) pavement structure (layer thicknesses and stiffnesses and amount and plasticity of clay in subgrade), (b) air temper-

ature during testing, (c) Thornthwaite index, and (d) annual precipitation.

13. When conducting backcalculations, the best fit between calculated and measured deflections does not imply that the most accurate set of layer moduli has been selected. In fact, such a set often includes modulus values that appear to be totally illogical.

It is important to remember that variations in layer thicknesses along a highway are common and can have major effects when moduli are backcalculated using average layer thicknesses throughout a test section. If the actual structure can be determined for a set of deflections at a point, much more accurate estimates of layer moduli can be backcalculated.

Because this is a limited study based on limited data, it will be possible in the future to learn much more about causes for variability in measured deflections, and thus perhaps for the sources of variability in the pavement itself. The ultimate objective is, of course, to be able to characterize the many variabilities in pavement structure and materials that lead to distress and loss of performance.

## ACKNOWLEDGMENTS

All of the data used in these studies originated from the Long-Term Pavement Performance Studies being conducted by the Strategic Highway Research Program. Permission for use of these data was granted by Neil Hawks.

Nick Coetzee with Dynatest Consulting, Inc., provided backcalculated moduli developed from the same data, but using Program ELMOD. This allowed comparisons of backcalculated moduli.

The correlation study and the multiple regressions were conducted using SAS, a software system for data analysis leased from the SAS Institute, Inc., SAS Circle, Box 8000, Cary, N.C. 27512-8000.

## REFERENCES

1. R. Briggs, T. Scullion, and K. Maser. Asphalt Thickness on Texas SHRP Sections and Effect on Backcalculated Moduli. Presented at a Symposium on Nondestructive Deflection Testing and Backcalculation for Pavements, Nashville, Tenn. Aug. 1991.

# Influence of Statistical Variation in Falling Weight Deflectometers on Pavement Analysis

RAJ SIDDHARTHAN, PETER E. SEBAALY, AND MOHAN JAVAREGOWDA

A relatively simple approach that is based on a Monte Carlo simulation procedure is presented to statistically investigate the influence of variation in falling weight deflectometer (FWD) measurements on pavement analysis. The factors considered are pavement moduli and pavement performance or response strains that correlate with pavement performance. From extensive FWD data obtained in Nevada, the variability of FWD deflections was statistically quantified at six sites for two seasons. The FWD tests were carried out at an interval of 50 ft within a uniform 1,000-ft test pavement section at every site. Using these data, as many as 900 FWD sensor deflections with normal distribution for each sensor were randomly generated for each of the 12 cases (six sites, two seasons) studied. The MODULUS program was used in the backcalculation of the pavement layer moduli. The FWD measurements show substantial variation within all of the uniform pavement sections investigated. Backcalculated pavement layer moduli using the generated deflection data show a large variation. The coefficient of variation for layer moduli vary from 5 to as much as 65 percent. Larger variations were computed for AC and base. However, the coefficient of variations for pavement performance strains are smaller, varying from 8 to 25 percent. Because the number of loading cycles to cause pavement distress is sensitive to pavement performance strains, the variation in pavement strain caused by the variation in FWD measurements has a significant influence on pavement life predictions.

As a consequence of the decreasing number of new highway construction projects, much attention is devoted to upgrading and maintaining existing highways. In this regard, effective and often customized overlay design procedures are being actively researched by state transportation departments. The primary objective of an overlay design analysis is whether a highway section requires overlaying and, if it does, by how much. If an overlay is needed, then the goal is to arrive at a pavement section that can withstand the expected traffic loads throughout the design life without excessive pavement failures such as cracking, rutting, or loss of serviceability.

The stiffness of the existing pavement layers is an important input parameter in the overlay design procedures. Although both laboratory and nondestructive testing (NDT) may be used to estimate the stiffness (modulus) of pavement layers, the NDT methods have become widely accepted because they are cheaper and more practical. Through the years, NDT methods have undergone changes because of the need to more realistically simulate wheel loading. The simulation of wheel loading has evolved from a static load to a more representative impulse loading using the falling weight deflectometer (FWD). The FWD is one of the most widely used NDT devices and is being used extensively in the Long-Term Pavement Performance (LTPP) evaluation that is being undertaken by the Strategic Highway Research Program (SHRP). The pavement layer moduli are computed using a "backcalculation procedure" in which the measured deflections on the pavement surface under FWD loading serve as input.

Department of Civil Engineering (258), University of Nevada, Reno, Nev. 89557.

In a typical pavement improvement project, a stretch of highway is divided into a number of representative pavement sections with similar pavement and traffic loading characteristics. Among other factors, important parameters such as age, construction data, layer thicknesses, and pavement condition are often used to determine the extent of representative pavement sections. Within a representative pavement section, FWD tests are carried out at an interval that typically varies from 500 to 1,000 ft. In Nevada, the interval is often 500 ft. The pavement layer properties near an FWD test location are assumed to be uniform. A deviation from this assumption will affect backcalculated moduli and, thus, introduce error in the subsequent pavement analysis procedures that use FWD-based results.

A number of sources of error are associated with FWD measurements. The influence of all of the error sources cannot be completely eliminated. For instance, human factors can influence FWD testing but cannot be predicted. An additional factor to be considered is the pavement section variability. Even though the asphalt concrete (AC) and base layers may have relatively constant properties, the subgrade conditions often vary erratically even within a short distance.

The University of Nevada, Reno, and the Nevada Department of Transportation (NDOT) have collected an extensive FWD data base on a variety of pavements located around the state during at least 4 years and for all four seasons. This data base, in which the FWD measurements were taken at 50-ft intervals within a representative uniform pavement section, has been used to study statistically the variability in pavement deflections caused by various error sources. FWD data collected at these much finer intervals are considered to reflect the true variation of the material properties within a pavement section that is assumed to be uniform. Under these circumstances, the FWD deflection measurements collected at finer intervals can be considered as random variables, and a probabilistic approach seems appropriate to interpret the results given by subsequent backcalculation analysis. This paper uses a Monte Carlo simulation procedure to quantify the

influence of error in FWD deflection measurements on pavement moduli. The data base of pavement moduli values generated by this approach can be used to study the corresponding layer moduli variation. One of the main purposes of estimating the pavement layer stiffnesses is to use them to compute the stresses and strains in the pavement under the design wheel loads. These stresses and strains can then be used as input to pavement distress (performance) models (e.g., rutting and fatigue). The investigation of the influence of the variation in FWD sensor deflections on pavement strains is also presented in this paper.

## BACKGROUND

The FWD causes the pavement to deflect by dropping a free-falling mass that strikes a spring buffered plate. By changing the mass, the drop height, or both, the impulse force on the pavement can be changed. The deflections of the pavement surface are measured at a number of predetermined locations using velocity transducers. These deflection data, along with the thickness of pavement layers and other pavement properties, are used to predict the resilient modulus of the layers using a certain backcalculation procedure. By far, the most widely used backcalculation procedures assume static layered elastic conditions. The pavement materials are characterized to be elastic, homogeneous, and isotropic, with full contact at layer interfaces. The bottom boundary may be assumed to be located at some depth below the top of the subgrade or at a very large depth (half-space).

A recent NCHRP research program on the nondestructive evaluation of pavement layer stiffnesses has assessed all types of NDT equipment for both project-level and network-level pavement condition evaluation (*1*). This extensive study clearly outlines the applicability and limitations of FWD testing to obtain pavement layer stiffnesses. The research concluded that FWD testing is the most suitable for both project- and network-level pavement evaluation. The study also outlines a much more efficient backcalculation procedure that is based on linear elastic theory in which the best values of the layer moduli are estimated using interpolation between calculated deflection basins. This backcalculation analysis method is incorporated into a program called MODULUS. This paper uses the MODULUS program to backcalculate pavement layer moduli. Several state transportation agencies and private firms are currently using MODULUS.

Mechanistic or mechanistic-empirical design procedures characterize the long-term performance of pavements in terms of basic performance or response parameters such as stresses and strains that are induced in the pavement. In these methods, the failure is normally defined in terms of specific mechanisms such as fatigue cracking, rutting, and low temperature cracking. Mechanistic-empirical methods depend in part on empirical relationships between pavement stresses and strains and the number of load applications that the pavement can support before failure. For example, the strain at the bottom of the existing asphalt layer is normally correlated to fatigue failure. In some instances, the stress or strain at the top of the subgrade has been used to correlate rutting failure. In general, mechanistic-empirical procedures have been widely accepted by practitioners and researchers in recent years because they have been proven to be somewhat more reliable and because the pavement performance parameters can be obtained easily.

One of the major uses of the layer stiffnesses is to obtain the pavement performance parameters mentioned above. Static multilayer linear elastic computer programs, such as ELSYM5 and CHEVRON, are often used to estimate these pavement performance parameters. It has been argued that, if both the pavement performance parameter evaluation and FWD backcalculation procedures are carried out under a consistent set of conditions (i.e., static layered elastic), the dynamic effects and nonlinear soil properties may not be important.

It will be clear from the next section that there are a number of sources of error in FWD deflection measurements that cannot be totally eliminated. The paper investigates the influence of the variation in FWD measurements caused by such errors on the backcalculated pavement layer moduli and also on the pavement performance parameters mentioned earlier.

## RESEARCH APPROACH

### Sources of Variability in FWD Testing

It is important that the sources of variability associated with FWD testing be identified and reduced to a minimum. In general, there are two kinds of errors: random and systematic. These error sources result in a variation in the FWD measurements even within a uniform pavement section. Systematic errors can be identified and may be quantified, whereas random errors are a result of random variations in the measurements or in the pavement materials. Random errors are present in measurements recorded by the load cell and velocity transducers. Although they may be reduced somewhat by repeated testing and averaging, random errors cannot be totally eliminated. For example, Dynatest FWD deflection sensors have an accuracy of approximately $\pm 2$ percent as provided by the manufacturer. Other sources of random error include spatial variation of the material properties, both with depth and along the pavement length, and distortion in the deflection caused by passing traffic in the adjacent lanes.

On the other hand, systematic errors are introduced by bias; therefore, their effects may be eliminated by removing the source of the bias. Lytton et al. (*1*) have documented a number of systematic error sources. These sources include (a) erroneous assumptions made in the backcalculation process (e.g., the applicability of the static linear elastic approach), (b) a deviation of the contact pressure from a uniform distribution, and (c) a temporal variation in material properties within one layer caused by significant thermal and suction gradients.

Existing pavements are seldom perfectly flat; therefore, when the FWD falling mass strikes the base plate, uniform contact pressure may not be present under the plate. Furthermore, to achieve uniform contact pressure, the plate should be substantially flexible enough to deform and match the pavement surface. Recent studies by Touma et al. (*2*) and Uzan and Lytton (*3*) show that significant errors may result in the backcalculated layer moduli values if full contact between the base plate and pavement is not present.

**Nevada FWD Data Base**

NDOT is sponsoring a research project at the University of Nevada, Reno, to develop a customized overlay design procedure that takes into account the localized conditions that exist throughout the state. The overlay design procedure that is being developed uses a mechanistic-empirical approach in which pavement performance is predicted on the basis of stresses and strains induced in the pavement. As a part of this project, a total of 27 representative highway sites were selected for monitoring on the basis of factors such as climate, traffic, age, and type of construction. At each of the sites, the test section consists of a 1,000-ft highly uniform section on the outside traffic lane. The uniformity of the test sections was checked through coring and testing all of the layers in the pavement structure. Each test section was subdivided into 21 stations at 50-ft intervals, and FWD testing using Dynatest FWD model 8000 was performed for each of the four seasons for at least 2 years. Tests were carried out at four load levels varying from 6,000 lb to as much as 20,000 lb. The data base that was generated by this project is quite substantial.

**Variation in FWD Deflection Data**

The influence of the variation of the material properties can be somewhat reduced by performing FWD testing at finer intervals within a test section, but it cannot be totally eliminated. In this paper no attempt is made to quantify the influence of the individual error sources identified earlier. The influences of all of the error sources on the FWD measurements are lumped together, and the variability of the measurements within a uniform pavement section is statistically quantified as described later.

From the FWD data base described above, the deflection data collected for six sites that have a thin to medium-thick AC layer were selected for an in-depth study in this paper. The pavement section thicknesses at these sites and the dates of the FWD measurements are shown in Table 1. Only measurements that were obtained for two seasons in 1988 and 1989 (summer and winter) were considered in this paper. Typical deflection results obtained below the center of the plate (D-1) and at a point 55.1 in. from the plate (D-6) in August 1988 (summer) and February 1989 (winter) at Site 16 are shown in Figure 1. The deflections that correspond to the FWD load that is closest to 9,000 lb were selected and normalized to an FWD load of 9,000 lb.

The deflections can be seen to vary substantially within a test section. Among other reasons, one of the primary causes behind the variation in the deflection between the stations is the variability in the subgrade. This is because the other factors, such as the pavement cross section, construction method, and material types used at the site are the same. The winter and summer deflections are similar in shape; however, the summer values at D-1 (Figure 1 (*top*)) are higher, whereas the winter values at D-6 (Figure 1 (*bottom*)) are higher. This difference is because the deflection at D-1 is affected by the material properties of all the pavement layers, whereas the deflection at D-6 is affected by the properties of subgrade only. A histogram obtained for the deflection data at D-1 is presented in Figure 2. This histogram was obtained with an interval of 0.5 mils for August 1988. The histogram shows that the variation of deflection can, for practical purposes, be considered to be normally distributed. The mean, standard deviation, and coefficient of variation of the deflections of all the FWD sensors have been computed, and the values associated with the first five transducers are presented for all the sites in Table 2.

The mean deflection at Site 28 is substantially higher than that at other sites because this site has the lowest AC and base thicknesses. The coefficient of variation (COV) of deflections varies between 9.0 percent and as much as 40.8 percent. Generally, higher COV values occur for sensors located farther away from the center of the plate, where measured deflections are small.

**Proposed Monte Carlo Simulation Procedure**

It is clear from the previous discussion that the FWD deflections can vary substantially within a short distance and may be represented by a normal distribution. It was decided to use the Monte Carlo simulation approach to investigate the influence of the variation in the FWD deflection (*4,5*). The variables investigated in the study are the backcalculated pavement layer moduli and pavement performance parameters.

A random number generator routine that is available in a computer library generates random numbers with a uniform density; therefore it was not used in the study. Random num-

**TABLE 1 Details of Selected Test Sites and Dates of FWD Measurement**

| Site No. | FWD Measured Dates | A.C. thickness (in) | Base thickness (in) |
|---|---|---|---|
| 11 | 8-09-88 and 2-06-89 | 4.00 | 11.00 |
| 12 | 8-09-88 and 2-06-89 | 7.25 | 16.00 |
| 16 | 8-10-88 and 2-07-89 | 7.75 | 11.00 |
| 24 | 6-08-88 and 12-12-88 | 7.75 | 9.00 |
| 26 | 3-08-88 and 6-07-88 | 7.50 | 9.00 |
| 28 | 3-11-88 and 6-09-88 | 3.00 | 6.00 |

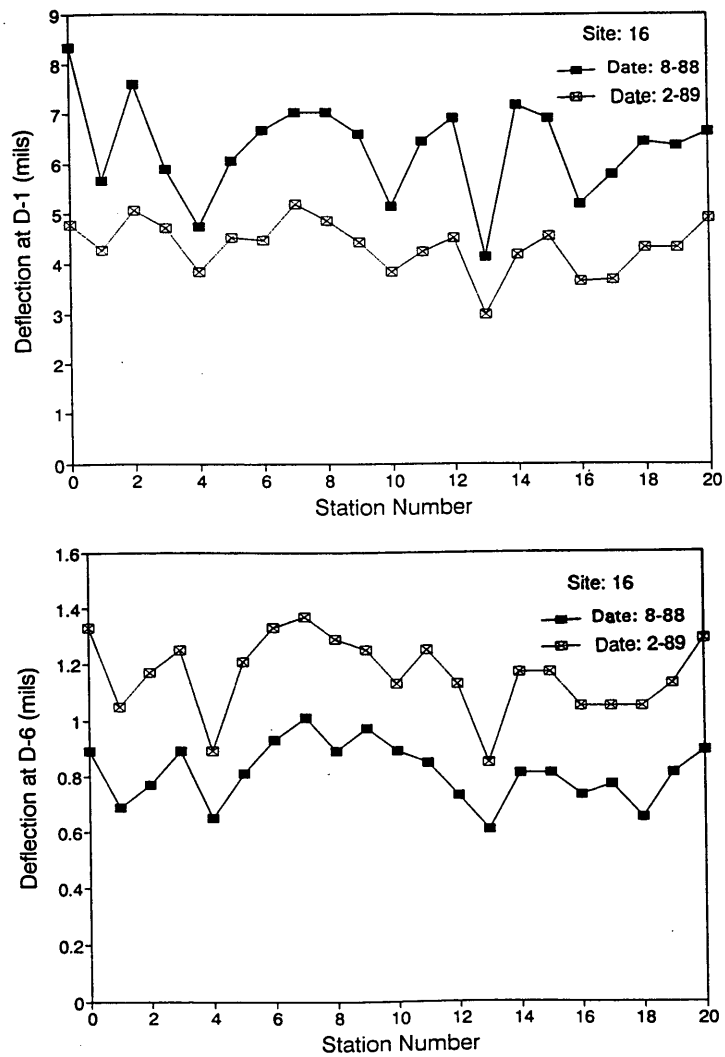


**FIGURE 1 Variation of D-1 (*top*) and D-6 (*bottom*) across Site 16.**

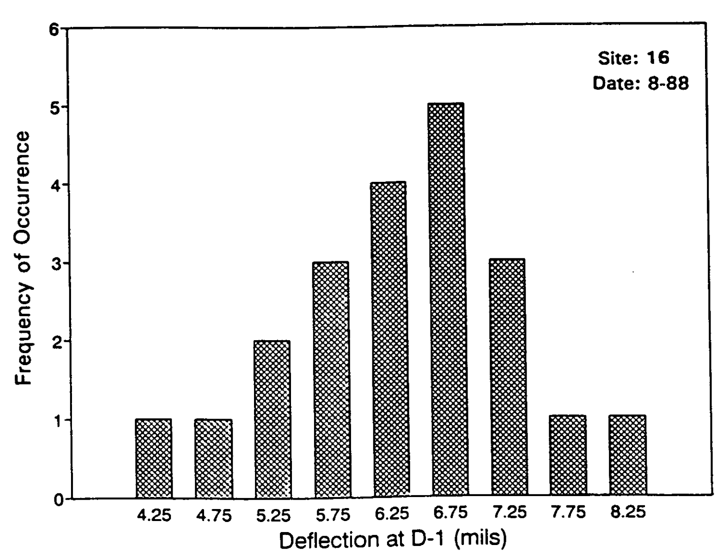


**FIGURE 2 Histogram of D-1 across Site 16.**

**TABLE 2 Summary of Mean and Standard Deviation of Measured Deflection for Selected Sites**

| Site | Date | Description | D1 | D2 | D3 | D4 | D5 |
|---|---|---|---|---|---|---|---|
| 11 | 8-88 | Mean | 5.81 | 4.02 | 2.94 | 1.18 | 0.69 |
| | | Std.Dev/C.O.V(%) | 0.67/11.5 | 0.59/14.7 | 0.51/17.2 | 0.26/22.3 | 0.13/19.5 |
| | 2-89 | Mean | 9.90 | 7.87 | 6.54 | 3.21 | 1.84 |
| | | Std.Dev/C.O.V(%) | 1.80/18.0 | 1.76/22.4 | 1.74/26.6 | 1.17/36.4 | 0.73/39.5 |
| 12 | 8-88 | Mean | 4.79 | 3.86 | 3.25 | 1.81 | 1.09 |
| | | Std.Dev/C.O.V(%) | 0.97/20.2 | 0.80/20.7 | 0.67/20.6 | 0.42/23.2 | 0.28/26.2 |
| | 2-89 | Mean | 4.33 | 3.60 | 3.10 | 1.84 | 1.21 |
| | | Std.Dev/C.O.V(%) | 1.41/32.7 | 1.10/30.6 | 0.85/27.1 | 0.50/27.1 | 0.36/29.5 |
| 16 | 8-88 | Mean | 6.65 | 5.04 | 4.15 | 2.43 | 1.57 |
| | | Std.Dev/C.O.V(%) | 0.99/14.8 | 0.78/15.5 | 0.67/16.1 | 0.42/17.3 | 0.26/16.5 |
| | 2-89 | Mean | 4.19 | 3.70 | 3.41 | 2.48 | 1.84 |
| | | Std.Dev/C.O.V(%) | 0.52/12.4 | 0.46/12.5 | 0.43/12.6 | 0.34/13.5 | 0.24/13.4 |
| 24 | 6-88 | Mean | 13.74 | 11.89 | 10.55 | 6.62 | 4.06 |
| | | Std.Dev/C.O.V(%) | 1.24/9.0 | 1.13/9.5 | 1.03/9.7 | 0.73/11.0 | 0.54/13.4 |
| | 12-88 | Mean | 9.25 | 8.30 | 7.61 | 5.38 | 3.67 |
| | | Std.Dev/C.O.V(%) | 0.89/9.6 | 0.82/9.8 | 0.78/10.1 | 0.62/11.5 | 0.49/13.4 |
| 26 | 3-88 | Mean | 8.12 | 7.24 | 6.63 | 4.82 | 3.33 |
| | | Std.Dev/C.O.V(%) | 1.27/15.6 | 0.91/12.6 | 0.82/12.4 | 0.54/11.2 | 0.36/10.9 |
| | 6-88 | Mean | 10.82 | 9.18 | 8.13 | 5.25 | 3.46 |
| | | Std.Dev/C.O.V(%) | 1.58/14.6 | 1.18/12.9 | 1.04/12.8 | 0.78/14.8 | 0.36/10.5 |
| 28 | 3-88 | Mean | 50.87 | 38.18 | 27.64 | 11.35 | 6.85 |
| | | Std.Dev/C.O.V(%) | 6.03/11.8 | 6.34/16.6 | 3.81/13.7 | 1.84/16.1 | 1.02/14.8 |
| | 6-88 | Mean | 51.26 | 38.60 | 28.23 | 11.42 | 6.80 |
| | | Std.Dev/C.O.V(%) | 6.21/12.1 | 4.71/12.2 | 3.70/13.0 | 1.82/15.9 | 1.15/16.9 |

bers with a normal distribution can be obtained using the following equation (*6,7*):

$$X = \sqrt{-2 \log (U)} \cos(2\pi V) \qquad (1)$$

where $U$ and $V$ are two independent random variables with uniform densities on [0,1]. $U$ and $V$ can be generated using the standard routines available in the computers. The variation of $X$ given by Equation 1 has a mean and a standard deviation of 0 and 1, respectively. Now the random variable $Z$ having a normal distribution with the mean of $\overline{Z}$ and a standard deviation of $\sigma$ can be obtained by using

$$Z = \overline{Z}X + \sigma \qquad (2)$$

This procedure was used to obtain all of the FWD sensor deflections independently for each site and each season using the means and standard deviations summarized in Table 2. In total, as many as 900 sets of deflection basins per case were generated for all 12 cases identified in Table 2. In each set, the sensor deflections were obtained independently of each other using Equations 1 and 2. Only the randomly generated deflections that fell within the mean ± standard deviation were used in the computations. Typical histograms obtained for Site 16 using the randomly generated deflections at D-1 and D-6 are shown in Figure 3. The variation indicated in Figure 3 (*top*) compares favorably with the measured variation in Figure 2; in addition, the mean of the deflections match with those given in Table 2.

## Results of Backcalculation Procedure

The deflection basins obtained using the Monte Carlo simulation procedure were used with the MODULUS program to backcalculate layer moduli (*1*). The input data for the MODULUS program include layer thicknesses, Poisson's ratio, $\nu$, for the layers, and estimated maximum and minimum resilient moduli values for the layers. These input parameters are shown in Figure 4. The sensor locations for D-1 through D-7 are located at 0, 7.9, 11.8, 23.6, 36.0, 55.1, and 70.9 in. from the center of the plate. The thickness of the subgrade layer is not required when using the MODULUS program because it is treated as an additional unknown variable. The program computes a series of deflection basins and tries to match the input deflection basin to arrive at the layer moduli

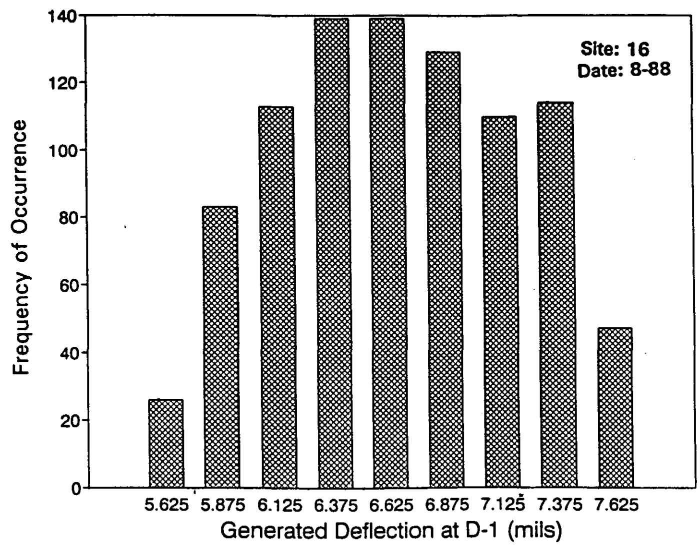


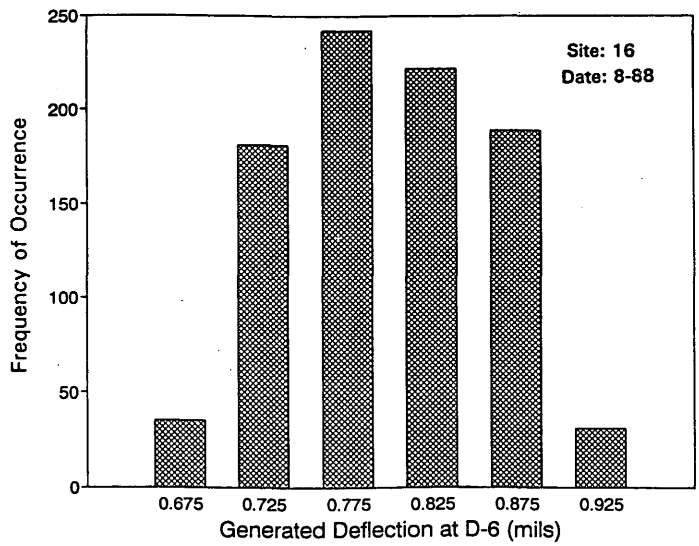


**FIGURE 3 Variation of randomly generated deflection at D-1 (900 values) (*top*) and D-6 (900 values) (*bottom*).**

values and the thickness of the subgrade. This program is much more efficient than other backcalculation programs and, in general, has been found to yield reasonable results.

Table 3 summarizes the backcalculated moduli values for all the sites and seasons considered in the study. The table gives results in terms of the mean, standard deviation, and coefficient of variation. Figure 5 shows the typical variation obtained for the AC resilient modulus at Site 16 (August 1988). These results clearly show that a substantial difference in the backcalculated moduli exists for the randomly generated deflection basins. In the case of AC and base, the coefficients of variation vary from 12 to as much as 65 percent. The coefficient of variation in the case of subgrade is smaller, varying between 5 and 13 percent. On the average, the mean AC modulus of thin pavement sections (Sites 11 and 28) is not affected by the seasonal variation. Site 16 showed the largest variation.

### Pavement Performance Parameters

Pavement performance criteria such as AC fatigue and pavement rutting can be investigated for anticipated traffic loadings of existing pavements using layered linear elastic models, with layer moduli obtained from FWD data. A comprehensive review of AC fatigue failure studies indicated that crack initiation in AC is related to the maximum tensile strain, $\varepsilon_a$, in the AC layer (*8,9*). Some models suggest that the AC modulus and the $\varepsilon_a$ are important factors that affect the AC fatigue life. However, the relative importance of the AC modulus is much less than that of the $\varepsilon_a$. The maximum tensile strain in medium-thick pavements occurs at the bottom of the AC layer.

The other major factor that affects pavement performance is surface rutting caused by permanent deformation in the pavement layers. Although the contribution of all the pave-

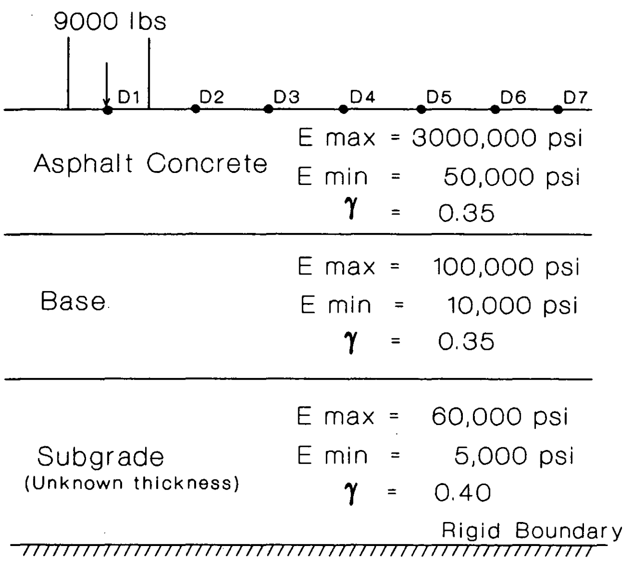


**FIGURE 4 Input data for MODULUS program.**

ment layers needs to be considered in rutting predictions, it is customary to pay the most attention to the contribution from the subgrade. This is because its contribution is frequently dominant. A number of widely used pavement rutting models use the maximum vertical compressive strain at the top of the subgrade, $\varepsilon_s$, as a measure of rutting in the subgrade (*9–11*). The design philosophy is that the pavement rutting can be reduced by controlling $\varepsilon_s$.

The backcalculated layer moduli values and the thickness of the subgrade given by the program MODULUS were input into the program NHELSYM5 to compute the pavement strains, $\varepsilon_a$ and $\varepsilon_s$ (*12*). This program, which is based on the well-known ELSYM5 program, is menu driven and user friendly. However, this program was further modified so that it can handle multiple data sets of layer properties. The single-axle dual-wheel configuration used with the modified NHELSYM5 program is shown in Figure 6. The tire pressures have substantially increased from 60 to 70 lb/in.$^2$ in the 1960s to as much as 90 to 120 lb/in.$^2$ in recent years (*11,13*). A value of 110 lb/in.$^2$ for the tire pressure was used in the computations. The strains $\varepsilon_a$ and $\varepsilon_s$ (principal strains) at the bottom of the AC layer and at the top of the subgrade, respectively, were computed at three vertical sections, as shown in Figure 6. These vertical sections are located along the center line of one tire midway between the centers of the tires and at the edge of a tire. Only the largest value out of these three values of $\varepsilon_a$ and $\varepsilon_s$ was noted and is presented in Table 4. All 900 cases per site per season that were considered in the backcalculations were used in the computations. Similar to earlier results, the variation in terms of the mean, standard deviation, and coefficient of variation are presented for all of the sites. Figure 7 presents a typical variation of $\varepsilon_a$ and $\varepsilon_s$ for Site 16 (August 1988).

A number of observations can be made from Table 4 and Figure 7. First, it appears that, except for Site 28, the strains strongly depend on the seasonal variation. This is mainly because Site 28 does not experience large environmental changes between the seasons for which the FWD measurements were made. Second, even though a large variation in the backcalculated moduli values was obtained [coefficient of variation (COV) as much as 65 percent], the COVs of the computed strain values are much lower with a maximum of 25 percent. The range of COV for both strains is between 8 and 25 percent. This means that the pavement strain computation is not very sensitive to variations in the pavement layer moduli. Third, the COV for the AC strain, $\varepsilon_a$, is much higher than the COV of the subgrade strain, $\varepsilon_s$. Finally, the strains developed for Site 28 are substantially larger than those obtained for the other sites. This can be traced to the substantially lower AC and base thicknesses at Site 28.

**TABLE 3 Backcalculated Resilient Moduli for Pavement Layers**

| Site | Date | Resilient Modulus of A.C (psi) | | | Resilient Modulus of Base (psi) | | | Resilient Mod. of Subgrade (psi) | | |
|---|---|---|---|---|---|---|---|---|---|---|
| | | Mean | Std. Dev | C.O.V (%) | Mean | Std. Dev | C.O.V (%) | Mean | Std. Dev | C.O.V (%) |
| 11 | 8-09-88 | 1,292,138 | 407,769 | 31.55 | 88,498 | 14,214 | 16.06 | 45,658 | 5822 | 12.75 |
| | 2-06-89 | 1,056,659 | 683,608 | 64.69 | 68,067 | 24,056 | 35.34 | 18,629 | 2629 | 14.11 |
| 12 | 8-09-88 | 895,965 | 357,775 | 39.93 | 92,074 | 13,565 | 14.73 | 19,292 | 2053 | 10.64 |
| | 2-06-89 | 1,378,614 | 727,555 | 52.77 | 94,484 | 15,795 | 16.71 | 19,180 | 2814 | 14.20 |
| 16 | 8-10-88 | 478,178 | 149,928 | 31.20 | 91,295 | 13,994 | 15.32 | 23,476 | 1509 | 6.42 |
| | 2-07-89 | 2,719,507 | 330,678 | 12.15 | 89,335 | 19,659 | 22.00 | 21,708 | 1759 | 8.00 |
| 24 | 6-08-88 | 454,426 | 138,486 | 30.47 | 32,485 | 17,490 | 53.84 | 7,712 | 575 | 7.45 |
| | 12-12-88 | 880,663 | 268,202 | 30.45 | 71,615 | 30,558 | 42.66 | 9,174 | 770 | 8.39 |
| 26 | 3-08-88 | 1,208,384 | 492,612 | 40.76 | 67,714 | 34,042 | 50.27 | 11,451 | 647 | 5.65 |
| | 6-07-88 | 583,480 | 283,299 | 48.55 | 61,773 | 29,722 | 48.11 | 9,722 | 520 | 5.34 |
| 28 | 3-11-88 | 267,919 | 155,529 | 58.05 | 18,482 | 9,517 | 51.49 | 5,549 | 296 | 5.33 |
| | 6-09-88 | 294,666 | 147,909 | 50.19 | 15,975 | 6,751 | 42.25 | 5,432 | 340 | 6.25 |

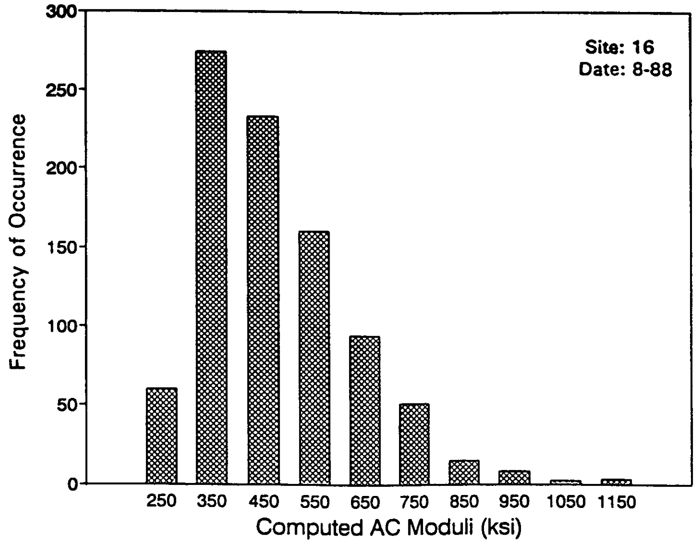


**FIGURE 5 Variation of backcalculated AC resilient moduli.**

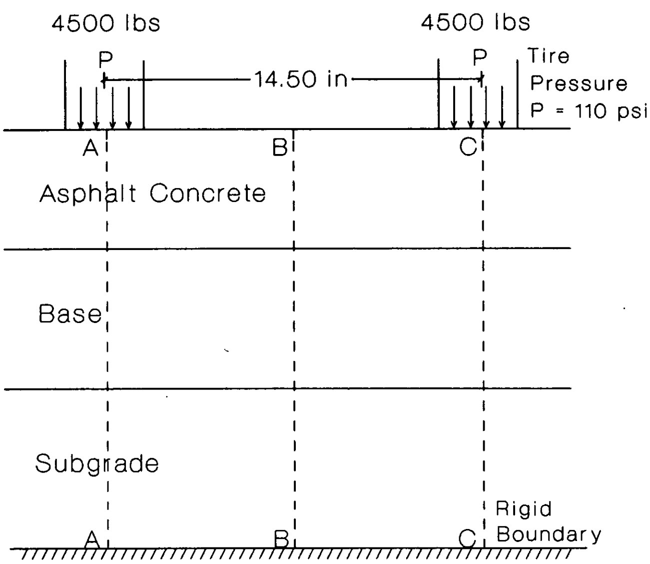


**FIGURE 6 Single-axle dual-wheel configuration used for pavement strain computations.**

### Consequence of the Variability in Pavement Strains

A number of fatigue failure models are reported in the literature (*14–16*). One of the most widely used models is that of Monismith and Epps (*16*), which can be written as

$$\log N_f = 14.82 - 3.291 \log(\varepsilon_a) - 0.854 \log (E_{AC}) \quad (3)$$

where $N_f$ is the number of cycles to fatigue failure (given in micro strain) and $E_{AC}$ is the asphalt concrete resilient modulus (in ksi). This equation can be rewritten as

$$N_f = a(\varepsilon_a)^b \quad (4)$$

where $a$ is a constant that depends on $E_{AC}$ and $b = -3.291$. The equation can be used to compare the relative increase (or decrease) in the number of load applications for various strain values.

Using a representative mean value of 100μ and a variation of ±10 percent for $\varepsilon_a$, the changes in the number of cycles to fatigue failure can be compared using Equation 4. The calculations reveal that the ±10 percent change in $\varepsilon_a$ corresponds to changes in the number of cycles of −27 and +41 percent, respectively.

Similar computations can be carried out for rutting using the Chevron equation (*10*). The Chevron equation gives the number of cycles, $N_r$, to cause a 0.75-in. rut depth as

$$N_r = 1.077 \times 10^{18} (\varepsilon_s)^{-4.483} \quad (5)$$

The $\varepsilon_s$ should be given in terms of micro strain. Using a representative mean value of 200μ and a variation of ±10 percent for $\varepsilon_s$, the changes in the number of cycles to cause rutting failure can now be computed using Equation 5. A ±10 percent change in $\varepsilon_s$ corresponds to changes in the number of loading cycles of −35 and +60 percent, respectively.

The changes in the number of loading cycles for both pavement failure models are substantial. This is because these models are sensitive to strain values.

## SUMMARY AND CONCLUSIONS

The FWD testing, which is a widely used NDT method, simulates traffic loading more closely than other NDT methods. The surface deflections measured by FWD testing are used to estimate pavement layer moduli values using a "backcalculation procedure." The pavement moduli values are, in turn, often used with pavement performance models to predict the remaining life of pavement sections. There are a

TABLE 4 Pavement Performance Strains Computed Using Modified NHELSYM5

| Site | Date | Max. Tensile Strain in AC (microns) | | | Max. Comp. Strain in Subgrade (microns) | | |
|---|---|---|---|---|---|---|---|
| | | Mean | Std. Dev | C.O.V(%) | Mean | Std. Dev | C.O.V(%) |
| 11 | 8-09-88 | 98.6 | 13.5 | 13.6 | - 145.2 | 12.0 | 8.3 |
| | 2-06-89 | 135.8 | 29.1 | 21.4 | - 273.2 | 23.6 | 8.6 |
| 12 | 8-09-88 | 62.9 | 10.2 | 16.3 | - 120.7 | 9.5 | 7.9 |
| | 2-06-89 | 51.2 | 12.6 | 24.6 | - 108.3 | 14.3 | 13.2 |
| 16 | 8-10-88 | 79.7 | 7.6 | 9.6 | - 158.5 | 8.8 | 5.6 |
| | 2-07-89 | 30.5 | 2.3 | 7.8 | - 88.6 | 6.4 | 7.2 |
| 24 | 6-08-88 | 141.6 | 11.9 | 8.4 | - 373.1 | 36.0 | 9.6 |
| | 12-12-88 | 74.3 | 6.4 | 8.6 | - 232.7 | 21.3 | 9.1 |
| 26 | 3-08-88 | 65.1 | 8.4 | 12.9 | - 196.4 | 28.6 | 14.5 |
| | 6-07-88 | 101.1 | 10.6 | 10.4 | - 286.9 | 32.4 | 11.3 |
| 28 | 3-11-88 | 660.3 | 132.2 | 20.0 | -1796.6 | 177.2 | 9.8 |
| | 6-09-88 | 682.4 | 116.5 | 17.0 | -1805.0 | 187.7 | 10.4 |

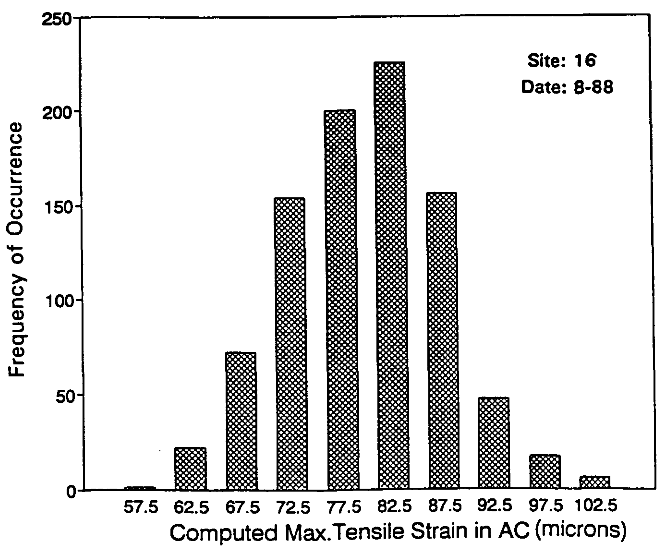


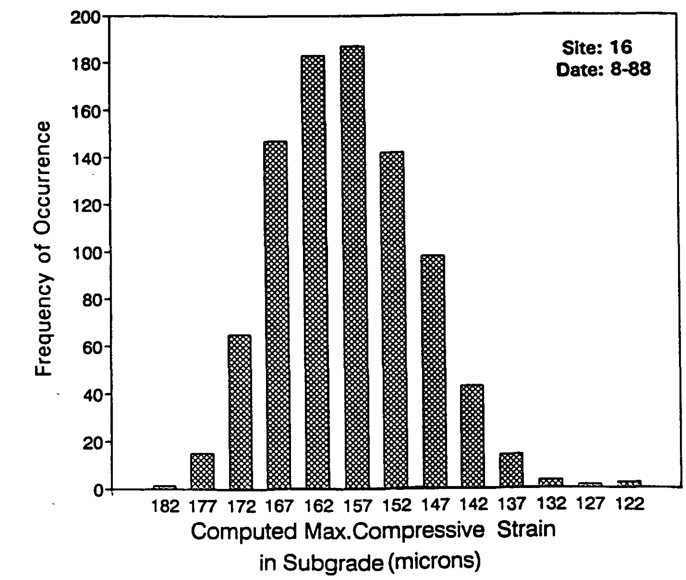


**FIGURE 7 Variation of maximum tensile strain in AC (*left*); variation of maximum compressive strain in subgrade (*right*).**

number of sources of error relative to FWD testing. These errors can be broadly divided into two types: systematic and random. Systematic errors include errors caused by assumptions made in the backcalculation process. Random errors are caused by, among other factors, deviations in sensor measurements, site variability, and passing traffic. Although they can be minimized by repeated testing and averaging, such errors cannot be totally eliminated. These error sources influence the FWD measurements taken even within a uniform pavement section. The study reported here investigates the influence of the variation in FWD deflection measurements on pavement moduli and pavement performance strain predictions.

As a part of the development of an overlay design procedure for Nevada, a total of 27 representative highway sites were selected and FWD tests were performed for each of the four seasons for at least 2 years. At each site, the test section consists of a 1,000-ft highly uniform pavement section, and FWD tests were carried out at 50-ft intervals. By selecting such fine testing intervals, the influence of the spatial variation in the material properties on the FWD measurements can be minimized. Deflection data from sites with thin to medium-thick pavements were selected to study the sensor deflection variability. The study reveals that the FWD measurements can be substantially influenced by the various error sources for all of the sites considered.

By varying the sensor deflections within its range, 900 sets of independent deflection basins using a random number generator with a normal distribution were obtained for the six selected sites and for two seasons. Backcalculation on these deflection basins was performed using the program MODULUS.

The data base of backcalculated moduli given by MODULUS for the generated deflection basins showed a substantial variation. In the case of AC and base, the coefficients of variation vary from 12 to as much as 65 percent. The coefficient of variation for subgrade is smaller, varying between 5 and 13 percent.

The pavement performance strains, such as the maximum tensile strain in the AC and the maximum compressive strain in the subgrade, were computed using a modified version of the computer program NHELSYM5. The backcalculated moduli and the subgrade thickness given by the program MODULUS were used as input. Even though the coefficient of variation was large for backcalculated moduli, the coefficients of variation of the computed strain were lower, with a maximum of 25 percent. The pavement performance strains were used to estimate the number of loading cycles required to cause pavement distress utilizing widely used pavement performance equations. This exercise suggests that the number of loading cycles to cause pavement distress is sensitive to pavement performance strains. This means that the variation in pavement strains caused by the variation in FWD measurements can have a substantial influence on the pavement life predictions.

Finally, the influence of other important factors such as the variation in the thickness of the AC and base have not been investigated in this paper. In the study, these thickness values, which were obtained from construction data and coring, were uniform across a test section. Studies investigating the influence of the changes in the thickness of the top layers may also be carried out using the proposed Monte Carlo approach.

## ACKNOWLEDGMENT

The research reported here was funded by a grant from the Nevada Department of Transportation, whose support is gratefully acknowledged.

## REFERENCES

1. R. L. Lytton, F. P. Germann, Y. J. Chou, and S. M. Stoffels. *NCHRP Report 327: Determining Asphaltic Concrete Pavement Structural Properties by Nondestructive Testing*. TRB, National Research Council, Washington, D.C., June 1990
2. B. E. Touma, J. A. Crovetti, and M. Y. Shahin. The Effects of Various Load Distributions on the Backcalculated Moduli Values in Flexible Pavements. Presented at 70th Annual Meeting of the Transportation Research Board, Washington, D.C., Jan. 1991.
3. J. Uzan and R. L. Lytton. Analysis of Pressure Distribution Under Falling Weight Deflectometer Loading. *Journal of Transportation Engineering*, ASCE, Vol. 116, No. 2, 1990, pp. 246–250.
4. I. A. Shreider. *The Monte-Carlo Method: The Method of Statistical Trials*. Pergamon Press, New York, 1966.
5. J. M. Hammerslay and D. C. Handscomb. *Monte-Carlo Methods*. John Wiley Publications, New York, 1964.
6. L. J. Snell. *Introduction to Probability*. Random House/Birkhouser Mathematics Series, New York, 1988.
7. M. Dwass. *Probability: Theory and Applications*. W. A. Benjamin Inc., New York, 1970.
8. M. Gomez and M. R. Thompson. *Mechanistic Design Concepts for Full Depth Asphalt Concrete Pavements*. Transportation Engineering Series, No. 41. University of Illinois, Urbana-Champaign, Aug. 1984.
9. *Research and Development of the Asphalt Institute's Thickness Design Manual (MS-1)*, 9th ed. Research Report 82-2. The Asphalt Institute, Aug. 1982.
10. L. E. Santucii. Thickness Design Procedure for Asphalt and Emulsified Asphalt Mixture. *Proc., 4th International Conference on the Structural Design of Asphalt Pavement*, University of Michigan, Ann Arbor, 1977, pp. 424–456.
11. O. K. Kim, C. A. Bell, and J. E. Wilson. Effect of Increased Truck Tire Pressure on Asphalt Concrete Pavement. *Journal of Transportation Engineering*, ASCE, Vol. 115, No. 4, July 1989, pp. 329–350.
12. R. Henry and C. Goodspeed. *NHELSYM5: Program for Pavement Analysis*. Department of Civil Engineering, University of New Hampshire, Oct. 1984.
13. D. R. Middleton, F. L. Roberts, and T. Chira-Chavala. Measurements and Analysis of Truck Tire Pressures in Texas Highways. In *Transportation Research Record 1070*, TRB, National Research Council, Washington, D.C., 1986, pp. 1–8.
14. A. A. Bu-Bushsait. *Development of a Flexible Pavement Fatigue Model for Washington State*. Ph.D. dissertation, University of Washington, Seattle, 1985.
15. P. S. Pell. *Special Report 140: Characterization of Fatigue Behavior: Structural Design of AC Pavements to Pavement Fatigue Cracking*. HRB, National Research Council, Washington, D.C., Jan. 1973.
16. C. C. Monismith and J. A. Epps. *Asphalt Mixture Behavior in Repeated Flexure*. Report TE-69-6. Institute of Transportation and Traffic Engineering, Berkeley, Calif., 1969.

# Correlation Between Backcalculated and Laboratory-Determined Asphalt Concrete Moduli

MUSTAQUE HOSSAIN AND LARRY A. SCOFIELD

Falling weight deflectometer (FWD) testing was done on eight test sections of an experimental overlay project in Arizona incorporating both virgin and recycled asphalt concrete mix and various overlay thicknesses as well as on a new pavement test section. The layer moduli were backcalculated by an elastic layer analysis program. Cores of the asphalt concrete layer retrieved from FWD test points were tested by ASTM Method D4123 to determine the resilient moduli. Visual distress surveys were also conducted on each test section in accordance with PAVER procedures, and pavement condition index (PCI) values were calculated. The results indicated that the laboratory-determined asphalt concrete moduli at individual test locations were not in good agreement with the backcalculated moduli. However, the average laboratory-determined moduli for sections with higher PCI values were close to the average backcalculated moduli. Linear regression between PCI values and average ratio of laboratory to backcalculated moduli indicated significant correlation between these two parameters. This shows that the condition of the existing pavement is a primary determinant in better agreement between laboratory-determined and backcalculated moduli. The finding was verified by comparing backcalculated asphalt concrete layer moduli from FWD test results on a new pavement section with the resilient moduli determined in the laboratory. It was found that the average backcalculated modulus of the asphalt concrete layer matches closely the average modulus of all the cores. It was recommended that the backcalculated asphalt concrete moduli instead of laboratory-determined moduli be used in rehabilitation design.

Nondestructive testing (NDT) is now widely recognized as an important tool for pavement structural evaluation. State-of-the-art NDT evaluation measures a pavement's deflection response to a known load. The load generated by an NDT device may be static (Benkelman beam), steady-state vibratory (Dynaflect and Road Rater) or impulse [falling weight deflectometer (FWD)]. Although surface deflection data analysis is a matter of continuing research, nondestructive testing for measuring surface deflection is accepted by most highway agencies as a standard practice. Currently, falling weight deflectometer has gained acceptance as the most developed deflection testing device for its ability to apply heavy load and to simulate actual truck traffic wheel loadings (*1–3*).

Deflections measured with an FWD are used to estimate the moduli of pavement layers. The pavement is modeled by a suitable approach, such as linear elastic theory or linear or nonlinear finite element methods. Moduli estimates are determined with a backcalculation technique. For a specific test load and pavement structure, computed deflections are compared with measured deflections. The moduli of the layers are varied until the computed and measured deflections are approximately equal. The surface layer and other asphaltic layer moduli thus obtained are modified to take into account the temperature at the time of testing. These moduli are then used to compute the effective structural capacity of the pavement according to a pavement design procedure such as the AASHTO guide (*4*).

Currently, a gap exists between analysis of the deflection data and application in practice. Part of the problem arises from the fact that there is no "guarantee" that the backcalculated layer moduli uniquely represent the in situ layer moduli. Ali and Khosla compared the backcalculated asphalt concrete moduli from several automated backcalculation schemes with laboratory resilient moduli (*5*). In general, good agreement was observed between the backcalculated layer moduli from two schemes and laboratory-determined asphalt concrete resilient moduli. Only four samples from two sites in North Carolina were used in their study. Also, the conditions of the pavements used in the study were not reported. Lee et al. reported a verification study of backcalculated layer moduli from an elastic layer analysis backcalculation program (*6*). Sixteen sites from the state of Washington were included in the study. Laboratory asphalt concrete resilient moduli were determined according to ASTM D4123 (*7*). In general, the backcalculated and laboratory asphalt concrete moduli ranged from being essentially similar to differing by over 400 percent. Overall, differences of 20 to 50 percent were common. Higher differences were found for sites with alligator and extensive longitudinal cracking. They also observed that the differences between the backcalculated and laboratory moduli were significantly less than the spatial variation of the layer moduli. Mamlouk et al. studied the correlation between the laboratory and backcalculated layer moduli for 19 sites in Arizona (*8*). The ratios of laboratory-determined asphalt concrete resilient moduli to backcalculated moduli varied from 0.07 to 0.70 with the mean ratio being 0.27. The coefficient of determination, $R^2$ value, for the linear regression between the laboratory and backcalculated moduli was found to be 0.002. Unfortunately the study did not include a detailed condition survey of the test sites, although the apparent discrepancy between the backcalculated and laboratory moduli was explained in terms of in situ pavement condition at the time

M. Hossain, Department of Civil Engineering, Seaton Hall, Kansas State University, Manhattan, Kans. 66506-2905. L. A. Scofield, Arizona Transportation Research Center, College of Engineering and Applied Sciences, Arizona State University, Tempe, Ariz. 85287.

of FWD testing. This paper addresses the correlation between laboratory-determined moduli of the asphaltic concrete layer and backcalculated layer moduli from FWD data collected on nine test sections in Arizona as a function of pavement condition.

## LAYOUT OF TEST SECTIONS AND DESCRIPTION

Eight test sections were selected from a project built in 1981 with virgin and recycled materials with various overlay thickness. The project is located in southwestern Arizona on Interstate 8. During a distress survey of this project in 1990, various sections exhibited various degrees of structural distress. Figure 1 shows the layout of the test sections and Figure 2 shows the structural sections. The existing new pavement section used in this study is on SR-87 in the Phoenix metropolitan area. This section was built in 1986 and currently shows no distress. Figure 2 also shows the structural section of this test section.

## DEFLECTION TESTING AND CORING

Deflection data were collected on each of the eight test sections on I-8 with a Dynatest 8000 FWD in May 1990. FWD tests on SR-87 were conducted during July 1990. Very high

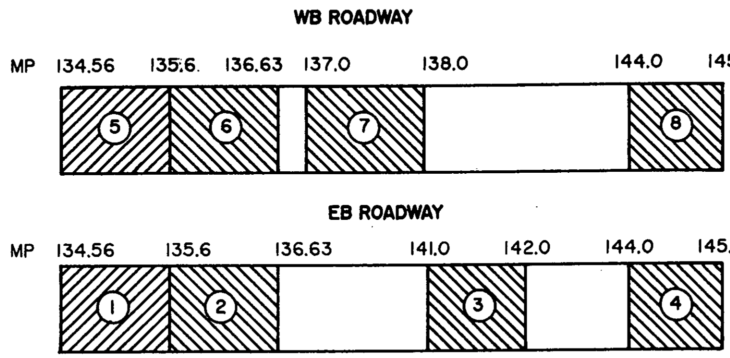


**FIGURE 1 Layout of test sections on I-8.**

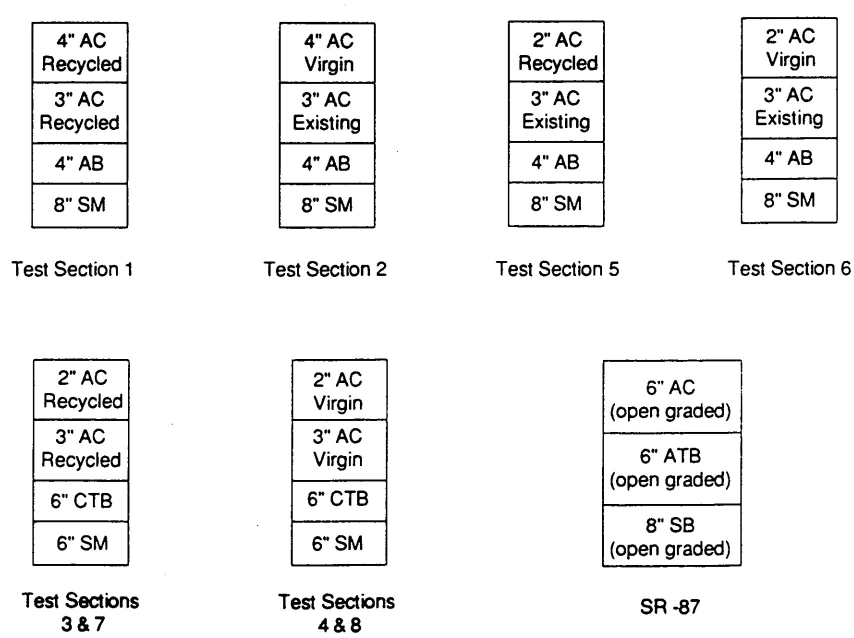


**Note: AC = Asphalt Concrete, AB = Aggregate Base, SM = Select Material/ Subbase**
**CTB = Cement Treated Base, ATB = Asphalt Treated Base, SB = Subbase**

**FIGURE 2 Pavement cross sections of test sections.**

pavement surface temperatures (up to 114°F) were encountered during most of the testings on I-8. Seven sensors were used, with the first sensor being at the center of the loading plate and six others at a uniform radial distance of 12 in. apart. Three drops of FWD load were used for target loadings of 6,000, 9,000 and 15,000 lb. Data were collected at five random locations on the outer wheel path of the travel lane for each section. Additional tests were also conducted in between-the-wheel-path locations for some sections. In total, FWD data were collected at 60 locations.

Cores of asphalt concrete were retrieved from the test points at each of the 60 locations. However, four cores were disintegrated during storage and handling. The cores were retrieved for the full depth of asphalt concrete layer.

## BACKCALCULATION ANALYSIS SCHEME

The FWD deflection data were used in a backcalculation scheme, BKCHEVM, to calculate the layer moduli. BKCHEVM is a microcomputer-based backcalculation program developed at Arizona State University (*8*). The program is a modification of the program CHEVDEF (*9*). The modifications have been relatively minor and designed primarily to simplify use and to improve convergence. In addition, the iterative scheme has been modified to obtain a closer match between measured and computed deflections for the inner three sensors so that a better estimate of asphalt concrete moduli is possible. Four distinct layers were assumed in the analysis and a rigid layer was introduced automatically (within the program) when it was judged appropriate, on the basis of the seventh-sensor deflection value. However, in this analysis no rigid bottom was encountered for any section. The default values of all the layer moduli were provided. The program yielded a solution in the form of a set of layer moduli whenever "convergence" was reached. If no convergence was possible, the "best-fit" set of layer moduli (based on the sum of errors of the computed deflections) was included as output (*8*).

BKCHEVM is part of the mechanistic overlay design procedure, CODA, being implemented by the Arizona Department of Transportation. In this study, the deflection basin corresponding to the second drop of FWD mass (with target load of 9,000 lb) was used in the backcalculation analysis. The asphalt concrete layer thickness used in backcalculation was determined from the core thickness at each location. Temperature correction was applied to the backcalculated asphalt concrete moduli using AASHTO (*4*) factors.

## LABORATORY TESTING

Asphalt concrete (AC) cores of the pavements for all sections with AC layer thickness greater than 4 in. were sliced to represent the top and bottom lifts in construction. The resilient moduli tests were performed at 104°F according to ASTM D4123 test procedures. This test temperature was selected because most of the FWD testing was done at a very high temperature. Also, the AASHTO temperature correction factors to be used were found to be very sensitive to higher temperatures (*10*). The backcalculated moduli on the test sections were also adjusted to 104°F using AASHTO temperature correction factors to compare with the laboratory-determined moduli. However, the resilient moduli tests on cores from SR-87 were conducted at 77°F. This temperature was used to minimize damage to the cores that were open graded asphalt concrete. The backcalculated moduli for the locations on SR-87 were adjusted to 77°F using AASHTO curves. Each specimen was tested at two positions (90 degrees apart) and at three different frequencies (1, 0.5, and 0.3 Hz) with a load duration of 0.1 sec. The applied load was between 90 and 120 lb, with the majority around 100 lb. The horizontal deformation was measured, and the resilient moduli computed assuming a Poisson ratio of 0.35 at 77°F and 0.40 at 104°F. For the test results of cores on I-8, both instantaneous and total resilient moduli were calculated and used in the analysis. The instantaneous and total resilient moduli of asphalt concrete cores on SR-87 were found to be essentially the same, and only instantaneous resilient moduli were used in the analysis. No frequency correction was applied to laboratory-determined resilient moduli to take into account the difference between the load duration of FWD and laboratory resilient moduli test load.

## PAVER CONDITION SURVEY

A PAVER condition survey was conducted on each test section during coring in May 1990 (*11*). Approximately 30 percent of the area in each test section was surveyed. The survey consisted of observing 19 distress types on asphalt concrete pavements on 200-ft sample units, at a rate of eight or nine for each section. The sample units contain most of the FWD test locations. The sample units were chosen systematically on each section, with the first sample unit being chosen at random. Five rut depth measurements were taken on each sample unit at 50-ft intervals. The predominant distresses were found to be alligator cracking, block cracking, and longitudinal and transverse cracking and weathering. Pavement condition index (PCI) was calculated for each sample unit using the Micro-PAVER program. Rutting was omitted from the calculation of PCI because of the difficulty in defining the actual rutted area. Also, cracking was considered to be the predominant distress type affecting FWD deflection test results. Table 1 summarizes the results of the PAVER survey for each test section. From the results it is evident that, once rutting is ignored, the load-associated deduct values dominate the PCI values for each test section.

## ANALYSIS AND RESULTS

### Test Sections 1 and 2

FWD testing was conducted at five locations in the outer-wheel-path and three locations in between-wheel-path locations in Sections 1 and 2. Resilient moduli testing was performed on the cores taken from the FWD test locations. The cores were sliced into two halves and each half was tested. The reported values are the average of two test results. Table 2 shows the comparison of the backcalculated and laboratory-determined instantaneous resilient moduli. The testing frequencies were

**TABLE 1 PAVER Survey Results**

| Test Section | PCI* Mean | PCI* S.D. | PCI* C.V. | Load Assoc. Deduct Values | Climate Assoc. Deduct Values | Other Deduct Values | Average Rut Depth (in) |
|---|---|---|---|---|---|---|---|
| 1,EB | 71 | 12 | 17 | 44 | 41 | 15 | 0.50 |
| 2,EB | 69 | 13 | 19 | 50 | 45 | 5 | 0.40 |
| 3,EB | 50 | 12 | 24 | 58 | 42 | 0 | 0.20 |
| 4,EB | 32 | 18 | 56 | 68 | 31 | 1 | 0.20 |
| 5,WB | 37 | 12 | 32 | 66 | 34 | 0 | 0.20 |
| 6,WB | 41 | 17 | 42 | 62 | 38 | 0 | 0.15 |
| 7,WB | 38 | 16 | 43 | 46 | 54 | 0 | 0.25 |
| 8,WB | 15 | 13 | 84 | 56 | 43 | 1 | 0.25 |

* excluding rutting

**TABLE 2 Comparison of Backcalculated and Laboratory AC Moduli for Test Sections 1 and 2**

| MP Location | Backcalc Modulus | Lab Modulus (1 Hz) | Ratio (lab/back) | Lab Modulus (0.3 Hz) | Ratio (lab/back) |
|---|---|---|---|---|---|
| (a) Test Section 1 | | | | | |
| 134.58 | 576 | 265 | 0.46 | 265 | 0.46 |
| 134.62 | 459 | 581 | 1.27 | 506 | 1.10 |
| 134.88 | 483 | 261 | 0.54 | 254 | 0.53 |
| 135.28 | 1200 | 350 | 0.29 | 313 | 0.26 |
| 135.36 | 800 | 190 | 0.24 | 213 | 0.27 |
| 134.58C | 576 | 607 | 1.05 | 537 | 0.93 |
| 134.66C | 833 | 579 | 0.70 | 549 | 0.66 |
| 134.79C | 565 | 619 | 1.10 | 600 | 1.06 |
| Mean | | | 0.70 | | 0.66 |
| $R^2$ (Linear Regression) | | 0.05 | | 0.05 | |
| (b) Test Section 2 | | | | | |
| | 0 | 234 | 0.26 | 225 | 0.25 |
| 135.76 | 294 | 425 | 1.45 | 317 | 1.08 |
| 136.03 | 951 | 119 | 0.13 | 207 | 0.22 |
| 136.17 | 542 | 311 | 0.57 | 302 | 0.56 |
| 136.46 | 244 | 381 | 1.56 | 396 | 1.62 |
| 135.65C | 233 | 117 | 0.50 | 106 | 0.45 |
| 135.82C | 400 | 368 | 0.92 | 333 | 0.83 |
| 136.06C | 435 | 409 | 0.94 | 344 | 0.79 |
| Mean | | | 0.79 | | 0.73 |
| $R^2$ (Linear Regression) | | 0.23 | | 0.08 | |

Note: C indicates between wheel path location

1 Hz and 0.3 Hz. It is evident that the between-wheel-path locations show better agreement between backcalculated and laboratory-determined moduli. The average ratios of laboratory-determined moduli to backcalculated moduli for Sections 1 and 2 were found to be 0.70 and 0.79, respectively. The ratios vary from as low as 0.13 to as high as 1.62. The PCI values ranged between 58 and 85, with a mean value of 71 for Section 1. The general rating of the section is very good. The percentage of load-related deduct values was 44 percent, and that for climate/durability was 41 percent. For Section 2, the mean PCI value was 69 with a range from 39 to 83; which was rated as good. The percentages of load-associated and climate-associated deduct values for this section were similar to those for Section 1 and were 50 percent and 45 percent, respectively. Distresses found on these two sections were alligator, block, longitudinal, and transverse cracking and weathering. Test Section 2 also showed a very high amount of rutting. The mean rut depth was 0.48 in., with ranges between 0.39 and 0.62 in.

## Test Sections 3 and 4

Test Sections 3 and 4 have 2-in. overlays over 3-in. mill and replace sections. FWD testing was done at five locations at the outer-wheel-path locations in both sections. Resilient modulus testing was done on the cores taken from the FWD test locations. The cores were sliced into two halves to represent the top and bottom layers of the existing pavement, and testing was done on each half. The reported results represent the average of two values. Table 3 shows the comparison of the backcalculated and laboratory-determined instantaneous resilient moduli. The testing frequencies were 1 Hz and 0.3 Hz. The average ratios of laboratory-determined moduli (at 1 Hz) to backcalculated moduli were found to be 1.70 and 2.33, respectively. The ratios vary from as low as 0.42 to as high as 4.76. For Section 3, the PCI values ranged between 20 and 67, with a mean value of 50. The general rating of the section is fair. The percentage of load-related deduct values was 58 percent and that for climate/durability was 42 percent. For Section 4, the mean PCI value was 32 with a range from 13 to 60; it was rated as poor. The percentages of load-associated and climate-associated deduct values for this section were 68 percent and 31 percent, respectively. Distresses found on these two sections were alligator, block, longitudinal, and transverse cracking and weathering. The amount and severity of alligator cracking on these sections were much higher than on Sections 1 and 2.

## Test Sections 5 and 6

Test Sections 5 and 6 have 2-in. overlays over the 3-in. existing AC pavements. The sections are in the westbound roadway. FWD testing was conducted at five locations in the outer wheel path and at one location between the wheel path for both sections. Resilient moduli testing was performed on the cores taken from the FWD test locations for the overlay layer only. Because of disintegration of the cores from the existing AC layer, this layer could not be tested. Table 4 shows the

**TABLE 3 Comparison of Backcalculated and Laboratory AC Moduli for Test Sections 3 and 4**

| MP Location | Backcalc Modulus | Lab Modulus (1 Hz) | Ratio (lab/back) | Lab Modulus (0.3 Hz) | Ratio (lab/back) |
|---|---|---|---|---|---|
| (a) Test Section 3 | | | | | |
| 141.06 | 522 | 742 | 1.42 | 989 | 1.89 |
| 141.26 | 209 | 613 | 2.93 | 523 | 2.50 |
| 141.54 | 1610 | 773 | 0.48 | 747 | 0.46 |
| 141.87 | 420 | 1355 | 3.23 | 1579 | 3.76 |
| 141.94 | 1325 | 552 | 0.42 | 528 | 0.40 |
| Mean | | | 1.70 | | 1.80 |
| $R^2$ (Linear Regression) | | 0.09 | | 0.12 | |
| (b) Test Section 4 | | | | | |
| 144.22 | 664 | 751 | 1.13 | 704 | 1.06 |
| 144.50 | 465 | 881 | 1.89 | 723 | 1.55 |
| 144.53 | 502 | 340 | 0.68 | 493 | 0.98 |
| 144.60 | 174 | 597 | 3.43 | 643 | 3.70 |
| 144.91 | 148 | 665 | 4.49 | 641 | 4.33 |
| Mean | | | 2.33 | | 2.32 |
| $R^2$ (Linear Regression) | | 0.01 | | 0.006 | |

**TABLE 4 Comparison of Backcalculated and Laboratory AC Moduli for Test Sections 5 and 6**

| MP Location | Backcalc Modulus | Lab Modulus (1 Hz) | Ratio (lab/back) | Lab Modulus (0.3 Hz) | Ratio (lab/back) |
|---|---|---|---|---|---|
| (a) Test Section 5 | | | | | |
| 134.68 | 155 | 550 | 3.55 | 501 | 3.23 |
| 134.78 | 153 | 485 | 3.17 | 417 | 2.73 |
| 135.15 | 314 | 250 | 0.80 | 250 | 0.74 |
| 135.20 | 242 | 414 | 1.71 | 386 | 1.60 |
| 135.30 | 230 | 335 | 1.46 | 406 | 1.77 |
| 134.68C | 145 | 722 | 4.98 | 802 | 5.53 |
| Mean | | | 2.61 | | 2.60 |
| $R^2$ (Linear Regression) | | 0.72 | | 0.57 | |
| (b) Test Section 6 | | | | | |
| 135.76 | 612 | 324 | 0.53 | 271 | 0.44 |
| 135.80 | 455 | 285 | 0.63 | 255 | 0.56 |
| 135.85 | 980 | 756 | 0.77 | 637 | 0.65 |
| 136.14 | 1138 | 285 | 0.25 | 255 | 0.22 |
| 136.51 | 2258 | 740 | 0.33 | 773 | 0.34 |
| 136.958C | 430 | 692 | 1.61 | 653 | 1.52 |
| Mean | | | 0.69 | | 0.62 |
| $R^2$ (Linear Regression) | | 0.18 | | 0.28 | |

Note: C indicates between wheel path location

comparison of the backcalculated and laboratory-determined instantaneous resilient moduli. The testing frequencies were 1 Hz and 0.3 Hz. The average ratios of laboratory-determined moduli (at 1 Hz) to backcalculated moduli for Sections 5 and 6 were found to be 2.61 and 0.69, respectively. The ratios vary from as low as 0.22 to as high as 5.53. For Section 5, the PCI values ranged between 23 and 50, with a mean value of 37. The general rating of the section is poor. The percentage of load-related deduct values was 66 percent and that for climate/durability was 34 percent. For Section 6, the mean PCI value was 41 with a range from 17 to 66. It was also rated as poor. The percentages of load-associated and climate/durability-associated deduct values were similar to those for Section 5.

### Test Sections 7 and 8

Test sections 7 and 8 have the same structural sections as Test Sections 3 and 4 but are located in the westbound direction. FWD testing was conducted at five locations on the outer wheel path. Resilient moduli testing was performed on the cores taken from the FWD test locations. The testing was done on the cores sliced into two halves. The reported laboratory-determined moduli represent the average of the moduli determined on the top and bottom half of the cores. Table 5 shows the comparison of the backcalculated and laboratory-determined instantaneous resilient moduli. The testing frequencies were 1 Hz and 0.3 Hz. The average ratios of laboratory-determined moduli (at 1 Hz) to backcalculated moduli for Sections 7 and 8 were found to be 2.02 and 2.97, respectively. The ratios vary from 1.10 to 4.16. The PCI values for Section 7 ranged between 4 and 61, with a mean value of 38. The general rating of the section is poor. The percentage of load-related deduct values was 46 percent and that for climate/durability was 54 percent. For Section 8, the mean PCI value was 15 with a range from 0 to 29. It was rated as very poor. Extensive high-severity alligator cracking was responsible for the poor rating of this section.

## COMPARISON OF LABORATORY-DETERMINED AND BACKCALCULATED MODULI

As mentioned earlier, FWD testing was conducted on a test section on SR-87 in the outer wheel path at four locations and in between-wheel-path locations at three places. The cores were taken from the FWD test locations. This pavement has an existing 6-in.-thick open graded asphalt concrete layer. The cores were sliced into two halves, and resilient moduli testing was conducted at 77°F on each half. The reported asphalt concrete moduli are the average of the resilient moduli determined on each half. Table 6 shows the comparison of backcalculated and laboratory-determined asphalt concrete

**TABLE 5 Comparison of Backcalculated and Laboratory AC Moduli for Test Sections 7 and 8**

| MP Location | Backcalc Modulus | Lab Modulus (1 Hz) | Ratio (lab/back) | Lab Modulus (0.3 Hz) | Ratio (lab/back) |
|---|---|---|---|---|---|
| (a) Test Section 7 | | | | | |
| 137.30 | 339 | 673 | 1.99 | 780 | 2.30 |
| 135.55 | 420 | 1600 | 3.81 | 1916 | 4.56 |
| 137.80 | 312 | 591 | 1.89 | 563 | 1.80 |
| 137.91 | 496 | 644 | 1.30 | 588 | 1.19 |
| 137.95 | 536 | 595 | 1.11 | 465 | 0.87 |
| Mean | | | 2.02 | | 2.14 |
| $R^2$ (Linear Regression) | | 0.0 | | 0.016 | |
| (b) Test Section 8 | | | | | |
| 144.25 | 185 | 769 | 4.16 | 749 | 4.05 |
| 144.47 | 410 | 778 | 1.90 | 747 | 1.82 |
| 144.82 | 303 | 834 | 2.75 | 765 | 2.52 |
| 144.93 | 410 | 778 | 1.90 | 747 | 1.82 |
| 144.98 | 185 | 769 | 4.16 | 749 | 4.05 |
| Mean | | | 2.97 | | 2.85 |
| $R^2$ (Linear Regression) | | 0.03 | | 0.01 | |

moduli. As evident from the table, the individual backcalculated moduli were different; the average ratio of backcalculated moduli to laboratory moduli was very close to unity (0.82 to 0.91). The coefficient of determination of linear regression between these two sets of moduli was 0.06. The project was surveyed for distresses in 1990 during the FWD testing. The survey was conducted as per PAVER, but no visible distresses were evident. The PCI value was computed to be 95, and the rating of this section was excellent. It is clear that although the correlation between the laboratory-determined and backcalculated AC moduli is poor, the average ratio is close to unity. The agreement between backcalculated and laboratory-determined AC moduli was similar for both outer-wheel-path and between-wheel-path locations.

## EFFECT OF PAVEMENT CONDITION

The data indicate that there is an apparent relationship between pavement condition and the average ratio of laboratory-

**TABLE 6 Comparison of Backcalculated and Laboratory AC Moduli for Test Section on SR-87**

| Station Location | Backcalc Modulus | Lab Modulus (1 Hz) | Ratio (lab/back) | Lab Modulus (0.3 Hz) | Ratio (lab/back) |
|---|---|---|---|---|---|
| 115+00 | 1053 | 815 | 0.77 | 748 | 0.71 |
| 121+00 | 720 | 1017 | 1.41 | 1034 | 1.44 |
| 126+00 | 1323 | 1125 | 0.85 | 780 | 0.59 |
| 134+00 | 864 | 1111 | 1.29 | 982 | 1.14 |
| 118+00C | 883 | 486 | 0.55 | 473 | 0.54 |
| 126+00C | 1276 | 818 | 0.64 | 666 | 0.52 |
| 136+00C | 702 | 703 | 1.00 | 614 | 0.87 |
| Mean | | | 0.91 | | 0.82 |
| $R^2$ (Linear Regression) | | 0.06 | | 0.03 | |

Note: C indicates between wheel path location

determined moduli to backcalculated asphalt concrete moduli. Table 7 shows the average ratio of backcalculated to laboratory-determined asphalt concrete moduli (at 1 Hz) and average PCI for all the sections included in the study. It is apparent that the higher the PCI value for a section, the better the agreement between the average laboratory-determined and the average backcalculated asphalt concrete moduli. However, the surface distresses may be limited to the top few inches of an asphaltic layer. The existing new pavement showed the best agreement between average backcalculated and average laboratory-determined asphalt concrete moduli. A linear regression analysis was conducted between the average PCI values of the sections and the average ratio of laboratory-determined and backcalculated asphalt concrete moduli. The coefficient of determination, $r_2$, was found to be 0.60. Student's *t*-test conducted on the correlation coefficient of these two variables confirmed significant correlation at 5 percent level of significance.

For pavements with lower PCI, the laboratory-determined moduli are usually higher than the backcalculated moduli. In the backcalculation process, the entire asphaltic concrete layer consisting of various sublayers was lumped into a single layer of an "equivalent" layer (*8*). However, in the laboratory, only intact samples from the layers were tested. Thus, for a pavement with poor surface condition, deflection tests capture the response of the pavement with surface distresses, whereas in the laboratory, the uncracked distress-free samples of the same pavement are tested. Testing these samples results in a higher ratio of laboratory to backcalculated moduli for pavements with lower PCI. Because the FWD captures the response of the entire pavement to the applied load, the backcalculated moduli from FWD data are more representative of the in situ layer moduli than laboratory-determined moduli on samples taken from crack-free areas of the pavement. Again, in the backcalculation process, a "homogeneous" asphaltic concrete layer was assumed. But, when the pavement

**TABLE 7 Relationship Between Ratio of Backcalculated to Laboratory-Determined Moduli and PCI**

| Section | Avg. Ratio | Avg. PCI | Pavement Rating |
|---|---|---|---|
| 1 | 0.70 | 71 | Very Good |
| 2 | 0.79 | 69 | Good |
| 3 | 1.70 | 50 | Fair |
| 4 | 2.33 | 32 | Poor |
| 5 | 2.61 | 37 | Poor |
| 6 | 0.69 | 41 | Poor |
| 7 | 2.02 | 38 | Poor |
| 8 | 2.85 | 15 | Very Poor |
| SR 87 | 0.91 | 95 | Excellent |

Note: $R^2$ (Linear Regression) = 0.6035

**TABLE 8 Comparison of Instantaneous and Total Resilient Moduli**

| Test | Inst E/Back E (@1 Hz) | Inst E/Back E (@0.3 Hz) | Total E/Back E (@1 Hz) | Total E/Back E (@0.3 Hz) |
|---|---|---|---|---|
| 1 | 0.70 | 0.66 | 0.59 | 0.60 |
| 2 | 0.79 | 0.73 | 0.78 | 0.73 |
| 3 | 1.70 | 1.80 | 1.53 | 1.34 |
| 4 | 2.33 | 2.32 | 1.71 | 1.95 |
| 5 | 2.61 | 2.60 | 2.19 | 2.14 |
| 6 | 0.69 | 0.62 | 0.62 | 0.61 |
| 7 | 2.02 | 2.14 | 1.74 | 1.55 |
| 8 | 2.97 | 2.85 | 2.65 | 2.78 |
| Mean | 1.73 | 1.72 | 1.48 | 1.46 |

is cracked, this assumption is fully violated. This homogeneity of a pavement section may be the contributing factor for the apparent agreement of average backcalculated and laboratory-determined AC resilient moduli for the new pavement section.

## INSTANTANEOUS VERSUS TOTAL RESILIENT MODULI OF ASPHALT CONCRETE

The instantaneous resilient modulus value of asphalt concrete is calculated using the recoverable deformation that occurs instantaneously during the unloading portion in one cycle of ASTM D4123. The total resilient modulus is calculated using the total recoverable deformation that includes both instantaneous recoverable and the time-dependent continuing recoverable deformation during the unloading and rest period portion of one cycle. There is considerable disagreement among the researchers as to which moduli are more representative. In this study, both moduli were correlated with the backcalculated layer moduli from FWD data for the eight test sections used in the study. Table 8 shows the average ratio of laboratory-determined to backcalculated asphalt concrete moduli. On the basis of the analysis of this set of data, it appears that the use of total resilient moduli provides a better correlation with the backcalculated layer moduli.

## VIRGIN VERSUS RECYCLED MATERIALS

Comparison was also made between the average ratio of laboratory-determined to backcalculated asphalt concrete moduli (at 1 Hz) of virgin and recycled overlays. Table 9 shows the ratios. The ratios are comparable for the two types of materials. The table also shows the ratios for overlays on both existing and mill and replaced sections. In general, the ratio of laboratory-determined to backcalculated moduli is higher for sections with mill and replace.

## CONCLUSIONS

On the basis of this study, the following conclusions can be drawn:

1. The average backcalculated asphalt concrete moduli for a section compares favorably with the average laboratory-determined moduli when the condition of the pavement is good. However, the backcalculated and laboratory-determined moduli are different at individual locations. Pavement condition is a primary determinant for good agreement between backcalculated and laboratory-determined moduli.
2. The FWD testing captures the response of the entire pavement to the applied load. Since FWD deflection testing is usually done for evaluating existing pavements, backcalculated asphalt concrete moduli can more realistically represent the in situ moduli of the asphalt concrete layer. This conclusion appears to be validated by the better agreement between backcalculated and laboratory-determined asphalt concrete moduli for new pavements and also for distress-free pavements in between-wheel-path locations on old pavements.

## RECOMMENDATIONS

This study shows that the backcalculated asphalt concrete moduli from FWD test results on existing pavements can represent more realistically the in situ layer moduli and should be used in pavement rehabilitation design. It is recommended that the backcalculated asphalt concrete moduli from FWD deflection testing for a certain analysis section be used in the mechanistic overlay design process. The backcalculated asphalt concrete moduli are more representative of in situ conditions than laboratory-determined asphalt concrete moduli on cores from existing pavements.

## ACKNOWLEDGMENTS

The authors wish to acknowledge the financial help for this study from the Arizona Transportation Research Center. The

**TABLE 9 Comparison of Backcalculated and Laboratory AC Moduli for Virgin and Recycled Overlays**

| Virgin Overlays | | | Recycled Overlay | | |
|---|---|---|---|---|---|
| 2 inches | | 4 inches | 2 inches | | 4 inches |
| 3" mill | Existing | | 3" mill | Existing | |
| 4 EB<br>8 WB | 6 WB | 2 EB | 3 EB<br>7 WB | 5 WB | 1 EB |
| 2.3 | 0.7 | 0.79 | 1.7 | 2.6 | 0.7 |
| 2.9 | | | 2.0 | | |

Note: Numbers on the body of the table indicate ($E_{lab}$/ $E_{backcalc}$)

PAVER survey was done by Sylvester Kalevela and Gregory Rollins of Arizona Transportation Research Center. Resilient moduli testing was done at the Highway Materials Laboratory of the Arizona State University. The assistance of M. S. Mamlouk in this regard is highly appreciated.

## REFERENCES


1. P. Ullidtz. *Pavement Analysis.* Elsvier, New York, 1987.
2. O. Tholen, J. Sharma, and R. L. Terrel. Comparison of Falling Weight Deflectometer with Other Deflection Testing Devices. In *Transportation Research Record 1007*, TRB, National Research Council, Washington, D.C., pp. 20–26.
3. M. S. Hoffman and M. R. Thompson. A Comparative Study of Selected Nondestructive Testing Devices. In *Transportation Research Record 852*, TRB, National Research Council, Washington, D.C., 1982, pp. 32–42.
4. *AASHTO Guide for Design of Pavement Structures.* AASHTO, Washington, D.C., 1986.
5. N. A. Ali and N. P. Khosla. Determination of Layer Moduli Using a Falling Weight Deflectometer. In *Transportation Research Record 1117*, TRB, National Research Council, Washington, D.C., 1987, pp. 1–10.
6. S. W. Lee, J. P. Mahoney, and N. C. Jackson. A Verification of Backcalculation of Pavement Moduli. Presented at 67th Annual Meeting of the Transportation Research Board, Washington, D.C., 1988.
7. *Road and Paving Materials: Pavement Management Technologies.* Annual Book of ASTM Standards, Section 4, Vol. 04.03. ASTM, Philadelphia, 1990.
8. M. S. Mamlouk, W. N. Houston, S. L. Houston, and J. P. Zaniewski. *Rational Characterization of Pavement Structures Using Deflection Analysis*, Vol. 1. Report FHWA-AZ88-254. Arizona Department of Transportation, Phoenix, 1988.
9. A. J. Bush III and D. R. Alexander. Pavement Evaluation Using Deflection Basin Measurements and Layered Theory. In *Transportation Research Record 1022*, TRB, National Research Council, Washington, D.C., 1985, pp. 16–22.
10. A. S. M. M. Hossain and J. P. Zaniewski. *Variability in Estimation of Structural Capacity of Existing Pavements from Falling Weight Deflectometer Data.* Report AZ-SP-9001. Arizona Department of Transportation, Phoenix, 1990.
11. M. Shahin and S. D. Kohn. *Pavement Maintenance Management for Roads and Parking Lots.* Technical Report M-294. Construction and Engineering Research Laboratory, Champaign, Ill., 1981.


*The contents of this paper reflect the views of the authors, who are responsible for the facts and the accuracy of the data presented herein. The contents do not necessarily reflect the official views or policies of the Arizona Department of Transportation or FHWA. The U.S. government and the state of Arizona do not endorse products or manufacturers.*

# Layer Moduli from Deflection Measurements: Software Selection and Development of Strategic Highway Research Program's Procedure for Flexible Pavements

G. R. RADA, C. A. RICHTER, AND P. J. STEPHANOS

Deflection basin measurements on flexible pavements for the purpose of structural capacity evaluation are a key component of the Strategic Highway Research Program's (SHRP's) Long-Term Pavement Performance monitoring program. In the near term, SHRP will apply a backcalculation procedure to these deflection measurements to estimate the in situ elastic moduli of the pavement layer materials. Because a standard method for evaluating the structural capacity of flexible pavements from deflection data does not presently exist, SHRP has undertaken a study to develop a layer moduli backcalculation procedure for use in the initial analysis of the SHRP deflection data. This procedure covers not only the software but also the rules, guidelines, and criteria used in applying the program. The process SHRP has followed in selecting software and developing a backcalculation procedure for flexible pavements is discussed, and the outcome of the software evaluation portion of the study is presented.

Deflection measurements on flexible pavements for the purpose of structural capacity evaluation are a key component of the Strategic Highway Research Program's (SHRP's) Long-Term Pavement Performance (LTPP) monitoring program. Since the spring of 1988, SHRP has completed an initial round of deflection testing on hundreds of in-service pavement test sections and begun a second round. Like the rest of the LTPP data, the raw deflection data are being stored in SHRP's National Pavement Performance Data Base and ultimately will be available to all researchers to use as they see fit.

In the near term, SHRP will apply a backcalculation procedure to these data for the sole purpose of meeting the immediate needs of the initial analysis of the LTPP data. The layer moduli derived from this endeavor will supplement, not replace, the raw deflection data stored in SHRP's data base. This endeavor is undertaken with the full expectation that it will be the first analysis, but not by any means the last. Too much remains to be learned about the art and science of backcalculation for this analysis to be regarded as definitive.

Numerous methods for evaluating the structural capacity of flexible pavements from deflection basin data are available, but a standard procedure does not presently exist. This paper will discuss the process SHRP has followed in selecting software and developing a backcalculation procedure for flexible pavements, and presents the outcome of the software evaluation portion of the study. Development of a procedure for rigid pavements is currently in progress and thus is not discussed in this paper.

SHRP's selection of backcalculation software does not constitute an endorsement and does not imply that the particular program selected is, in any sense, the "best" program available. Indeed, given the present state of the art, it is probable that the best program for use in any given circumstance depends on a number of factors, including, but not limited to, the level of expertise of the user, the nature of the pavement being evaluated, and the intended use of the results.

Before embarking on a detailed discussion, it is important to clarify the authors' terminology. In using the term "backcalculation software," the authors mean just that—the computer programs used in backcalculation. However, it is the authors' contention that the manner in which a backcalculation program is used is as important and, in some cases, more important than which program is used. Hence, in referring to backcalculation procedures, the authors are referring to not only the software, but also the "rules" by which that software is applied.

## DEVELOPMENT PROCESS

The objective of the SHRP study summarized in this paper was to develop a backcalculation procedure for flexible pavements, on the basis of existing backcalculation software, that will provide the most accurate, repeatable, and reliable results possible, given the present state of the art. It was anticipated that this procedure would involve the development of detailed guidelines and specifications for the application of that software.

With this objective in mind, the process by which SHRP has pursued the selection and development of a flexible pavement backcalculation procedure for use in the LTPP data analysis involves the following steps, which will be discussed in greater detail in the ensuing sections of this paper.

G. R. Rada and P. J. Stephanos, PCS/Law Engineering, 12240 Indian Creek Court, Suite 120, Beltsville, Md. 20705-1242. C. A. Richter, Strategic Highway Research Program, 818 Connecticut Ave., N.W., Suite 400, Washington, D.C. 20006.

1. Software identification,
2. Development of preliminary software selection criteria,
3. Preliminary software selection,
4. Software evaluation,
5. Compilation of evaluation results,
6. Final software selection, and
7. Procedure development and documentation.

To date, this process has been completed through the sixth step outlined above. The procedure development and documentation stage of the process currently is in progress and will be finalized after a review of the preliminary rules by the SHRP Expert Task Group (ETG) for Deflection Testing and Backcalculation.

**Software Identification and Preliminary Software Selection**

The first three steps in the process outlined earlier were quite straightforward. Software identification involved a review of the literature to identify a number of the programs available and their pertinent features. The second and third steps were accomplished through discussions at a meeting of SHRP's Deflection Testing and Backcalculation ETG in November 1990. The ETG recommended that software selected for detailed evaluation meet the following criteria:

- Use layered elastic theory;
- Allow variable slip conditions at layer interfaces;
- Have flexible plate boundary conditions;
- Require user input for seed moduli but program results independent of seed moduli;
- Report goodness of fit for each deflection measurement;
- Have capability for user-defined depth to rigid layer;
- Have nonlinear modeling capability for base and subgrade materials (desirable);
- Provide the capability for the user to fix a layer modulus;
- Be able to model at least five layers; and
- Have capability for applying a weighing function to the error tolerances (desirable, but not essential).

On the basis of the above criteria (which were relaxed in a few cases), four programs were selected for further evaluation. They are ISSEM4 (*1*), MODCOMP3 (*2*), MODULUS (*3*), and WESDEF (*4,5*).

**Software Evaluation: The Plan**

The purpose of SHRP's flexible pavement backcalculation software evaluation exercise was twofold: (a) to provide a basis for selecting a program for use in the SHRP backcalculation and (b) to provide a basis for development of the procedures to be used with that software. For this endeavor a group composed of ETG members, the software developers, and SHRP contractors was assembled. Each evaluator was requested to work independently of the others to run all of the backcalculation programs using the same data sets from a number of actual SHRP test sections.

By having a spectrum of users from "informed" to "expert" for each program, SHRP hoped to gain some insight into what was required in terms of user input and application rules to be successful with each program and thus obtain information for the development of the SHRP backcalculation procedure document. To judge the "success" of a program, several criteria were planned. First, the participants were to make informed estimates of the material moduli, on the basis of laboratory test results for the materials involved, for comparison with the backcalculation results. In addition, results were to be evaluated on the basis of reasonableness, robustness, stability, goodness of fit, and general suitability for SHRP's purposes.

Deflection data and other pertinent information from eight SHRP pavement test sections were extracted from the SHRP data base for use in this software evaluation exercise. A primary consideration in the selection of these data sets was coverage of the wide range of pavement structures that make up the SHRP experiments. Other considerations included the distribution of these sections by climatic region, SHRP region, and geographical location within the United States. Figure 1 shows the pavement structures, and Table 1 gives typical measured deflections for these pavements.

**Software Evaluation: The Reality**

The SHRP backcalculation software evaluation exercise did not progress entirely according to plan. The first problem encountered was related to data availability. Laboratory materials data on which the "informed estimates" of the layer moduli were to be based were not available until after completion of the study, and hence that basis for evaluation of analysis results was lost. Since these data would have also helped the evaluators determine appropriate seed moduli and other input values, their efforts were also hindered by the lack of laboratory materials data. The other significant deviation from the plan was that the evaluation process turned out to be sufficiently time consuming that several of the evaluators were not able to complete the evaluation of all of the software. However, enough of the work was completed to provide a basis for decision making and procedure development.

**Evaluation Results**

*Overview of Evaluators' Comments and Recommendations*

Before proceeding with the detailed evaluation, an overview of the comments and recommendations provided by the evaluators was undertaken to determine how they viewed each program. Although the ranking of the programs varied from one evaluator to another, MODCOMP3, MODULUS, and WESDEF were overwhelmingly ranked as the top three backcalculation programs. Program ISSEM4 was consistently given the lowest rating for the following reasons:

- Not able to achieve a reasonable solution for several of the sections analyzed,

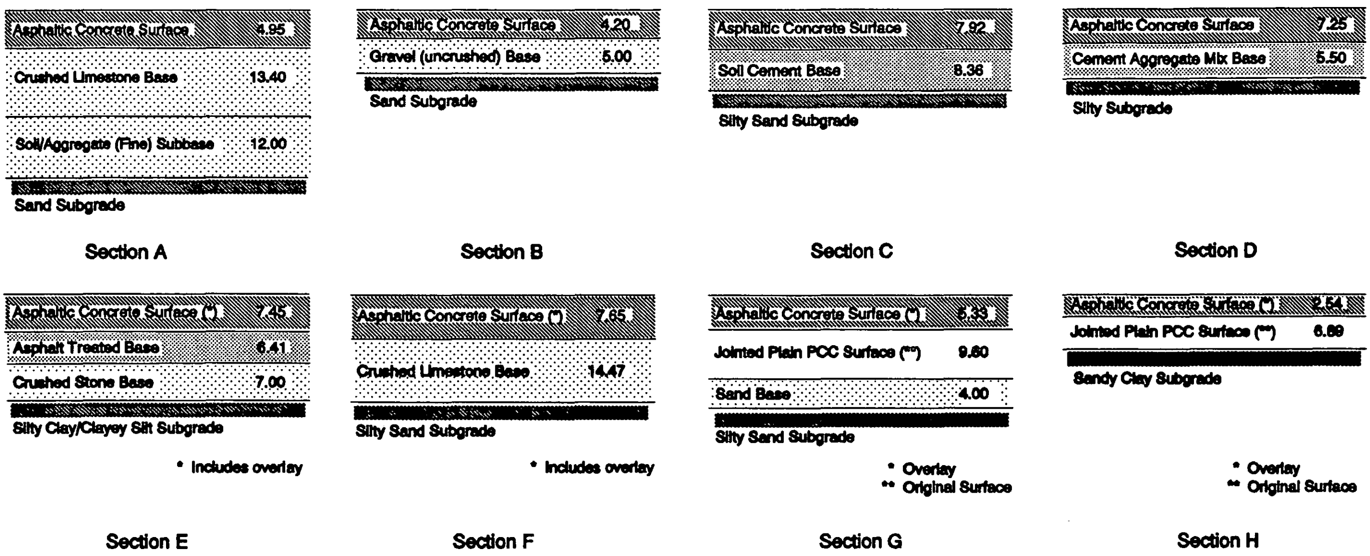


**FIGURE 1 AC surfaced pavement structures.**

**TABLE 1 Typical Deflection Data**

| Section ID | Load (lbs) | Deflection (mils) @ | | | | | | |
|---|---|---|---|---|---|---|---|---|
| | | r=0" | r=8" | r=12" | r=18" | r=24" | r=36" | r=60" |
| A | 10006 | 9.47 | 7.43 | 6.31 | 4.90 | 3.82 | 2.48 | 1.24 |
| B | 9596 | 12.21 | 9.43 | 7.65 | 5.72 | 4.32 | 2.62 | 1.36 |
| C | 9522 | 4.87 | 3.89 | 3.40 | 2.95 | 2.57 | 2.03 | 1.31 |
| D | 9474 | 5.67 | 5.27 | 4.97 | 4.50 | 4.10 | 3.42 | 2.38 |
| E | 9752 | 3.67 | 2.88 | 2.60 | 2.23 | 1.95 | 1.29 | 0.65 |
| F | 9512 | 5.07 | 4.32 | 3.67 | 2.99 | 2.40 | 1.69 | 1.01 |
| G | 9398 | 2.81 | 2.41 | 2.33 | 2.24 | 2.14 | 1.90 | 1.40 |
| H | 9704 | 5.77 | 4.79 | 4.66 | 4.26 | 3.75 | 2.80 | 1.49 |

Note: Deflections shown correspond to a nominal 9,000 lb load. Deflection measurements were also taken at 3 additional load levels.

- Has convergence problems with several of the sections analyzed,
- Not capable of handling a rigid base layer, and
- Does not calculate deflections at the set sensors for comparison with the measured deflections.

Because a preliminary evaluation of the backcalculation results confirmed the evaluator's findings, ISSEM4 was eliminated from further study. Thus, the remainder of the software evaluation focused on MODCOMP3, MODULUS, and WESDEF.

*Program-to-Program Comparison*

Several analyses were conducted to aid in the selection of software for use by SHRP. First, a very broad program-to-program comparison of the backcalculated moduli was conducted. Figure 2 illustrates the results of this analysis for MODCOMP3 versus MODULUS. Although there was considerable variation, it was also apparent that an excellent correlation exists between these programs. The best agreement exists between MODULUS and WESDEF ($R^2$ = 0.89), followed by MODCOMP3 and MODULUS ($R^2$ = 0.85), and MODCOMP3 and WESDEF ($R^2$ = 0.83).

The data also showed that MODCOMP3 tends to predict higher subgrade moduli but lower base/subbase moduli. Although several reasons can be offered to explain these global differences, it is postulated that they were primarily related to the inclusion or omission of a rigid base layer in the analysis. MODULUS computes a hypothetical depth to a rigid layer and WESDEF uses a default depth of 20 ft—in each case, the user can override the program value, but this was not done by most of the evaluators. Since MODCOMP3 allows for up to 15 layers, the user can easily specify a rigid base layer having fixed modulus. However, boring data for each

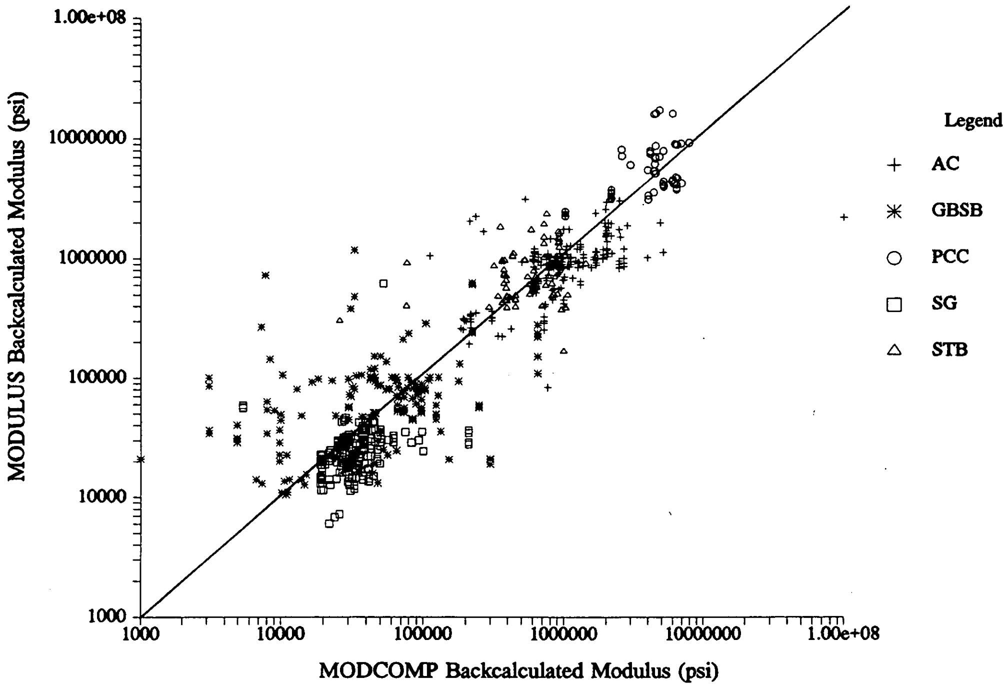


**FIGURE 2 Comparison of MODCOMP and MODULUS programs.**

section showed that bedrock was not present within the top 20 ft; thus most evaluators modeled the subgrade as a semi-infinite layer.

If a rigid base layer is included in the analysis, the subgrade moduli tend to be lower when compared with a solution in which such layer is not included. In turn, there is a compensating moduli effect on the remaining pavement layers; i.e., higher surface and base layer moduli. Hence, the better correlation of results between MODULUS and WESDEF and the higher subgrade moduli for MODCOMP3. Unfortunately, this rigid base question cannot be put to rest by this SHRP exercise, because true moduli or approximately true values are not known.

### *User Sensitivity*

The next analysis in the software evaluation involved a comparison of the results generated by each individual evaluator to assess user variability. Because all three program developers were a part of the evaluation panel, their results were used as the reference datum in this comparison. It was assumed that the program developers were experts in the use of their program and hence would arrive at the "best" set of results.

Plots of the moduli predicted by the program developer versus those predicted by the other evaluators were developed for each program and are illustrated in Figure 3. The degree of correlation ($R^2$) found for each developer-evaluator comparison by program averaged 0.92 for MODULUS, 0.87 for MODCOMP3, and 0.72 for WESDEF. Thus, it appears that MODULUS is less user dependent than the other programs. However, this observation must be tempered by the fact that the degree of versatility and hence degree of sophistication required on the part of the user varies from program to program; this is particularly true when comparing MODCOMP3 to MODULUS and WESDEF.

The variability of the MODCOMP3 results is primarily associated with the unbound granular base/subbase layers. In the case of MODULUS, the variability is mostly related to the subgrade and granular base/subbase layers; lower subgrade moduli and higher base/subbase moduli were generally predicted by the evaluators compared with the program developer. For WESDEF, all material types contribute to the variability, with the exception of the subgrade layer, which shows excellent agreement among all evaluators. For all three programs, it is hypothesized that the variability is primarily associated with the modeling of the pavement by each evaluator. More importantly, these findings clearly emphasize the need to develop detailed guidelines and specifications for the application of the selected software to achieve consistent results from one program user to another.

### *Reasonableness of Results*

Although true moduli or approximately true values are not known, an analysis aimed at determining the reasonableness of the predicted moduli was undertaken. Using data generated by the program developers, a series of bar charts comparing the backcalculated moduli by program and pavement section were developed for each material type and are shown in Figures 4 through 7 for all materials, except portland cement concrete. Each bar shown in these charts was generated from the analysis of four load levels—nominal 6,000-, 9,000-, 12,000-, and 16,000-lb loads.

Figure 4 shows that the backcalculated moduli for the asphaltic concrete layer appear reasonable for all three programs, except as follows. Layer moduli predicted by MODCOMP3 for Sections D and G seem high whereas that for Section H

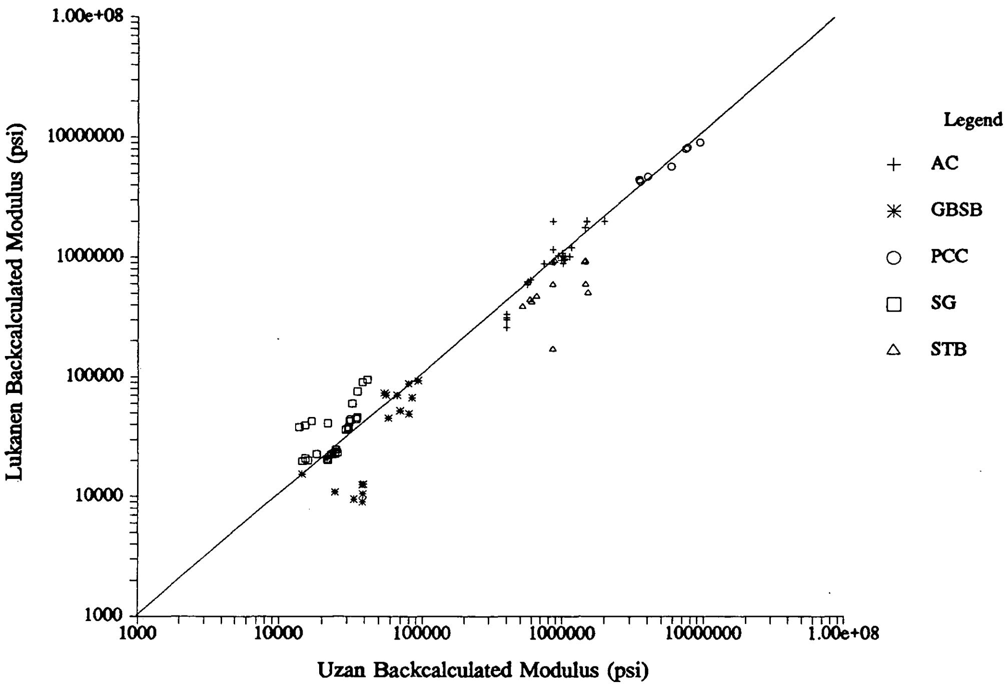


FIGURE 3 User comparison: MODULUS.

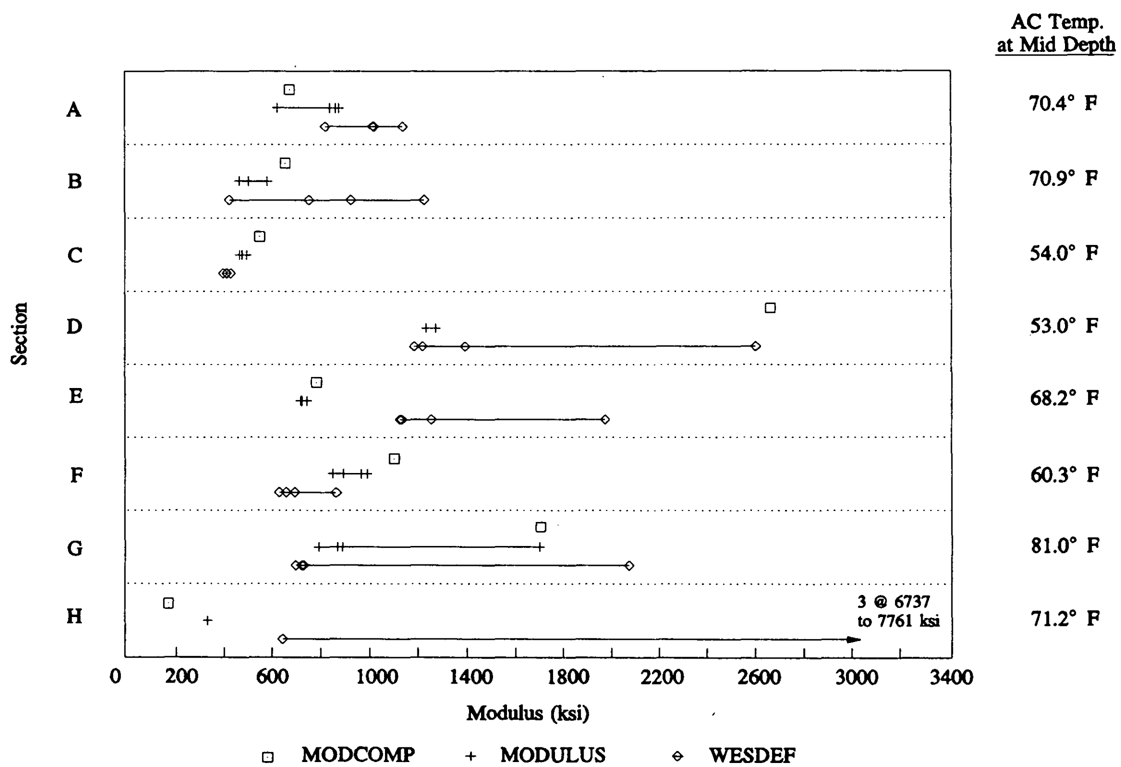


FIGURE 4 Comparison of backcalculated moduli: asphalt concrete (no temperature correction).

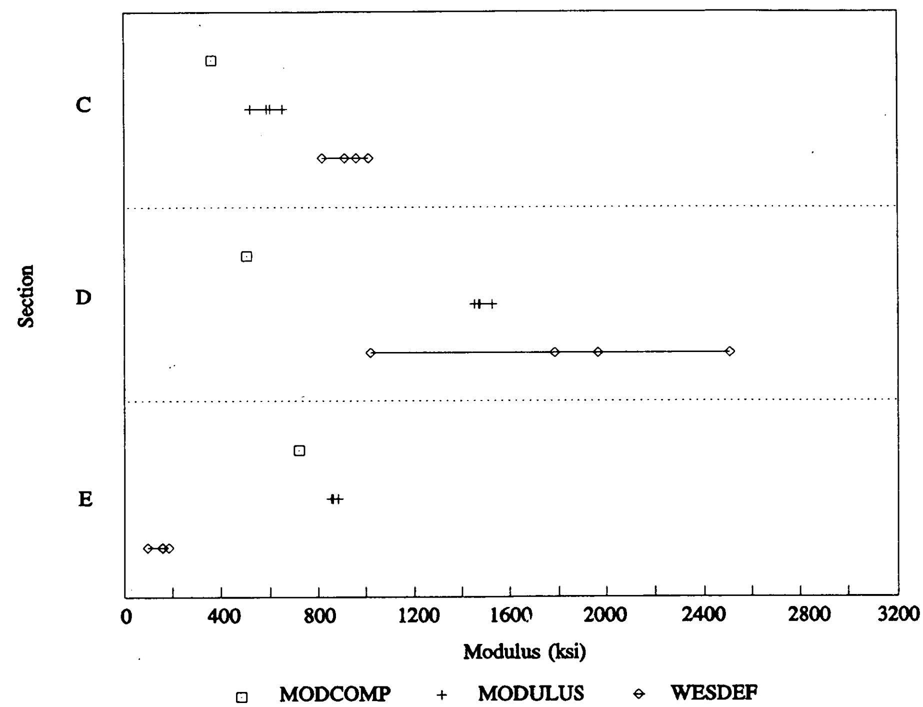


**FIGURE 5** **Comparison of backcalculated moduli: stabilized base.**

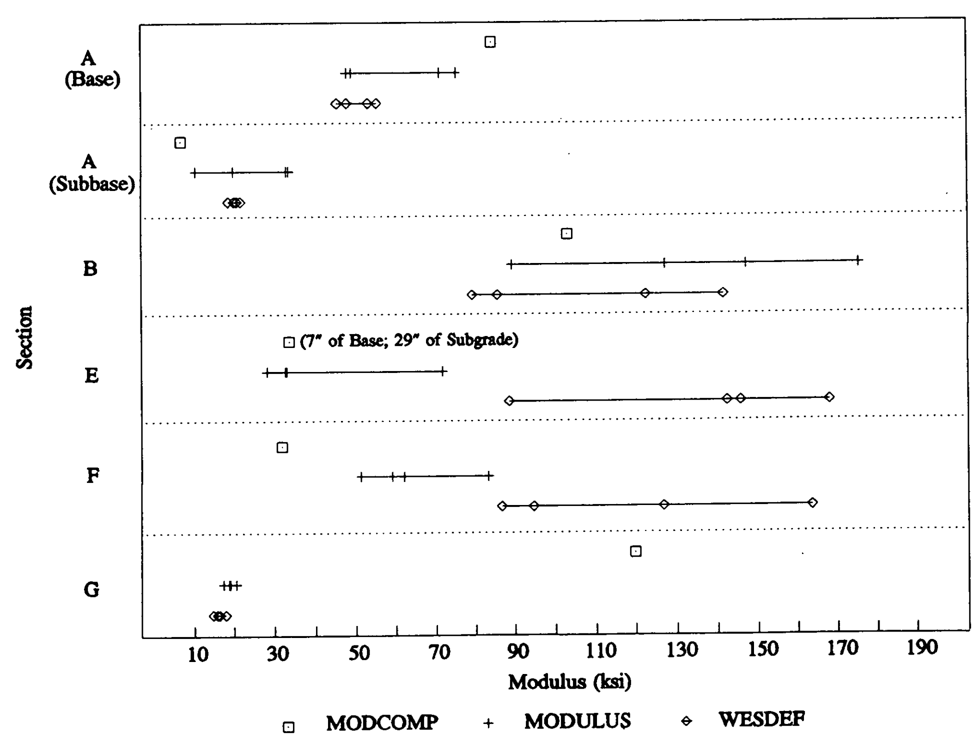


**FIGURE 6** **Comparison of backcalculated moduli: unbound base/subbase.**

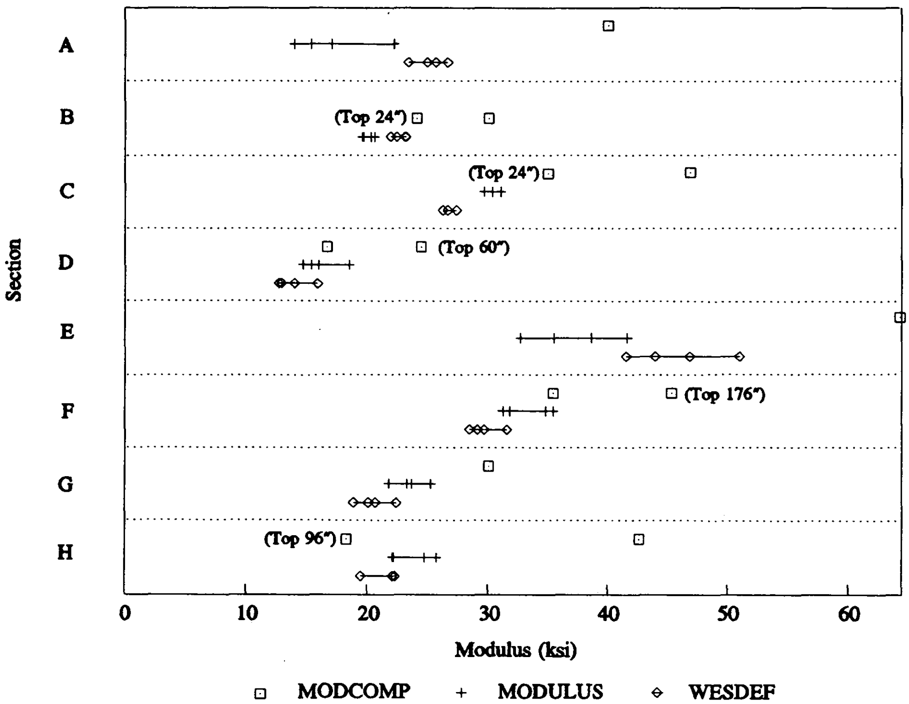


**FIGURE 7 Comparison of backcalculated moduli: subgrade.**

appears low. For Section G, the value predicted by MODULUS for the lowest load level appears to be high, especially when compared with the moduli for the remaining load levels. WESDEF results corresponding to the lowest load level for Sections D, E, and G seem unusually high as do the results for the three highest load levels in Section H. Also, the degree of variability associated with Section B seems high. In all fairness to the three programs, it should also be noted that Section G contained nondecreasing deflections, a situation these programs were not developed to handle.

Although only two of the eight sections had a portland cement concrete layer, the MODCOMP3 predicted values appeared reasonable for both sections. The MODULUS results appeared reasonable for Section H but high and variable for Section G. WESDEF, on the other hand, seemed to have a problem with this material type; three of the four values for Section G seem unusually high whereas all of those for Section H were very low.

Figure 5 shows that the backcalculated moduli for the stabilized base and subbase materials appeared reasonable, except as follows. For Section D, the MODCOMP3 modulus value seem somewhat low for a cement aggregate base, especially when compared with that of the soil cement in Section A or with the values obtained by the other two programs for this same section. The MODULUS results for Section E appear high at first glance, but this is because this layer was combined with the AC surface layer in the analysis. Hence, the values reflect a composite response of the two layers. WESDEF results for Section D are unusually variable, and some of the values appear to be high. In addition, predicted moduli for Section E seem low.

Compared with the previous material types, the results for the unbound granular base and subbase materials are considerably more variable, as shown in Figure 6, and thus more difficult to assess. MODCOMP3 results are mostly in the range of expected values, with the exception of Section G, which has an unusually high modulus value, especially when compared with those from the two other programs. All MODULUS predicted values appear reasonable, although somewhat high and variable for Section B. Likewise, WESDEF predicted moduli appear reasonable, although somewhat high and variable for Sections B, E, and F.

With regard to the backcalculated subgrade moduli, Figure 7 shows that MODCOMP3 consistently predicted higher modulus values than both MODULUS and WESDEF, which had similar values. On the basis of an earlier analysis, this difference between MODCOMP3 and the other two programs was attributed to the inclusion or omission of a rigid base layer.

Overall, the results of this analysis appear to indicate that both MODCOMP3 and MODULUS generate reasonable moduli more consistently than WESDEF. However, this conclusion must be tempered by the fact that reasonableness, as defined here in the absence of true moduli, refers to the subjective judgment of the authors.

### *Deflection Matching Errors*

The most objective measure of the performance of a backcalculation program is how well it matches the measured deflection basin. As with the previous analysis, only the results generated by the program developers were used to evaluate the goodness of fit obtained with the programs. Table 2 summarizes the results of the analysis in terms of the absolute sum of errors and the root mean square parameters. On the basis of the work done for this evaluation, it appears that MODULUS does a better job of matching the measured deflection basin. This program, however, did not consider all of the deflections for some basins; for example, deflections

**TABLE 2 Summary of Deflection Errors**

| Section | Load | Absolute Sum of Errors (%) | | | Root Mean Square (%) | | |
|---|---|---|---|---|---|---|---|
| | | MODCOMP | MODULUS | WESDEF | MODCOMP | MODULUS | WESDEF |
| A | 1 | | 3.73[1] | 11.80 | | 0.73[1] | 2.24 |
| | 2 | | 2.80[1] | 6.00 | | 0.57[1] | 1.22 |
| | 3 | | 4.43[1] | 5.54 | | 0.82[1] | 0.92 |
| | 4 | 4.57 | 3.02[1] | 7.18 | 1.09 | 0.61[1] | 1.36 |
| B | 1 | | 2.81[2] | 76.88 | | 0.61[2] | 12.15 |
| | 2 | | 2.72[2] | 59.21 | | 0.60[2] | 10.30 |
| | 3 | | 2.70[2] | 52.87 | | 0.61[2] | 9.11 |
| | 4 | 14.71 | 2.63[2] | 49.43 | 4.35 | 0.63[2] | 8.44 |
| C | 1 | | 21.37 | 37.26 | | 3.95 | 6.23 |
| | 2 | | 17.21 | 24.92 | | 3.25 | 4.42 |
| | 3 | | 13.76 | 20.63 | | 2.53 | 3.23 |
| | 4 | 8.25 | 13.76 | 21.01 | 2.02 | 2.61 | 3.52 |
| D | 1 | | 12.71 | 11.32 | | 2.30 | 1.96 |
| | 2 | | 11.30 | 16.23 | | 1.81 | 2.44 |
| | 3 | | 8.21 | 9.05 | | 1.36 | 1.52 |
| | 4 | 10.72 | 9.44 | 9.04 | 3.61 | 2.01 | 1.54 |
| E | 1 | | 12.35[1] | 23.03 | | 3.11[1] | 3.84 |
| | 2 | | 9.41[1] | 13.89 | | 2.08[1] | 3.15 |
| | 3 | | 13.41[1] | 9.30 | | 2.69[1] | 1.47 |
| | 4 | 22.31 | 18.19[1] | 11.86 | 5.80 | 3.88[1] | 1.91 |
| F | 1 | | 4.47[1] | 30.73 | | 0.81[1] | 6.11 |
| | 2 | | 8.75[1] | 21.56 | | 1.70[1] | 3.72 |
| | 3 | | 12.52[1] | 13.61 | | 3.99[1] | 2.48 |
| | 4 | 3.94 | 2.22[1] | 12.90 | 0.85 | 0.44[1] | 1.97 |
| G | 1 | | 13.49 | 5.89 | | 2.07 | 1.11 |
| | 2 | | 2.73 | 5.12 | | 0.49 | 0.94 |
| | 3 | | 1.85 | 8.86 | | 0.33 | 1.39 |
| | 4 | 5.45 | 1.73 | | 1.71 | 0.31 | |
| H | 1 | | 10.50 | 12.36 | | 1.71 | 2.21 |
| | 2 | | 12.46 | 7.09 | | 2.17 | 1.22 |
| | 3 | | 10.43 | 7.06 | | 1.77 | 1.30 |
| | 4 | 30.38 | 9.85 | 10.54 | 10.75 | 1.71 | 1.92 |
| Average | | 12.54 | 8.66 | 19.75 | 3.77 | 1.70 | 3.40 |
| Std. Dev. | | 9.47 | 5.50 | 17.77 | 3.30 | 1.13 | 2.96 |
| COV | | 0.76 | 0.64 | 0.90 | 0.87 | 0.67 | 0.87 |
| Min | | 3.94 | 1.73 | 5.12 | 0.85 | 0.31 | 0.92 |
| Max | | 30.38 | 21.37 | 76.88 | 10.75 | 3.99 | 12.15 |

[1] Excludes deflection at r=60 inches
[2] Excludes deflection at r=36 and 60 inches

at 60 in. from the center of the load plate were excluded from the analysis of Sections A, E, and F, and those at 60 in. were excluded from Section B. Thus, it is postulated that the deflection matching errors would be worse for this program if the excluded deflections were considered.

A theoretical analysis was conducted in an attempt to further assess the accuracy of the moduli predicted by each program. Specifically, the BISAR layered elastic computer code was used to simulate deflection basins for nine pavement structures with varying material types and layer thicknesses. In turn, these basins were analyzed with the programs in question to backcalculated layer moduli for comparison with those assumed in the BISAR runs.

All simulated deflection basins were generated by R. Briggs (Texas Department of Transportation). These data were provided to the authors, along with information on the pavement structures (layer thicknesses and material types), but not the moduli used in the generation of the basins. These assumed moduli were later provided to the authors, after all backcalculation analyses had been completed. Thus, seed moduli or moduli ranges were assigned for each pavement layer on the basis of material type. In the absence of knowledge or algorithms to compute the depth to rigid layer, a semi-infinite subgrade was assumed in this simulated analysis.

Table 3 presents the pavement structure and simulated deflection basins used in the analysis; Table 4 summarizes the backcalculated moduli and the comparison of assumed and predicted values; and Table 5 gives the corresponding deflection matching errors. In general, the analysis results show that all three programs do an excellent job of matching the assumed moduli as well as the corresponding deflection basins. However, MODULUS is given higher marks on the basis that it more closely and consistently matched the simulated moduli and deflections.

In all fairness to MODCOMP3, which uses the CHEVRON code, it should be noted that differences in deflection cal-

**TABLE 3 BISAR Simulated Deflection Data**

| ID | Layer | Material | Thickness (inches) | Surface Deflection (mils) r=0" | r=8" | r=12" | r=18" | r=24" | r=36" | r=60" |
|---|---|---|---|---|---|---|---|---|---|---|
| 1 | 1 | Asphalt Concrete | 3 | 32.90 | 23.20 | 17.80 | 12.60 | 9.51 | 6.15 | 3.57 |
| | 2 | Granular Base | 6 | | | | | | | |
| | 3 | Subgrade | | | | | | | | |
| 2 | 1 | Asphalt Concrete | 6 | 30.10 | 24.50 | 21.70 | 18.50 | 15.90 | 12.20 | 7.73 |
| | 2 | Granular Base | 12 | | | | | | | |
| | 3 | Subgrade | | | | | | | | |
| 3 | 1 | Asphalt Concrete | 8 | 8.97 | 7.95 | 7.56 | 7.07 | 6.57 | 5.61 | 4.00 |
| | 2 | Cement Stab. Base | 6 | | | | | | | |
| | 3 | Subgrade | | | | | | | | |
| 4 | 1 | PCC Slab | 9 | 8.94 | 8.41 | 8.05 | 7.48 | 6.91 | 5.80 | 4.02 |
| | 2 | Lime Stab. Base | 6 | | | | | | | |
| | 3 | Subgrade | | | | | | | | |
| 5 | 1 | PCC Slab | 6 | 18.10 | 16.60 | 15.50 | 13.70 | 11.90 | 8.97 | 5.26 |
| | 2 | Subgrade | | | | | | | | |
| 6 | 1 | PCC Slab | 12 | 8.38 | 8.06 | 7.91 | 7.71 | 7.50 | 7.05 | 6.10 |
| | 2 | Cement Stab. Base | 6 | | | | | | | |
| | 3 | Subgrade | | | | | | | | |
| 7 | 1 | Asphalt Concrete | 3 | 7.50 | 6.13 | 5.87 | 5.43 | 4.97 | 4.09 | 2.72 |
| | 2 | PCC Slab | 9 | | | | | | | |
| | 3 | Subgrade | | | | | | | | |
| 8 | 1 | Asphalt Concrete | 5 | 6.56 | 5.48 | 5.27 | 5.01 | 4.73 | 4.14 | 3.08 |
| | 2 | PCC Slab | 10 | | | | | | | |
| | 3 | Lime Stab. Base | 8 | | | | | | | |
| | 4 | Subgrade | | | | | | | | |
| 9 | 1 | Asphalt Concrete | 4 | 6.89 | 5.87 | 5.74 | 5.59 | 5.42 | 5.05 | 4.28 |
| | 2 | PCC Slab | 12 | | | | | | | |
| | 3 | Asphalt Stab. Base | 8 | | | | | | | |
| | 4 | Subgrade | | | | | | | | |

Load = 16,000 lbs Load Radius = 5.91 inches

culations, particularly near the load plate, exist between the CHEVRON and BISAR codes. Thus, some of the poorer fit obtained with MODCOMP3, as compared with MODULUS, could be caused by differences between the two forward calculation routines.

## *Other Factors and Program Features*

It is clear from the preceding discussion, and the analyses that support it, that MODCOMP3, MODULUS, and WESDEF, are useful tools for backcalculation that can produce good results. The programs do, however, have various strengths and weaknesses. On the basis of work done for this evaluation, it can be concluded that MODCOMP3 produces results that match quite well the measured deflection basins, are reasonably independent of the user, and are generally "reasonable." In addition, MODCOMP3 is the most flexible of the programs evaluated because it allows the user to model up to 15 layers (although not more than 5 should be modeled as having unknown moduli that are to be backcalculated), with the deepest layer treated as a layer of known high modulus (i.e., bedrock or a "rigid" layer) or not, as the user desires, and because it is the only program of those evaluated that allows the user to model stress sensitivity of the pavement layers. This ability was not significant in the analyses conducted for this evaluation, because the pavement investigated did not demonstrate significant nonlinear materials behavior, but it could be important in some circumstances.

In the same analyses, MODULUS does a slightly better job of matching the measured deflections basins, is slightly more independent of the user, and also produces results that are generally reasonable. It is postulated that the closer fit of the measured deflection basins is partially due to the use of an algorithm in MODULUS to calculate effective depth to rigid layer and to the exclusion of some of the outer deflections from the calculations for some of the deflection basins. Although it is widely recognized that the presence of a true or effective rigid layer in the pavement cross section can have a significant effect on measured deflections and, hence, back-

**TABLE 4 Comparison of Assumed Versus Backcalculation Moduli**

| Material Type | Layer Thickness (inches) | Assumed Moduli (BISAR) (psi) | Backcalculated Moduli | | | % Difference | | |
|---|---|---|---|---|---|---|---|---|
| | | | Modcomp | Modulus | Wesdef | Modcomp | Modulus | Wesdef |
| AC | 3 | 500000 | 553118 | 481700 | 480658 | -10.62% | 3.66% | 3.87% |
| GB | 6 | 50000 | 49520 | 51100 | 60371 | 0.96% | -2.20% | -20.74% |
| SG | --- | 20000 | 19973 | 20000 | 18723 | 0.14% | 0.00% | 6.39% |
| AC | 6 | 300000 | 288840 | 311000 | 254599 | 3.72% | -3.67% | 15.13% |
| GB | 12 | 60000 | 65227 | 59100 | 75465 | -8.71% | 1.50% | -25.77% |
| SG | --- | 10000 | 9854 | 10000 | 9359 | 1.46% | 0.00% | 6.41% |
| AC | 8 | 1000000 | 1100365 | 969700 | 960804 | -10.04% | 3.03% | 3.92% |
| CTB | 6 | 2000000 | 1610059 | 2130900 | 2436563 | 19.50% | -6.54% | -21.83% |
| SG | --- | 20000 | 19826 | 20100 | 18433 | 0.87% | -0.50% | 7.84% |
| PCC | 9 | 4000000 | 3572500 | 3118800 | 3645284 | 10.69% | 22.03% | 8.87% |
| LTB | 6 | 60000 | 118685 | 237300 | 176950 | -97.81% | -295.50% | -194.92% |
| SG | --- | 20000 | 19808 | 19700 | 18268 | 0.96% | 1.50% | 8.66% |
| PCC | 6 | 3000000 | 2622308 | 2970800 | 3257227 | 12.59% | 0.97% | -8.57% |
| SG | --- | 15000 | 15495 | 15100 | 13978 | -3.30% | -0.67% | 6.81% |
| PCC | 12 | 4000000 | 4000000 * | 4246400 | 3757139 | 0.00% | -6.16% | 6.07% |
| CTB | 6 | 2000000 | 1794517 | 1829600 | 2406254 | 10.27% | 8.52% | -20.31% |
| SG | --- | 10000 | 9907 | 10000 | 8594 | 0.93% | 0.00% | 14.06% |
| AC | 3 | 300000 | 298462 | 304000 | 256023 | 0.51% | -1.33% | 14.66% |
| PCC | 9 | 4000000 | 3240565 | 3883500 | 4899980 | 18.99% | 2.91% | -22.50% |
| SG | --- | 30000 | 31381 | 30300 | 26828 | -4.60% | -1.00% | 10.57% |
| AC | 5 | 600000 | 946524 | 649300 | 591949 | -57.75% | -8.22% | 1.34% |
| PCC | 10 | 4000000 | 2223404 | 2764400 | 3871242 | 44.41% | 30.89% | 3.22% |
| LTB | 8 | 100000 | 234554 | 254900 | 174140 | -134.55% | -154.90% | -74.14% |
| SG | --- | 25000 | 24056 | 24700 | 22760 | 3.78% | 1.20% | 8.96% |
| AC | 4 | 500000 | 500000 * | 447900 | 493080 | 0.00% | 10.42% | 1.38% |
| PCC | 12 | 4000000 | 4000000 * | 7096600 | 3733876 | 0.00% | -77.42% | 6.65% |
| STB | 8 | 1000000 | 940431 | 367300 | 1300568 | 5.96% | 63.27% | -30.06% |
| SG | --- | 15000 | 14796 | 15100 | 12996 | 1.36% | -0.67% | 13.36% |
| AC | 6 | 300000 | 261094 | 303700 | 288906 | 12.97% | -1.23% | 3.70% |
| GB | 12 | 60000 | 73236 | 59900 | 61677 | -22.06% | 0.17% | -2.80% |
| SG | 36 | 10000 | 7817 | 10000 | 10175 | 21.83% | 0.00% | -1.75% |

Note: (1) AC = Asphalt Concrete, GB = Dense Graded Aggregate, PCC = Portland Cement Concrete, SG = Subgrade
CTB = Cement Stabilized Base, LTB = Lime Stabilized Base, ATB = Asphalt Stabilized Base
* Fixed Modulus Value

**TABLE 5 Summary of Deflection Errors: Simulated Data**

| Section | Absolute Sum of Errors (%) | | | Root Mean Square (%) | | |
|---|---|---|---|---|---|---|
| | MODCOMP | MODULUS | WESDEF | MODCOMP | MODULUS | WESDEF |
| 1 | 11.62 | 0.85[1] | 14.20 | 2.36 | 0.16[1] | 2.32 |
| 2 | 1.74 | 0.82 | 7.20 | 0.34 | 0.17 | 1.12 |
| 3 | 4.03 | 1.27 | 1.60 | 0.81 | 0.22 | 0.26 |
| 4 | 4.13 | 3.06 | 1.40 | 0.81 | 0.52 | 0.23 |
| 5 | 18.71 | 1.29 | 4.70 | 3.68 | 0.20 | 0.91 |
| 6 | 25.97 | 0.63 | 1.40 | 6.80 | 0.12 | 0.21 |
| 7 | 14.19 | 0.75 | 8.60 | 3.24 | 0.15 | 1.47 |
| 8 | 1.59 | 2.06 | 4.00 | 0.37 | 0.37 | 0.58 |
| 9 | 21.72 | 1.11 | 3.90 | 5.42 | 0.19 | 0.57 |
| Average | 11.52 | 1.32 | 5.22 | 2.65 | 0.23 | 0.85 |
| Std. Dev. | 9.20 | 0.78 | 4.21 | 2.34 | 0.13 | 0.70 |
| COV | 0.80 | 0.59 | 0.81 | 0.88 | 0.56 | 0.82 |
| Min | 1.59 | 0.63 | 1.40 | 0.34 | 0.12 | 0.21 |
| Max | 25.97 | 3.06 | 14.20 | 6.80 | 0.52 | 2.32 |

[1] Excludes deflection at r=60 inches

calculated moduli, the book on how to address this effect in the analysis of pavement deflection data clearly has not been completed. Also, it is logical to conclude that the lower degree of user dependence of MODULUS, as compared with MODCOMP3, comes about as a result of fewer options with respect to modeling of the pavement structure.

The performance of WESDEF was similar to that of MODCOMP3 (i.e., not quite as good as MODULUS) with respect to the ability to match measured deflection basins. However, the results are somewhat less independent of the user, and are subjectively judged to be slightly less reasonable for the sections evaluated. Again, it may be postulated that these results are at least partially attributed to the manner in which the presence or absence of a rigid layer in the subgrade is handled.

On the basis of evaluations that have been performed, the demonstrated performance of MODULUS is somewhat superior to that of the other programs, although one or both of the other programs may be better for an individual section. Thus, MODULUS has been selected as the primary backcalculation program to be used in the initial analysis of the SHRP deflection data.

### Procedure Development and Application

The procedure development stage of this study is currently in progress. SHRP's goal in this stage of the process is to glean from the results of the software evaluation exercise as much information as possible about what input criteria to apply to make the backcalculation process straightforward, productive, successful, and consistent. However, the limited size of the data set used in the evaluation, and the evolving nature of the science (or art) of backcalculation, make it likely that early experience with this procedure will bring to light areas in which further refinement is needed. Hence, it is anticipated that the initial release of the SHRP backcalculation procedure will be followed up, as we learn more about the strengths, weaknesses, and requirements of the process.

SHRP has a distinct advantage over most agencies that have done backcalculation in the past, because the SHRP data base contains a wealth of information that can and will be used to generate the input data for the backcalculation process. The SHRP backcalculation procedure will make use of data base queries to extract the information needed as input for the backcalculation procedure from the SHRP data base. For example, SHRP can draw on the laboratory materials data in the data base to determine ranges of moduli for each of the pavement layers. In instances in which the surface layer is thin, a conditional query can be established to set the surface modulus as a known value, on the basis of the temperature at the time of testing and other known properties of the asphalt concrete.

Initially, the SHRP backcalculation procedure will be applied to the data from one test point on each of the SHRP test sections—the "test pit location"—a point for which SHRP has deflection data and accurate layer thickness information, as well as field and laboratory materials data. Eventually, the procedure will be applied to all of the SHRP deflection data.

## SUMMARY AND CONCLUSIONS

The objective of the study discussed in this paper was to evaluate existing software for the purpose of developing an SHRP flexible pavement backcalculation procedure for the initial analysis of the LTPP deflection data. Using ETG recommended criteria, four programs were selected for detailed evaluation: ISSEM4, MODCOMP3, MODULUS, and WESDEF. These programs, along with SHRP deflection data and other pertinent information, were provided to each member of a group of evaluators that also included the program developers.

On the basis of initial review of the backcalculation results and evaluator's comments, ISSEM4 was eliminated from further study. The three remaining programs—MODCOMP3, MODULUS, and WESDEF—were analyzed for user repeatability, reasonableness of results, deflection matching errors, ability to match assumed moduli from simulated deflection basins, and versatility. It was concluded from these analyses that the performance of MODULUS was superior to that of the other programs; hence, MODULUS has been selected as the primary program to be used by SHRP in the initial data analysis.

## ACKNOWLEDGMENTS

The work reported herein was funded by the Strategic Highway Research Program, National Research Council. The authors gratefully acknowledge the assistance of the SHRP Expert Task Group for Deflection Testing and Backcalculation for their efforts on behalf of this endeavor. Special thanks are due to Robert Briggs, Albert J. Bush, Billy G. Connor, William Edwards, John P. Hallin, Anastasios Ioannides, Lynne H. Irwin, Erland Lukanen, Joe P. Mahoney, Richard N. Stubstad, Marshall Thompson, Jacob Uzan, Wes Yang, and their associates, who participated in the evaluations.

## REFERENCES

1. *Description of and User's Guide for the Dynatest ISSEM4 Computer Program*. Dynatest Consulting, Inc., Ojai, Calif., April 1988.
2. L. Irwin and T. Szebenyi. *User's Guide to MODCOMP3, Version 3.2*. CLRP Report 91-4. Cornell University Local Roads Program, Ithaca, N.Y., March 1991.
3. *MODULUS: Preliminary User's Manual—Version 4.0.* Texas Transportation Institute, Texas A&M University, College Station, 1990.
4. D. R. Alexander, S. D. Kohn, and W. P. Grogan. Nondestructive Testing Techniques and Evaluation Procedures for Airfield Pavements. In *Nondestructive Testing of Pavements and Backcalculation Moduli.* (A. J. Bush III and G. Y. Baladi, eds.), ASTM STP 1026, ASTM, Philadelphia, Pa., 1989, pp. 502–524.
5. F. J. Van Cauwelaert, D. R. Alexander, T. D. White, and W. R. Barker. Multilayer Elastic Program for Backcalculating Layer Moduli in Pavement Evaluation. In *Nondestructive Testing of Pavements and Backcalculation of Moduli* (A. J. Bush III and G. Y. Baladi, eds.), ASTM STP 1026, ASTM, Philadelphia, Pa., 1989, pp. 171–188.

# Comparison of Backcalculated Moduli from Falling Weight Deflectometer and Truck Loading

PETER E. SEBAALY, NADER TABATABAEE, AND TOM SCULLION

Historically, the in situ resilient moduli of pavement layers have been evaluated from nondestructive deflection testing (NDT) devices such as the Dynaflect, Road Rater, or falling weight deflectometer (FWD). Even though the FWD is the best NDT device available, it still does not fully represent the loading conditions generated by a moving truck. Therefore, the moduli values, backcalculated from FWD deflections, may be different from those that are backcalculated from truck loading data. The in situ resilient moduli of the pavement layers were backcalculated from FWD, multidepth deflectometers (MDD), and strain gauge data. In the case of the FWD loading, the backcalculated moduli from the FWD deflection basins are compared with the ones backcalculated from the MDD deflections. In the truck loading case, the backcalculated moduli from the MDD deflections are compared with the ones backcalculated from the strain gauge data.

A large number of the nation's highways are approaching the end of their service lives. Consequently, there is an urgent need to upgrade and maintain these highways. By applying a well-designed overlay to a deteriorated pavement section, its functional and structural performances can be greatly improved.

The key word in the preceding discussion is the well-designed overlay: What does this mean? On the basis of the classical pavement design approach, a well-designed overlay is one that is designed using the most representative (a) material properties of the existing pavement structure and (b) traffic load distributions throughout the expected design life. The evaluation of materials properties has been a great concern for the pavement design community for a long time. Very often, the engineer asks, What is the most appropriate way of evaluating material properties that is consistent with current design procedures?

## BACKGROUND

Historically, the in situ resilient moduli of pavement layers have been evaluated from various nondestructive deflection testing devices. Currently, the falling weight deflectometer (FWD) is considered the best NDT device available to simulate actual traffic loading conditions. Even though the FWD is the best NDT device available, it still does not fully represent the loading conditions generated by a moving truck. The major discrepancies exist in the differences between the frequency content of the FWD signal (2 to 100 Hz) and the signal imparted from a truck moving at 50 to 60 mph (1 to 20 Hz). It is well known that the resilient modulus of the asphalt concrete material is highly dependent on the frequency of the loading (*1*). Therefore, the moduli values, backcalculated from FWD deflections, may be different from those that are backcalculated from truck loading data.

In recent years, several backcalculation automated search routines have been developed that minimize the error between the measured and calculated surface deflection bowls (*2–5*). Christison and Shields developed an iterative procedure by which layer moduli can be evaluated from pavement instrumentation for a two-layer pavement system (*6*). They used surface deflections and the strains at the bottom of the asphalt concrete layer to backcalculate the modulus of the asphalt and the subgrade under truck and nondestructive testing equipment. The study presented in this paper will focus on backcalculating layer moduli for four-layer pavement systems from measurements collected by strain gauges, multidepth deflectometers (MDD), and surface deflection sensors.

## DESCRIPTION OF TEST SECTIONS

As a part of the research project, In Situ Instrumentation for Resilient Moduli Measurements, various types of pavement instrumentation were selected for field evaluation under actual truck loading (*7*). Three different types of strain gauges were selected to measure the longitudinal strain at the bottom of the asphalt concrete layer, including the Kyowa H gauge, the Dynatest H gauge, and instrumented core gauges. The multidepth deflectometer device was selected to measure the vertical deflection throughout the depth of the pavement structure (*8*).

The gauges were installed at the test track at Pennsylvania State University in two newly constructed sections (*7*). The structures of the constructed sections consisted of a thin section (6 in. of asphalt concrete over 8 in. of crushed aggregate base and 12 in. of subbase) and a thick section (10 in. of asphalt concrete over 10 in. of crushed aggregate base and 12 in. of subbase). The loading of the test sections was conducted with a single-axle tractor and tandem-axle trailer combination. The experimental plan for field testing is shown in Table 1. The test sections were also tested by the FWD.

P. E. Sebaaly, Department of Civil Engineering, University of Nevada, Reno, Nev. 89557. N. Tabatabaee, Pennsylvania Transportation Institute, Research Building B, University Park, Pa. 16802. T. Scullion, Texas Transportation Institute, Texas A&M University, College Station, Tex. 77843.

TABLE 1 Experimental Plan for Field Testing

| Variable | Levels |
|---|---|
| Pavement section | Thin and thick |
| Load | Empty, intermediate, fully loaded |
| Tire pressure | 100, 125 psi |
| Speed | 20, 35, 50 mph |
| Replicate measurements | 4 |

## DESCRIPTION OF GENERALIZED MODULUS BACKCALCULATION PROCEDURE

A key requirement of this study was to be able to convert the output of pavement instrumentation under known loadings to appropriate layout moduli. The instrumentation to be used includes strain gauges and multidepth deflectometers. The conversion will be made using calculations made with linear elastic theory. A search routine is used to minimize error between the measured readings (strains or deflections) and the computed values. In the search routine, the solution is the set of layer moduli that produces the best fit between measured and calculated values. The scope of the system developed by Uzan et al. (*9*) was expanded to permit strain bowl and depth deflections, in addition to surface deflection, to be used in the backcalculation process.

The procedure is designed to find the set of parameters that correspond to the best fit of the measured pavement response (i.e., strain or deflection). The best fit is achieved by minimizing the error between the measured and the calculated pavement response curves. The objective function can, therefore, be written as

Minimize

$$\sum_{i=1}^{n} \varepsilon^2 = \sum_{i=1}^{n} \left[ \frac{W_i^m - W_i^c}{W_i^m} \right] W_{ei}$$

where

$\varepsilon^2$ = squared error,
$W_i^m$ = measured pavement response (i.e., deflection or strain) at distance $i$ away from load,
$W_i^c$ = calculated pavement response (i.e., deflection or strain) at distance $i$ away from load,
$n$ = number of distances away from load, and
$W_{ei}$ = user-supplied weighing factor for distance $i$.

## INPUTS TO GENERALIZED BACKCALCULATION PROCEDURE

The generalized backcalculation procedure permits flexible input of measured pavement responses. Measured values can be taken from various sensors, which is the case with surface or depth deflection sensors, or from multiple loading positions on a single sensor.

### Strain Gauge

Strain gauges are typically installed at the bottom of the asphalt layer. Therefore, to analyze strain gauge data, it is necessary to calculate the strains induced as the wheel approaches the single gauge. An example of this can be seen in Figure 1; the tensile strains at offsets of 0, 6, 12, 18, 24, and 30 in. are extracted from the strain pulse. Using these offsets and the relevant gauge depth (6 in.), a data base of strain values will be generated for the user-supplied range of acceptable moduli. The measured tensile strains, as shown in Figure 1, are then compared with the calculated strains in the data base.

### Multidepth Deflectometer

Multidepth deflectometers can be located at various depths within each layer of the pavement. However, these devices present an added complication because they measure the relative movement between the sensor location and an anchor buried at some depth (in this project, 73 in.) below the surface. The anchor movement must be taken into consideration. This is done within the generalized backcalculation procedure by calculating the theoretical anchor movement for each combination of layer moduli within the data base. Then, on entering the pattern search, the theoretical relative deflection (theoretical deflection at depth minus theoretical anchor movement) can be compared with the MDD readings.

## BACKCALCULATION OF LAYER MODULI

To evaluate the layer moduli for the test sections, pavement responses were measured using FWD and truck loading. Multiple backcalculation analyses were conducted under each loading condition.

### Backcalculation of Layer Moduli from FWD Data

The FWD was positioned directly over the multidepth deflectometer, and drops were made at three different load levels. Deflections were simultaneously measured on the surface and at MDD locations; the results are shown in Tables 2 and 3.

| Offset Distance (ins) | 0 | 6 | 12 | 18 | 24 | 30 |
|---|---|---|---|---|---|---|
| Tensile Strain (microstrain) | 95 | 82 | 40 | -10 | -40 | -40 |

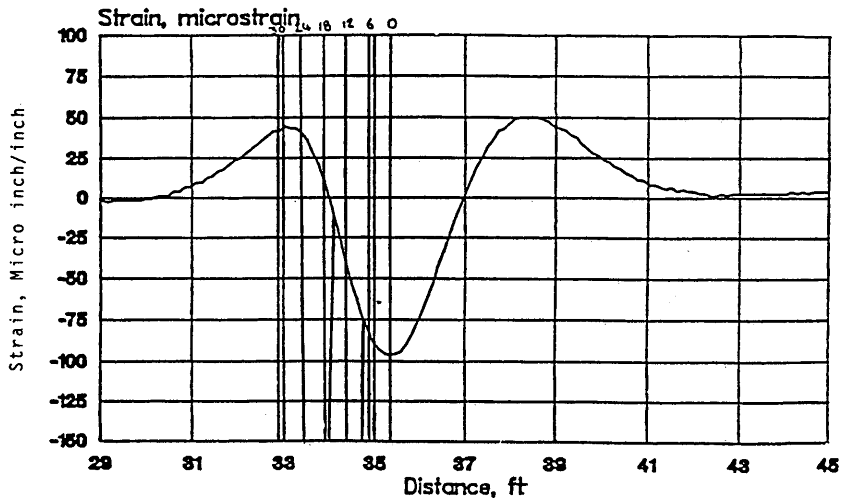


**FIGURE 1** Typical strain response from strain gauge at bottom of asphalt concrete layer: thin section, Dynatest, Station 9, 50 mph.

**TABLE 2** FWD and MDD Test Results From Thin Pavement Section

| Drop # | Load (lbs) | FWD Deflections (mils) | | | | | | MDD (mils) | | |
|---|---|---|---|---|---|---|---|---|---|---|
| | | 0 | 12 | 24 | 32.5 | 48 | -12 | 6.5 | 14.5 | 26.5 |
| 1 | 7,310 | 12.68 | 8.46 | 4.74 | 3.03 | 1.26 | 8.54 | 11.19 | 7.64 | 2.57 |
| 2 | 8,606 | 15.47 | 10.51 | 5.94 | 3.74 | 1.52 | 10.59 | 13.68 | 9.78 | 3.18 |
| 3 | 10,271 | 18.54 | 12.64 | 7.21 | 4.53 | 1.85 | 12.79 | 16.67 | 12.04 | 3.81 |

**TABLE 3** FWD and MDD Test Results From Thick Pavement Section

| Drop # | Load (lbs) | FWD Deflections (mils) | | | | | | MDD (mils) | | | |
|---|---|---|---|---|---|---|---|---|---|---|---|
| | | 0 | 12 | 24 | 32.5 | 48 | -12 | 3 | 10 | 20 | 32 |
| 1 | 7,495 | 5.51 | 3.15 | 1.97 | 1.34 | 1.26 | 3.38 | 4.74 | 3.71 | 2.05 | 1.09 |
| 2 | 8,698 | 6.85 | 3.98 | 2.44 | 1.65 | 1.52 | 4.33 | 5.81 | 4.58 | 2.56 | 1.36 |
| 3 | 10,271 | 8.07 | 4.84 | 2.95 | 2.01 | 1.10 | 5.24 | 6.91 | 5.54 | 3.02 | 1.59 |

### *Backcalculation of In Situ Moduli from Surface Deflections*

Backcalculation of in situ moduli from surface deflections consisted of the traditional backcalculation of layer moduli from surface deflections. The results of this analysis are shown in Table 4. These results indicated extremely low values for the subbase and subgrade layers of the thin sections. The large difference between the subbase and subgrade moduli of the two sections is unusual because both sections are within 100 ft of the test track.

### *Backcalculation of In Situ Moduli from MDD Deflections*

Backcalculation of in situ moduli from MDD deflections consisted of backcalculating the layer moduli from the MDD deflections. Table 5 summarizes the layer moduli values obtained from this analysis.

The data in Tables 4 and 5 show that there are major disagreements between the backcalculated moduli from surface deflections and those calculated from MDD deflections. However, both analyses agree that the subbase on the thin section is very weak.

## Modulus Backcalculation Using Sensor Data Collected Under Truck Loading

The generalized backcalculation procedure was used to process the strain basins and MDD deflections under truck loading to backcalculate the in situ resilient moduli. All of the backcalculation analyses are conducted on the basis of measurements under the single drive axle.

### *Backcalculation of In Situ Moduli from Measured Strain Basins*

Table 6 summarizes the values of the backcalculated moduli as a function of the truck speed and axle load for the thick section. The data show good agreement between the two types of gauges (i.e., Kyowa and core gauges). The effect of speed on the moduli of the asphalt concrete layer ($E_1$) is very noticeable under all load levels. The effect of load magnitude on the backcalculated moduli is insignificant, which indicates that the nonlinearity of the base and subgrade materials is insignificant.

Table 7 summarizes the backcalculation results of the thin section on the basis of measurements from all three types of gauges. In this case, there is less agreement among the results of the various gauges compared with the thick section data. The effect of truck speed on the backcalculated moduli of the asphalt concrete layer is very significant, whereas the effect of load level is insignificant.

### *Backcalculation of In Situ Moduli from Measured MDD Deflections*

As discussed earlier in the paper, one MDD was installed in each test section (thick and thin). The MDD in the thick section had four modules at depths of 3, 10, 20, and 32 in.;

**TABLE 4 Layer Moduli Backcalculated Using Surface Deflections**

| Pavement | AC Modulus (ksi) | Base Modulus (ksi) | Subbase Modulus (ksi) | Subgrade Modulus (ksi) |
|---|---|---|---|---|
| Thin | 301 | 67 | 7 | 6 |
| Thick | 271 | 81 | 76 | 22 |

**TABLE 5 Layer Moduli Backcalculated Using MDD Deflections**

| Pavement | AC Modulus (ksi) | Base Modulus (ksi) | Subbase Modulus (ksi) | Subgrade Modulus (ksi) |
|---|---|---|---|---|
| Thin | 455 | 25 | 6 | 25 |
| Thick | 402 | 29 | 34 | 46 |

**TABLE 6 Backcalculated Moduli for Thick Section Under Single-Drive Axle, on Basis of Strain Measurements**

| Speed (mph) | Load (k) | Station (Strain gauge) | $E_1$ (ksi) | $E_2$ (ksi) | $E_3$ (ksi) | $E_4$ (ksi) |
|---|---|---|---|---|---|---|
| 50 | 20 | 6 (k) | 545 | 10 | 7 | 60 |
| | | 12 (c) | 461 | 10 | 5 | 60 |
| | 12 | 6 (k) | 556 | 10 | 7 | 60 |
| | | 12 (c) | 640 | 10 | 13 | 60 |
| | 8 | 6 (k) | 534 | 10 | 7 | 60 |
| | | 12 (c) | 641 | 10 | 13 | 60 |
| 35 | 20 | 6 (k) | 350 | 10 | 5 | 44 |
| | | 12 (c) | 366 | 10 | 5 | 60 |
| | 12 | 6 (k) | 347 | 10 | 5 | 39 |
| | | 12 (c) | 349 | 10 | 5 | 41 |
| | 8 | 6 (k) | 393 | 10 | 11 | 60 |
| | | 12 (c) | 361 | 10 | 5 | 60 |
| 20 | 20 | 6 (k) | 258 | 10 | 16 | 60 |
| | | 12 (c) | 230 | 10 | 11 | 60 |
| | 12 | 6 (k) | 214 | 18 | 40 | 60 |
| | | 12 (c) | 200 | 22 | 40 | 60 |
| | 8 | 6 (k) | 200 | 21 | 40 | 60 |

k = Kyowa gauge

c = core gauge

and the MDD in the thin section had three modules at depths of 6.5, 14.5, and 26.5 in. In the case of the MDD, the peak deflections at each level were used to backcalculate the in situ moduli. Tables 8 and 9 summarize the in situ moduli for the thick and thin sections, respectively.

### *Backcalculation of In Situ Moduli from Combination of Measured Strain Basins and MDD Deflections*

The data set chosen for evaluation is shown in Table 10. These data were measured on the thick pavement section using a fully loaded truck with a single-drive axle and 125 lb/in.$^2$ tire pressure. The data represent the peak depth deflections and strain bowls (Kyowa gauge) under single axle (19.6 kips per axle).

A four-layer structure was assumed, as shown in Figure 2. The procedure consists of using the generalized backcalculation method as follows:

1. Fix the $E_1$ value calculated from the strain bowl; use the MDD data to calculate $E_2$, $E_3$, and $E_4$ values.
2. Fix the $E_2$, $E_3$, and $E_4$ values calculated in Step 1; use the strain data to calculate an $E_1$ value.

Steps 1 and 2 are repeated until the error between measured and computed deflection and strain values are reduced to an acceptable level. The results of this analysis are shown in Table 11. At each speed, two iterations were used. The surfacing modulus showed some distinct speed effects; the base and subbase were weak, and the subgrade was relatively strong.

## IMPACT OF VARIOUS MODULI VALUES

Analysis of the pavement response data indicates that the backcalculated layer moduli are affected by various factors, including

1. Type of loading—FWD or truck,
2. Measured pavement response—surface deflection, MDD, and strain gauges, and
3. Analysis approach—single response or multiple responses.

**TABLE 7 Backcalculated Moduli for Thin Section Under Single-Drive Axle, on Basis of Strain Measurements**

| Speed (mph) | Load (k) | Station (Strain gauge) | $E_1$ (ksi) | $E_2$ (ksi) | $E_3$ (ksi) | $E_4$ (ksi) |
|---|---|---|---|---|---|---|
| 50 | 20 | 30 (d) | 758 | 10 | 5 | 10 |
| | | 29 (k) | 675 | 10 | 5 | 10 |
| | | 12 (c) | 1170 | 10 | 5 | 18 |
| | 12 | 30 (d) | 900 | 12 | 5 | 10 |
| | | 29 (k) | 896 | 10 | 5 | 10 |
| | | 12 (c) | 1500 | 44 | 5 | 35 |
| | 8 | 30 (d) | 900 | 15 | 5 | 10 |
| | | 29 (k) | 764 | 10 | 5 | 10 |
| | | 12 (c) | 1500 | 23 | 5 | 38 |
| 35 | 20 | 30 (d) | 511 | 10 | 5 | 10 |
| | | 29 (k) | 425 | 10 | 5 | 10 |
| | | 12 (c) | 828 | 10 | 5 | 10 |
| | 12 | 30 (d) | 700 | 10 | 5 | 10 |
| | | 29 (k) | 568 | 10 | 5 | 10 |
| | | 12 (c) | 1368 | 10 | 8 | 60 |
| | 8 | 30 (d) | 855 | 10 | 5 | 10 |
| | | 29 (k) | 703 | 10 | 5 | 10 |
| | | 12 (c) | 1339 | 10 | 6 | 60 |
| 20 | 20 | 30 (d) | 329 | 10 | 10 | 60 |
| | | 29 (k) | 298 | 10 | 8 | 60 |
| | | 12 (c) | 368 | 10 | 12 | 60 |
| | 12 | 30 (d) | 329 | 14 | 40 | 60 |
| | | 29 (k) | 302 | 10 | 10 | 60 |
| | | 12 (c) | 420 | 20 | 40 | 60 |
| | 8 | 30 (d) | --- | -- | -- | -- |
| | | 29 (k) | 233 | 19 | 15 | 10 |
| | | 12 (c) | 431 | 10 | 15 | 50 |

d = Dynatest gauge
k = Kyowa gauge
c = core gauge

**TABLE 8 Backcalculated Moduli for Thick Section Under Single-Drive Axle, on Basis of MDD Measurements**

| Speed (mph) | Load (k) | $E_1$ (ksi) | $E_2$ (ksi) | $E_3$ (ksi) | $E_4$ (ksi) |
|---|---|---|---|---|---|
| 50 | 20 | 363 | 10 | 24 | 50 |
| 35 | 20 | 340 | 10 | 23 | 50 |
| 20 | 20 | 200 | 12 | 23 | 50 |

**TABLE 9 Backcalculated Moduli for Thin Section Under Single-Drive Axle, on Basis of MDD Measurements**

| Speed (mph) | Load (k) | $E_1$ (ksi) | $E_2$ (ksi) | $E_3$ (ksi) | $E_4$ (ksi) |
|---|---|---|---|---|---|
| 50 | 20 | 200 | 12 | 9 | 47 |
| | 12 | 900 | 10 | 13 | 41 |
| | 8 | 900 | 25 | 25 | 50 |
| 35 | 20 | 551 | 10 | 9 | 50 |
| | 12 | 900 | 12 | 19 | 41 |
| | 8 | 900 | 11 | 18 | 50 |
| 20 | 20 | 201 | 11 | 9 | 44 |
| | 12 | 900 | 10 | 11 | 41 |
| | 8 | 900 | 13 | 22 | 50 |

**TABLE 10 Strain and Deflection Data Used in Analysis**

| MPH | MDD DEPTHS (in.) 3 | 20 | 32 | STRAIN OFFSET (in.) 0 | 6 | 12 | 24 |
|---|---|---|---|---|---|---|---|
| 20 | 8.46 | 3.36 | 1.56 | 155.4 | 100.7 | 10.7 | -45.4 |
| 35 | 7.50 | 2.81 | 1.34 | 120.8 | 99.6 | 38.7 | -41.5 |
| 50 | 6.98 | 2.74 | 1.37 | 79.9 | 69.1 | 40.9 | -23.5 |

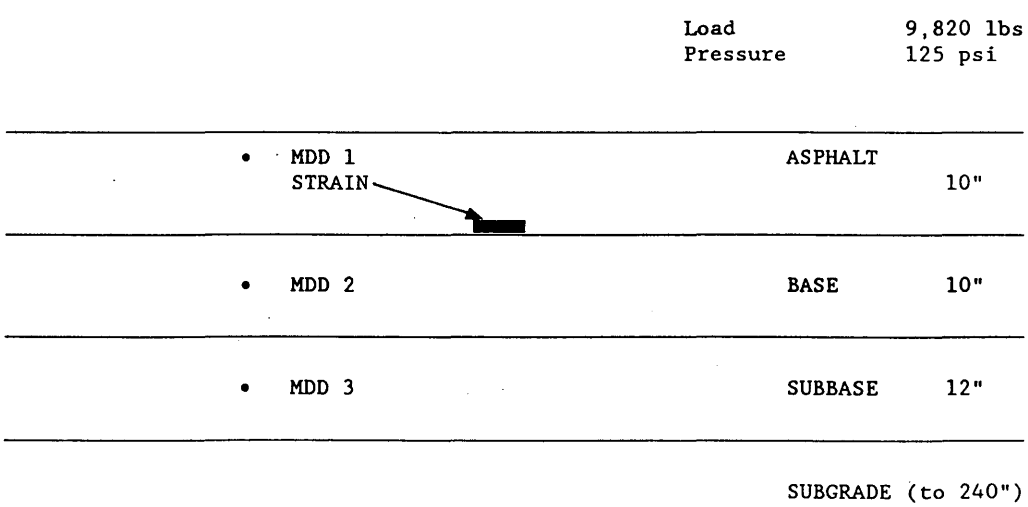


**FIGURE 2 Setup of MDD and strain gauge for moduli evaluation of pavement layers.**

**TABLE 11 Layer Moduli Values Backcalculated Using Deflection and Strain Data**

| Speed (mph) | Description | MDD (mils) Depths | | | Max. Strain | Moduli (ksi) | | | | No. Iteration |
|---|---|---|---|---|---|---|---|---|---|---|
| | | 3" | 20" | 32" | (microstrain) | $E_1$ | $E_2$ | $E_3$ | $E_4$ | |
| | Measured | 8.46 | 3.36 | 1.56 | 155.4 | 291 | 9 | 19 | 44 | 2 |
| 20 | Calculated | 8.46 | 3.36 | 1.56 | 171.0 | | | | | |
| | % Error | 0.0 | 0.0 | 0.0 | -10.0 | | | | | |
| | Measured | 7.50 | 2.81 | 1.34 | 120.8 | 414 | 8 | 21 | 48 | 2 |
| 35 | Calculated | 7.31 | 2.74 | 1.34 | 132.5 | | | | | |
| | % Error | 2.6 | 2.4 | 0.0 | -9.7 | | | | | |
| | Measured | 6.98 | 2.74 | 1.37 | 79.9 | 751 | 5 | 14 | 36 | 2 |
| 50 | Calculated | 6.79 | 2.69 | 1.36 | 88.8 | | | | | |
| | % Error | 2.7 | 1.7 | 0.6 | -11.2 | | | | | |

One fundamental way to evaluate the significance of the differences between the moduli values from the various analyses is to study their influence on the end product, i.e., equivalent single axle loads (ESALs). It is very common that the backcalculated moduli will be used in either of the following two analyses:

1. To evaluate the capacity of the existing pavement section using the AASHTO design guide (*10*), or

2. To evaluate the capacity of the existing pavement section using a mechanistic-empirical approach (*11*).

The end product of the two analyses is the number of ESALs that the pavement section can handle before the ultimate failure of the pavement.

The AASHTO design guide procedure consists of evaluating the structural number (SN) of the existing pavement section and determining the ESALs for specific values of re-

**TABLE 12 Impact of Various Backcalculated Moduli for Thin Sections**

| Method of Backcalculation Analysis | Standard Number (SN) | AASHTO ESAL's (millions) | Critical Strains (Micro) | Cracking ESAL's (millions) |
|---|---|---|---|---|
| 1. FWD Load & Surface Deflection | 4.5 | 2.4 | 168 | 3.2 |
| 2. FWD Load & MDD Deflections | 4.3 | 30.0 | 208 | 1.1 |
| 3. Truck Load & Strain Gauge, 50 mph | 3.6 | 2.0 | 198 | 0.9 |
| 4. Truck Load & Strain Gauge, 35 mph | 3.4 | 1.7 | 277 | 0.5 |
| 5. Truck Load & Strain Gauge, 20 mph | 3.3 | 31.0 | 325 | 0.4 |
| 6. Truck Load & MDD, 50 mph | 4.4 | 50.0 | 139 | 2.4 |
| 7. Truck Load & MDD, 35 mph | 5.0 | 50.0 | 132 | 2.8 |
| 8. Truck Load & MDD, 20 mph | 4.3 | 50.0 | 141 | 2.2 |
| Mean | | 27.1 | | 1.7 |
| Standard Deviation | | 20.9 | | 1.0 |
| Coefficient of Variation (%) | | 77 | | 59 |

liability, standard deviation, loss of pounds per square inch, and subgrade moduli. In this analysis, the following values were used:

- Reliability, 95 percent;
- Standard deviation, 0.35; and
- Loss of pounds per square inch, 1.5.

On the basis of the thickness of the pavement section and the backcalculated moduli, the SN value was evaluated for each combination of pavement type (i.e., thin or thick) and for each method of backcalculation analysis. When using the AASHTO nomograph, a maximum value for the effective roadbed soil resilient modulus of 40,000 lb/in.$^2$ and a maximum value of 50 million ESALs were used.

The second analysis consisted of evaluating the capacity of the existing pavement section using a mechanistic-empirical approach. The following fatigue performance equation, developed by Finn et al., was selected for this analysis (*11*):

$$\log N_f = 15.947 - 3.291 \log\left(\frac{\varepsilon}{10^{-6}}\right) - 0.854 \log\left(\frac{E}{10^3}\right)$$

where

$N_f$ = number of load applications required to cause 10 percent Class 2 cracking of wheel tracks;
$\varepsilon$ = tensile strain at bottom of asphalt concrete layer; and
$E$ = resilient modulus of asphalt concrete layer.

The tensile strains at the bottom of the asphalt concrete layer were evaluated from the multilayer elastic solution, and the resilient modulus value was obtained from the backcalculated moduli.

The data shown in Tables 12 and 13 indicate that there are significant differences among the predicted ESALs from various methods of backcalculation analyses. Figures 3 and 4 show the distribution of AASHTO and cracking ESALs for the thin and thick sections, respectively.

**TABLE 13 Impact of Various Backcalculated Moduli for Thick Sections**

| Method of Backcalculation Analysis | Standard Number (SN) | AASHTO ESAL's (millions) | Critical Strains (Micro) | Cracking ESAL's (millions) |
|---|---|---|---|---|
| 1. FWD Load & Surface Deflection | 6.1 | 50 | 72 | 57.1 |
| 2. FWD Load & MDD Deflections | 8.0 | 50 | 93 | 17.6 |
| 3. Truck Load & Strain Gauge, 50 mph | 5.7 | 50 | 101 | 10.3 |
| 4. Truck Load & Strain Gauge, 35 mph | 4.7 | 50 | 146 | 4.5 |
| 5. Truck Load & Strain Gauge, 20 mph | 5.1 | 50 | 166 | 3.8 |
| 6. Truck Load & MDD, 50 mph | 6.1 | 50 | 127 | 6.9 |
| 7. Truck Load & MDD, 35 mph | 5.9 | 50 | 134 | 6.1 |
| 8. Truck Load & MDD, 20 mph | 5.1 | 50 | 188 | 3.2 |
| 9. Truck Load, MDD, & Strain Gauge, 50 mph | 6.5 | 50 | 82 | 15.6 |
| 10. Truck Load, MDD, & Strain Gauge, 35 mph | 6.4 | 50 | 120 | 7.4 |
| 11. Truck Load, MDD, & Strain Gauge, 20 mph | 5.5 | 50 | 155 | 4.3 |
| Mean | | 50 | | 12.4 |
| Standard Deviation | | 0 | | 14.8 |
| Coefficient of Variation (%) | | 0 | | 119 |
| Excluding the FWD Load & Surface Deflection Analysis | | | | |
| Mean | | | | 8.0 |
| Standard Deviation | | | | 4.8 |
| Coefficient of Variation | | | | 60 |

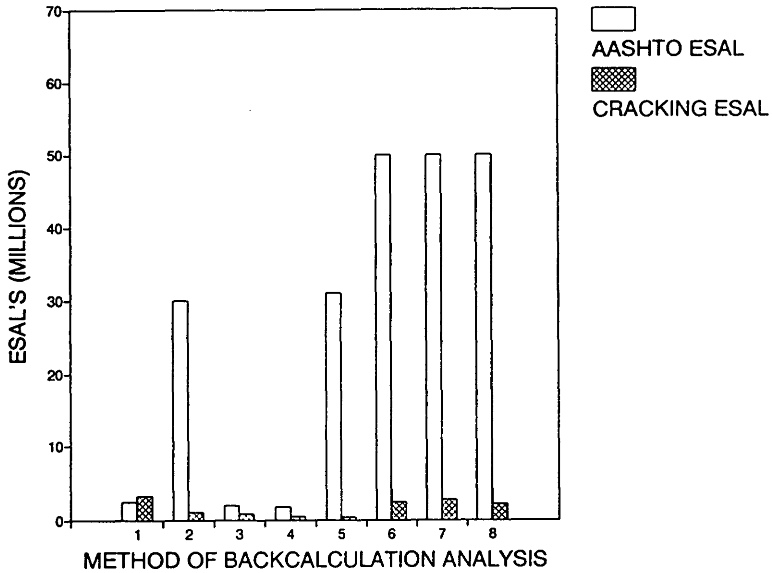


**FIGURE 3 Distribution of predicted ESALs from various analyses, thin section (see Table 12 for method).**

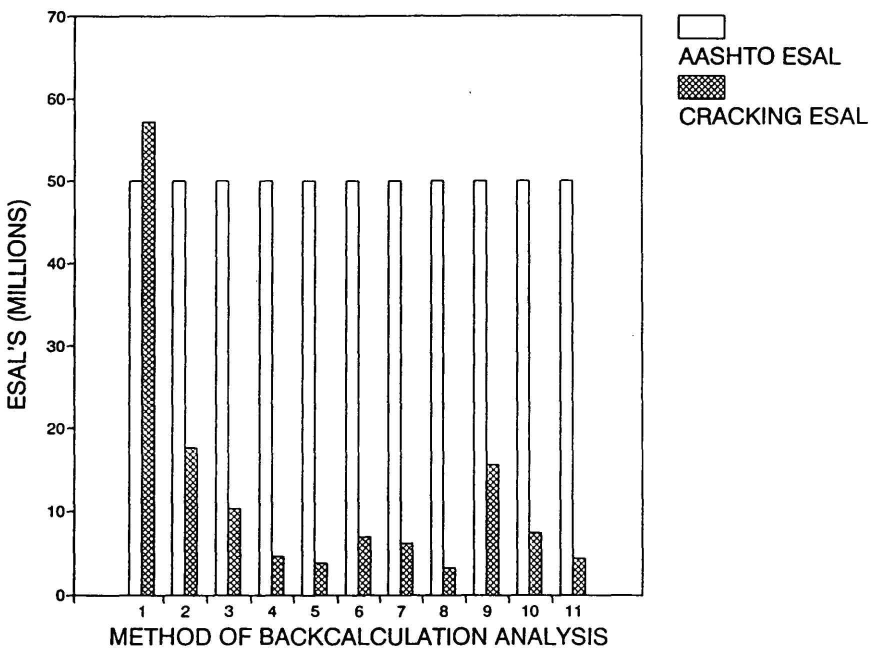


**FIGURE 4 Distribution of predicted ESALs from various analyses, thick section (see Table 13 for method).**

## CONCLUSIONS AND RECOMMENDATIONS

On the basis of an appraisal of the backcalculated moduli from the various analyses, the following conclusions and recommendations can be made.

- The backcalculated moduli of all the pavement layers are significantly affected by the mode of loading (i.e., FWD or truck). The modulus of the asphalt concrete layer was reduced by 50 percent as a function of reducing the speed from 50 to 20 mph. The effect of truck speed on the granular and subgrade layers was insignificant.
- The effect of the magnitude of the axle load on the backcalculated moduli of all the pavement layers was insignificant. This observation indicates that for the data collected in this experiment and the methods of analyses used, the effect of the material's nonlinearity is very small.
- The combined analysis of strain and MDD data show that the speed has a significant effect on the modulus of the asphalt concrete layer. The backcalculated moduli from these com-

bined analyses have high merit because they satisfy two independently measured pavement response parameters (strains and depth deflections).

- The effect of the various backcalculation analysis on the predicted ESALs was very significant. The coefficients of variations of the predicted ESALs were 77, 59, and 119 percent for the AASHTO and cracking ESALs of the thin and thick sections, respectively. The coefficient of variation of the cracking ESALs on the thick section was dramatically improved by the removal of FWD load and surface deflection analysis.
- The FWD load and surface deflection backcalculation analysis has shown the closest agreement between the AASHTO ESALs and the cracking ESALs. However, the set of moduli generated from this analysis did not satisfy the independently measured depth deflections (Table 4).

On the basis of the findings of the research presented in this paper, it is almost impossible to produce one set of layer moduli that satisfies all of the pavement response parameters. The combined analysis of MDD deflections and strain gauge measurements represents a major step forward toward the appropriate solution. However, it does not represent the complete solution because it did not satisfy the FWD load and surface deflection case. In the meantime, it seems appropriate to use the FWD load and surface deflection analysis while the research for the perfect solution continues because it is the only analysis that provided a close agreement between the AASHTO and the cracking ESALs.

## ACKNOWLEDGMENT

The authors would like to thank FHWA for the financial support for this research.

## REFERENCES


1. E. J. Yoder and M. W. Witczack. *Principles of Pavement Design*, 2nd ed. John Wiley and Sons, Inc., New York, N.Y.
2. L. H. Irwin. *User's Guide to MODCOMP2*. Cornell Local Roads Report 83-8. Cornell University, Ithaca, N.Y., Nov. 1983.
3. M. S. Mamlouk. *Development of Microcomputer Program for Moduli Prediction of Pavement Layers*. CART, Arizona State University, Tempe, Aug. 1986.
4. S. W. Lee. *Backcalculation of Pavement Moduli by Use of Pavement Surface Deflection*. Ph.D. dissertation, University of Washington, Seattle, 1988.
5. A. J. Bush. Nondestructive Testing of Light Aircraft Pavements, Phase II, Development of the Nondestructive Evaluation Methodology. Report FHWA-RD-80-9-11. FHWA, U.S. Department of Transportation, Washington, D.C., 1980.
6. J. T. Christison and B. P. Shields. Pavement Elastic Moduli by the Surface Wave Method Correlated with In-Situ Measurements of Elastic Response Under Moving Vehicle Loads. *Proc., 19th Annual Conference of the Canadian Technical Asphalt Association*, Regina, Saskatchewan, Canada.
7. P. E. Sebaaly and B. T. Kulakowski. In Situ Instrumentation for Resilient Moduli Measurements. FHWA; Pennsylvania Transportation Institute, University Park, June 1988–June 1992.
8. P. E. Sebaaly, N. Tabatabaee, and T. Scullion. Instrumentation for Flexible Pavements. Report FHWA-RD-89-084. FHWA, U.S. Department of Transportation, Washington, D.C., 1989.
9. J. Uzan, T. Scullion, C. H. Michelek, M. Parades, and R. L. Lytton. *A Microcomputer-Based Procedure for Backcalculating Layer Moduli from FWD Data*. Research Report 1123-1. Texas Transportation Institute, Texas A&M University, College Station, July 1988.
10. *AASHTO Guide for Design of Pavement Structures*. AASHTO, Washington, D.C., 1986.
11. F. Finn, C. L. Saraf, R. Kulkarni, K. Nair, W. Smith, and A. Abdullah. *NCHRP Report 291: Development of Pavement Structural Subsystems*. TRB, National Research Council, Washington, D.C., 1986.

# Modeling Material Nonlinearity in a Pavement Backcalculation Procedure

J. M. BRUNTON AND J. R. DE ALMEIDA

The development of improved procedures for the computation of effective stiffnesses of pavement layers from deflection bowls measured using the falling weight deflectometer (FWD) with particular emphasis given to the behavior of granular materials and subgrades is described. So far, the interpretation of FWD data at the University of Nottingham has been carried out using the computer program PADAL. In this program the pavement is represented by a series of linear elastic layers. The nonlinear properties of the subgrade are incorporated by dividing the subgrade into a series of sublayers, each having a different stiffness based on a stress-dependent elastic model derived from the results of laboratory repeated load triaxial tests. PADAL 2, an updated version of PADAL in which the nonlinearity of the subgrade is approximately modeled in the horizontal direction, has been developed. This modification allows for a more realistic description of the variability of elastic stiffnesses throughout the pavement. A comparison is made between two models incorporated in the back-analysis program to simulate the resilient behavior of fine-grained soils. FENLAP, a new finite element code for the structural analysis of pavements has been developed. The program includes a number of different nonlinear constitutive relationships. The finite element analysis may serve for calibrating the simpler layered elastic analysis approach. A pavement section is analyzed using the two computer programs, PADAL 2 and FENLAP.

The computer program PADAL was developed at Nottingham in 1985 (*1*) for the backcalculation of elastic stiffnesses of the pavement layers from deflection bowls measured using the falling weight deflectometer (FWD). Since then it has been extensively used to evaluate the condition of existing pavements in situ. Meanwhile, research has continued to develop and improve analytical methods for interpreting the results of FWD surveys on road pavements with thick granular layers. To pursue these objectives, two numerical techniques have been considered for the analysis of pavement structures, multilayered elastic systems, and finite elements.

In PADAL the pavement is represented by a series of linear elastic layers. The nonlinear properties of the subgrade are incorporated by dividing the subgrade into a series of sublayers, each having a different stiffness based on a stress-dependent elastic model derived from the results of laboratory repeated load triaxial tests. Extensive use of PADAL over the last 7 years to evaluate in situ pavements has shown this backcalculation technique to be generally satisfactory; however, experience has shown that it has some limitations, especially for pavements with thick granular bases. Recent development has continued to enhance the back-analysis procedure; in particular, consideration has been given to a new constitutive relationship for the subgrade, a nonlinear elastic model for granular materials, and a scheme for taking into account the stress dependency of stiffnesses in the horizontal direction.

With reference to the finite element method, a new computer program for the nonlinear analysis of pavements (FENLAP) has been developed. A pavement section backcalculated through PADAL is recomputed in FENLAP using the elastic stiffnesses obtained in PADAL. The results are used to compare the two programs.

Department of Civil Engineering, University of Nottingham, University Park, Nottingham, England NG7 2RD.

## DEVELOPMENTS ON COMPUTER PROGRAM PADAL

### Nonlinear Elastic Subgrade Models

For the structural analysis of pavements, accurate modeling of the behavior of the subgrade is important because the subgrade has a major influence on the pavement performance, particularly when considering deflections under wheel loading. For a realistic description of the subgrade condition, it is desirable to adopt nonlinear stress-strain relationships.

The computer program PADAL, which performs the backcalculation of stiffnesses of the individual pavement layers on the basis of FWD data, uses Brown's nonlinear elastic model for the subgrade, developed from laboratory testing (*2*).

$$E_r = A\left(\frac{p'_o}{q_r}\right)^B \tag{1}$$

where

$E_r$ = resilient modulus;
$p'_o$ = effective mean normal stress caused by overburden;
$q_r$ = deviatoric stress caused by wheel loading;
$A$ = material constant, typically in the range of 20 to 200 MPa; and
$B$ = material constant, typically in the range of 0 to 0.5.

Subsequent laboratory testing of fine-grained soils has resulted in the development of a new model at Nottingham by Loach in a paper by Brown et al. (*3*), expressed by

$$E_r = Cq_r\left(\frac{p'_o}{q_r}\right)^D \tag{2}$$

where $C$ is a material constant, typically in the range of 10 to 100, and $D$ is a material constant, typically in the range of 1 to 2.

This relationship should constitute an improvement to Equation 1, because it was formulated after a comprehensive set of cyclic triaxial tests on samples more representative of soil in the ground. Therefore, Loach's model was incorporated in PADAL. All the essential characteristics of the representation of the subgrade in PADAL have been retained as for the model of Brown et al. (*1*). Hence, the subgrade is divided into five sublayers, and stresses at the middepth of each sublayer are considered for the calculation of stiffnesses and successive adjustments of the material constants, depending on the matching between measured and computed deflections at two outer points of the FWD deflection bowl. Figure 1 shows a typical deflection bowl and corresponding structure with the subgrade subdivision layers.

The only modification in the new algorithm is the implementation of a different procedure for adjusting stiffness between successive iterations. Using Brown's model, the stiffness of the upper layers and the elastic parameters of the subgrade were adopted in each iteration as follows (*1*):

$$E_{ni} = E_{oi}\left(\frac{dc_j}{dm_j}\right)^k \tag{3}$$

$$A_n = A_o\left(\frac{dc_l}{dm_l}\right)^k \tag{4}$$

$$B_n = B_o\left(\frac{dc_m}{dm_m}\right)^k \tag{5}$$

where

$E_{ni}$, $E_{oi}$ = new and old computed stiffnesses for layer $i$,
$A_n$, $A_o$, $B_n$, $B_o$ = new and old values of subgrade parameters $A$ and $B$,
$dc_j$, $dm_j$, $dc_l$, $dm_l$, $dc_m$, $dm_m$ = computed and measured deflections at sensors $j$, $l$, $m$, and
$k$ = integer exponent that initially is equal to 1 but may vary as iterations proceed.

Because of the greater difficulty in achieving convergence for Loach's model, it was found necessary to adopt different values for the power index $k$. The exponent adopted used for the subgrade is half the value previously adopted ($k/2$ in Equations 4 and 5). Hence, the variation of the subgrade stiffness throughout the iterations is much smoother than before, making this approach more stable. However, the reduced power index for the subgrade implies that the convergence rate will be slower. To overcome this, the exponent of the upper layers is increased from $k$ to $2k$ in Equation 3. Even so, the rate of convergence is usually slower for Loach's model than for Brown's model.

## Comparison of Nonlinear Subgrade Models

The same pavement was back-analyzed with both Brown's and Loach's models. Details of the structure analyzed are presented in Figure 2. Brown's model took 31 iterations to perform the back-analysis, whereas with Loach's model convergence was reached after only 78 iterations. Additionally, the input parameters $C$ and $D$ used in this example were not very different from the values eventually determined; otherwise the number of iterations required by Loach's model would have been greater.

The output is summarized in Table 1. The results obtained using each of the models are very similar, for both deflections and stiffnesses. These results confirm that PADAL tends to unique solutions even when different constitutive relationships are compared. However, in Loach's model the exponent $D$ of Equation 2 is slightly lower than 1. That is, according to the relationship, the subgrade shows a stress hardening behavior because its stiffness increases with increasing deviatoric stress. This was not expected, since fine-grained soils have always been regarded as stress softening materials.

The experimental data that led to Loach's model were based on tests at high $(q/p'_o)$ ratios compared with those that occur at depth in the subgrade. In fact, for stress pulse durations of 1s and 0.1s (representative of the stress pulses induced in the subgrade by the FWD), Loach used 0.2 for the minimum value of $(q/p'_o)$. However, when using PADAL, this ratio for the lower part of the subgrade was found to be substantially smaller (0.008 in the preceding example). Therefore, the stress conditions that exist in the deep subgrade were not reproduced, so it is possible that the model is not appropriate for these situations.

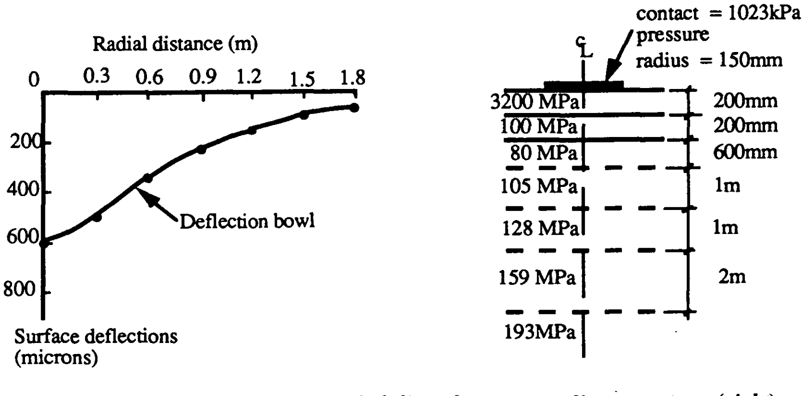


**FIGURE 1 Typical deflection bowl (*left*) and corresponding structure (*right*).**

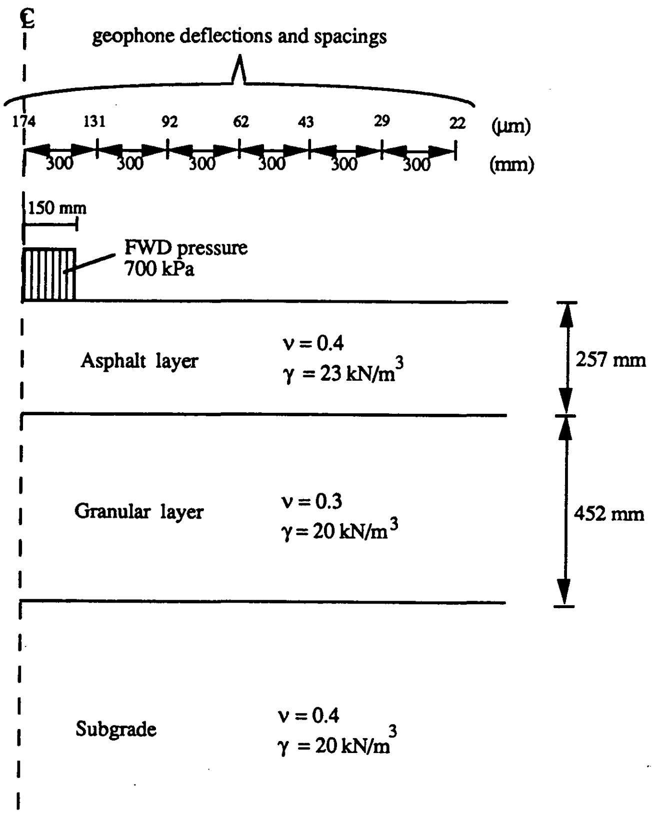


**FIGURE 2 FWD data for full-scale pavement.**

When an unstressed state is approached, Loach's model tends to predict infinite stiffnesses. However, most soils exhibit a finite maximum stiffness even when tested at low deviatoric stress. This seems to point out the inadequacy of Loach's model for low values of $(q/p'_o)$, which may explain the odd values obtained for the constant $D$ (<1).

### Nonlinearity of Subgrade in Radial Direction

The original version of PADAL, despite incorporating a nonlinear elastic relationship for the subgrade, is unable to model nonlinearity in the horizontal direction. This shortcoming is common to all packages that are based on layered elastic analysis, because it is assumed that each layer or sublayer has a unique stiffness. Thus, although the stresses vary with radius, the stress dependency of the materials in the radial direction cannot be reproduced.

For a generic point in the subgrade at depth $z$ and radius $r$, PADAL assigns a stiffness $E(z,r)$ that is based on the stresses calculated at a point located underneath the load center ($r = 0$) and at the middepth $Z$ of the sublayer considered, that is,

$$E(z,r) = A\left(\frac{p'_o}{q_r}\right)^{B}_{(Z,0)} \tag{6}$$

An approximate procedure has been devised to overcome this restriction, that is, to make the subgrade stiffness variable with radius. Clearly, this procedure can be accurately achieved

**TABLE 1 Comparison of Models in PADAL and PADAL 2**

| | PADAL | | PADAL 2 | |
|---|---|---|---|---|
| | Brown's Model | Loach's Model | Brown's Model | Loach's Model |
| No. Iterations | 31 | 78 | 36 | 39 |
| $d_2$ Error (%) | -2.65 | -2.78 | -3.16 | -2.62 |
| $d_3$ Error (%) | -2.48 | -2.60 | -2.69 | -2.52 |
| $d_6$ Error (%) | 4.62 | 4.65 | 4.49 | 4.68 |
| $E_{as}$ (MPa) | 5041 | 5009 | 4814 | 5068 |
| $E_{sb}$ (MPa) | 245 | 251 | 337 | 229 |
| $E_{sg\text{-}l1}$ (MPa) | 174 | 170 | 148 (220) | 180 (162) |
| $E_{sg\text{-}l2}$ (MPa) | 232 | 232 | 199 (249) | 243 (229) |
| $E_{sg\text{-}l3}$ (MPa) | 301 | 303 | 260 (295) | 316 (306) |
| $E_{sg\text{-}l4}$ (MPa) | 399 | 403 | 345 (372) | 418 (411) |
| $E_{sg\text{-}l5}$ (MPa) | 582 | 587 | 507 (524) | 603 (600) |

*Notes:* $d_1$,...,$d_7$ = deflections at the geophone locations.

$E_{as}$, $E_{sb}$, $E_{sg}$ = stiffnesses of asphalt, sub-base and subgrade layers (subgrade with 5 sub-layers).

Deflections $d_1$, $d_4$, $d_5$ and $d_7$ were adopted for the matching of computed and measured deflection bowls, hence their errors are negligible.

The "-" sign means that the computed deflection is lower than the measured one.

The subgrade stiffnesses out of "( )" refer to locations beneath the load whereas the values within "( )" refer to a distance of 1.80 m away from the load axis.

only through finite element techniques, so simplifications have had to be adopted for the layered analysis. Essentially, this new approach computes the surface deflection at a certain radial position using a set of stiffnesses for the subgrade corresponding to the stresses in the subgrade at the same radial position. Thus, adopting Brown's relationship, the surface deflection at a distance $R$ from the load center is calculated on the assumption that each sublayer of the subgrade has a stiffness given by

$$E(z,r) = A\left(\frac{p_o'}{q_r}\right)^B_{(z,R)} \tag{7}$$

This procedure is not entirely correct because a unique stiffness is still assumed for each layer in each deflection computation. Nevertheless, the adoption of stiffnesses taken from the stress state of points directly beneath the location where surface deflection ($d$) is to be computed can be justified by the following expression:

$$d = \int_{-\infty}^{0} \frac{1}{E} [\sigma_z - \nu(\sigma_r + \sigma_\theta)]\, dz \tag{8}$$

where

$E,\nu$ = Young's modulus and Poisson's ratio, respectively,
$\sigma_z, \sigma_r, \sigma_\theta$ = vertical, radial, and tangential stresses, respectively, and
$z$ = depth.

From Equation 8 it can be concluded that the deflection depends mainly on the stiffnesses that exist below the point considered, for the integration variable is $z$ ($r$ is kept constant). However, because the stresses are calculated using constant moduli in the radial direction, there will be an error because the evaluation of stresses does not take into account the variation of stiffness with radius. This limitation is inevitable in layered analysis, in which a unique stiffness must be assigned for each layer to proceed with the computation. In spite of that, the new approach seems to be much more appropriate than the earlier one.

The subgrade stiffnesses used for adjusting each deflection are then different and the analysis is carried out at each stage using a set of subgrade moduli corresponding to the radial position being considered. The stresses required for the calculation of the subgrade stiffnesses are computed every 10th iteration only, because they do not vary significantly between iterations. A summary of the procedure adopted is as follows:

1. Assume initial stiffnesses of individual layers and subgrade constants.
2. Calculate stresses in the subgrade (for first iteration and subsequent 10th iterations only).
3. Calculate deflections at each radial position (using subgrade stiffnesses at corresponding radii for all but first iteration).
4. Compare calculated and measured deflections at each radius.
5. Adjust subgrade constants on the basis of deflection comparison.
6. Having calculated stresses and elastic constants of the subgrade, determine subgrade stiffnesses at selected radial positions.
7. Adjust stiffnesses of upper layers on the basis of deflection match.
8. Repeat Steps 2 through 7 until convergence is achieved.

When convergence has been reached, it is possible to reproduce the spatial variation of the subgrade stiffness, both vertically and horizontally, according to Equation 7.

The iteration process involves only calculation of the stresses at the radial positions where the deflections have been selected for matching purposes. For other locations, the evaluation of subgrade stiffnesses must be preceded by the calculation of the stresses at those locations. By linear interpolation of the stiffnesses already determined at the selected points, estimates of the subgrade stiffness at any radial location can be obtained. These may then be used to calculate the stresses at the same radial position and consequently the actual stiffnesses from Equation 7. The use of linear interpolation is acceptable as variations in stiffness do not significantly affect the values of stress.

The consideration of stresses outside the symmetry axis also implies that the three-dimensional equivalent of the mean normal stress, $p$, and deviatoric stress, $q$, should be used. For the axisymmetric system adopted in PADAL, these stresses take the following form:

$$p = \frac{\sigma_z + \sigma_r + \sigma_\theta}{3} \tag{9}$$

$$q = \sqrt{\frac{(\sigma_z - \sigma_r)^2 + (\sigma_z - \sigma_\theta)^2 + (\sigma_r - \sigma_\theta)^2 + 6\tau_{zr}^2)}{2}} \tag{10}$$

where $\sigma_z$, $\sigma_r$, $\sigma_\theta$ are vertical, radial, and tangential stress, respectively, and $\tau_{zr}$ is the shear stress in the $zr$ plane.

To obtain convergence when using both Brown's and Loach's models, the subgrade constants ($A$ and $B$ or $C$ and $D$) were adjusted as shown in Equations 4 and 5, but restricting the value of the power $k$ to 1. For the upper layers, the stiffnesses were adjusted using the same method as in the original PADAL program (Equation 3 with $k$ varying in accordance with the pattern of convergence) (*1*). With this approach convergence was achieved and no special modifications were required for Loach's model.

### Comparison of PADAL and PADAL 2

The modifications described earlier were incorporated in a new version of PADAL named PADAL 2. This new program has been tested for the same typical example analyzed earlier, using both Brown's and Loach's models. The results are also presented in Table 1. The computed deflections match quite well against the measured ones (as shown by the low relative errors), and their values were practically equal to the deflections obtained when constant stiffnesses with radius were assumed. The introduction of a radial variation in stiffness has little effect on the overall magnitude of stiffnesses.

Once again, the value obtained for the exponent $D$ of Loach's relationship in this example is <1. This implies that the subgrade stiffnesses decrease with increasing radial distance from the load, contrary to what was expected.

### Nonlinear Model for Granular Layers

PADAL is unable to adequately represent the behavior of granular subbases, for it adopts a linear elastic relationship for these materials. To overcome this limitation and provide a more useful package for the back-analysis of pavements for which granular layers are structurally relevant, improved constitutive relationships are necessary. After examining several possibilities, the $K$-$\theta$ model (*4*) was chosen to describe the nonlinear response of unbound granular layers. In this model, the resilient modulus $E_r$ is given by

$$E_r = k_1\theta^{k2} \tag{11}$$

where

- $\theta$ = sum of peak values of principal stresses (first stress invariant);
- $k_1$ = material constant, typically in the range of 100 to 1,000; and
- $k_2$ = material constant, typically in the range of 0 to 0.8 (these values of $k_1$ and $k_2$ apply for stiffnesses and stresses in MPa).

This model has been widely used in structural analysis of pavements because its simplicity makes it very attractive for numerical applications. However, the $K$-$\theta$ model is often inaccurate when compared with more complex resilient models. The simple fact of ignoring the influence of the deviatoric stress on the state of deformation of the material shows its limitations. An assessment of this model led to the conclusion that its performance was generally unsatisfactory (*5*).

Despite these limitations, the $K$-$\theta$ model is perhaps the most suitable nonlinear elastic relationship for granular materials that can be implemented successfully in PADAL, for the following reasons:

1. Only two parameters, $k_1$ and $k_2$, are considered in the definition of the material behavior, whereas other models generally involve a greater number of constants. This property is very important in PADAL, since the number of deflections that must be calculated in each iteration should equal the number of material constants to be determined. Thus, an excessive number of material constants will increase the amount of computation and make it more difficult to converge toward a unique solution.
2. The $K$-$\theta$ model assumes a constant Poisson's ratio for the granular layer. Although this assumption is usually regarded as a drawback, this simplification is beneficial to the back-analysis procedure. In fact, the limited number of elastic parameters that can be backcalculated in PADAL implies that only the most important ones, that is, the elastic stiffnesses, can be taken as unknowns. Therefore, a model with stress-dependent Poisson's ratio is inappropriate to be implemented in PADAL.
3. It was shown that, although it is inadequate when predicting stresses and strains in granular layers, the $K$-$\theta$ model gives reasonable results in terms of vertical displacements (*5*). For the back-analysis of a pavement, the requirements of accuracy essentially concern the surface deflection (because the evaluation of the elastic stiffnesses is made on the basis of these deflections).

At the current stage of the research, the method for incorporating the stress-dependent constitutive relationship in PADAL 2 consists of steps similar to those adopted for the subgrade modeling, that is,

1. Division of the granular layer into sublayers, each one having a stiffness consistent with its stress level according to Equation 11.
2. Successive adjustments of the values of parameters $k_1$ and $k_2$ of Equation 11, by matching the measured and the calculated FWD deflections at two preselected radial locations.
3. Consideration of the nonlinearity of the granular material in the horizontal direction, by using an approximate approach analogous to the one followed for the subgrade.

Taking into account the range of thicknesses of granular layers that can be found in real pavement structures, it is thought that two sublayers should be sufficient to model the behavior of these materials. Finer subdivision would not result in any significant benefits but would increase the computational procedure.

## FENLAP—NEW FINITE ELEMENT CODE FOR PAVEMENT ANALYSIS

### General Description

To overcome some of the drawbacks inherent to layered analysis, the mainframe computer program FENLAP (Finite Element Nonlinear Analysis of Pavements) was developed. The program performs a finite element calculation of an axisymmetric solid and is designed for the structural analysis of pavements. A version for use on microcomputers has also been implemented.

The domain is modeled using eight-node rectangular elements, with the loading applied as concentrated forces at the nodes. All nodes along the bottom of the mesh are fixed. All nodes on both sides of the mesh are assumed to be on rollers, allowing vertical displacements but preventing radial displacements (see Figure 3).

FENLAP has been devised to allow for easy incorporation of various stress-strain models. Several material models have been adopted, including linear elastic, Brown's (*2*) and Loach's (*3*) nonlinear models for fine-grained soils, and the $K$-$\theta$ model for granular materials (*4*).

### Analysis Procedure

In FENLAP the initial stress conditions are obtained directly from the specific weights of the materials, the level of the water table, the estimated suction values, and the residual lateral stresses. Having determined the initial stresses, the program calculates the starting values of Young's modulus and Poisson's ratio for each nonlinear element that is based on the mean normal effective stress, the deviatoric stress, and the stress-strain relationships adopted. Then, the vehicle loads are applied and the corresponding stresses computed. Using the sum of the initial and load-induced stresses, a new set of elastic parameters is obtained.

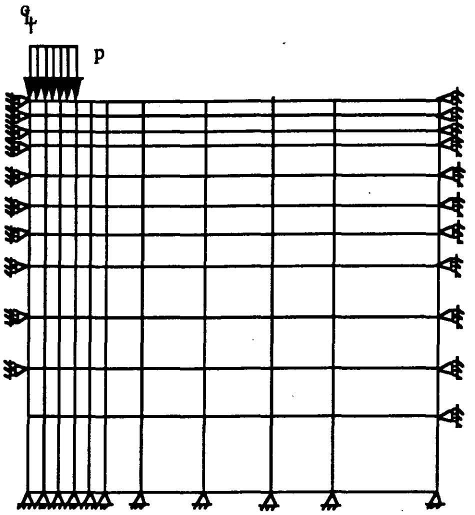


**FIGURE 3 Finite element mesh and boundary conditions in FENLAP.**

The program continues to iterate until sequential resilient modulus calculations for all nonlinear elements agree within a specified tolerance. Once a stable solution is reached, nodal displacements, strains, and stresses can be printed out.

Knowing the transient stresses and strains, it is possible to obtain equivalent values of elastic stiffness and Poisson's ratio associated with the passing of the wheel load alone. These elastic parameters are referred to as "chord" moduli, for they are obtained from the difference between loaded and unloaded conditions. Chord moduli are particularly useful, for they provide an estimation of the resilient response of the layers (*5,6*) and can be compared directly with the nonlinear elastic stiffnesses determined in the program PADAL.

## COMPARISON BETWEEN PROGRAMS PADAL 2 AND FENLAP

### Numerical Example

To test the approach introduced in PADAL 2 for modeling the radial variation of stiffness as well as to further validate FENLAP, both programs were used to analyze the same pavement. PADAL 2 is a back-analysis program that returns the values of stiffnesses corresponding to the surface deflections recorded by the FWD, whereas FENLAP is a forward analysis program that evaluates displacements, strains, and stresses in a pavement with given elastic constants. Hence, a comparison between the two programs cannot be made directly; it must be carried out by running program FENLAP on a pavement with a set of elastic parameters obtained through PADAL 2 for the same pavement and then comparing the surface deflections and the subgrade stiffnesses obtained with both methods.

Data obtained from the same full-scale pavement as was used previously was chosen for this comparison. Both Brown's and Loach's models were considered in the finite element analysis. The respective elastic constants of the subgrade determined in PADAL 2 were taken as input parameters in FENLAP. Linear elastic behavior was assumed for the upper layers, their elastic stiffnesses being taken from the PADAL output.

The results obtained using both programs showed a poor match between PADAL 2 and FENLAP solutions. Because the pavement analyzed in FENLAP assumed a rigid boundary at a depth of 10 m, it was decided to rerun PADAL 2 with a rigid layer at that depth. The new elastic parameters were then input to FENLAP and the program was rerun. The calculated deflections at the geophone locations and subgrade stiffnesses are presented in Table 2.

This second match resulted in an improved comparison between the two programs. However, some differences were still found in both stiffnesses and deflections. The following reasons may explain the differences:

1. The finite element method is, by nature, an approximate technique, in which factors such as the mesh size and the convergence criteria influence the results.
2. The approach followed in PADAL 2 to model the stress dependency of stiffnesses in the radial direction is based on a simplification, as described above. Therefore, the procedure is approximate.
3. Although the finite element lower boundary can be simulated in PADAL 2 by assigning a rigid layer at the corresponding depth, PADAL 2 is unable to reproduce the truncation of the domain at a certain radial distance, as it is required by the finite element method.

Nevertheless, the trends of the solutions obtained with both programs are not very different. Hence, despite the limitations point out, the approximate nonlinear modeling procedure adopted in PADAL 2 for the subgrade has been shown to satisfactorily match the output from the more accurate FENLAP analysis.

### Finite Elements in Pavement Backcalculation

Because the finite element method has advantages over the layered analysis in modeling the nonlinear behavior of materials, it could potentially provide a framework for a backcalculation procedure. However, finite element techniques use much more computing time than programs that are based on layered analysis. For instance, in the mainframe computer of University of Nottingham, a FENLAP iteration on a typical pavement system can last more than 30 sec (if a mesh is used that is sufficiently fine to guarantee accuracy), whereas a PADAL iteration of the same system takes only about 3 sec. Considering the backcalculation is a trial-and-error process that implies many runs, the difference in computing time between the two approaches would be substantial.

Finite element calculations require a rigid boundary placed at some finite distance below the surface. Although various procedures have been proposed to estimate the depth of a rigid layer (*7,8*), none appears to apply satisfactorily to a wide spectrum of pavements. Hence, unless some geological information enables the approximate location of the bedrock to be known, a subgrade with infinite depth is usually assumed. The assignment of an arbitrary depth for the rigid bottom then can be a potential source of inaccuracy in a finite

**TABLE 2 Comparison Between PADAL 2 and FENLAP for Full-Scale Pavement**

| | FWD | PADAL 2 | | FENLAP | |
|---|---|---|---|---|---|
| | Data | Brown's Model | Loach's model | Brown's Model | Loach's Model |
| $d_1$ (μm) | 174.0 | 174.0 | 174.0 | 168.5 | 180.1 |
| $d_2$ (μm) | 131.0 | 127.3 | 128.1 | 122.2 | 133.6 |
| $d_3$ (μm) | 92.0 | 89.6 | 89.9 | 85.7 | 94.0 |
| $d_4$ (μm) | 62.0 | 62.0 | 62.0 | 59.5 | 64.4 |
| $d_5$ (μm) | 43.0 | 43.0 | 43.0 | 41.8 | 44.1 |
| $d_6$ (μm) | 29.0 | 30.3 | 30.4 | 30.4 | 30.6 |
| $d_7$ (μm) | 22.0 | 22.0 | 22.0 | 23.2 | 22.0 |
| $E_{sg\text{-}l1}$ (MPa) | --- | 179 (219) | 228 (163) | 183 (220) | 228 (162) |
| $E_{sg\text{-}l2}$ (MPa) | --- | 209 (233) | 264 (220) | 221 (241) | 267 (216) |
| $E_{sg\text{-}l3}$ (MPa) | --- | 239 (254) | 297 (269) | 258 (276) | 295 (254) |
| $E_{sg\text{-}l4}$ (MPa) | --- | 275 (285) | 338 (322) | 302 (307) | 332 (304) |
| $E_{sg\text{-}l5}$ (MPa) | --- | 331 (337) | 402 (393) | 329 (326) | 438 (431) |

*Notes:* PADAL 2 backcalculates elastic stiffnesses from measured values whereas FENLAP determines the deflections from the stiffnesses obtained using PADAL 2.

The subgrade stiffnesses without "( )" refer to locations beneath the load whereas the values within "( )" refer to a distance of 1.80 m away from the load axis.

element backcalculation scheme, because two different positions of the lower boundary will necessarily lead to different solutions. The shortcoming of finite element programs being limited to solve finite domain problems in both vertical and horizontal directions can be overcome by the use of infinite elements. However, it is doubtful whether the supplementary effort required to consider them would be worthwhile.

In summary, at this stage of the investigation no conclusions can yet be made about the usefulness of a finite element backcalculation method, although the amount of computing time associated would probably rule out its implementation for practical purposes. However, it is certain that finite elements can provide valuable information to assist with a backanalysis procedure, particularly in connection with the following points:

1. To assess the significance of considering nonlinear models for a range of various pavements.
2. To compare the performance of several constitutive relationships tested.
3. To determine average resilient moduli that may describe the global response of the pavement layers in an accurate way.

## CONCLUSIONS

The investigations carried out to date essentially have been concerned with developing and improving computational techniques for the nonlinear structural analysis and evaluation of pavements, paying particular attention to the modeling of the stress-dependent constitutive relationships of the foundation layers. The examples given in the paper have been selected as representative of a number of structures investigated. Further validation studies are ongoing, with particular consideration being given to the use of various load levels to determine material nonlinearity.

Loach's relationship for fine-grained soils was incorporated into program PADAL. The results obtained with this model and with Brown's (previously adopted) were similar. However, when applying Loach's relationship to PADAL, the well-known stress softening behavior of clays was not reproduced.

PADAL 2, an updated version of PADAL in which the nonlinearity of the subgrade is approximately modeled in the horizontal direction, was developed. This development allows for a more realistic description of the variability of elastic stiffnesses throughout the pavement. Loach's model was also tested on PADAL 2, but the inconsistency outlined above remained. In view of that, Brown's relationship is considered preferable for modeling the subgrade in PADAL.

Attention was given to the nonlinear modeling of granular layers in PADAL. Among the available models, the $K$-θ model seems the most adequate for this purpose. FENLAP, a new finite element code for the structural analysis of pavements, was implemented and validated. FENLAP includes a range of various nonlinear constitutive relationships and is a valuable tool for pavement design and evaluation.

The viability and utility of a finite element backcalculation procedure was discussed. Although more appropriate for nonlinear problems, this approach would be much more time consuming than the current one, which is based on layered elastic analysis.

## ACKNOWLEDGMENTS

The research described in this paper was made possible by the financial support of Commission of the European Com-

munities, the U.K. Science and Engineering Research Council, and the U.K. Transport and Road Research Laboratory. The authors are also grateful for the assistance rendered by SWK Pavement Engineering Ltd., United Kingdom.

## REFERENCES

1. S. F. Brown, W. S. Tam, and J. M. Brunton. Structural Evaluation and Overlay Design: Analysis and Implementation. *Proc., 6th International Conference on the Structural Design of Asphalt Pavements*, Ann Arbor, Mich., 1987, pp. 1013–1028.
2. S. F. Brown. The Characterisation of Cohesive Soils for Flexible Pavement Design. *Proc., 7th European Conference on Soil Mechanics and Foundation Eng.*, Vol. 2, 1979, pp. 15–22.
3. S. F. Brown, S. C. Loach, and M. P. O'Reilly. *Repeated Loading of Fine Grained Soils*. Contractors Report CR 72. U.K. Transport and Road Research Laboratory, Crowthorne, Berkshire, England, 1987.
4. R. G. Hicks and C. L. Monismith. Factors Influencing the Resilient Response of Granular Materials. In *Highway Research Record 345*, TRB, National Research Council, Washington, D.C., 1971, pp. 15–31.
5. S. F. Brown and J. W. Pappin. Modeling of Granular Materials in Pavements. In *Transportation Research Record 1022*, TRB, National Research Council, Washington, D.C., 1985, pp. 45–51.
6. G. T. H. Sweere, A. Penning, and E. Vos. Development of a Structural Design Procedure for Asphalt Pavements with Crushed Rubbled Base Courses. *Proc., 6th International Conference on Structural Design of Asphalt Pavements*, Vol. I, Ann Arbor, Mich., 1987, pp. 34–49.
7. W. Uddin, A. H. Meyer, and W. R. Hudson. Rigid Bottom Considerations for Nondestructive Evaluation of Pavements. In *Transportation Research Record 1070*, TRB, National Research Council, Washington, D.C., 1986, pp. 21–29.
8. G. T. Rohde, W. Yang, and R. E. Smith. Inclusion of Depth to a Rigid Layer in Determining Pavement Layer Properties. *Proc., 3rd International Conference on Bearing Capacity of Roads and Airfields*, Trondheim, Norway, 1990, pp. 475–486.

# Backcalculation of Design Parameters for Rigid Pavements

J. UZAN, R. BRIGGS, AND T. SCULLION

Current rigid pavement backcalculation procedures use only interior or center slab deflection bowls that are measured far from any crack or joint. Usually two parameters—the rigidity of the slab and the modulus of subgrade reaction—are evaluated. The backcalculated subgrade modulus is recommended for design subject to a correction/calibration factor. However, since the modulus of subgrade reaction depends on the size of the loaded area, various calibration factors may be required for various loading conditions at the time of the testing and for various assumptions in the design procedure concerning the loading condition, namely interior or edge loading conditions. Furthermore, when a stabilized layer is used beneath the concrete slab it is not clear what the backcalculated parameters represent. Does the backcalculated rigidity of the slab include the stabilized layer or is it included in the backcalculated subgrade modulus of reaction? The answers to these questions have an impact on the computation of stresses that are the basis of any rigid pavement design procedure. A procedure for backcalculating the slab rigidity and the modulus of subgrade reaction for either the center slab or the free-edge loading condition is briefly described. The material parameters and the slab rigidity were backcalculated using the plate on Winkler foundation for interior and free-edge loading conditions. The center slab results are compared with those that are backcalculated using linear elastic layer models. The proposed method uses the MODULUS computer program framework in which a data base of theoretical deflection bowls is generated and used thereafter with a pattern search algorithm to find the set of parameters (the characteristic length $\ell$ and the subgrade modulus of reaction $k$) that minimizes the error between measured and computed deflections. Results backcalculated from five Strategic Highway Research Program jointed concrete monitor sites are presented. The slab thicknesses range between 9.3 and 11.4 in., and the base layers are either granular, asphalt, or cement stabilized. Deflection tests were made at three load levels using a falling weight deflectometer. Results include (a) a comparison of $\ell$ and $k$ values backcalculated at the center slab and at the edge (it is clearly seen that the $k$-values derived from free-edge condition are two to four times larger than those obtained from center slab deflections) and (b) a comparison of results computed using both the Hogg model and the linear elastic layered model. It is clearly seen that the Hogg model produces subgrade moduli similar to those produced using the linear elastic model. Furthermore, with the Hogg model the effect of the stabilized base layer is included in the $\ell$-parameter.

The evaluation of the load-deformation characteristics from deflection-based nondestructive deflection testing (NDT) is, in essence, similar for flexible and rigid pavements (*1*). However, because of the existence of joints, cracks, and free edges, the boundary conditions prevailing in rigid pavements are more complex than those in flexible pavements. These conditions are best treated with finite element solutions of plates resting on one- or two-layer systems or on a Winkler foundation. When load transfer characteristics are included in the evaluation, the problem becomes too complicated for standard backcalculation procedures.

The approach is presented in Uzan (*1*) and some is repeated here for completeness. The backcalculation scheme makes use of simple solutions that assume that the cracks or joints are far from the load and do not affect the deflection bowl. These solutions are applicable for plain or simply reinforced concrete pavements in which cracks are widely separated, in contrast to continuously reinforced concrete pavements in which cracks are fairly close. In general, the distance between joints and cracks would be less than eight times the characteristic length of the system [in which case the size of the plate may be considered as infinite (*2,3*)], and the use of the simple solutions constitutes an approximation. The framework presented in the paper is general and finite element programs instead of the simple solutions could be used for deflection computations.

In this paper a backcalculation procedure is described to determine the appropriate layer properties from field deflection measurements. The procedure involves two steps: in the first step, a factorial deflection data base is built using multiple runs of a theoretical model; in the second step, a pattern search and interpolation scheme are used to match field measured and theoretical deflection bowls. The output is the set of layer properties that minimizes the error between measured and computed deflections. In this paper the authors compare the results from three different theoretical pavement models: (a) a multilayer linear elastic model; (b) Hogg model, and (c) Hertz-Westergaard model. Furthermore, calculations with deflections measured near a free edge can be compared with those made with deflections measured at the center of the slab. This analysis enables an examination of the significance of the $k$-subgrade modulus of reaction and the procedures of modeling rigid pavements with stabilized base layers.

## THEORETICAL MODELS FOR COMPUTING SLAB DEFLECTIONS

Three types of models are used for evaluating the load-deformation characteristics of pavement materials. These are the multilayer linear elastic model, the Hogg model of a slab supported by an elastic foundation, and the Hertz-Westergaard model of a slab supported by a liquid foundation. These models all use linear load-deformation characteristics, implying con-

J. Uzan and T. Scullion, Texas Transportation Institute, Texas A&M University, College Station, Tex. 77843. R. C. Briggs, Texas Department of Transportation, 125 East 11th Street, Austin, Tex. 78701.

stant moduli of elasticity, Poisson's ratios, and modulus of subgrade reaction.

In the multilayer elastic system model, the pavement is represented by linear elastic layers that extend to infinity in the horizontal direction. This model, widely used in flexible pavement evaluation, corresponds to the interior loading case in which both the load and the deflection sensors are far from any joint or crack. The boundary conditions at the interfaces from the layers can be varied from completely rough to smooth (*4,5*). In the case of a concrete pavement with unbound base material, the interface conditions have negligible effects on deformations and stresses. However, when the base layer is stabilized, the effects of interface conditions on stresses and deformations may be significant.

The second model considered is the Hogg model (*6,7*). With this model the pavement is represented by an infinite slab resting on an elastic foundation. This model, like the linear elastic model, corresponds to the interior loading case only. The model is in essence a two-layer system with additional assumptions concerning the first layer, which is represented by a slab (*8*). In this model, the pavement parameters are the subgrade modulus of elasticity, $E_{sg}$, and the radius of relative stiffness of the slab subgrade system $\ell_e$ (which is a function of the elastic parameters of the concrete and of the subgrade and the slab thickness).

The third model used is the Hertz-Westergaard model (*9,10*). With this model the pavement is represented by an infinite or semiinfinite slab resting on a dense liquid foundation (also known as a Winkler foundation). In this model, two loading cases are considered: (a) the interior loading case (known as the Hertz model) in which the slab is infinite and the load and deflection sensors are far from any joint or crack; and (b) the free-edge case (known as the Westergaard model) in which the slab is semiinfinite and the load and deflection sensors are near a free joint and far from any additional joint or crack. The pavement parameters are the subgrade modulus of reaction, $k$, and the radius of relative stiffness of the slab-subgrade system $\ell_k$ (which is a function of the elastic parameters of the concrete, the subgrade modulus of reaction and the slab thickness).

Closed-form solutions for deflection bowls exist only for the case of a concentrated load (*9,11*). In the case of a uniform pressure distributed over a circular area, the solution of the concentrated load may be integrated numerically. In the interior loading case, a computer program given by Selvadurai (*11*) was used to compute the deflections at the surface. In the free-edge loading case, Westergaard equations (*12*) were integrated over the loading area using the procedure presented by Uzan and Sides (*13*).

In the three-layer and Hogg models, a rigid base at any depth in the subgrade can be easily included. The Hertz-Westergaard model does not have this capability because the subgrade is represented by a spring or a liquid that is dimensionless.

## BACKCALCULATION PROCEDURE

The backcalculation of layer properties for rigid pavement follows the MODULUS backcalculation framework already developed for flexible pavements. It is described in detail elsewhere (*14,15*). For flexible pavements the outputs are the set of layer moduli that minimize the error between measured and theoretically calculated deflection bowls. The existing system is a two-step process. In the first step, a linear elastic program is run for a range of layer moduli, and the resulting deflections are stored in a deflection data base. In the second step, a pattern search and interpolation scheme are used to minimize the error between measured and computed deflection bowls.

The multilayer system model described in this paper is essentially the same as the flexible pavement system. The data base is built by varying the moduli of each pavement layer in turn and storing the computed deflections.

In both the Hogg and the Hertz-Westergaard models, the data base is built by varying the subgrade modulus $E_{sg}$ (or the subgrade modulus of reaction $k$) and the radius of relative stiffness $\ell_e$ (or $\ell_k$). In the analysis discussed for the Hogg model, 10 values of subgrade modulus (range 2,000 to 75,000 lb/in.$^2$) and 10 values of $\ell_e$ (range, 10 to 210 in.) were computed. This resulted in 100 theoretical deflection bowls being generated and stored. For Hertz-Westergaard, a $10 \times 10$ factorial was again stored with ranges of $k$ for 25 to 1,500 lb/in.$^3$ and $\ell_k$ from 10 to 140 in. These ranges are intended to represent the limits of possible values.

The program can handle any sensor arrangement. In all cases deflections are computed at the sensor locations used in the field measurements. For the SHRP testing program this is at 0, 8, 12, 18, 24, 36, and 60 in. from the center of the load. Only one data base of computed surface deflections is required for each sensor arrangement, and the first step of the procedure need not be repeated if the data base is already available. The procedure used in this paper can handle any number of sensors or any sensor arrangement. Moreover, the Hogg model includes both the infinite and finite subgrade thickness cases. The procedure presented is unique in that both center and free-edge deflection bowls can be analyzed to backcalculate the modulus of subgrade reaction and the modulus of elasticity of the concrete.

The results of the numerical integration have been checked against other analysis methods, such as the FE results presented in the appendix, and have been found to be comparable. A direct comparison of the results of backcalculation obtained with the procedure described in the paper (named JUSLAB) and with the ILLI-BACK computer program follows. Table 1 presents results of backcalculation for eight rigid pavement sections at three different load levels. The procedures and objective functions of the backcalculation are usually different in JUSLAB and ILLI-BACK programs. For the sake of comparison, the procedure and objective function in JUSLAB were changed to resemble those in ILLI-BACK. In ILLI-BACK, the computation procedure is (a) to obtain the characteristic length from the basin area; (b) to compute a $k$-value for each sensor; and (c) to compute a mean value. It appeared that in several cases analyzed the computed $k$-value from the last sensor deflection was much lower than the other $k$-values obtained from the other six sensors. The procedure of taking the mean is then similar to dropping the last sensor. The results of backcalculation using JUSLAB were obtained by fitting the first six sensors (by means of weighting factors) and minimizing the squared error between measured and computed deflections at these six sensors. The results obtained with JUSLAB and ILLI-BACK compare very well; different

**TABLE 1 Comparison of Backcalculation Results**

| Section | Subgrade Modulus of Reaction in pci, for Load Level | | | | | |
|---|---|---|---|---|---|---|
| | 1 | | 2 | | 3 | |
| | JUSLAB | ILLI-BACK | JUSLAB | ILLI-BACK | JUSLAB | ILLI-BACK |
| I | 564 | 505 | 555 | 518 | 533 | 508 |
| J | 249 | 252 | 341 | 328 | 288 | 272 |
| K | 162 | 144 | 262 | 323 | 250 | 268 |
| L | 125 | 143 | 126 | 139 | 131 | 149 |
| M | 296 | 302 | 283 | 288 | 292 | 299 |
| N | 252 | 241 | 238 | 233 | 248 | 244 |
| O | 161 | 161 | 146 | 146 | 196 | 202 |
| P | 591 | 501 | 592 | 618 | 552 | 590 |

results will be obtained if the seventh sensor is not dropped from the analysis and if the objective function to be minimized is changed, for example, from squared error to absolute error.

## CASE STUDY DESCRIPTION

To evaluate the backcalculation procedure, Strategic Highway Research Program (SHRP) falling weight deflectometer (FWD) data were processed on five SHRP general pavement study sites in Texas. Average slab thicknesses and other information are given in Table 2. All the pavements were jointed concrete with asphalt shoulders.

In the SHRP deflection testing procedure, deflections are taken at midslab, edge, corner, and pavement joints. In this analysis the center slab and the edge FWD deflection data were used. SHRP uses three loading levels for rigid pavements (approximately 9, 12, and 16 kips) and collects four replicate drops at each test point. In the analysis that follows the four replicate drops were normalized to the average load and then averaged so that a single deflection bowl was processed for each load level. This procedure takes care of the random errors, as planned by SHRP. Therefore, the averaging process used includes (a) computing the average load, (b) normalizing each of the four deflection bowls to the average load, and (c) averaging the normalized bowls.

In general, 60 deflection bowls were processed for each site, three load levels at 20 positions. In all cases the load was applied on a 12-in.-diameter FWD load plate. Deflection sensors were located at 0, 8, 12, 18, 24, 36, and 60 in. from the center of the plate.

## PRESENTATION OF RESULTS

The results of this analysis are shown in Figures 1 through 5, details of which follow. The results from all five sites are presented on a single diagram. Within each site the results from various locations and load levels are presented. In each analysis all seven sensors were used in matching measured

**TABLE 2 Layer Characteristics of Study Pavements**

| SHRP ID # | Pavement Characteristics | Joint Spacing | Slab Thickness (Inches) | Base | | Subbase | | Subgrade |
|---|---|---|---|---|---|---|---|---|
| | | | | Type* | Thickness (Inches) | Type* | Thickness (Inches) | |
| 3003 | Plain | 15 ft | 9.3 | AC | 3.7 | LT | 7.2 | Clay |
| 3589 | Reinforced | 15 ft | 10.1 | GR | 6.0 | -- | -- | Sandy/ Clay |
| 3699 | Reinforced | 60 - 20 ft+ | 10.1 | CT | 5.8 | LT | 6.0 | Sandy/ Clay |
| 4142 | Reinforced | 60 - 20 ft+ | 9.6 | AC | 7.9 | SS | 8.8 | Sand |
| 4152 | Reinforced | 30 ft++ | 11.4 | CT | 6.3 | LT | 5.6 | Sandy/ Clay |

*Codes
AC Asphaltic Concrete
GR Crushed Gravel
CT Cement Treated
LT Lime Treated
SS Select Sand

+ 60 ft 6 in between construction joints with towels 20 ft between warping joints.

++ with transverse cracks in each slab.

and theoretical bowls, and the average error per sensor was computed. Figure 1 shows the percent error per sensor between measured and computed deflection. It is seen that the error is very large, approaching 10 percent in the cases of the Hertz and Westergaard models compared with the Hogg or layered linear elastic model. In the following analysis, all solutions that resulted in more than 6 percent error per sensor (and solutions that resulted in unacceptable results) have been excluded for Figures 2 through 5.

Figure 2 shows the results for the linear elastic layered analysis in terms of the backcalculated modulus of the subgrade and modulus of concrete at center slab. In modeling the pavement, the complete layering shown in Table 2 was used. For example, for section 4152 the pavement was modeled as four layers (11.4 in. of concrete resting on a 6.3-in. cement-treated base over a 5.6-in. lime-treated subbase over a semi-infinite depth subgrade). In all modeling, the subgrade depth was set at semi-infinite. The backcalculated subgrade moduli ranged from 20 to 45 ksi and concrete moduli ranged from 4 to 8 million lb/in.$^2$ (8 million lb/in.$^2$ was set as maximum).

Figure 3 shows the backcalculated results from using the Hogg model on the center slab deflections. The subgrade was assumed to be semi-infinite. The backcalculated subgrade moduli ranged from 20 to 50 ksi and characteristic length $\ell_e$ ranged from 25 to 45 in.

Figure 4 shows the backcalculated results obtained using the Hertz model with the center slab deflections. The modulus of subgrade reactions ranged typically from 50 to 200 lb/in.$^3$, with a few readings reaching 300 lb/in.$^3$. The characteristic lengths ranged typically from 40 to 70 in.

Figure 5 shows the backcalculated results obtained using the Westergaard edge solution. The modulus of subgrade reactions ranged typically from 200 to 700 lb/in.$^3$ with characteristic lengths ranging from 35 to 60 in.

## DISCUSSION OF RESULTS

The following observations are made with regard to the results presented in Figures 1 through 5.

1. Even after screening, the error in the fitting of the deflection bowl seems to be very large in the Hertz and Westergaard models. However, the error is acceptable for the

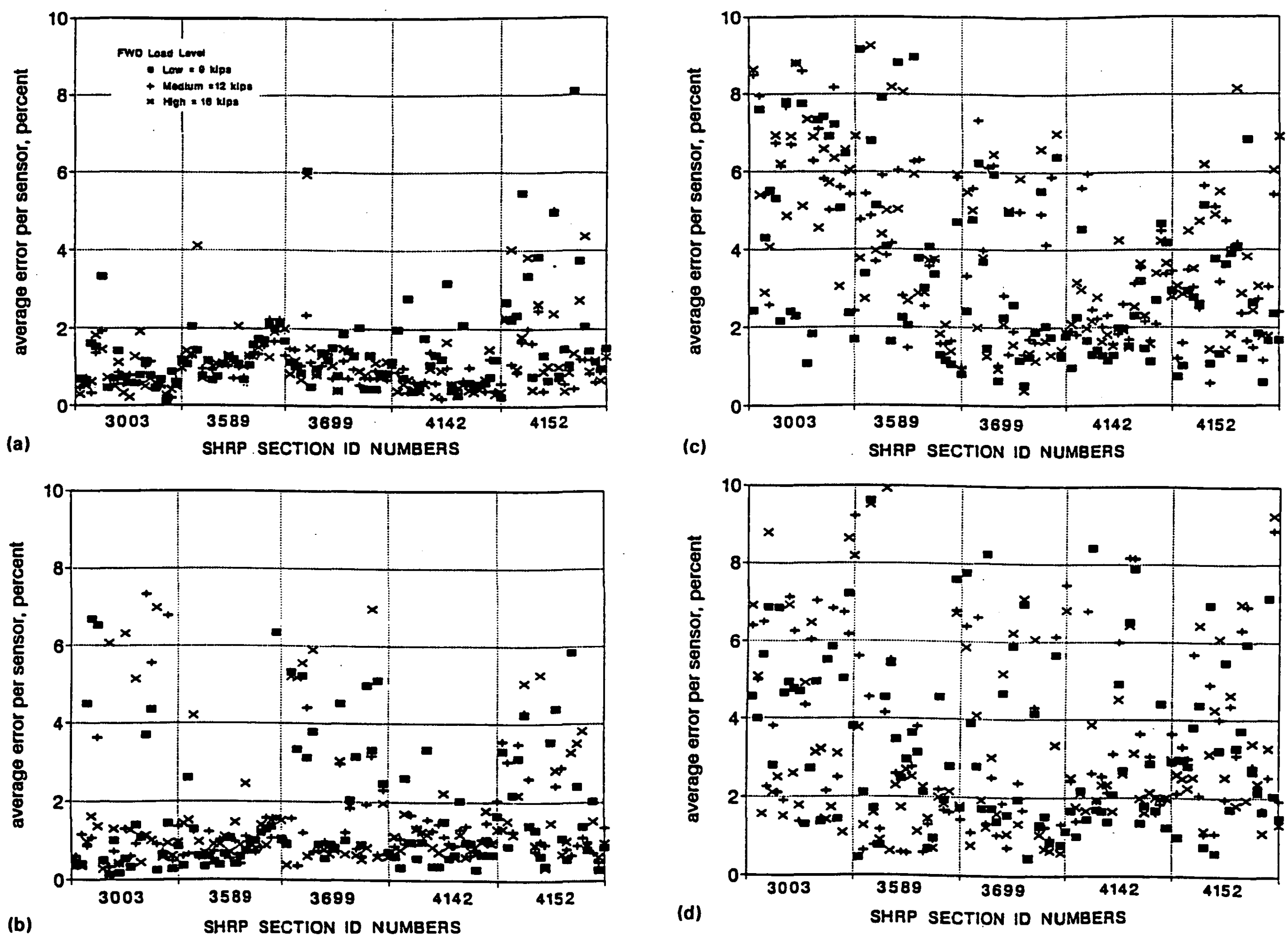


**FIGURE 1 Average error per sensor between computed and measured deflection: (*a*) linear layered elastic model; (*b*) Hogg with center deflections; (*c*) Hertz with center deflections; and (*d*) Westergaard with edge deflections.**

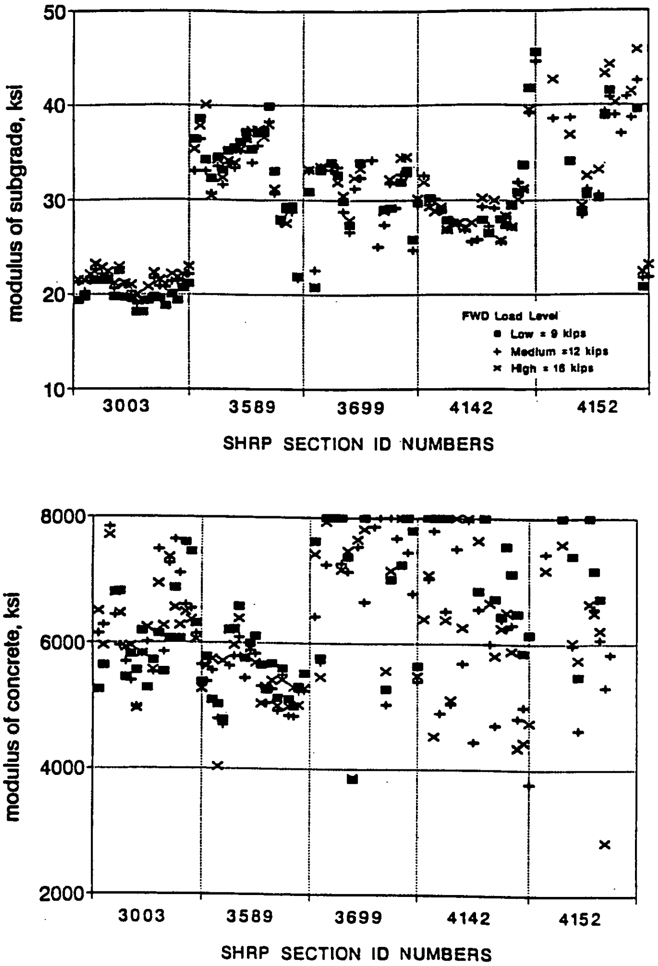


**FIGURE 2 Subgrade (*top*) and concrete (*bottom*) modulus backcalculated using linear layered elastic model for each SHRP test section.**

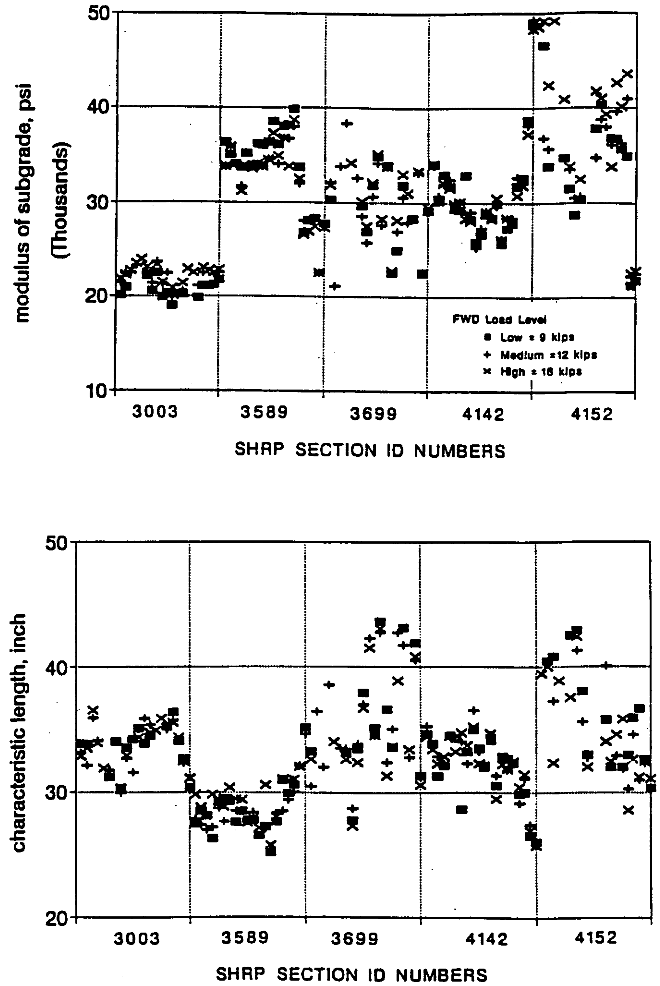


**FIGURE 3 Subgrade modulus (*top*) and slab characteristic length (*bottom*) backcalculated using Hogg model with center slab deflections.**

Hogg and layered linear elastic models. In the case of rigid pavements, material behavior is very close to linear and does not induce appreciable systematic error. It may be argued that the error is caused by the boundary conditions that are not fulfilled because of the proximity of the cracks and joints. However, this deficiency exists for both the Hertz and Westergaard models, as well as for the Hogg and layered linear elastic models. It is the authors' opinion that the bad fitting is the result of systematic errors induced by the model representation of the subgrade support, namely, that in the cases of strong subgrade, with elastic moduli of 20 to 45 ksi, the subgrades cannot be simulated as liquid or spring. The above hypothesis should be checked with weaker subgrade materials. If this is found to be the case, the use of the $k$ model should be questioned in rigid pavement design. The backcalculation was made using all sensors, including the seventh sensor, which was found in several cases to be underpredicted. A similar trend is found in ILLI-BACK results in which the error caused by the seventh sensor may be in excess of 30 percent.

2. The modulus of subgrade reaction at the edge is two to four times higher than that obtained from the center slab. A discussion of this finding together with a comparison of earlier results, such as those of Teller and Sutherland (*16*), is given in the appendix to the paper. The $k$-values at the center of the slab appear very low. As will be discussed later, the modulus of subgrade reaction represents the subgrade layer and does not include the stabilized base material on top of the subgrade. This result suggests that the modulus of subgrade reaction is not an adequate material property for modeling slab response because it is a function of the loading geometry. Using linear elastic theory, one can find that the subgrade modulus of reaction is proportional to the modulus of elasticity and inversely proportional to the size of the loaded area.

3. From Figures 2 and 3 it is observed that the modulus of the subgrade is identical for both the linear layered elastic model and the Hogg model. The Hogg model is a simplified two-layered system, whereas the linear elastic is either a three- or four-layered system. This difference implies that in the Hogg model, the base-subbase layers are included in the plate rigidity to give a composite plate that rests on the subgrade. This result is very important for choosing the computation scheme of the bending stresses. In this case the method of equivalent moment of inertia or thickness should be used in

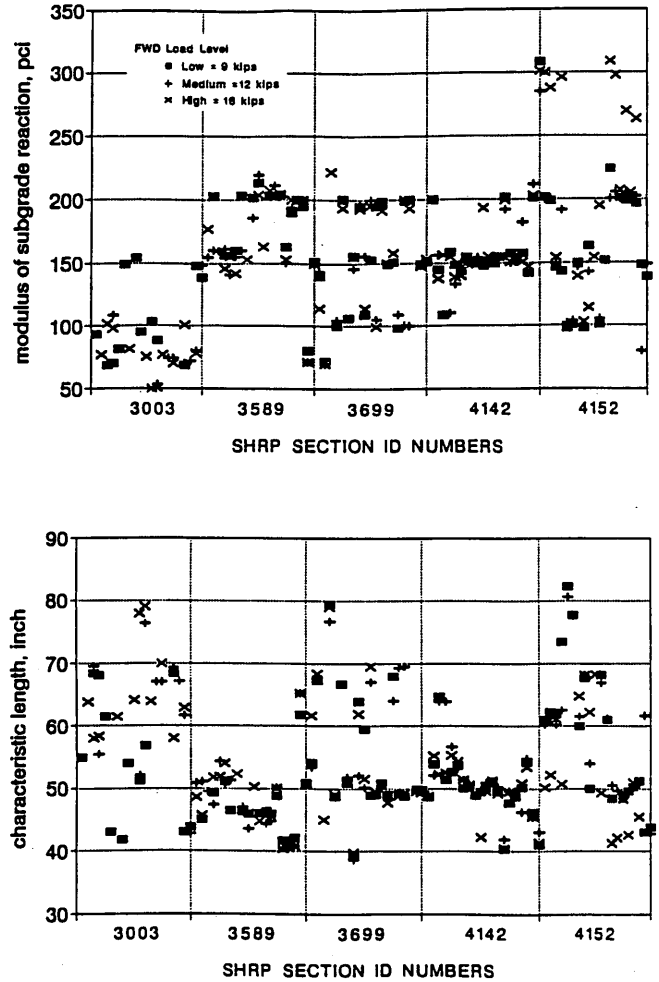


FIGURE 4 Modulus of subgrade reaction (*top*) and slab characteristic length (*bottom*) backcalculated using Hertz model with center slab deflections.

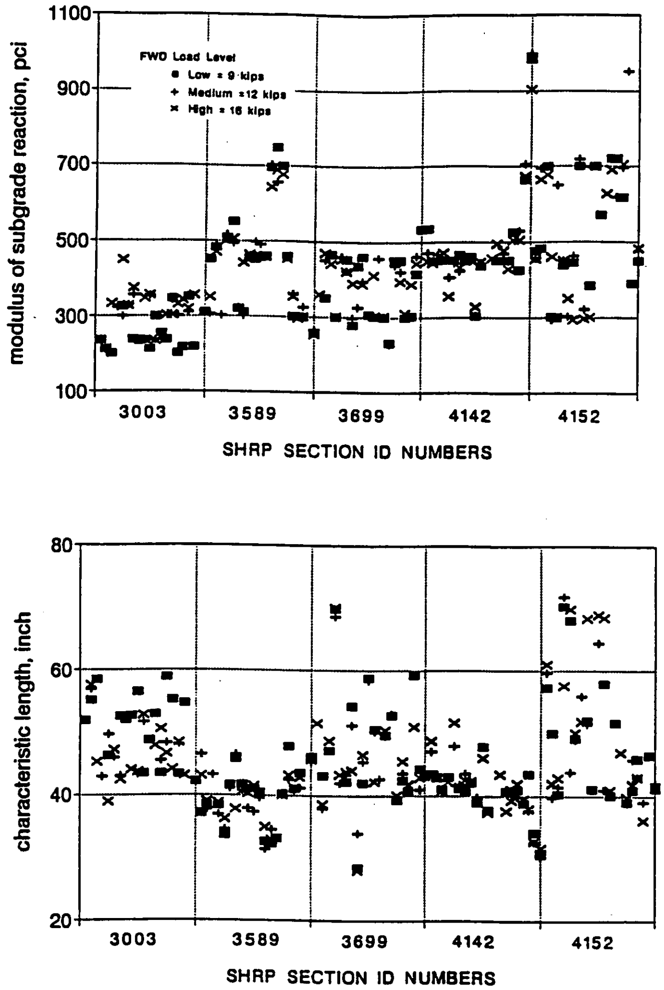


FIGURE 5 Modulus of subgrade reaction (*top*) and slab characteristic length (*bottom*) backcalculated using Hertz-Westergaard model with edge deflections.

computing the bending stresses. Similar behavioral effect is assumed to occur for the Hertz-Westergaard model, namely that the stiffness effect of the base and subbase layers is included in the plate (pavement) rigidity (*1*).

4. In all cases the $\ell$ values backcalculated are relatively large. However, as mentioned earlier, it appears that this value includes a contribution from the base and subbase layers. To evaluate this contribution the equivalent thickness $h_{eg}$ for the slab was calculated using the following formula:

$$h_{eg}^3 = \frac{\ell_k^4\, 12(1 - \nu_c^2)k}{E_c} \tag{1}$$

for the Hertz-Westergaard model and

$$h_{eg}^3 = 2C\,\frac{12(1 - \nu_c^2)}{E_c}\,\ell_e^3 \tag{2}$$

$$C = \frac{E_2\,(1 - \nu_2)}{(1 + \nu_2)\,(3 - 4\nu_2)} \tag{3}$$

for the Hogg model,

where

$E_c$ = modulus of elasticity of concrete (an average value of 6,500,000 lb/in.$^2$ was used in the calculation),
$E_2$ = modulus of elasticity of subgrade,
$\nu_c$ = Poisson's ratio of concrete (a value of 0.2 was used), and
$\nu_2$ = Poisson's ratio of subgrade (a value of 0.4 was used).

The equivalent thickness was computed for each location and load level. In Table 3 the average equivalent thicknesses for each section are compared with the actual thicknesses. The equivalent thickness is much larger than the actual concrete thickness (except for the second sections in which a lower $E_c$ should have been used). It approaches the combined thickness of the concrete and the cement-treated base together. This result indicates that there is a good bond between the layers. To derive a relationship between equivalent thickness $h_{eq}$ and pavement variables, it is important to know the exact layer thickness and to collect data on a wider range of pavement sections.

5. The relationship between subgrade elastic modulus $E_{sg}$ and the subgrade $k$-value was developed by the Corps of

**TABLE 3 Comparison of Actual Slab Thickness with Calculated Equivalent Slab Thickness**

| Section ID | Actual Slab Thickness (inches) | Base | | Equivalent Slab Thickness | | |
|---|---|---|---|---|---|---|
| | | Type | Thickness (inches) | Figure 3 Hogg (center) | Figure 4 Hertz (center) | Figure 5 Westergaard (edge) |
| 3003 | 9.3 | AC | 3.7 | 12.60 | 12.62 | 14.03 |
| 3589 | 10.1 | GR | 6.0 | 9.59 | 11.63 | 12.27 |
| 3699 | 10.1 | CT | 5.8 | 16.29 | 13.20 | 14.48 |
| 4142 | 9.6 | AC | 7.9 | 14.29 | 12.15 | 13.18 |
| 4152 | 11.4 | CT | 6.3 | 14.28 | 14.56 | 17.40 |

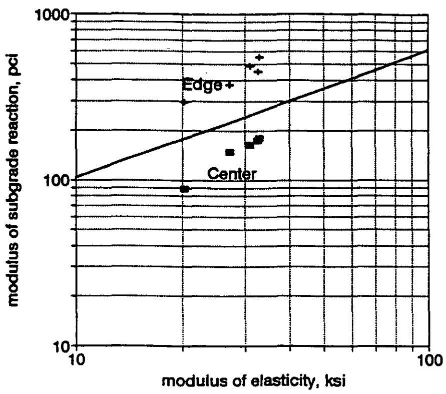


**FIGURE 6 Relationship between modulus of elasticity and modulus of subgrade reaction.**

Engineers (*17*) and is shown in Equation 4 ($k$ in pounds per cubic inch and $E_{sg}$ in pounds per square inch):

$$\log k = \frac{(\log E_{sg} - 1.415)}{1.284} \tag{4}$$

This equation is shown graphically in Figure 6 together with the correlations obtained from edge and center slab conditions. As can be seen, the Corps of Engineers line lies between the lines generated for edge and center slab and therefore represents an average correlation.

## CONCLUSIONS AND RECOMMENDATIONS

The use of four different models to backcalculate rigid pavement material parameters has led to the following conclusions:

1. The Winkler foundation model for rigid pavements may be not appropriate for the cases analyzed with strong subgrades. Similar analyses should be conducted on weak subgrades to further evaluate this conclusion.
2. The subgrade modulus of reaction does not seem to be a material property. The $k$-value for edge conditions is two to four times larger than that for center conditions for the same site. One should then use the values obtained only for the same conditions that prevailed in their derivations. For example, the values obtained for the center conditions can be used only with a procedure (design procedure, for example) that uses the same infinite slab size conditions. This result makes the edge condition backcalculation necessary for use with design procedures that uses the edge conditions.
3. Bending stress computations should be made using the method of equivalent thicknesses. It is recommended that the deflection bowls and the backcalculation method be used with SHRP data to develop and calibrate the method.

## ACKNOWLEDGMENTS

This work is sponsored by the Texas Department of Transportation. Jerome F. Daleiden of Brent Rauhut Engineering supplied the deflection data and pavement layer data used in the study.

# APPENDIX

The dependence of the backcalculated $k$ on the location of load (center versus free edge) may be questioned, according to earlier results. For example, on the basis of four slabs and one set of basin measurements on each slab (using an average of 12 observations), Teller and Sutherland (*16*) concluded, "for conditions that are comparable there is rather good agreement between the values of modulus of subgrade reactions, $k$, as determined by pavement deflection, for the interior and edge loadings but the value for the corner loadings is consistently lower." However, Carlton and Behrmann (*18*) stated, "from the data obtained in this study, it appears that the effective subgrade modulus is the same for both corner and edge loadings. In previous model tests, however, determinations of the subgrade modulus for the model had shown that for interior loadings, the effective $k$ was 35 pounds per cubic inch. This is approximately half the value of $k$ measured at the edge and at the corner. It is believed that this apparent increase in $k$ near the boundaries of the slab may be explained by additional support derived from the subgrade outside the limits of the slab."

Despite the above contradictory results, it appears that a gradual increase in the subgrade modulus as the load moves from the center to the edge and then to the corner would be acceptable [see work by Ioannides et al. (*3*)]. The question would then be, How much increase would be acceptable? The results presented in the paper suggested that the ratio of the

backcalculated *k* values from edge and interior loading can be as large as 2 to 4. As mentioned in the paper, these results are based on field deflections collected by the Long Term Pavement Performance program of SHRP.

The difference between Teller and Sutherland and SHRP deflection results is seen very clearly from the ratios of the maximum deflections per unit load in the center and edge loadings. In the case of Teller and Sutherland, the ratio is about 1 to 4, whereas in the SHRP section case, the ratio is about 1 to 1.3. In the case study reported by Uzan (*1*), the ratio of the edge to center loading deflections did not exceed 2. It is not clear what the cause is of the discrepancy of the deflection ratios. It may be attributed to any of the following: the dynamic FWD loading as compared with the static loading condition used by Teller and Sutherland, warping of the plates, or the presence of the voids. Readers are given the opportunity to make their own judgments about which value of *k* to use in the design.

## REFERENCES


1. J. Uzan. *Rigid Pavement Evaluation Using NDT—A Case Study.* ASCE, in press (in preparation).
2. A. M. Ioannides, M. R. Thompson, and E. J. Barenberg. Finite Element Analysis of Slabs-on-Grade Using a Variety of Support Models. *Proc., 3rd International Conference on Concrete Pavement Design and Rehabilitation*, Purdue University, West Lafayette, Ind., 1985, pp. 309–324.
3. A. M. Ioannides, M. R. Thompson, and E. J. Barenberg. Westergaard Solutions Reconsidered. In *Transportation Research Record 1043*, TRB, National Research Council, Washington, D.C., 1985, pp. 13–23.
4. D. L. De Jong, M. G. F. Pentz, and A. R. Korswagen. *Computer Program BISAR: Layered Systems Under Normal and Tangential Surface Loads.* External Report AMSR 0006.73. Koninklijke/Shell Laboratorium, Amsterdam, the Netherlands, 1973.
5. J. Uzan. The Influence of the Interface Condition on Stress Distribution in a Layered System. In *Transportation Research Record 616*, TRB, National Research Council, Washington, D.C., 1976, pp. 71–73.
6. A. H. A. Hogg. Equilibrium of a Thin Plate, Symmetrically Loaded, Resting on an Elastic Foundation of Infinite Depth. *Philosophical Magazine*, Vol. 25, No. 168, 1958, pp. 576–582.
7. A. H. A. Hogg. Equilibrium of a Thin Slab on an Elastic Foundation of Finite Depth. *Philosophical Magazine*, Vol. 35, No. 243, 1944, pp. 265–276.
8. A. M. Ioannides. Dimensional Analysis in NDT Rigid Pavement Evaluation. *Journal of Transportation Engineering*, ASCE, Vol. 116, No. 1, Jan., 1990, pp. 23–36.
9. H. Hertz. On the Equilibrium of Floating Elastic Plates. In *Miscellaneous Papers by Heinrich Hertz* (authorized English translation; (D. E. Jones and G. A. Schott, translators). MacMillan Co., Ltd., London, England, 1896, pp. 266–272.
10. H. M. Westergaard. New Formula for Stresses in Concrete Pavements of Airfields. *Transactions*, ASCE, Vol. 113, 1948, pp. 425–439.
11. A. P. S. Selvadurai. *Elastic Analysis of Soil-Foundation Interaction, Developments in Geotechnical Engineering*, Vol. 17. Elvesier, Amsterdam, the Netherlands, 1979.
12. G. Pickett and G. K. Ray. Influence Charts for Concrete Pavements. *Transactions*, ASCE, Vol. 116, 1951, pp. 49–73.
13. J. Uzan and A. Sides. The Effect of Contact Area Shape and Pressure Distribution on Multilayer System Response. In *Transportation Research Record 1117*, TRB, National Research Council, Washington, D.C., 1987, pp. 21–24.
14. J. Uzan, R. L. Lytton, and F. P. German. General Procedure for Backcalculating Layer Moduli. *ASTM Special Technical Publication 1026*, 1988, pp. 217–228.
15. J. Uzan, T. Scullion, C. H. Michalek, M. Parades, and R. L. Lytton. *A Microcomputer-Based Procedure for Back-calculating Layer Moduli from FWD Data.* Report FHWA/TX-88-1123-1. Texas Transportation Institute, Texas A&M University, College Station, Sept. 1988.
16. L. W. Teller and E. C. Sutherlands. The Structural Design of Concrete Pavements, Part 5—An Experimental Study of the Westergaard Analysis of Stress Conditions in Concrete Pavement Slabs of Uniform Thickness. *Public Roads*, Vol. 23, No. 8, 1943, pp. 143–212.
17. F. Parker, Jr., W. R. Barker, R. C. Gunkel, and E. C. Odem. *Development of a Structural Design Procedure for Rigid Pavements.* U.S. Army Engineers Waterways Experiment Station, Vicksburg, Miss., April 1979.
18. P. F. Carlton and R. M. Behrmann. A Model Study of Rigid Pavement Behavior Under Corner and Edge Loadings. *Proc., 35th Annual Meeting of the Highway Research Board*, HRB, National Research Council, Washington, D.C., 1956, pp. 139–146.

# Asphalt Thickness Variation on Texas Strategic Highway Research Program Sections and Effect on Backcalculated Moduli

ROBERT C. BRIGGS, TOM SCULLION, AND KENNETH R. MASER

Four Long Term Pavement Performance monitoring sites, part of the Strategic Highway Research Program (SHRP), were investigated in Texas with ground penetrating radar (GPR) to determine asphalt and base layer thicknesses as well as base moisture content. It was found that, with coring, the GPR could determine asphalt layer thicknesses to ± 0.11 in. This accuracy is reduced to ± 0.32 if the GPR results are not calibrated with cores. The base thicknesses could be determined to ± 0.99 in. The data obtained during this survey indicated that significant variations in layer thicknesses were present within the 500-ft SHRP sections. Practical limitations in the data collection process have forced SHRP personnel to treat pavement thicknesses as shown on plans, or obtained during the drilling and sampling process, as representative of the entire section, even though it is recognized that this may not be true. Deflection data currently are being gathered on the SHRP sites and will be used to backcalculate the material properties of the pavement layers. Values for material properties obtained through the backcalculation of deflection basins are extremely sensitive to pavement layer thickness. It was the intent of this study to quantify the errors introduced by variations in pavement layer thicknesses that are not accounted for in the backcalculation process. It was found that errors of up to 100 percent in pavement layer moduli were possible when comparing the moduli obtained using GPR measured thicknesses and moduli obtained using the SHRP data base thicknesses. It was also found that deflection basins alone are not a good indicator of layer thickness variations and that a good fit between measured and calculated deflection basins is not a good indicator of the correctness of the moduli values. The paper concludes by recommending that some method be investigated to quantify layer thickness variations on SHRP sites before using the deflections for backcalculation purposes.

The Strategic Highway Research Program (SHRP) as part of the Long Term Pavement Performance (LTPP) study, is currently performing deflection testing on over 1,000 in-service pavement sections located around the United States and Canada with falling weight deflectometers (FWDs). Measurements of pavement deflections under load are a generally accepted method of determining the material properties of the pavement layers and subsequent performance under traffic. Information obtained during this effort will be used to improve existing or formulate new equations for the design of pavements and overlays as well as pavement performance models for pavement management systems.

R. C. Briggs, Texas Department of Transportation, 125 East 11th Street, Austin, Tex. 78701. T. Scullion, Texas Transportation Institute, Texas A&M University, College Station, Tex. 77843. K. R. Maser, Infrasense, Inc., 765 Concord Avenue, Cambridge, Mass. 02138.

The SHRP staff has committed significant resources to ensuring that the deflection data obtained are complete, accurate, and meaningful before placement in the National Pavement Data Base. To achieve this end, numerous quality assurance practices have been developed. Manuals detailing the FWD data collection procedures on GPS rigid and flexible, as well as the SPS sections have been compiled and used to train FWD operators (*1*). Variables such as pavement surface temperature, as well as temperature gradients within the pavement structure, both of which heavily affect pavement deflections, are recorded by the FWD operator at the time of test. The FWD data collection program has been modified to include a subroutine that calculates the variance of multiple deflections taken at the same point and allows the operator to reject those deflections if the variance is too high. Programs such as FWDCHECK and FWDSCAN (*2*) have been written by SHRP contractors and distributed to the regional coordinating offices to identify FWD data files that are incomplete, contain questionable data, or contain deflections that indicate that the SHRP section is composed of variable pavement structure. An absolute calibration process has been developed by SHRP contractors and is scheduled to be implemented in four locations around the United States to ensure that the SHRP-owned FWDs have not drifted out of calibration and to certify state-owned FWDs for SHRP LTPP data collection. This calibration process is intended to ensure that the FWDs are measuring deflections at the accuracy published by their manufacturers (2 percent of the deflection $\pm 2\mu$). These quality assurance practices are considered vital in determining accurate moduli of the pavement layers.

There is a variable within the structural evaluation process in SHRP (a) that cannot be controlled in the design of the experiment, (b) can be quantified only in an indirect sense, (c) whose variance or standard deviation cannot be measured at all, and (d) that has a tremendous impact on the accuracy of the backcalculated material properties of the constituent pavement layers. This variable is pavement layer thickness.

SHRP pavement layer thickness data is obtained from two sources: (a) plan sheets and (b) measurements taken during the LTPP material sampling activities at the test pit locations on either end of the SHRP section. Obvious disadvantages

are inherent in both sources. Plan sheets do not always reflect what was actually constructed, particularly when field changes have not been recorded on the plans. Normal variations in layer thicknesses as a result of construction activities are not reflected in the plans. Although layer thicknesses can be measured directly during the material sampling activities at both ends of the test section, there is no guarantee that these measurements are representative of the pavement structure located within the 500 ft between the test pits. To make matters worse, the plans often do not agree with the results obtained from the test pit. Layer thicknesses cannot be measured within the confines of the test section because drilling and trenching would disturb the structural integrity of the pavement and render the section useless for the study of pavement distress propagation. Thus, one is forced to assume that the pavement structure at either end of the SHRP section is representative of the entire section.

The Texas Department of Transportation (TxDOT) has faced this dilemma for years. Deflection testing equipment has been used for more than 20 years for design of new pavements and overlays. Recent acquisition of FWDs has expanded the role of deflection testing to determination of load zoning requirements, pavement evaluation for superheavy permit loads, and network level deflection testing for pavement management. In every case, the engineer is forced to assume that the pavement structure found on the cross-section drawings of the plan sheets is representative of the entire section under test. Experience has shown that this is not always true, as many pavements have been overlaid multiple times, increasing significantly the thickness of the asphalt surfacing. Deviations from the plans often are necessary during construction and are not shown on the drawings. Variations in layer thicknesses are commonplace as a result of variations in the construction process.

To overcome this problem, TxDOT has sponsored several research projects with the Texas Transportation Institute with the objective of developing a swift, accurate, nondestructive method for measuring pavement layer thicknesses and their variations along the roadway. This test technique is intended to be used in conjunction with the FWD. Ground penetrating radar (GPR) is one of the technologies currently under study.

As a result of these studies, recent improvements in hardware and signal processing techniques have boosted GPR capabilities and accuracy. A report recently submitted to TxDOT indicates that GPR, as developed in this study, has the capability of measuring the thickness of asphaltic concrete with an accuracy of ± 0.1 in. and determining base thickness on asphaltic pavements to within ± 0.99 in. if cores are obtained to calibrate the radar (*3*). Without coring (using only radar), the accuracy drops to ± 0.32 in. for asphalt concrete.

## GPR SURVEY OF SHRP SITES

During June 1990, a GPR survey was performed on four SHRP LTPP sites near College Station, Tex. (*3*). These sites were Sections 481178, 483559, 481109, and 481050. The purpose of the survey was to determine how closely the GPR apparatus could predict asphalt and base thicknesses as well as determine moisture content of the base material. SHRP sites were selected as the pavement structure was reasonably well documented. Each test run consisted of 1,500 ft of pavement, 500 ft before the SHRP section, the SHRP section itself, and 500 ft after the test section. This provided 1,000 ft of pavement from which materials could be extracted for determination of dielectric constant. It also allowed the researchers to core the pavement and check the accuracy of the radar predictions. Four passes were made at each SHRP test section, one at 5 mph in the left wheel path, and one at 5, 15, and 40 mph over the right wheel path. Three types of destructive testing was performed to verify GPR results: (a) 4-in.-diameter wet cores were taken to verify asphalt concrete pavement (ACP) thickness; (b) 6-in.-diameter dry cores were obtained to verify base moisture content predictions; and (c) cone penetrometer tests were performed to measure GPR base thickness predictions. As a result of this study it was determined that GPR could predict asphalt thicknesses to within ± 0.11 in. with verification and calibration by coring, and to ± 0.32 in. without coring. Base thicknesses could be predicted within ± 0.99 in. and base moisture could be predicted within 2 percent by weight. Furthermore, the radar data indicated that significant variations in layer thicknesses were present on most of the SHRP sections tested.

Tables 1 through 4 compare the thicknesses measured with GPR on the four sites and that obtained from the SHRP data base, and Figure 1 illustrates this graphically. As can be seen

**TABLE 1 Assumed Versus Measured Thicknesses, Section 481109**

| ASSUMED THICKNESSES: 7.0 in. HMAC, 6.0 in. Granular Base | | |
|---|---|---|
| MEASURED THICKNESSES | | |
| DISTANCE (ft.) | HMAC (in.) | BASE (in.) |
| 0 | 6.5 | 5.2 |
| 50 | 6.0 | 5.3 |
| 100 | 6.4 | 4.9 |
| 150 | 6.6 | 5.0 |
| 200 | 6.6 | 5.0 |
| 250 | 6.5 | 4.8 |
| 300 | 6.3 | 5.8 |
| 350 | 6.5 | 5.5 |
| 400 | 6.5 | 6.1 |
| 450 | 6.5 | 5.4 |
| 500 | 7.0 | 5.5 |

**TABLE 2 Assumed Versus Measured Thicknesses, Section 481050**

| ASSUMED THICKNESSES: 2.3 in. HMAC, 8.3 in. Granular Base | | |
|---|---|---|
| MEASURED THICKNESSES | | |
| DISTANCE (ft.) | HMAC (in.) | BASE (in.) |
| 0 | 2.0 | 10.4 |
| 50 | 2.4 | 11.8 |
| 100 | 2.3 | 13.0 |
| 150 | 2.0 | 11.2 |
| 200 | 2.4 | 10.2 |
| 250 | 2.7 | 10.3 |
| 300 | 2.7 | 10.1 |
| 350 | 2.2 | 10.0 |
| 400 | 2.4 | 10.0 |
| 450 | 2.1 | 11.0 |
| 500 | 2.1 | 11.8 |

**TABLE 3 Assumed Versus Measured Thicknesses, Section 481178**

| ASSUMED THICKNESSES: 8.8 in. HMAC, 10.2 in. Granular Base | | |
|---|---|---|
| MEASURED THICKNESSES | | |
| DISTANCE (ft.) | HMAC (in.) | BASE (in.) |
| 0 | 8.6 | 10.3 |
| 50 | 8.4 | 9.7 |
| 100 | 8.1 | 10.5 |
| 150 | 8.0 | 10.5 |
| 200 | 8.0 | 10.8 |
| 250 | 8.2 | 8.9 |
| 300 | 8.3 | 10.4 |
| 350 | 8.6 | 10.0 |
| 400 | 8.4 | 8.7 |
| 450 | 8.3 | 8.2 |
| 500 | 8.5 | 9.6 |

**TABLE 4 Assumed Versus Measured Thicknesses, Section 483559**

| ASSUMED THICKNESSES: 7.0 in. HMAC, 6.O in. Base | | |
|---|---|---|
| MEASURED THICKNESSES | | |
| DISTANCE (ft.) | HMAC (in.) | BASE (in.) |
| 0 | 8.2 | 7.2 |
| 50 | 9.0 | 7.0 |
| 100 | 9.1 | 7.0 |
| 150 | 8.2 | 7.8 |
| 200 | 8.7 | 7.5 |
| 250 | 8.3 | 7.2 |
| 300 | 7.6 | 7.0 |
| 350 | 7.1 | 8.0 |
| 400 | 7.4 | 7.8 |
| 450 | 7.2 | 7.8 |
| 500 | 7.4 | 8.0 |

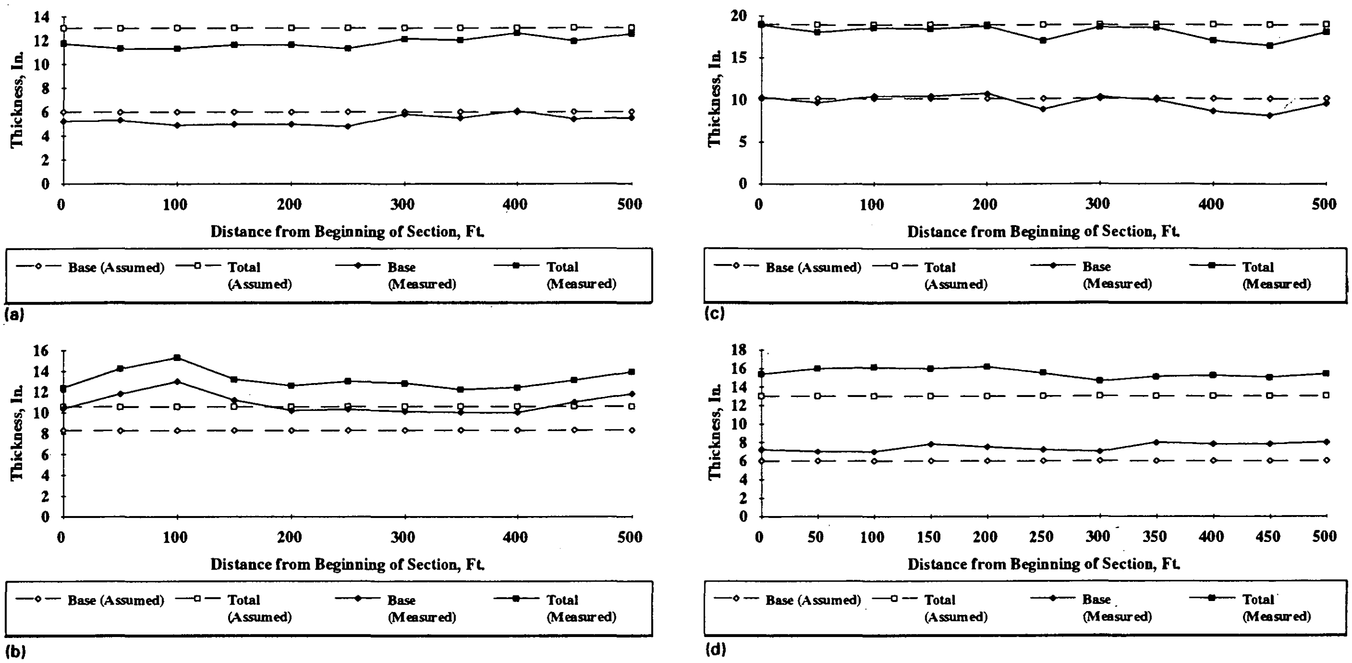


FIGURE 1 Assumed layer thicknesses for SHRP data base versus layer thicknesses obtained from GPR measurements: (*a*) Section 481109, (*b*) Section 481050, (*c*) Section 481178, and (*d*) Section 483559.

from the figure, the differences approached 2 in. on 481109, 481178, and 483559, whereas on 481050 a difference of up to 5 in. occurred at 100 ft from the beginning of the section. This led to the question of how these variations in pavement structure could possibly affect the backcalculated moduli of the paving materials if the pavement structure was assumed to be that which is stored in the SHRP data base. To quantify these variations, the FWD deflections were obtained from the data base. Pavement layer moduli were backcalculated using the SHRP layer thicknesses and the thicknesses obtained with GPR. The remainder of this report documents the results of this comparison.

## DEFLECTION TESTS RESULTS

FWD deflection files were obtained for each of the SHRP sites: 481109, 481050, 481178, and 483559 from the South-eastern RCO. Only the midlane deflections were used in this comparison to avoid the effects of any distresses that may have been present in the wheel paths. Although deflections are obtained at 25-ft intervals on the test sections, the radar data were reported in 50-ft intervals; thus only deflections at 50-ft intervals were used in this analysis. A total of 16 deflection tests were performed at each test point, with four drops at four separate load levels. The 16 deflection basins at each point were normalized to 10,000 lb and then averaged for presentation in Tables 5 through 8, as well as graphically in Figure 2. However, for backcalculation purposes, the basins were neither normalized nor averaged.

No correlation was apparent between the variations in pavement thickness and the variations in deflections obtained along the section, as evidenced in a comparison of Figures 1 and 2, with the exception of the 100-ft position on 481050. Here, the deflections seemed to reduce as the base thickness increased. The deflections indicate that significant variation, either in

TABLE 5 Average Normalized Deflections, Section 481109

| Distance | R=0" | R=8" | R=12" | R=18" | R=24" | R=36" | R=60" |
|---|---|---|---|---|---|---|---|
| 0 | 11.18 | 10.06 | 9.25 | 7.86 | 6.58 | 4.57 | 2.43 |
| 50 | 8.46 | 7.53 | 6.86 | 5.84 | 4.93 | 3.48 | 1.96 |
| 100 | 8.92 | 7.81 | 7.02 | 5.80 | 4.72 | 3.07 | 1.35 |
| 150 | 8.08 | 7.09 | 6.36 | 5.29 | 4.32 | 2.81 | 1.15 |
| 200 | 7.12 | 6.13 | 5.47 | 4.56 | 3.74 | 2.51 | 1.18 |
| 250 | 8.77 | 7.80 | 7.10 | 5.97 | 4.97 | 3.46 | 1.87 |
| 300 | 10.18 | 8.98 | 8.19 | 6.94 | 5.79 | 4.03 | 2.05 |
| 350 | 11.22 | 9.96 | 9.06 | 7.62 | 6.32 | 4.26 | 2.01 |
| 400 | 8.34 | 7.14 | 6.42 | 5.36 | 4.42 | 3.00 | 1.42 |
| 450 | 7.64 | 6.61 | 5.93 | 4.93 | 4.03 | 2.67 | 1.17 |
| 500 | 5.96 | 5.11 | 4.51 | 3.60 | 2.83 | 1.73 | 0.69 |
| Avg | 8.71 | 7.66 | 6.92 | 5.80 | 4.79 | 3.24 | 1.57 |
| Std | 1.55 | 1.46 | 1.38 | 1.22 | 1.06 | 0.79 | 0.50 |

**TABLE 6 Average Normalized Deflections, Section 481050**

| Distance | R=0" | R=8" | R=12" | R=18" | R=24" | R=36" | R=60" |
|---|---|---|---|---|---|---|---|
| 0 | 20.65 | 13.51 | 8.95 | 6.03 | 4.47 | 2.91 | 1.63 |
| 50 | 27.46 | 17.73 | 11.68 | 7.40 | 5.01 | 3.01 | 1.93 |
| 100 | 15.96 | 10.59 | 7.31 | 5.26 | 4.21 | 3.09 | 1.84 |
| 150 | 14.89 | 9.72 | 7.04 | 5.26 | 4.18 | 3.12 | 1.91 |
| 200 | 21.34 | 12.29 | 7.98 | 5.41 | 3.98 | 2.73 | 1.69 |
| 250 | 17.87 | 11.93 | 8.38 | 5.82 | 4.20 | 2.75 | 1.61 |
| 300 | 25.70 | 16.32 | 10.90 | 7.43 | 5.36 | 3.57 | 1.93 |
| 350 | 25.68 | 16.20 | 10.47 | 7.07 | 5.14 | 3.37 | 1.99 |
| 400 | 23.09 | 14.75 | 9.85 | 6.64 | 4.84 | 3.22 | 1.94 |
| 450 | 17.93 | 11.35 | 7.92 | 5.56 | 4.13 | 2.79 | 1.71 |
| 500 | 20.97 | 13.59 | 8.78 | 5.84 | 4.26 | 2.89 | 1.70 |
| Avg | 21.05 | 13.45 | 9.02 | 6.16 | 4.52 | 3.04 | 1.81 |
| Std | 3.96 | 2.45 | 1.45 | 0.80 | 0.45 | 0.26 | 0.13 |

**TABLE 7 Average Normalized Deflections, Section 481178**

| Distance | R=0" | R=8" | R=12" | R=18" | R=24" | R=36" | R=60" |
|---|---|---|---|---|---|---|---|
| 0 | 7.97 | 6.99 | 6.28 | 5.42 | 4.49 | 3.06 | 1.74 |
| 50 | 5.73 | 4.73 | 4.16 | 3.61 | 3.11 | 2.47 | 1.65 |
| 100 | 6.70 | 5.53 | 4.90 | 4.32 | 3.75 | 3.04 | 2.00 |
| 150 | 6.76 | 5.72 | 5.08 | 4.49 | 3.90 | 3.18 | 2.08 |
| 200 | 5.77 | 4.63 | 4.07 | 3.60 | 3.17 | 2.62 | 1.83 |
| 250 | 5.92 | 4.84 | 4.25 | 3.73 | 3.25 | 2.69 | 1.84 |
| 300 | 5.07 | 4.12 | 3.61 | 3.16 | 2.77 | 2.29 | 1.56 |
| 350 | 7.40 | 6.10 | 5.28 | 4.48 | 3.74 | 2.83 | 1.77 |
| 400 | 4.57 | 3.79 | 3.36 | 3.02 | 2.71 | 2.29 | 1.59 |
| 450 | 5.36 | 4.48 | 3.96 | 3.49 | 3.05 | 2.47 | 1.70 |
| 500 | 6.17 | 4.96 | 4.34 | 3.81 | 3.31 | 2.66 | 1.80 |
| Avg | 6.13 | 5.08 | 4.48 | 3.92 | 3.39 | 2.69 | 1.78 |
| Std | 0.96 | 0.89 | 0.80 | 0.66 | 0.51 | 0.29 | 0.15 |

**TABLE 8 Average Normalized Deflections, Section 483559**

| Distance | R=0" | R=8" | R=12" | R=18" | R=24" | R=36" | R=60" |
|---|---|---|---|---|---|---|---|
| 0 | 6.22 | 5.51 | 5.07 | 4.25 | 3.66 | 2.69 | 1.33 |
| 50 | 5.60 | 5.06 | 4.68 | 4.10 | 3.54 | 2.57 | 1.28 |
| 100 | 5.73 | 5.10 | 4.50 | 4.20 | 3.75 | 2.62 | 1.37 |
| 150 | 5.24 | 4.64 | 4.20 | 3.56 | 3.02 | 1.98 | 0.85 |
| 200 | 3.90 | 3.47 | 3.14 | 2.58 | 2.08 | 1.30 | 0.50 |
| 250 | 4.76 | 4.24 | 3.66 | 3.17 | 2.41 | 1.55 | 0.53 |
| 300 | 5.31 | 4.58 | 4.07 | 3.29 | 2.57 | 1.50 | 0.49 |
| 350 | 6.07 | 5.40 | 4.81 | 3.86 | 3.03 | 1.73 | 0.50 |
| 400 | 5.32 | 4.59 | 4.04 | 3.35 | 2.56 | 1.51 | 0.43 |
| 450 | 5.74 | 5.04 | 4.34 | 3.45 | 2.63 | 1.48 | 0.42 |
| 500 | 5.72 | 4.92 | 4.37 | 3.54 | 2.74 | 1.66 | 0.51 |
| Avg | 5.42 | 4.78 | 4.26 | 3.58 | 2.91 | 1.87 | 0.75 |
| Std | 0.62 | 0.55 | 0.51 | 0.48 | 0.52 | 0.49 | 0.37 |

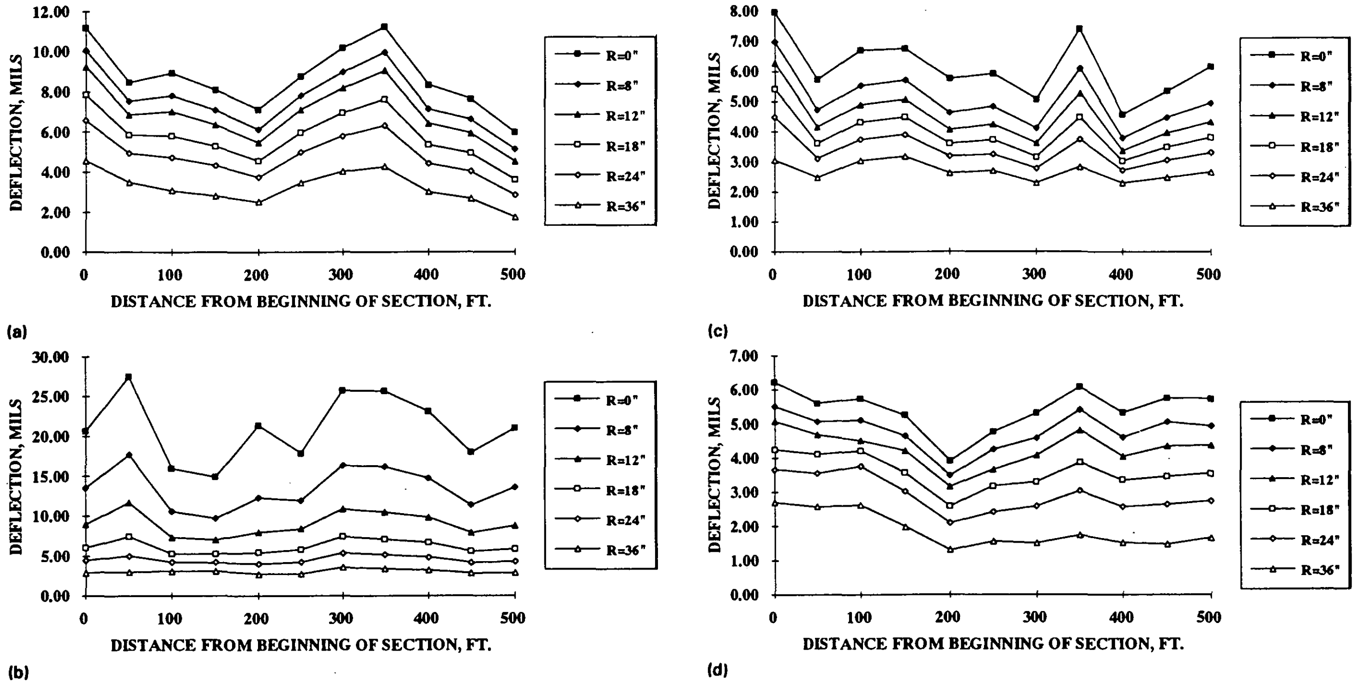


**FIGURE 2 Average normalized deflections obtained on SHRP sites: (*a*) Section 481109, (*b*) Section 481050, (*c*) Section 481178, and (*d*) Section 483559.**

strength or structure, can be found within each of these SHRP sites.

## BACKCALCULATION OF MATERIAL PROPERTIES

The backcalculation effort for each section consisted of two runs. The first run was performed using thicknesses obtained from the SHRP data base. The second run was performed using thicknesses obtained from the GPR survey. The MODULUS program (*4*) was used for the backcalculation process. All other variables were held constant between the two runs, including the upper and lower ranges for the moduli. A rigid layer was assigned at 240 in. from the pavement surface. Poisson ratios were selected on the basis of commonly used values obtained from the literature.

For the MODULUS runs using the assumed layer thicknesses, the program was run iteratively with the goal of achieving an average error of 2 percent or less per geophone when comparing the backcalculated versus measured deflection basins while restricting the upper and lower ranges of moduli to reasonable limits.

Each test point consisted of 16 deflection basins, four drops at each of four load levels. The modulus program was run on each of the 16 deflection basins, and the average of the results is reported in the tables. The material types and associated thicknesses can be found in Tables 1 through 4.

## RESULTS

In almost every case, using measured thicknesses in place of assumed thicknesses resulted in a better fit when comparing the measured versus backcalculated deflection basins. Figure 3 illustrates this clearly. In virtually every case, except for several points on Section 481178, the utilization of the GPR measured thicknesses improved the deflection basin fit; in the case of 481050 and 483559, it improved it dramatically. Note however, that on Section 481178, using the assumed thicknesses, the average error per sensor was already below the 3 percent range, and from Figure 1 we can observe that the measured versus assumed thicknesses were not significantly different compared with those in the other three sections. Thus, for this section, the introduction of GPR measured thicknesses did not improve by much the results of the analysis.

Tables 9 through 12 indicate that by introducing GPR-measured thickness in lieu of the SHRP data base thicknesses, the overall average error per sensor decreased from 1.41 to 1.01 on Section 481109, decreased from 6.38 to 2.94 for Section 481050, increased from 2.7 to 2.92 on Section 481178, and decreased from 3.96 to 1.73 on Section 483559. The standard deviation increased or decreased accordingly. It should be reiterated here that nothing was changed between the MODULUS runs using measured versus assumed layer thicknesses except the thicknesses themselves.

### ACP Moduli

Tables 13 through 16 present the average backcalculated moduli for the ACP, base, and subgrade layers for all four SHRP sections, using both assumed and measured thicknesses. The modulus values are shown at 50-ft intervals beginning at the zero point on the section. Each cell on the table represents the average results for 16 deflection basins.

Tables 17 through 20 summarize the average percent difference between the backcalculated moduli using assumed

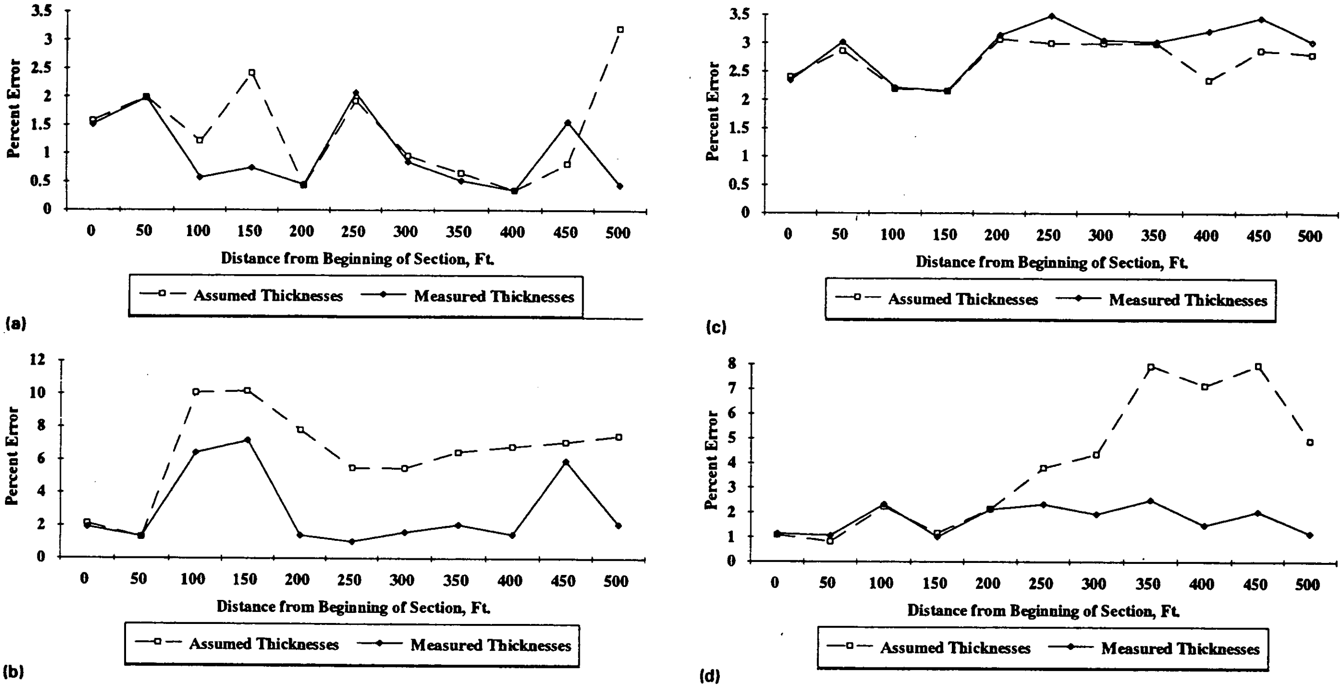


**FIGURE 3** Average error per sensor for backcalculation using measured versus assumed layer thicknesses: (*a*) Section 481109, (*b*) Section 481050, (*c*) Section 481178, and (*d*) Section 483559.

**TABLE 9** Average Error per Sensor, Section 481109

| DISTANCE | ASSUMED THICKNESSES | MEASURED THICKNESSES |
|---|---|---|
| 0 | 1.58 | 1.51 |
| 50 | 1.99 | 1.98 |
| 100 | 1.21 | 0.57 |
| 150 | 2.41 | 0.74 |
| 200 | 0.43 | 0.45 |
| 250 | 1.93 | 2.08 |
| 300 | 0.96 | 0.85 |
| 350 | 0.66 | 0.52 |
| 400 | 0.35 | 0.35 |
| 450 | 0.82 | 1.57 |
| 500 | 3.21 | 0.45 |
| Avg | 1.41 | 1.01 |
| Std | 0.94 | 0.65 |

**TABLE 10** Average Error per Sensor, Section 481050

| DISTANCE | ASSUMED THICKNESSES | MEASURED THICKNESSES |
|---|---|---|
| 0 | 2.11 | 1.90 |
| 50 | 1.31 | 1.33 |
| 100 | 10.06 | 6.42 |
| 150 | 10.17 | 7.17 |
| 200 | 7.80 | 1.38 |
| 250 | 5.50 | 1.04 |
| 300 | 5.48 | 1.59 |
| 350 | 6.46 | 2.05 |
| 400 | 6.79 | 1.47 |
| 450 | 7.07 | 5.93 |
| 500 | 7.46 | 2.08 |
| Avg | 6.38 | 2.94 |
| Std | 2.71 | 2.27 |

**TABLE 11 Average Error per Sensor, Section 481178**

| DISTANCE | ASSUMED THICKNESSES | MEASURED THICKNESSES |
|---|---|---|
| 0 | 2.40 | 2.35 |
| 50 | 2.87 | 3.02 |
| 100 | 2.20 | 2.22 |
| 150 | 2.15 | 2.16 |
| 200 | 3.07 | 3.15 |
| 250 | 3.00 | 3.49 |
| 300 | 3.00 | 3.06 |
| 350 | 3.00 | 3.03 |
| 400 | 2.35 | 3.22 |
| 450 | 2.87 | 3.45 |
| 500 | 2.80 | 3.02 |
| Avg | 2.70 | 2.92 |
| Std | 0.41 | 0.51 |

**TABLE 12 Average Error per Sensor, Section 483559**

| DISTANCE | ASSUMED THICKNESSES | MEASURED THICKNESSES |
|---|---|---|
| 0 | 1.09 | 1.14 |
| 50 | 0.82 | 1.06 |
| 100 | 2.23 | 2.32 |
| 150 | 1.16 | 1.01 |
| 200 | 2.14 | 2.11 |
| 250 | 3.80 | 2.32 |
| 300 | 4.35 | 1.93 |
| 350 | 7.93 | 2.49 |
| 400 | 7.13 | 1.48 |
| 450 | 7.95 | 2.02 |
| 500 | 4.90 | 1.15 |
| Avg | 3.96 | 1.73 |
| Std | 3.19 | 0.83 |

**TABLE 13 Average Backcalculated Moduli Values, Section 481109**

| DISTANCE | ASSUMED THICKNESSES | | | MEASURED THICKNESSES | | |
|---|---|---|---|---|---|---|
| | ACP | BASE | SUBGR | ACP | BASE | SUBGR |
| 0 | 1270861 | 33664 | 14124 | 1502636 | 44736 | 14151 |
| 50 | 1202360 | 142277 | 17825 | 1462478 | 250581 | 18052 |
| 100 | 1217483 | 22513 | 22511 | 1551991 | 27447 | 22202 |
| 150 | 1320798 | 24936 | 24933 | 1605450 | 31070 | 24155 |
| 200 | 1395401 | 60562 | 26715 | 1434563 | 111030 | 26503 |
| 250 | 1286523 | 79352 | 18388 | 1707190 | 88442 | 18712 |
| 300 | 1226050 | 46981 | 16237 | 1507749 | 67952 | 16190 |
| 350 | 1171804 | 16987 | 16120 | 1452957 | 16457 | 16154 |
| 400 | 1166171 | 62700 | 22207 | 1281846 | 82963 | 22046 |
| 450 | 1452738 | 27851 | 26153 | 1687505 | 43427 | 25592 |
| 500 | 1355823 | 38777 | 38772 | 1422720 | 38138 | 38134 |
| Avg | 1278728 | 50600 | 22180 | 1510644 | 72931 | 21990 |
| Std | 89538 | 34393 | 6672 | 117626 | 62714 | 6425 |

**TABLE 14 Average Backcalculated Moduli Values, Section 481050**

| DISTANCE | ASSUMED THICKNESSES | | | MEASURED THICKNESSES | | |
|---|---|---|---|---|---|---|
| | ACP | BASE | SUBGR | ACP | BASE | SUBGR |
| 0 | 690852 | 38840 | 23374 | 1036038 | 37344 | 22922 |
| 50 | 692701 | 22517 | 19550 | 616998 | 21775 | 19486 |
| 100 | 320045 | 90470 | 23662 | 521148 | 64469 | 22657 |
| 150 | 502121 | 99999 | 23725 | 228976 | 93773 | 22897 |
| 200 | 214275 | 47506 | 25471 | 291054 | 39058 | 26469 |
| 250 | 609746 | 58961 | 22897 | 619669 | 43219 | 23755 |
| 300 | 315167 | 38452 | 18270 | 328046 | 29480 | 19024 |
| 350 | 307956 | 36833 | 19163 | 558852 | 29177 | 20026 |
| 400 | 354099 | 43090 | 20134 | 522756 | 32926 | 21108 |
| 450 | 285640 | 68302 | 24029 | 723510 | 50631 | 24137 |
| 500 | 440044 | 44734 | 22681 | 960286 | 33068 | 24013 |
| Avg | 430240 | 53609 | 22087 | 582485 | 43174 | 22409 |
| Std | 161801 | 22720 | 2265 | 243727 | 19467 | 2170 |

**TABLE 15 Average Backcalculated Moduli Values, Section 481178**

| DISTANCE | ASSUMED THICKNESSES | | | MEASURED THICKNESSES | | |
|---|---|---|---|---|---|---|
| | ACP | BASE | SUBGR | ACP | BASE | SUBGR |
| 0 | 865565 | 41414 | 19925 | 892935 | 44140 | 19849 |
| 50 | 583858 | 328485 | 22116 | 581501 | 386996 | 22446 |
| 100 | 501303 | 316250 | 17800 | 511040 | 339547 | 17906 |
| 150 | 558158 | 291878 | 16907 | 577812 | 320001 | 17020 |
| 200 | 459003 | 597719 | 19922 | 461585 | 599727 | 20046 |
| 250 | 492775 | 467289 | 19809 | 467628 | 739099 | 20460 |
| 300 | 554894 | 565781 | 23353 | 555878 | 592894 | 23498 |
| 350 | 482413 | 155280 | 20348 | 486347 | 165743 | 20424 |
| 400 | 664908 | 817949 | 21823 | 763059 | 999997 | 23086 |
| 450 | 634126 | 432760 | 21238 | 600036 | 782441 | 22130 |
| 500 | 463280 | 396455 | 20396 | 455242 | 476503 | 20708 |
| Avg | 569117 | 401024 | 20331 | 577551 | 495190 | 20688 |
| Std | 114055 | 204306 | 1761 | 130768 | 269049 | 1936 |

**TABLE 16 Average Backcalculated Moduli Values, Section 483559**

| DISTANCE | ASSUMED THICKNESSES | | | MEASURED THICKNESSES | | |
|---|---|---|---|---|---|---|
| | ACP | BASE | SUBGR | ACP | BASE | SUBGR |
| 0 | 2073723 | 116974 | 24749 | 1639274 | 46312 | 25452 |
| 50 | 3119528 | 70918 | 26140 | 1802766 | 22659 | 27467 |
| 100 | 2619711 | 183844 | 24385 | 1688967 | 51458 | 25258 |
| 150 | 2805006 | 16771 | 39117 | 1934697 | 15621 | 40157 |
| 200 | 3117260 | 18814 | 62457 | 1902148 | 18764 | 61693 |
| 250 | 2354590 | 16206 | 54012 | 1681229 | 15783 | 52440 |
| 300 | 1815968 | 15994 | 53306 | 1601528 | 15862 | 52561 |
| 350 | 1456681 | 15000 | 45964 | 1649556 | 15000 | 45502 |
| 400 | 1717293 | 16289 | 54288 | 1739869 | 16072 | 53568 |
| 450 | 1440741 | 15864 | 52876 | 1509539 | 16015 | 53377 |
| 500 | 1677222 | 15039 | 49402 | 1636301 | 15377 | 49642 |
| Avg | 2199793 | 45610 | 44245 | 1707807 | 22629 | 44283 |
| Std | 606908 | 53725 | 12943 | 122163 | 12599 | 12261 |

**TABLE 17 Percentage Difference in Backcalculated Moduli, Section 481109**

| Distance | ACP | BASE | SUBGR |
|---|---|---|---|
| 0 | 18.29 | 32.89 | 0.19 |
| 50 | 21.63 | 76.12 | 1.27 |
| 100 | 27.48 | 21.92 | -1.37 |
| 150 | 21.55 | 24.60 | -3.12 |
| 200 | 2.81 | 83.33 | -0.80 |
| 250 | 32.70 | 11.46 | 1.76 |
| 300 | 22.98 | 44.64 | -0.29 |
| 350 | 23.99 | -3.12 | 0.22 |
| 400 | 9.92 | 32.32 | -0.73 |
| 450 | 16.16 | 55.93 | -2.14 |
| 500 | 4.93 | -1.65 | -1.65 |
| Avg | 18.14 | 44.13 | -0.86 |

**TABLE 18 Percentage Difference in Backcalculated Moduli, Section 481050**

| Distance | ACP | BASE | SUBGR |
|---|---|---|---|
| 0 | 49.97 | -3.85 | -1.93 |
| 50 | -10.93 | -3.29 | -0.33 |
| 100 | 62.84 | -28.74 | -4.25 |
| 150 | -54.40 | -6.23 | -3.49 |
| 200 | 35.83 | -17.78 | 3.92 |
| 250 | 1.63 | -26.70 | 3.75 |
| 300 | 4.09 | -23.33 | 4.13 |
| 350 | 81.47 | -20.79 | 4.51 |
| 400 | 47.63 | -23.59 | 4.84 |
| 450 | 153.29 | -25.87 | 0.45 |
| 500 | 118.23 | -26.08 | 5.87 |
| Avg | 35.39 | -19.46 | 1.46 |

**TABLE 19 Percentage Difference in Backcalculated Moduli, Section 481178**

| Distance | ACP | BASE | SUBGR |
|---|---|---|---|
| 0 | 3.16 | 6.58 | -0.38 |
| 50 | -0.40 | 17.81 | 1.49 |
| 100 | 1.94 | 7.37 | 0.59 |
| 150 | 3.52 | 9.64 | 0.66 |
| 200 | 0.56 | 0.33 | 0.62 |
| 250 | -5.10 | 58.17 | 3.29 |
| 300 | 0.18 | 4.79 | 0.62 |
| 350 | 0.82 | 6.74 | 0.37 |
| 400 | 14.76 | 22.26 | 5.79 |
| 450 | -5.38 | 80.80 | 4.20 |
| 500 | -1.73 | 20.19 | 1.53 |
| Avg | 1.48 | 23.48 | 1.76 |

**TABLE 20 Percentage Difference in Backcalculated Moduli, Section 483559**

| Distance | ACP | BASE | SUBGR |
|---|---|---|---|
| 0 | -20.95 | -60.41 | 2.84 |
| 50 | -42.21 | -68.05 | 5.08 |
| 100 | -35.53 | -72.01 | 3.58 |
| 150 | -31.03 | -6.86 | 2.66 |
| 200 | -38.98 | -0.27 | -1.22 |
| 250 | -28.60 | -2.61 | -2.91 |
| 300 | -11.81 | -0.82 | -1.40 |
| 350 | 13.24 | 0.00 | -1.00 |
| 400 | 1.31 | -1.33 | -1.33 |
| 450 | 4.78 | 0.96 | 0.95 |
| 500 | -2.44 | 2.25 | 0.49 |
| Avg | -22.37 | -50.39 | 0.09 |

versus measured thicknesses for the 16 basins at each test point.

These tables indicate that the backcalculated moduli of the ACP layers, being highly sensitive to assumptions regarding the pavement structure, are adversely affected by normal layer thickness variations found on these SHRP sections. In the case of Section 481109, the average backcalculated modulus of the ACP increased from 1,278,728 lb/in.$^2$ to 1,510,644 lb/in.$^2$ when substituting the measured layer thicknesses for the SHRP data base thicknesses. Figure 4 illustrates this graphically. In each of these plots, the ACP moduli value obtained utilizing the assumed thicknesses is plotted against the $x$-axis, whereas the modulus value obtained utilizing the GPR measured thicknesses is plotted against the $y$-axis. The straight line on the graph represents the line of equality. Each point on the graph represents one deflection basin. From this graph, it is apparent that by using assumed thicknesses from the SHRP data base, one runs the risk of consistently over- or underpredicting the modulus of the ACP layer.

For Section 481050, the average ACP modulus increased from 430,240 lb/in.$^2$ to 582,425 lb/in.$^2$, or 35 percent, when comparing assumed versus measured thicknesses. However, from Figure 4 it is apparent that the differences are far worse when considering individual deflection basins. Several deflection basins exhibited changes in backcalculated moduli of over 100 percent.

Section 481178, having less difference between the assumed versus the measured layer thicknesses, exhibited little change in ACP modulus. In fact, the average difference, as can be seen in Table 19, was only 1.48 percent, the largest change occurring at 400 ft from the beginning of the section and that being 14.76 percent. Furthermore, most of the points fell on the line of equality in Figure 4.

Section 483559 exhibited an interesting phenomenon near the beginning of the section, in which the ACP moduli reached the somewhat questionable value of 4,000,000 lb/in.$^2$ while using the SHRP assumed thicknesses. Note that the average error per sensor between the measured and calculated de-

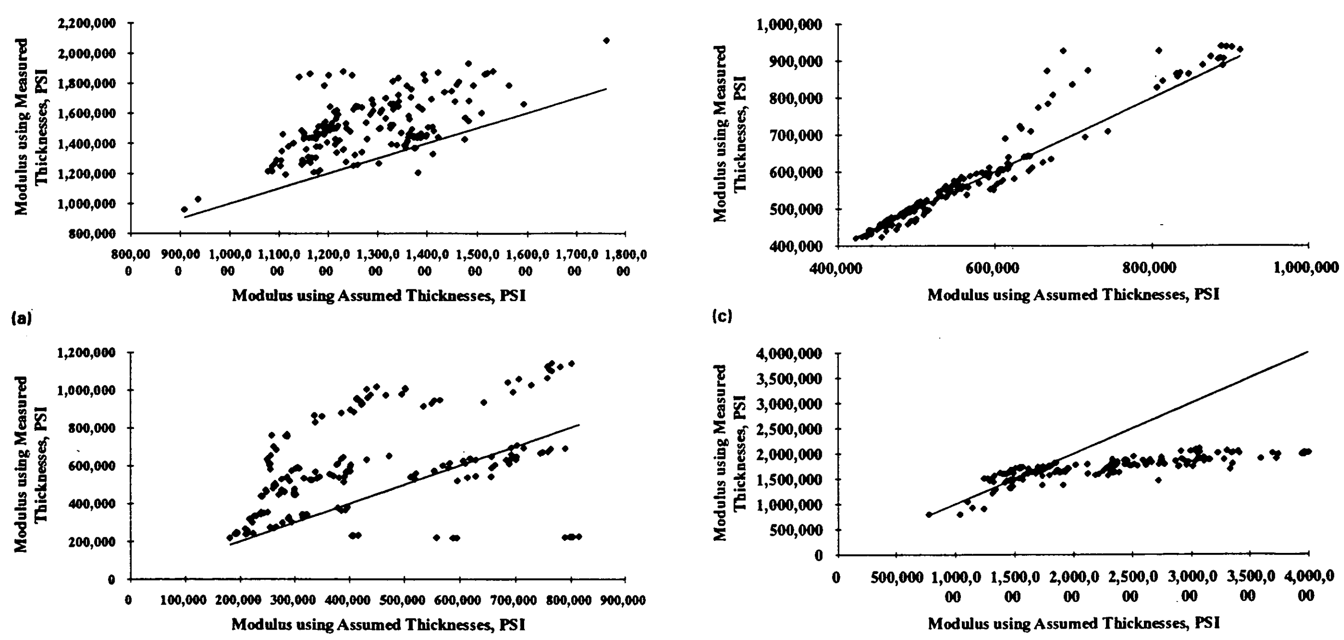


**FIGURE 4 Backcalculated asphalt moduli using assumed versus measured layer thicknesses: (*a*) Section 481109, (*b*) Section 481050, (*c*) Section 481178, and (*d*) Section 483559.**

flection basin was in most cases less than or near 2 percent. By using the GPR-measured thicknesses, the moduli were reduced to near 2,000,000 lb/in.$^2$, which is more consistent with values found elsewhere on the section, and the average error per sensor was similar to that obtained using the SHRP data base thicknesses. Table 4 provides insight into the cause of this apparent discrepancy. By examining Table 4 we find that between Test Points 0 and 300, substantial differences exist between the assumed and the measured ACP thicknesses. Differences of up to 2 in. were found at points 50 and 100. By taking this discrepancy into account, the backcalculated moduli on these points were not only more realistic, but the standard deviation of the moduli values over the section were reduced from 606,908 lb/in.$^2$ to 122,163 lb/in.$^2$, as can be seen in Table 16. This illustrates that the error between the measured and calculated basin in the backcalculation process is not always a good indicator of the accuracy of the layer moduli obtained during the process.

The standard deviations of the ACP moduli increased for Sections 481109, 481050, and 481178 when substituting GPR measured thicknesses with those from the SHRP data base. In two instances, for Sections 481178 and 481109, the increase is considered by the authors to be negligible. However, for Section 481050 a dramatic increase from 161,801 to 243,727 can be seen. The ACP thicknesses, both measured and assumed, are less than 3 in. The FWD is relatively insensitive to variations in ACP modulus when the layer is this thin. That is, the deflections obtained do not vary significantly with changes in ACP modulus at this level of thickness. Thus when performing the backcalculation, one may expect a wide variation in the predicted ACP modulus when attempting to fit the basins. For instance, by varying the difference between the measured and calculated deflection basin by only a few tenths of a mil, wide variations in ACP modulus will result. It is standard practice in Texas to fix the ACP modulus to some temperature corrected value during the backcalculation process. For these reasons, the increase in standard deviation of the ACP modulus values for Section 481050 cannot be considered significant.

The ACP moduli values seem high for Sections 481109 and 483559. This can be explained as the result of combining the thin ACP surface layer with the underlying asphalt stabilized base layer that was present on both sections.

### Base Course Moduli

The base course moduli were affected by the changes in thicknesses as well. Figure 5 illustrates the affect of including the GPR measured thicknesses in the analysis. Generally, by using assumed layer thicknesses, one underpredicts the base course modulus on Sections 481109 and 481178. On Section 481050 the reverse is true. From Tables 17 through 20 it is apparent that, on average, the modulus is underpredicted by 44.13 and 23.48 percent on 481109 and 481178, respectively. For Sections 481050 and 483559, it is overpredicted by 19.46 and 50.39 percent, respectively.

Another interesting finding was that the base course modulus for Section 483559 was substantially less than the subgrade modulus (22,629 versus 44,283 lb/in.$^2$), suggesting the presence of nonlinearity in the subgrade or the presence of a rigid layer. This trend was evident regardless of whether the assumed layer thicknesses or the GPR-measured thicknesses were used in the backcalculation procedure.

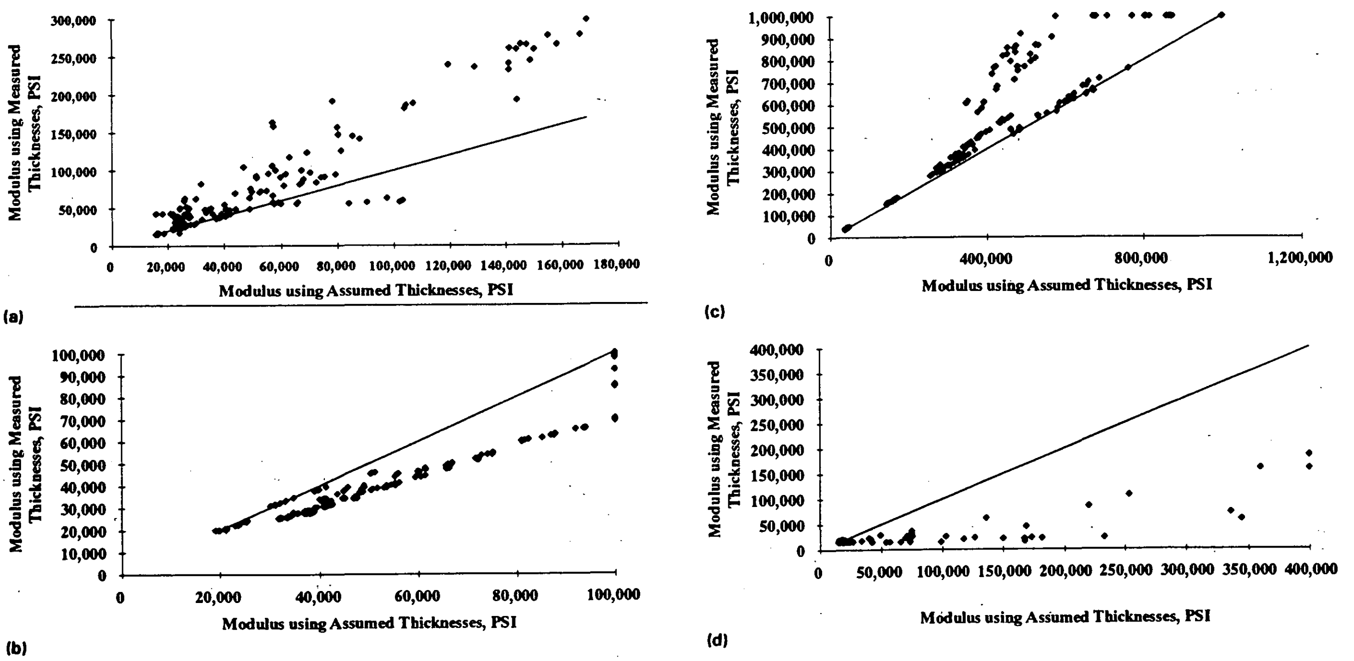


**FIGURE 5 Backcalculated base moduli using assumed versus measured layer thicknesses: (*a*) Section 481109, (*b*) Section 481050, (*c*) Section 481178, and (*d*) Section 483559.**

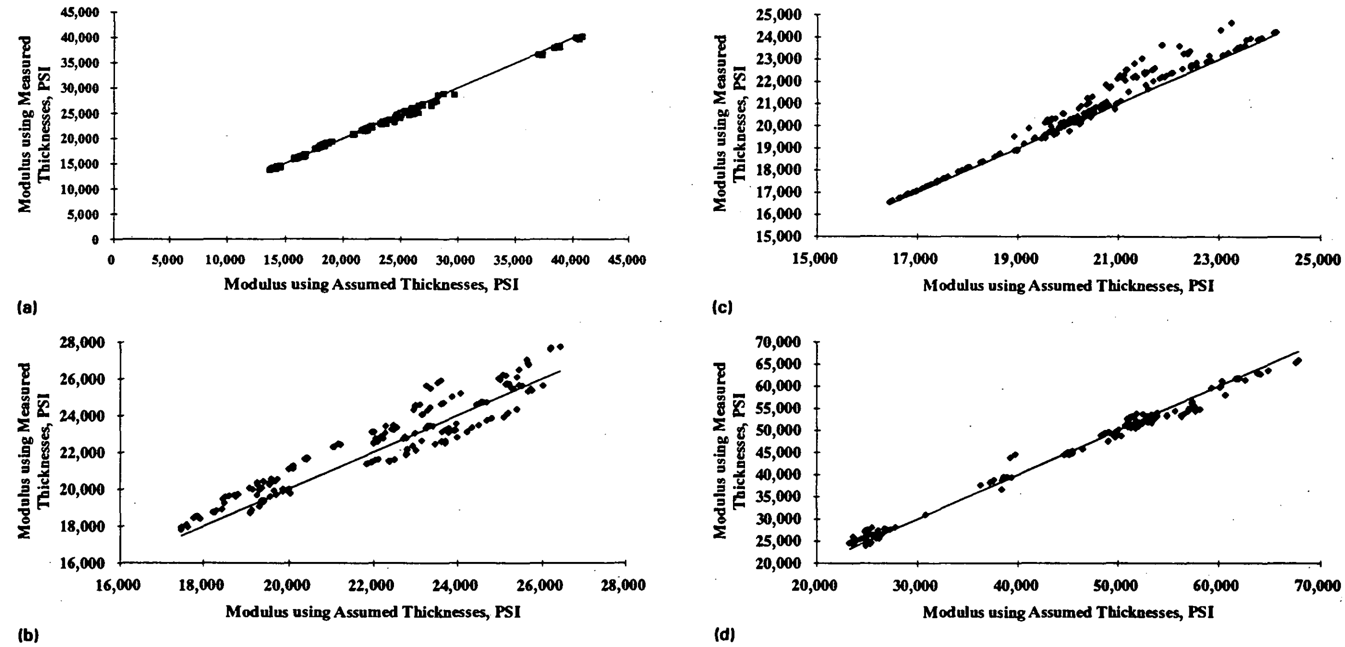


**FIGURE 6 Backcalculated subgrade moduli using assumed versus measured layer thicknesses: (*a*) Section 481109, (*b*) Section 481050, (*c*) Section 481178, and (*d*) Section 483559.**

### Subgrade Modulus

As can be seen in Figure 6, the subgrade modulus value was affected very little by the variation in pavement thicknesses. Tables 17 through 20 show that the differences were less than 2 percent. Because this result was expected before the analysis, and because it is consistent with backcalculation theory, no further discussion is deemed necessary.

## DISCUSSION OF RESULTS

Since at this time no laboratory testing of the materials obtained from the test pits on the sections has been performed by the SHRP contractors, it is difficult to determine the accuracy of the moduli, whether obtained using assumed thicknesses or GPR measured thicknesses. However, it is safe to say that if variations in layer thicknesses exist on SHRP sections, and the results of the GPR survey indicate that they do, and these variations are ignored in the backcalculation process, one can expect erroneous backcalculation results. Regardless of the complexity of the backcalculation scheme, the quality of the deflection data, or the thoroughness and care expended in the process, the magnitude of the errors probably will be along the lines of those found here.

With regard to backcalculation errors, they may not be significant with respect to the overlay design process. In certain cases, there may be compensating effects between layers. A 20 to 30 percent error in the backcalculation process may not have a great effect on overlay requirement, since the "error" is compensated for by thickness, that is, the total stiffness of both systems is essentially the same. The effect of the error is, of course, dependent on the design procedure being used. Any design procedure that uses tensile strain at the bottom of the ACP layer would be sensitive to these errors in the backcalculation process.

## CONCLUSIONS

The results of this study indicate that

1. Variations found in layer thicknesses on SHRP sites in Texas are large enough to cause up to 100 percent error in the backcalculated modulus of the surface layer of the pavement, if not taken into account.
2. These variations also resulted in up to 80 percent error in the base materials.
3. These variations did not appreciably affect the backcalculated modulus of the subgrade.
4. Deflection basins alone cannot be used to identify or quantify changes in pavement layer thicknesses, which are severe enough to adversely affect the accuracy of the backcalculated moduli.
5. If reliable backcalculated moduli values are to be obtained on SHRP sites, or for that matter any pavement section, some method of identifying and quantifying layer thickness variations must be used before the backcalculation process.
6. The success with which a calculated deflection basin is "matched" with a measured basin is not a good indicator of the accuracy of the backcalculated moduli. It is possible to obtain small error terms with inaccurate moduli values.

## REFERENCES

1. P-001 Technical Assistance Staff. *SHRP-LTPP Manual for FWD Testing*. Strategic Highway Research Program, TRB, National Research Council, Washington, D.C., Jan. 1989.
2. P-001 Technical Advisory Staff. *Analysis of Section Homogeneity, Non-Representative Test Pit and Section Data, and Structural Capacity*. Strategic Highway Research Program, TRB, National Research Council, Washington, D.C., Sept. 1990.
3. K. Maser. *Automated Detection of Pavement Layer Thickness and Subsurface Moisture Using Ground Penetrating Radar*. Infrasense Inc., Cambridge, Mass., Nov. 1990.

# Validation of Moduli Backcalculation Procedure Using Multidepth Deflectometers Installed in Various Flexible Pavement Structures

Y. R. KIM, N. P. KHOSLA, S. SATISH, AND T. SCULLION

Falling weight deflectometer (FWD) data collected during June 1990 and May 1991 from test sections along US-421 Bypass near Siler City, North Carolina are presented. The test road consists of 12 types of pavement sections (different materials and thicknesses, but all with asphalt concrete surface course), two of each type in two directions of traffic, for a total of 48 test sections. Twenty-four northbound sections are installed with strain gauges, pressure cells, thermocouples, and moisture sensors. The multidepth deflectometers (MDDs) are installed in eight sections with varying layer materials and thicknesses. FWD testing was performed on some sections with the MDDs, seven sections in June 1990 and four sections in May 1991. FWD loading was applied on top of the MDDs for both of the trips. During the June 1990 trip, the FWD load plate was placed on one or two additional locations with offset distances up to 32 in. At each position, three FWD drops were applied, and the resulting surface deflections and depth deflections were measured simultaneously using FWD geophones and the MDDs, respectively. The MODULUS backcalculation program developed by the Texas Transportation Institute was used to backcalculate the moduli values of each section. Then the backcalculated moduli values were entered into a forward calculation program with known pavement layer thicknesses, assumed Poisson's ratios, and the magnitude and geometry of FWD loading to calculate the surface and depth deflections. The surface and depth deflections were finally used to calculate the average vertical strains of different layers at the centerline of loading. In the validation process, the comparison between the measured and predicted depth deflections was first used to evaluate the influence of different assumptions made before backcalculation. The validity of the backcalculation program based on the multilayered elastic theory was investigated by comparing the measured and predicted pavement responses, such as surface deflections, depth deflections, and average vertical strains within the layers. Finally, the influence of different flexible pavement designs with varying thicknesses and layer material types was studied using the average vertical strains within various layers.

Nondestructive testing has become a powerful tool for determining in situ properties of pavement layers needed for pavement design and rehabilitation. Numerous deflection-based methods have been developed to backcalculate layer moduli for multilayered flexible pavements, mostly dependent on the theory of linear elasticity. These deflection-based backcalculation programs can be divided into two groups. One is the iterative approach, in which a set of moduli that minimizes an error between the measured deflection and calculated deflection from a forward calculation scheme is determined iteratively. The other group uses a data base approach that uses a forward calculation scheme to build a deflection data base from sets of assumed moduli. Then regression equations with interpolation techniques are used to determine a set of moduli that minimizes the error between the measured and calculated surface deflections. Some advantages of the data base approach have been documented (*1,2*).

One of the major concerns of many practicing engineers has been how valid the deflection-based backcalculation programs are in measuring accurate, dependable layer moduli of flexible pavements with not only varying thicknesses and material types, but also with different levels of damage in pavements due to traffic and environmental conditions. One way of checking the validity is to backcalculate the layer moduli from an instrumented pavement section with known layer thicknesses and material types and calculate responses of the same pavement with the forward calculation method used in the backcalculation program. Comparing these calculated pavement responses against the measured values from the instrumented test sections will allow one to evaluate how significantly the assumptions made in the forward calculation scheme and backcalculation approach violate in situ behavior of layer materials.

The purpose of this paper is (a) to evaluate one of the deflection-based backcalculation programs using the multilayered elastic analysis, MODULUS, by comparing actual measurements of surface and depth deflections and average vertical strains with the predicted values from the WES5 forward calculation scheme used in the MODULUS program and (b) to investigate the effect of different flexible pavement designs on the response of various layers under the FWD loading.

## INSTRUMENTED PAVEMENT TEST SECTIONS

A research project, "A Comparative Study of Performance of Different Designs for Flexible Pavements," sponsored by the North Carolina Department of Transportation, is under way at the North Carolina State University. As a part of this

Y. R. Kim, N. P. Khosla, and S. Satish, Department of Civil Engineering, North Carolina State University, Box 7908, Raleigh, N.C. 27695-7908. T. Scullion, Texas Transportation Institute, Texas A&M University, College Station, Tex. 78743.

project, a 7.5-mi-long test road consisting of 48 test sections was constructed along US-421 Bypass near Siler City, North Carolina, in June 1990. In each direction of traffic, 12 types of flexible pavements (Table 1), typical in North Carolina, were constructed with 2 replications. This resulted in 12 pavement designs, 2 replicates, and 2 traffic levels (i.e., 2 traffic directions), for a total of 48 test sections.

All 24 northbound test sections were instrumented with the following in situ gauges: subgrade pressure transducers, subgrade moisture cells, subgrade thermocouples, base course moisture cell (for aggregate base only), base course thermocouple (except for asphalt base), asphalt strain gauges, and asphalt thermocouples. No instrumentation was provided for the southbound roadway, although the performance of these sections would also be monitored.

In selected sections (Sections 1–3, 6–9, and 11), the multidepth deflectometers (MDDs) were installed after completion of the construction. The MDD is an LVDT deflection measuring device that is retrofitted into pavement layers (*3,4*). Under the passage of a single load the MDD can be used to measure the depth deflection profile and the induced average vertical compressive strains. After repeated loads the MDD can be used to measure the permanent deformations in each of the pavement layers. A schematic of a typical MDD after installation is shown in Figure 1. Figure 2 presents the MDD locations in the test sections.

The traffic level (passes and weights) along the highway is monitored using the CMI weigh-in-motion device. Furthermore, the longitudinal profiles of all the sections have been monitored, along with rut depth measurements and periodic surface condition surveys. More detailed information on the test sections can be found elsewhere (*5*).

## TEST PROTOCOL

The data presented in this paper were generated from two trips made in June 1990 and May 1991. A falling weight deflectometer (FWD) was used for both trips. During the trip in June 1990, surface deflections with FWD geophones and depth deflections with the MDDs were measured simultaneously from seven MDD sections (Sections 1, 2, 3, 6, 7, 8, and 9). Since only one lane was open to traffic during the FWD testing, limited time was available for field testing, and therefore testing of only seven MDD sections could be completed.

The testing sequence for the June 1990 trip was as follows. The FWD load plate was placed directly on top of the MDD top cap. An offset distance of approximately 3 in. from the center of the load plate was used to prevent the center geophone from sitting directly on the brass top cap. Three drops of approximately 9,000 lb were applied, and the resulting surface and depth deflections were measured simultaneously.

The tests were repeated at other offset distances (Positions A and B). On Section 1, as an example, Position A has the distance from the center of the load plate to the middle of the MDD hole set at 20 in.; in Position B the distance was 32 in. At both the locations deflection data were collected using three drops of approximately 9,000 lb. When the FWD load plate was not over the MDD hole (Positions A and B), the movement of the anchor was monitored by measuring the movement on the center core of the MDD system. This was achieved by placing one of the FWD surface geophones (the geophone at 60 in.) on top of a pedestal mounted on the center core. Different offset distances were used in each section.

During the May 1991 trip, the limitation in testing time and difficulties with the MDD data acquisition program encountered in some sections prevented conducting FWD tests on all the MDD sections. As a result, deflection data from only five sections (Sections 3, 6, 7, 8, and 9) are presented in this paper. FWD loading was applied on top of the MDDs using the same method as in June 1990, but no offset FWD testing was conducted. During both the trips, MDD deflection measurements were made by a data acquisition program installed in a Compaq 386 portable computer.

**TABLE 1 Section Descriptions**

| Section No. | I-1* | H* | HB* | ABC* | CTB* | Stabilized Subgrade |
|---|---|---|---|---|---|---|
| 1, 23 | 2" | 1.5" | | 12" | | No |
| 2 | 2" | | | 12" | | Cement |
| 24 | 2" | | | 12" | | Lime |
| 3, 16 | 2" | 3" | | 8" | | No |
| 4, 18 | 2" | 1.5" | | | 7.5" | No |
| 5 | 2" | 1.5" | | 8" | | Cement |
| 17 | 2" | 1.5" | | 8" | | Lime |
| 6, 21 | 2" | 3" | | | 5.5" | No |
| 7, 20 | 2" | 1.5" | 5.5" | | | No |
| 8, 19 | 2" | | | | 7.5" | Lime |
| 9, 22 | 2" | 3" | 4" | | | No |
| 10, 15 | 2" | 1.5" | | | 5.5" | Lime |
| 11, 14 | 2" | | 5.5" | | | Lime |
| 12, 13 | 2" | 1.5" | 4" | | | Lime |

Note: *I-1 = Asphalt surface course
H = Asphalt binder course
HB = Asphalt-stabilized base course
ABC = Granular base course
CTB = Cement-treated base course

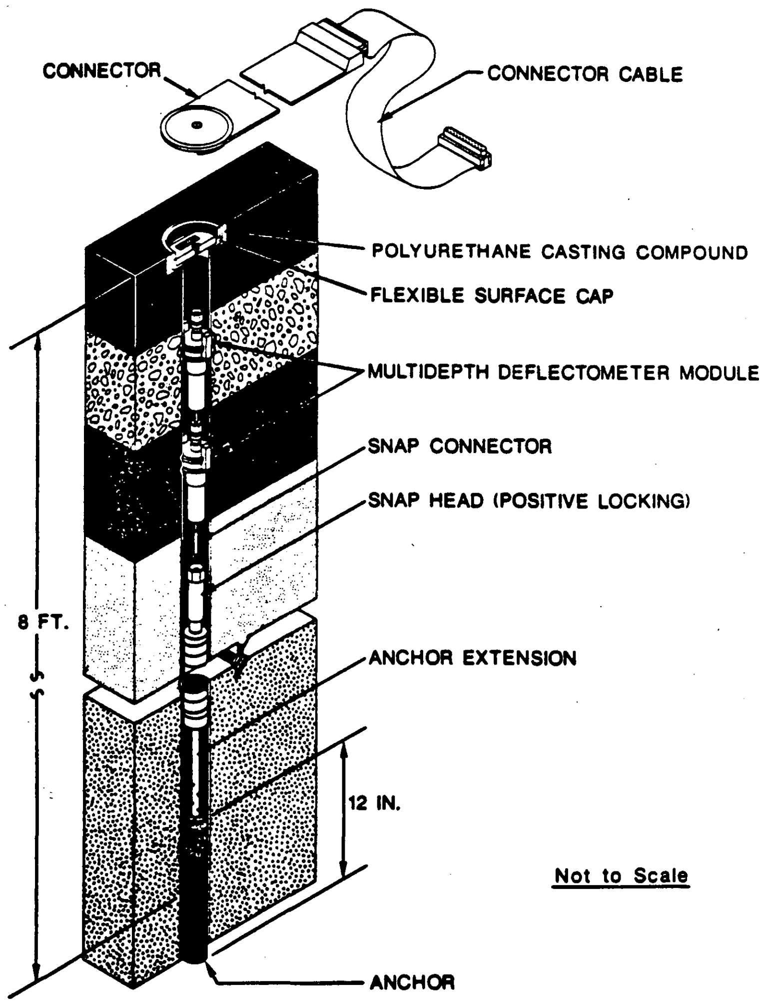


**FIGURE 1 Typical cross section of MDD after installation (*4*).**

## ANALYSIS AND DISCUSSION

### Moduli Backcalculation

Typical MDD signal and normalized surface and depth deflections in Section 1 are presented as an example in Figures 3(a) and 3(b), respectively. In Figure 3(a), the traces are smooth for each of the MDDs. Duration of the pulse is approximately 30 msec. Figure 3(b) contains extremely valuable information for validating backcalculation schemes based on surface deflections. The surface deflection is represented by the solid line, and the other symbols represent depth deflections measured by the various MDDs. The "+" symbols at the bottom of the graph are the measured anchor movements.

The surface deflection data were entered into the MODULUS backcalculation program, Version 4.0, to calculate the layer moduli for all seven sections. The "best" sets of backcalculated moduli of seven sections for the June 1990 and May 1991 trips are presented in Table 2. In processing the FWD surface deflection data to determine the moduli values in Table 2, the following assumptions were made:

1. The moduli of all thin surfacing less than 4 in. thick were fixed constant. These moduli were determined by the MODULUS program on the basis of the type of coarse aggregate used in the surface course and the asphalt concrete temperature at the time of FWD testing. For the June 1990 trip, the asphalt concrete temperature was calculated from the air temperature. For the May 1991 trip, it was measured from the thermocouple at a 1-in. depth from the surface.
2. For the sections with the asphalt concrete base, both the surface and base were counted as a single layer.
3. Depths to bedrock were left to be calculated by the MODULUS program for all the sections.
4. The stabilized subgrade was assumed to be 7 in. thick.

Assumptions 1 and 2 were made on the basis of knowledge from the literatures and the authors' experience with the backcalculation technique. Although actual depths to bedrock were measured during the construction of the test sections, it was determined not to use these values because the drilling locations in the sections could have been different from where the MDDs were installed. The validation of these assumptions is discussed later in this paper.

The following observations were made from Table 2:

1. The calculated asphalt concrete moduli values for the given temperatures seemed reasonable except for Section 8

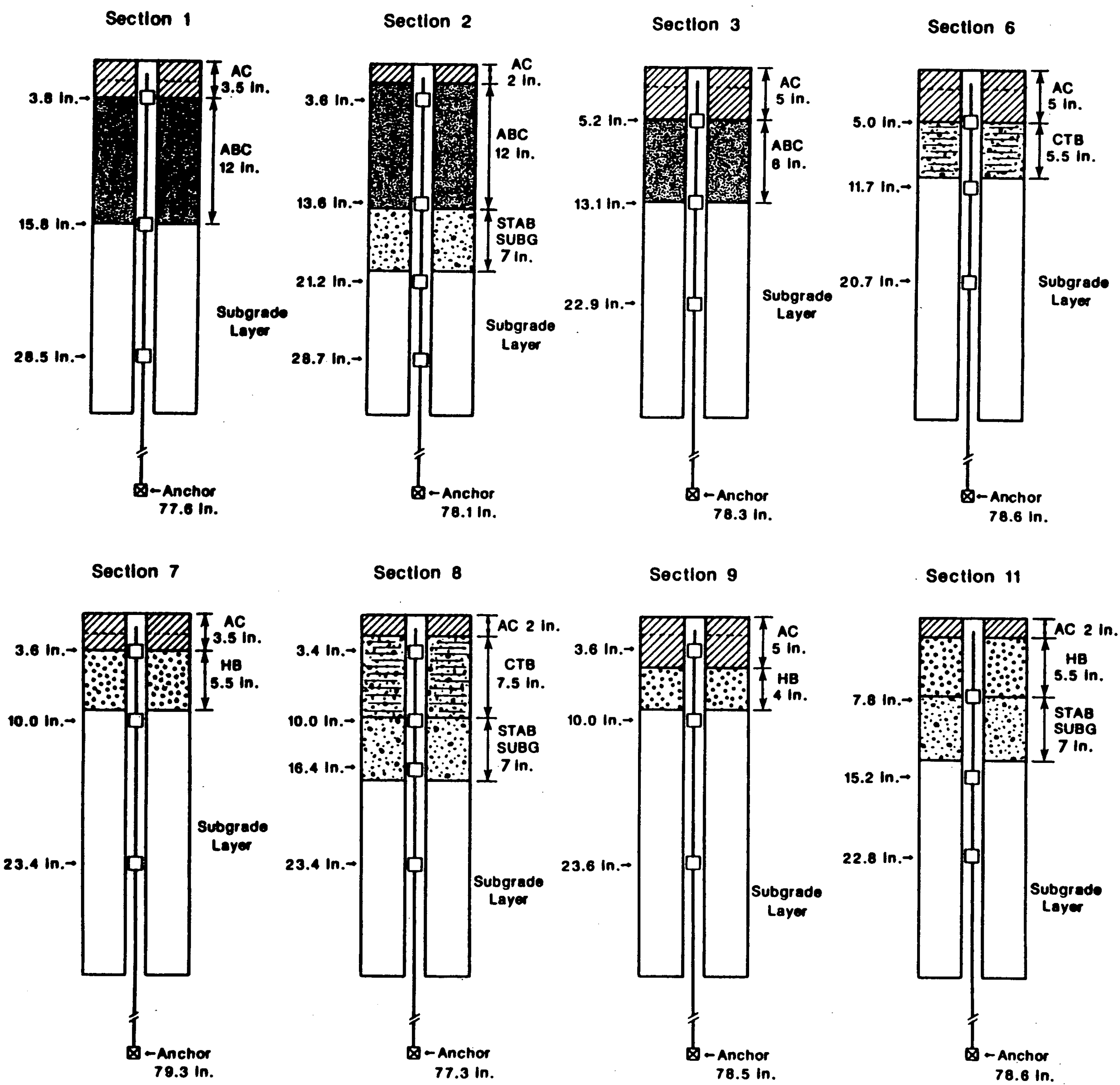


**FIGURE 2 MDD locations (AC = asphalt concrete, ABC = aggregate base course, CTB = cement-treated base, and STAB SUBG = stabilized subgrade).**

in May 1991. The AC surface modulus value of Section 8 was calculated from the MODULUS program on the basis of temperature and coarse aggregate type.

2. For both trips, the granular base over the stabilized subgrade in Section 2 had a much higher modulus than the granular base over the soft subgrade in Sections 1 and 3, demonstrating the effect of confinement and support on granular layer modulus.

3. The modulus of the cement-treated base (CTB) in Section 6 was much higher than that of the CTB in Section 8 for both trips. This could be explained by the appearance of random longitudinal and transverse cracks on the surface a short time after the construction of Section 8, perhaps indicating that the CTB was cracked, resulting in a lower effective modulus.

4. The subgrade moduli values for Sections 1, 3, 7, and 9 were very low (3 to 7 ksi) for both trips, indicating that the subgrade on these sections was saturated. The subgrade moduli values on the sections with the stabilized subgrade (Sections 2 and 8) were unreasonably high. Perhaps this was due to the low stress state in these layers, but most likely it was due to the limitation of the multilayered elastic theory used in the backcalculation procedure.

5. The analysis of data from both trips revealed that the cement-stabilized subgrade in Section 2 was much stiffer than the lime-stabilized subgrade in Section 8. This is generally

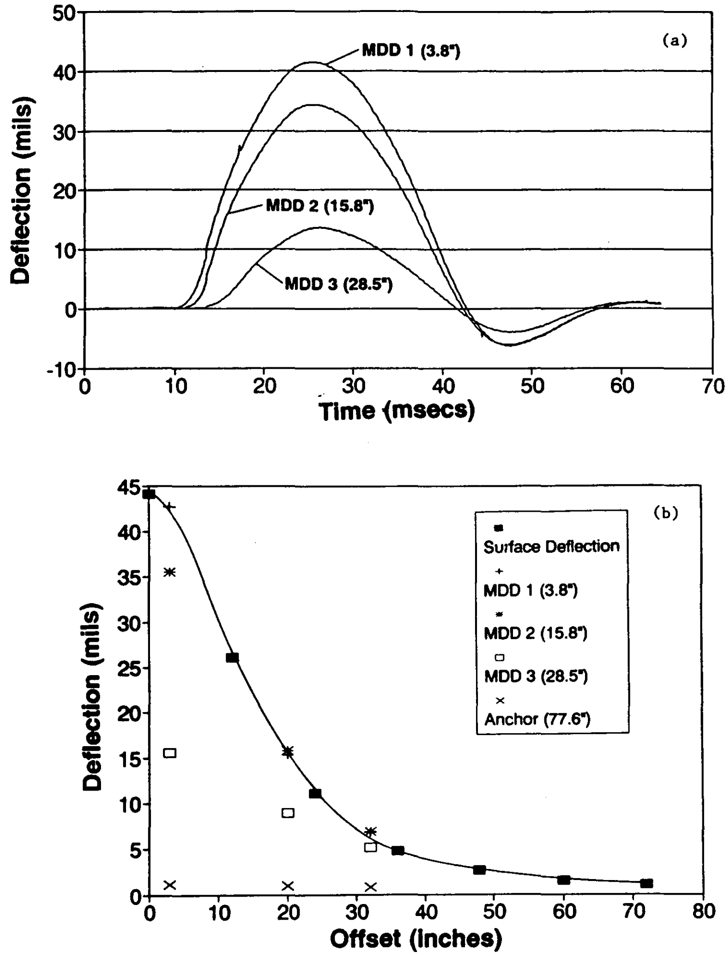


**FIGURE 3** (*a*) **Raw MDD data under FWD loading on Section 1;** (*b*) **normalized surface and depth deflections from Section 1.**

expected because the strength gain due to lime stabilization is mainly dependent on pozzolanic reaction, whereas cement stabilization provides additional important cementitious reaction forming hydrates of calcium silicate.

6. In most cases, calculated depths to bedrock from the MODULUS program were smaller than the actual depths to bedrock measured during the construction of the project, although this comparison might not be fair due to different locations in drilling and FWD testing.

Unreasonably high moduli values of the aggregate base course and subgrade over or under the stabilized subgrade reported in Observations 2 and 4 indicate the limitation of the multilayered elastic theory. It must be recognized by practicing engineers that the deflection-based moduli backcalculation schemes built on the multilayered elastic theory measure the effective modulus, not the modulus as the material property.

## Validation by Comparing Surface and Depth Deflections

The traditional approach to backcalculating layer strength relies solely on the surface deflection. Various schemes are available for performing the backcalculation, but little effort has been expended in validating the numbers calculated in such schemes.

One way of validating backcalculation schemes is using the MDD depth deflections. Once the modulus of each layer has been determined, deflections at different depths can be calculated from the WES5 forward calculation program using the thicknesses of layers, assumed Poisson's ratios used in the backcalculation, the backcalculated layer moduli values, and the magnitude and geometry of FWD loading. The discrepancy between the measured depth deflections and the predicted depth deflections can be used as an estimate of how valid the backcalculated moduli are for various design types.

This validation process has been applied to the backcalculated moduli values in Table 2 and resulted in Figures 4 through 10. The following observations can be made from these figures:

1. Stabilized layers in Sections 2, 6, and 8 lowered the surface and depth deflections considerably.
2. Except for Section 8 in May 1991, surface deflections were predicted very accurately for both trips, as shown in Figures 4a through 10a. The larger discrepancy of Section 8 from the May 1991 trip might be due to the poor condition

**TABLE 2 Layer Moduli Backcalculated Using FWD Data Collected on Each Section**

(a) June 1990

| Section | Moduli in ksi | | | | Calculated | Actual | Temp.[b] |
|---|---|---|---|---|---|---|---|
| | Surface | Base | Stabilized Subgrade | Subgrade | DB[a] (ft) | DB[a] (ft) | (°F) |
| 1 | 201[c] | 12.4 | ... | 4.7 | 5.4 | > 20 | 107 |
| 2 | 201[c] | 80.8 | 404.9 | 40.5 | 18.1 | 18 | 107 |
| 3 | 115 | 10.0 | ... | 4.1 | 3.4 | 15 | 107 |
| 6 | 183 | 1709.6 | ... | 10.1 | 7.3 | N/M[d] | 107 |
| 7 | 102[e] | ... | ... | 3.1 | 3.4 | > 15 | 107 |
| 8 | 201[c] | 307.4 | 170.3 | 30.7 | 7.9 | > 20 | 107 |
| 9 | 101[e] | ... | ... | 3.3 | 4.3 | 16 | 107 |

(b) May 1991

| Section | Moduli in ksi | | | | Calculated | Actual | Temp.[f] |
|---|---|---|---|---|---|---|---|
| | Surface | Base | Stabilized Subgrade | Subgrade | DB[a] (ft) | DB[a] (ft) | (°F) |
| 1 | 314[c] | 12.0 | ... | 4.4 | 4.9 | > 20 | 93 |
| 2 | 168[c] | 51.5 | 215.1 | 21.5 | 7.3 | 18 | 114 |
| 3 | 125 | 5.6 | ... | 4.7 | 3.2 | 15 | 100 |
| 6 | 223 | 1133.9 | ... | 12.3 | 13.9 | N/M[d] | 108 |
| 7 | 235[e] | ... | ... | 5.6 | 6.1 | > 15 | 82 |
| 8 | 508[c] | 184.5 | 67.5 | 18.3 | 7.9 | > 20 | 80 |
| 9 | 352[e] | ... | ... | 6.6 | 9.8 | 16 | 83 |

Note: [a]Depth to bedrock.
[b]Temperature assumed.
[c]Fixed modulus based on the temperature.
[d]Not measured.
[e]Calculated value for AC surface and AC base layer combined.
[f]Temperature measured from the thermocouple at 1 inch depth from the surface.

of Section 8 described earlier. The pavement condition survey conducted in July 1991 revealed severe rutting and fatigue cracking in Section 8.

3. The maximum surface deflections of full-depth asphalt concrete pavements in Sections 7 and 9 were much lower in May 1991 than in June 1990. This could be mainly due to lower testing temperatures in May 1991 as indicated in Table 2.

4. The surface deflection of Section 8 increased significantly in May 1991, indicating severe deterioration of the section.

5. For the June 1990 trip, the measured deflections at the interfaces of different layers were larger than the predicted deflections, as shown in Figures 4b through 10b, 4c through 10c, and 5d through 9d. The trend was somewhat reversed for the May 1991 data in Figures 6b through 10b and 6c through 10c.

6. However, the deflections within the subgrade for the June 1990 trip were predicted accurately except in Sections 7 and 9 (Figures 8 and 10) of full-depth asphalt concrete pavements.

7. The accuracy of deflection prediction became much worse in the May 1991 data, especially for the subgrade.

Whether the discrepancy between the measured and predicted depth deflections is acceptable depends on how and where the backcalculated moduli are to be used. If a pavement engineer were to measure relative stiffnesses of different layers in pavements, deflection-based backcalculation schemes based on the multilayered elastic analysis could be sufficiently accurate. However, the comparison between the measured and predicted depth deflections made earlier indicates that great caution has to be used should the purpose of the backcalculation be more detailed analysis of pavement responses in different layers.

### Validation by Comparing Strains

Since the interface deflection is the sum of deformations in all the layers below that interface, it is difficult to study which layer is more responsible for the discrepancy between the measured and predicted values. This can be better accomplished by using either the deformation or the strain in each layer. Once the surface and depth deflections are measured, one can calculate the deformation within each layer by subtracting the LVDT reading at the bottom of the layer from that at the top of the layer. The average vertical strain can then be determined by dividing the deformation within the layer by the distance between two LVDTs.

The calculated average vertical strains due to the FWD loading right on top of the MDDs in June 1990 and May 1991 are plotted in Figures 11 through 13. In these figures, compressive strains are presented on the positive axis. Large errors between the measured and predicted strains within different layers were noticeable. In general, it was difficult to conclude from these figures which layer the strain values were predicted more accurately for.

In Figure 11, the average vertical AC layer strains calculated from the measured depth deflections increased considerably in 1991, which might indicate the lower structural bearing capacities of these layers due to the accumulation of damage between June 1990 and May 1991. There was a unique trend in the 1991 data of the strains calculated from the measured deflections being higher than the predicted average vertical strains. Also, the accuracy in predicting the average vertical strains became poorer in 1991, which could demonstrate the limitations of the multilayered elastic theory.

Figure 12 shows the average vertical strains within the base layers. In Sections 6 and 8 with the cement-treated bases, the average vertical strains calculated from the measured deflections were much smaller than those in other sections. Comparison of the strains in 1990 and 1991 indicated that there was almost no change in the magnitudes of the strains calculated from the measured deflections. The most important finding from Figure 12 was the larger discrepancies between the strains from the measured and the predicted depth deflections in Sections 1 and 3 with the aggregate base courses. This may be because unbound aggregate materials dilate when they are subjected to compressive loading. The dilatation of aggregate materials causes higher confining pressure around them that eventually yields lower strain values in the layer than the predicted ones from the multilayered elastic theory.

The subgrade strains in Figure 13 seemed to have a unique trend of the measured strains calculated from the deflections being larger than the predicted strains for all the cases. This indicates that pavement design or rehabilitation methods based on the multilayered elastic analysis underestimate the compressive strain within the subgrade, which is an important parameter in the prediction of rutting.

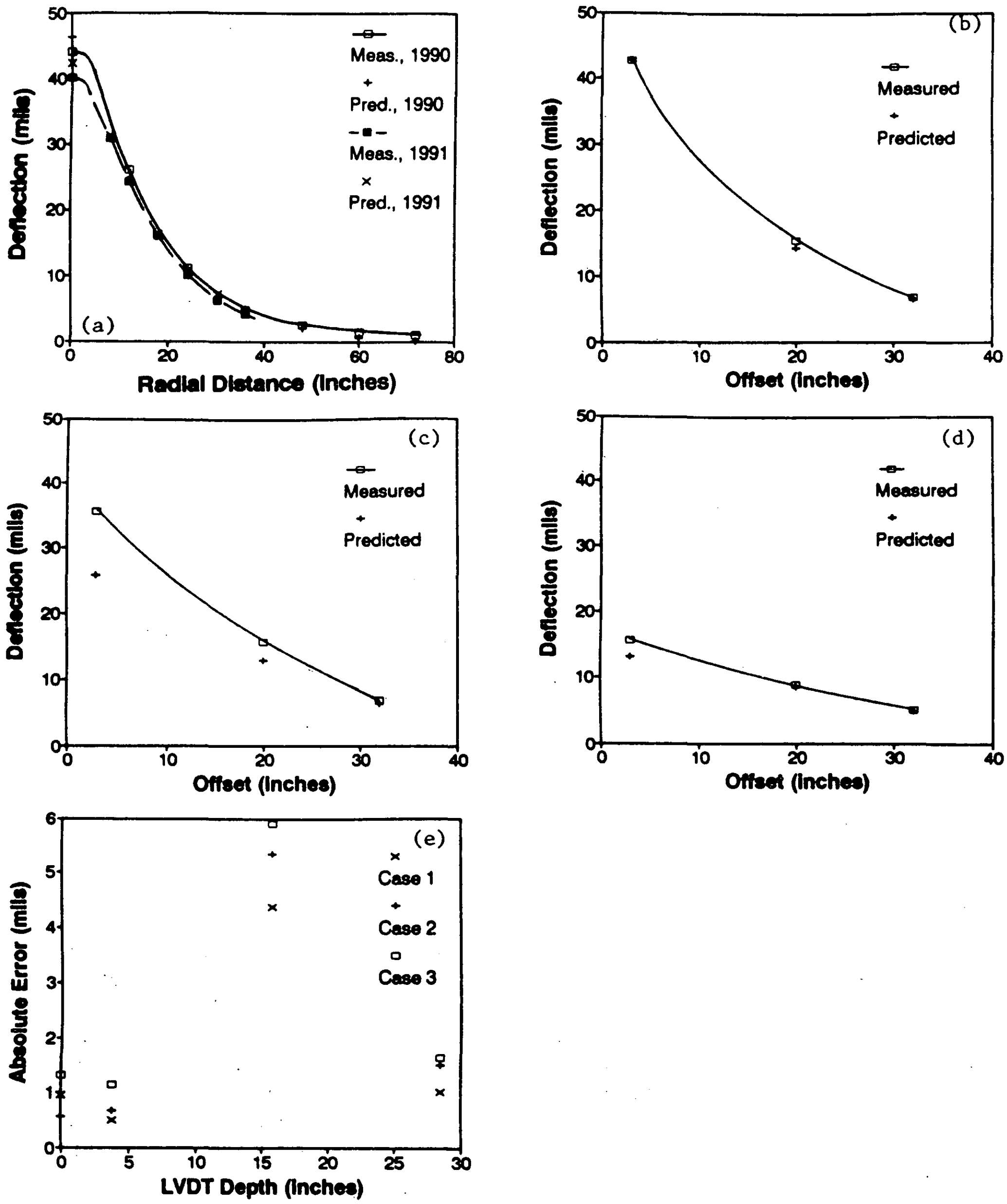


**FIGURE 4 June 1990 and May 1991 results of Section 1: (*a*) surface deflection, (*b*) deflection at top of the base, (*c*) deflection at top of the subgrade, (*d*) deflection 13 in. into the subgrade, and (*e*) absolute errors from different assumptions (June 1990).**

The same conclusion on the subgrade strain prediction can be drawn from Figure 14 with the offset loading conditions. In the asphalt concrete layers [Figure 14(a)], large vertical tensile strains were developed in most sections except Sections 6 and 9. The average vertical strains calculated from the measured deflections indicated that all the layers in Section 8 were in a tensile mode except the subgrade. This different response of Section 8 could be explained again by the early damage in this section. That is, the stress-strain behavior of the layers in Section 8 could be difficult to predict from the forward calculation program based on the multilayered elastic analysis.

### Validation of Assumptions 1 through 3

There are various backcalculation schemes available today with different deflection-matching algorithms. The differences among these algorithms result in different moduli values for the same deflection data. A more discouraging fact to inexperienced pavement engineers is that, even with the same backcalculation program, one can get very different results from the same deflection basin. Some of the basic reasons why backcalculation programs fail to give reasonable values are summarized by Chou et al. (*6*) as follows:

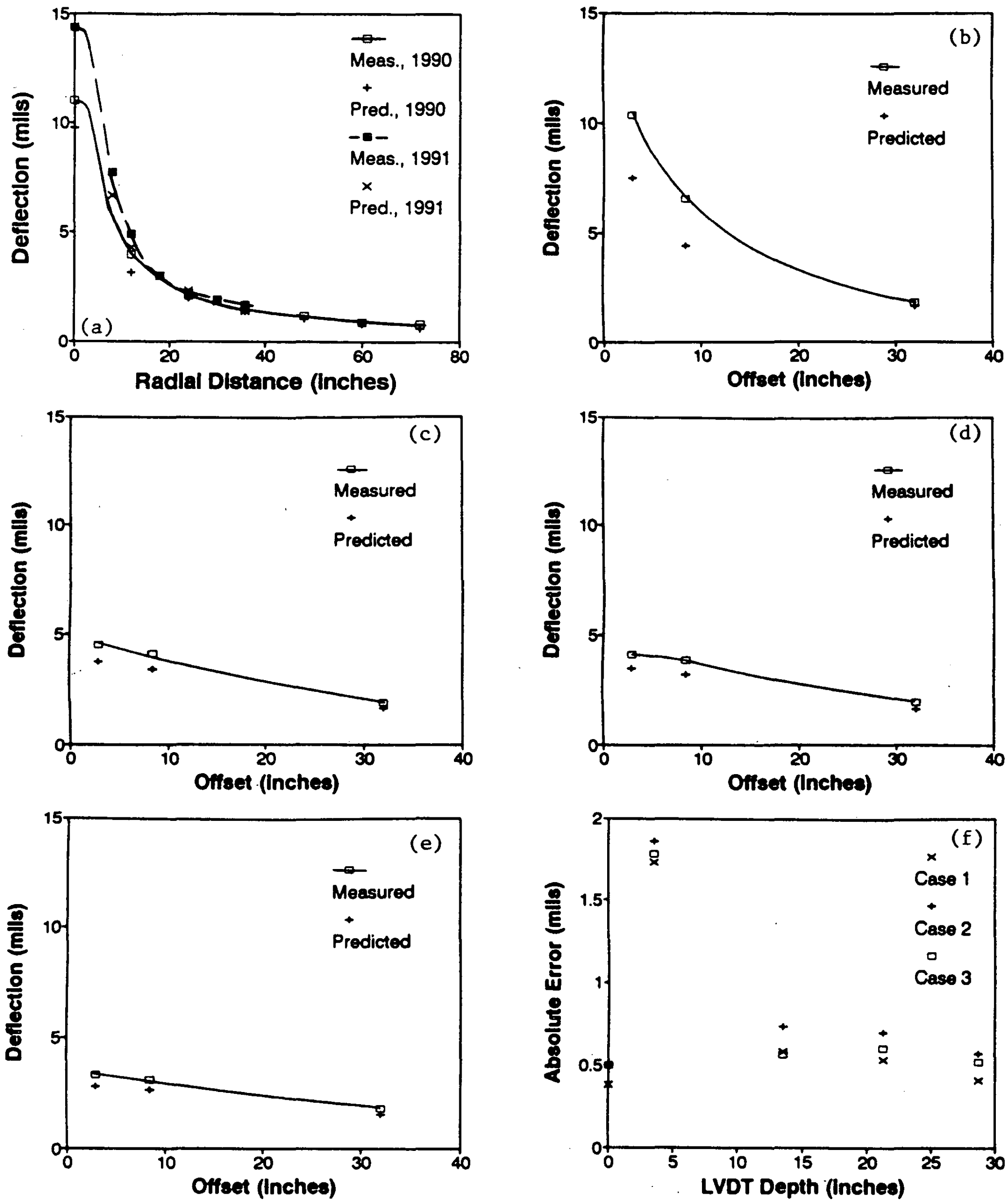


**FIGURE 5 June 1990 and May 1991 results of Section 2: (*a*) surface deflection, (*b*) deflection at top of the base, (*c*) deflection at top of the stabilized subgrade, (*d*) deflection at top of the subgrade, (*e*) deflection 7.7 in. into the subgrade, and (*f*) absolute errors from different assumptions (June 1990).**

1. Pavement materials consist of a very large range of possible properties that may not always comply well with the linear elastic, homogeneous, and isotropic assumptions used in elasticity theory.
2. The accuracy of backcalculated moduli values is dependent on the accuracy of input parameters, such as the thickness of each layer, Poisson's ratio of layer materials, and the depth of subgrade to bedrock. Loading condition and how well sensors are resting on the pavement also affect the accuracy of moduli values.

In spite of difficulties from these nonideal conditions, a few analysts with specialized or private knowledge often can produce more reasonable results. This knowledge may be related to the experience of a particular pavement section or may exist in research reports, textbooks, general experience, common sense, and engineering rules of thumb (*6*). The assumptions made earlier for the sections studied in this paper are based on this type of knowledge.

Since the depth deflections measured by MDDs could be used in evaluating the accuracy of the backcalculation technique, the influence of making different assumptions with the MODULUS program could be investigated. The same deflection basins used to generate moduli values in Table 2 were input to the MODULUS program with different combinations of Assumptions 1, 2, and 3. The moduli values were back-

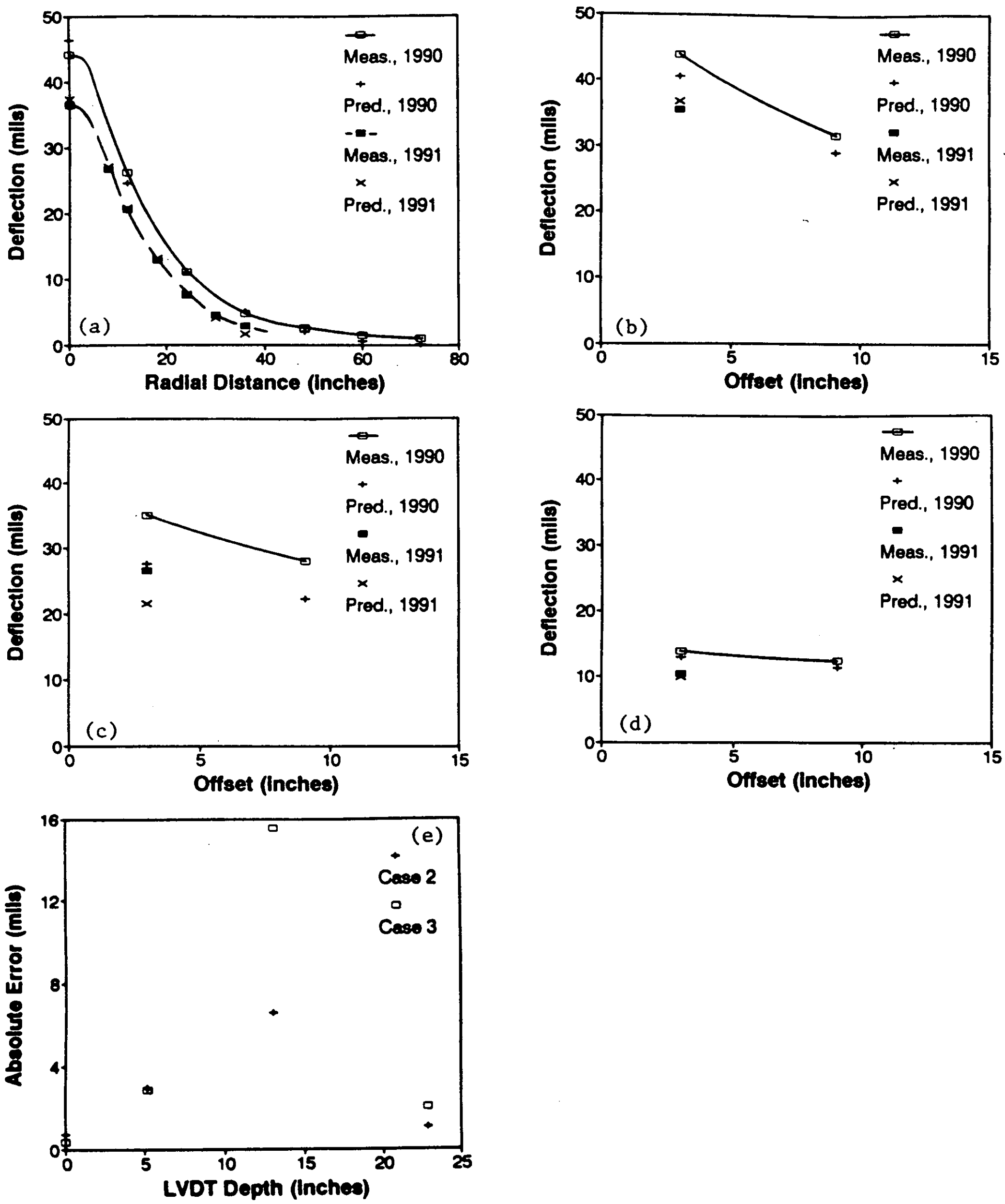


**FIGURE 6 June 1990 and May 1991 results of Section 3: (*a*) surface deflection, (*b*) deflection at top of the base, (*c*) deflection at top of the subgrade, (*d*) deflection 9.9 in. into the subgrade, and (*e*) absolute errors from different assumptions (June 1990).**

calculated from the surface deflections with different assumptions, and depth deflections were calculated from the WES5 forward calculation program. The absolute errors for different cases were calculated and plotted against the depth of LVDT in the last subfigures of Figures 4 through 10. Five cases were studied with the following conditions:

1. The surface modulus of thin surfacing was fixed. Other conditions were the same as in Case 2.
2. The surface modulus of thin surfacing was not fixed. The depth to bedrock was left to be calculated by the MODULUS program.
3. The measured depth to bedrock was input to the MODULUS program. Other conditions were the same as in Case 2.
4. Top 24 in. of subgrade was considered as a separate layer. Other conditions were the same as in Case 2.
5. Asphalt concrete base layer was separated from the surface and binder courses in Sections 7 and 9. Other conditions were the same as in Case 2.

The first assumption, fixing the modulus for thin surfacing, was applicable to Sections 1, 2, and 8. As could be seen by comparing Cases 1 and 2 of these sections in Figures 4, 5, and

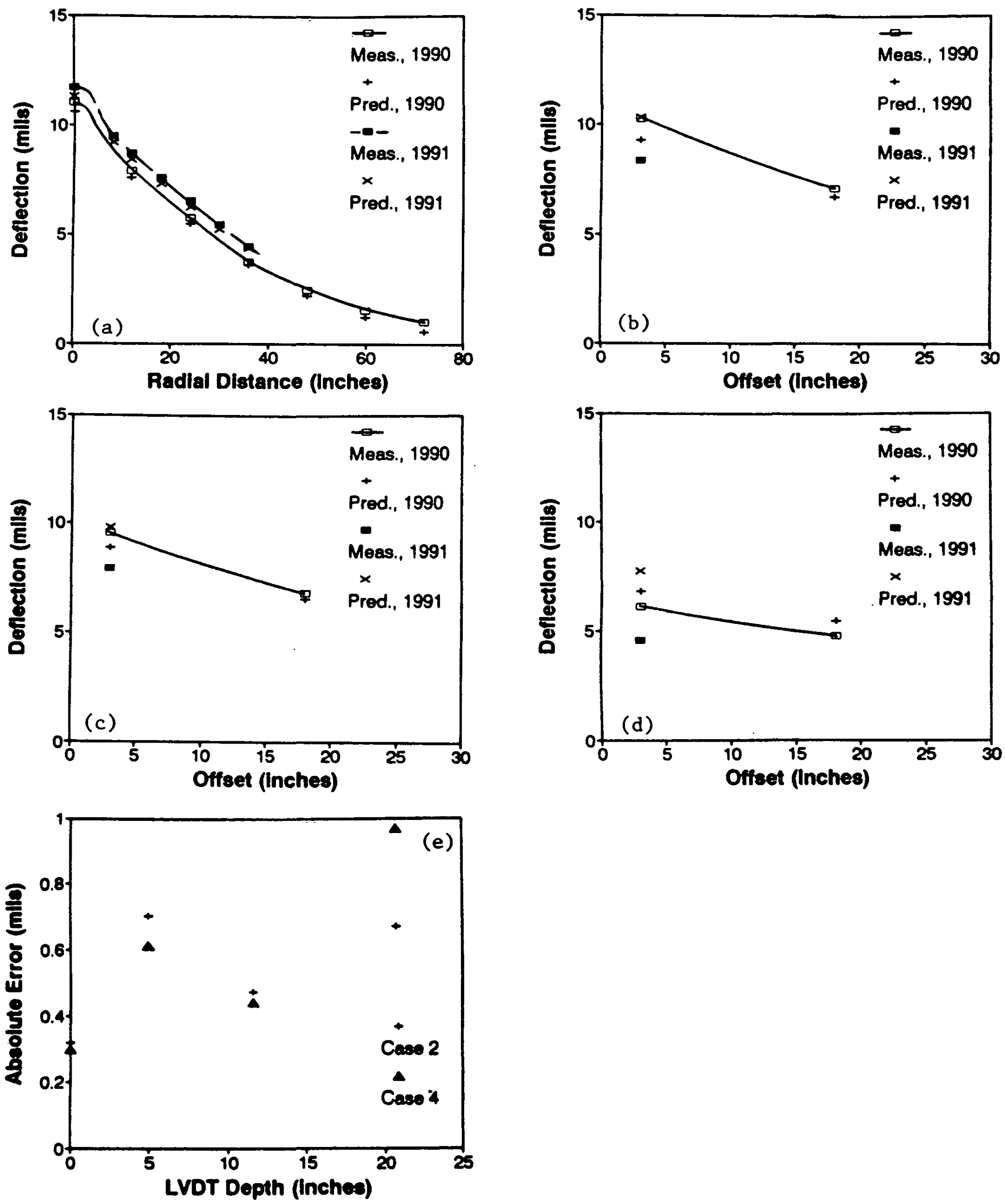


**FIGURE 7 June 1990 and May 1991 results of Section 6: (*a*) surface deflection, (*b*) deflection at top of the cement-treated base, (*c*) deflection at top of the subgrade, (*d*) deflection 10.2 in. into the subgrade, and (*e*) absolute errors from different assumptions (June 1990).**

9, the absolute errors were smaller when the surface modulus was fixed. In Figures 8 and 10 for Sections 7 and 9, respectively, combining the asphalt concrete base layer with asphalt concrete surface course (Case 2) also resulted in better prediction than splitting these layers (Case 5). The effect of forcing the measured depth to bedrock in the MODULUS program, Case 3, produced larger errors in predicting depth deflections than in Case 2 (Figures 4 through 6 and 8 through 10). Also, the consideration of the top 24 in. of subgrade as a separate layer (Case 4) increased the absolute error, as shown in Figures 7, 8, and 10. These observations verified the validity of the assumptions made in backcalculating the moduli values in Table 2.

## Effect of Various Designs on Average Layer Vertical Strains

All the test sections were designed such that a comparative study of the performance of various flexible pavement designs could be conducted. The data obtained from the instrumented gauges under the FWD loading and the standard vehicle loading, pavement condition survey, and the weigh-in-motion will produce invaluable information for the pavement design and rehabilitation. In this section, the average vertical strains of multilayers in Figures 11 through 13 were used in evaluating the effect of different designs (i.e., varying thicknesses and material types) on the pavement response.

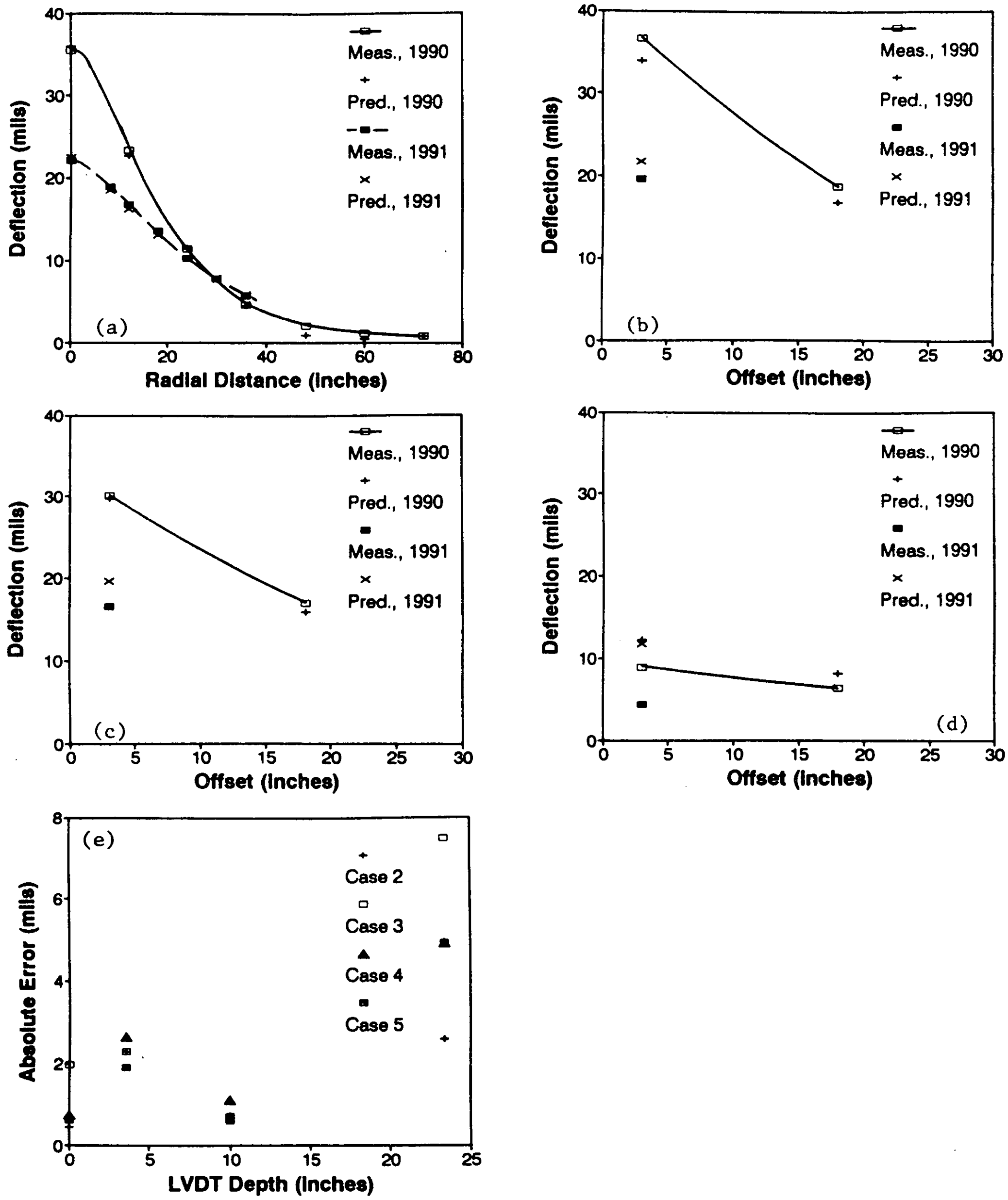


**FIGURE 8 June 1990 and May 1991 results of Section 7: (*a*) surface deflection, (*b*) deflection at top of the asphalt concrete base, (*c*) deflection at top of the subgrade, (*d*) deflection 14.4 in. into the subgrade, and (*e*) absolute errors from different assumptions (June 1990).**

The first noteworthy observation made from Figures 11 through 13 was the beneficial effect of stabilized layers in Sections 2, 6, and 8. In Figure 13, the average vertical strain values in the subgrade of Sections 2, 6, and 8 were much lower than those of other sections due to the stiffening effect of stabilization. The comparison of the subgrade strains in Sections 1 and 2 yielded more detailed information on the beneficial effect of subgrade stabilization. Section 1 has 3.5-in.-thick AC surfacing with no stabilization, and in Section 2, the surface course is only 2 in. thick but the top 7 in. of the subgrade is stabilized with the cement. Although the average vertical strains in the aggregate base layer were almost the same for both the sections in Figure 12, the strains in the asphalt concrete and in the subgrade were reduced considerably in Section 2, which is an important factor in minimizing rutting in pavements.

The same type of comparison could be made with Sections 6 and 8. Section 6 has 5-in.-thick AC surfacing with no subgrade stabilization, and Section 8 has only 2-in.-thick AC surfacing but with the lime-stabilized subgrade. Although the beneficial effect of the stabilized subgrade could not be fully recognized because of the cement-treated base layers in both sections, still the average vertical strains in the base layer and subgrade of Section 8 with the stabilized subgrade were smaller than those in Section 6 without subgrade stabilization.

The influence of base stabilization could also be studied by comparing the strains of Sections 2 and 8. Sections 2 and 8 have identical designs except for the material type and thick-

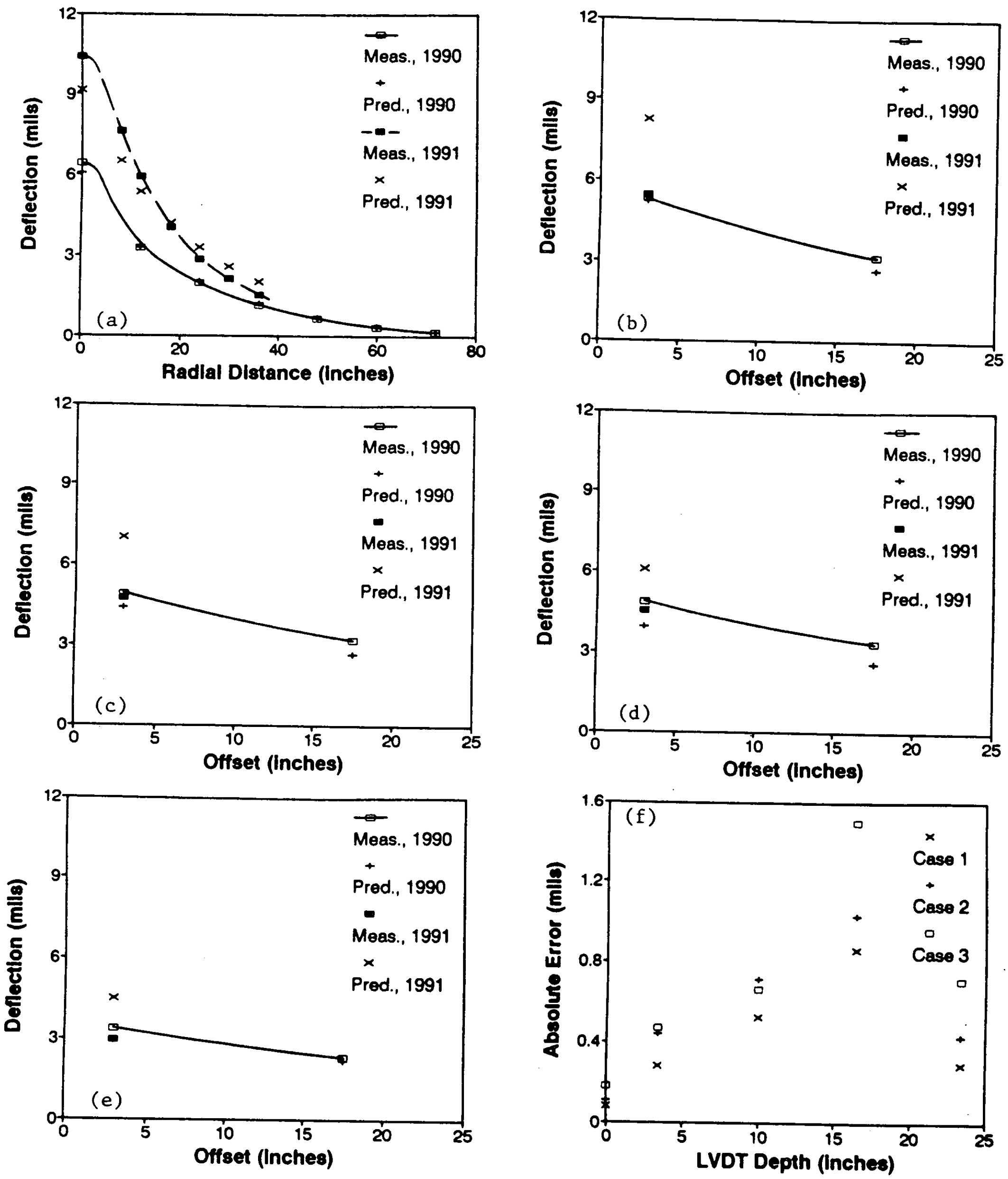


**FIGURE 9 June 1990 and May 1991 results of Section 8: (*a*) surface deflection, (*b*) deflection at top of the cement-treated base, (*c*) deflection at top of the stabilized subgrade, (*d*) deflection at top of the subgrade, (*e*) deflection 6.9 in. into the subgrade, and (*f*) absolute errors from different assumptions (June 1990).**

ness of the base layer. The results in Figures 11 and 13 show that the strains in the AC layer and in the subgrade were lower in Section 2. Furthermore, some block cracking observed in the sections with the cement-treated base courses after the construction makes the researchers question the benefits of the cement-treated base course.

The comparison of Sections 1 and 3 in Figures 11 through 13 can also give an interesting finding. In Section 1, the thicknesses of the surfacing and the aggregate base layer are 3.5 and 12 in., respectively, whereas Section 3 has 5-in.-thick AC surfacing and 8-in.-thick aggregate base course. As a result, the average vertical strain in the AC surfacing was much lower in Section 3 with a thicker AC layer, but the vertical strains in the aggregate base layer and in the subgrade were lower in Section 1. Therefore, a 1.5-in. increase in the AC layer thickness with a 4-in. reduction of the base layer thickness increased the average vertical strains in the base layer and in the subgrade.

The effect of replacing 12-in.-thick aggregate base course with 5.5-in.-thick asphalt concrete base course was investigated by comparing the vertical strains of Sections 1 and 7 in Figure 13. The average vertical strains in the subgrade were almost the same for both sections. This observation indicates that, as far as the vertical compressive strain in the subgrade is concerned, the structural capacity of 5.5-in.-thick asphalt concrete base is almost the same as that of 12-in.-thick unbound aggregate base course.

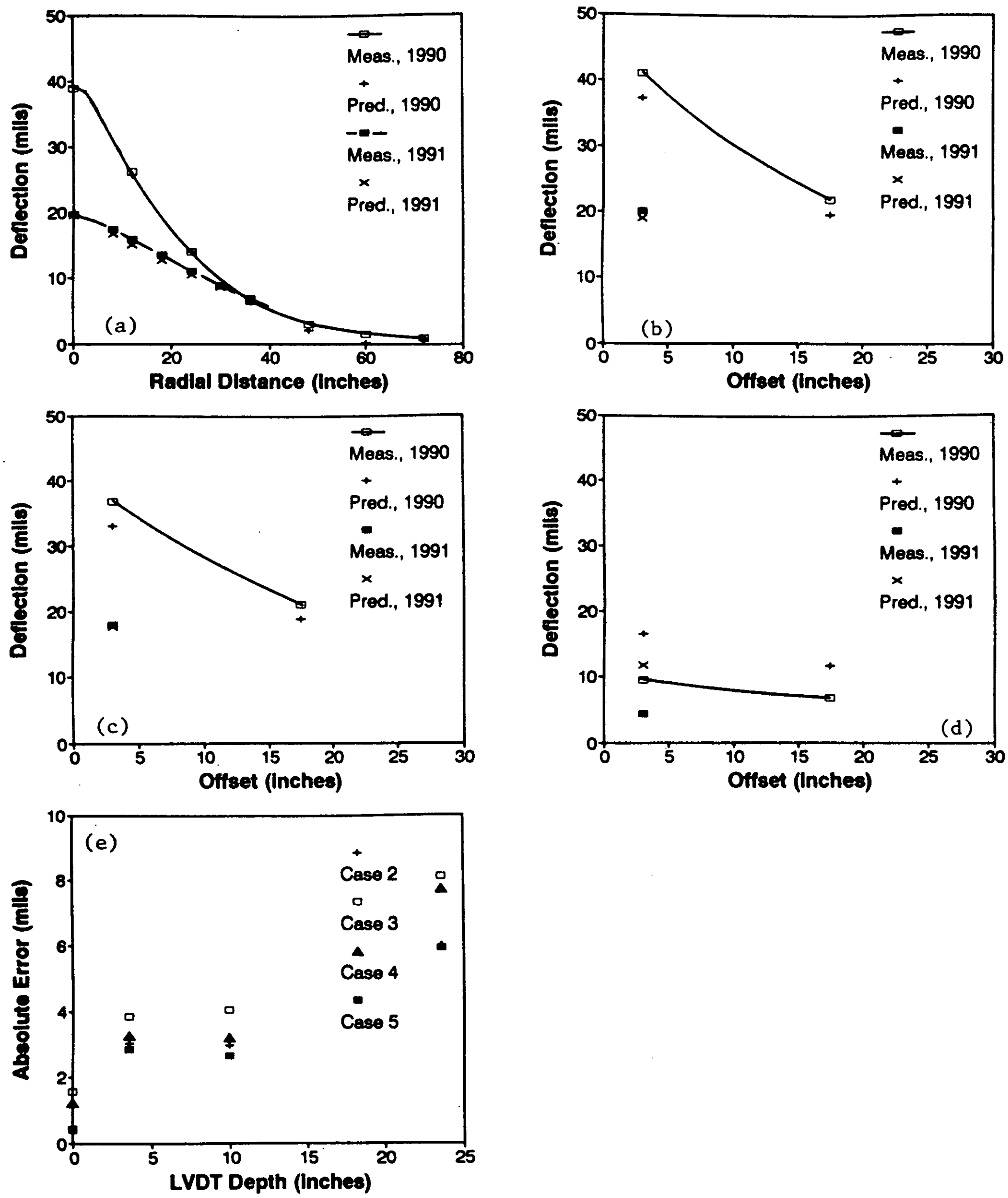


**FIGURE 10** **June 1990 and May 1991 results of Section 9: (*a*) surface deflection, (*b*) deflection at top of the asphalt concrete binder course, (*c*) deflection at top of the subgrade, (*d*) deflection 14.6 in. into the subgrade, and (*e*) absolute errors from different assumptions (June 1990).**

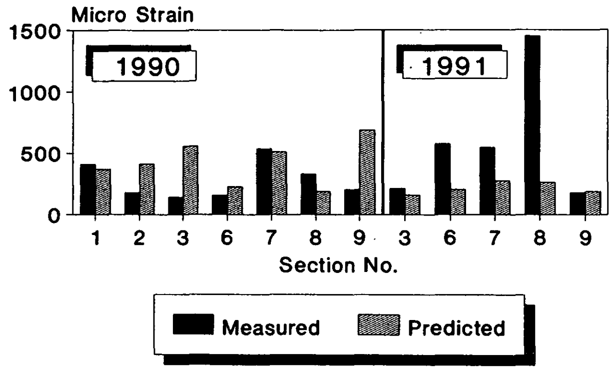


**FIGURE 11 Average vertical strains within the asphalt concrete surface layers.**

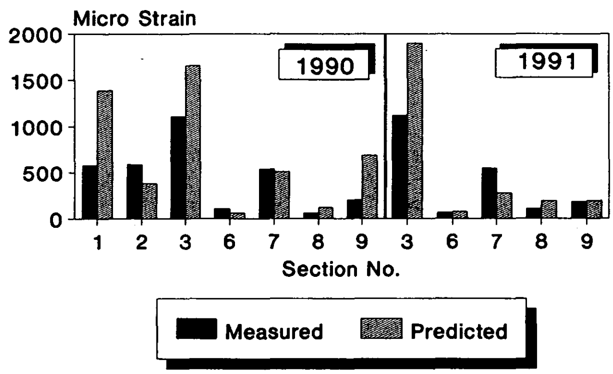


**FIGURE 12 Average vertical strains within the base layers.**

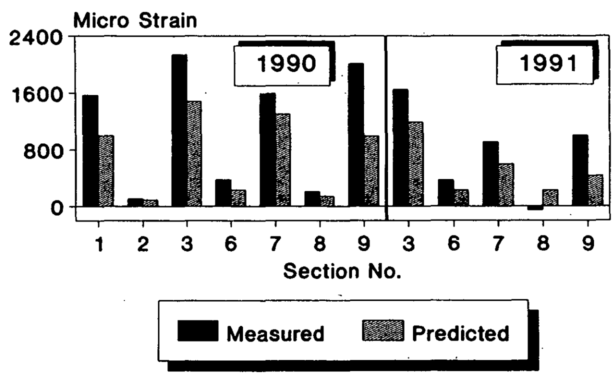


**FIGURE 13 Average vertical strains within the subgrades.**

The vertical strain values from Sections 3, 6, and 9 could be compared to evaluate the effect of different base materials. Sections 3, 6, and 9 have the same design except 8-in.-thick unbound aggregate base, 5.5-in.-thick cement-treated base, and 4-in. asphalt concrete base, respectively. The average vertical strain in the subgrade was highest in Section 3 and lowest in Section 6, demonstrating the beneficial effect of base layer stabilization. This was evident for both trips in Figure 13.

In general, Section 2 resulted in the lowest average vertical strain in the subgrade. Although the thickness of the AC surface was only 2 in., cement stabilization of the top 7 in. of subgrade reduced the subgrade strain very effectively. This emphasizes the importance of taking care of poor subgrade on the pavement design and rehabilitation.

## CONCLUSIONS

FWD testing was performed on the instrumented test sections during June 1990 and May 1991. The MODULUS backcalculation program generally resulted in reasonable effective moduli values considering the material types and environmental conditions except in Section 8, which had severe damage. The validation process using the WES5 forward calculation program revealed that the error-minimizing technique used in the MODULUS program provided fast and accurate fitting of surface deflection basins in various designs of flexible pavements.

The depth deflections measured from the multidepth deflectometers can be a powerful tool in evaluating the accuracy and dependability of backcalculated moduli values. The following conclusions were made from the validation of the backcalculated moduli values using depth deflections and average vertical layer strains:

1. The assumptions made in this paper during the backcalculation appeared to reduce the errors between the measured and calculated depth deflections.
2. According to the comparison between the measured and calculated depth deflections of both trips, great caution has to be exercised when the backcalculated moduli are used in predicting response of pavements at different depths.
3. The accuracy in predicting depth deflections became poorer in 1991, especially for the subgrade. This could be an indicator of the additional systematic errors in 1991 due to the accumulated damage of the pavements.
4. The multilayered elastic analysis overpredicted the average vertical compressive strains within the aggregate base layers, demonstrating the effect of higher confining pressure developed from the dilatation of the aggregate materials under the compressive loading.
5. The average vertical subgrade strains were underestimated by the multilayered elastic analysis in all the sections of both trips.
6. The comparative study of the structural capacities of various designs also revealed the importance of stabilizing a poor subgrade in reducing the average vertical subgrade strain. Further study with the data from gauges and more field testing will yield invaluable information in pavement design and rehabilitation.

## ACKNOWLEDGMENT

The authors are grateful to the North Carolina Department of Transportation for its support and sponsorship of this research. Special thanks are due to B. Todd Roberts, Judith B. Corley-Lay, and Thomas M. Hearne for their assistance in the FWD testing.

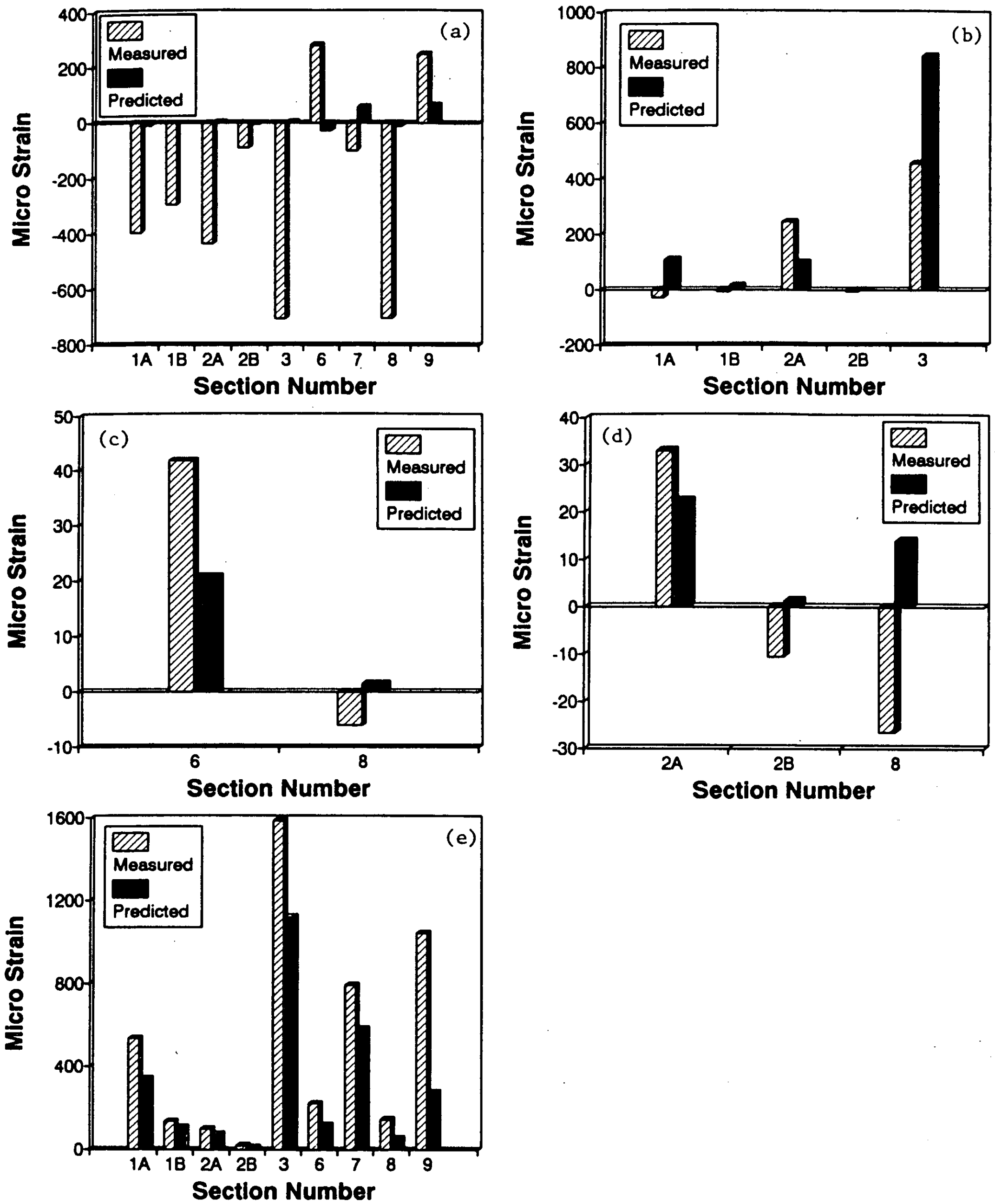


**FIGURE 14 Average vertical strains determined from MDD deflections with FWD loading at offset distances of 20 in. for 1A, 8.5 in. for 2A, and 32 in. for 1B and 2B (June 1990) within (*a*) the asphalt concrete layer, (*b*) the aggregate base layer, (*c*) the cement-treated base layer, (*d*) the stabilized subgrade, and (*e*) the subgrade.**

## REFERENCES


1. R. L. Lytton. Backcalculation of Pavement Layer Properties. In *Nondestructive Testing of Pavements and Backcalculation of Moduli*, Special Technical Publication 1026, American Society for Testing and Materials, 1989, pp. 7–38.
2. K. N. Chua. Evaluation of Moduli Backcalculation Programs for Low-Volume Roads. In *Nondestructive Testing of Pavements and Backcalculation of Moduli*, Special Technical Publication 1026, American Society for Testing and Materials, 1989, pp. 398–414.
3. T. Scullion, J. Uzan, J. I. Yazdani, and P. Chan. *Field Evaluation of the Multi-Depth Deflectometers*. Research Report 1123-2. Texas Transportation Institute, Sept. 1988.
4. T. Scullion, R. C. Briggs, and R. L. Lytton. Using the Multidepth Deflectometer To Verify Modulus Backcalculation Procedures. In *Nondestructive Testing of Pavements and Backcalculation of Moduli*, Special Technical Publication 1026, American Society for Testing and Materials, 1989, pp. 90–101.
5. R. N. Stubstad, N. P. Khosla, and W. W. Wynn. Construction of Fully Instrumented Test Pavements in North Carolina. *CRREL Symposium Proceedings on State of the Art of Pavement Response Monitoring Systems for Roads and Airfields*, West Lebanon, N.H., 1989.
6. Y. J. Chou, J. Uzan, and R. L. Lytton. Backcalculation of Layer Moduli from Nondestructive Pavement Deflection Data Using the Expert System Approach. In *Nondestructive Testing of Pavements and Backcalculation of Moduli*, Special Technical Publication 1026, American Society for Testing and Materials, 1989, pp. 341–354.

# Implementation of Falling Weight Deflectometer Load-Zoning Procedure in Texas

JEFF JACKSON AND MIKE MURPHY

The Texas Transportation Institute, on behalf of the Texas Department of Transportation (TxDOT), has developed a computer program, LOADRATE (Project 473) to be used as a load-zoning analysis tool for two-layer pavements. A comparison study was undertaken of the solutions generated by LOADRATE and those obtained using the Texas triaxial classification methodology for determining allowable wheel load capacity. The Texas triaxial method historically has been used to determine whether load zoning is warranted on a given roadway and is also used as a "check" for pavement designs generated by the flexible pavement design system computer program when used for low-traffic-volume roadways. For this comparison, deflection data were collected on all load-zoned roads (228.68 mi) in Ellis County of the Dallas district using the falling weight deflectometer. The LOADRATE program was used to compute both unadjusted and adjusted base moduli using the temperature/moisture correction features of the LOADRATE program. An allowable axle load for single, tandem, and tridem axles was then computed by the program using an allowable rut depth of 0.5 in. as the failure criteria. The results generated by the LOADRATE program do not give reasonable allowable loads as a function of pavement thickness. Additional field calibration of the LOADRATE program is warranted.

Of the more than 78,000 centerline-mi of roadway on the state-maintained highway network in Texas, approximately 17,250 mi, or slightly more than 22 percent, is load zoned. This load-zoned mileage is primarily made up of light-duty pavements within the farm-to-market (FM) road system and typically are constructed of unbound base materials with a thin wearing surface of asphalt and aggregate. In areas exhibiting especially weak subgrade soils, some load-zoned roadways are constructed of stabilized materials, including hot-mix asphalt concrete surface courses and asphalt, lime, or cement-treated bases and subgrades.

Load zoning is almost exclusively accomplished by limiting gross vehicle weight to 58,420 lb, the maximum legal load in Texas when many of these roads were constructed. The Texas triaxial load capacity method currently is used to determine whether load zoning is warranted on a roadway segment and provides a means for computing the required thickness of the pavement structure to prevent rutting of the subgrade caused by excessive wheel loads (*1*). On the basis of a need for an improved method of analyzing load-zoned roadways using mechanistic analysis of nondestructive test data, the Texas Department of Transportation (TxDOT) sponsored a research project with the Texas Transportation Institute at Texas A&M University to develop a computer program for determining the allowable axle load and remaining life of light-duty pavements. This program, LOADRATE, uses either falling weight deflectometer (FWD) or dynaflect deflection data to backcalculate moduli values for base and subgrade layers and then uses pavement layer and traffic information to determine the allowable axle load to ensure a minimum 10-year design life that is based on failure caused by rutting (*2*).

Texas Department of Transportation, 125 East 11th Street, Austin, Tex. 78701-2483.

## OBJECTIVE AND SCOPE

The LOADRATE computer program is currently being evaluated by TxDOT, and the results are being compared with those from the Texas triaxial load capacity method. The objective of this paper is to present findings of one such comparison, involving an analysis of FWD and soil triaxial classification data that were collected for all load-zoned roads in Ellis County (Dallas district). The results of this analysis will be given and the strengths and limitations of each method will be discussed. Conclusions will be drawn on the basis of these results, subject to inferences that can be made using the field data that were collected.

## TEXAS TRIAXIAL METHOD

Developed in the late 1940s, the Texas triaxial classification method is used to determine the required thickness of a pavement structure to ensure against subgrade compression failure caused by a design wheel load for either a 10- or 20-year design life. This method is currently used to check pavement designs generated by the flexible pavement design system (FPS) and is used in determining the allowable wheel load for load-zoning purposes (*1*).

The Texas triaxial method classifies paving materials on a scale from 1 to 6 (1 being considered a good flexible base material and 6 being considered a very weak subgrade). These classifications are based on a triaxial test that determines the shearing resistance of soils, soil aggregate mixtures, and base materials. The test consists of applying an axial load to cylindrical specimens of specified dimensions, supported by various, known lateral pressures until failure occurs. The test is run on saturated specimens that yield conservative results, especially for materials in West Texas, where saturated conditions rarely occur (*3,4*).

A chart that is based on empirical data has been developed that relates the triaxial class and pavement thickness to design wheel load. The pavement thickness necessary to prevent subgrade compression failure (rutting) is determined by reading the design wheel load on the horizontal axis of the chart, intersecting this value with the material classification and then reading the required material thickness in inches off the vertical axis (see Figure 1). For load-zoning purposes, the thickness of the pavement structure and the subgrade soil triaxial classification are known and the allowable wheel load for a 10-year design life is determined on the basis of these values. Allowable wheel loads less than 10,000 lb warrant road load zoning.

For pavement design purposes, a thickness reduction is allowed for pavement layers that are stabilized. The method for determining the allowable thickness reduction is based on the type of stabilizing agent used (cement, asphalt, lime, etc.) and the thickness of the stabilized layer. In determining the allowable wheel load, stabilized layers are accounted for by increasing the effective thickness of the pavement structure. The theory is that stabilized materials, being stiffer than nonstabilized materials, spread the load more and therefore reduce vertical compressive stresses to the subgrade, resulting in a higher allowable wheel load. The allowable thickness reduction is dependent on the cohesiometer value for the material. Table 1 gives recommended cohesiometer values for various stabilized layer types and thicknesses. To determine the equivalent pavement thickness, the cohesiometer value for the stabilized layer is determined from available data or selected on the basis of estimates in Table 1. Referring to Figure 2, the allowable thickness reduction is determined by entering the chart on the vertical axis with the pavement thickness, intersecting the appropriate cohesiometer value line and reading the thickness reduction on the horizontal scale. The equivalent pavement thickness equals the actual pavement thickness plus the allowable thickness reduction (*3*). If a stabilized subgrade exists, only the equivalent thickness reduction resulting from the stabilized layer is included in the equivalent pavement thickness—the actual thickness of the stabilized subgrade is not included.

As an example, the equivalent thickness of the following pavement structure will be determined:

| *Surface course* | *Base course* | *Subbase* |
|---|---|---|
| Asphalt surface treatment (1 in.) | 10-in. limestone flexible base | 6-in. lime stabilized subgrade |

Entering Figure 2 with a depth of pavement structure of 17 in. and a cohesiometer value of 250, the allowable thickness reduction is computed as 2.5 in. The equivalent pavement thickness would then be computed as

| *Surface course* | *Base course* | *Equivalent thickness reduction* |
|---|---|---|
| Asphalt surface treatment (1 in.) | 10-in. limestone flexible base | 2.5 in. |

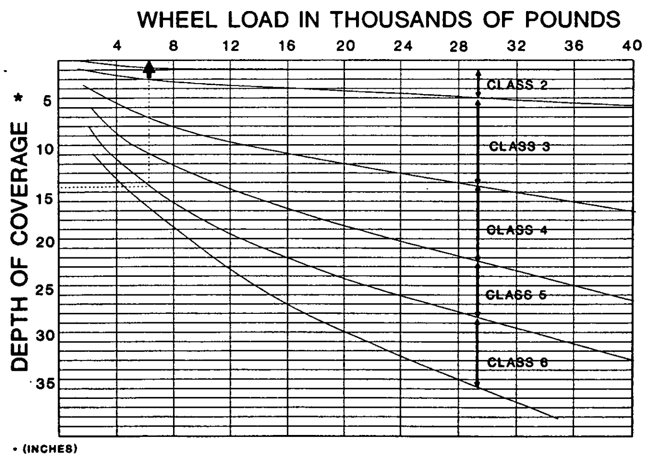


**FIGURE 1 Triaxial classification lead capacity chart.**

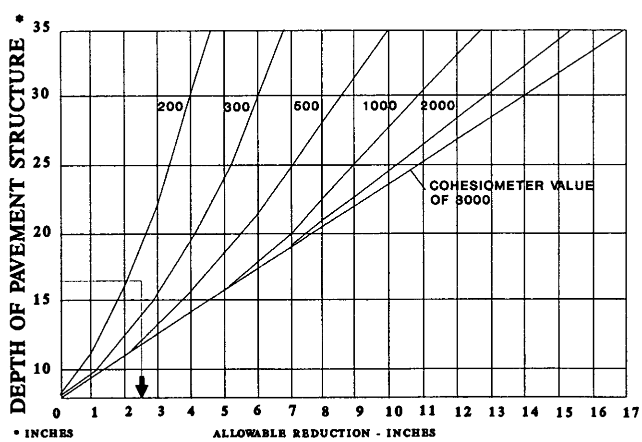


**FIGURE 2 Thickness reduction chart for stabilized layers.**

**TABLE 1 Cohesiometer Values for Stabilized Materials**

| STABILIZED MATERIAL TYPE | COHESIOMETER VALUE |
|---|---|
| Lime Treated Base > than 3" Thick | 300 |
| Lime Treated Subgrade > than 3" Thick | 250 |
| Cement Treated Base > than 3" Thick | 1000 |
| Cold Mixed Bituminous Materials > 3" Thick | 300 |
| Hot Mixed Bituminous Materials > 6" Thick | 800 |
| Hot Mixed Bituminous Materials 4" to 6" Thick | 550 |
| Hot Mixed Bituminous Materials 2" to 4" Thick | 300 |

The equivalent pavement thickness would then be 13.5 in. If we assume a soil triaxial classification of 6.0 and refer to Figure 1, we determine that this pavement structure provides sufficient depth of coverage for a wheel load capacity of approximately 6,000 lb (for an estimated design life of 10 years). We would then conclude that this pavement warrants load zoning because the allowable wheel load is less than 10,000 lb.

## LOADRATE

The LOADRATE computer program was developed by the Texas Transportation Institute at Texas A&M University. LOADRATE provides a mechanistic modeling approach for analyzing light-duty pavements using backcalculated moduli for the base and subgrade, base course thickness, subgrade material type, and traffic data (*4*). The program is able to correct base moduli for temperature and moisture variation and can predict rutting for three subgrade types; heavy clays (CH), clayey silt/silty clay (CL-ML), and clayey/silty sand (SC-SM). However, the program is flexible and gives the user the option to specify parameters that are based on laboratory data for soil types specific to the roadway being evaluated (*4*).

LOADRATE determines remaining life and allowable axle loads on the basis of a specified limiting rut depth. The program was designed to analyze two-layer problems (base and subgrade) and cannot determine remaining life on the basis of failure from fatigue cracking of an asphalt surface course.

Remaining life calculations require the user to provide either (a) the current annual traffic in 18-kip equivalent single axle loads (ESALs), traffic growth rate, and length of analysis period in years or (b) the 1st and 20th year average daily traffic (ADT) and the total number of 18-kip ESALs in 20 years. The rut depth prediction model relates accumulated permanent strain to number of load applications and subgrade type. The model is of the form

$$\log \varepsilon_p = \log a + b \log N \qquad (1)$$

where

$\varepsilon_p$ = accumulated permanent strain,
$a,b$ = material constants based on soil type, and
$N$ = number of 18-kip load applications.

The determination of the remaining life then becomes a straightforward calculation that is based on a predetermined allowable rut depth, traffic, and subgrade soil type. TxDOT has established criteria that require a remaining life of at least 10 years for FM roads. If the LOADRATE program determines that 100 percent of the test sections analyzed can accommodate the projected number of 18-kip ESALs without exceeding the predetermined rut depth, then the program reports that legal axle load limits are allowed and load zoning is not required. If the remaining life is computed to be less than 10 years, the program then determines the allowable axle load limits for single, tandem, and tridem axles that would ensure a minimum life of 10 years and reports these reduced axle load limits in the output.

## ROADWAYS USED FOR COMPARISON

All load-zoned roadway sections in Ellis County of the Dallas district were tested with the FWD. A total of 31 FM roadways totaling 228.680 mi were measured in this county. Of the 31 FMs measured, only 20 FMs totaling 135.260 mi were either fully or partly compatible for use with LOADRATE. Some were compatible over their entire length and some contained sections within the length of the roadway that were compatible for analysis using the LOADRATE program. Compatibility in this case is defined as a roadway containing only a two-layer pavement structure (a subgrade and a base with a thin surfacing material) or a pavement that could, for practical purposes, be considered as a two-layer pavement structure, as can be seen in Table 2. This limitation is an inherent one and is totally acceptable as the program was designed within this limitation.

The 20 FMs were segmented into roadway sections that were based on changes in the typical sections of the pavements (changes in the structural composition of the layers of the pavements) or changes in traffic volume for a total of 49 roadway sections. Finally, of the 49 sections, 40 sections totaling 114.566 mi were compatible for analysis using the LOADRATE program. This amounted to approximately 50 percent of the measured mileage being compatible for analysis using the LOADRATE program, which is not much different from that stated by the LOADRATE developers in their report (*2*). Although this percentage does not appear to be significant, if it were assumed to represent the percentage of all mileage of load-zoned FMs in the state that could be analyzed using LOADRATE this would amount to an approximate total of 8,625 mi of the approximate 17,250 mi of current load-zoned roadways in the state (a sizeable contribution to load-zone analysis of low-volume roadways).

## LIMITS ON INFERENCE SPACE

The subgrade soil of all load-zoned roadways in Ellis County were in the relatively poor category (triaxial class 5.4 to 5.2), as can be seen in Table 2. Obviously, this very limited range inhibits the accuracy of extrapolation of results to the fair and good ranges (triaxial class 4.0 to 1.0). In addition, the deflection collected was taken primarily in the summer months, which may generate moduli of elasticity that are stronger than those that have been generated from deflection data taken during the spring thaw period. Therefore, the results obtained in this comparison and the subsequent observations and conclusions drawn are for a small range of the subgrade triaxial class scale and for moduli values that have been revised or adjusted by the LOADRATE temperature/moisture correction routine from a summer condition to a spring-thaw condition.

## WHEEL LOAD CAPACITIES BASED ON TEXAS TRIAXIAL METHOD

The Division of Materials and Tests (D-9) of TxDOT provided the subgrade triaxial class data and the Texas triaxial wheel

**TABLE 2 Original Input Data for Texas Triaxial and LOADRATE Methods**

| | SURFACE | | BASE | | SUBGRADE SOIL | | TRAFFIC | | |
|---|---|---|---|---|---|---|---|---|---|
| S# | TYPE | THICK (IN.) | TYPE | THICK (IN.) | DESCRIPTION | TRIAXIAL CLASS | 1990 ADT | 2010 ADT | 20 YEAR ESALS |
| 1 | 1-C.S.T. | 0.50 | FLEXBASE | 12 | SILTY CLAY | 5.4 | 1,150 | 2,500 | 436,000 |
| 2 | 2-C.S.T. | 1.00 | FLEXBASE | 14 | SILTY CLAY | 5.4 | 1,150 | 2,500 | 436,000 |
| 3 | 1-C.S.T. ON 1-C.S.T. | 1.00 | FLEXBASE | 10 | SILTY CLAY | 5.2 | 1,200 | 1,700 | 461,000 |
| 4 | 2-C.S.T. | 1.00 | FLEXBASE | 12 | SILTY CLAY | 5.4 | 1,450 | 2,900 | 485,000 |
| 5 | 1-C.S.T. | 0.50 | FLEXBASE | 10 | SILTY CLAY | 5.4 | 610 | 1,050 | 255,000 |
| 6 | 2-C.S.T. | 1.00 | LIME TRTD FOUND CRSE | 7 | SILTY CLAY | 5.2 | 370 | 710 | 85,000 |
| 7 | 2-C.S.T. | 1.00 | FLEXBASE | 6 | CHALK W/ SILTY CLAY | 5.2 | 5,400 | 11,100 | 1,472,000 |
| 8 | 2-C.S.T. | 1.00 | FLEXBASE | 6 | CHALK W/ SILTY CLAY | 5.2 | 910 | 1,800 | 356,000 |
| 9 | 2-C.S.T. | 1.00 | FLEXBASE | 12 | SILTY CLAY | 5.3 | 1,000 | 2,200 | 183,000 |
| 10 | 2-C.S.T. | 1.00 | FOUND CRSE | 15 | SILTY CLAY | 5.3 | 1,000 | 2,200 | 183,000 |
| 11 | 2-C.S.T. | 1.00 | FOUND CRSE | 15 | SILTY CLAY | 5.3 | 1,000 | 2,200 | 183,000 |
| 12 | 1-C.S.T. ON 1-C.S.T. | 1.00 | FLEXBASE | 10 | SILTY CLAY | 5.2 | 590 | 1,200 | 120,000 |
| 13 | 1-C.S.T. | 0.50 | FLEXBASE | 6 | SILTY CLAY | 5.2 | 590 | 1,200 | 120,000 |
| 14 | 1-C.S.T. | 0.50 | FLEXBASE | 6 | CHALK W/ SILTY CLAY | 5.2 | 440 | 910 | 100,000 |
| 15 | 1-C.S.T. | 0.50 | FLEXBASE | 6 | CHALK W/ SILTY CLAY | 5.2 | 1,100 | 2,200 | 185,000 |
| 16 | 2-C.S.T. | 1.00 | FLEXBASE | 12 | SILTY CLAY | 5.3 | 740 | 1,400 | 303,000 |
| 17 | 1-C.S.T. ON 1-C.S.T. | 1.00 | FLEXBASE | 12 | SILTY CLAY | 5.3 | 1,100 | 2,400 | 427,000 |
| 18 | 1-C.S.T. | 0.50 | FLEXBASE | 6 | SILTY CLAY | 5.3 | 450 | 940 | 133,000 |
| 19 | 2-C.S.T. | 1.00 | FLEXBASE | 8 | SILTY CLAY | 5.4 | 1,050 | 2,300 | 143,000 |
| 20 | A.S.B. | 1.25 | FLEXBASE | 6 | SILTY CLAY | 5.4 | 3,600 | 7,400 | 299,000 |
| 21 | 2-C.S.T. | 1.00 | A.S.B. | 6 | SILTY CLAY | 5.4 | 3,300 | 6,700 | 539,000 |
| 22 | ACP | 1.00 | FLEXBASE | 8 | SILTY CLAY | 5.4 | 1,000 | 1,700 | 258,000 |
| 23 | 2-C.S.T. | 1.00 | A.S.B. | 6 | SILTY CLAY | 5.4 | 1,000 | 1,700 | 258,000 |
| 24 | ACP | 1.00 | SOIL ASPH BASE | 6 | SILTY CLAY | 5.4 | 90 | 180 | 20,000 |
| 25 | 2-C.S.T. | 1.00 | LIME STAB BASE | 12 | SILTY CLAY | 5.4 | 540 | 1,000 | 253,000 |
| 26 | 2-C.S.T. | 1.00 | FLEXBASE | 12 | SILTY CLAY | 5.4 | 90 | 180 | 50,000 |
| 27 | 2-C.S.T. | 1.00 | FLEXBASE | 10 | SILTY CLAY | 5.4 | 190 | 370 | 46,000 |
| 28 | 1-C.S.T. | 0.50 | SOIL ASPH BASE | 6 | SILTY CLAY | 5.4 | 1,550 | 2,900 | 491,000 |
| 29 | 1-C.S.T. | 0.50 | SOIL ASPH BASE | 6 | SILTY CLAY | 5.4 | 830 | 1,700 | 342,000 |
| 30 | 2-C.S.T. | 1.00 | FLEXBASE | 12 | SILTY CLAY | 5.4 | 830 | 1,700 | 342,000 |
| 31 | 2-C.S.T. | 1.00 | FLEXBASE | 6 | SILTY CLAY | 5.1 | 830 | 1,700 | 342,000 |
| 32 | 1-C.S.T. | 0.50 | FLEXBASE | 6 | CHALK W/ SILTY CLAY | 5.2 | 5,100 | 12,200 | 1,608,000 |
| 33 | 1-C.S.T. | 0.50 | FLEXBASE | 6 | CHALK W/ SILTY CLAY | 5.2 | 2,500 | 4,900 | 911,000 |
| 34 | 1-C.S.T. | 0.50 | FLEXBASE | 6 | CHALK W/ SILTY CLAY | 5.2 | 1,050 | 2,200 | 583,000 |
| 35 | 2-C.S.T. | 1.00 | FLEXBASE | 6 | CHALK W/ SILTY CLAY | 5.2 | 570 | 1,150 | 138,000 |
| 36 | 2-C.S.T. | 1.00 | FLEXBASE | 9 | CHALK W/ SILTY CLAY | 5.2 | 1,000 | 2,000 | 200,000 |
| 37 | 2-C.S.T. | 1.00 | FLEXBASE | 8 | SILTY CLAY | 5.3 | 630 | 1,100 | 266,000 |
| 38 | 2-C.S.T. | 1.00 | FLEXBASE | 6 | SILTY CLAY | 5.2 | 490 | 950 | 104,000 |
| 39 | 1-C.S.T. ON 1-C.S.T. | 1.00 | FLEXBASE | 10 | SILTY CLAY | 5.3 | 3,500 | 6,700 | 360,000 |
| 40 | 1-C.S.T. ON 1-C.S.T. | 1.00 | FLEXBASE | 10 | SILTY CLAY | 5.3 | 1,050 | 2,000 | 171,000 |

load capacity for each of the given roadway sections on the basis of the engineering data given to them concerning each section. The wheel loads provided by D-9 were for a 20-year pavement life and, according to the Texas triaxial method, the allowable wheel loads were adjusted by a factor of two to obtain a 10-year pavement life for comparison with LOADRATE output. In addition, the pavement thickness used for the Texas triaxial method is actually an effective thickness, as previously discussed, and not the actual thickness as used by LOADRATE (see Table 3). These allowable wheel load capacities ranged from 3,000 lb to over 13,000 lb/wheel. Because of the basis of the Texas triaxial method, the allowable wheel loads increased with an increase in the effective pavement thickness, as expected. The variability in strength or load-carrying capacity of the base course was not a consideration in this method except, as previously outlined, in the cases in which there existed a stabilized layer. This method assumes a worst-case (saturated) condition and, although it provides a conservative design, does not always represent the conditions in the field. The degree of conservativism is dependent on the conditions at a given site and therefore is not a constant. However, until an acceptable and reliable replacement is decided on, this method is the standard accepted method of load-zone analysis for TxDOT because conservativism is preferred when there is a lack of a better process or methodology.

**TABLE 3 Results of Texas Triaxial and LOADRATE Methods**

| | TEXAS TRIAXIAL METHOD | | | | LOADRATE METHOD | | | |
|---|---|---|---|---|---|---|---|---|
| S# | SOIL CLASS USED | THICK. USED (IN.) | 20 YEAR ALLOW. WHEEL LOAD CAPACITY (LBS.) | 10 YEAR ALLOW. WHEEL LOAD CAPACITY (LBS.) | SOIL GROUP | THICK. USED (IN.) | ALLOW. AXLE LOAD CAPACITY (LBS.) | ALLOW. WHEEL LOAD CAPACITY (LBS.) |
| 1 | 5.4 | 13.5 | 4,600 | 9,200 | 2) SILTY CLAY | 12.5 | 22,000 | 11,000 |
| 2 | 5.4 | 15.5 | 5,400 | 10,800 | 2) SILTY CLAY | 15.0 | 20,000 | 10,000 |
| 3 | 5.2 | 11.5 | 3,800 | 7,600 | 2) SILTY CLAY | 11.0 | 20,000 | 10,000 |
| 4 | 5.4 | 13.5 | 4,600 | 9,200 | 2) SILTY CLAY | 13.0 | 20,000 | 10,000 |
| 5 | 5.4 | 11.5 | 3,200 | 6,400 | 2) SILTY CLAY | 10.5 | 22,000 | 11,000 |
| 6 | 5.2 | 10.5 | 3,200 | 6,400 | 2) SILTY CLAY | 7.0 | 26,000 | 13,000 |
| 7 | 5.2 | 7.5 | 1,600 | 3,200 | 2) SILTY CLAY | 7.0 | 17,000 | 8,500 |
| 8 | 5.2 | 7.5 | 1,600 | 3,200 | 2) SILTY CLAY | 7.0 | 22,000 | 11,000 |
| 9 | 5.3 | 13.5 | 4,800 | 9,600 | 2) SILTY CLAY | 13.0 | 23,000 | 11,500 |
| 10 | 5.3 | 16.5 | 7,100 | 14,200 | 2) SILTY CLAY | 16.0 | 23,000 | 11,500 |
| 11 | 5.3 | 16.5 | 7,100 | 14,200 | 2) SILTY CLAY | 16.0 | 24,000 | 12,000 |
| 12 | 5.2 | 11.5 | 3,800 | 7,600 | 2) SILTY CLAY | 11.0 | 25,000 | 12,500 |
| 13 | 5.2 | 7.5 | 1,600 | 3,200 | 2) SILTY CLAY | 6.5 | 26,000 | 13,000 |
| 14 | 5.2 | 7.5 | 1,600 | 3,200 | 2) SILTY CLAY | 6.5 | 26,000 | 13,000 |
| 15 | 5.2 | 7.5 | 1,600 | 3,200 | 2) SILTY CLAY | 6.5 | 24,000 | 12,000 |
| 16 | 5.3 | 13.5 | 4,800 | 9,600 | 2) SILTY CLAY | 13.0 | 22,000 | 11,000 |
| 17 | 5.3 | 13.5 | 4,800 | 9,600 | 2) SILTY CLAY | 13.0 | 20,000 | 10,000 |
| 18 | 5.3 | 7.5 | 1,550 | 3,100 | 2) SILTY CLAY | 6.5 | 25,000 | 12,500 |
| 19 | 5.4 | 9.5 | 2,300 | 4,600 | 2) SILTY CLAY | 9.0 | 24,000 | 12,000 |
| 20 | 5.4 | 9.0 | 2,100 | 4,200 | 2) SILTY CLAY | 7.3 | 22,000 | 11,000 |
| 21 | 5.4 | 7.5 | 1,500 | 3,000 | 2) SILTY CLAY | 7.0 | 20,000 | 10,000 |
| 22 | 5.4 | 10.5 | 2,800 | 5,600 | 2) SILTY CLAY | 9.0 | 22,000 | 11,000 |
| 23 | 5.4 | 7.5 | 1,500 | 3,000 | 2) SILTY CLAY | 7.0 | 23,000 | 11,500 |
| 24 | 5.4 | 12.0 | 3,600 | 7,200 | 2) SILTY CLAY | 7.0 | 30,000 | 15,000 |
| 25 | 5.4 | 16.5 | 6,600 | 13,200 | 2) SILTY CLAY | 13.0 | 22,000 | 11,000 |
| 26 | 5.4 | 13.5 | 4,600 | 9,200 | 2) SILTY CLAY | 13.0 | 28,000 | 14,000 |
| 27 | 5.4 | 11.0 | 3,000 | 6,000 | 2) SILTY CLAY | 11.0 | 28,000 | 14,000 |
| 28 | 5.4 | 10.5 | 2,800 | 5,600 | 2) SILTY CLAY | 6.5 | 20,000 | 10,000 |
| 29 | 5.4 | 10.5 | 2,800 | 5,600 | 2) SILTY CLAY | 6.5 | 22,000 | 11,000 |
| 30 | 5.4 | 13.5 | 4,600 | 9,200 | 2) SILTY CLAY | 13.0 | 21,000 | 10,500 |
| 31 | 5.1 | 7.5 | 1,700 | 3,400 | 2) SILTY CLAY | 7.0 | 22,000 | 11,000 |
| 32 | 5.2 | 7.5 | 1,600 | 3,200 | 2) SILTY CLAY | 6.5 | 23,000 | 11,500 |
| 33 | 5.2 | 7.5 | 1,600 | 3,200 | 2) SILTY CLAY | 6.5 | 23,000 | 11,500 |
| 34 | 5.2 | 7.5 | 1,600 | 3,200 | 2) SILTY CLAY | 6.5 | 20,000 | 10,000 |
| 35 | 5.2 | 7.5 | 1,600 | 3,200 | 2) SILTY CLAY | 7.0 | 25,000 | 12,500 |
| 36 | 5.2 | 10.5 | 3,200 | 6,400 | 2) SILTY CLAY | 10.0 | 26,000 | 13,000 |
| 37 | 5.3 | 9.5 | 2,400 | 4,800 | 2) SILTY CLAY | 9.0 | 22,000 | 11,000 |
| 38 | 5.2 | 7.5 | 1,600 | 3,200 | 2) SILTY CLAY | 7.0 | 26,000 | 13,000 |
| 39 | 5.3 | 11.5 | 3,500 | 7,000 | 2) SILTY CLAY | 11.0 | 21,000 | 10,500 |
| 40 | 5.3 | 11.5 | 3,500 | 7,000 | 2) SILTY CLAY | 11.0 | 24,000 | 12,000 |

## WHEEL LOAD CAPACITIES BASED ON LOADRATE METHOD

The Dallas district (District 18) in conjunction with the Division of Transportation Planning (D-10) of TxDOT provided the traffic data for the given roadway sections. District 18 also provided the subgrade soil type and collected the FWD data on the given roadway sections (see Table 2). The soil types given were best represented by choosing the No. 2, silty clay option within the program for this method. The solution generated by the LOADRATE program was an allowable axle load. To compare on an equal basis, this allowable axle load was decreased by a factor of two to an allowable wheel load for this comparison. The legal wheel load in Texas is 10,000 lb/wheel. The allowable wheel loads generated by LOADRATE seem to indicate that load-zoning could be removed for almost all roadway sections without failures occurring within 10 years (see Table 3). The allowable wheel loads tended to vary to some degree yet appear to oscillate around an almost horizontal line at approximately 10,500 to 11,500 lb/wheel (see Figures 3 and 4). The LOADRATE program also prints out the backcalculated moduli it generated that was the basis for its allowable wheel load capacity along with traffic, pavement thickness, and subgrade soil type.

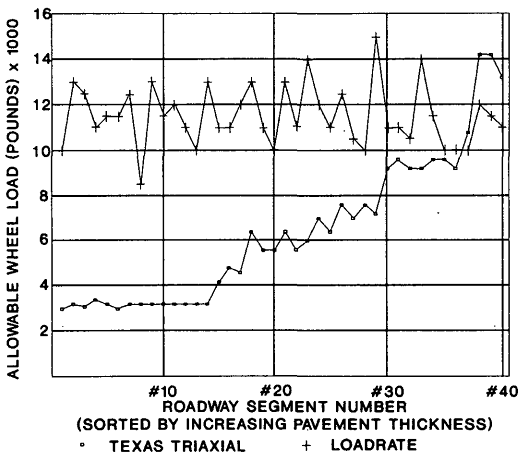


**FIGURE 3 LOADRATE method versus Texas triaxial method.**

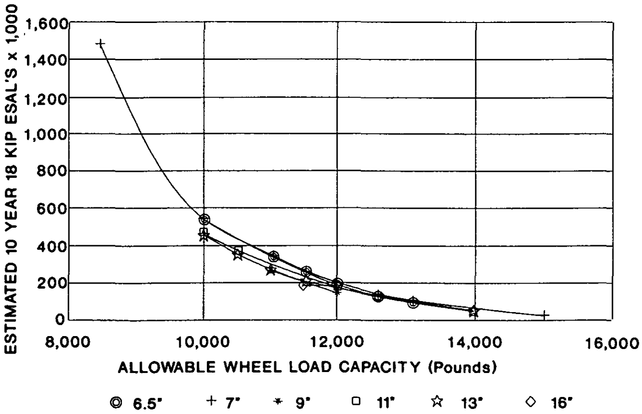


**FIGURE 4 LOADRATE allowable wheel load versus accumulated traffic.**

## LOADRATE RESULTS COMPARED WITH TEXAS TRIAXIAL RESULTS

Currently, the backcalculated moduli generated by the LOADRATE program do not correlate with any degree of confidence with the Texas triaxial method. This is primarily because the Texas triaxial method is measured in the laboratory by testing under worst-case conditions (saturated), whereas the backcalculated moduli of elasticity are measured in the field and are a time-dependent (seasonal) characteristic of the soil. The LOADRATE program does allow for adjustment of the backcalculated moduli values that are based on moisture and temperature. The existing moisture conditions on these roadways, however, were not measured for various reasons; therefore, maximum adjustment allowed by LOADRATE was used to ensure that the most conservative results would be obtained from LOADRATE for comparison with the Texas triaxial method. The moisture and temperature corrections did not change the original allowable axle load in almost all instances. When the corrections did change the allowable axle load (there were only three cases) two sections received increases of 1,000 lb each in allowable axle load and one section received a decrease of 1,000 lb allowable axle load. Even after making this adjustment, the LOADRATE results suggest removal of load zoning on all but two roadway sections. Because of the inconsistency of results from the correction routines, the results reported herein are for the original input and output to the LOADRATE program.

## RESULTS AND OBSERVATIONS

The two methods place different significance on input factors such as traffic, moduli values, and soil type (subgrade triaxial class). Traffic is not a standard consideration in the Texas triaxial method but it is a primary input in the LOADRATE method. The moduli values are of no use in the Texas triaxial method but are a necessity in the LOADRATE method. The subgrade triaxial class is a required input in the Texas triaxial method but it is not a user input to the LOADRATE method.

The Texas triaxial method appears to give conservative allowable wheel loads when the effective thickness is less than 15 in. The LOADRATE method appears to give conservative allowable wheel loads when the effective pavement thickness is greater than 15 in. This observation in itself would not lend either method unacceptable. However, the LOADRATE method's liberal allowable wheel loads coupled with the fact that the LOADRATE method tends to suggest removal of load zoning on almost all sections that are currently load zoned lead the authors to believe that more work needs to be done to establish the reasons for this discrepancy and possibly to calibrate or modify, or both, the LOADRATE program for final acceptance and subsequent use by TxDOT.

## SUMMARY AND CONCLUSIONS

As mentioned, the Texas triaxial method does have limitations and is a conservative method for a large percentage of load-zoned roadways. However, until an acceptable alternative procedure is developed, tested, and confirmed as a standard method of pavement load-zone analysis, the Texas triaxial method will still remain the standard method used by TxDOT, especially because it is a conservative method for the most part and also because it has been in use for many years in Texas with acceptable results (partially because of its conservative approach).

The results indicate that, although the LOADRATE method allows for a more precise manner of measuring a pavement's load capacity in the field and at any given point in time, the latter could be a disadvantage without readily available information relating to the existing moisture condition and the effect of moisture change along a particular roadway section on the variation of moduli values because they are heavily dependent on moisture conditions. In addition, the backcalculated subgrade moduli values in general appear to be slightly lower than was expected with other backcalculation procedures. Although the LOADRATE method does take traffic into account, the percent error inherent in traffic predictions combined with the fact that the pavement engineering community currently has established no standard, nationwide backcalculation procedure as the most acceptable or realistic, further highlights the need for more work on the LOADRATE program before implementation can be considered.

## REFERENCES

1. Flexible Pavement Design Procedures. *Proc., Pavement Managers Workshop, Aug. 1985.* Pavement Design Section, Division of Highway Design, Texas Department of Transportation, Austin, 1985.
2. B. L. Santha, W. Yang, and R. L. Lytton. *A Microcomputer Based Procedure for Load-Zoning Determination on Low-Volume Roads.* Report FHWA/TX-90/473-3F. Texas Transportation Institute, Texas A&M University, College Station; Texas Department of Transportation, Austin, Nov. 1989.
3. *Test Method Tex-117-E Rev: December 1982 Triaxial Compression Tests for Disturbed Soils and Base Materials.* Division of Materials and Tests, Texas Department of Transportation, Austin, 1982.
4. A. W. Smith and K. A. Dyer. *Triaxial Classification of the Surface Soils of Texas as Grouped by Soil Conservation Service Series.* Publication 3-05-71-035. Division of Materials and Tests, Texas Department of Transportation, Austin, 1973.
5. S. M. and J. F. Young. *Concrete.* Prentice-Hall, Inc., Englewood Cliffs, N.J., 1981.
6. *The Aggregate Handbook* (R. D. Barksdale, ed.). National Stone Association, Washington, D.C., 1991.
7. E. J. Yoder and M. W. Witczak. *Principles of Pavement Design.* John Wiley and Sons, Inc., New York, N.Y., 1975.

# Implementation of Backcalculation in Pavement Evaluation and Overlay Design in Oregon

HAIPING ZHOU, JIM HUDDLESTON, AND JAMES LUNDY

The implementation of the BOUSDEF backcalculation program with emphasis on the comparison between the laboratory-tested and backcalculated moduli and in using the backcalculated moduli in overlay design is presented. In doing so, two projects, both conventional flexible pavement structures, were evaluated for overlay design requirement. The deflections were measured with a KUAB falling weight deflectometer, and pavement temperature was measured during the deflection tests. The laboratory tests included determination of modulus for asphalt concrete (AC) cores and base materials. For the AC cores, the diametral test procedure (ASTM D4123) was followed. The cores were tested at three temperatures—42°F, 73°F, and 95°F—to determine the AC modulus-temperature relationship. For the base material, the triaxial test procedure (AASHTO T-274) was used. The comparison showed that for the AC materials, the backcalculated moduli are generally lower than those that are laboratory tested and also seemed to be less susceptible to temperature variations. For the base material, the backcalculated modulus slope ($k_2$) is slightly higher than that determined from laboratory testing. However, in the range in which pavement stresses generally fall, a satisfactory comparison is observed. On the basis of the backcalculated and the laboratory results, inputs were developed for pavement overlay design using a mechanistic approach. The overlay design recommendation on these two projects were also compared with those from the ODOT (Oregon Department of Transportation) standard overlay design procedure. The results from both the mechanistic approach and the ODOT procedure were very close, implying that the backcalculated moduli provided a reasonable estimate of the existing pavement properties.

Using backcalculation techniques to determine pavement layer moduli has received increasing interest among the pavement engineering community. To date, a number of computer programs have been developed that use various algorithms. Oregon Department of Transportation (ODOT) has been using a backcalculation program, BOUSDEF, developed at Oregon State University (*1*). The BOUSDEF program is based on the method of equivalent thicknesses together with Boussinesq's theory. The program, because of its extremely fast computing speed and capability of determining nonlinearity of granular base and fine subgrade, has been used to assist ODOT pavement engineers in evaluating existing pavement structural properties and in developing inputs for pavement or overlay design using a mechanistic approach. The BOUSDEF program was initially evaluated by three approaches: (a) comparing the backcalculated moduli with theoretical moduli, (b) comparing the backcalculated moduli with results from other developed backcalculation programs,and (c) comparing backcalculated moduli with those from the laboratory tests. The evaluation indicated that the moduli backcalculated using the BOUSDEF program compared very well with the theoretical moduli and also are very similar to those from other developed programs. The moduli determined from the backcalculation and the laboratory tests were also compared on a limited scale and the results were promising.

H. Zhou, Nichols Consulting Engineers, 1885 South Arlington Avenue, Suite 111, Reno, Nev. 89509. J. Huddleston, Oregon Department of Transportation, 800 Airport Road, Salem, Oreg. 97310. J. Lundy, Department of Civil Engineering, Oregon State University, Corvallis, Oreg. 97331.

This paper presents the implementation of the BOUSDEF program with emphasis on the comparison between the laboratory-tested and backcalculated moduli for asphalt concrete (AC) and base materials and the use of the backcalculated moduli in overlay design. Two projects, both conventional flexible pavement structures, were selected for this purpose. To verify the backcalculated results, pavement materials were obtained and tested in the laboratory for determining resilient modulus. On the basis of the backcalculated and laboratory-tested values, a set of design inputs was developed and used in a mechanistic approach for the development of overlay thickness. The overlay thickness was then compared with that from the standard procedure currently used in Oregon. The procedures used in this study are as follows:

1. Select project sites for evaluation.
2. For selected sites, perform pavement condition survey and deflection test.
3. Backcalculate pavement layer moduli from deflection basin data.
4. Obtain samples from same road section where deflections were measured.
5. Perform laboratory tests on samples.
6. Compare results from backcalculated and laboratory tests.
7. Determine pavement layer moduli and other inputs for overlay design.
8. Perform overlay design using a mechanistic approach and the ODOT procedure.

## BACKCALCULATION AND LABORATORY TESTING PROGRAM

### Project Descriptions

Two project sites were selected for this study. These two projects are typical conventional pavement structures con-

sisting of an asphalt concrete surface layer over an aggregate base and subgrade. Project 1 is located by the Columbia River, in northern Oregon. The pavement was constructed in 1969 and has an average thickness of 6.8 in. of AC and 18 in. of aggregate base on the subgrade. In 1989 a pavement condition survey was conducted. The pavement had moderate rutting, extensive cracking, and apparent delamination and was rated fair to poor. The subgrade was identified in the field as sandy gravel, brown in color, nonplastic, damp, and very dense. Project 2 is situated at the south end of the Willamette Valley in western Oregon. The pavement was constructed in 1967 and has 4 in. of AC and 16 in. of aggregate base on the subgrade. The condition survey results showed that the pavement had light to moderate alligator cracking and moderate transverse cracking. The pavement was rated fair to poor. The subgrade is fine-coarse sandy gravel and dense.

### Deflection Test

Deflection tests were performed in both travel directions of the selected projects using KUAB falling weight deflectometer (FWD). The impulse force is created by dropping a set of two weights from various heights. By varying the drop height, the load at the pavement surface was varied from approximately 3,000 to 15,000 lb. A smooth load pulse similar to that created by a moving wheel load is generated by using the two-mass system (*2,3*). Surface deflections were measured with seismic transducers that are lowered automatically with the loading plate. The sensor locations may be adjusted for the project requirement. For Project 1, the sensors were set at distances of 0, 8, 12, 24, 36, and 58 in. For Project 2, the sensors were set at distances of 0, 12, 24, 36, 60, and 99 in. Although the sensor settings were arbitrary for this study, it is important to have one sensor that is far enough away from the load to obtain the pavement response from the subgrade. For these projects, this distance is approximately 36 in. from the load.

Project 1 is approximately 1 mi long. The deflections were measured at 250-ft intervals in both travel directions. Three FWD load levels, ranging from approximately 3,000 to 12,000 lb, were applied at each test spot. There were 45 test spots for this project. Deflections were automatically recorded with a personal computer. Pavement surface temperatures were measured immediately before the deflection testing was performed. Eastbound, the measured pavement surface temperature was 66°F. Westbound, the measured pavement surface temperature was 78°F.

Project 2 is approximately 1.3 mi long. The deflections were measured at 200-ft intervals. At each test location, two load levels were applied ranging from 8,000 to 14,000 lb. There were 70 test locations for this project. Recorded data at each test location included pavement surface temperature, load applied, and deflection at each sensor location. For this project, the pavement surface temperatures were measured during the deflection testing with a thermometer mounted on the FWD. The pavement surface temperature varied from 50°F to 92°F.

### Backcalculation of Layer Moduli

The BOUSDEF program was used to backcalculate the modulus for each pavement layer from the deflection data. All raw data, without correcting for temperature, were used to calculate the pavement moduli at the time of testing. This was intended to obtain a whole picture of pavement layer properties for the project. During backcalculation, typical modulus range and initial modulus values for AC, aggregate base, and subgrade were used. Poisson's ratios for AC, aggregate base, and subgrade were set at 0.35, 0.4, and 0.45, respectively. Deflections measured at various load levels were used to backcalculate layer moduli at various stress levels to determine nonlinearity of the base and subgrade materials. Table 1 presents the summary of the backcalculated results. The backcalculated results show that the base material is stress sensitive whereas the subgrade material appears not to be.

### Materials Sampling

Pavement materials sampled at both project sites included asphalt concrete cores and base aggregates. Subgrade soil was not obtained because of difficulties in getting undisturbed soil samples.

For each project, eight 4-in.-diameter asphalt concrete cores were obtained for the determination of resilient modulus. Bag samples of aggregate materials were also obtained for the modulus testing.

### Laboratory Tests

Laboratory tests were performed on the pavement samples for resilient modulus. For the AC cores, the diametral test (ASTM D-4123) was followed. For the aggregate base ma-

**TABLE 1 Summary of Backcalculated Modulus**

| Project | AC Modulus (ksi) | Base Modulus (psi) | Subgrade Modulus (ksi) |
|---|---|---|---|
| 1 | 480[1]<br>221[2] | For westbound: $MR = 11{,}100*\theta^{0.33}$<br>For eastbound: $MR = 9{,}800*\theta^{0.29}$ | 21[1]<br>6[2] |
| 2 | 678[3]<br>287[2] | For westbound: $MR = 5{,}100*\theta^{0.72}$<br>For eastbound: $MR = 9{,}700*\theta^{0.42}$ | 15[3]<br>5[2] |

[1] Average modulus based on a total of 135 deflection readings
[2] Standard deviation
[3] Average modulus based on a total of 140 deflection readings

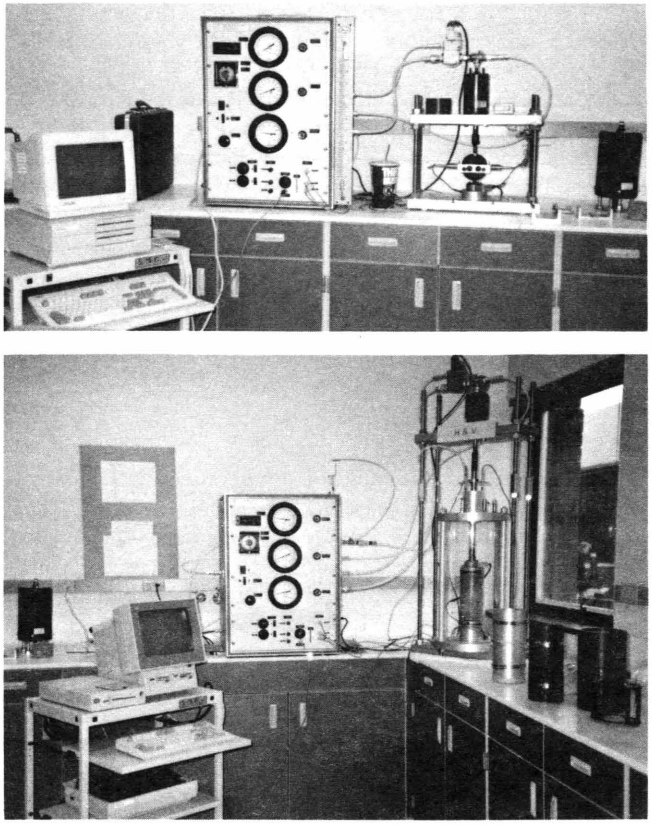

**FIGURE 1 Resilient modulus testing system: *top*, diametral testing system; *bottom*, triaxial testing system.**

terial, the triaxial test (AASHTO T-274) was used. The AC core samples for the purpose of testing were trimmed to a height of approximately 1.5 to 2.5 in., depending on the thickness of the surface lift. The resilient modulus test was then performed on the surface cores.

The AC cores were tested at three temperatures—42°F, 73°F, and 95°F—to determine the influence of the temperature on the modulus of the asphalt concrete. A diametral testing system was employed for the test (*4*). This testing system can be used for both diametral and triaxial resilient modulus test. The set up of the system is illustrated in Figure 1. For the diametral test, a temperature chamber was used for the control of the temperature. The data acquisition and modulus calculation were accomplished by a microcomputer that is connected to the testing system. Table 2 summarizes the test results for both projects. Actual temperatures at time of testing were recorded. The measured resilient modulus at 73°F and 95°F from Project 2 are much higher than those from Project 1 and also appear to be higher than those for conventional AC at the same temperature range. The cause of these higher moduli is not known. It is very likely that a stiff asphalt could have been used in this project.

The triaxial resilient modulus test on aggregate base material was performed by following AASHTO T-274. For Project 1, the moisture-density relationship for the aggregate base material was determined in accordance with the AASHTO T-99 Method C. The samples for the resilient modulus test were then prepared at the maximum density with the optimum moisture content. The actual moisture content at time of testing was slightly less than the optimum, indicating a slight loss of moisture during the testing. The density and actual mois-

**TABLE 2 Summary of Laboratory-Tested AC Resilient Modulus**

| Project | Sample ID | Resilient Modulus (ksi) | | |
|---|---|---|---|---|
| | | 42°F | 73°F | 95°F |
| 1 | 1-1 | 2,521 | 477 | 183 |
| | 1-2 | 2,886 | 834 | 516 |
| | 1-3 | 3,563 | 728 | 538 |
| | 1-4 | 2,316 | 848 | 601 |
| | 1-5 | 2,733 | 624 | 262 |
| | 1-6 | 3,441 | 718 | 404 |
| | 1-7 | 2,536 | 811 | 560 |
| | 1-8 | 2,054 | 654 | 159 |
| | Average | 2,756 | 712 | 403 |
| | STD | 491 | 117 | 167 |
| 2 | 2-1 | 2,874 | 1,634 | 792 |
| | 2-2 | 2,673 | 1,296 | 469 |
| | 2-3 | 2,898 | 1,725 | 841 |
| | 2-4 | 2,262 | 1,373 | 515 |
| | 2-5 | 2,723 | 1,384 | 696 |
| | 2-6 | 2,369 | 1,482 | 602 |
| | 2-7 | 2,794 | 1,678 | 715 |
| | 2-8 | 2,794 | 1,754 | 752 |
| | Average | 2,674 | 1,541 | 673 |
| | STD | 219 | 167 | 124 |

ture content were measured right after the triaxial test and are summarized in Table 3. Resilient modulus test results for both samples are plotted in Figure 2. The test results from this project indicate that for the same material the resilient modulus values increase proportionally to the sample density.

For Project 2, the samples were prepared at the field moisture condition. The aggregate materials were delivered to the laboratory directly from the field, and samples were made immediately. Four samples were made and similar compaction efforts were applied to each sample. Table 4 presents the moisture content and density results that were measured immediately after the modulus testing, whereas the resilient modulus test results are summarized in Figure 3. The test results from this project seem to indicate that for the same material, when compacted with similar effects, the relationship between the modulus and bulk stress would be similar.

## Comparison of Backcalculated and Laboratory-Tested Resilient Moduli

For AC material, comparisons between the backcalculated and laboratory-tested results are provided in Figures 4 and 5. The comparisons show that for asphalt concrete, the backcalculated moduli are generally lower than the laboratory-tested moduli and also seem to be less susceptible to tem-

**TABLE 3 Density Results, Project 1**

| Sample ID | Optimum Moisture (%) | Maximum Dry Density (pcf) | Actual Moisture (%) | Actual Dry Density (pcf) | Relative to Max Density (%) |
|---|---|---|---|---|---|
| A | 5.2 | 136.6 | 5.1 | 136.3 | 99.8 |
| B | 5.2 | 136.6 | 5.0 | 131.3 | 96.1 |

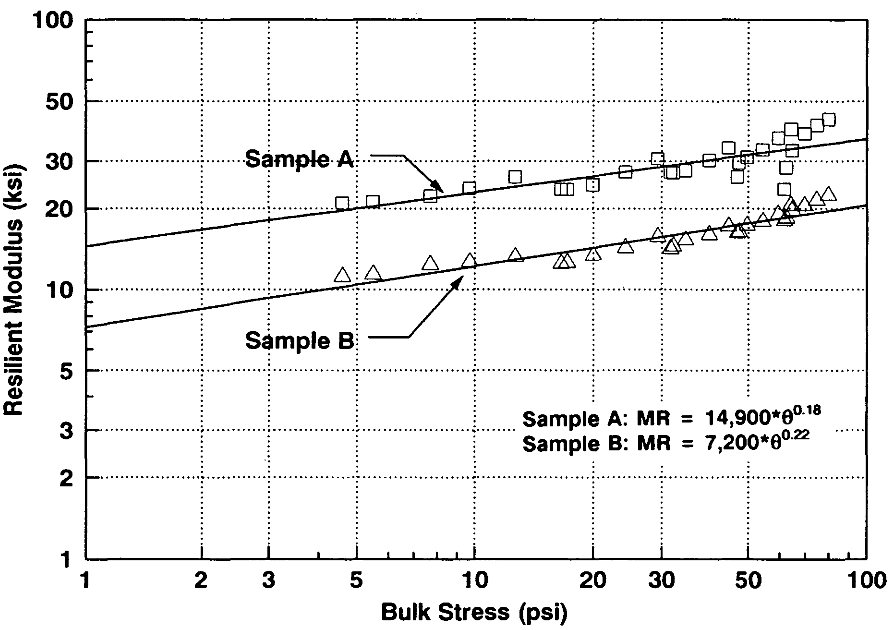


**FIGURE 2 Laboratory-tested moduli for Project 1.**

**TABLE 4 Density Results, Project 2**

| Sample ID | Moisture Content (%) | Dry Density (pcf) |
|---|---|---|
| A | 5.3 | 125.0 |
| B | 4.8 | 126.0 |
| C | 7.7 | 121.8 |
| D | 6.7 | 124.3 |

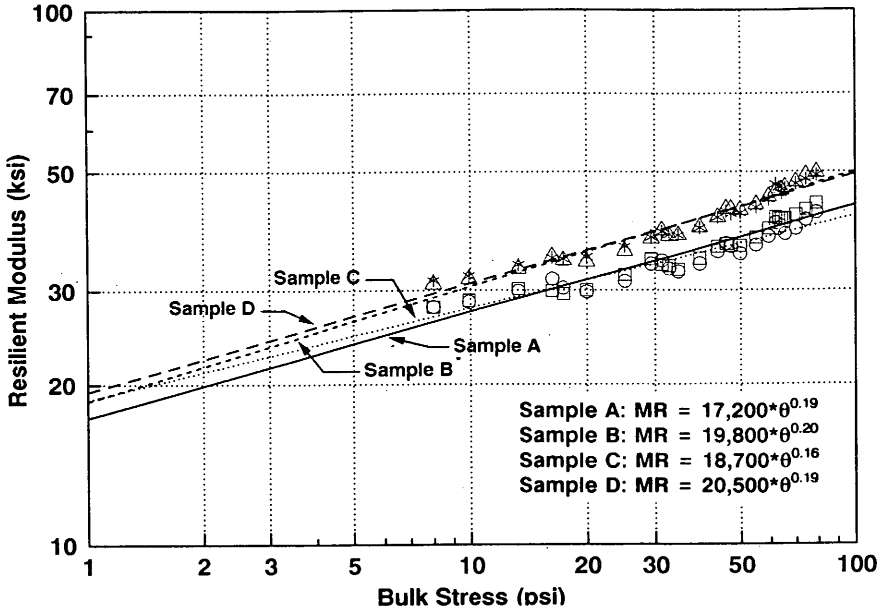


**FIGURE 3** Laboratory-tested moduli for Project 2.

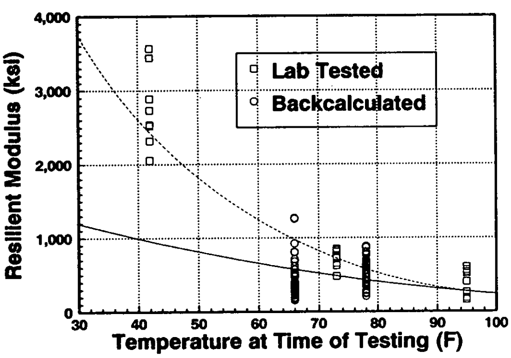


**FIGURE 4** Comparison between laboratory-tested and backcalculated AC moduli, Project 1.

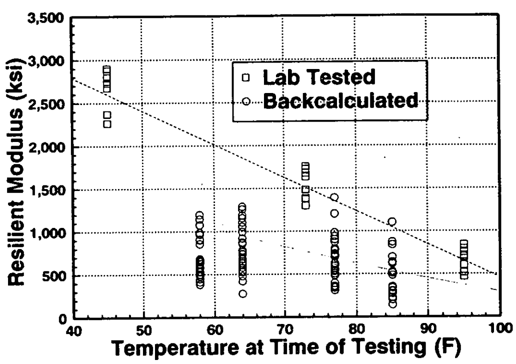


**FIGURE 5** Comparison between laboratory-tested and backcalculated AC moduli, Project 2.

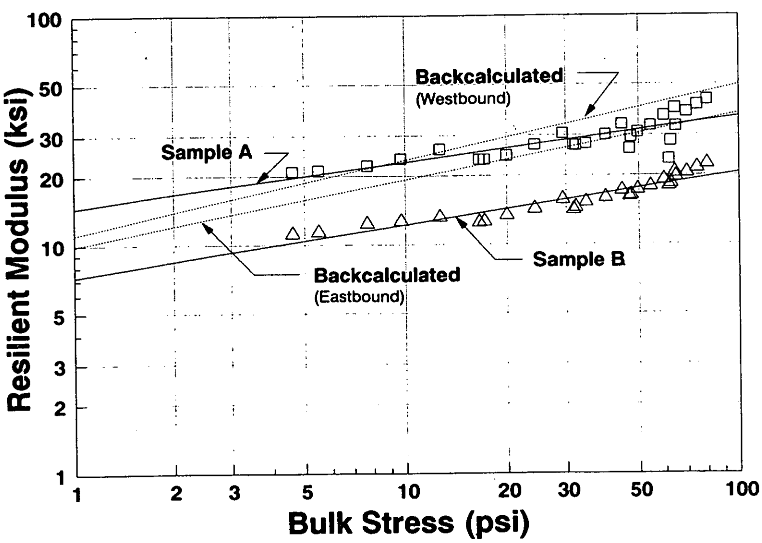


**FIGURE 6** Comparison between laboratory-tested and backcalculated base moduli, Project 1.

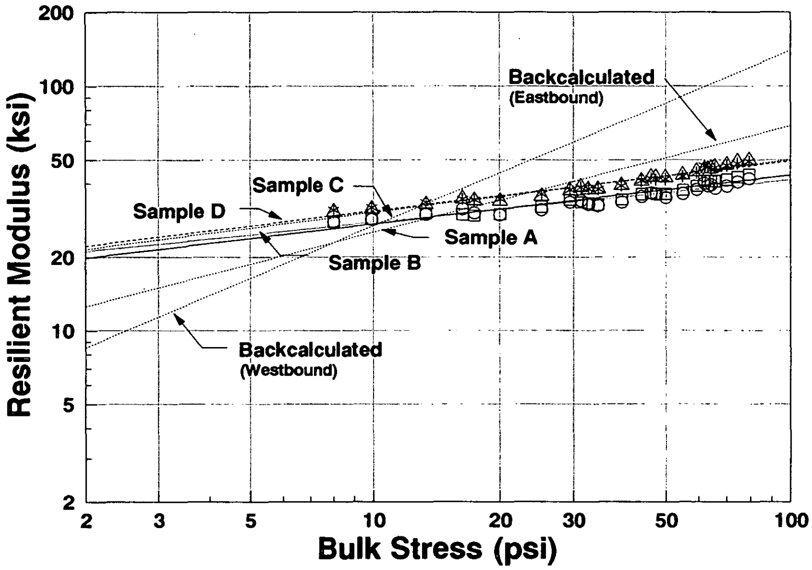


**FIGURE 7 Comparison between laboratory-tested and backcalculated base moduli, Project 2.**

perature variation. At the same temperature, the average difference can be expected to be 20 to 30 percent. The existing pavements had moderate to extensive cracking; these factors may contribute to the lower backcalculated AC moduli.

The difference may also result from the method used in moduli determination. The backcalculated AC moduli are more of a weighted average value for an entire layer, whereas the laboratory-tested moduli, which were measured on intact surface cores, are more representative of resilient modulus of the specimen. If the cores were taken from an uncracked portion of the AC layer and were of good quality, a higher resilient modulus would be expected. However, this may not truly reflect the entire AC layer material property. For the aggregate base material, the backcalculated modulus slope ($k_2$) is slightly higher than the laboratory-tested moduli, as can be seen in Figures 6 and 7. However, in the range of bulk stress in which actual pavement stresses generally fall (e.g., 5 to 20 lb/in.$^2$), a favorable comparison can be found.

## DEVELOPMENT OF DESIGN INPUTS FOR OVERLAY DESIGN

### Pavement Layer Moduli

The backcalculated moduli represent the pavement material properties corresponding to the temperature at the time of deflection testing. These modulus values may be converted to a standard design temperature or to other temperatures to consider temperature effects, similar to seasonal effects, on the pavement materials. For this study an attempt was made to consider environmental effects on the two projects. To do so, a representative temperature for each season was determined on the basis of local weather data. This representative temperature as used in this study was an average temperature for each season. The pavement temperatures used for characterizing the material properties within each season are presented in Table 5, along with modulus values corrected for

**TABLE 5 Representative Temperature and Corresponding Modulus**

| Project | Description | Spring | Summer | Fall | Winter |
|---|---|---|---|---|---|
| 1 | Temperature (°F) | 49 | 70 | 48 | 37 |
| | AC modulus (ksi) | 872<br>(0.50)[1] | 436<br>(1.00) | 908<br>(0.48) | 1,282<br>(0.34) |
| | Base modulus (ksi) | 20[2] | 26 | 27[2] | 20[2] |
| | Subgrade modulus (ksi) | 15[2] | 21 | 21[2] | 15[2] |
| 2 | Temperature (°F) | 50 | 64 | 49 | 42 |
| | AC modulus (ksi) | 1,240<br>(0.52) | 777<br>(0.83) | 1,290<br>(0.50) | 1,573<br>(0.41) |
| | Base modulus (ksi) | 44 | 50[2] | 45[2] | 40[2] |
| | Subgrade modulus (ksi) | 15 | 20[2] | 21[2] | 16[2] |

[1] Conversion Factor relative to 70°F (from Figure 6). For Project 1, modulus at 70°F is 436 ksi. For Project 2, modulus at 70°F is 645 ksi.

[2] Adjusted based on backcalculated results for considering seasonal effects.

temperature for the asphalt concrete. The resilient modulus for each season was determined by adjusting the backcalculated asphalt concrete modulus to the corresponding temperature, using a relationship shown in Figure 8. The modulus values at various temperatures may also be determined from either the laboratory-tested or the backcalculated results, as shown in Figures 4 and 5. For this study, the laboratory-tested moduli at the same temperatures appear to be high, whereas the backcalculated moduli are more close to those from using the relationship shown in Figure 8.

It should be noted that engineering judgment may be necessary to determine what moduli to be used in the overlay design. In this study, the base moduli were adjusted on the basis of the backcalculated modulus-bulk stress relationship and anticipated pavement stresses. For subgrade, because the soil is not stress sensitive, a single value determined from backcalculation was used. Variation of moisture content in base and subgrade was also a factor considered in developing the layer moduli for each season. In Oregon, summer and fall seasons are much dryer than winter and spring. It was assumed that moisture condition in the base and subgrade would be slightly dryer in summer and fall; therefore, slightly higher moduli were used. If the deflections were measured and moduli were backcalculated for each season, the resilient moduli determined could be directly used in overlay design.

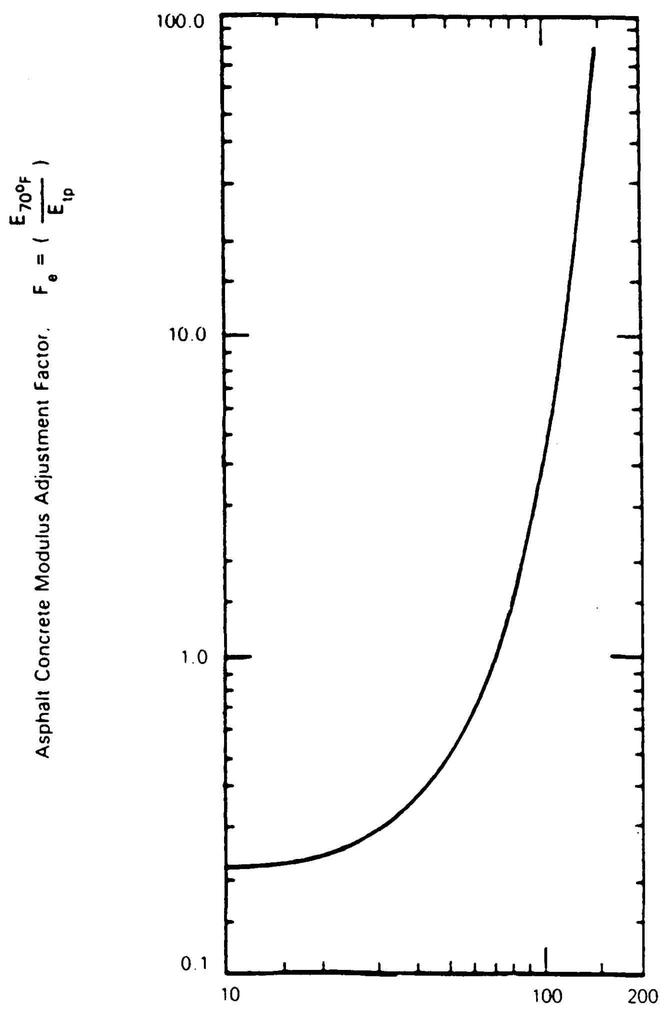


**FIGURE 8 Asphalt modulus temperature adjustment factor.**

### Traffic Data

Projected traffic repetitions were expressed in terms of 18-kip equivalent axial loads (EALs). It is ideal if the historical traffic data are available. These data may help the designer evaluate the remaining life of an existing pavement before an overlay. However, the historic traffic data are usually difficult to obtain. In this study, the historic traffic applications were unknown; therefore, the remaining life of the pavements was not evaluated.

Traffic data for both projects was furnished by the Oregon State Highway Division (OSHD) traffic section. The data came from a 16-hr manual count taken in 1988 and projected for a 20-year design period. The traffic applications were then broken down for each season. The length of each season was determined on the basis of the location of the project.

### Overlay Design Using Mechanistic Approach

After establishing the appropriate inputs for overlay design, a mechanistic design program, MECHOD (MECHanistic Overlay Design), was used to determine the thickness of overlay. The MECHOD program was developed at Oregon State University (*5*). The program uses ELSYM5 as its subroutine to calculate critical strains at the bottom of AC layer and on the top of subgrade (*6*). The strains were then used to evaluate fatigue and the subgrade rutting using the relationships developed by Finn and Monismith (*7*) and The Asphalt Institute (*8*), respectively. In MECHOD, pavement damage for each season is determined and the total pavement damage for all seasons in the analysis is summed. The inputs required to run MECHOD included design load, load radius, moduli, and Poisson ratios for each pavement layer, number of seasons in analysis, and historical and projected traffic applications for each season. The modulus value of overlay material and projected traffic applications for each season are presented in Table 6. The modulus values were determined using the representative temperature data shown in Table 5.

During calculation, the MECHOD program first uses the given data to evaluate the existing pavement. If an overlay is needed, on the basis of total pavement damage, the program would ask for the modulus of overlay material. For these two projects, an overlay modulus value of 450 ksi (at 70°F), was used.

The overlay thickness design is an iterative process. For practical purposes, an initial overlay thickness of 1 in. is used in the MECHOD program, with a ½-in. increment for each iteration. The process is repeated until the total pavement damage is less than unity. The design results for the two projects are summarized in Table 7. Total pavement damage for both fatigue and subgrade rutting is also presented in the table. These values indicate that after 20 years of service, the traffic loadings would consume a certain percentage of the

**TABLE 6 Inputs for Overlay Design**

| Project | Description | Spring | Summer | Fall | Winter |
|---|---|---|---|---|---|
| 1 | Traffic | 4,526,428 | 11,275,413 | 4,526,428 | 6,776,089 |
| | Length of season (mon.) | 2[1] | 5 | 2 | 3 |
| | % distribution | 16.7[2] | 41.6 | 16.7 | 25.0 |
| | Overlay modulus (ksi) | 900 | 450 | 938 | 1,324 |
| 2 | Traffic | 1,151,132 | 1,533,307 | 768,956 | 1,151,132 |
| | Length of season (mon.) | 3 | 4 | 2 | 3 |
| | % distribution | 25.0 | 33.3 | 16.7 | 25.0 |
| | Overlay modulus (ksi) | 865 | 542 | 900 | 1,098 |

Note: Poisson's ratio was assumed to be 0.35 for AC material for all seasons.

**TABLE 7 Overlay Design Results, MECHOD**

| Project | Overlay Thickness (in) | Total Pavement Damage (%) | |
|---|---|---|---|
| | | AC Fatigue | Subgrade Rutting |
| 1 | 4 | 96.5 | 2.2 |
| 2 | 2 | 98.3 | 11.3 |

design life of the pavement. For the projects evaluated, the results show that fatigue damage in the asphalt concrete layer will be a major concern, over 95 percent, whereas the rutting in the subgrade is not significant, less than 12 percent, after overlay is placed. This analysis used a reliability level of 50 percent because ODOT's present overlay design procedure does not take reliability into consideration during overlay design.

### Overlay Design Using ODOT Procedure

The present procedure used to determine overlay requirements in Oregon is based on deflection measurements of the existing pavement (*9*). The design procedure is essentially that of the California Department of Transportation, with modifications for Oregon's Traffic and Crushed Base Equivalencies. The procedure suggests that tolerable deflection is a function of traffic and pavement thickness and that additional overlay thickness will reduce measured deflection. The deflections can be measured using either an FWD or the Dynaflect test equipment. Deflections are typically measured every 250 ft within a section. The measured deflections are normalized to an equivalent deflection for a 9,000-lb load at 70°F. For deflections measured using the FWD, the equivalent deflections are determined by interpolating between the deflections measured at loads above and below 9,000 lb. The equivalent deflections are adjusted to account for the in-place pavement temperature. This adjustment is a function of both the pavement temperature at the time the deflections were measured and the thickness of the existing AC layer. For an AC layer greater than 6 in., this procedure does not recommend temperature correction. For an AC layer less than 6 in., the equivalent deflections are multiplied by the temperature correction factor to establish the final normalized deflection.

The normalized deflection is determined for each location where deflections were measured. Statistical analysis is performed to determine average and standard deviation. The 80th-percentile deflection was then calculated and used as a design value to determine the overlay thickness. The 80th-percentile deflection is computed using the equation

$$D_{80} = X + 0.84 * S$$

where

$D_{80}$ = design deflection value (80th-percentile deflection),
$X$ = mean deflection, and
$S$ = standard deviation of deflections.

The 80th-percentile deflection was then compared with a tolerable deflection, which is a function of future equivalent axle load repetitions and the thickness of the in-place pavement. If the 80th-percentile deflection is less than the tolerable deflection, then an overlay is not needed. If the 80th-percentile deflection is greater than the tolerable deflection, then the percentage reduction in deflection is calculated as

$$\% \text{ reduction} = 100 * (D_{80} - D_t)/D_{80}$$

where $D_t$ is tolerable deflection. The value of percent reduction is used to determine the crushed base equivalence factor, meaning the 1-in.-thick asphalt concrete is equivalent to a certain thickness of gravel. The equivalent factor ranges from 1.52 to 2.5. A factor of 2.0 is used by ODOT for overlay design. The determined overlay thicknesses using the ODOT method is summarized in Table 8.

### Comparison of Overlay Design Results

The comparison of design results, presented in Tables 7 and 8, indicated that both procedures recommended similar overlay thicknesses. These results may indicate that for these two projects the backcalculated layer moduli are reasonable and can be used in mechanistic approach for overlay design purposes. The basis for this statement is that the two procedures

**TABLE 8 Overlay Design Results, ODOT Procedure**

| Project | $D_{80}$ (mils) | $D_t$ (mils) | % Deflection Reduction | Overlay Thickness (in) |
|---|---|---|---|---|
| 1 | 14.1 | 8.0 | 43.3 | 3 |
| 2 | 22.1 | 14.0 | 36.8 | 2 |

yield similar overlay results. The final recommendation for rehabilitation treatment would be determined on the basis of both the required overlay thickness and the existing pavement condition.

## FUTURE ACTIVITIES

Implementation of a backcalculation technique to determine pavement layer properties and the use of the backcalculated layer moduli in overlay design provide the practicing engineers a useful tool in understanding and characterizing pavement materials properties. For the state agency, because of the need of future rehabilitation activities, a cost-effective method for determining the structural capacity of existing pavements will provide a tremendous benefit in developing rehabilitation strategies. ODOT has recently purchased a new FWD made by Dynatest, Inc. This equipment has the capacity to obtain a large amount of deflection data quickly; this demands a means to evaluate these data. To automate the backcalculation process and analyze as many test data as possible, the BOUSDEF program is being modified to meet the demand by providing two options: one option allows the engineer to analyze a single set of deflection basin data as it does now and the other to directly access the FWD machine output and consequently perform backcalculation analysis. It is envisioned that this modification should significantly reduce the amount of time needed for the data entry process and provide considerable amount of information for pavement evaluation. It is hoped that with the availability of more information, a better assessment of pavement layer materials can be achieved.

## CONCLUSIONS AND RECOMMENDATIONS

This paper has described the implementation of the backcalculation technique and the use of backcalculated results in pavement overlay design in Oregon. The results of the two projects appeared very promising and encouraging. The overlay design results from both the mechanistic approach and the ODOT method were very close, implying that the backcalculated moduli provided a reasonable estimate of the existing pavement layer properties. This conclusion is preliminary and is based on the results from these two projects. Further study on more projects may be necessary to evaluate the reasonableness of the backcalculated pavement layer moduli. In addition, other overlay design procedures may be used to verify the reasonableness of the designed overlay thicknesses.

As a recommendation, backcalculation on deflection basin data should be performed on as many test data as possible. This would avoid biased backcalculation results from using a single test datum. To consider seasonal effects on pavement layer properties, it is recommended that deflection testing be performed for each season and that the deflection data be backcalculated for layer moduli. Finally, limited laboratory tests also should be performed. These tests would provide necessary information for the engineer to verify the backcalculated results and increase the confidence in determining modulus values to be used in pavement design.

## REFERENCES


1. H. Zhou, R. G. Hicks, and C. A. Bell. BOUSDEF: A Backcalculation Program for Determining Moduli of a Pavement. In *Transportation Research Record 1260*, TRB, National Research Council, Washington, D.C., 1990.
2. O. Tholen. *Falling Weight Deflectometer: A Device for Bearing Capacity Measurements: Properties and Performance*. Department of Highway Engineering, Royal Institute of Technology, Stockholm, Sweden, 1980.
3. O. Tholen, J. Sharma, and R. Terrel. Comparison of Falling Weight Deflectometer with Other Deflection Testing Devices. In *Transportation Research Record 1007*, TRB, National Research Council, Washington, D.C., 1985, pp. 20–26.
4. H&V Materials and Development Inc. Resilient Modulus Repeated Load Test System. *Proc., Workshop on Resilient Modulus Testing*, Oregon State University, Corvallis, March 1989.
5. R. G. Hicks, H. Zhou, and B. Connor. *Development of an Improved Overlay Design Procedure for the State of Alaska*, Vol. 3, Field Manual. Report FHWA-AK-RD-88-06B, FHWA, 1989.
6. R. G. Hicks. Use of Layered Theory in the Design and Evaluation of Pavement Systems. Report FHWA-AK-RD-83-8, July 1982.
7. F. N. Finn and C. L. Monismith. *NCHRP Synthesis of Highway Practice 116: Asphalt Overlay Design Procedures*. TRB, National Research Council, Washington, D.C., Dec. 1984.
8. *Research and Development of the Asphalt Institute's Thickness Design Manual (MS-1)*, 9th ed., Research Report 82-2. The Asphalt Institute, Aug. 1982.
9. *Flexible Pavement Design Procedure*. Oregon State Highway Division, 1951.

# Rapid Determination of Layer Properties of Pavements from Surface Wave Method

DEREN YUAN AND SOHEIL NAZARIAN

The spectral analysis of surface waves (SASW) method has been used as a nondestructive test method for determining elastic modulus profiles of pavement systems. To perform the test, a disturbance is applied to the pavement surface to generate stress waves that propagate mostly as surface waves of various wavelengths. The waves are monitored and captured with a data acquisition system. Signal and spectral analyses are used to determine a dispersion curve (variation in phase velocity with wavelength). The last step is to determine the elastic modulus of various layers from the dispersion curve. Several alternatives are available. First, a trial-and-error (forward modeling) process can be carried out. Second, optimization techniques can be used. Finally, generalized inverse theory can be implemented. In most applications, the backcalculation of layer moduli is accomplished using a manual trial-and-error matching process between the theoretical and experimental dispersion curves. Unfortunately, this process is rather time consuming and requires engineering judgment. To improve this aspect of SASW testing, a backcalculation technique that is based on the generalized inverse theory is developed. The technique provides a fast and automated procedure for simultaneously determining layer elastic moduli and thickness of pavements. In addition, some description of uncertainty in the backcalculated results is provided. The development of this algorithm is discussed and the speed and accuracy as well as the limitations of the algorithm are demonstrated. An actual field case history is included to exhibit the usefulness of the method in actual field testing.

As a nondestructive test method, the spectral analysis of surface waves (SASW) method has been used to determine elastic modulus profiles of pavements (*1,2*). The SASW method is based on the dispersive characteristic of seismic surface waves in layered media. To perform the test, three major steps are followed: (a) field testing, (b) determination of experimental dispersion curve, and (c) determination of stiffness profile.

The in situ testing consists of generating and detecting surface waves by affecting the surface of the pavement and monitoring and capturing the motion of the pavement surface at several points. The captured signals are manipulated using the Fourier and spectral analyses to determine the cross-power spectra and the coherence functions.

Determining the experimental dispersion curve consists of processing the cross-power spectra and the coherence functions to construct an experimental dispersion curve. This curve represents the dependence of phase velocity on frequency or wavelength.

Determining the elastic modulus profile from the experimental dispersion curve is the last but the most time-consuming and complicated step. This process is known as inversion or backcalculation. To accomplish this task, a manual trial-and-error (forward modeling) procedure has been successfully employed for years (*3*). A merit of the forward modeling procedure is that common sense notions can be incorporated into the trial-and-error stage. This, however, implies that a fairly experienced person is needed to conduct this task efficiently. Therefore, one of the major shortcomings of the procedure is probably the time required to reduce the data. To remedy this shortcoming, an automated procedure is desirable.

To turn the SASW method to a practical testing equipment, all aspects of testing and data reduction should be automated. A device for conducting the field tests rapidly (in about 1 min) is under development for SHRP (*4*, p. 128). An algorithm for automatically determining the dispersion curve has been developed by Desai (*5*). Finally, an automated backcalculation process has been developed and is described in this paper. The process, which is based on the general linear inverse theory (*6,7*), provides an automated algorithm for rapidly determining modulus profiles from dispersion curves. At the same time, the algorithm yields information needed for uncertainty analysis of backcalculated results. Synthetic (theoretically derived) data and actual case studies are included to illustrate some aspects of the strengths and limitations of the process.

## BACKGROUND

Any algorithm for determining the modulus profile of a pavement system from an experimental dispersion curve contains two fundamental components. First, a proper algorithm that is based on wave propagation theory is needed to construct a theoretical dispersion curve from a trial profile. Second, an algorithm is needed to minimize the error between the theoretical dispersion curve and the experimental one. Each step will be discussed.

Shown in Figure 1 is an idealized cross section of a pavement. To apply the theory of wave propagation to this pavement section, two major simplifying but realistic assumptions are usually made. First, it is assumed that only the in-plane waves (P- and SV-waves) are involved so that the problem can be approximated as a plane strain problem. Second, it is assumed that the system is composed of a stack of flat layers with homogeneous and isotropic properties and that each layer extends horizontally to infinity (as compared with the dimension of source-receiver configuration). The effects of these two assumptions either are minor (*8*) or can be minimized with proper setup in field testing (*9*). Because of these as-

Department of Civil Engineering, University of Texas at El Paso, El Paso, Tex. 79968.

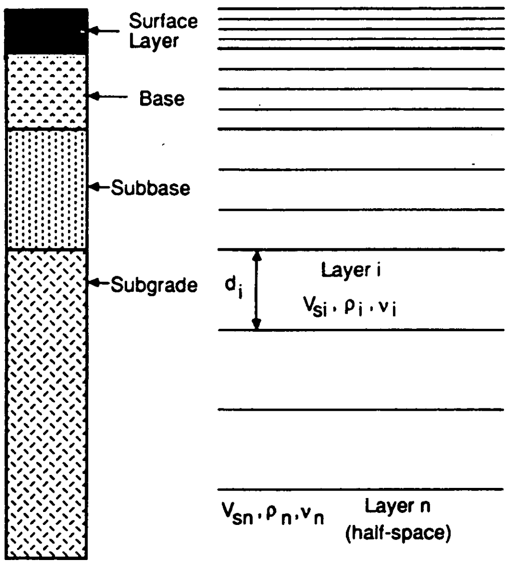


**FIGURE 1 Idealized profile of pavement system: *left*, traditionally assumed layering; *right*, sublayering assumed in SASW analysis.**

sumptions, the solution to the wave equation reduces to a simple two-dimensional problem in the Cartesian coordinate system.

With these assumptions, the parameters needed to define the properties of each layer are thickness ($h$), Young's modulus ($E$), Poisson's ratio ($\nu$), and mass density ($\rho$). Alternatively, Young's modulus can be replaced by shear or $S$-wave velocity ($V_s$). One way of demonstrating this relationship is

$$E - 2\rho V_s^2(1 + \nu) \quad (1)$$

Among these parameters, shear wave velocity (or Young's modulus) has the dominant effect on the dispersion characteristics of surface waves, and the effects of density and Poisson's ratio are rather small. Nazarian has numerically shown that the effects of these two parameters, in most practical cases, are less than 5 percent (*3*). Therefore, to simplify the inversion process, one can assume that density and Poisson's ratio for each layer are known parameters. Reasonable values can be assigned to these parameters on the basis of past experience. Shear wave velocity of each layer is the only active pavement strength parameter that should be backcalculated.

To estimate layer thicknesses, two procedures can be followed. They can be either assumed to be known or backcalculated. If layer thicknesses are assumed as known parameters, it is necessary to include many layers (on the order of 10) in the trial profile to minimize the biased effect of interfaces on resulting profile. This is necessary because the interpretation of layer thickness is done by determining layer interfaces with significant modulus contrast. If both thicknesses and moduli need to be simultaneously determined, only a few (on the order of five) layers will be required.

## THEORETICAL DISPERSION CURVE

In the development of the theory of surface waves and its application to determining shear wave velocity or stiffness profiles, much attention has been paid to the situation in which velocity or stiffness generally increases with depth. This situation typically covers most geophysical and geotechnical investigations. However, for the reverse case, such as pavements, where modulus decreases with depth, very limited theoretical analyses have been made. These analyses are mainly reflected in the works of Jones (*10*), Vidale (*11*), and Nazarian (*3*). Therefore, it is thought that a brief discussion regarding the characteristic and computation of dispersion for pavements is necessary.

Dispersion curves for soil deposits demonstrate a continuous relationship between phase velocity and frequency; that is, phase velocity is a continuous function of frequency or wavelength. In the contrary, a characteristic of the theoretical dispersion curve for a layered system resembling a pavement structure is that the curve is composed of multiple branches or limbs (see Figure 2, which is based on a Poisson's ratio of 0.25).

The existence of discontinuities in dispersion curves was first recognized by Sezawa and Kanai (*12*). On the basis of both theoretical analyses and actual observations, Jones (*10*) and Vidale (*11*) reported this characteristic of dispersion curves for pavement constructions.

To apply properly any analytical backcalculation technique, the theoretical dispersion curve should be very accurately determined. Several methods have been suggested for the computation of the theoretical dispersion curve. These methods include transfer matrix method (*13,14*), stiffness matrix method (*15*), finite element method (*16*), and finite difference method (*17*). However, the results from most of these methods in original form (as applied to pavement systems) face problems with accuracy or with numerical difficulties, or both.

In the work presented in this paper, the transfer matrix method as modified by Dunkin (*18*) has been chosen to calculate the theoretical dispersion curves. This method was selected because of its flexibility and potential accuracy. The computer program used is based on the major routines of program INVERT developed by Nazarian (*3*) with major im-

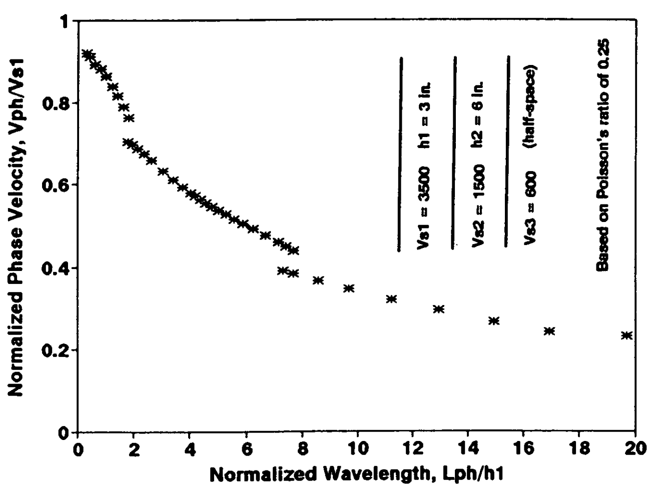


**FIGURE 2 Theoretical dispersion curve for typical pavement section.**

provements in mode isolation and root refinement. These refinements are discussed elsewhere (*3*) and are omitted from here for brevity.

## INVERSION PROCESS

### Description of Problem

Let us assume that a series of SASW tests has been carried out on a pavement section with $M$ assumed layers. As a result, an experimental dispersion curve containing $N$ data points has been constructed; that is, at each frequency, $f_i$, phase velocity, $V_i^{\text{obs}}$, is determined. To initiate the backcalculation process, an initial shear wave velocity profile, $\mathbf{p}^0$, is assumed. Mathematically, $\mathbf{p}^0$ is a vector whose elements, $p_j^0$, contain the shear wave velocity and thickness of each layer. The initial profile $\mathbf{p}^0$, is then used to determine the theoretical phase velocity, $V_i^{\text{thr}}$, at each frequency, $f_i$. The goal is to determine a vector $\mathbf{p}^f$ that minimizes the difference between the theoretical and observed data.

The inversion process can be categorized as a nonlinear problem with respect to the unknowns to be determined. To simplify the procedure, the problem is linearized. As a result, several iterations are necessary before the final profile is obtained. This procedure is defined below.

The initial profile, $\mathbf{p}^0$, is used to calculate the theoretical phase velocity, $V_i^{\text{thr}}$, and the partial derivatives, $\partial V_i^{\text{thr}}/\partial p_j^0$, at each frequency. The governing equations of the inversion problem can then be expressed as

$$V_i^{\text{obs}} - V_i^{\text{thr}} = \sum_{j=1}^{K} \frac{\partial V_i^{\text{thr}}}{\partial p_j} \Delta p_j \qquad i = 1, \ldots, N \tag{2}$$

or in matrix form

$$\mathbf{A}\Delta\mathbf{p} - \Delta\mathbf{c} \tag{3}$$

where

$\Delta\mathbf{c}$ = $(\Delta c_1, \Delta c_2, \ldots, \Delta c_N)^T$ where $\Delta c_i = V_i^{\text{obs}} - V_i^{\text{thr}}$;

$\Delta\mathbf{p}$ = $(\Delta p_1, \Delta p_2, \ldots, \Delta p_K)^T$ is defined as a correction or modification vector that is added to vector $\mathbf{p}^0$ to determine the vector of unknowns $\mathbf{p}^i$ for the next iteration. In the vector, $K$ equals $M$, if layer thicknesses are assumed to be fixed, and $2M - 1$, if both shear wave velocity and thickness of each layer need to be determined simultaneously; and

$\mathbf{A}$ = $N$-×-$K$ matrix of partial derivatives whose elements $A_{ij} = \partial V_i^{\text{thr}}/\partial p_j^0$.

Vector $\mathbf{p}^i$ considered as the solution to the unknowns when it yields a vector $\Delta\mathbf{c}$ in Equation 3 that is sufficiently small. This is elaborated in the next section.

The choice of the number of experimental dispersion data points (parameter $N$) depends on the quality of the field data and the number of layers (parameter $M$) in the trial profile. In practice, it is assumed that $N$ (number of dispersion data points) is greater than $K$ (number of unknowns). Thus, the problem defined by Equation 3 is overconstrained. Typically, parameter $N$ is limited to 20 to 40 data points. As indicated before, parameter $M$ is limited to about five layers when both thickness and stiffness should be determined and is about 10 when only stiffness has to be determined.

### Construction of Shear Wave Velocity Profile

In general, Equation 3 cannot be solved through calculating the conventional inverse of matrix $\mathbf{A}$, $\mathbf{A}^{-1}$. Matrix $\mathbf{A}^{-1}$ exists only if $\mathbf{A}$ is square and nonsingular. An approach to solving Equation 3 is to construct its normal or Gaussian-Newton equation. This results in the classical least-squares solution

$$\Delta\mathbf{p} = (\mathbf{A}^T A)^{-1}\,\mathbf{A}^T\Delta\mathbf{c} \tag{4}$$

subject to minimization of $(\Delta\mathbf{c} - \mathbf{A}\Delta\mathbf{p})^T(\Delta\mathbf{c} - \mathbf{A}\Delta\mathbf{p})$ with respect to $\Delta\mathbf{p}$. This solution is also known as the optimization solution.

The computation of matrix $\mathbf{A}^T\mathbf{A}$ may involve numerical inaccuracy that can be troublesome when the number of dispersion data or the number of layers is large. To avoid this drawback, the singular value decomposition of a matrix (*19*) approach has been used to develop the generalized inverse solution of Equation 3.

The decomposition of matrix $\mathbf{A}$ leads to a product of three matrices

$$\mathbf{A} = \mathbf{U}\mathbf{S}\mathbf{V}^T \tag{5}$$

where

$\mathbf{U}$ = $N$-×-$K$ matrix whose columns are eigenvectors, $\mathbf{u}_j$ ($j = 1, \ldots, K$), of length $N$ associated with the columns (observations) of $\mathbf{A}$,

$\mathbf{V}$ = $K$-×-$K$ matrix whose columns are eigenvectors, $\mathbf{v}_j$ ($j = 1, \ldots, K$), of length $K$ associated with the rows (parameters) of $\mathbf{A}$, and

$\mathbf{S}$ = $K$-×-$K$ diagonal matrix with diagonal entries, $s_{jj}$ ($j = 1, \ldots, K$), which are the nonnegative square roots of the eigenvalues of symmetric matrix $\mathbf{A}^T\mathbf{A}$ and known as the singular values of $\mathbf{A}$.

By substituting Equation 5 into Equation 4 and utilizing the orthonormal property of $\mathbf{U}$ and $\mathbf{V}$ [i.e., $\mathbf{U}^T\mathbf{U} = \mathbf{V}^T\mathbf{V} = \mathbf{V}\mathbf{V}^T = \mathbf{I}$ (unit matrix)], it is easy to show that

$$\Delta\mathbf{p} = \mathbf{V}\mathbf{S}^{-1}\mathbf{U}^T\Delta\mathbf{c} \tag{6}$$

This expression gives the generalized inverse solution of Equation 3.

Adding $\Delta\mathbf{p}$ to $\mathbf{p}_0$ yields an updated profile from which a new set of phase velocities and a new set of partial derivatives can be calculated. This procedure is repeated until $\Delta c_i$'s (elements of vector $\Delta\mathbf{c}$ described in Equation 3) are "sufficiently small." At this time, a profile that satisfies the given data is found. The term sufficiently small is defined in the next paragraph.

The convergence of successive iterations is monitored by the following root-mean-squares (*RMS*) error criterion:

$$\varepsilon = \sqrt{\frac{1}{N}\sum_{i=1}^{N} \Delta c_i} \tag{7}$$

The iteration procedure is terminated when $\varepsilon$ reaches an acceptably small value or when all elements of vector $\Delta\mathbf{c}$ are within the standard error bounds of each experimental datum or other prespecified limits.

In many applications, a physically acceptable shear wave velocity profile cannot be determined from Equation 6 because of the lack of numerical stability; that is, a small change in the data can lead to unacceptably large changes in the derived profile. The remedy to this problem is as follows.

Let us rewrite Equation 6 in the from of a linear combination or weighted sum of eigenvectors, $\mathbf{v}_j$,

$$\Delta\mathbf{p} = \sum_{j=1}^{K} \frac{\mathbf{u}_j^T\Delta\mathbf{c}}{s_j}\mathbf{v}_j \tag{8}$$

Vectors $\mathbf{v}_j$ are finite in magnitude and increasingly oscillatory as $j$ increases. Hence, the stability of the solution is controlled by the magnitude of $\mathbf{u}_j^T\Delta\mathbf{c}/s_{jj}$. As $j$ increases, $s_{jj}$ becomes significantly smaller than $\mathbf{u}_j^T\Delta\mathbf{c}$. This can result in very large numbers, which can cause instability in the solution. To remedy this instability, the singular value decomposition algorithm has been combined with Marquardt's technique as described by Jupp and Vozoff (*20*). In this approach, $s_{jj}$ in Equation 8 is replaced by $(s_{jj} + \gamma/s_{jj})$. The solution can then be written as

$$\Delta\mathbf{p} = \sum_{j=1}^{K} \frac{s_{jj}}{s_{jj}^2 + \gamma}\mathbf{u}_j^T\Delta\mathbf{c}\mathbf{v}_j \tag{9}$$

where $\gamma$ is a "small" (in comparison with the largest singular value) positive number. Parameter $\gamma$, known as Marquardt's factor, dampens or eliminates the undesirable effects that small singular values can have on the solution.

### Evaluation of Uncertainty

In addition to the representative shear wave velocity profile, the level of uncertainty associated with each unknown parameter is determined. To evaluate uncertainty in the profile, the variance or standard error associated with each parameter is determined according to the statistics of experiment errors (*7*). The stability constraints shown in Equation 9 have to be taken into account. The variance of each parameter can then be estimated through the following formulation:

$$\mathrm{var}[\Delta\mathbf{p}_j] = \sigma^2 \sum_{k=1}^{K} \left[ V_{jk}\frac{s_k}{(s_k^2 + \gamma)} \right]^2 \tag{10}$$

where $V_{jk}$ are the elements of matrix $\mathbf{V}$, and $\sigma^2$ is associated with the random errors in the experimental data. The approximate value of $\sigma^2$ is given by Draper and Smith (*21*):

$$\sigma^2 = \frac{1}{N - K}(\Delta\mathbf{c} - \mathbf{A}\Delta\mathbf{p})^T(\Delta\mathbf{c} - \mathbf{A}\Delta\mathbf{p}) \tag{11}$$

The square root of each variance gives the standard error for the corresponding profile parameter.

The uncertainties obtained are caused by only the random error in the field data. Other factors, such as errors in the assumed profile (Poisson's ratio and mass density), simplifying assumptions in the algorithm, and systematic errors in the observed data, cannot be included. Therefore, these estimates should be considered as the lower limits of the level of uncertainty.

## PARAMETRIC STUDY

In this section, results from the analysis of a set of "synthetic" (theoretically determined) dispersion data are presented to illustrate the applicability and limitation of the inversion process presented. The dispersion data correspond to a three-layer pavement section. The profile consists of 3 in. of asphalt concrete (AC) (shear wave velocity of 3,000 ft/sec), over 6 in. of high-quality base (shear wave velocity of 2,000 ft/sec), over subgrade (shear wave velocity of 1,000 ft/sec). A Poisson's ratio of 0.33 and a uniform mass density were assigned to each layer.

Twenty-one data points were theoretically calculated using the pavement properties described above. These dispersion data were then input into the inversion program to backcalculate the shear wave velocity profile.

As the dispersion data are theoretically calculated, they are not contaminated with systematic errors or random scatter usually contained in the field data. The same theoretical algorithm used for calculating the dispersion curve was used as a subroutine in the inversion program. In addition, the exact properties of each layer are known. As such, any differences between the real and backcalculated profiles are a result of the weaknesses of the inversion algorithm.

Various seed profiles were used to examine the convergence in each simulation. In most instances, the same results were achieved. However, a reasonable setup of initial profile is important to reduce the computation time. In the remainder of this section, several different testing scenarios are considered and studied. In almost all cases, the final results were obtained in less than 1 min using an 80386-based 20-MHz personal computer.

### Simulation 1

In Simulation 1, it was assumed that the number and thicknesses of layers were known. Only shear wave velocity for each layer had to be determined. The initially assumed (seed) and the backcalculated profiles are shown in Table 1. The backcalculated profile is identical to the true profile. The "observed" (the synthetic dispersion is called that for simplicity) and the "final" (refers to the dispersion curve obtained

**TABLE 1 True, Seed, and Backcalculated Values of Shear Wave Velocities, Simulation 1**

| Layer Number | Thickness(in.) | Shear Wave Velocity (fps) | | |
|---|---|---|---|---|
| | | True | Seed | Backcalculated |
| 1 | 3.0 | 3000. | 2500. | 3000. |
| 2 | 6.0 | 2000. | 1500. | 2000. |
| 3 | ∞ | 1000. | 500. | 1000. |

Data Misfit (%): Min. = 0.0, Max. = 0.0, Average = 0.0

from the profile after the completion of inversion) dispersion curves are compared in Figure 3. For each data point at a given wavelength, the percent data misfit is calculated by simply determining the relative errors between the observed and final dispersion data, $\Delta c_i/V_i^{obs}$. The maximum, minimum, and average misfit among the 21 data points are also given in Table 1. The complete convergence in data matching after backcalculation demonstrates the effectiveness and accuracy of the process.

The same exercise with the same trial profile but using less (eleven and nine) observed data points were repeated. The results obtained were the same as those given in Table 1.

**Simulation 2**

In Simulation 2, it was assumed that only the number of layers was known. Shear wave velocity for each layer was backcalculated with the arbitrarily fixed layer thicknesses. The seed and backcalculated profiles are shown in Table 2. At a first sight, the differences between the true and backcalculated shear wave velocities may seem small. However, as indicated before, the dispersion data used in the inversion process are "accurate" (i.e., error- and scatter-free). Therefore, the differences are rather significant. This emphasizes that, similar to any other nondestructive deflection testing (NDT) method, to obtain an accurate stiffness profile, the thickness of the layers should be accurately known.

The observed and final dispersion data are compared in Figure 3 and Table 2. The two dispersion curves deviate significantly from one another. The maximum misfit is more than 8 percent.

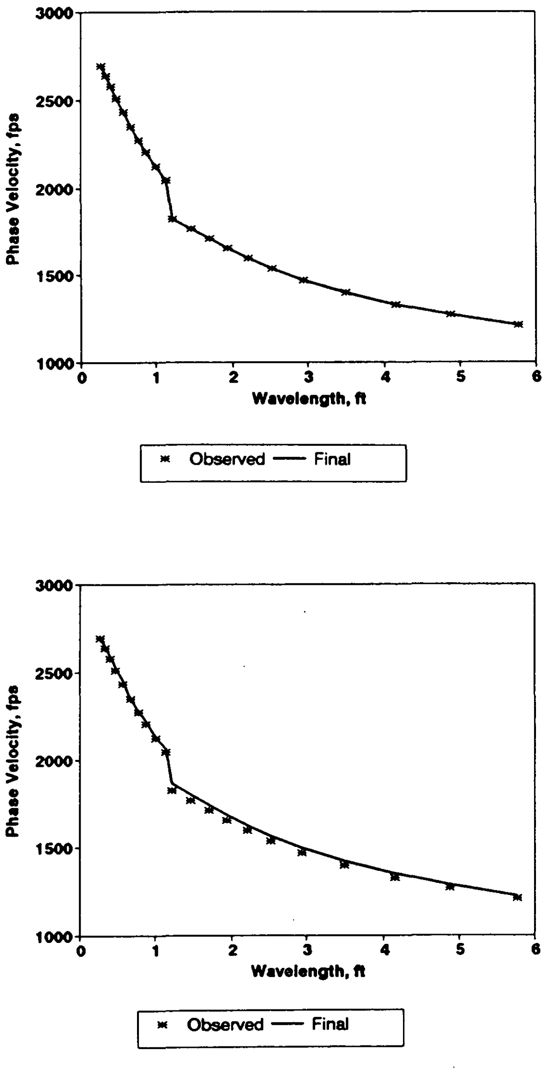


**FIGURE 3 Comparison of observed and final dispersion curves: *top*, Simulation 1; *bottom*, Simulation 2.**

**Simulation 3**

In Simulation 3, the same seed velocities and layer thicknesses used in Simulation 2 were used. However, both thickness and shear wave velocity for each layer were determined through the inversion process. The results from this simulation are reflected in Table 3. Once again, the thicknesses and velocities are perfectly determined. The mismatch between the observed and final dispersion curves is practically zero. The results obtained in this simulation demonstrate the effectiveness and accuracy of the backcalculation technique.

**Simulation 4**

Simulation 4 corresponds to a practical situation usually encountered. It was assumed that thicknesses and shear wave velocities of layers, as well as the number of layers, are all unknown. Thicknesses and shear wave velocities were estimated by assuming that the profile contains five layers. The thicknesses of the layers in the seed profile were assumed to be equal.

**TABLE 2 True, Seed, and Backcalculated Values of Shear Wave Velocities, Simulation 2**

| Layer Number | Thickness (in.) | | Shear Wave Velocity (fps) | | |
|---|---|---|---|---|---|
| | True | Seed | True | Seed | Backcalculated |
| 1 | 3.0 | 3.6 | 3000. | 2500. | 2915. |
| 2 | 6.0 | 4.8 | 2000. | 1500. | 1870. |
| 3 | ∞ | ∞ | 1000. | 800. | 1093. |

Data Misfit (%): Min. = 0.06, Max. = 8.20, Average = 1.16

**TABLE 3 True, Seed, and Backcalculated Values of Shear Wave Velocities, Simulation 3**

| Layer Number | True | | Seed | | Backcalculated | |
|---|---|---|---|---|---|---|
| | h (in.) | $V_s$ (fps) | h (in.) | $V_s$ (fps) | h (in.) | $V_s$ (in.) |
| 1 | 3.0 | 3000. | 3.6 | 2500. | 3.0 | 3000. |
| 2 | 6.0 | 2000. | 4.8 | 1500. | 6.0 | 2000. |
| 3 | ∞ | 1000. | ∞ | 800. | ∞ | 1000. |

Data Misfit (%): Min. = 0.02, Max. = 0.08, Average = 0.05

The final profile after inversion is included in Table 4 and is compared with the true profile in Figure 4. The thickness and velocity of the surface layer are determined relatively accurately. The thickness of the second layer of the true profile is determined accurately, provided that the second and third layers of the backcalculated profile are combined. This is justified because the velocities of the second and third layers of the final profile are rather close. The velocity of the half space is predicted rather well, if the fourth layer is ignored.

The velocity of the fourth layer from the final profile is significantly higher than the actual value. This corresponds to one of the weaknesses of the present inversion process. This discrepancy can be attributed to the change of branch patterns (five layers against three layers) in dispersion curves. Means of resolving this problem are being studied.

## Simulation 5

In every simulation represented up to this point, the result was obtained on the assumption that the Poisson's ratio and density for each layer are known. The effects of misestimation of Poisson's ratio on backcalculated profile is demonstrated here.

**TABLE 4 True, Seed, and Backcalculated Values of Shear Wave Velocities, Simulation 4**

| Layer Number | True h (in.) | True V, (fps) | Seed h (in.) | Seed V, (fps) | Backcalculated h (in.) | Backcalculated V, (fps) |
|---|---|---|---|---|---|---|
| 1 | 3.0 | 3000. | 3.0 | 2500. | 3.07 | 2966. |
| 2 | 6.0 | 2000. | 3.0 | 2000. | 1.06 | 2153. |
| 3 | ∞ | 1000. | 3.0 | 1500. | 4.83 | 2025. |
| 4 | | | 3.0 | 1000. | 1.44 | 1206. |
| 5 | | | ∞ | 800. | ∞ | 1036. |

Data Misfit (%): Min. = 0.35, Max. = 2.18, Average = 1.26

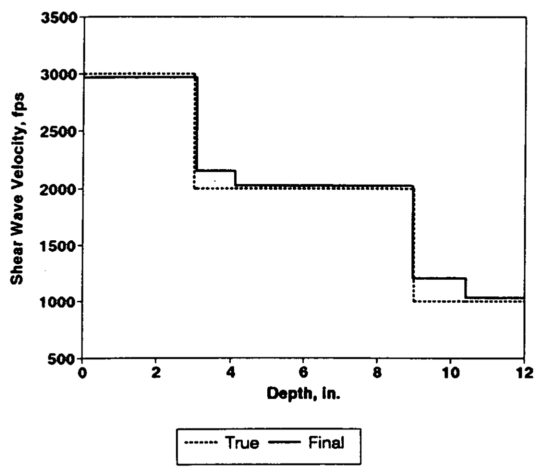


**FIGURE 4 Comparison of true and final shear wave velocity profiles from Simulation 4.**

**TABLE 5 True, Seed, and Backcalculated Values of Shear Wave Velocities, Simulation 5**

| Layer Number | Thickness (in.) | Shear Wave Velocity (fps) True | Seed | Backcalculated |
|---|---|---|---|---|
| 1 | 3.0 | 3000. | 2500. | 3006. |
| 2 | 6.0 | 2000. | 1500. | 2092. |
| 3 | ∞ | 1000. | 800. | 1002. |

Data Misfit (%): Min. = 0.51, Max. = 3.63, Average = 1.45

A Poisson's ratio of 0.25, rather than 0.33, was assumed for all layers. For simplicity, the number and thicknesses of layers have been assumed to be known parameters. The backcalculated velocities are shown in Table 5.

Decreasing the Poisson's ratio from 0.33 to 0.25 should naturally result in an increase of about 1.5 percent in the velocity of each layer. It can be seen that velocities of all layers are predicted closely. This confirms that Poisson's ratio has a minor influence on the backcalculated results.

## CASE STUDY

A series of tests was carried out on Highway US-69 in Angelina County near Lufkin, Tex. The cross section of the road consisted of two 12-ft-wide driving lanes and two 8-ft-wide paved shoulders. The pavement section reportedly consisted of a 6-in.-thick AC layer. On the basis of construction drawings, the AC layer consisted of three different lifts placed at various times. The base course consisted of 10 in. of flexible ash base, below which the subgrade existed. The results from one site are discussed here.

The dispersion curve from the site is shown in Figure 5. To backcalculate elastic moduli, 31 data points were sampled from the experimental dispersion curve. The automated method suggested by Desai (*5*) was used to select these representative data points. A relatively large number of data is incorporated in the inversion process so that the discontinuity in the experimental dispersion curve can be sufficiently defined. The

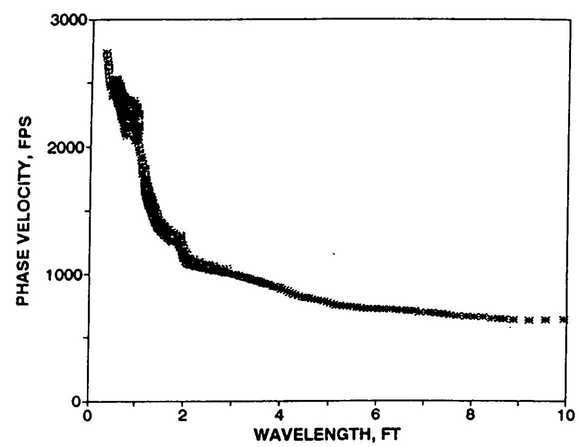


**FIGURE 5 Dispersion curve from flexible pavement section tested.**

statistical standard errors in the data range from 15 to 50 ft/sec (equivalent to a relative error of about 2 percent).

The seed profile is shown in Figure 6. The selection of the proper seed profile is rather simple for the top layer and the half space. A convenient method for determining the seed values for other layers is given by Nazarian (*3*). The final profile after simultaneous (thickness and velocity) inversion is also presented in Figure 6.

The idealized dispersion curve used in the inversion process is compared with the theoretical one obtained from the back-calculated profile in Figure 7. The two curves compare quite favorably showing the appropriateness of the final profile.

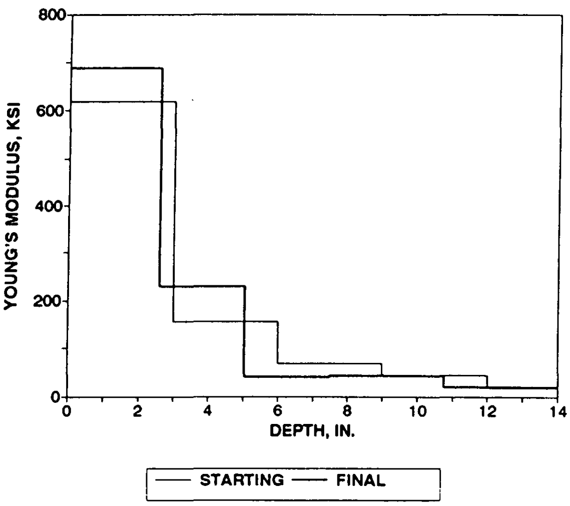


**FIGURE 6 Seed (starting) and final modulus profiles.**

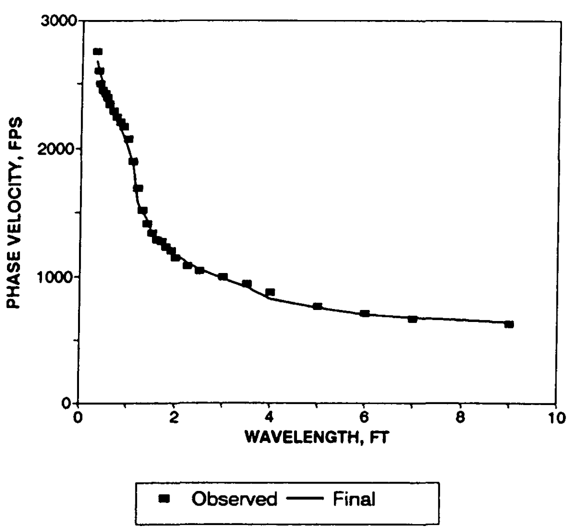


**FIGURE 7 Comparison of observed and final dispersion curves.**

The final profile along with the estimated 95 percent confidence interval bounds associated with the modulus and thickness are shown in Figure 8. The confidence interval bounds are rather narrow, corresponding to small scatter in the field data and good fit between the dispersion curves.

The thickness of the AC layer is estimated at about 2.6 in., underlying a softer layer down to a depth of about 5.5 in. The thickness of the base layer was found to be about 6 in. also. As mentioned before, the as-built thickness of the AC layer was reported as 7 in. On the basis of actual coring after the completion of the analysis, it was found that the AC layer was severely stripped. Actually only about 2.5 to 3 in. of the core could be recovered and the rest of the AC layer had lost its binding agent.

The FWD tests were also carried out at the site. Because of time constraints, the drop load was limited to 10,000 lb (nominally). Program MODULUS 4.0 (*22*,p.72) was used to backcalculate the moduli. Three different pavement profiles were used. In the first profile, the layering obtained from construction drawings was used. In this case, the thickness of the AC and base were assumed to be 7 and 10 in., respectively. The backcalculated moduli from this layering are reported in Table 6. Also shown in the table are the moduli obtained

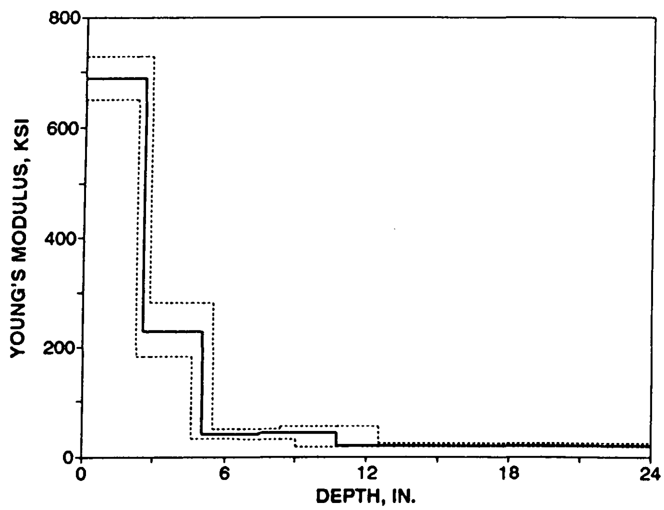


**FIGURE 8 Final modulus profile with 95 percent confidence bounds.**

**TABLE 6 Comparison of Moduli Obtained from SASW and FWD**

| Method | Modulus, ksi | | | | Absolute Average Errors (%) |
|---|---|---|---|---|---|
| | AC* | | Base | Subgrade | |
| | Layer 1 | Layer 2 | | | |
| SASW | 688 | 229 | 41 | 21 | 1.8 |
| FWD (Construction Drawings)* | 193 | | 6 | 21 | 0.9 |
| FWD (SASW)* | 500 | 286 | 4 | 21 | 1.3 |
| FWD (Coring)* | 323 | 273 | 4 | 21 | 1.0 |

* Source for Determining Layer Thickness

from SASW tests. The modulus of the subgrade from both methods are comparable; however, the moduli of the base and AC layers are quite different. It would be difficult to derive any conclusions from the FWD moduli of the top two layers, because the actual layer thicknesses were significantly different from those assumed in the backcalculation process.

The second pavement profile used was the one obtained from the SASW tests. In this case, the modulus values are much closer. The modulus of base seems unreasonably low (4 ksi). The reason for this matter is not known at this time.

The final pavement profile used was the one obtained from the actual coring of the site. The thickness of the intact AC layer was reported as 2.5 to 3 in. and the thickness of the base was reported between 6 and 7 in.

This profile yields moduli that are similar to those of the SASW profile. This result is expected because the layering from the SASW tests and coring are relatively close.

## SUMMARY AND CONCLUSIONS

On the basis of the general inverse theory, a backcalculation technique for estimating layer properties of pavements from surface wave dispersion data has been developed. The theoretical principle and numerical considerations of this technique are briefly described and discussed. Results from both synthetic (theoretically derived) and actual field dispersion data are presented. These preliminary and limited results demonstrate that the technique may be an effective tool for estimating elastic modulus profiles of pavement systems. More work is under way to improve and accelerate the method.

Because a pavement structure contains only a few material layers, and certain prior information about them is always available, simultaneous backcalculation for both layer thicknesses and elastic moduli may provide more reliable results.

## ACKNOWLEDGMENTS

This work has been mainly funded by the Texas Department of Transportation, and the authors would like to thank that organization. Robert C. Briggs and Jeff Jackson have been the project coordinators. The Strategic Highway Research Program is also acknowledged. The case history was carried out for that organization under Project H-104B. The efforts of Bob Briggs to reduce the FWD data are highly appreciated.

## REFERENCES


1. S. Nazarian and K. H. Stokoe, II. *In Situ Determination of Elastic Moduli of Pavement Systems by Spectral-Analysis-of-Surface-Waves Method (Practical Aspects)*. Research Report 368-1F. Center for Transportation Research, University of Texas, Austin, 1986.
2. S. Nazarian and K. H. Stokoe, II. *In Situ Determination of Elastic Moduli of Pavement Systems by Spectral-Analysis-of-Surface-Waves Method (Theoretical Aspects)*. Research Report 437-2. Center for Transportation Research, University of Texas, Austin, 1987.
3. S. Nazarian. *In Situ Determination of Elastic Moduli of Soil Deposits and Pavement Systems by Spectral-Analysis-of-Surface-Waves Method*. Ph.D. dissertation. University of Texas, Austin, 1984.
4. S. Nazarian, M. Baker, and R. E. Smith. *Measurement Concepts and Technical Specifications of Seismic Pavement Analyzer*. Center for Geotechnical and Highway Materials Research, University of Texas, El Paso, 1991.
5. M. Desai. *An Automated Method for Construction of Surface Wave Dispersion Curve*. M. S. thesis. University of Texas, El Paso, 1991.
6. R. A. Wiggins. The General Linear Inverse Problem: Implications of Surface Waves and Free Oscillations on Earth Structure. *Reviews of Geophysics and Space Physics*, Vol. 10, 1972, pp. 251–285.
7. D. D. Jackson. Interpretation of Inaccurate, Insufficient and Inconsistent Data. *Geophysical Journal of the Royal Astronomical Society*, Vol. 28, 1972, pp. 97–109.
8. I. Sanchez-Salinero, J. M. Roësset, K.-Y. Shao, K. H. Stokoe, II, and G. J. Rix. Analytical Evaluation of Variables Affecting Surface Wave Testing of Pavements. In *Transportation Research Record 1136*, TRB, National Research Council, Washington, D.C., 1987, pp. 86–95.
9. J. C. Shue, K. H. Stokoe, II, and J. M. Roësset. Effect of Reflected Waves on SASW Testing of Pavements. In *Transportation Research Record 1196*, TRB, National Research Council, Washington, D.C., 1989, pp. 51–61.
10. R. Jones. Surface Wave Technique for Measuring the Elastic Properties and Thickness of Roads: Theoretical Development. *British Journal of Applied Physics*, Vol. 13, 1962, pp. 21–29.
11. R. F. Vidale. *The Dispersion of Stress Waves in Layered Media Overlying a Half Space of Lesser Acoustic Rigidity*. Ph.D. thesis. University of Wisconsin, 1964.
12. K. Sezawa and K. Kanai. Discontinuity in the Dispersion Curves of Rayleigh Waves. *Bulletin of Earthquake Research Institute*, Vol. 13, 1935, pp. 237–244.
13. W. T. Thomson. Transmission of Elastic Waves Through a Stratified Solid Medium. *Journal of Applied Physics*, Vol. 21, 1950, pp. 89–93.
14. N. A. Haskell. The Dispersion of Surface Waves in Multilayered Media. *Bulletin of the Seismological Society of America*, Vol. 43, 1953, pp. 17–34.
15. E. Kausel and J. M. Roësset. Stiffness Matrices for Layered Soils. *Bulletin of the Seismological Society of America*, Vol. 71, 1981, pp. 1743–1761.
16. J. Lysmer and L. A. Drake. A Finite Element Method for Seismology. In *Methods in Computational Physics*, Vol. 11, Academic Press Inc., New York, N.Y., 1972, pp. 181–216.
17. M. M. Hossain and V. P. Drnevich. Numerical and Optimization Techniques Applied to Surface Waves for Backcalculation of Layer Moduli. *Nondestructive Testing of Pavements and Backcalculation of Moduli*, ASTM Special Technical Publication 1026, Baltimore, Md., 1989.
18. J. E. Dunkin. Computation of Modal Solutions in Layered, Elastic Media at High Frequencies. *Bulletin of Seismological Society of America*, Vol. 55, 1965, pp. 335–358.
19. G. H. Golub and C. Reinsch. Singular Value Decomposition and Least Squares Solution. *Numerische Mathemetik*, Vol. 14, 1970, pp. 403–420.
20. D. L. B. Jupp and K. Vozoff. Stable Iterative Methods for Inversion of Geophysical Data. *Geophysical Journal of the Royal Astronomical Society*, Vol. 42, 1975, pp. 957–976.
21. N. R. Draper and H. Smith. *Applied Regression Analysis*. John Wiley and Sons, New York, N.Y., 1980.
22. J. Uzan, T. Scullion, C. H. Michalek, M. Parades, and R. L. Lytton. A Microcomputer-Based Procedure for Backcalculating Layer Moduli from FWD Data. Research Project 1123-1. Texas Transportation Institute, Texas A&M University, College Station, 1988.

# Interpretation of Backcalculated Layer Moduli of Crack-and-Seat Pavement from Falling Weight Deflectometer Data

MUSTAQUE HOSSAIN AND LARRY A. SCOFIELD

In 1986 the Arizona Department of Transportation rehabilitated a section of Interstate 40 using a crack-and-seat technique. The project, in north-central Arizona, consisted of cracking the existing jointed plain concrete pavement in a 3- × 3-ft pattern and seating these areas before placing a 4-in. asphalt concrete overlay. Two test sections, each 0.1-mi long, were constructed on the project. One of these test sections used a nominal crack spacing of 4- × 6-ft, and the other a spacing of 2- × 2-ft to investigate the effect of crack spacing on the performance of this project. To establish the changes in effective modulus of cracked portland cement concrete (PCC), falling weight deflectometer (FWD) testing was conducted for 5 years after construction. Layer moduli were backcalculated from the FWD deflection test results using an elastic layer analysis program. The structural layer coefficients for the cracked PCC layer were analyzed to establish a difference in structural characteristics of sections with various crack spacings. Large variations in the effective modulus of the cracked PCC layer were obtained from the backcalculation technique. Unreasonably high moduli were computed through this process. The backcalculated concrete moduli tended to fluctuate over time, but no definite trends were established. The structural layer coefficients of the cracked PCC layer were also analyzed. This analysis showed that there is no remarkable difference in structural response of cracked and seated concrete pavement corresponding to various crack spacings.

Interstate 40 is one of Arizona's major east-west trucking routes. It is a four-lane divided highway in the northern part of the state. Approximately 4 percent of its 718 mi (total, both directions) consists of plain jointed concrete pavements (JPCP). As I-40 concrete pavements attain their 20-year design lives, they require extensive rehabilitation. One form of rehabilitation used was cracking and seating the existing concrete pavement followed by an asphalt concrete (AC) overlay. In 1986 Project I-40-3(31) was designed for rehabilitation with the cracking and seating before the placement of a 4-in. hot-mix asphalt concrete (HMAC) overlay. This strategy was selected because of structural deterioration of the existing concrete pavement. Two test sections and three crack spacing intervals were incorporated into the project as part of the experiment with optimum crack spacing. The objective was to study the effectiveness of the crack-and-seat strategy and the effect of crack spacing on the mitigation of reflective cracking. The changes in the effective modulus of broken concrete was planned to be evaluated through backcalculation of layer moduli from falling weight deflectometer (FWD) test data. This paper describes the structural analysis of this project using FWD data.

M. Hossain, Department of Civil Engineering, Seaton Hall, Kansas State University, Manhattan, Kans. 66506. L. A. Scofield, Arizona Transportation Research Center, College of Engineering and Applied Sciences, Arizona State University, Tempe, Ariz. 85287.

## PROJECT LOCATION AND DESCRIPTION

The project is located on I-40 approximately 10 mi west of Williams in north-central Arizona. Soils in this area are residual soils derived from volcanic parent rock and range from well-graded sand (SW) to clays (CH). Mean annual precipitation is approximately 20 in. The mean daily temperature is 60°F with extremes between 97°F and −22°F (*1*).

### Existing Pavement Section

The original concrete construction project extended from Milepost (MP) 152.1 to 158.6 and included both eastbound (EB) and westbound (WB) roadways. Each roadway consisted of two 12-ft concrete lanes with 4-ft and 10-ft asphalt concrete shoulders on the inside and outside, respectively. The project incurs approximately 12,000 average daily traffic, with 38 percent truck traffic. The pavement section consisted of 8 in. of JPCP on 4 in. of cement-treated base (CTB) over 6 in. of subgrade seal (engineering fill), as shown in Figure 1. The existing EB roadway was opened to traffic in 1968, whereas the WB roadway was opened in 1967. Transverse joints were established at 15-ft intervals. Both transverse and longitudinal joints were sawed at the time of construction.

### Design Consideration and Layout

Two test sections were established on this project to evaluate the effect of crack spacing. The two test sections, each 0.1 mi in length, were constructed at the extreme west end of the project, as shown in Figure 2. The crack-and-seat spacings for the test sections were selected as 2 × 2 ft and 4 × 6 ft. These spacings represented crack intervals that were both larger and smaller than the originally specified 3- × 3-ft spacing. The 3- × 3-ft spacing was considered the "control" section. The 2- × 2-ft and 4- × 6-ft spacings represented intervals previously used in other states.

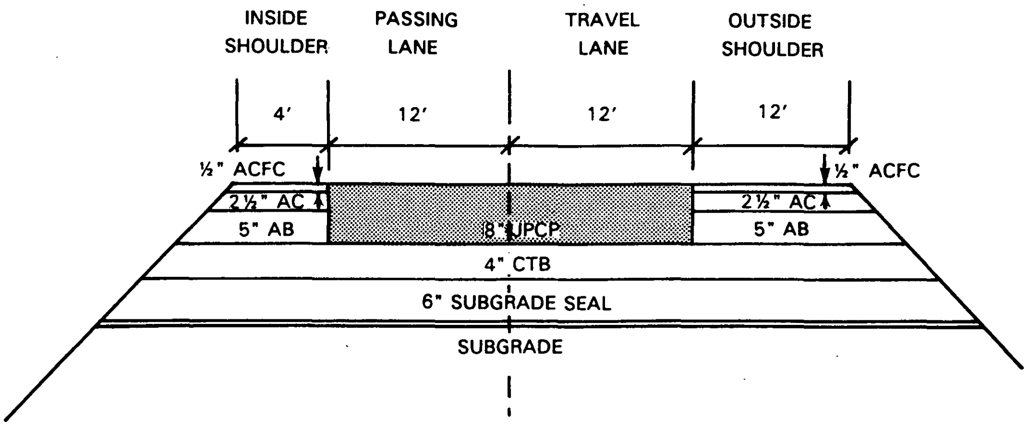


FIGURE 1 Original pavement section.

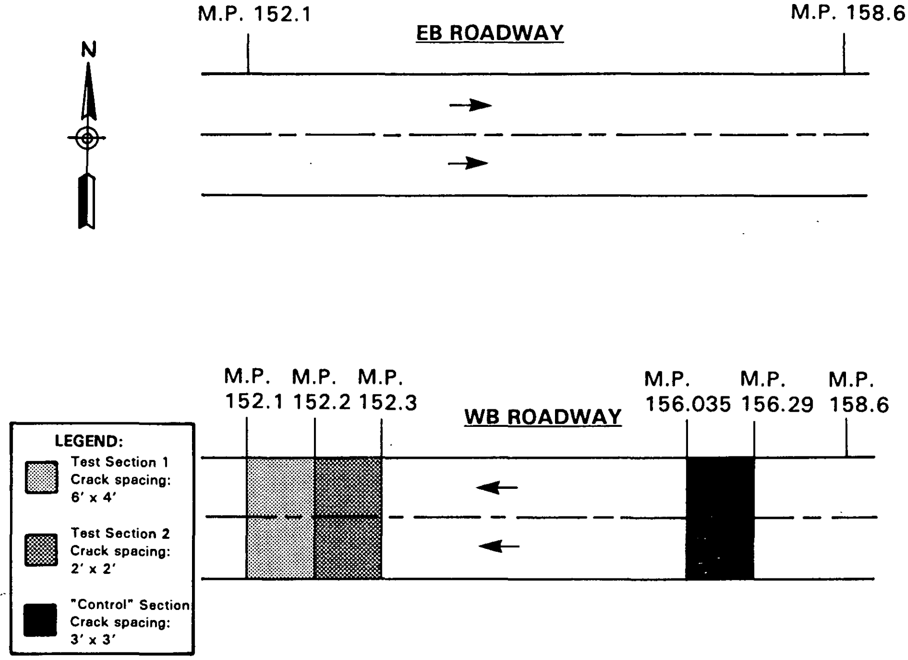


FIGURE 2 Layout of test sections.

## CONSTRUCTION FEATURES

The project consisted of cracking and seating the existing 8-in. JPCP, installing edge drains adjacent to the outside shoulder, and placing a 4-in. HMAC overlay across the entire roadway, including both shoulders.

The cracking required that the specified crack spacing would be obtained by cracking the existing portland cement concrete (PCC) slab with a method that produced full-depth, generally transverse, hairline cracks at a nominal longitudinal spacing of 3 × 3 ft. The only exception was at MP 152.1 to 152.2 (WB) and at MP 152.2 to 153.3 (WB) where the nominal spacing was 4 × 6 ft and 2 × 2 ft, respectively. Inspection of the cracking effectiveness was performed by applying water to a test section once each day. Also, cores were retrieved to make sure that the cracking had progressed full depth. A Michigan whip hammer was used to perform the cracking operation. Construction specifications required seating to be accomplished by at least two passes of a 50-ton pneumatic roller or until the concrete pieces were assured of being seated. During construction, this was accomplished by a "wagon-like" tire roller fitted with sand ballast.

Cracked pavement segments were required to be seated not more than 24 hr before receiving the asphalt concrete overlay and not more than 72 hr after cracking. Traffic was allowed on the cracked and seated concrete for no more than 72 hr. Evaluation of the seating effectiveness was based on the judgment of the engineer. After seating was complete, the 4-in. overlay was placed in two lifts. The project was completed in November 1986 (*2*).

## FALLING WEIGHT DEFLECTOMETER TESTING

FWD was conducted every year from 1987 through 1991. The FWD testing was performed with a Dynatest model 8000 with sensor locations of 0, 12, 24, 36, 48, 60, and 72 in. from the center of the load at target load levels of 6,000, 9,000, and 12,000 lb. The FWD testing was performed at the same 18 locations on the test and "control" sections each year on the outer wheel path, and usually, 2 to 3 ft from the edge of the lane. The tests were performed in summer from late morning to early afternoon.

As mentioned before, the FWD test was done to establish how the effective moduli of broken concrete pavement changed with time. Since the Michigan whip hammer imparted so little fracture energy into the pavement during construction, it was assumed that the effective modulus would decrease with time as the effects of thermal changes and freeze-thaw acted to reduce the aggregate interlock at the fracture locations.

### Analysis Methodology

The FWD deflection data were analyzed using the BKCHEVM elastic layer computer program to backcalculate the layer moduli (*3*). BKCHEVM is a minor modification of CHEVDEF program (*4*). Backcalculations were performed on FWD test results from four locations within Section 1 and four locations within Section 2. Ten test locations were analyzed for the control section.

The pavement was assumed to be a four-layer flexible pavement system. Layer 1 was the AC overlay, Layer 2 was the cracked and seated PCC pavement (PCCP), Layer 3 was the CTB, and Layer 4 was the subgrade that generally was assumed to be semi-infinite. However, BKCHEVM automatically introduced a rigid layer at 20 ft below the top of the subgrade when it detected a rigid layer. The rigid layer was detected by using the seventh sensor deflection value. Details of BKCHEVM are discussed by Bush and Alexander (*4*). The subgrade seal layer was considered as part of the subgrade. The subgrade seal layer can be considered as an engineering fill layer consisting of soil-aggregate mixtures. The deflection values corresponding to the load level closest to 9,000 lb were used for backcalculation of layer moduli.

### Backcalculation Results

*Asphalt Concrete*

Table 1 shows the backcalculated asphalt concrete moduli for all the test sections. The moduli have been adjusted for temperature at 77°F using AASHTO correction factors. From the table it is clear that the backcalculated AC moduli for various test sections fluctuate over the years. The average modulus varies from 69 to 978 ksi. The average backcalculated AC moduli for Test Section 3 or control section is higher than that for the other test sections.

*Broken PCC Layer*

The results of the backcalculated cracked PCC layer moduli are shown in Table 2. Figure 3 illustrates the results. Very high concrete pavement moduli were obtained for every year that was included in the analysis. The average PCC moduli typically ranged between 3.3 and 7 million lb/in.². Individual test results ranged from a low of 140,000 lb/in.² to a high of 11.7 million lb/in.². The large standard deviation and coefficient of variation existed for every year. The average moduli for Test Sections 1 and 2 and the control section suggest a fluctuation of cracked PCCP layer moduli with time. Test Sections 1 and 2 show a decrease of cracked PCCP layer modulus since 1989. But the control section does not show any trend.

**TABLE 1 Backcalculated AC Moduli for Crack-and-Seat Project**

| Year | Section 1 Modulus (ksi) | | | Section 2 Modulus (ksi) | | | Control Section Modulus (ksi) | | |
|---|---|---|---|---|---|---|---|---|---|
| | Mean | Std. Dev. | C.V. | Mean | Std. Dev. | C.V. | Mean | Std. Dev. | C.V. |
| 1987 | 412 | 281 | 55 | 441 | 95 | 22 | 451 | 100 | 22 |
| 1988 | 69 | 15 | 21 | 89 | 5 | 5 | 149 | 123 | 83 |
| 1989 | 638 | 328 | 47 | 656 | 358 | 55 | 978 | 298 | 30 |
| 1990 | 379 | 180 | 48 | 379 | 157 | 41 | 470 | 201 | 43 |
| 1991 | 129 | 33 | 25 | 246 | 268 | 109 | 259 | 305 | 118 |

**TABLE 2 Backcalculated Cracked PCC Moduli for Crack-and-Seat Project**

| Year | Section 1 Modulus (ksi) | | | Section 2 Modulus (ksi) | | | Control Section Modulus (ksi) | | |
|---|---|---|---|---|---|---|---|---|---|
| | Mean | Std. Dev. | C.V. | Mean | Std. Dev. | C.V. | Mean | Std. Dev. | C.V. |
| 1987 | 6491 | 3316 | 51 | 6672 | 3484 | 52 | 5772 | 3500 | 61 |
| 1988 | 3910 | 2197 | 56 | 4876 | 3598 | 74 | 6224 | 3585 | 58 |
| 1989 | 8083 | 4152 | 51 | 5676 | 5553 | 98 | 3344 | 3107 | 93 |
| 1990 | 4407 | 5078 | 115 | 4602 | 4938 | 107 | 2936 | 3335 | 114 |
| 1991 | 3125 | 3924 | 126 | 1592 | 1729 | 109 | 4255 | 4093 | 96 |

*Comparison with Laboratory Test Results*

Four 4-in.-diameter cores were retrieved from the PCC layer during the design phase. Compression tests with strain measurements were conducted on these cores to assess the structural integrity of the concrete. The results of this testing are shown in Table 3. The laboratory test results indicated that even though the compressive strength was 7,000 to 9,000 lb/in.², the modulus was only 2 million lb/in.². This rather low modulus was reported in the project design summary as an indication of the poor concrete condition. The Asphalt Concrete Institute relationship between compressive strength and modulus suggests that the modulus is of the order of 5 million lb/in.² (*5*).

The backcalculation results suggest that little reduction in effective modulus has resulted from the crack-and-seat process. The backcalculated moduli are comparable to the results calculated from the compressive strength test results (5 million lb/in.²) of the concrete cores obtained during the design phase. The results suggest that the cracking of the PCC layer did not result in a reduction of this layer modulus.

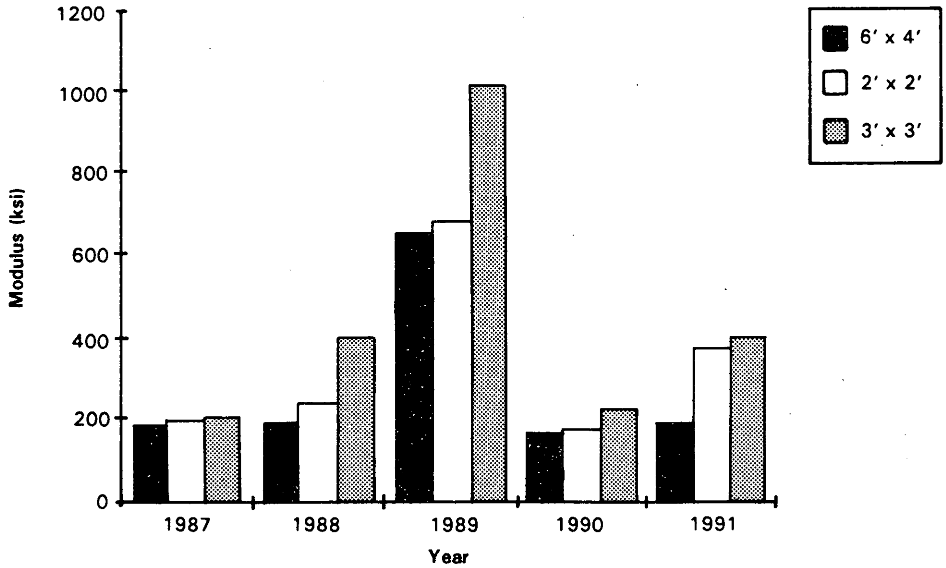


FIGURE 3 Backcalculated cracked PCC moduli.

TABLE 3 Concrete Test Results

| Location of Core | Compressive Strength (psi) | Laboratory Determined Modulus (psi) | Calculated Modulus (57000/√f'c) (psi) |
|---|---|---|---|
| 153.02 EB | 7180 | $2.12\times10^6$ | $5.1\times10^6$ |
| 159.98 EB | 9019 | $2.41\times10^6$ | |
| 152.1 WB | 6614 | $1.54\times10^6$ | $5.0\times10^6$ |
| 159.0 WB | 8860 | $1.31\times10^6$ | |

### *Cement-Treated Base*

Table 4 shows the average moduli for cement-treated base layer. The backcalculated moduli for this layer were also quite variable. The coefficient of variation of backcalculated layer moduli varies from 16 to 194 percent. The average layer modulus varies from 27 to 123 ksi over the last 5 years. The CTB was observed to be severely deteriorated at the time of construction of a subsurface drainage trench in this project. Also, energy imparted for cracking concrete might have led to more deterioration and apparently contributed to the very low moduli of CTB layer for most of the cases.

TABLE 4 Backcalculated Cement-Treated Base Moduli

| Year | Section 1 Modulus (ksi) | | | Section 2 Modulus (ksi) | | | Control Section Modulus (ksi) | | |
|---|---|---|---|---|---|---|---|---|---|
| | Mean | Std. Dev. | C.V. | Mean | Std. Dev. | C.V. | Mean | Std. Dev. | C.V. |
| 1987 | 70 | 11 | 16 | 58 | 11 | 19 | 82 | 63 | 77 |
| 1988 | 44 | 7 | 16 | 43 | 9 | 20 | 78 | 27 | 35 |
| 1989 | 43 | 16 | 37 | 56 | 13 | 24 | 123 | 167 | 136 |
| 1990 | 27 | 5 | 19 | 27 | 5 | 19 | 70 | 135 | 194 |
| 1991 | 118 | 155 | 131 | 38 | 15 | 41 | 76 | 97 | 127 |

### *Subgrade*

The backcalculated subgrade moduli for all test sections as well as the control section are shown in Table 5. Minimum variability was obtained in backcalculated subgrade moduli. The coefficient of variation ranged between 8 and 30 percent. All sections except the control section showed a minor variation in subgrade moduli over time. The average subgrade moduli for the control section varied between 18 ksi and 34 ksi over the last 5 years.

## DETERMINATION OF STRUCTURAL LAYER COEFFICIENTS

The structural layer coefficients for the cracked concrete layer was analyzed to establish the difference in structural characteristics of sections with various crack spacings. The results of the backcalculation analysis were used to calculate the structural layer coefficients using both the 1986 AASHTO guide procedures and the modified National Asphalt Pavement Association (NAPA) procedures (*6,7*). AASHTO procedures are explained in the guide. The AASHTO procedure is valid for cracked and seated concrete moduli up to 950,000

TABLE 5 Backcalculated Subgrade Moduli

| Year | Section 1 Modulus (ksi) | | | Section 2 Modulus (ksi) | | | Control Section Modulus (ksi) | | |
|---|---|---|---|---|---|---|---|---|---|
| | Mean | Std. Dev. | C.V. | Mean | Std. Dev. | C.V. | Mean | Std. Dev. | C.V. |
| 1987 | 20 | 2 | 8 | 23 | 4 | 18 | 28 | 3 | 9 |
| 1988 | 24 | 4 | 15 | 27 | 3 | 12 | 18 | 6 | 30 |
| 1989 | 23 | 3 | 14 | 27 | 6 | 23 | 34 | 7 | 27 |
| 1990 | 20 | 4 | 19 | 26 | 2 | 9 | 18 | 5 | 27 |
| 1991 | 21 | 3 | 16 | 29 | 7 | 24 | 21 | 3 | 16 |

lb/in.$^2$. Because most of the backcalculated PCCP layer moduli values of this project were far above 950,000 lb/in.$^2$, the layer coefficients corresponding to the moduli values greater than 950,000 lb/in.$^2$ have been taken as 0.44, the maximum layer coefficient for cracked and seated concrete in the AASHTO guide.

In the NAPA method used for this analysis, backcalculation for determination of effective modulus of cracked and seated concrete was done by BKCHEVM. Only the equation for computing the structural layer coefficient of cracked and seated concrete in the NAPA procedure has been used. The cement-treated base layer coefficient and modulus were assumed to be 0.12 and 500,000 lb/in.$^2$, respectively. The NAPA equation for computing the structural layer coefficient of cracked and seated concrete is as follows:

$$a_{cs} = a_2(E_{cs}/E_2)^{1/3}$$

where

$a_{cs}$ = structural layer coefficient of cracked and seated concrete,
$E_{cs}$ = effective modulus of cracked and seated layer (lb/in.$^2$),
$a_2$ = layer coefficient for the base (CTB), and
$E_2$ = layer modulus of the base (CTB) (lb/in.$^2$).

The cement-treated base layer coefficient and modulus were held fixed throughout the analysis for a valid comparison of change in effective modulus over time and also between the crack spacings.

The calculated structural layer coefficients for both the AASHTO procedures and the modified NAPA procedures are shown in Table 6. These results indicate the variation in layer coefficients with both time and spacing. It is obvious that the modified NAPA procedures resulted in decreased coefficients with time for the 6- × 4-ft and the 2- × 2-ft crack patterns.

The NAPA coefficients were generally lower than the magnitude of the AASHTO coefficients. In most of the cases,

**TABLE 6 Variation of PCCP Structural Layer Coefficients with Crack Spacing and Time**

| Year | Crack Spacing | PCCP Structural Layer Coefficient (AASHTO) | PCCP Structural Layer Coefficient (NAPA) |
|---|---|---|---|
| 1987 | 2'x2' | 0.44 | 0.27 |
| | 3'x3' | 0.44 | 0.255 |
| | 6'x4' | 0.42 | 0.24 |
| 1988 | 2'x2' | 0.44 | 0.23 |
| | 3'x3' | 0.44 | 0.26 |
| | 6'x4' | 0.44 | 0.24 |
| 1989 | 2'x2' | 0.44 | 0.29 |
| | 3'x3' | 0.44 | 0.206 |
| | 6'x4' | 0.39 | 0.229 |
| 1990 | 2'x2' | 0.44 | 0.206 |
| | 3'x3' | 0.43 | 0.203 |
| | 6'x4' | 0.395 | 0.208 |
| 1991 | 2'x2' | 0.435 | 0.197 |
| | 3'x3' | 0.43 | 0.218 |
| | 6'x4' | 0.41 | 0.161 |

AASHTO coefficients have been taken as the highest coefficient tabulated in the guide. A comparison of the structural layer coefficients with those from any procedure yields no definite conclusions about the difference in structural characteristics of the sections with various crack spacings.

## CONCLUSIONS

Large variations in the effective modulus of the cracked concrete pavement were obtained from the backcalculation procedures using elastic layer analysis. Unreasonably high PCCP moduli values appear to have been computed through this process. PCCP moduli for various crack spacings tended to fluctuate over time. No consistent trends were evident.

The AASHTO procedure for computing structural layer coefficients was not applicable to most of the data for this project because of unusually high cracked and seated concrete moduli. The AASHTO procedure has tabulated values of structural layer coefficients for cracked and seated concrete moduli up to 950,000 lb/in.$^2$. The structural layer coefficients predicted by the modified NAPA procedures appear to decrease with time for 6- × 4-ft spacing.

## RECOMMENDATIONS

Future crack and seat projects should include a control section that is not cracked and seated, and an FWD test should also be conducted on the control section. An FWD test should be conducted before cracking, just after cracking and seating, and also after overlaying. An alternative analysis method to elastic layer analysis may be helpful for analyzing crack-and-seat pavements.

## REFERENCES

1. *Climates of the States, Volume 1: Alabama–New Mexico*, 3rd ed., Gale Research Company, Detroit, Mich., 1985, pp. 40–58.
2. A. H. Osseiran. *Crack and Seat Pavement*. Report FHWA-AZ-EP8604. Arizona Department of Transportation, Phoenix, Sept. 1987.
3. M. Mamlouk, W. Houston, S. Houston, and J. Zaniewski. *Rational Characterization of Pavement Structures Using Deflection Analysis*, Vol. 1, Report FHWA-AZ88-254. Arizona Department of Transportation, Phoenix, Dec. 1988.
4. A. J. Bush III and D. R. Alexander. Pavement Evaluation Using Deflection Basin Measurements and Layered Theory. In *Transportation Research Record 1022*, TRB, National Research Council, Washington, D.C., 1985, pp. 16–22.
5. *ACI Building Code*. American Concrete Institute, Detroit, Mich., 1977.
6. *AASHTO Guide for Design of Pavement Structures*. AASHTO, Washington, D.C., 1986.
7. *Structural Evaluation of Cracked and Seated PCC Pavements for Overlaying with Hot Mix Asphalt*. Information Series 100. National Asphalt Pavement Association, 1987.

# Comparison of Theoretical and In Situ Behaviors of a Flexible Pavement Section

SOHEIL NAZARIAN AND Y. E. CHAI

The use of nondestructive testing (NDT) devices has provided pavement engineers with a simple method for determining pavement layer moduli. Moduli obtained with the NDT devices are used in mechanistic pavement design. Therefore, it is important to determine accurately the elastic moduli of pavement systems. Through a case study, some concerns with the deflection-based NDT of pavements are examined. The main objectives were (a) to establish the accuracy of a backcalculation methodology, (b) to determine the closeness of the theoretical and measured deformations within a pavement cross section, and (c) to assess the impact of the established accuracies on the design of pavement sections. These items are discussed through an example from one instrumented site. The instrumentation and algorithm used to determine in situ deflections are briefly described. A total of seven state-of-the-art NDT devices were employed. Particular attention was devoted to the effects of the load-induced nonlinearity associated with the large magnitude of loads imparted by the NDT devices to the pavement. On the basis of the case study, it was found that some differences in the deflections predicted the use of backcalculated moduli and measured deflections. It was also shown that load-induced nonlinearity may be one of the reasons for the poor match between the measured and theoretical deflection basins.

Mechanistic pavement design has been used more frequently in recent years than in earlier years. The backbone of mechanistic pavement design is nondestructive testing (NDT). To confirm the validity of mechanistic models and NDT methods, it has become important to monitor the behavior and performance of pavements under actual loads. As such, much effort has been focused on instrumenting pavements. One response parameter usually measured is the deflection within the body of the pavement. Multidepth deflectometer (*1*) or geophone units (*2*) can be used to obtain this information.

One site was instrumented with geophones and tested with seven NDT devices. The main objective of this study was to determine how well layered elastic theory in conjunction with NDT devices can predict the behavior of pavements. To achieve this objective, several steps were taken. The first step was to determine the effects that the load level and the sensor locations might have on backcalculated moduli. For each NDT device, and each load level, up to 19 deflections were available, 12 within the pavement section and the rest on the surface. Eight combinations of deflections were used in backcalculation. On the basis of these results, a thorough discussion of the effects that the load level, location, and number of deflection sensors and type of NDT device may have on backcalculated moduli was carried out.

Department of Civil Engineering, University of Texas at El Paso, El Paso, Tex. 79968.

The second goal was to determine how well the deformations, stresses, and strains are determined. A comprehensive comparison of stresses and strains from various types of NDT devices used is also included in this paper.

## BACKGROUND

Seven commercially available dynamic deflection measuring devices, including four falling weight deflectometer (FWD) devices and three vibratory loading devices (Dynaflect, Road Rater, WES 16-kip), were used in this study. These devices are well described by Bentsen et al. (*3*) and others.

An experimental study of these seven nondestructive testing devices by Bentsen et al. (*3*) shows that each device is capable of producing and collecting nondestructive pavement test data consistently and reliably. However, they also indicated that, as with any type of test equipment, the data should not be considered error-free. Care should be taken when field data are employed for pavement evaluation purposes, such as in the determination of allowable loads, overlay thicknesses, and layer moduli.

A side-by-side evaluation of deflection measuring equipment was carried out by Hudson et al. (*4*). Three FWD devices, a Road Rater, and a Dynaflect were evaluated. The report indicated that the results from these devices are satisfactory.

## TESTING PROGRAM AND DATA COLLECTION

### Description of Site

The site was located in the apron of Sheppard Air Force Base in Wichita Falls, Tex. As shown in Figure 1, the profile consisted of a 7-in. asphaltic concrete (AC) surface layer, a base layer of about 20 in. of granular material, underlain by a sandy clay subgrade.

### Instrumentation

The installation process is described in detail by Nazarian et al. (*5*). Four two-dimensional geophone units were installed at the site. Each geophone unit consisted of two geophones (one horizontal and one vertical). The two were carefully placed inside a 2-in.-long, 4-in. outside-diameter polyvinyl chloride (PVC) pipe. The geophones were then covered with

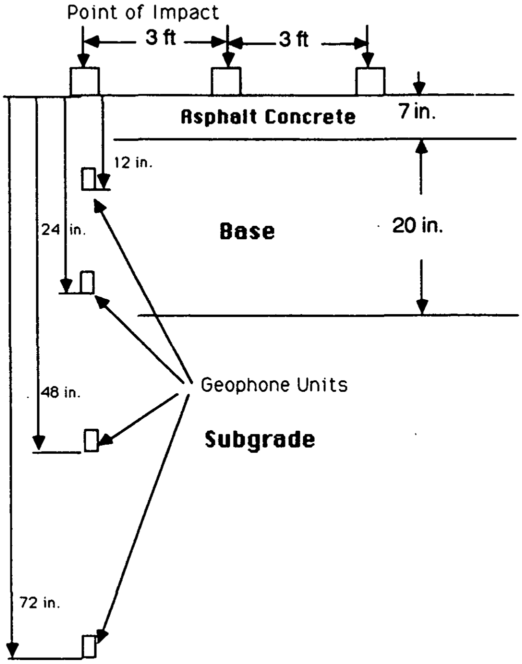


**FIGURE 1 Schematic of testing program.**

an epoxy-resin mix using the PVC pipe as the mold to eliminate the possibility of corrosion and moisture damage.

### Testing Program

A schematic of the testing program is illustrated in Figure 1. The loading mechanism of the NDT device was placed on top of the borehole containing the four geophone units. Data were collected with both vertical and horizontal receivers. The NDT device was then moved about 3 ft and the testing was repeated. Once again, the device was moved colinearly another 3 ft (total of 6 ft from the borehole) and tests were repeated. The voltage output of the geophones was monitored, captured, and stored using two Hewlett-Packard two-channel spectral analyzers.

### Determination of Field Deflections

The procedures adopted for determining the deflections from the geophone records are described here. The data reduction procedure is described in detail in Tandon and Nazarian (*2*). A frequency-domain solution is employed. Any function in the time domain can be easily expressed by a limited number of harmonic functions, if Fourier transform is utilized.

Shown in Figure 2 are the actual vertical displacement time histories sensed by the vertical geophones caused by a 25-kip load applied with an FWD. All figures are plotted to the same scale to demonstrate the variation in amplitude with distance from the point of impact. It can be seen that the deflections decrease rapidly with both radial and horizontal distance.

## DETERMINATION OF MODULI

Moduli obtained from the backcalculation process are included in Table 1 for all load levels applied by all devices. The average absolute differences between the theoretical and measured basins after completion of deflection basin fitting vary between 0.9 and 5.7 percent, with an average of about 2 to 3 percent. Therefore, the matching has been done in a reasonable fashion.

### Asphalt Layer

The thickness of the asphalt layer was 7 in. Therefore, theoretically speaking, one should be able to determine reasonably well the modulus of this layer.

The modulus of the asphalt layer varies from a minimum of 220 ksi to a maximum of about 1,080 ksi (619 ksi, if the result from the Road Rater is considered as an outlier). Overall, the coefficient of variation is equal to about 47 percent (29 percent without a modulus from the Road Rater).

### Base Layer

As indicated before, the base was about 20 in. thick. Theoretically, the modulus of such a thick layer should be determined with no difficulty at all. Practically speaking, assuming a constant modulus for this layer may not be appropriate. The load-induced nonlinearity and method of construction might have caused significant heterogeneity in the base layer. The modulus varies between a minimum of 23 ksi and a maximum of approximately 63 ksi. The average modulus is about 37 ksi with a standard deviation of about 10 ksi.

Nonlinear behavior in terms of reduction in modulus with increase in load levels is not evident from the falling weight devices except for the KUAB device. However, for the vibratory devices the effects of nonlinearity is (at least) qualitatively evident. The Dynaflect, which applies 1 kip of load, has the highest modulus. Also for the WES vibrator, the modulus values increase as the load decreases.

### Subgrade Layer

The modulus of the subgrade determined from deflection basins measured by various devices falls in a narrow range. The minimum and maximum values are approximately equal to 14 ksi and 20 ksi, respectively. The average modulus is about 16.5 ksi with a standard deviation of 1.4 ksi. The coefficient of variation is relatively small, about 8.5 percent; this indicates that the modulus of the subgrade layer, unlike the other two pavement layers, is more or less independent of the testing device.

### Moduli from Alternative Sensor Configurations

Practically speaking, only surface sensors should be used in routine pavement evaluation. However, to understand the behavior of pavements under large loads and to determine

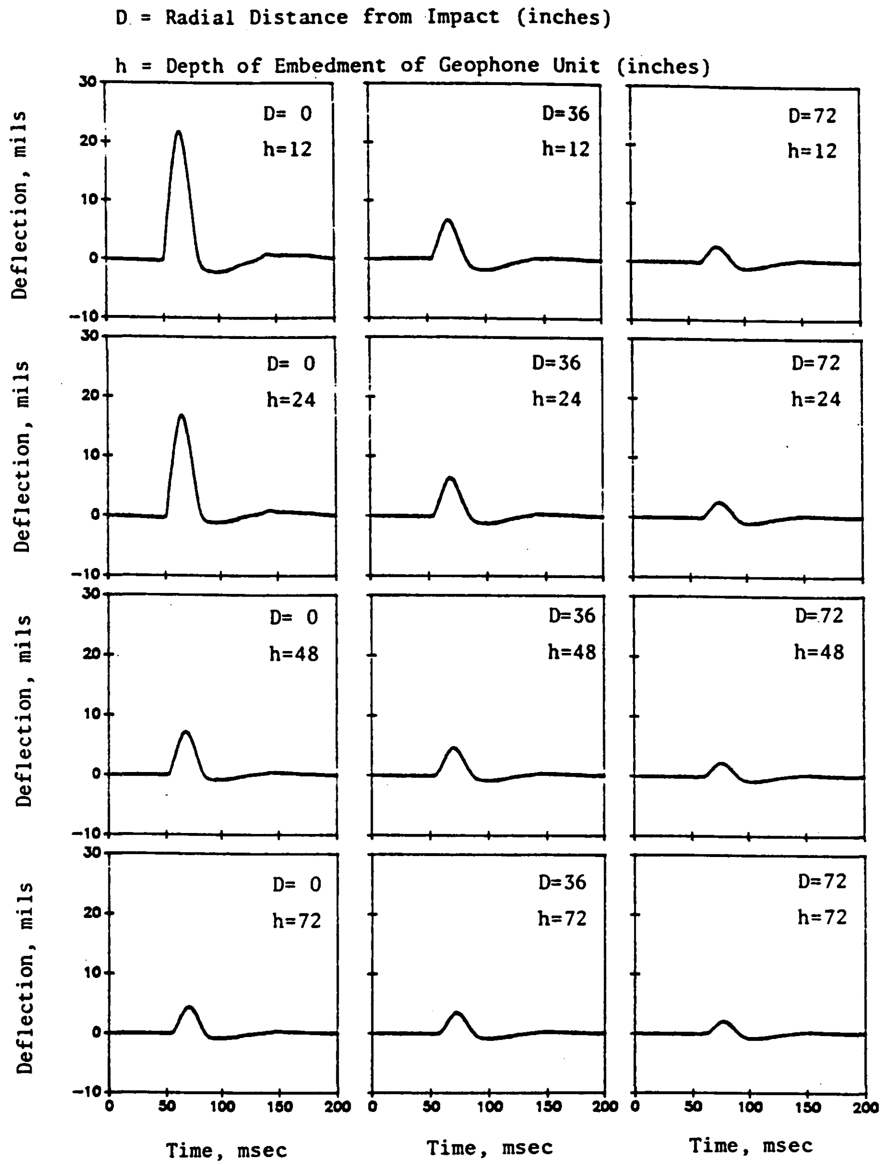


**FIGURE 2 Vertical displacement time histories from embedded geophone units caused by effects of FWD.**

the limitations of the NDT tests, it is desirable to determine moduli from other sensors embedded in the pavement. Eight different data sets were used for backcalculation, as shown in Figure 3. Data Set 1 corresponds to the surface deflections. Data Sets 2 through 5 contain only three deflection sensors. Each set represents the three sensor readings obtained at a given depth. Data Sets 6 through 8 correspond to a rather comprehensive set of deflections, as reflected in the figure.

### Effects of Load-Induced Nonlinearity

To study the effect of load-induced nonlinearity on backcalculated moduli, deflection data from various depths were used to determine the moduli of various layers. Data Sets 2 through 5, described in Figure 3, correspond to this exercise.

The backcalculated moduli for the base and subgrade for each data set are shown in Figure 4 for one FWD. The results from six other NDT devices are presented in Chai (*6*). For the sake of brevity, they are not represented here. However, the conclusions drawn here are more or less applicable to other devices.

In the backcalculation methodology, the modulus of the AC layer was fixed as 400 ksi. This was a good average based on the backcalculation of the surface deflections. The reason for not backcalculating the modulus of AC layer was the scarcity of deflection data in some cases.

Strain contour lines for a 6-in.-radius plate used by several NDT devices are shown in Figure 5. The computer program BISAR was used to determine the strains and stresses. The average moduli obtained from all NDT devices using the surface deflections were input in to the program (see Table 1).

**TABLE 1 Moduli Backcalculated from Surface Deflection Bowls Using Program BISDEF**

| Device, Load | Modulus of Asphalt (psi) | Modulus of Base (psi) | Modulus of Subgrade (psi) | Avg. Abs. Difference (Percent) |
|---|---|---|---|---|
| Dynatest 25 k | 260,756 | 30,882 | 16,142 | 5.0 |
| Dynatest 15 k | 221,778 | 33,881 | 16,548 | 4.7 |
| Dynatest 10 k | 249,457 | 33,860 | 17,735 | 4.7 |
| KUAB 15 k | 496,736 | 32,494 | 18,379 | 1.0 |
| KUAB 10 k | 414,194 | 36,848 | 17,766 | 0.9 |
| KUAB 5 k | 341,198 | 41,816 | 16,745 | 1.2 |
| Heavy FWD 45 k | 468,549 | 22,647 | 14,109 | 5.7 |
| Heavy FWD 25 k | 333,651 | 23,794 | 16,121 | 4.4 |
| Heavy FWD 15 k | 353,214 | 23,202 | 16,560 | 2.8 |
| Phoenix 20 k | 364,974 | 33,719 | 16,792 | 4.5 |
| Phoenix 15 k | 343,811 | 34,303 | 16,990 | 4.5 |
| Dynaflect 1 k | 287,299 | 63,141 | 15,564 | 2.8 |
| Road Rater 5 k | 1080,891 | 35,809 | 19,669 | 1.8 |
| WES 15 k | 442,919 | 39,537 | 14,295 | 5.2 |
| WES 10 k | 517,562 | 46,221 | 14,953 | 5.2 |
| WES 5 k | 619,770 | 54,623 | 15,793 | 5.2 |
| AVG | 424,797 | 36,788 | 16,501 | - |
| STD | 198,894 | 10,531 | 1,388 | - |
| COV | 46.8 | 28.6 | 8.4 | - |

| Deflection Data Set | Sensors Utilized |
|---|---|
| 1 | Surface Sensors only |
| 2 | 11, 12, 13 |
| 3 | 21, 22, 23 |
| 4 | 31, 32, 33 |
| 5 | 41, 42, 43 |
| 6 | 01, 02, 03, 11, 12, 13, 21, 22, 23, 31, 32, 33, 41, 42, 43 |
| 7 | 11, 12, 13, 21, 22, 23, 31, 32, 33, 41, 42, 43 |
| 8 | Surface Sensor, 11, 12, 13, 21, 22, 23, 31, 32, 33, 41, 42, 43 |

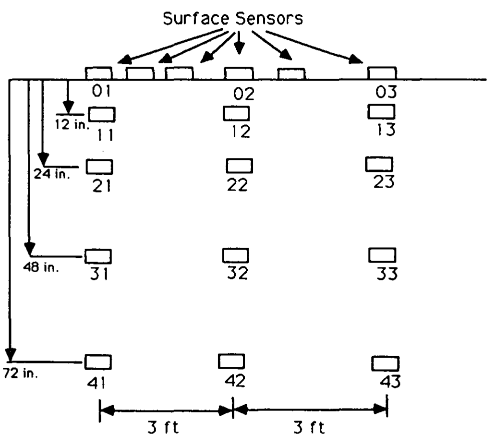


**FIGURE 3 Deflection data sets used in backcalculation.**

It is understood that utilizing a linear-elastic program for determining the contour levels may introduce some inaccuracies in the upcoming discussions. However, as demonstrated by Chai (*6*), the regions in which stresses and strains are relatively large are rather localized and limited to a small region close to the point of impact. Therefore, for regions several diameters away from the point of impact, the nonlinear and linear solutions should be similar.

To facilitate the upcoming discussion, for strain levels below 0.003 percent, it is assumed that the materials behave linearly. This region is called linear region. Any region in which the strain level lies between 0.003 and 0.01 percent is called a quasi-linear region. In this strain range, the reduction in moduli is typically less than 15 percent. The nonlinear region is the region in which the strains are greater than 0.01 percent. These ranges are selected on the basis of the terminology used in the earthquake geotechnical engineering.

In Table 2, the influence of load-induced nonlinearity as a function of the location of sensors is demonstrated. It can be seen that the sensors at a radial distance of zero are in either the nonlinear or quasi-linear range, and the sensors at radial distances of 72 in. are all in the linear range. One interesting point is that, for the sensors at radial distances of 36 in., deflections from Data Set 4 (depth of 48 in.) experience more load-induced nonlinearity than those from Data Set 3 (depth of 24 in.). This is because the sensors at the depth of 24 in. are embedded in the stiff base layer; whereas the sensors at a depth of 48 in. are located in the relatively soft subgrade soil. This matter is well reflected in the modulus of base layer (Figure 4).

The backcalculated moduli from this series is shown in Figure 4. From Data Set 3, one obtains smaller moduli than from Data Set 2. This is true for all three load levels. On the other hand, the modulus of the subgrade layer increases as the data sets from deeper strata are used.

For any given data set, moduli of the base and subgrade increase as the load level decreases. The increase in the modulus of the base under the lowest load is significantly higher for Data Sets 2 through 4. The reason for this matter is not known at this time.

Although not shown here, for data sets in which all three sensors are outside the nonlinear region, the average absolute difference is small (less than 3.5 percent); whereas, as soon as one or two of the sensors are located in the nonlinear range, a good basin fitting cannot be achieved. In the latter cases, the minimum value for the average absolute difference is about 7.8 percent. This can at least partially describe why in many pavement sections, the basic fitting cannot be carried out satisfactorily.

## Effects of Increased Number of Sensors

Typically, in the nondestructive evaluation of pavement deflections, from four to seven surface sensors are used to backcalculate the moduli of two to four layers. In the program BISDEF, the least-squares criterion is used to evaluate the closeness of the theoretical deflections to the measured ones. Typically, when the least-squares criterion is used, the more overcompensated the problem is (i.e., the larger the number

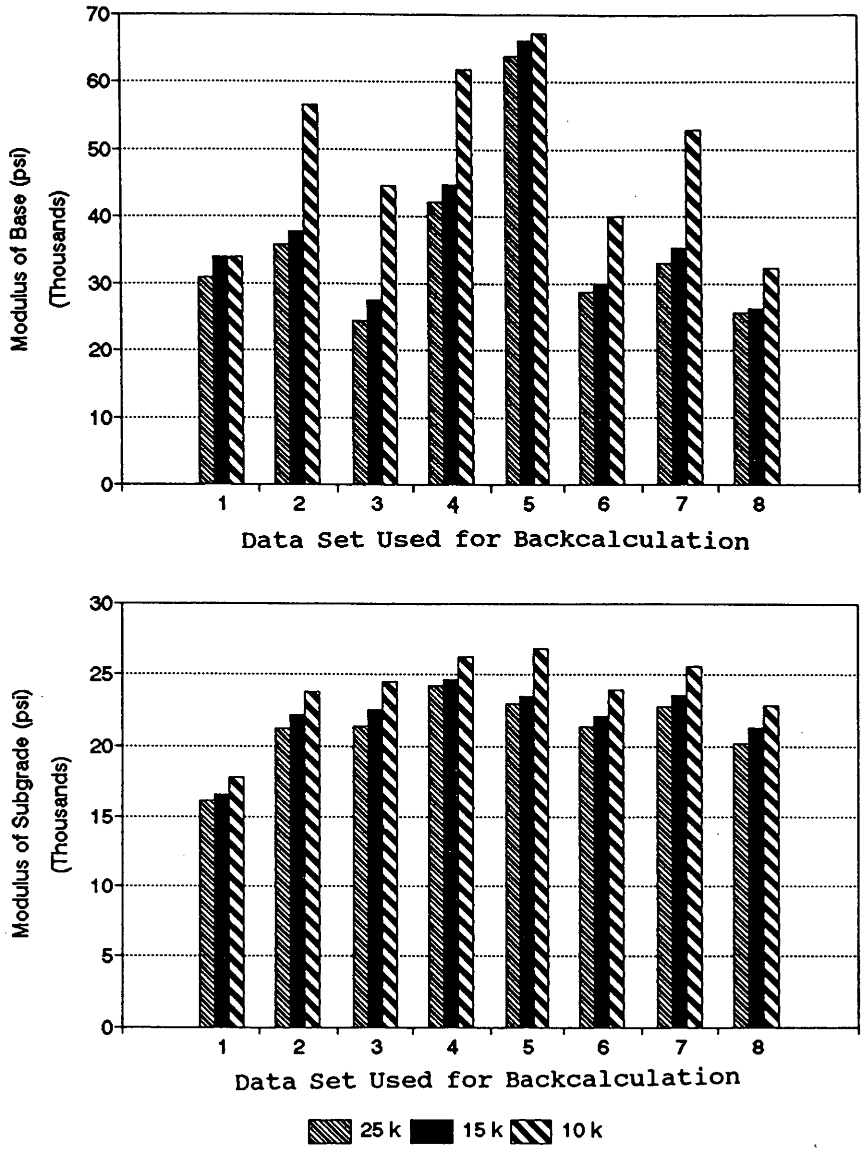


**FIGURE 4 Comparison of layer moduli of base (*top*) and subgrade (*bottom*) backcalculated from various data sets imparted by one FWD.**

of known data points relative to the number of parameters to be determined), the more statistically appropriate the outcome will be. This matter was investigated.

In Figure 4, three other data sets are presented. Moduli reported for Data Set 6 correspond to moduli backcalculated utilizing a total of 14 or 15 deflections. For Data Set 7, data from the embedded receivers were used. Twelve deflection points were available (see Figure 3). For the last series, Data Set 8, deflection from all surface sensors plus the 12 deflection points used in Data Set 7 were used (i.e., a total of 16 to 19 deflections).

To backcalculate moduli from these data sets, the pro gram BISDEF had to be slightly modified. Generally, the deflection basin fitting for Data Sets 6 and 8 did not yield satisfactory results (average absolute differences of greater than 10 percent). However, deflections from Data Set 7 could be matched relatively close (average absolute differences of about 5 percent). Once again, as the deflections from the nonlinear regions were minimized, the quality of basin fitting improved.

Because of an unsatisfactory deflection basin-fitting process, it would be difficult to draw definite conclusions. However, using deflections from Data Set 6 generally yields base moduli that are approximately equal to or slightly less than those obtained from surface sensors. However, the subgrade moduli are always greater from Data Set 6 compared with those backcalculated from surface sensors.

Typically, moduli obtained for the base and subgrade employing Data Set 7 are greater than those obtained from Data Set 1 (surface deflection data only). The reason for this matter is that deflections for Data Set 7 are from regions that are less affected with the load-induced nonlinearity.

Base moduli from Data Set 8 are always less than those determined from the surface deflections. By way of contrast,

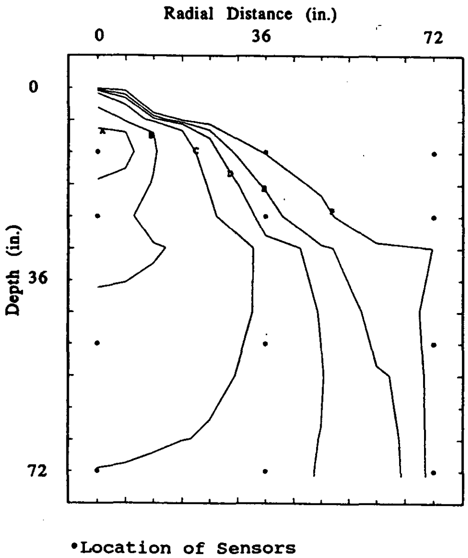


Description of Contours (Numbers in percent strain)

| Load, kip | A | B | C | D | E | F |
|---|---|---|---|---|---|---|
| 25 | 0.05 | 0.03 | 0.01 | 0.005 | 0.003 | 0.001 |
| 20 | 0.04 | 0.024 | 0.008 | 0.004 | 0.0024 | 0.0008 |
| 15 | 0.03 | 0.018 | 0.006 | 0.003 | 0.0018 | 0.0006 |
| 10 | 0.02 | 0.012 | 0.004 | 0.002 | 0.0012 | 0.0004 |
| 5 | 0.01 | 0.006 | 0.002 | 0.001 | 0.0006 | 0.0002 |

**FIGURE 5 Strain distribution in pavement section used in this study caused by loads applied to a 6-in.-radius plate.**

**TABLE 2 Degree of Load-Induced Nonlinearity at Sensor Locations for Load Plate with 6-in. Radius**

| Data Set | Sensor | Load Level, kips | | | |
|---|---|---|---|---|---|
| | | 5 | 10 | 15 | 25 |
| 2 | 11 | N | N | N | N |
| | 12 | L | L | L | L |
| | 13 | L | L | L | L |
| 3 | 21 | Q | N | N | N |
| | 22 | L | L | L | Q |
| | 23 | L | L | L | L |
| 4 | 31 | Q | Q | Q | N |
| | 32 | L | Q | Q | Q |
| | 33 | L | L | L | L |
| 5 | 41 | L | Q | Q | Q |
| | 42 | L | L | Q | Q |
| | 43 | L | L | L | L |

N: Nonlinear
Q: Quasi-Linear
L: Linear

the subgrade moduli are always greater than those obtained from surface deflections.

## COMPARISON OF DEFLECTIONS

A good indication of the quality of the backcalculation techniques is how well the measured deflections and the deflections determined from the backcalculated moduli compare. If the two compare closely, one can conclude that the existing processes are adequate.

Another motivation for comparing the measured and calculated deflections is to verify a widely implemented assumption that accurate design parameters can be obtained from elastostatic backcalculation programs provided that heavy loads (corresponding to expected traffic loads) are applied to the pavement. In other words, if one imparts large loads to the pavement surface and measures deflections affected with load-induced nonlinearity; and if one backcalculates moduli from an algorithm (such as BISDEF), which is based on the assumption that materials behave linear elastically; and finally, if the backcalculated moduli are used to determine the stresses, strains, and deformations using an elastostatic algorithm (similar to BISAR), the measured and calculated stresses, strains, and deformations at that load level will be similar. This matter is investigated next.

The comparison of measured and calculated deflections from one data set is presented in Figure 6. The calculated deflections are determined from a layer modulus backcalculated from deflection Data Set 1 (surface sensors only) caused by 25 kips of load applied by an FWD. The comparison of deflections from all devices and all load levels is included in Chai (*6*).

The deflection contour lines obtained from the deflections measured with one FWD at a load level of 25 kips is shown in Figure 6*a*. The contour lines are rather coarse because of the scarcity of deflection data. The points where data were collected are marked with a small solid point. Next to each data point, the measured deflections in mils are reflected. The contour lines are depicted as solid lines, and the contour value is reflected in bold numbers next to each line.

At a depth of about 27 in., a sharp change in the slope of the contour lines can be observed. This depth corresponds to the thickness of the AC and base layers. Sharp changes in the slopes at this level are expected because of the differences between the modulus of the base and subgrade layers. Had the data been collected with more resolution (i.e., utilizing more geophone units) a similar change in slope would have been observed at the interface of the asphalt and the base layers.

To compare the theoretical and experimental results, contour lines were again determined. However, instead of using measured deflections, deflections calculated from BISAR using backcalculated moduli were used. The contour lines for this case are presented in Figure 6*b*. Basically, the two deflection contours vary significantly. This variation is summarized and quantified in the next paragraph.

Shown in Figure 7*a* is the average percentage difference between the calculated and measured deflections for each device and each load level for Data Set 1 (surface deflections only). To obtain this value for a given device and load level, the corresponding absolute difference between the measured and calculated deflections from 15 sensor locations (12 embedded and 3 on the surface) were averaged. A small value will indicate overall agreement between the measured and calculated value.

In Figure 7*b*, the average absolute difference from deflection-basin fitting for each device and load level is shown. The two parameters (average percent difference in deflections and av-

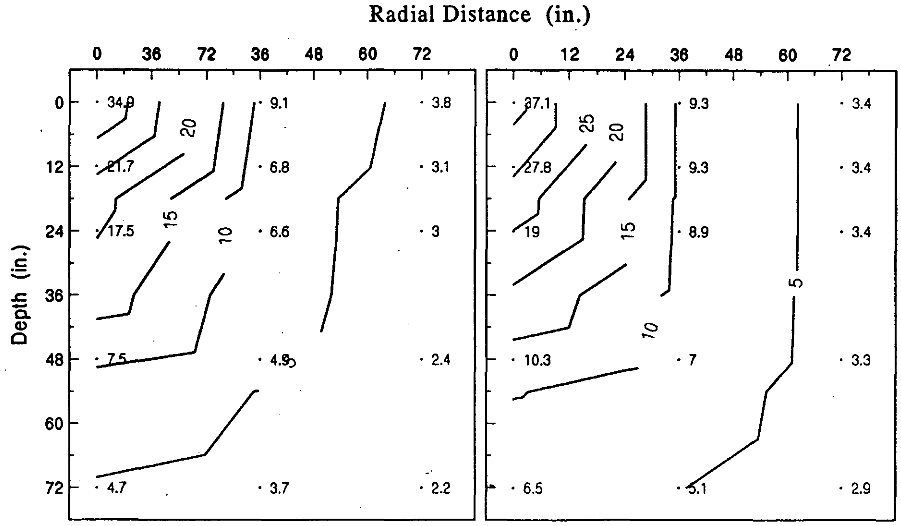


**FIGURE 6 Comparison of measured (*left*) and calculated (*right*) deflections from one FWD.**

| Device | 1 | 2 | 3 | 4 | 5 | 6 | 7 |
|---|---|---|---|---|---|---|---|
| Equipment | Dynatest | Kuab | WES 16-kip | Road Rater | Dynaflect | HWD | Phoenix |

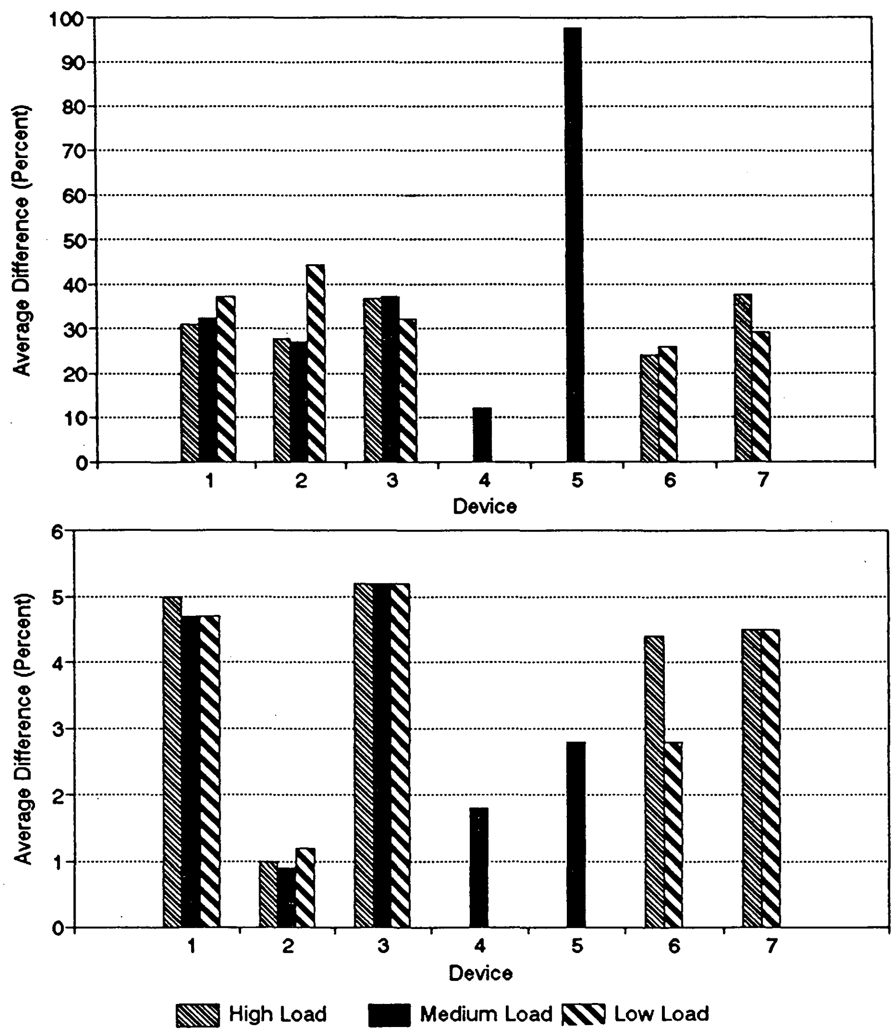


**FIGURE 7 Comparison of measured deflections with deflections calculated from backcalculated moduli using Data Set 1: *top*, measured versus calculated; *bottom*, from basin fitting.**

erage absolute difference in the basin fitting) go hand in hand. It is not appropriate to compare experimental deflections with theoretical deflections obtained from backcalculated moduli where the basin fitting is not done closely.

For the surface deflections, the basin fitting is done reasonably well for every case. The minimum and maximum average absolute differences in basin fitting are 0.9 percent and 5.7 percent, respectively (Figure 7*b*). However, the theoretical and experimental deflections within the body of pavement do not compare well at all. The average percent differences from Figure 7*a* vary from a minimum of about 24 percent to a maximum of about 98 percent.

Results from other data sets are not shown here, for the sake of brevity. For Data Sets 2 through 4 as deeper data sets were used, the difference among various devices and load levels were less pronounced. This may suggest that the discrepancy between the measured and calculated data is caused by the inherent problems in the data reduction instead of the type and magnitude of load. The agreements between the measured and theoretical deflections for Data Set 5 are much better than those obtained from surface deflections as reflected in the figure. The average difference is always less than 20 percent.

The last three data sets (Data Sets 6 through 8) should logically yield relatively good agreement between the measured and calculated deflections. Basically, data from all data points were used in deflection basin fitting. For Data Set 6, the average absolute differences are less than 20 percent. Such a relatively good agreement may be fortuitous because of large absolute differences found from deflection basin fitting. Similar results were obtained from Data Sets 7 and 8.

## DETERMINATION OF STRESSES

The modulus of each layer backcalculated from various deflection data sets can be used to calculate stresses at interface directly under the load from progam BISAR. The normalized radial tensile stresses and normalized vertical stresses at Interface 1 (AC and base layers) and Interface 2 (base and subgrade layers) are computed. To obtain normalized stresses, the stress calculated from BISAR at each interface was divided by the loading stress applied at the surface. These data can be used to estimate the amount of stress generated in the pavement system by each device.

### Vertical Stresses

Vertical stresses determined from various data sets are reported in Chai (*6*). For one FWD, the calculated vertical stresses are shown in Figure 8. For Interface 1, the highest vertical stresses were obtained when backcalculated moduli from Data Set 1 (surface sensors) or Data Set 5 (deepest three sensors) were used. For Interface 2, the stresses are more or less independent of the data set used or the level of load applied.

Stresses in a pavement section are directly related to the Young's moduli of different layers. This matter is well reflected in Figure 8. Considering the fact that the modulus of the AC layer was assumed to be constant for Data Sets 2 through 5, the vertical stress at Interface 1 increases as the modulus of the base layer increases (see Figure 4). Similarly, the stress at Interface 2 decreases with an increase in the modulus of subgrade.

For the other three falling weight devices, similar trends occur. For these three devices, the highest vertical stress at Interface 1 occurs when Data Set 5 was used. Data Set 5 corresponds to the three deflections least affected by the load-induced nonlinearity. This trend is significantly important from a design point of view. Vertical stresses calculated using the conventional surface sensors are in the order of 25 to 100 percent lower than those determined from Data Set 5. It is premature to make any conclusions on the basis of one site. However, this may suggest that (against popular belief), for the study of rutting, the use of moduli obtained from techniques using lower load intensities may be desirable. More study of this phenomenon is highly recommended.

On the other hand, the stresses obtained at Interface 2 are usually most critical from surface deflections. However, for most data sets (except Data Set 5), the vertical stress at Interface 2 is reasonably independent of the data set used in backcalculation or the load level applied to the pavement.

For WES 16-kips vibrator and the Road Rater, the trends in variation in vertical stresses at the two interfaces as a function of data set used follow trends that are similar to those of the falling weight devices described above.

The results from the Dynaflect device indicate that the stresses obtained from Data Sets 1 through 4 are similar and independent of data set used. One possible explanation for this closeness is that deflections from all four data sets correspond to the linear range and therefore yield similar moduli and stresses. Deflections from Data Set 5 for Dynaflect suffer from a low signal-to-noise ratio and therefore are not as reliable.

In general, the maximum values for the first interface vary between about 20 and 42 lb/in.$^2$, and for the second interface between 2.5 and 3.6 lb/in.$^2$. The minimum vertical stresses varied from 10 to 18 lb/in.$^2$ for Interface 1, and from 1 to 3.4 lb/in.$^2$ for Interface 2. This figure may be an indication of the device dependency and load dependency of the results obtained from the deflection-based NDT devices.

### Radial Stresses

Radial stresses determined from various data sets from one FWD are presented in Figure 9. Basically, stresses from all devices (except the Dynaflect) exhibit similar behaviors. For Interface 1, Data Set 5 yields the smallest radial tensile stresses. Simultaneously, radial stresses at Interface 2 affected by the same set of data (Data Set 5) result in the largest tensile stresses. Practically speaking, moduli obtained from deflection data less affected by the load-induced nonlinearity may result in higher radial stresses at the base-subgrade interface.

For Interface 1, the variability in the results is large for Data Set 1 because of a large variation in the modulus of AC layer. As for Data Sets 2 through 5, a constant modulus value was assigned to the AC layer, and the stresses follow a predictable pattern. Basically, moduli from Data Set 3 are the most critical values in terms of stresses at Interface 1.

As for the vertical stresses, the signal-to-noise ratio for the data collected with the Dynaflect is small, and this matter may have caused the amount of scatter seen in the data.

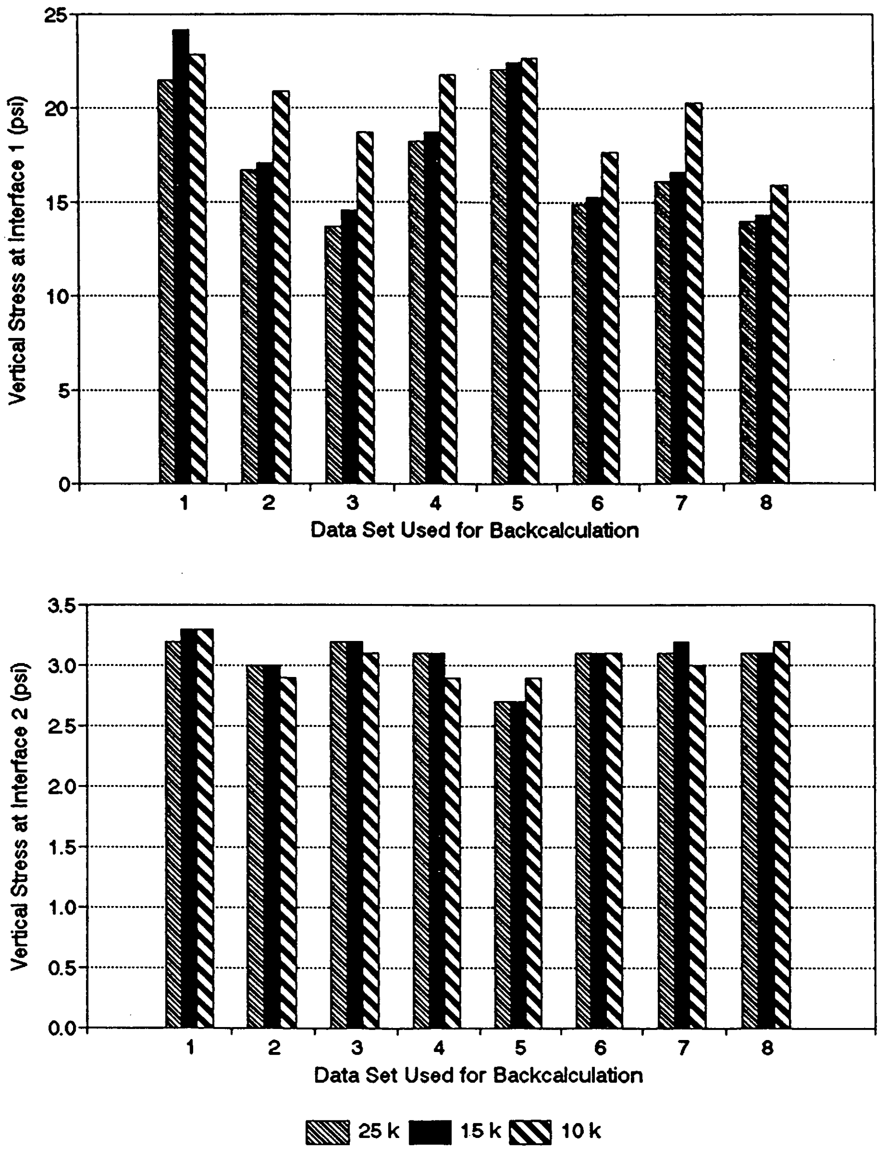


**FIGURE 8 Variation of vertical stresses at two interfaces for various data sets caused by a 9,000-lb load applied using moduli backcalculated from Dynatest FWD: *top*, Interface 1; *bottom*, Interface 2.**

Large variations in the minimum and maximum values of tensile radial stresses at both interfaces as a function of the type of device used and the nature of load imparted were evident.

## SUMMARY AND CONCLUSIONS

Backcalculation methods for determining elastic moduli from deflection profiles obtained by nondestructive testing devices have provided researchers with a tool to improve pavement design. Nevertheless, it is important to verify the accuracy of backcalculating methods. The use of a relatively low-cost geophone system to achieve this goal is described in this paper.

The process of installation of the geophone system is presented. An explanation of the approach used to determine deflections using geophones is reviewed. Deflections from seven NDT devices were used to determine the closeness between the measured and calculated responses of a pavement section. The limitations of one backcalculating algorithm as a function of amplitude of loads imparted and the type of device used were examined. The capability of modeling the behaviors of pavements from backcalculated moduli using elastostatic programs was investigated. The stresses critical to design were also examined.

Because only one site was used, it may be premature to make any conclusions. However, the results from this study reveal some items that may be of interest for further theoretical and experimental investigations. These items are

1. Deflection basin fitting would not yield a close match between the theoretical and measured deflections when some

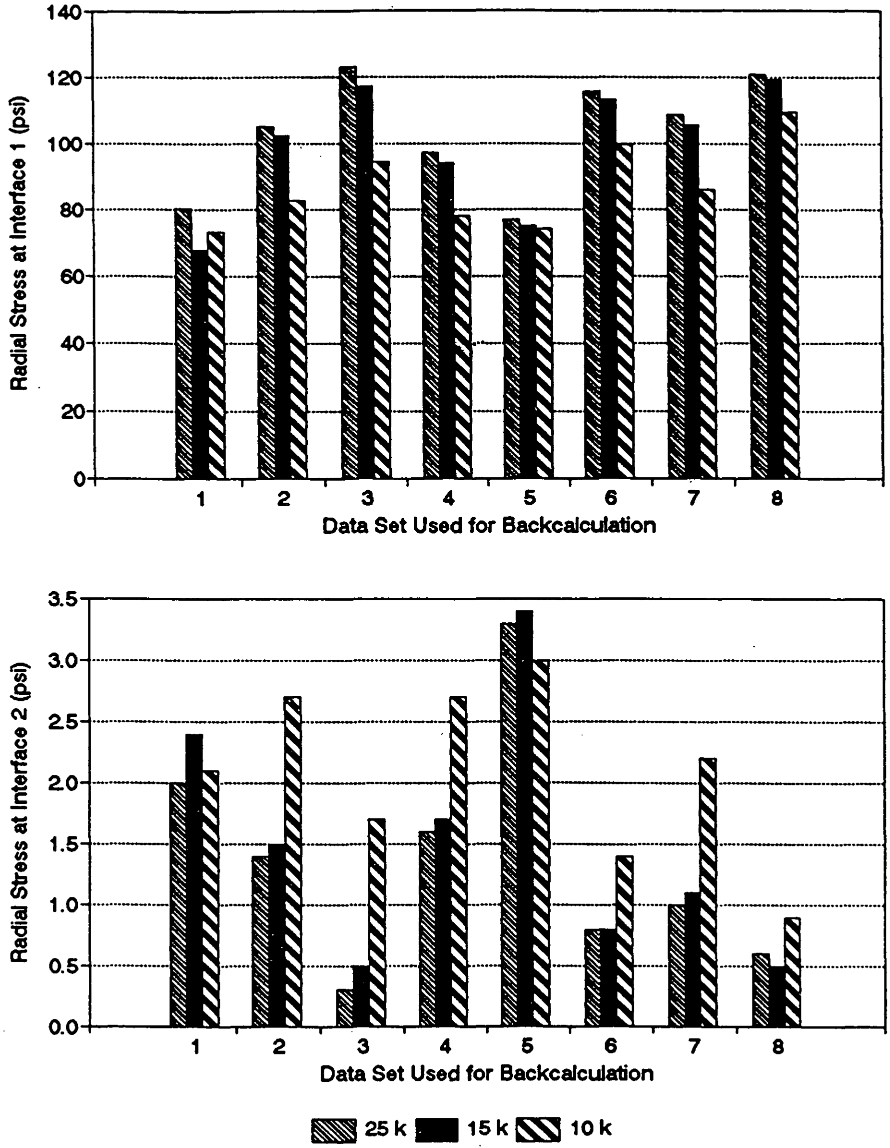


**FIGURE 9 Variation in radial stresses at two interfaces for various data sets caused by a 9,000-lb load using moduli backcalculated from one FWD: *top*, Interface 1; *bottom*, Interface 2.**

of the deflections are obtained from the regions contaminated with load-induced nonlinearity; conversely, the deflection basin fitting may yield a close match when none of the deflections are measured in the nonlinear region;

2. Theoretical deflections within the body of a pavement from backcalculated NDT moduli (using surface deflections), may not be representative of deflections measured at similar points;

3. Theoretical deflections, calculated from measured deflections away from the load (not affected with load-induced nonlinearity), may be close to measured deflections at similar points;

4. Vertical compressive and radial tensile stresses determined from moduli backcalculated from conventional surface deflections may be conservative.

Finally, many of the conclusions and statistics made here are further analyzed and substantiated in Chai (*6*). Because of space limitations, only the major steps are highlighted herein. The interested readers are referred to that publication for a comprehensive discussion.

## ACKNOWLEDGMENTS

This work was supported by the University of Texas at El Paso. The instrumentation of the site and the collection of the raw data were done with the technical and monetary assistance of the Army Corps of Engineers Waterways Experiment Station. Al Bush, Don Alexander, and Ross Bensten of that organization are acknowledged for their technical as-

sistance, hard work, and friendship. Dennis Hiltunen of Penn State was of great help in collecting the field data.

## REFERENCES

1. T. Scullion, R. C. Briggs, and R. L. Lytton. *Using the Multidepth Deflectometer to Verify Modulus Backcalculation Procedures*. ASTM Special Technical Publication 1026, Philadelphia, Pa., 1989, pp. 90–101.
2. V. Tandon and S. Nazarian. *Comprehensive Evaluation of Sensors Used for Pavement Monitoring*. Research Report 913-1F. University of Texas at El Paso, 1991.
3. R. A. Bensten, S. Nazarian, and J. A. Harrison. *Reliability Testing of Seven Nondestructive Pavement Testing Devices*. ASTM Special Technical Publication 1026, Philadelphia, Pa., 1989, pp. 278–290.
4. W. R. Hudson, G. E. Elkins, W. Uddin, and K. T. Reilley. *Pavement Condition Monitoring Methods and Equipment, Phase I—Part 1 Evaluation of Deflection Measuring Equipment*. Report FH67/1. ARE Inc., Austin, Tex., 1986.
5. S. Nazarian, E. Y. Chai, and D. R. Alexander. Pavement Instrumentation for Verifying Elastic Theory. *Proc., 2nd International Symposium on State-of-the-Art of Pavement Response Monitoring Systems for Roads and Airfields*, West Lebanon, N.H., Sept. 1991.
6. Y. E. Chai. *In Situ Verification of Layer Theory for Pavement Design and Rehabilitation*. Master's thesis. University of Texas at El Paso, 1990.

# Nondestructive Testing with Falling Weight Deflectometer on Whole and Broken Asphalt Concrete Pavements

FRIEDRICH W. JUNG AND DIETER F. E. STOLLE

Extensive testing of flexible pavements with the falling weight deflectometer on various test sites in Ontario has aided the development of a rational method of deflection basin interpretation. The goal is a fast computer program (PROBE) that calculates important mechanistic response parameters and determines the quality of data and the degree of structural integrity of the pavement layers. Using the theory of Boussinesq and Odemark's method of equivalent layer thickness, two quantities are defined to help interpret deflection bowl data: (a) the effective modulus of measured surface deflection and (b) the effective modulus of subgrade deflection. Both moduli change with their radial distance from the test load. When plotted they may briefly be referred to as the surface modulus profile and the subgrade modulus profile, respectively. Both moduli provide apparent values of elastic stiffnesses, using uniform elastic half-space solutions. They are parameters for a systematic study of the difference between the theoretically expected and the observed behavior of asphalt concrete pavements. The surface modulus profile evaluates the quality and integrity of pavement layers. Both the surface and subgrade modulus profile are used to estimate the subgrade modulus near the test load, which is the base for further calculations of primary response parameters by the Odemark method. Examples are presented, ranging from very good to poor and broken conditions. Computer simulations with various programs suggest two major points: (a) dynamic effects have only a comparatively minor influence, so that elastostatic modeling appears to be feasible; and (b) deflections die away faster than expected with radial distance, probably because of an increase in the subgrade modulus with depth, an unrecorded presence of a bedrock face, or—more likely—discontinuities of unbound or cracked layer materials. In short, the new approach tries to obtain information and interpretations on system features of field cases by systematically studying the deviation from simple elastostatic modeling.

Owing to the popular use of the falling weight deflectometer (FWD), a great deal of effort has gone into interpreting FWD-generated deflection data. Such efforts have mainly centered around the backcalculation of layer material properties within the framework of continuum mechanics, in particular, the elastic layer theory.

This theory, however, implies that a certain condition be met, namely that the pavement layers are continuous and are not broken or cracked, or that at least the FWD test is carried out on a spot of unbroken or uncracked pavement. Continuum mechanics assumes continuous layer materials and cannot describe cracked or broken pavements. Unfortunately, this fact has diminished the usefulness of backcalculated results. For this reason more emphasis should be placed on interpretation rather than on backcalculation.

F. W. Jung, Pavements and Roadway Office, Research and Development Branch, Ministry of Transport of Ontario, Downsview, Ontario, Canada. M3M 1J8. D. F. E. Stolle, Department of Civil Engineering and Engineering Mechanics, McMaster University, Hamilton, Ontario, Canada L8S 4L7.

Many tests in Ontario have been carried out on flexible pavements that were severely cracked or broken, and it was found that no elastostatic analysis method could interpret the results. Such experience with respect to analyzing data, gathered at severely damaged sections, has confirmed the inappropriateness of using elastic theories in the usual way. Therefore, an alternative backcalculation and interpretation methodology has been investigated. Instead of emphasizing more realistic modeling of the boundary value problem, the new approach, incorporated into the new PROBE program, uses differences between the real problem and the idealized problem, to estimate a "weighted average" of in situ properties and to obtain other important information on the integrity and the state of deterioration of layer materials.

## EFFECTIVE MODULUS OF MEASURED SURFACE DEFLECTION

The FWD is an instrument that measures the peaks of a deflection wave from an impulse load created by a falling weight. The test load is distributed over a circular contact pressure area 300 mm in diameter and thus resembles, also in its duration in time, a passing heavy single-tire wheel load from a truck. An essential feature is that the peak deflections, measured at various distances from the load, superficially resemble the deflections created by a corresponding elastostatic load.

The first step of the new approach is to assume that the FWD-generated deflections correspond to elastostatic deflections on a uniform elastic half space. Then, to interpret the data, effective moduli are calculated that are apparent, but well-defined, values of surface stiffness.

### Definition

The effective modulus of measured surface deflection of a flexible pavement in an FWD test is defined as follows: it is the modulus that a uniform elastic half space would have under a corresponding static load, having the same deflection as measured by the FWD sensor, at the same distance from

the load axis on a layered flexible pavement. This term is sometimes called the surface modulus. It is a function of the distance from the load axis.

### Derivation

The concept is derived from a paper by Yoder and Witczak (*1*, p.29), which contains an equation for the vertical deflections in a uniform elastic half space, loaded by a circular distributed load. For the surface deflections ($Z = 0$) the equation can be written as follows:

$$Y = P(1 - \mu^2)A\ H/E \tag{1}$$

where

$Y$ = vertical surface deflection,
$P$ = contact pressure (force per unit area),
$\mu$ = Poisson's ratio (assumed to be 0.35),
$A$ = radius of loaded area,
$E$ = modulus of linear elastic material,
$H$ = a function of ratio $X/A$, and
$X$ = distance from load axis.

Solving Equation 1 for $E$, one obtains the function of the effective modulus of surface deflection, $E_x$, in which the deflections, $Y$, are now regarded as the result of FWD deflection measurements.

$$E_x = P(1 - \mu^2)A\ H/Y \tag{2}$$

Note that for distant deflections ($X > 5A$) the factor, $H$, merges into $H = A/X$. This means Equation 1 becomes identical to the Boussinesq equation for a concentrated load, $L$ (with $L = \pi P\ A^2$), and Equation 2 is then identical to the one offered by Ullidtz (*2*).

### Characteristics of Surface Modulus Profile, $E_x$

Characteristics of the surface modulus profile are illustrated in Figures 1 through 6 and have been drawn after studying many field tests of flexible pavements in Ontario; in the figures, $X$ is the point of FWD measurement. The following features have been observed:

1. Near the load, the stiffening effect of the upper structural layers is strongest, and the effective modulus is large, because at and around the load position the effective modulus represents the overall stiffness of all the pavement layers.

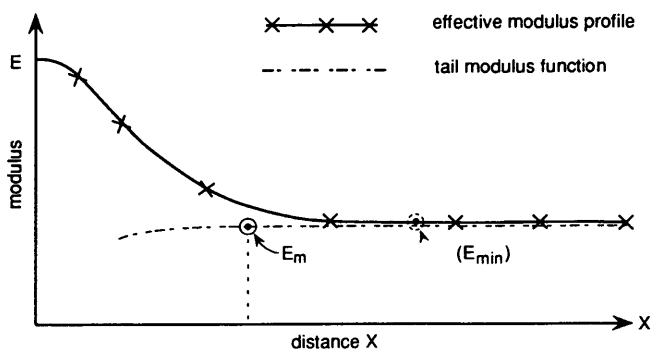


**FIGURE 1 Effective and tail modulus for elastic layer systems.**

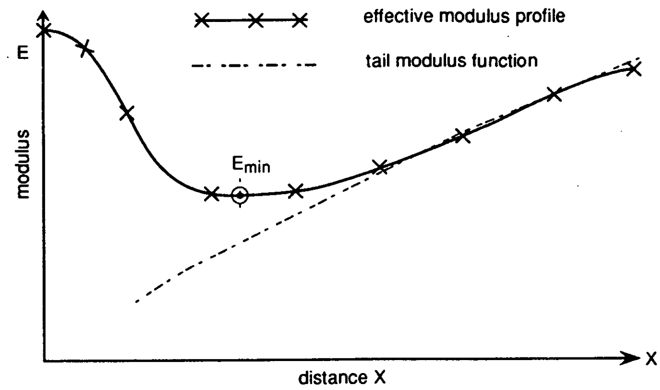


**FIGURE 2 Effective and tail modulus for whole AC pavements.**

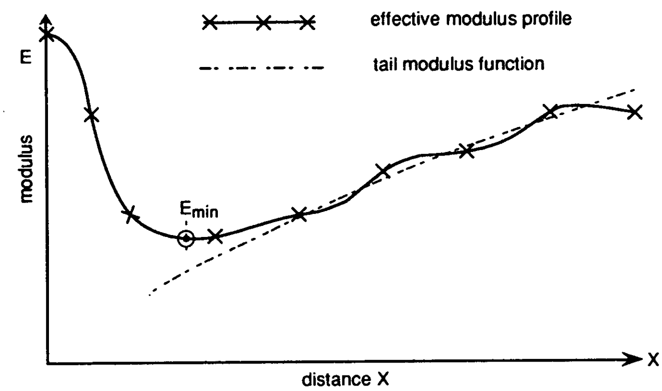


**FIGURE 3 Effective and tail modulus for cracked AC pavements.**

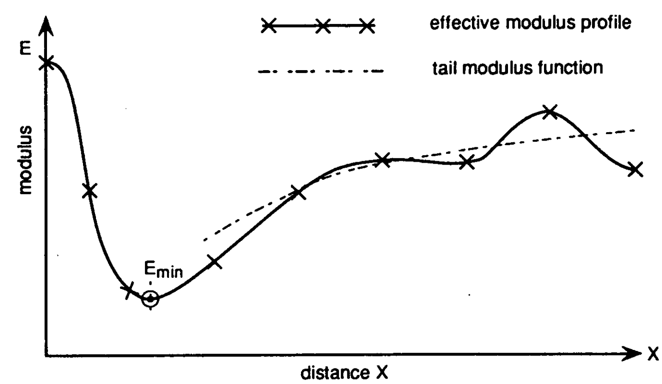


**FIGURE 4 Effective and tail modulus for broken AC pavements.**

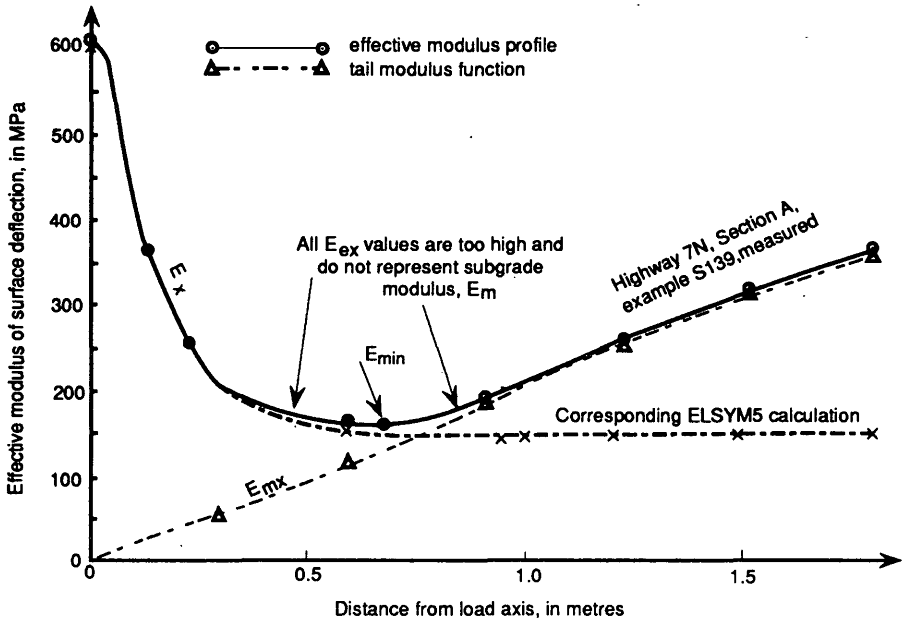


**FIGURE 5 Concept of effective modulus of surface deflection: Highway 7N, Section A example.**

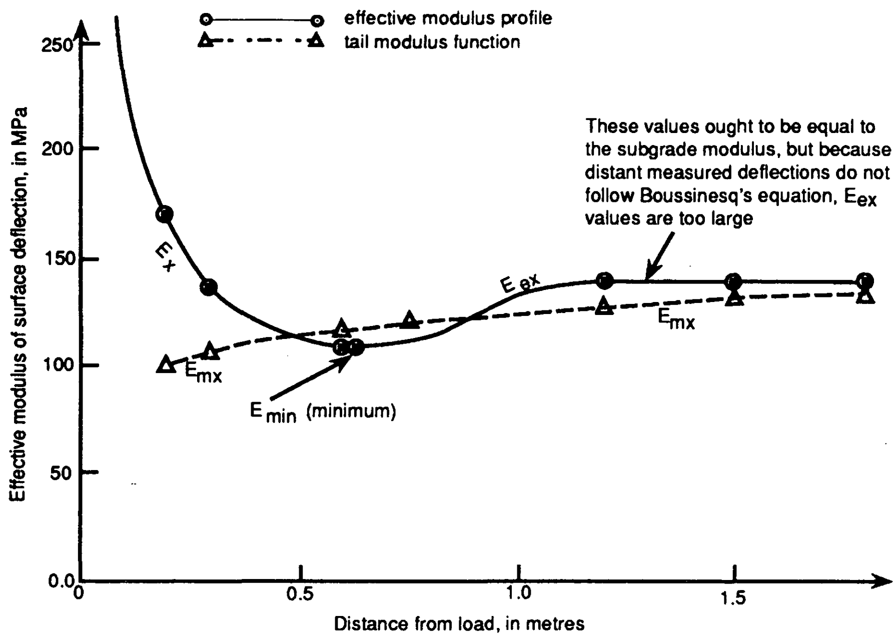


**FIGURE 6 Concept of effective modulus of surface deflection: Highway 7N, test pit example, Highway 80 Near Sarnia, 1989, partly broken AC.**

2. When using computer-generated data (ELSYM5) of a layered pavement structure, for linearly elastic materials and for an "infinitely" deep subgrade with constant elastic stiffness, the distant tail of the effective modulus profile merges into a horizontal asymptote at the level of the subgrade modulus, $E_m$, as shown in Figure 1.

3. When using real data from the tested flexible pavements, this asymptote is not horizontal any more, but becomes a line or curve with a positive gradient, as illustrated in Figures 2 through 5. The reason is that the measured deflections die away faster with increasing distance than the elastostatic model would allow. A faster decrease in deflections means an increase in the computed surface modulus values.

4. Because of the characteristics in Items 1 and 3 on all field-tested flexible pavements, the profile of the effective modulus of surface deflection has a minimum, usually not too far from the load (within a meter or less). The location of the minimum signifies that the stiffening effect of the upper layers

has faded away, and the stiffness at and beyond this distance is determined by the subgrade.

5. The magnitude of this minimum value of the effective modulus and its distance from the load axis both have been observed to diminish with a decrease in pavement integrity, or wholeness, usually manifested by cracks.

6. On flexible pavements of good or fair condition (Figures 2, 3, and 5) the distant values of the effective moduli are located on a line or curve that can be called the tail modulus function. On pavements in severely cracked or broken condition, the tail modulus function cannot be determined (Figure 4). The tail modulus function is discussed next.

### Quality Indicators from Curve Fitting of Tail Modulus Function

The tail modulus function, $E_{mx}$, is derived by modifying Equation 8 from Jung (*3*):

$$E_{mx} = \frac{P\,A^2(1 - \mu^2)X^{(\eta - 1)}}{\zeta} = C \cdot X^{(\eta - 1)} \tag{3}$$

where

$E_{mx}$ = tail modulus function, as established below;
$A$ = radius of contact pressure area;
$C$ = constant;
$X$ = distance from load; and
$\eta$, $\zeta$ = constants found by curve-fitting deflection data (*3*).

In the earlier version of PROBE that is based on consistency tests on data collected in Ontario (*3,4*), the value of the tail modulus function, at $X_t$ = 0.75 m, was considered an approximation of the subgrade modulus, $E_m$, valid at and around the test load. This approximation yielded consistent results on various test sections in Ontario, although values often are too high.

A comparison with MODULUS, a layer analysis program developed in Texas, was important. The modulus, $E_m$, as calculated by the original PROBE program (Equations 3 and 4 with $X = X_t = 0.75$), compares well with the subgrade modulus computed by MODULUS in Lytton et al. (*5*, p.77). The comparison is illustrated in Figure 7. The values $E_4$, from the MODULUS program, are about 10 to 25 percent larger than the values $E_m$. The correlation coefficient of the linear regression analysis for 21 reliable data points (out of 25 total) is $r = 0.984$.

In the current version of PROBE, the curve fitting is carried out by linear regression analysis of the logarithms of Equation 3:

$$\log E_{mx} = \log C + (\eta - 1)\log X \tag{4}$$

To establish the constants, $C$ and $\eta$, with some confidence, three or four valid points from the tail of the deflection basin are needed.

In the current version of the PROBE program, poor quality of pavement is indicated by a group of information items, such as

1. The number and the location of sensor readings discarded at the tail of the basic (for instance, two values at 1.5 m and 1.8 m in the case of broken pavement),

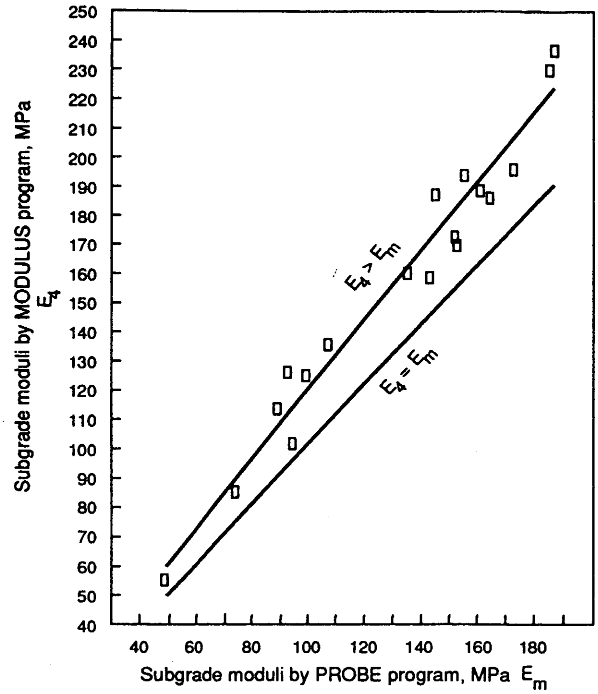


**FIGURE 7 Comparison of subgrade moduli [21 points (*5*)].**

2. Several deflection sensor readings with large errors of fit (errors of fit >10 percent),
3. A large value of $\eta$(>2.5), and
4. Low correlation coefficient (<0.85).

All four items should be considered. The correlation coefficient is the last and the weakest criterion because it is optimized by discarding sensor locations that exhibit too large an error of fit.

## EFFECTIVE MODULUS OF SUBGRADE DEFLECTION

The effective modulus of subgrade deflection is derived from Boussinesq's equation for vertical deflections in a uniform half space at the depth $Z = H_{em}$.

$$E_{mz} = \frac{P(1 - \mu^2)\,A^2}{XY_s}\left[\frac{1}{\sqrt{1 + \left(\frac{z}{x}\right)^2}} + \frac{\left(\frac{z}{x}\right)^2}{2(1 - \mu)\left(\sqrt{1 + \left(\frac{z}{x}\right)^2}\right)^3}\right] \tag{5}$$

where

$E_{mz}$ = subgrade modulus profile, effective modulus of subgrade deflection (MPa);

$Z = \Sigma H_{em}$ = sum of equivalent layer thicknesses, with respect to subgrade modulus; and
$Y_s$ = vertical deflection on top of subgrade (mm) (refer to Equation 6).

$$Y_s = Y\left[1 - (1 - K) \cdot \frac{E_m}{E_{1\text{eff}}} \cdot \frac{H_1 + H_2 + H_3}{Z}\right] \qquad (6)$$

where

$K$ = expression in square bracket of Equation 5,
$E_m$ = subgrade modulus,
$E_{1\text{eff}}$ = combined effective modulus of upper layers, and
$H_1 + H_2 + H_3$ = sum of thicknesses of upper layers.

Equation 6 is an approximate correction for establishing the deflection on top of the subgrade, $Y_s$. The value $Y_s$ (unknown) is computed from the measured surface deflection ($Y$).

By means of an iterative procedure, Equations 5 and 6 are used to calculate the subgrade modulus profile, $E_{mz}$, which is similarly defined as the surface modulus profile, $E_x$. The $E_{mz}$ profile has its lowest value under the test load and starts with a horizontal tangent. In normal flexible pavements (asphaltic concrete and unbound granular bases), the $E_{mz}$ profile increases with radial distance, $X$, from the test load, and the gradient of this increase is steeper for cracked and broken pavements. For continuous elastic materials (such as portland cement concrete on cement-treated bases) the $E_{mz}$ profile is virtually a horizontal straight line. Thus, the shape of the $E_{mz}$ profile was found to be indicative of material characteristics.

However, the main purpose of this profile is to estimate a value for the subgrade modulus, $E_m$, an in situ "weighted average," to be used for the calculation of subgrade parameters by the Odemark method.

## DISCUSSION ON SURFACE AND SUBGRADE MODULUS PROFILES, $E_x$ and $E_{mz}$

As shown in Figures 1 through 6, the surface modulus profile at and around the load position has large values caused by the stiffening effect of the structural layers [asphalt concrete (AC), base, and/or subbase]. For pavements that are whole and in good condition, the minimum values of the effective modulus profile, $E_{\min}$, are larger than the subgrade modulus, $E_m$, because of the residual stiffening effect of the structural layers. This keeps the overall stiffness at the minimum point above that of the subgrade, which is assumed to have the lowest modulus value of all layers.

It has been observed in pavements that are cracked or broken that the minimum value of the effective modulus profile decreases. When the pavement is very severely cracked and completely broken, this minimum must finally approach a value that represents the subgrade modulus, i.e., the modulus near the top of the subgrade at and around the test load. This is illustrated in Figure 8 where the point ($X_{\min}$, $E_{\min}$) has moved very close to the subgrade modulus curve.

Equation 5 is used by the current PROBE program to calculate the effective modulus of subgrade deflection, and it

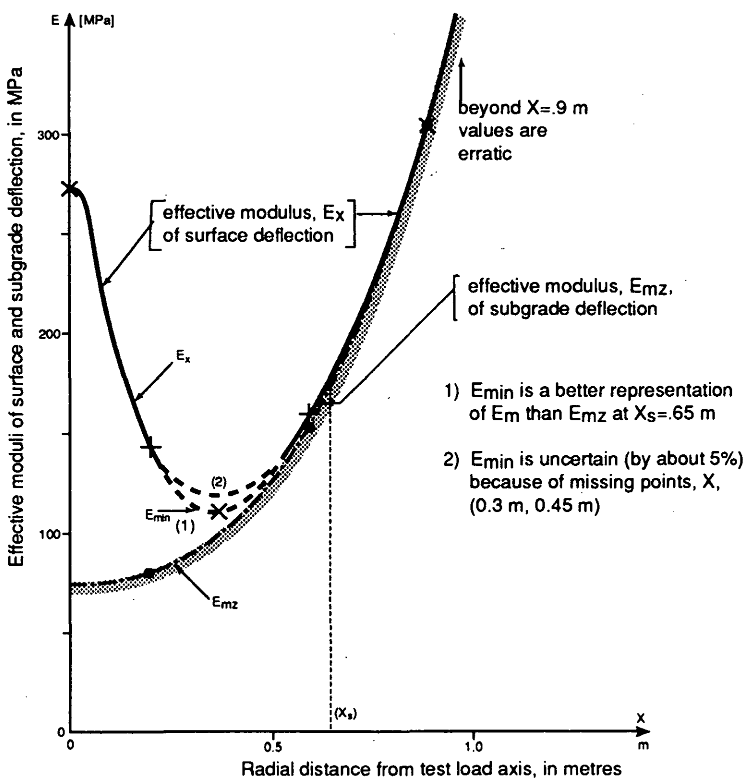


**FIGURE 8 Effective modulus of surface and subgrade deflection of a "bad" data example, File S430-0.**

must do so within the process of iteration of the backcalculation procedure. At each step of iteration, there is a slight change in $E_m$ and $H_{em}$, until the deflections under the test load match. The subgrade modulus profiles in Figures 8 and 9 were calculated in this way.

The old PROBE version used the tail modulus function to estimate $E_m$ at a selected distance, $X_t = 0.75$ m. This value was found by establishing consistency between the 1987 fall FWD tests, on neighboring points of Sections A and B on Highway 7N, stipulating that the subgrade modulus must be equal in both sections, except for statistical scattering. The sections were unequal in strength.

The new PROBE version also uses the tail modulus function. A similar calibration procedure leads to a smaller selected radial distance of about $X_s = 0.66$ m, because the procedure is now more complex.

Several "candidates" of the average in situ value of subgrade modulus $E_m$ are compared:

1. The minimum value of the surface modulus profile, $E_x$, found by Lagrange interpolation (smallest value selected for broken pavements),
2. The value at $X_s = 0.66$ m of the tail modulus function, $E_{mz}$ (often smallest value selected for whole pavements),
3. The value at $X_s = 0.72$ m of the subgrade modulus profile, $E_{mz}$ (sometimes smallest value for pavements in fair condition), and
4. The average of the subgrade modulus profile up to $X = 1$ m, times a calibration factor (often smallest value for pavements in fair condition).

Figure 9 shows two examples of unbroken, whole AC pavements from a strong and weak design section of Highway 7N. Note that, in spite of the various $E_x$ profiles, the subgrade modulus profiles $E_{mz}$ converge near the test load.

## NUMERICAL INDICATORS OF QUALITY AND STRENGTH

Further, the new PROBE program provides two indicators of relative strength or stiffness, in relation to the existing strength or stiffness of the soil. One of them, structural strength index (SSI), is based on the computed values of the surface modulus values only, before and independent of any computation or decision on the subgrade modulus. The other, structural integrity index (SII), uses the estimated subgrade modulus $E_m$. Both are based on the (approximate) area ($A_x$) under the surface modulus profile ($E_x$), from the load axis to $X_s$, or to the minimum value ($E_{min}$) at $X = X_{min}$. The two

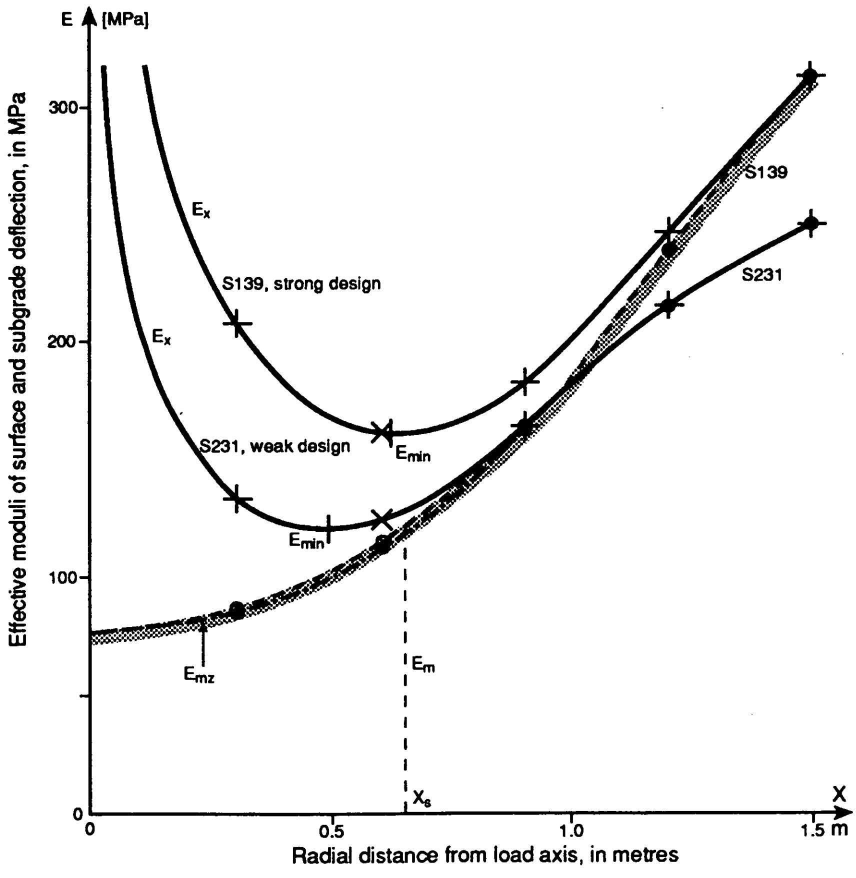


**FIGURE 9 Convergence of effective modulus of subgrade deflection near the test load of strong (S139) and weaker section (S231) of Highway 7N test section.**

indexes are

1. $SSI = A_x/(X_{min} \cdot E_{min})$ and
2. $SII = A_x/(X_s \cdot E_m)$

The index, SSI, can identify structurally weak or broken pavements that have values of SSI equal to or smaller than 1.5 (according to present experience).

The index, SII, is the more potent of the two. It measures the relative strength, stiffness, or integrity of the upper structural layers relative to the strength or stiffness of the subgrade. It is much affected by cracks at and near the load position, especially when the cracks run transversely to the direction of the FWD measurement. According to present experience, values can range from slightly below one (for severely cracked conditions) to above two (for pavements in good condition). SII is also subject to a small temperature adjustment with regard to a chosen standard temperature (such as 21°C). The SII is recommended to monitor flexible pavements for rehabilitation planning and overlay design, and valuable information can be obtained by chain-plotting SII along the whole pavement section. Note that SSI and SII quantify only a relative stiffness or strength under the load.

## UNDERSTANDING FIELD DATA: COMPUTER SIMULATIONS

The increase of the effective modulus profile at distances from the load beyond the minimum value is concordant with the exponent, $\eta$, being larger than one, observed on all flexible pavements tested. Even values of $\eta$ larger than two were measured on the major test section, Highway 7N, Toronto bypass. Observing and even trying to account for the fact does not mean that one fully understands it (*3*, *4*); therefore, computer simulations are helpful.

As indicated previously, a comparison of effective modulus profiles, using data from computer-generated and measured deflection bowls, clearly indicates that differences exist between actual field conditions and what is assumed for modeling. To investigate possible reasons for the observed differences, an idealized two-layer pavement was studied, taking into account the effects of bedrock location and impact loading, respectively. The problem case consisted of a 150-mm-thick plate with an elastic modulus of 2,250 MPa and a Poisson's ratio of 0.35, supported by a homogeneous subgrade with a modulus of 45 MPa and a Poisson's ratio of 0.50.

The deflection bowls were generated using the Bessel Fourier Series approach, described previously (*6,7*), assuming a peak load uniformly distributed over a 15-cm radius base plate. For the dynamic analysis, the impact load was applied as a half sine wave over an interval of 25 multisec, and a unit weight of 20 kN/m$^3$ was assumed.

Figure 10 provides a comparison of effective modulus profiles that were calculated using the generated deflection data, for various depths ($D$) of subgrade. As expected, the effective modulus for the elastostatic case, in which the subgrade extends to infinity ($D \rightarrow \infty$), approaches 45 MPa as the radial distance from the load get larger.

The dip below 45 MPa and the subsequent small gradual increase in effective modulus is caused by Poisson's ratio of the plate, which is different from that of the subgrade. For the elastodynamic case ($D \rightarrow \infty$), the effective modulus continuously decreases. This is not surprising, since the decay rate of surface wave amplitude for the semi-infinite half-space problem is known to be less than that of an elastotatic deflection bowl.

Figure 10 suggests that the increase in the effective modulus, observed when using real data, possibly can be attributed to the presence of bedrock. The strength of the increase of the effective modulus, with depth, depends on the subgrade thickness $D$. As $D$ decreases, both the minimum effective modulus and the distant effective modulus increase. In the simulations, the distance at which the modulus is a minimum is approximately equal to the effective thickness of the pavement structure, i.e., $H_{em} \cong H_1\sqrt[3]{E_1/E_m}$.

The evidence from the analysis of the real and idealized deflection bowls indicates that the interpretation of the effective modulus profiles provides hints with respect to the deviation of assumed and actual behavior. This can be used

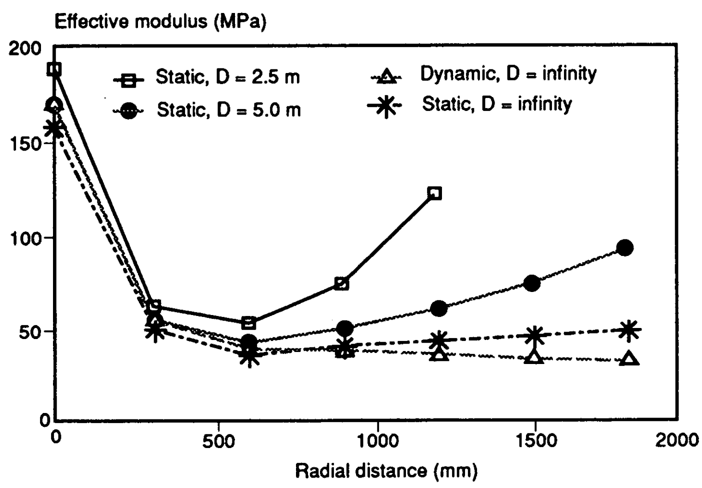


**FIGURE 10 Dynamic and elastostatic computer simulation.**

to evaluate the possible presence of unexpected features with respect to material properties or dimensions, or both, such as the presence of a bedrock face or harder layers of subgrade in its lower strata.

The presence of bedrock, at a finite distance below the pavement, represents a sudden change in the subgrade stiffness with depth. The increases in the effective modulus at larger radial distances from the load, observed in the field, can also be explained by a more gradual increase in the subgrade modulus with depth, which is almost certain to occur.

The surface deflections at larger distances from the load, used for the effective modulus calculations, are more sensitive to modulus increases with depth than those close to the load. Close to the load, the observed deflections are largely caused by the subgrade deformations in the upper zone of the subgrade, whereas the surface deflections farther away are caused by straining the deeper strata within the subgrade.

On the basis of the results from the two-layer problem, it appears that the effective modulus profile provides considerable information for characterizing a pavement structure, such as an estimate of subgrade modulus close to the load (close to $E_{min}$ in broken pavements, smaller than $E_{min}$ in whole pavements), strength of subgrade modulus increase with depth as indicated by $\eta - 1$, and stiffness of the upper pavement layer structure are reflected by $H_{em}$.

The results suggest that the effect of the subgrade modulus increase, with depth on the effective modulus profile, is more important than the influence associated with the dynamic nature of FWD loading. Most recently, however, Der-Wen et al. (*8*) have demonstrated that dynamic effects cannot be neglected when bedrock is close to the surface, i.e., within 2 to 5 m. Fortunately, often these effects are small and should not prevent an analytical solution, provided that deflections in the vicinity of the load are used for backcalculation analysis, i.e., not those much beyond a radius of $H_{em}$.

It is clear that the use of distant sensor readings can lead to considerable nonconservative errors in the subgrade modulus prediction, if the increases in subgrade stiffness with depth or the presence of bedrock, or both, are not properly taken into account. Other possible reasons for the positive

| | | |
|---|---|---|
| Standard test load, in kN: | 40.034 | Radius, in mm: 150 |
| Standard contact pressure, in kPa: | 566.4 | |
| Layer thicknesses, in mm: | 140, 169, 513 | |
| Total: | Z = 822 mm | |
| Temperatures, at test (and standard), in degrees Celsius: | 8 ( 21 ) | |
| Preliminary estimate of subgrade modulus:. | E = 129.39 MPa (at X = .66 m) | |
| $\eta$ from regression analysis: | 2.0818 | |
| Average absolute % error of fit: | 0.46 | |
| Number of tail-sensors dropped in curve-fitting: | 0 | |
| Correlation coefficient: | .9998507 | 4 sensors, first at I = 4 |
| Maximum effective modulus, in MPa: | 604.91 | |
| Minimum effective modulus, in MPa: | 160.01, at a distance of X = 0.64 m | |
| Structural Strength Index: | 1.927 | |

| | Temperature | |
|---|---|---|
| **Primary Response parameters:** | **Unadjusted** | **Adjusted** |
| Structural Integrity Index: | 2.31 | 2.00 |
| Total deflection, in mm: | 0.2465 | 0.3031 |
| Radius of AC curvature, in m: | 579.7 | 471.4 |
| AC tensile micro-strain: | 120.8 | 148.5 |
| Subgrade deflection, in mm: | 0.1259 | 0.1378 |
| Subgrade stress, in kPa: | 15.97 | 19.18 |
| Subgrade micro-strain: | 123.4 | 148.3 |

| | | | | |
|---|---|---|---|---|
| Equivalent thickness, $H_{em}$, in m: | 1.263 | | | |
| Subgrade modulus: | 129.39 MPa | | | |
| Subgrade modulus candidates: | 160.01 | 129.39 | 134.59 | 135.43 |
| Layer moduli, in MPa: | 7539.1 | 3486.2 | 260.3 | 129.4 |
| Layer moduli are: | AC-mod | adjusted AC-mod | base & subbase | subgrade |

| Sensor | Distance, mm | Deflection, mm | Hyperbola, mm | Error of Fit, % | Effective Moduli MPa | |
|---|---|---|---|---|---|---|
| 1 | 0 | 0.24647 | 0.00000 | 0.00 | 604.91 | 0.00 |
| 2 | 300 | 0.18657 | 0.67598 | 262.32 | 206.52 | 86.56 |
| 3 | 600 | 0.11638 | 0.15968 | 37.21 | 160.54 | 116.41 |
| 4 | 900 | 0.06838 | 0.06866 | 0.41 | 181.71 | 161.85 |
| 5 | 1200 | 0.03792 | 0.03772 | -0.52 | 245.75 | 238.71 |
| 6 | 1500 | 0.02380 | 0.02371 | -0.40 | 313.22 | 315.68 |
| 7 | 1800 | 0.01614 | 0.01622 | 0.51 | 385.00 | 393.78 |

**FIGURE 11 Output file of PROBE-A run, File A:S139; example of good data, whole pavement.**

subgrade modulus gradient at distant radii, not studied by the computer simulation, is the pressure dependence and anisotropy of granular, or AC materials, as they are composed of bonded or unbonded discrete particles (*2*).

## NEW PROBE PROGRAM

As before, the program processes FWD deflection data from a sequential input file. The file contains geometrical information, such as radius of load distribution, layer thicknesses, and distances of sensors from the load axis. Further, for any number of target load levels (usually four), the file must provide the readings of pressures of the load cell and the deflections at each of the transducers or geophones, usually seven or more. The file contains also the mean temperature of the bitumen-bound layers, a normal temperature, and a standard load level chosen by the user.

The deflections, pressures, and loads from each target load level (in the quasi-elastic range) are already processed within the file creation program to one normal or standard load level (usually 9,000 lb or 40.034 kN) by adding the values and multiplying them by a factor. The PROBE program processes only values pertaining to the chosen normal load level.

Two examples of PROBE results are presented in the form of printed output in Figures 11 and 12. One is from a pavement of normal Ontario design (File S139), and the other is from a deteriorated section scheduled to be rehabilitated by an overlay (File S430), Section D on Highway 7N, 1990 data. Figures 11 and 12 correspond to the graphical representations in Figures 9 and 8, respectively.

The tables list all relevant information from one test location, and items can be chain plotted for a string of test locations along a section. In particular, the tensile strain and curvature under the load are computed in accordance with a method presented in 1988 (*9*). The subgrade parameters were computed by Odemark's method of equivalent layer thickness.

Vertical subgrade stresses and strains are modified by applying Froehlich's concentration factor, ranging from 3 to 4. The factor can be conceived as a function of the parameter, $\eta$, ranging from one to above two. This results in stresses and

| | | |
|---|---|---|
| Standard test load, in kN: | 40.034 | Radius, in mm: 150 |
| Standard contact pressure, in kPa: | 566.4 | |
| Layer thicknesses, in mm: | 90, 172, 340 | |
| Total: | Z = 602 mm | |
| Temperatures, at test (and standard), in degrees Celsius: | 26 ( 21 ) | |
| Preliminary estimate of subgrade modulus | E = 192.14 MPa (at X = .66 m) | |
| η from regression analysis: | 3.4232 | |
| Average absolute % error of fit: | 14.37 | |
| Number of tail-sensors dropped in curve-fitting: | 1 | |
| Correlation coefficient: | .9818988 | 4 sensors, first at I = 3 |
| Maximum effective modulus, in MPa: | 272.26 | |
| Minimum effective modulus, in MPa: | 111.35, at a distance of X = .37 m | |
| Structural Strength Index: | 1.482 | |

| Primary Response parameters: | Temperature Unadjusted | Temperature Adjusted |
|---|---|---|
| Structural Integrity Index: | 0.83 | 0.86 |
| Total deflection, in mm: | 0.5476 | 0.5182 |
| Radius of AC curvature, in m: | 133.7 | 141.3 |
| AC tensile micro-strain: | 336.7 | 318.6 |
| Subgrade deflection, in mm: | 0.2150 | 0.2123 |
| Subgrade stress, in kPa: | 46.61 | 44.10 |
| Subgrade micro-strain: | 418.6 | 396.0 |

| | | | | |
|---|---|---|---|---|
| Equivalent thickness, Hem, in m: | 0.739 | | | |
| Subgrade modulus: | 111.35 MPa | | | |
| Subgrade modulus candidates: | 111.35 | 192.14 | 226.90 | 228.10 |
| Layer moduli, in MPa: | 798.3 | 1161.5 | 225.8 | 111.3 |
| Layer moduli are: | AC-mod | adjusted AC-mod | base & subbase | subgrade |

| Sensor | Distance, mm | Deflection, mm | Hyperbola, mm | Error of Fit, % | Effective Moduli MPa | |
|---|---|---|---|---|---|---|
| 1 | 0 | 0.54763 | 0.00000 | 0.00 | 272.26 | 0.00 |
| 2 | 200 | 0.41101 | 5.25226 | 1177.87 | 143.57 | 74.06 |
| 3 | 600 | 0.11710 | 0.12220 | 4.35 | 159.55 | 150.54 |
| 4 | 900 | 0.03669 | 0.03050 | -16.88 | 338.63 | 341.42 |
| 5 | 1200 | 0.00898 | 0.01139 | 26.89 | 1037.98 | 1060.03 |
| 6 | 1500 | 0.00585 | 0.00531 | -9.36 | 1273.25 | 1300.52 |
| 7 | 1800 | 0.00859 | 0.00284 | -66.89 | 723.44 | 736.95 |

**FIGURE 12 Output file of PROBE-A run, File A:S430-o; example of bad data, broken pavement.**

strains often larger (up to 30 percent) than those computed by elastic layer programs such as ELSYM5.

Besides those mechanistic parameters, there is plenty of information about quality and strength presented to give an indication of structural integrity or deterioration.

The upper-layer moduli are no more than rough estimates; they are needed only for adjustments to normal temperature. Such adjustment is required for any comparison of tests carried out at various temperatures. This adjustment makes the FWD method useful and feasible in the design and monitoring of flexible pavements (compared with other methods with less distinct temperature adjustment).

Note that moduli are not material properties, but are model parameters of the pavement structure/subgrade system as measures (i.e., "perceived") by the FWD instrument at the surface. However, the values of these model parameters should be consistent with those of the average material properties under investigation.

## CONCLUSIONS AND RECOMMENDATIONS

The need to analyze FWD deflection data on severely cracked and broken flexible pavements and the differences between the theoretical modeling of fast workhorse programs and observed field performance of materials have spurred the development of new concepts with regard to deflection analysis:

1. The function of the effective modulus of measured surface deflection or the surface modulus profile,
2. The tail modulus function, and
3. The profile of the effective modulus of subgrade deflection.

All of these are used to calculate representative values of subgrade moduli, valid at and around the test load, and to provide valuable information on structural strength and integrity.

A computer simulation on a two-layer system has revealed that the deviation of field behavior from elastostatic modeling is not so much caused by dynamic influences, but can be traced better to certain properties of layer materials. Some of these are the increase of subgrade stiffness with depth, the presence of an often unrecorded bedrock face, or the anisotropy or pressure dependence of bounded or unbounded granular materials, especially the discontinuity of these materials. The aforementioned effective modulus profiles can serve as a key to obtain information regarding these items. The new revised PROBE program is a first attempt to quantify such information. Research is being continued to provide a better understanding of the relationship between the effective modulus profile and in situ properties of materials and design features.

Deflections beyond the minimum of the effective modulus profile cannot be used directly to calculate a representative estimate of the subgrade modulus, only indirectly, via the tail modulus function (*3*,*4*).

If they are used directly, estimates of subgrade moduli may be excessively high. The subgrade modulus must be calculated from deflections closer to the load. The deflections beyond the minimum effective modulus, however, are used to provide information on the condition of the pavement structure.

Flexible pavements of usual design (bitumen-bound layers on granular bases) behave very differently from those designed with elastic continuum materials. Backcalculation of all layer moduli using distant deflections is futile. In the approach presented here, backcalculation is used only with regard to the deflection under the load and only to obtain an estimate of the subgrade modulus. Emphasis is given to interpretation, which is more useful than backcalculation for the practicing engineer.

## REFERENCES


1. E. J. Yoder and M. W. Witczak. *Principles of Pavement Design*, 2nd ed., John Wiley and Sons, Inc., New York, N.Y.
2. P. Ullidtz. *Pavement Analysis*. Elsevier, Amsterdam, the Netherlands, 1987.
3. F. W. Jung. *Interpretation of Deflection Basin for Real-World Materials in Flexible Pavements*. Research Report RR-242. Ministry of Transport, Ontario, Canada, 1990.
4. F. W. Jung et al. Testing and Interpretation with the Falling Weight Deflectometer (FWD) in Ontario. Presented at 70th Annual Meeting of the Transportation Research Board, Washington, D.C., 1991.
5. R. L. Lytton et al. *NCHRP Report 327*: Determining Asphaltic Concrete Pavement Structural Properties by Nondestructive Testing. TRB, National Research Council, Washington, D.C., June 1990.
6. D. Stolle, D. Hein, and Y. Wang. *Elastostatic Analysis and Backcalculation Estimates of Pavement Layer Moduli*. C39-C59. Roads and Transportation Association of Canada, 1988.
7. D. Stolle. Modelling of Dynamic Response of Pavements to Impact Loading. In *Computers and Geotechnics*, 1991, pp. 83–94.
8. Der-Wen et al. Effect of Depth to Bedrock on Deflection Basin Obtained with Dynaflect and FWD Tests. Presented at the 71st Annual Meeting of the Transportation Research Board, Washington, D.C., 1992.
9. F. W. Jung. Direct Calculation of Maximum Curvature and Strain in AC-Layers of Pavements from Load Deflection Basin Measurements. In *Transportation Research Record 1169*, TRB, National Research Council, Washington, D.C., 1988.

# Effect of Thickness and Temperature Corrections on Prediction of Pavement Structural Capacity Using Falling Weight Deflectometer Data

JOHN P. ZANIEWSKI AND MUSTAQUE HOSSAIN

Deflection measurements are commonly used for evaluating the structural capacity of pavements. Prediction of pavement performance from these measurements requires estimating the modulus of the pavement layers through backcalculation, estimating the critical response parameters, and using limiting criteria for determining the life of the pavement. In addition to the deflection data, the thickness of the pavement layers must be known, and the type of layer materials is used as a guide in the selection of the moduli values. The influence of two variables on the performance predictions generated in the pavement evaluation process were studied. These variables are the thicknesses of the pavement layers and the temperature correction factor used to adjust the modulus of bituminous materials from the test temperature to a standard temperature. The study demonstrated that for thick pavement structures, compensating effects of the analysis procedure make the prediction of pavement performance relatively insensitive to the thicknesses used in the analysis. Criteria are presented for the need for coring of the pavement structure on the basis of the variability of the thicknesses as recorded in construction quality control tests. On the other hand, the performance predictions are very sensitive to the temperature correction factor as presented in the AASHTO *Guide for Design of Pavement Structures*. The test procedures used to establish the temperature sensitivity of the asphalt concrete modulus in the laboratory may overestimate the sensitivity of the asphalt in field conditions. This is an area requiring further research.

Nondestructive testing (NDT) for deflection measurement is now widely recognized as an important tool for pavement structural evaluation. State-of-the-art NDT evaluation measures a pavement's deflection response to a known load. The load generated by an NDT device may be static (Benkelman beam), steady-state vibratory (Dynaflect and Road Rater), or impulse [falling weight deflectometers (FWDs)]. Although surface deflection data analysis is a matter of continuing research, nondestructive testing for measuring surface deflection is accepted by most highway agencies as a standard practice for the advantages of being fast and reliable in most of the cases. The new AASHTO *Guide for Design of Pavement Structures* (*1*) recommends the use of "dynamic" NDT deflection measuring devices for surface deflection measurements. With deflection testing, a thorough evaluation pavement response can be obtained by closely spacing test sites.

J. P. Zaniewski, Department of Civil Engineering, College of Engineering and Applied Sciences, Arizona State University, Tempe, Ariz. 85287. M. Hossain, Department of Civil Engineering, Seaton Hall, Kansas State University, Manhattan, Kans. 66506.

The deflections measured with NDT are used to estimate the moduli of pavement layers. The pavement is modeled by a suitable approach such as linear elastic theory, or linear or nonlinear finite element methods. Moduli estimates are determined with a "backcalculation" technique. For the test load-pavement combination, computed deflections are compared with measured deflections. The moduli of the layers are varied until the computed and measured deflections are approximately equal. The surface layer and other asphaltic layer moduli thus obtained are modified to take into account the temperature at the time of testing. These moduli are then used to compute the effective structural capacity of the pavement according to a pavement design procedure such as the AASHTO guide (*1*).

The FWD employs a mass falling onto a buffered circular load plate. Developed in Europe, FWDs have become popular in the United States. The load pulse shape of FWDs simulates traffic loads better than other deflection devices (*2,3*). FWDs can transmit relatively heavy loads to the pavements compared with the other deflection testing devices. Usually the load range is 1,500 to 35,000 lb, depending on the FWD model. The magnitude of the dropping mass and drop height are altered to change the applied load levels. The FWD has a small preload, 3 to 14 per cent of the maximum load. The applied load is measured by a load cell. The load pulse is approximately of a half sine waveform with a duration of 30 to 40 msec.

The Dynatest FWD uses velocity transducers to measure the peak deflection under the load and at several locations away from the load. The sensors are mounted on a bar that is automatically lowered with the loading plate. Measured deflections can be plotted as deflection basins.

The Arizona Department of Transportation (ADOT) purchased a Dynatest Model 8000 FWD unit in 1982 and updated it in 1987. The operating sequence of the Dynatest FWD is fully automated. The load is applied by a single falling mass. Factory-calibrated geophones register the peak deflections from an applied load. The load range is from 1,500 to 27,000 lb.

## PROBLEM DEFINITION

Calculating the pavement structural capacity in terms of the ability to carry 18-kip equivalent single axle load (ESAL)

repetitions from FWD data is a three-step procedure. First, the layer moduli are backcalculated from the FWD, layer type, and thickness data. Second, the critical pavement response, usually the tensile strain at the bottom of the asphalt concrete (AC) layer, is calculated. Finally, empirical relationships are used for estimating the number of 18-kip ESALs on the basis of the critical pavement response. The relationship estimates the number of 18-kip ESAL repetitions the pavement can carry before fatigue failure. Evidently, the variability in layer thickness affects the estimation of structural capacity by the mechanistic-empirical method.

## OBJECTIVES

This paper reports the study to determine the coring needs to extract thickness information about pavement cross sections at FWD test points on existing pavements. The effect of the temperature correction factor for asphaltic layer moduli on the estimated structural capacity was also examined.

## DATA COLLECTION

Table 1 lists the sites selected in this study, and Table 2 shows the pavement sections of these sites. All deflection data were collected with a Dynatest Model 8000 FWD. The deflection sensors were spaced at 12-in. intervals, with the first sensor located at the center of the load. The target load was 9,000 lb. At Sites 1 through 3, deflections were measured in the outer wheel path at 10 locations spaced at 10-ft intervals. For Site 4, deflection data were collected every tenth of a mile.

**TABLE 1 Location of Test Sites and Pavement Types**

| Site | Location | Route | Mile Post | Pavement Type | Test Type |
|---|---|---|---|---|---|
| 1 | Benson East | I10W | 303.00 | 4-layer | 10 tests/90 ft. |
| 2 | Flagstaff | I17N | 337.00 | 4-layer | 10 tests/90 ft. |
| 3 | Morristown | US60W | 120.00 | 4-layer | 10 tests/90 ft. |
| 4 | Tombstone | U80E | 316.50 | 4-layer | 10 tests/mile |

**TABLE 2 Layer Type and Thickness at Various Sites**

| Site/ Sta | Layer 1 Mat | Layer 1 Thk (in) | Layer 2 Mat | Layer 2 Thk (in) | Layer 3 Mat | Layer 3 Thk (in) | Layer 4 Mat | Layer 4 Thk (in) |
|---|---|---|---|---|---|---|---|---|
| 1/1 | AC | 6 | AB | 6 | SB | 18 | SC-SM* | -- |
| 2/1 | AC | 9 | AB | 4 | SB | 12 | - | - |
| 3/1 | AC | 4.25 | AB | 4 | SB | 15 | - | - |
| 4/1 | AC | 3.0 | AB | 4 | SB | 15 | - | - |

* Subgrade Classification based on Unified Method.

Note: AC: Asphalt Concrete, AB: Aggregate Base, SB: Sub Base (Select Material)

## ANALYSIS METHOD

The analysis process consists of (a) backcalculation of layer moduli of the pavements from FWD data and (b) computation of structural capacity of the existing pavement through fatigue analysis. Backcalculation of layer moduli was done with the Arizona deflection analysis method (ADAM) developed by Hossain (*4*). ADAM uses the CHEVRON (*5*, *6*) computer program for pavement response analysis. A robust optimization routine iterates the moduli values to minimize the squared error between the measured and calculated deflection basins. The backcalculated layer moduli were used to determine the tensile strain at the bottom of the asphalt concrete layer. The structural capacity of the pavement in terms of the theoretical number of 18-kip ESALs was determined using the following equation for fatigue analysis developed by Hossain (*4*):

$$N = (2.265 \times 10^{-7})\,(1/e_{ac})^{3.84} \tag{1}$$

where $N$ is the theoretical number of 18-kip ESAL repetitions to fatigue failure and $e_{ac}$ is the tensile strain at the bottom of AC layer (μin./in.). Figure 1 shows the flow chart of the analysis process.

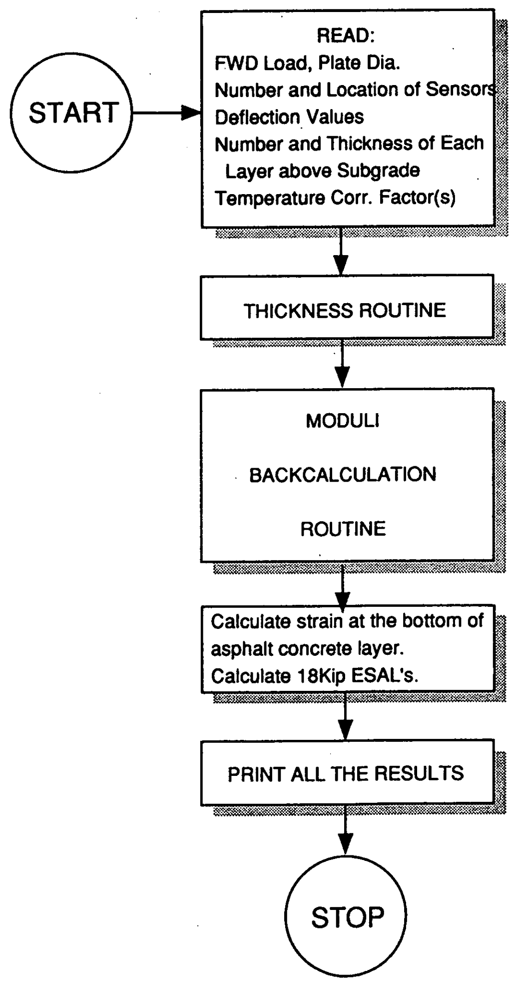


**FIGURE 1 Flow chart of analysis process.**

## EFFECT OF VARIATION IN LAYER THICKNESS ON STRUCTURAL CAPACITY

Pavement layer thickness is a primary input of all backcalculation procedures. Thickness data can be obtained from either construction data or cores taken from the pavement. These thicknesses may vary from the design thickness because of variability in the construction process. Also, existing pavements may receive treatments, such as an AC friction course, that are not expected to increase the structural capacity but contribute to the total thickness of the AC layer. Little information is available in the literature about the effect of thickness variation on the estimated structural capacity from FWD deflection data. Rwebangira et al. (*7*) concluded that variation of AC and base layer thicknesses affect the backcalculated layer moduli. However, the backcalculated layer moduli are more sensitive to AC thickness than base layer thickness. Irwin et al. (*8*) showed that random deflection measurement errors combined with random variability of pavement layer thickness can lead to a high degree of "pseudovariability" in the backcalculated layer moduli. They recommend accurate determination of layer thicknesses to reduce the inaccuracy of the resultant backcalculated layer moduli.

To study the effect of layer thickness on the calculated structural capacity of the pavements, Sites 1 through 3 from Table 1 were selected. The thickness for the AC layer for these sites ranges from 4.3 to 9.0 in., whereas the aggregate base (AB) layer thickness ranges from 4.0 to 6.0 in. The subbase layer thickness ranges from 12.0 to 18.0 in. Two sets of deflection basins from 10 stations within each site were analyzed for each site, representing deflection basins with the highest and lowest first sensor deflections (normalized to 9,000 lb).

The experiment was designed to capture the effect of layer thickness on the response parameter or the theoretical structural capacity (expressed in terms of 18-kip ESALs) of the pavement section from backcalculated layer moduli and fatigue analysis. The factors and levels selected to capture the effect of variability of layer thickness on the calculated structural capacity of Site 1 are

| *Thickness (in.)* | *Levels* |
|---|---|
| Surface | −1.0, −0.5, 0.0, 0.5, 1.0 |
| Base | −2.0, −1.0, −0.5, 0.0, 0.5, 1.0, 2.0 |
| Subbase | −2.0, −1.0, −0.5, 0.0, 0.5, 1.0, 2.0 |

Thus, a $7^3$ factorial was designed for this site.

Analysis of variance (ANOVA) was used to describe the variation in calculated 18-kip ESALs with the following variance components:

| *Source of Variation* | *Definition* |
|---|---|
| ACT | Thickness of AC layer |
| ABT | Thickness of AB layer |
| SMT | Thickness of SM layer |
| ACT*ABT | Interaction of thickness of AC and AB layers |
| ACT*SMT | Interaction of thickness of AC and SM layers |
| ABT*SMT | Interaction of thickness of AB and SM layers |
| ACT*ABT*SMT | Interaction of thickness of AC, AB, and SM layers |

The following model was proposed for Site 1:

$$\begin{aligned} N18_{ijkl} = {} & \mu + ACT_i + ABT_j + SMT_k \\ & + ACTABT_{ij} + ACTSMT_{ik} \\ & + ABTSMT_{jk} + ACTABTSMT_{ijk} \\ & + \varepsilon_{(ijkl)} \\ & i = 1, \ldots, 7, j = 1, \ldots, 7, \\ & k = 1, \ldots, 7, l = 1,2 \end{aligned} \quad (2)$$

where

- $N_{18ijkl}$ = theoretical 18-kip ESALs calculated from $l$th deflection basin at $i$th level of AC thickness, $j$th level of AB thickness, and $k$th level of SM thickness;
- $\mu$ = overall mean;
- $ACT_i$ = effect of $i$th level of (fixed) treatment AC thickness;
- $ABT_j$ = effect of $j$th level of (fixed) treatment AB thickness;
- $SMT_k$ = effect of $k$th level of (fixed) treatment AB thickness;
- $ACTABT_{ij}$ = interaction effect between $i$th level of AC thickness and $j$th level of AB thickness;
- $ACTSMT_{ik}$ = interaction effect between $i$th level of AC thickness and $k$th level of SM thickness;
- $ABTSMT_{jk}$ = interaction effect between $j$th level of AB thickness and $k$th level of SM thickness;
- $ACTABTSMT_{ijk}$ = interaction effect between $i$th level of AC thickness, $j$th level of AB thickness, and $k$th level of SM thickness; and
- $\varepsilon_{(ijkl)}$ = (random) within error. The $\varepsilon_{(ijkl)}$'s are assumed to be normally and independently distributed with mean zero and variance $\sigma^2$.

It is important to note that the replicate of deflection basins used in the backcalculation of layer moduli made it possible to estimate the error in the model. Table 3 shows the ANOVA

**TABLE 3 ANOVA for Site 1**

| Source of Variation | Sum of Squares | Degrees of Freedom | Mean Squares | Fo |
|---|---|---|---|---|
| ACT | 4.9E14 | 6 | 8.1E13 | 4.3* |
| ABT | 3.8E14 | 6 | 6.3E13 | 3.3* |
| SMT | 6.1E12 | 6 | 1.0E12 | 0.05 |
| ACT*ABT | 1.4E14 | 36 | 3.9E12 | 0.20 |
| ACT*SMT | 2.4E13 | 36 | 6.5E11 | 0.03 |
| ABT*SMT | 3.4E13 | 36 | 9.6E11 | 0.05 |
| ACT*ABT*SMT | 2.9E14 | 216 | 1.3E12 | 0.07 |
| Error | 6.6E15 | 343 | 1.9E13 | |
| Total | 7.96E15 | 685 | | |

* Significant at $\alpha$ = 5%

table for Site 1. From this table, it is evident that various levels of AC and AB thickness result in a significantly different structural capacity for Site 1.

The quality of the estimate of variation of structural capacity for each thickness level depends on the stability of the variation in structural capacity across thickness combinations. This variation depends on how much the estimate of structural capacity variance calculated from the two deflection basins for each thickness combination fluctuates. To test this statistically, Bartlett's test for constant variance was applied. The Bartlett's chi-square statistic was found to be 353. The critical value applicable to this statistic at the 5 percent level of significance is approximately 124, so the hypothesis of homogeneity of variance assumed in this test was rejected. Transformation of 18-kip ESAL data was necessary to make the variances stable. The correlation coefficient between means of N18 for each thickness combination and the corresponding variance was +0.89. The suggested transformation in this case of positive correlation between mean and variance is the square root of original data (*9*). This transformation was applied to N18 data, and Bartlett's test was repeated. The test statistic for the transformed data was 125, which is significant at 5 percent but insignificant at 2.5 percent. Anderson and McLean (*10*) state that the *F*-test used in the analysis of variance is robust against minor deviation from homogeneity of variance; thus the square root transformation appeared to be appropriate.

The ANOVA was repeated for the transformed data, as shown in Table 4. The degrees of freedom for the error were reduced by 1 because of the transformation applied to the data (*9*). It is clear that levels of thickness of AC and AB layers significantly affect the structural capacity estimated by the mechanistic method.

To determine the levels of AC and AB thickness that are significantly different from each other, Duncan's multiple range test (*9*) was applied to the means of 18-kip ESALs corresponding to various levels of AC and AB thickness.

Figure 2 illustrates the results. The means that do not share a common underline are statistically different. It is evident from the results that if the thickness for the AC layer is decreased by more than 1 in., the corresponding calculated 18-kip ESALs are significantly different; however, if it is increased by 1 in., the calculated 18-kip ESALs remain statistically the same.

**TABLE 4 ANOVA of Transformed Data for Site 1**

| Source of Variation | Sum of Squares | Degrees of Freedom | Mean Squares | Fo |
|---|---|---|---|---|
| ACT | 1.2E7 | 6 | 2.0E6 | 2.5* |
| ABT | 1.1E7 | 6 | 1.9E6 | 2.4* |
| SMT | 0.4E6 | 6 | .06E6 | 0.07 |
| ACT*ABT | 3.2E7 | 36 | .09E6 | 0.11 |
| ACT*SMT | 0.9E6 | 36 | .02E6 | 0.03 |
| ABT*SMT | 1.3E7 | 36 | .04E6 | 0.05 |
| ACT*ABT*SMT | 1.03E7 | 216 | .05E6 | 0.06 |
| Error | 2.7E8 | 342 | .08E6 | |
| Total | 3.5E8 | 685 | | |

* Significant at $\alpha = 5\%$

| Asphalt Concrete: | LEVEL | | | | | | |
|---|---|---|---|---|---|---|---|
| Variable | 1 | 2 | 3 | 4 | 5 | 6 | 7 |
| 18-kip ESALs (millions) | 6.5 | 5.7 | 5.4 | 5.0 | 4.8 | 4.7 | 4.7 |
| Thickness (inches) | (5) | (5.5) | (5.75) | (6.0*) | (6.25) | (6.5) | (7.0) |

| Aggregate Base: | LEVEL | | | | | | |
|---|---|---|---|---|---|---|---|
| Variable | 1 | 2 | 3 | 4 | 5 | 6 | 7 |
| 18-kip ESALs (millions) | 6.1 | 5.9 | 5.7 | 5.2 | 4.9 | 4.54 | 4.56 |
| Thickness (inches) | (4.0) | (5.0) | (5.5) | (6.0*) | (6.5) | (7.0) | (8.0) |

* Control Thickness

**FIGURE 2 Duncan's multiple range test for means of 18-kip ESALs for Site 1. (Means that do not share a common underline are statistically different.)**

For AB, a 2-in. deviation from the control thickness of 6-in. AB does not affect the calculation of 18-kip ESALs. However, there is significant difference between means of 18-kip ESALs computed from 5 in. AB and 7-in. AB. Thus, this site needs only knowledge of AC thickness within 0.5 in. of actual thickness to estimate the structural capacity.

On the basis of the analysis for Site 1, the number of levels for layer thickness for Sites 2 and 3 were decreased by 2, and the factorial was redefined to have five levels of thickness. The layer thicknesses for the AC layer for both sites varied by ±0.5 and ±1.0 in., whereas for AB and SM layers they varied by ±1.0 and ±2.0 in., producing $5^3$ combinations.

The model assumed for ANOVA was similar to the one for Site 1. Two deflection basins from a 90-ft span of each site were selected that correspond to maximum and minimum first-sensor deflections normalized to a 9,000-lb load. The ANOVA tables for the 18-kip ESALs computed from these deflection basins are shown in Table 5.

From the tables it is clear that only AC and AB thicknesses significantly affect the structural capacity calculation. The homogeneity of variances in each of the various layer thickness combinations for these sites were checked using Bartlett's test. Site 2 had a Bartlett's chi-square statistic of 116, whereas for Site 3 the statistic was 55. The critical value of this statistic at the 5 percent level of significance for the data from both sites was 124. So, the variances for the 18-kip ESALs computed for these sites were homogeneous, and no transformation of data was necessary.

To determine the levels of AC and AB thickness that predicted significantly different 18-kip ESALs, Duncan's multiple range test was applied. Figure 3 shows the test results for both sites. The means of 18-kip ESALs corresponding to various levels of AC and AB thickness that do not share a common underline were found to be statistically different. For Site 2, an AC thickness of 8 in. produced significantly different 18-kip ESALs when compared with other levels of thickness. Here also, a decrease in 1 in. of AC thickness from the control thickness (9 in.) resulted in significantly different 18-kip ESALs, whereas an increase of 1 in. of AC thickness did not significantly affect the calculated 18-kip ESALs. For AB, a

**TABLE 5 ANOVA for Sites 2 and 3**

SITE 2

| Source of Variation | Sum of Squares | Degrees of Freedom | Mean Squares | Fo |
|---|---|---|---|---|
| ACT | 2.90E17 | 4 | 7.2E16 | 6.5* |
| ABT | 1.20E17 | 4 | 3.0E16 | 2.7* |
| SMT | 8.50E16 | 4 | 2.1E16 | 1.9 |
| ACT*ABT | 1.50E17 | 16 | 9.5E15 | 0.86 |
| ACT*SMT | 9.70E16 | 16 | 6.1E15 | 0.55 |
| ABT*SMT | 1.30E16 | 16 | 7.9E14 | 0.07 |
| ACT*ABT*SMT | 6.80E16 | 64 | 1.1EE15 | 0.10 |
| Error | 1.40E18 | 125 | 1.1E16 | |
| Total | 2.23E18 | 249 | | |

SITE 3

| Source of Variation | Sum of Squares | Degrees of Freedom | Mean Squares | Fo |
|---|---|---|---|---|
| ACT | 6.48E15 | 4 | 1.62E15 | 7.7* |
| ABT | 4.70E15 | 4 | 1.20E15 | 5.7* |
| SMT | 7.20E13 | 4 | 1.79E13 | 0.09 |
| ACT*ABT | 2.64E15 | 16 | 1.65E14 | 0.77 |
| ACT*SMT | 4.38E14 | 16 | 2.74E13 | 0.13 |
| ABT*SMT | 2.40E14 | 16 | 1.49E13 | 0.07 |
| ACT*ABT*SMT | 1.70E15 | 64 | 2.64E13 | 0.13 |
| Error | 2.62E16 | 125 | 2.10E14 | |
| Total | 3.25E16 | 249 | | |

* Significant at $\alpha = 5\%$

**SITE 2:**

| Asphalt Concrete: | LEVEL | | | | |
|---|---|---|---|---|---|
| Variable | 1 | 2 | 3 | 4 | 5 |
| 18-kip ESALs (millions) | 300 | 367 | 395 | 392 | 362 |
| Thickness (inches) | (8.0) | (8.5) | (9.0*) | (9.5) | (10.0) |

| Aggregate Base: | LEVEL | | | | |
|---|---|---|---|---|---|
| Variable | 1 | 2 | 3 | 4 | 5 |
| 18-kip ESALs (millions) | 327 | 349 | 371 | 384 | 384 |
| Thickness (inches) | (2.0) | (3.0) | (4.0*) | (5.0) | (6.0) |

**SITE 3:**

| Asphalt Concrete: | LEVEL | | | | |
|---|---|---|---|---|---|
| Variable | 1 | 2 | 3 | 4 | 5 |
| 18-kip ESALs (millions) | 23.9 | 15.9 | 11.1 | 10.3 | 11.5 |
| Thickness (inches) | (3.3) | (3.8) | (4.3*) | (4.8) | (5.3) |

| Aggregate Base: | LEVEL | | | | |
|---|---|---|---|---|---|
| Variable | 1 | 2 | 3 | 4 | 5 |
| 18-kip ESALs (millions) | 7.7 | 11.3 | 17.1 | 19.3 | 17.5 |
| Thickness (inches) | (2.0) | (3.0) | (4.0*) | (5.0) | (6.0) |

* Control thickness

**FIGURE 3 Duncan's multiple range test for means of 18-kip ESALs for Sites 2 and 3. (Means that do not share a common underline are statistically different.)**

2-in. deviation from a control thickness of 4 in. yielded significantly different 18-kip ESALs, whereas overestimation of thickness by 2 in. did not affect the calculation.

For Site 3, an AC thickness of 3.3 in., which is 1 in. less than the control thickness of 4.3 in., gave significantly different 18-kip ESALs, whereas 5.3 in. of AC did not yield significantly different 18-kip ESALs. There was a significant difference between the 18-kip ESALs computed for 3.8 in. of AC and 3.3 in. of AC, implying that a 0.5-in. decrease in AC thickness for pavements having 3.8 in. or less of AC thickness will produce significantly different 18-kip ESALs. For AB thickness, a 1-in. decrease from the control thickness of 4 in. resulted in significantly different 18-kip ESALs, whereas overestimation of thickness by 2 in. did not produce any 18-kip ESALs that were significantly different from control thickness.

From the results of ANOVA analysis of these sites it is evident that for pavements with AC thickness of 4.0 to 9.0 in., a 1-in. decrease in AC thickness will produce significantly different 18-kip ESALs. For thin pavements, a 1-in. decrease in base thickness would result in different 18-kip ESALs, whereas for thick pavements the calculated 18-kip ESALs may or may not be affected by a 2-in. decrease in base layers, depending on the thickness of the AC layers. These results support the greater effect of base layer thickness on the calculation of 18-kip ESALs for thin pavements as outlined earlier. Again, the overestimation of thickness of these layers above the actual layer thickness for which deflection test results are available do not affect the calculated 18-kip ESALs.

If construction records for quality control show that as built thicknesses of AC and AB layers are varying by more than 1 in., then coring will be necessary to have an accurate thickness of AC and AB layers at the FWD test locations for pavements having an AC thickness of 4.0 to less than 6.0 in. and AB thickness of 4.0 in. For pavements having an AC thickness less than 4.0 in., only a 0.5-in. deviation from the mean value of AC thickness can be allowed, and variation of AB thickness should be less than 1 in. However, the base thickness variation may be more than 1 in. for thick pavements having an AC thickness of 6 in. or more.

## EFFECT OF TEMPERATURE CORRECTION FACTOR ON COMPUTED STRUCTURAL CAPACITY

Asphalt properties, especially the modulus of elasticity, are highly dependent on temperature. Since modulus affects the deflection measurements, the modulus of the layers that are temperature-dependent (such as AC, and hot-mix asphalt concrete base) must be corrected to a standard temperature, usually 70°F (*1*). The AASHTO guide (*1*) has a graph for temperature corrections of the asphaltic layer moduli to this standardized temperature that is based on

1. The air temperature at the time of FWD testing,
2. Five-day mean air temperature before the testing date, and
3. Thickness of the asphalt bound layer.

The backcalculated asphalt concrete or asphalt-treated base layer moduli are multiplied by these factors. These adjusted

moduli can be used for determination of the structural layer coefficient from the nomographs in the AASHTO guide (*1*).

In the mechanistic analysis, the moduli are used as inputs for critical response calculation in fatigue analysis. Because there is no limit on the value of layer moduli, the resulting structural capacity analysis from fatigue criterion could result in a very high number of 18-kip ESAL repetitions. This is particularly true when the temperature at the time of the test is greater than the reference temperature, resulting in an upward adjustment of the asphalt modulus. At high modulus values there are low strains calculated corresponding to a stiff asphaltic layer.

To study the effect of the temperature correction factor on the estimated structural capacity by mechanistic analysis developed in this study, the pavement section in Site 4 was evaluated. The pavement temperature of this site was calculated from the nomograph in the AASHTO guide (*1*) corresponding to air temperature at the time of deflection testing plus a 5-day mean air temperature before deflection testing and thickness of AC layer. The temperature adjustment factor of 2.5, corresponding to the pavement temperature of 88°F, was determined from the nomograph in the guide. The backcalculated AC layer modulus was corrected with this factor and six other factors, which are derived by varying the actual temperature correction factor by ±25, ± 50, and ±75 percent. The corresponding temperature correction factors were 4.375, 3.75, 3.125, 1.875, 1.25, and 0.625. The theoretical number of 18-kip ESALs calculated corresponding to the temperature adjusted moduli are shown in Table 6.

A close inspection of a temperature correction factor nomograph shows that the correction factor is very sensitive to the changes in temperature, thus making the surface modulus very sensitive to test temperature. Consequently, the calculated structural capacity of the pavement becomes very sensitive to the temperature factor. By varying the temperature correction factor from −75 to +75 percent, the estimated 18-kip ESALs vary from −69 to +153 percent.

**TABLE 6 Effect of Temperature Correction Factor on Estimated Structural Capacity**

| Var.[1] (%) | Factor[2] | Temp.[3] (°F) | EAC[4] (ksi) | 18-kip ESALs[5] (millions) | Diff[6] (%) |
|---|---|---|---|---|---|
| +75 | 4.375 | 101 | 897 | 14.7 | +153 |
| +50 | 3.750 | 98 | 780 | 11.1 | +91 |
| +25 | 3.125 | 94 | 650 | 8.2 | +41 |
| 0.0 | 2.50* | 88 | 520 | 5.8 | 0.0 |
| -25 | 1.875 | 83 | 390 | 3.9 | -33 |
| -50 | 1.250 | 80 | 260 | 2.6 | -55 |
| -75 | 0.625 | 62 | 130 | 1.8 | -69 |

* Actual value

Note: Uncorrected asphalt concrete modulus = 208 ksi

[1] Variation between the actual value and the level of the factor used in the analysis.

[2] Factor = 2.5 x (1 + VAR/100)

[3] Temperature corresponding to the correction factor.

[4] Elastic modulus of asphalt concrete corrected for temperature effect. EAC = 520 x FACTOR/2.5

[5] Predicted fatigue life of the pavement for different values of EAC.

[6] Diff = (18-kip ESAL - 5.8)/5.8 x 100

To find a relationship between the 18-kip ESALs and temperature adjustment factor (*Fc*) for the pavement in Site 4 an exponential curve of the following form was fitted:

$$N_{18} = 1.315 \times e^{0.568 \times Fc} \qquad R^2 = .996, n = 7, SEE = 0.055$$

From the previous relation it is obvious that if the temperature correction factor changes by one-tenth of a unit, that is, from 2.4 to 2.5, the calculated 18-kip ESALs change by 0.08 millions for the pavement in Site 4. The temperature correction factor is a very sensitive parameter, especially in the calculation of 18-kip ESALs. It is apparent that the temperature correction factors for asphaltic layer moduli are major sources of variation in structural capacity estimation of pavements by the mechanistic method. It is questionable at this time whether this factor is a very good adjustment parameter for the AC modulus to represent the field condition, especially when the pavement temperature is very high (greater than 130°F).

## CONCLUSIONS

In this paper, the variability of the structural capacity determination by the mechanistic methods was presented with respect to layer thicknesses and the temperature correction factor for asphaltic layer moduli.

The variability in thickness of AC and AB layers affects the estimated structural capacity, but their interaction is not significant. This happens because in a deflection-matching backcalculation scheme, the thickness variation is compensated by a corresponding increase or decrease in modulus. For pavements with AC thickness of 4 in. or more, input thickness in FWD data analysis should not vary from the actual thickness by more than 1 in., whereas for pavements with less than 4 in. of AC thickness, the AC thickness should be known within 0.5 in. The AB thickness for such pavements should be known within less than 1.0 in. of actual thickness. For thick pavements with AC thickness of 6 in. or more, base thickness should be known within less than 2.0 in. of actual thickness. Thus, coring of FWD test locations is necessary for only AC layers for thick pavements and AC and AB layers for thin pavements.

The temperature correction factor suggested in the AASHTO guide for correcting asphalt-bound layer moduli was found to be very sensitive to the temperature of the pavement and has a tremendous effect on the estimated structural capacity of the pavement.

## RECOMMENDATIONS

The thickness sensitivity analysis should be extended to include more projects with granular bases and with AC layer thicknesses different from those used in this study. The findings will supplement the suggested coring requirements for pavements with a wide range of AC thickness. The study should also include pavements with stabilized bases so that coring needs for extracting thickness information for these types of pavements can also be addressed.

The temperature correction factors from the AASHTO guide for asphaltic layer moduli should be studied in detail to find a better correlation between temperature and in situ layer moduli.

## ACKNOWLEDGMENTS

The authors wish to acknowledge the financial support of this study provided by the Arizona Transportation Research Center, ADOT. The computing facilities, especially CRAY supercomputing facilities, were provided by Arizona State University. Thanks are due to Larry Scofield and John Eisenberg of ADOT, and Dwayne Rollier and Rohan Perera of Arizona State University for their help in this study.

## REFERENCES

1. *Guide for Design of Pavement Structures*, AASHTO, Washington, D.C., 1986.
2. P. Ullidtz. *Pavement Analysis*. Elsevier, New York, 1987.
3. M. S. Hoffman and M. R. Thompson. A Comparative Study of Selected Nondestructive Testing Devices. In *Transportation Research Record 852*, TRB, National Research Council, Washington, D.C., 1982, pp. 32–42.
4. A. S. M. M. Hossain. *Deflection Analysis of Flexible Pavements Using Nondestructive Test Data*. Ph.D. dissertation. Department of Civil Engineering, Arizona State University, Tempe, July 1990.
5. L. J. Painter. *CHEVRON N-layer Program—Improved Accuracy*. California Research Corporation, Richmond, 1980.
6. J. Michelow. *Analysis of Stresses and Displacements in an N-layered Elastic System Under a Uniformly Distributed Load on a Circular Area*. California Research Corporation, Richmond, 1963.
7. T. Rwebangira, R. G. Hicks, and M. Truebe. Sensitivity Analysis of Selected Backcalculation Procedures. In *Transportation Research Record 1117*, TRB, National Research Council, Washington, D.C., 1987.
8. L. H. Irwin, W. S. Yang, and R. N. Stubstad. *Deflection Reading Accuracy and Layer Thickness Accuracy in Backcalculation of Pavement Layer Moduli*. Special Technical Publication 1026, ASTM, Philadelphia, PA., 1989, pp. 229–244.
9. D. C. Montgomery. *Design and Analysis of Experiments*, 2nd ed., John Wiley and Sons, New York, N.Y., 1984.
10. V. L. Anderson and R. A. McLean. *Design of Experiments: A Realistic Approach*. Marcel Dekker Inc., New York, N.Y., 1974.